Facultad de Farmacia

Departamento de Farmacología

Síntesis de Protoberberinas y Ciclopentil-isoquinoleínas Dopaminérgicas, y Síntesis de Indenopiridinas Melatoninérgicas.

Synthesis of Dopaminergic Protoberberines and Cyclopentyl-isoquinolines, and Synthesis of Melatoninergic Indenopyridines

Tesis Doctoral

Presentada por:

Javier Párraga Vidal

Valencia, Enero 2015

PROGRAMA DE DOCTORADO DE BIOMEDICINA Y FARMACIA

D. **Diego M. Cortes Martínez** Catedrático, Dña. **Mª Dolores Ivorra Insa**, Catedrática, y Dña. **Nuria Cabedo Escrig**, Investigadora, del Departamento de Farmacología de la Universitat de València.

CERTIFICAN:

Que el trabajo presentado por el Ldo. **Javier Párraga Vidal**, titulado ***"Síntesis de Protoberberinas y Ciclopentil-isoquinoleínas dopaminérgicas, y Síntesis de Indenopiridinas melatoninérgicas"***, ha sido realizado en el Departamento de Farmacología de la Facultad de Farmacia de Valencia, bajo nuestra dirección y asesoramiento.

Concluido el trabajo experimental y bibliográfico, autorizamos la presentación de la Tesis, para que sea juzgado por el tribunal correspondiente.

Lo que firmamos en Valencia, el doce de Enero de dos mil quince.

D. Diego M. Cortes Martínez **Dña. Mª Dolores Ivorra Insa** **Dña. Nuria Cabedo Escrig**

Laboratoire Cobra
Chimie organique, Bioorganique, Réactivité et Analyse.

Pr. Pierre-Yves RENARD
Bio-organic chemistry team
Ph : (+33) 02 35 52 24 76
F : (+33) 02 35 52 29 71
Pierre-yves.renard@univ-rouen.fr

Rouen, August 26th, 2013

To whom it may concern

Object : Mr Javier Parraga placement in UMR 6014 CNRS COBRA - Rouen

This is to certify that Mr Javier Parraga spent three month (February-April 2013) in my Laboratory to conduct research on the synthesis of cadiolide analogues.

Sincerely,

Prof. Pierre-Yves RENARD

COBRA – UMR CNRS 6014
Bâtiment IRCOF
1, rue Tesnière
76821 Mont Saint Aignan Cedex
Tél. : (+33) 02.35.52.24.76
Fax. : (+33) 02.35.52.29.71
http://ircof.crihan.fr

CNRS INSA UNIVERSITÉ DE ROUEN

VNIVERSITAT DE VALÈNCIA

Facultad de Farmacia

Departamento de Farmacología

La presente Tesis Doctoral ha sido financiada con los siguientes proyectos y ayudas:

a) Proyectos públicos:

- Proyecto concedido por el Ministerio de Educación y Ciencia (SAF2007-63142).
  "Síntesis de Isoquinoleínas dopaminérgicas"

- Proyecto concedido por el Ministerio de Ciencia y Tecnología (SAF2011-23777).
  "Estudio de los mecanismos moleculares y celulares en la disfunción endotelial asociada a enfermedades con inflamación sistémica que pondrían inducir desórdenes cardiovasculares"

b) Proyectos financiados por empresas:

- Proyecto concedido por Fundación Medina, 2010.
  "Aislamiento de Acetogeninas"

- Proyecto concedido por Laboratorios Servier, 1997-2012.
  "Semisíntesis de estiril-lactonas antitumorales"

- Proyecto concedido por Valentia Biopharma, 2011-2013.
  "Síntesis de moléculas bioactivas"

c) Becas

- "Beca de colaboración" con cargo al proyecto Semisíntesis de Estiril-Lactonas Antitumorales, dirigido por el profesor Diego M. Cortes Martínez, y financiado por Laboratorios Servier.

- "Beca de investigación" con cargo al proyecto Semisíntesis de Estiril-Lactonas Antitumorales, dirigido por el profesor Diego M. Cortes Martínez, y financiado por Laboratorios Servier.

Agradecimientos

Por mucho que me esfuerce en este pequeño pero más que importante apartado de mi Tesis Doctoral, no será suficiente para poder expresar el merecido agradecimiento a todas aquellas personas que han hecho posible uno de mis sueños académicos.

En primer lugar, me gustaría agradecerles a mis directores de Tesis, la confianza depositada en mí y la dedicación y colaboración que me han demostrado a lo largo de todos estos años. Particularmente, agradecer y valorar la capacidad que, Diego Cortes, tiene para transmitir el amor por lo que uno hace en su trabajo, así como sus charlas de tan diferente ámbito que me han hecho crecer tanto profesionalmente como personalmente. A Nuria Cabedo agradecer sus inagotables ganas de colaborar, trabajar y seguir luchando para conseguir lo máximo que uno puede dar, y a Loles Ivorra por su paciencia a la hora de hacerme entender ciertos aspectos de los estudios farmacológicos.

En segundo lugar, quiero dar las gracias a María Jesús Ferrando (Facultad de Medicina) y a Xavier Franck (Universidad de Rouen) por haber hecho posible mis estancias en sus laboratorios y haberme dado la oportunidad de ampliar mis conocimientos tanto químicos como farmacológicos.

Además, agradecer a todo el personal de secretaria (Mamen e Irene) y técnicos de laboratorio (Carlos y Ángel "en paz descanse") por toda la ayuda y magnífico trabajo que han realizado, haciendo posible y facilitando las tareas de los demás, así como las conversaciones amigables y chistosas que haya podido tener con cada uno de ellos.

A todos aquellos con los que he compartido laboratorio durante este tiempo, muchísimas gracias; porque sin vuestra presencia, compañía y vuestros "chismorreos" todo hubiera sido mucho más aburrido. Gracias a Paloma, por perder su tiempo en enseñarme todo lo básico que debes saber para desenvolverte correctamente en un laboratorio. Gracias a Laura, por mostrarme en todo momento el camino a seguir, porque sabes que para mí eres la hermana mayor que no tenía. Gracias Abraham, por haber estado siempre pendiente y ayudando en todo lo que era necesario, por esos momentos de carcajadas y por tantas anécdotas que has contado para amenizar las tardes en el laboratorio.

También quiero agradecer el trato inmejorable que he recibido de todos aquellos que forman parte del Departamento de Farmacología, y que hacen que uno se sienta como en casa desde el mismo día que empiezas a formar parte de él.

Quería hacer mención especial y merecida a mi familia, porque ellos siempre han estado apoyándome, porque en momentos difíciles han estado firmes y han querido que terminara lo que en su día empecé; porque para ellos nada se empieza sino es para terminarlo, porque para ellos no hay nada más importante que el convencimiento de éxito en el trabajo que uno mismo desempeña; y esto es para dar las gracias de corazón. Gracias por haberme enseñado tanto y por haberme educado de este modo.

A mi hermano Rubén, mi mejor amigo, por ser mi fiel compañero de batallas futbolísticas y por enseñarme cosas como "en los pequeños detalles se gana el partido", frase aplicable a cualquier aspecto de la vida.

A mis amigos, muchísimas gracias por todo lo compartido durante estos años vividos, por tantos felices e inolvidables momentos. Gracias Pepe, Paola, Javi, Carles, Marta, Carlos, Alberto, David y Alfonso, mis compañeros de piso en estos nueve años de estudios universitarios en Valencia, porque convivir y crecer como personas junto a ellos ha sido todo un honor y un placer. Especialmente, a Cintia, Javi, Pepe y Paola por ser como sois, por ser pilares fundamentales a lo largo de mi vida y por estar ahí siempre, pase lo que pase.

Y gracias a todas aquellas personas que no he nombrado pero que me han ayudado de un modo u otro durante este tiempo.

MUCHISIMAS GRACIAS A TODOS.

Abreviaturas utilizadas

ADHD:	Síndrome de Déficit de atención e Hiperactividad
ADP:	Adenosín difosfato
AMPc:	Adenosín monfosfato cíclico
AMS:	Ácido Metansulfónico
Asp:	Ácido Aspártico
ATP:	Adenosín trifosfato
CI_{50}:	Concentración Inhibitoria 50
COMT:	Catecol-*O*-metil transferasa
CoQ:	Coenzima Q
CRM:	Cadena Respiratoria Mitocondrial
DAT:	Transportador de Dopamina
DDQ:	2,3-Dicloro-5,6-diciano-1,4-benzoquinona
DHFAA:	Dihidroxifenilacetaldehído
DFT:	Teoría Funcional de la Densidad
HCPIQ:	Hexahidrociclopentilisoquinoleína
HFAA:	Hidroxifenilacetaldehído
HHIP:	Hexahidroindenopiridina
IQ:	Isoquinoleína
LAH:	Hidruro de aluminio y litio
MAO:	Monoamino Oxidasa
MD:	Dinámica Molecular
MS:	Metabolito Secundario
MSA:	Metabolito Secundario Activo
MT:	Melatonina
MTT:	Bromuro de 3-(4,5 dimetiltiazol-2-ilo)-2,5-difeniltetrazol
NADH:	Nicotinamida adenina dinucleótico
PARP:	Poli(ADP-ribosa) polimerasa

Phe:	Fenilalanina
PLP:	Fosfolipasa
PNMT:	Feniletanolamin-*N*-metil-transferasa
PPA:	Ácido Polifosfórico
QM:	Mecánica Cuántica
QTAIM:	Teoría Cuántica de Atomos en Moléculas
RD:	Receptor Dopaminérgico
REA:	Relación Estructura-Actividad
RL:	Radioligando
RMN:	Resonancia Magnética Nuclear
RMT:	Receptor Melatoninérgico
SDH:	Succinato-deshidrogenasa
Ser:	Serina
SNC:	Sistema Nervioso Central
THIQ:	Tetrahidroisoquinoleína
THPB:	Tetrahidroprotoberberina

Índice

Pág.

Introducción

Introducción

1.- Introducción y Objetivos

El estudio de compuestos de origen natural constituye una de las principales vías de obtención de nuevos productos farmacológicamente activos, tanto por aislamiento directo como por semisíntesis. Además, la naturaleza sigue siendo una fuente de inspiración inextinguible para químicos y farmacólogos en el diseño de nuevos fármacos. Numerosos organismos naturales, ya sean vegetales, animales o microorganismos, son capaces de biosintetizar una extensa diversidad de metabolitos secundarios (MS), los cuales se utilizan directamente como fármacos, pueden ser útiles en la síntesis de nuevos compuestos o pueden ayudarnos a diseñar nuevas moléculas utilizándolas como fuente de inspiración. De hecho, una gran cantidad de metabolitos secundarios activos (MSA) y sus correspondientes análogos estructurales constituyen el arsenal terapéutico, mientras algunos de los que no poseen actividad por si solos, son utilizados por la industria como productos de partida en la síntesis de nuevos compuestos bioactivos. La Farmacoquímica Natural se define como la rama de las ciencias farmacéuticas que se encarga del estudio de los principios activos de origen natural, es decir, de los MSA mencionados anteriormente.

En nuestro grupo de investigación se ha trabajado durante los últimos años en el campo de la Farmacoquímica Natural, basándose en el estudio de plantas de la familia Annonáceas y utilizando los compuestos que poseen estas especies como fuente de inspiración para desarrollar diferentes moléculas potencialmente activas.

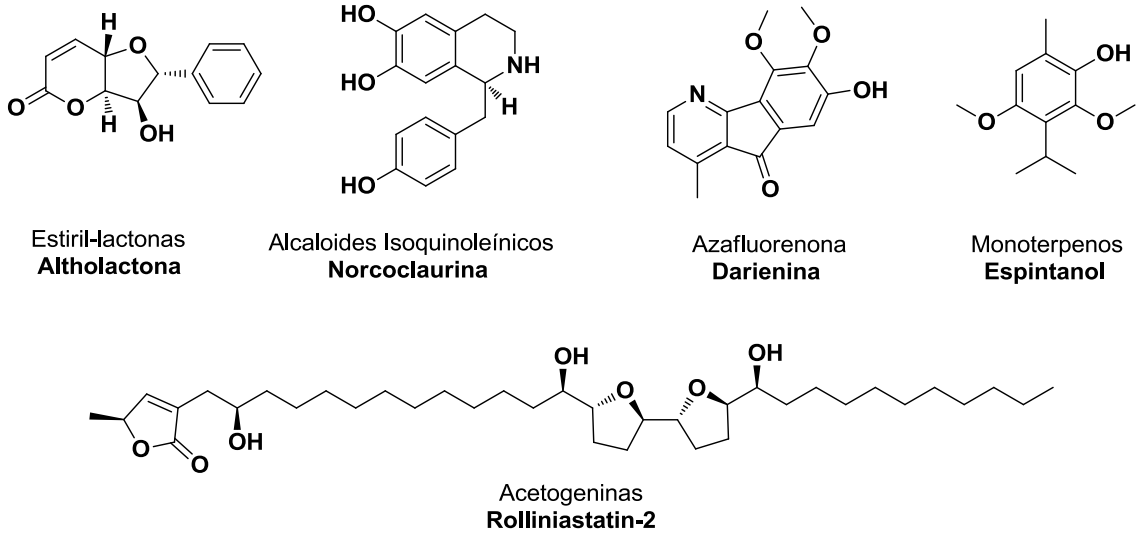

Figura 1. Ejemplos de MSA presentes en Annonáceas

Las especies vegetales que pertenecen a la familia Annonáceas son conocidas desde hace tiempo tanto por su interés económico (productoras de frutos comestibles, condimentos alimentarios, especias y aceites esenciales) como por su utilización en medicina tradicional y popular (pesticida y antiparasitaria) [1]. Los MSA presentes en estas plantas se utilizan debido a las propiedades y actividades farmacológicas que poseen (**Figura 1**).

A.- Acetogeninas: Moléculas presentes exclusivamente en especies de la familia Annonáceas interesantes por presentar actividad citotóxica, antitumoral, insecticida y antiparasitaria. Se caracterizan por poseer una estructura de cadena larga (entre 32 y 34 átomos de carbono) con varios grupos oxigenados y una lactona terminal. Su actividad citotóxica se debe principalmente a la inhibición selectiva que ejercen sobre el complejo I de la cadena respiratoria mitocondrial (CRM) [2 y 3].

B.- Estiril-lactonas: Compuestos caracterizados por presentar una estructura de 13 átomos de carbono que forman un esqueleto estiril unido a un anillo lactona. Estos compuestos, utilizados en medicina tradicional, están presentes en especies del género *Goniothalamus* y se han descrito como moléculas con actividad citotóxica. Los ensayos *in vitro* de estos compuestos demostraron que la crassalactona B presenta una elevada capacidad de inhibición sobre el crecimiento de la línea celular T de la leucemia [4 y 5].

C.- Monoterpenos: Metabolitos secundarios presentes en una amplia diversidad de especies vegetales, entre ellas las Annonáceas, que presentan importancia farmacológica por poseer diversas actividades biológicas como antiparasitaria, antibacteriana e insecticida, entre otras. El espintanol es un monoterpeno conocido por su actividad antimalárica [6 y 7].

D.- Alcaloides Isoquinoleínicos: Principios activos presentes en multitud de familias botánicas dentro del orden de las Magnoliales, donde se incluye a la familia Annonáceas. Este tipo de alcaloides se caracteriza por poseer un átomo de nitrógeno formando un anillo piperidínico adyacente a un anillo bencénico, dando lugar así al "scaffold" característico y común de todos los alcaloides isoquinoleínicos (IQs). Estas moléculas son importantes desde el punto de vista farmacológico, debido a la gran variedad de actividades biológicas que poseen.

En estos últimos años, nuestro grupo de investigación ha puesto a punto la síntesis de ciertos cabezas de serie de naturaleza nitrogenada con diferentes esqueletos químicos, basándose en estudios de Relación Estructura Química – Actividad Biológica (REA) efectuados previamente con moléculas naturales aisladas, generalmente de especies vegetales tropicales. De esta forma, se llevó a cabo la síntesis de alcaloides IQs y esqueletos relacionados con afinidad por los receptores dopaminérgicos (RD), a la luz de los resultados obtenidos años atrás con diferentes compuestos bencilisoquinoleínicos, aporfínicos, protoberberínicos, cularínicos y bis-bencilisoquinoleínicos naturales y sintéticos (**Figura 2**).

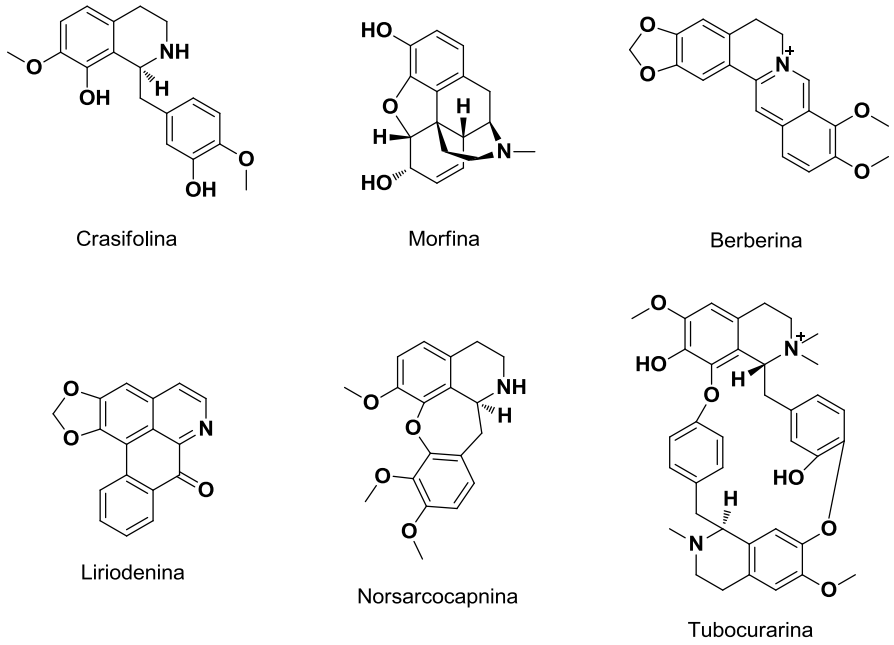

Figura 2. Alcaloides Isoquinoleínicos

E.- Azafluorenonas: Productos que se encuentran en pocas especies de la familia de las Annonáceas, como en *Oxandra longipetala, O. xylopioides*, *O. espintana, O. asbeckii* y *O. major* [8-11]. Este tipo de alcaloides son farmacológicamente interesantes debido a la elevada actividad antifúngica y antibacteriana que poseen [12]. La estructura química que presenta este tipo de moléculas se conoce como azafluorenonas, y consiste en un esqueleto tricíclico en el que se encuentran fusionados un anillo piridínico, una ciclopentanona y un anillo bencénico (**Figura 3**).

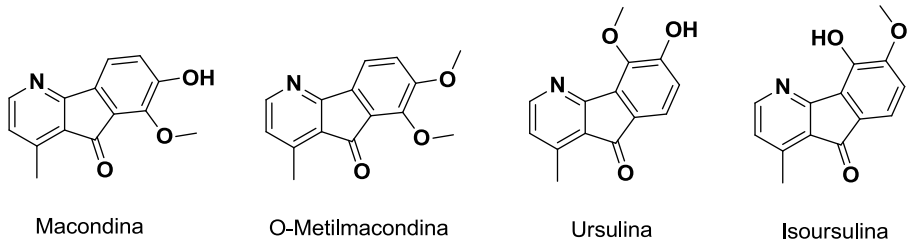

Figura 3. Azafluorenonas

Nuestro grupo de investigación se ha inspirado en este tipo de estructuras y en otras con esqueletos relacionados, como la melatonina, ramelteón y agomelatina, para desarrollar una ruta sintética que nos permita la obtención de hexahidroinderopiridinas (HHIP). La melatonina es una hormona que regula el ciclo diurno/nocturno, por lo que fármacos con estructura similar podrán tener cierta actividad melatoninérgica y ser potenciales fármacos contra el insomnio, como es el caso del hipnótico ramelteón (Rozerem©), un potente agonista de los receptores melatoninérgicos (RMT). La agomelatina (Thymanax©, Valdoxan©) es un fármaco antidepresivo usado actualmente en el tratamiento de depresiones mayores en adultos que presenta una estructura química relativamente parecida a la de las moléculas señaladas anteriormente. Las HHIP pueden considerarse análogos de la melatonina, por lo que se pretenderá estudiar la afinidad que poseen dichas HHIP sobre los RMT, con la finalidad de diseñar y obtener nuevos fármacos contra el insomnio y/o depresión (**Figura 4**).

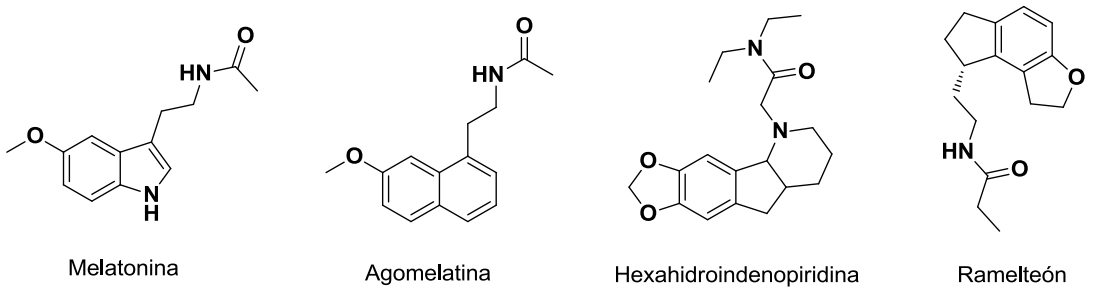

Figura 4. Melatonina, HHIP y moléculas relacionadas

Objetivos

Los objetivos propuestos en la presente Tesis Doctoral son:

1.- Síntesis y estudios de afinidad por los receptores dopaminérgicos de Isoquinoleínas:

- Tetrahidroprotoberberinas (THPB).
- 7-Fenil-hexahidrociclopenta-[*ij*]-isoquinoleínas (HCPIQ).

- Estudios de citotoxicidad, mediante ensayos de MTT y citometría de flujo.
- Estudio de la interacción ligando-receptor mediante Modelización Molecular.

2.- Síntesis y estudios de afinidad por los receptores melatoninérgicos de HHIP.

3.- Síntesis y estudios de actividad antimicrobiana y citotóxica de Isoquinoleínas lactámicas y benzoquinolizidinas.

2.- Los Alcaloides Isoquinoleínicos

Los alcaloides IQs son metabolitos secundarios, principalmente de origen vegetal. Presentan una estructura compleja nitrogenada, por lo que generalmente son básicos. Desde el punto de vista farmacológico se trata de un grupo de compuestos muy interesante, ya que presentan variadas acciones, caracterizándose por su gran actividad a dosis bajas, aunque también pueden presentar una toxicidad significativa. De hecho, en mamíferos, se ha observado que algunos alcaloides son capaces de ejercer una acción fisiológica intensa con efectos psicoactivos aún a dosis bajas, por lo que son muy usados en medicina para tratar diversos problemas neurofisiológicos. Otras actividades biológicas de interés son la actividad antitumoral, antiespasmódica, hipnoanalgésica y antifúngica. Además de su capacidad de inhibición de transporte y/o recaptación de neurotransmisores, así como la capacidad de unión a receptores de membrana, ya que presentan afinidad sobre receptores dopaminérgicos, adrenérgicos, canales de calcio voltaje-dependientes y sobre segundos mensajeros, como el AMPc [13].

2.1.- Biosíntesis de los Alcaloides Isoquinoleínicos

Los alcaloides son sustancias orgánicas nitrogenadas de origen natural, generalmente biosintetizadas a partir de aminoácidos, de carácter básico y de estructura química diversa y compleja. Los alcaloides con esqueleto IQ constituyen uno de los grupos más abundantes en la naturaleza, se encuentran principalmente distribuidos en el reino vegetal y abarcan una amplia variedad de tipos estructurales.

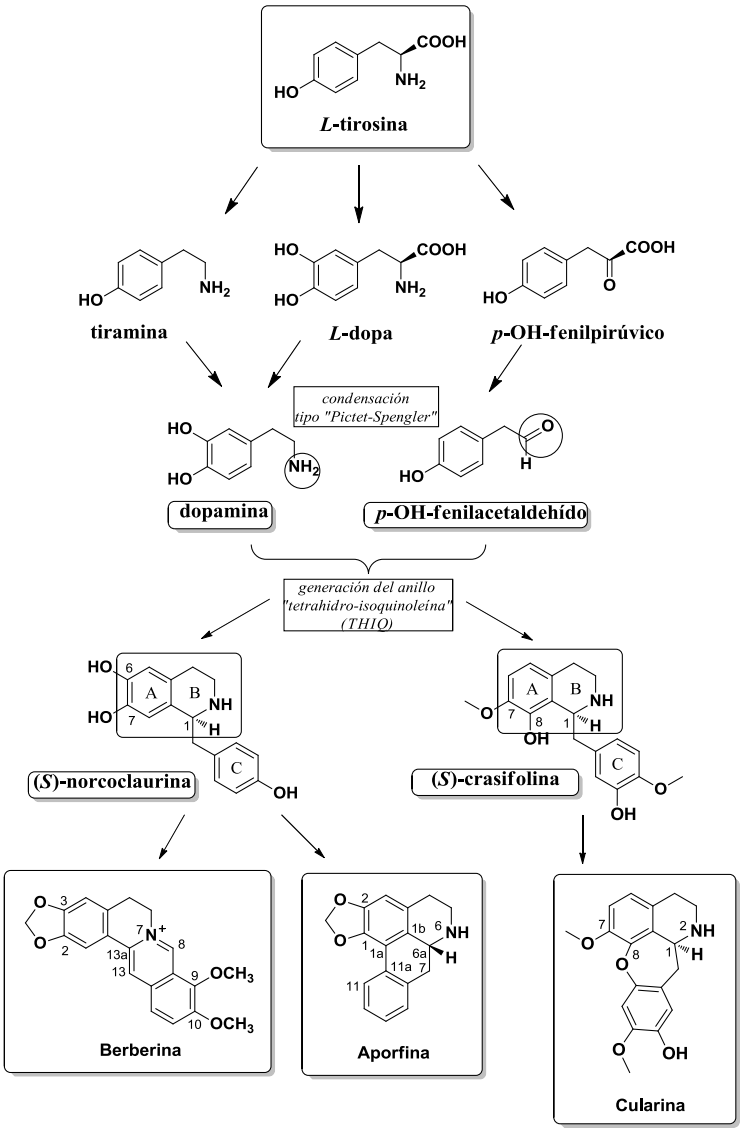

Esquema 1. Biosíntesis de Alcaloides Isoquinoleínicos

Los alcaloides IQs se biosintetizan a partir de la L-tirosina. Esta sufre una hidroxilación en posición 3 para dar lugar a la L-dopa, cuya descarboxilación conduce a la formación de dopamina. Esta descarboxilación la realiza una enzima fosfolipasa (PLP)-dependiente puesto que necesita fosfato de piridoxal como coenzima (**Esquema 2**) [14 y 15].

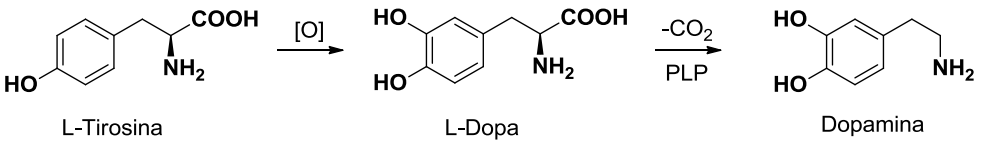

Esquema 2. Hidroxilación y descarboxilación de L-tirosina

Por otro lado, una molécula de L-tirosina sufre una desaminación oxidante para generar el ácido 4-hidroxifenilpirúvico o el ácido 3,4-dihidroxifenilpirúvico, que mediante una descarboxilación se transforma en el 4-hidroxi- (4-HFAA) o 3,4-dihidroxifenilacetaldehído (3,4-DHFAA) (**Esquema 3**) [14 y 15].

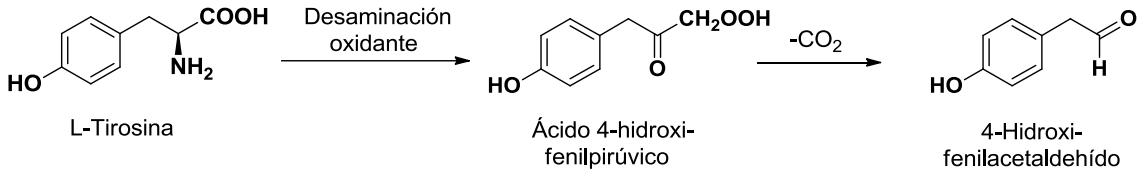

Esquema 3. Desaminación oxidante y descarboxilación de L-tirosina

A continuación y mediante una reacción de tipo Pictet-Splenger, la dopamina se condensa estereoespecíficamente con 4-HFAA o 3,4-DHFAA, reacción que puede ser catalizada por diferentes enzimas tipo sintasas y que dará lugar a diferentes alcaloides con estructura isoquinoleínica, como la (S)-norcoclaurina, la (S)-norlaudanosolina y la (S)-crasifolina (**Figura 5**). En el curso de esta reacción se genera una base de Schiff, que tiene la capacidad de captar protones del medio, y tras un movimiento característico de pares de electrones consigue la ciclación del anillo piperidínico propio de los alcaloides IQs, donde está presente el estereocentro típico de este tipo de moléculas (posición 1) (**Esquema 4**) [14].

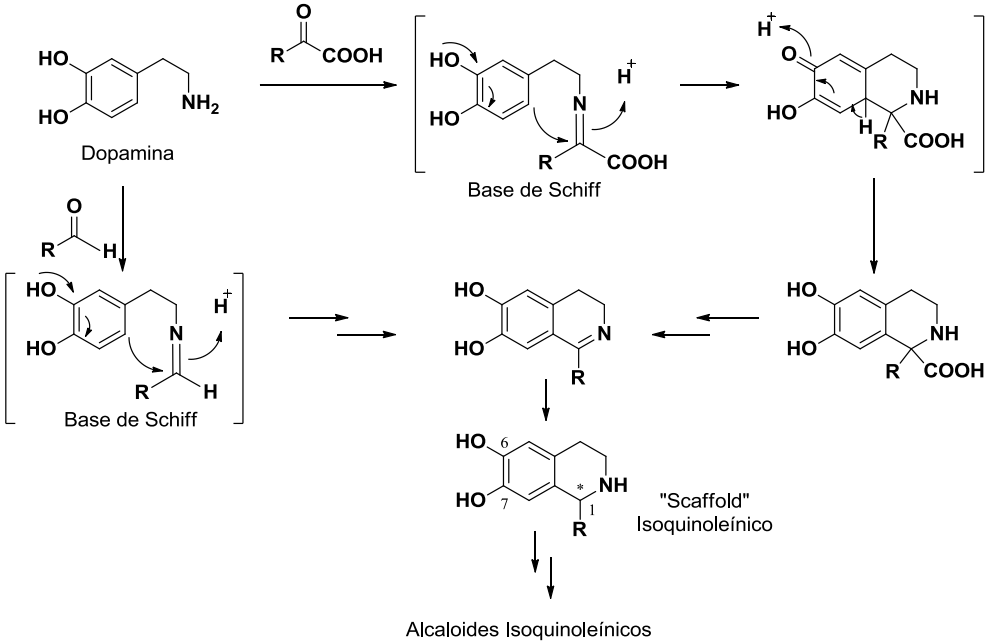

Esquema 4. Biosíntesis del "Scaffold" Isoquinoleínico

Una vez biosintetizado el "scaffold" IQ, se podrán obtener los diferentes alcaloides pertenecientes a esta familia, mediante diversos métodos y reacciones. Podemos observar que las 1-bencil-1,2,3,4-tetrahidroisoquinoleínas (1-bencil-THIQ) ocupan un lugar privilegiado dentro de este grupo, ya que a partir de ellas se biosintetizan multitud de análogos estructurales como las protoberberinas, aporfinas, cularinas, alcaloides morfínicos, bis-bencil-IQs, entre otros (**Esquema 1**).

2.2.- Tipos de Derivados Isoquinoleínicos

En las últimas décadas, diversos grupos de investigación han tenido como principal objetivo el aislamiento de alcaloides a partir de seres vivos, tanto vegetales, como animales, microorganismos e incluso insectos [16]. En la presente Tesis Doctoral se van a abordar diferentes tipos de derivados IQ, entre ellos:

A.- IQs naturales, derivadas de las 1-bencil-THIQs: En el **Esquema 1** se puede observar que las 1-bencil-THIQs son precursores naturales de diferentes tipos de alcaloides IQ, cada uno de los cuales va a presentar un esqueleto característico. La importancia de muchos de estos compuestos versa sobre las potentes actividades farmacológicas que poseen, como por ejemplo, la actividad antimicrobiana y antifúngica de las protoberberinas (berberina), la actividad analgésica de los alcaloides morfínicos (morfina), el poder antitusígeno de algunos de los alcaloides morfínicos (codeína), la capacidad relajante muscular de las 1-bencil-IQ (crasifolina) y bis-bencil-IQ (tubocurarina), los efectos cardiovasculares de las cularinas (norsarcocapnina) y la actividad antiparasitaria de oxoaporfinas (liriodenina) (**Figura 2**).

- **Protoberberinas**: Los alcaloides tetrahidroprotoberberínicos (THPB) son alcaloides IQ de origen natural presentes, entre otras, en especies de las familias Annonáceas, Berberidáceas y Ranunculáceas, como *Hydrastis canadensis* (sello de oro), *Coptis chinensis* (coptis o hebra de oro), *Berberis aquifolium* (uva de Oregón), *B. vulgaris* (agracejo) y *B. aristata* (árbol de cúrcuma). Este tipo de alcaloides presentan un esqueleto tetracíclico originado a partir de un sistema 1-bencil-THIQ. Por lo tanto, su ruta biosintética comparte el mismo origen que dichos alcaloides 1-bencil-THIQ y se inicia a partir del aminoácido *L*-tirosina (**Esquema 1**). Las THPB destacan por presentar actividades farmacológicas muy interesantes y variadas. En los últimos años se ha observado que pueden actuar tanto sobre receptores de membrana dopaminérgicos, como inhibiendo la acetilcolinesterasa y butirilcolinesterasa, además de tener actividad bactericida y ser incluso útiles para tratar la diabetes [17 y 18].

- **Aporfinas**: Los alcaloides aporfínicos constituyen uno de los grupos más amplios y más abundantes en la naturaleza dentro de los alcaloides IQ, encontrándose distribuidos en especies vegetales de las familias Annonáceas, Ranunculáceas, Lauráceas, Hernandiáceas y Monimiáceas [19]. Este tipo de alcaloides presentan un esqueleto tetracíclico muy variado, incluyendo los esqueletos de oxoaporfina o proaporfina. Todos ellos son originados a partir de un sistema 1-bencil-THIQ. Por lo tanto, su ruta biosintética será muy similar a la de los alcaloides protoberberínicos (**Esquema 1**). Las aporfinas presentan una elevada importancia farmacológica, puesto que poseen actividades como antioxidante, antiagregante plaquetario, antineoplásico y antiparkinsoniano [20]. Además cabe destacar dentro de este tipo de IQ, la apomorfina, obtenida por semisíntesis a partir de la morfina, ya que su aplicación terapéutica frente a la enfermedad de Parkinson es importante, debido a que es un potente agonista de los RD tipo D_2. La bulbocapnina también tiene efecto sobre el mismo tipo de RD, pero esta actuará como antagonista de los mismos, por lo que su aplicación versará sobre trastornos psicóticos como la esquizofrenia.

- **Cularinas**: Los alcaloides cularínicos pertenecen a uno de los grupos de IQ más escaso en la naturaleza, no obstante, se conoce que están presentes en especies de los géneros *Corydalis*, *Sarcocapnos*, *Ceratocapnos* y *Dicentra* [21-24]. La (+)-cularina fue aislada por Manske en 1938 a partir de especies de la familia Fumareáceas y su estructura fue determinada en 1950. La biosíntesis de este grupo de alcaloides IQ es diferente a la de los compuestos vistos anteriormente. En este caso se parte de una 1-bencil-IQ con un grupo funcional oxigenado en posición 8, para poder dar lugar al esqueleto benzoxepínico característico de los alcaloides cularínicos (**Esquema 1**).

B.- IQs sintéticas, las 7-fenil-1,2,3,7,8,8a-hexahidrociclopenta-[*ij*]-isoquinoleínas (HCPIQ): Este tipo de compuestos se puede definir como IQ sintéticas, puesto que se caracterizan por presentar un novedoso esqueleto IQ diversificado que no está presente en la naturaleza. Su estructura contiene un anillo de cinco átomos de carbono fusionado con el "scaffold" IQ y un grupo fenilo como sustituyente en el ciclopentano, en posición 7. Entre los alcaloides IQ, este tipo de moléculas no han sido observadas en ninguna especie animal, vegetal, ni en microorganismos, por lo que se pueden considerar IQ sintéticas. Además, se puede decir que es un esqueleto novedoso porque hay muy poco descrito sobre este tipo de compuestos en la literatura. No obstante, existen alcaloides de estructura similar en especies de esponjas marinas como la *Aaptos aaptos*, a partir de la cual se han aislado alcaloides IQ que poseen actividades farmacológicas interesantes como antitumoral, antimicrobiana y afinidad por adrenoreceptores. Las HCPIQs son análogos sintéticos de proaporfinas como la

pronuciferina, además de estar estructuralmente relacionados con los azafluorantenos [25-30] (**Figura 5**). En los últimos años, se han sintetizado derivados de HCPIQ con actividad inhibidora sobre la feniletanolamin-N-metil-transferasa (PNMT) [31], poli(ADP-ribosa) polimerasas (PARPs) [32] y con actividad antiprotozoaria [33]. Estos alcaloides presentes en especies vegetales y marinas, y sus análogos sintetizados con diversas actividades interesantes desde un punto de vista farmacológico, nos han inspirado al desarrollo de este tipo de moléculas con la finalidad de encontrar nuevos esqueletos IQs con afinidad por los RD.

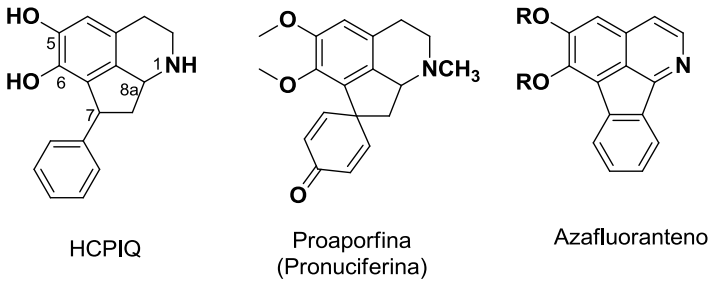

Figura 5. Hexahidrociclopenta[*ij*] isoquinoleína (HCPIQ), proaporfina y azafluoranteno

3.- Las Indenopiridinonas y Hexahidroindenopiridinas

Podemos encontrar en la naturaleza la estructura tricíclica de indenopiridinonas, en compuestos tipo azafluorenonas (*véase* **Figura 3**), la cual consiste en un anillo bencénico fusionado a una ciclopentanona y una piridina. En cambio, aunque las hexahidroindenopiridinas (HHIP) son moléculas de síntesis muy similares a las indenopiridinonas, se caracterizan por presentar en su estructura un esqueleto tricíclico nitrogenado, en el que destaca un anillo bencénico fusionado a un ciclopentano (anillo indeno) y una piperidina (**Figura 6**).

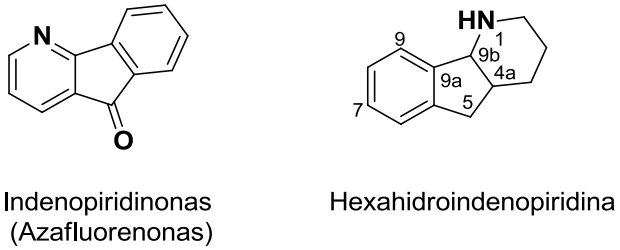

Figura 6. Similitud estructural

El esqueleto de las HHIP podría ser considerado como un análogo tricíclico del ligando *trans*-2-amino-3-fenil-2,3-dihidro-1*H*-indeno-5-ol con afinidad por los receptores dopaminérgicos D_1 y D_2, importante en el tratamiento de diferentes enfermedades neurodegenerativas y en el envejecimiento cerebral [34-36]. También habría que destacar la proximidad estructural de las HHIP con el aminoindano rasagilina, (1*R*)-*N*-propargil aminoindano [37], fármaco utilizado en la enfermedad del Parkinson (**Figura 7**).

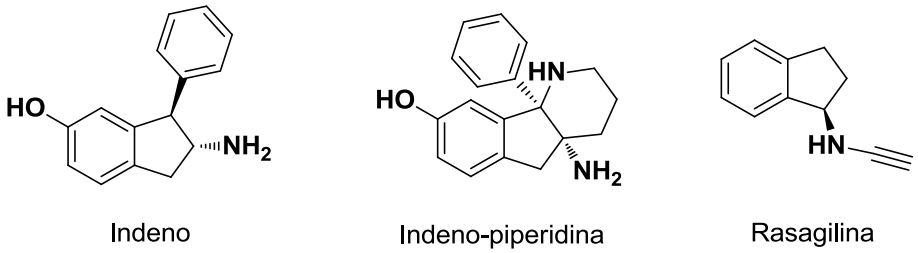

Figura 7. Estructura del indeno (*trans*-2-amino-3-fenil-2,3-dihidro-1*H*-indeno-5-ol), del análogo indeno-piperidina y de rasagilina

3.1.- Tipos de Hexahidroindenopiridinas

Este tipo de alcaloides sintéticos no han sido tan estudiados como los vistos anteriormente, por lo que el conocimiento sobre ellos es mucho menor. No obstante, se puede establecer una clasificación de las hexahidroindenopiridinas en función de la posición del nitrógeno en el anillo de piperidina (**Figura 8**).

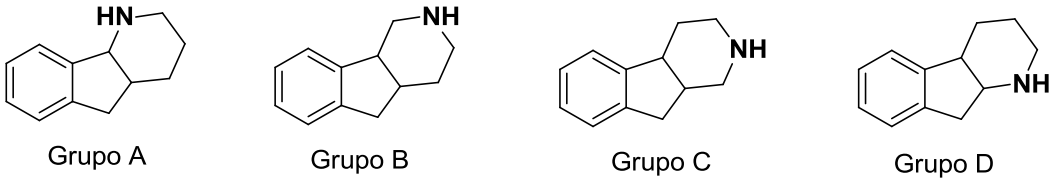

Figura 8. Clasificación de las hexahidroindenopiridinas (HHIP)

1.- **Grupo A**: Presenta el átomo de nitrógeno en posición relativa 1 dentro del anillo de piperidina y contiene tanto una unidad de fenilmetilamina como fenilpropilamina en su estructura. Como veremos más adelante, varios grupos de investigación han desarrollado diferentes rutas sintéticas para la obtención de este tipo de HHIP, a partir de cianoalquil-indanonas [38], 5-oxo-fenilvaleronitrilos [39], indanonas [34] e indenos [40] (**Esquema 5**).

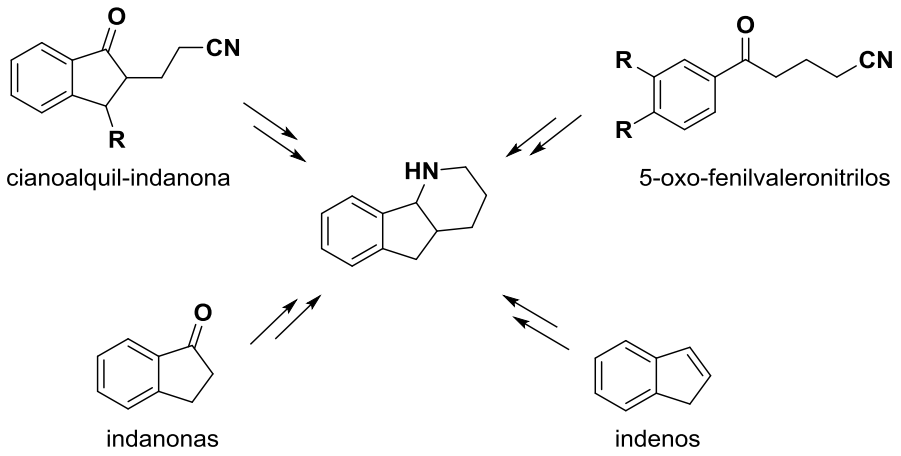

Esquema 5. Síntesis de HHIP del grupo A

2.- **Grupo B**: Contiene el átomo de nitrógeno en posición relativa 2 dentro del anillo de piperidina y en su estructura existe una unidad feniletilamina. Diversos grupos de investigación han desarrollado y patentado una serie de HHIP feniletilamínicas usados para el tratamiento de trastornos metabólicos, desórdenes en el sistema nervioso, alteraciones gastrointestinales y como analgésicos. Estas HHIP han sido sintetizadas a partir de etil-3-(*p*-tolil)-piperidina o ethyl-1,2,3,6-tetrahidropiridina, y mediante una serie de reacciones, diferentes según el compuesto a sintetizar, se obtuvieron toda una gama de indenopiridinas (**Esquema 6**) [41].

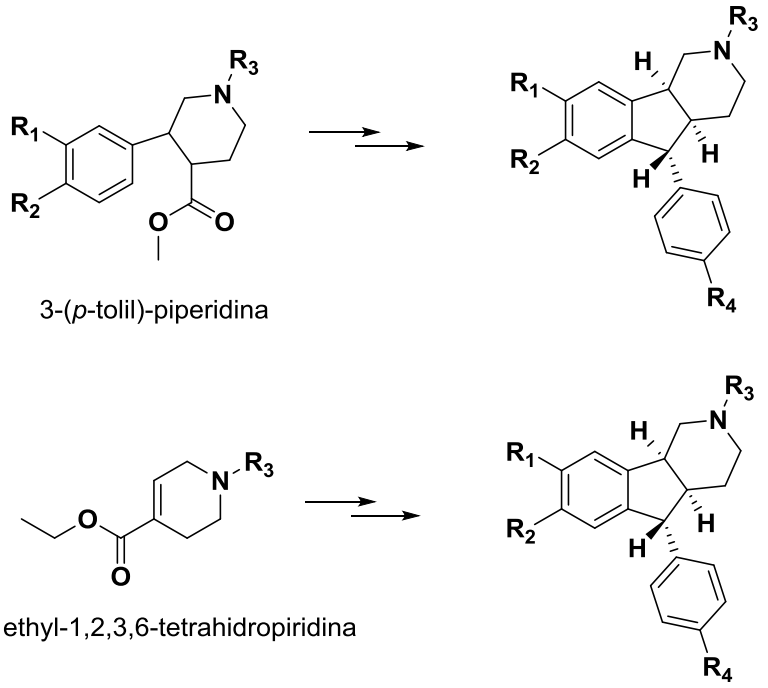

Esquema 6. Síntesis de HHIP del grupo B

3.- **Grupo C**: Son HHIP que presentan el átomo de nitrógeno del anillo piperidínico en posición relativa 3 y contiene una unidad fenilpropilamina en su estructura. Sobre este tipo de HHIP no se ha encontrado ninguna referencia bibliográfica que haya desarrollado una síntesis química ni tampoco que se hayan detectado y/o aislado de la naturaleza.

4.- **Grupo D**: Son compuestos indenopiridínicos que poseen el nitrógeno piperidínico en posición relativa 4, y presentan en su estructura una unidad de feniletilamina. Se han diseñado multitud de rutas sintéticas para la formación de este tipo de HHIP con actividad antidiabética y antidislipémica, destacando entre ellas la síntesis que utiliza como productos de partida un anillo bencénico y una piridina convenientemente sustituidos. Además, con esta misma actividad biológica se obtuvieron otros análogos que se sintetizaron a partir de 3,4-dihidronaftalen-2(1H)-ona (**Esquema 7**) [42].

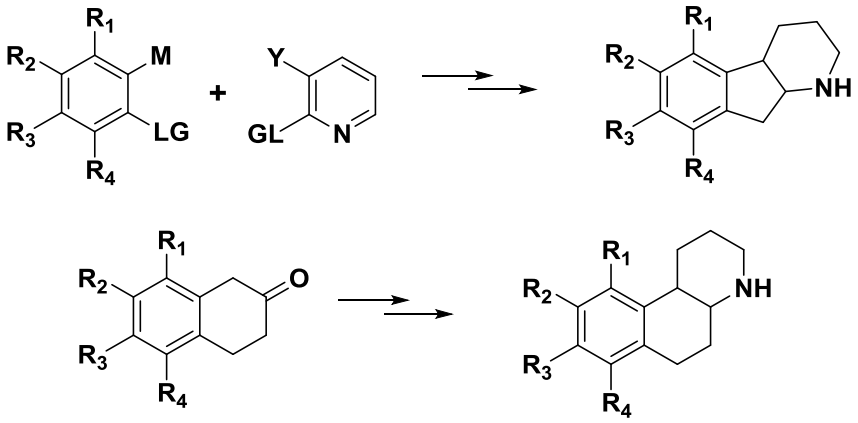

Esquema 7. Síntesis de HHIP del grupo D

4.- Antecedentes del Grupo de Investigación. Síntesis de Isoquinoleínas Dopaminérgicas

Actualmente, el avance tanto en síntesis química como en nuevas técnicas y metodología de determinación estructural, ha hecho posible el desarrollo de nuevas moléculas formadas por un esqueleto nitrogenado complejo diferentemente sustituido. Además, ha progresado el conocimiento de los lugares de unión de los diferentes receptores sobre los cuales van a interaccionar los fármacos sintetizados, gracias al desarrollo de técnicas como la modelización molecular. Esta nos ayudará a determinar posibles farmacóforos, es decir, la parte de la molécula responsable de la unión al receptor, puesto que nos permite conocer con mayor precisión los restos de aminoácidos que configuran el sitio de unión de un receptor y, por lo tanto, nos dará una gran información sobre qué tipo de estructura molecular, así como los sustituyentes, que debe tener el fármaco para mejorar y optimizar al máximo la unión de la molécula activa al receptor en cuestión.

Una de las líneas de investigación que mayor relevancia ha adquirido a lo largo de estos años en nuestro grupo de trabajo, ha sido la síntesis de diversas moléculas nitrogenadas y determinación de la afinidad por diferentes tipos de receptores celulares [43-51]. Los resultados que se han obtenido a lo largo de estos años nos permiten concluir que las THIQ 1-sustituidas presentan afinidad por los RD (subfamilias tipo D_1 y tipo D_2), y en algunos casos son capaces de inhibir la recaptación de dopamina.

En trabajos anteriores, se describió la síntesis enantioselectiva de pares de enantiómeros 1-bencil-THIQs dopaminérgicas (*1S*) y (*1R*), utilizando como auxiliar quiral el (*R*) o (*S*) fenilglicinol, respectivamente. En este trabajo se determinó que los enantiómeros (*1S*) eran de 5 a 15 veces más afines por los RD tipo D_1 y tipo D_2 que los enantiómeros (*1R*) (**Figura 9**) [46].

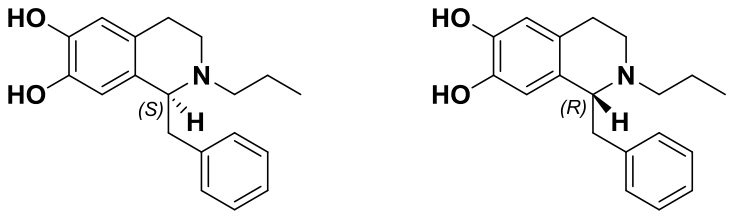

Figura 9. 1-Bencil-THIQ (*1S*) y (*1R*)

Posteriormente, se prepararon THIQs diferentemente sustituidas y se observó la importancia de la sustitución tanto en el anillo A, como en posición 1 y sobre el nitrógeno, para así mejorar la afinidad sobre los RD e incluso inhibir la recaptación de dopamina en alguno de los casos.

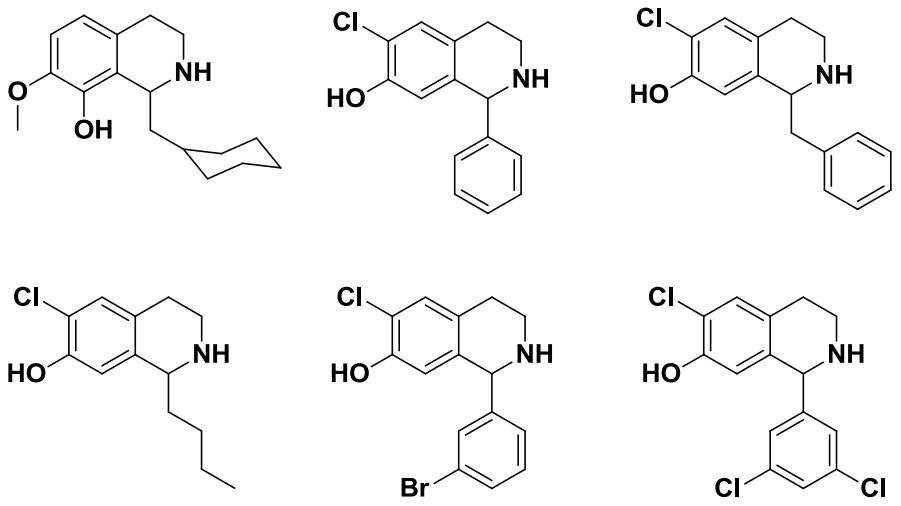

Figura 10. THIQ dopaminérgicas 1-sustituidas

En cuanto a la sustitución en posición 1 y sobre el nitrógeno, se observó que la presencia del grupo ciclohexilmetil en posición 1 cuando el nitróge no está en forma de amina secundaria, es decir, nitrógeno no sustituido; provocaba una elevada afinidad por el RD tipo D_2, mientras que si este compuesto presentaba un grupo metilo sobre el nitrógeno, aumentaba su afinidad por los RD D_1 [47]. También se observó que la presencia de una cadena alifática, tipo *n*-butil, sobre la posición 1, aumentaba considerablemente la afinidad por RD tipo D_2 (Ki = 66nM), mientras que otros sustituyentes en la misma posición como el grupo bencilo y fenilo no eran capaces de provocar una afinidad tan elevada. En cuanto a la sustitución en el anillo A, se confirmó que la presencia de un átomo de cloro y un grupo hidroxilo, en posición *meta* y *para* de la feniletilamina, aumenta la afinidad por los RD tipo D_2 [50]. También se observó que la presencia de halógenos en el sustituyente en posición 1 puede aumentar la afinidad por dichos RD [51] (**Figura 10**).

A través de los resultados obtenidos, se han podido preparar nuevos alcaloides IQs y diversificar los esqueletos para mejorar los valores de afinidad por los RD. Además, los estudios de modelización molecular han sido útiles para confirmar la presencia de diferentes farmacóforos en este tipo de moléculas, tales como: la sustitución alquílica del nitrógeno, la existencia de grupos halogenados y/o hidroxilados en el anillo A, y la de grupos hidrofóbicos sobre la posición 1 de las THIQ [48-51].

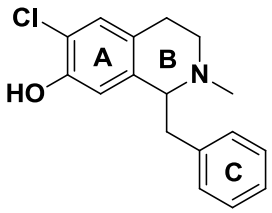

Esquema 8. 1-Bencil-THIQ dopaminérgica

5.- Síntesis de Derivados Isoquinoleínicos

La obtención de los diferentes alcaloides con estructura IQ se puede conseguir mediante distintas rutas sintéticas. A lo largo de los años, numerosos grupos de investigación han conseguido preparar una gran variedad de IQ y análogos estructurales a través de reacciones químicas de complejidad muy variada. Como ya hemos mencionado en la introducción, la fuente de inspiración en el diseño de estas rutas sintéticas es, en la mayoría de los casos, la naturaleza y las rutas biosintéticas que se producen en los seres vivos que contienen dichos compuestos.

5.1.- <u>Síntesis de Tetrahidroprotoberberinas</u>

Las aproximaciones sintéticas utilizadas para la obtención de THPB están indicadas en la siguiente figura (**Figura 11**):

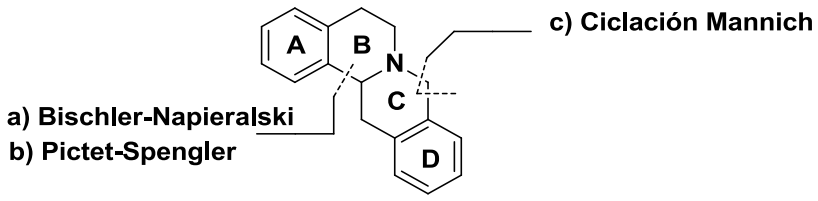

Figura 11. Aproximaciones sintéticas de THPB

Las estrategias sintéticas basadas en las desconexiones (a) y (b) tienen en común que la formación del anillo B de las THPB es la etapa de mayor importancia, mientras que en la desconexión (c), la etapa clave consiste en la generación del anillo C.

Analizaremos de forma general los aspectos más destacables de las distintas aproximaciones sintéticas indicadas.

a) Ciclodeshidratación de Bischler-Napieralski: el anillo B de las THPB se forma por ciclación de una amida, obtenida mediante el ataque de una feniletilamina a una 3-isocromanona, ambas convenientemente sustituidas, y una posterior reducción de la imina. Mediante la utilización de este método los rendimientos alcanzados no han superado el 20% y la mayor dificultad radica en la preparación de las isocromanonas de partida [52] (**Esquema 9**).

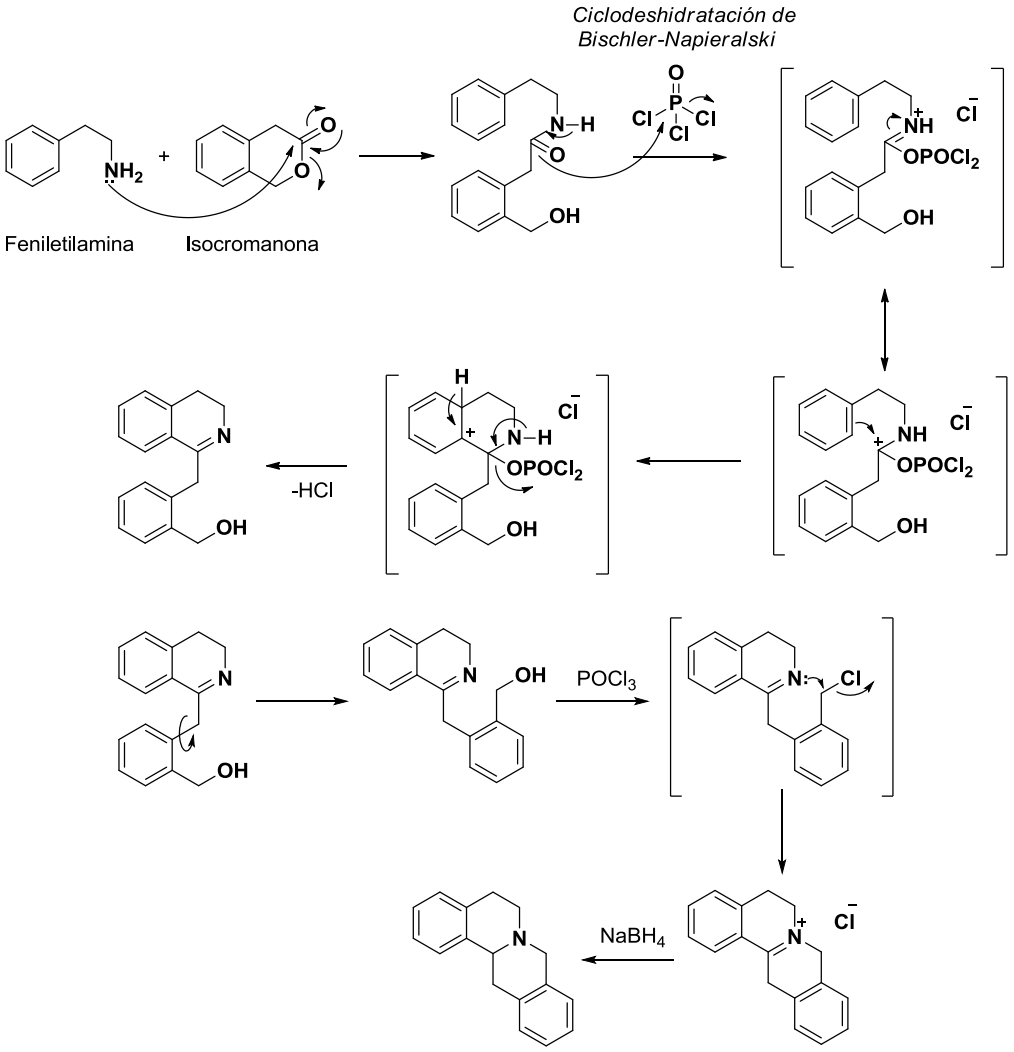

Esquema 9. Ciclodeshidratación de Bischler-Napieralski

b) Ciclación de Pictet-Spengler: el anillo B de las THPB se forma mediante una ciclación intramolecular de una sal de iminio, obtenida vía descarboxilación de un aminoácido funcionalizado en las posiciones apropiadas. El inconveniente de este método es el bajo rendimiento, puesto que en ninguno de los casos estudiados supera el 30%, y además, la accesibilidad a la THIQ-1,3-disustituida de partida va a estar muy condicionada por el modelo de sustitución deseado [53] (**Esquema 10**).

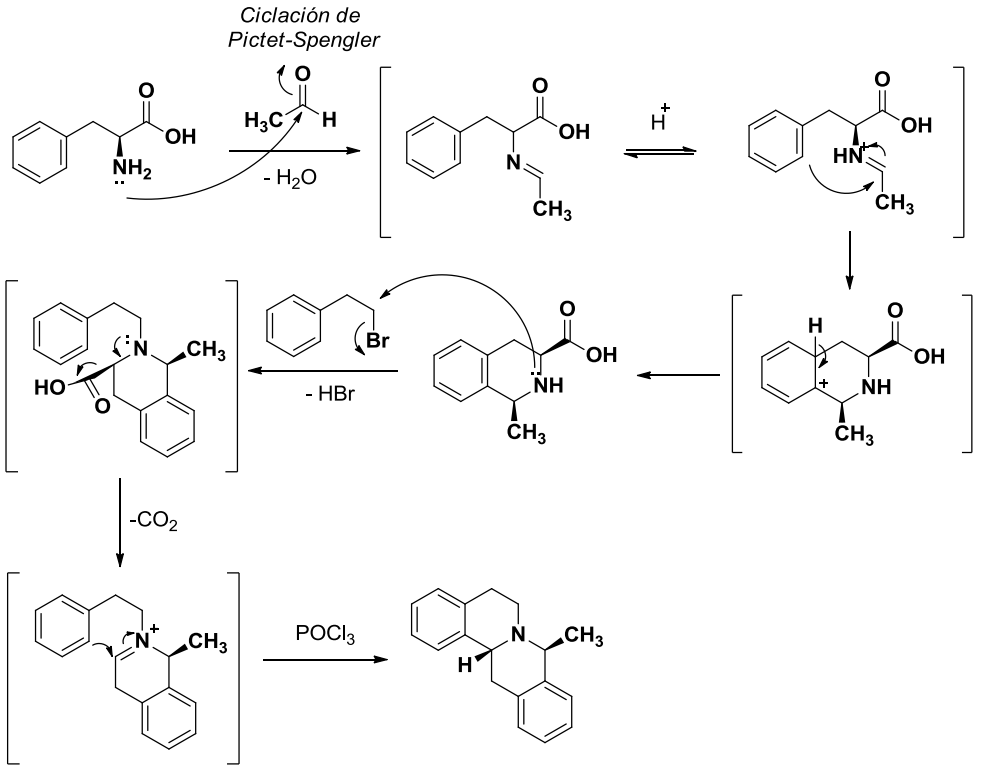

Esquema 10. Ciclación Pictet-Spengler

c) Ciclación de Mannich: la ciclación de Mannich intramolecular de 1-bencil-IQ con aldehídos bajo condiciones ácidas, de acuerdo con el modelo biosintético, es un método directo y efectivo de formación de THPB. Sin embargo, esta reacción requiere la presencia de un grupo activante en el anillo C de la 1-bencil-THIQ correspondiente. Este método presenta una baja estereoselectividad y en función de la naturaleza y posición de los sustituyentes del anillo bencílico puede variar la regioselectividad [54-56] (**Esquema 11**).

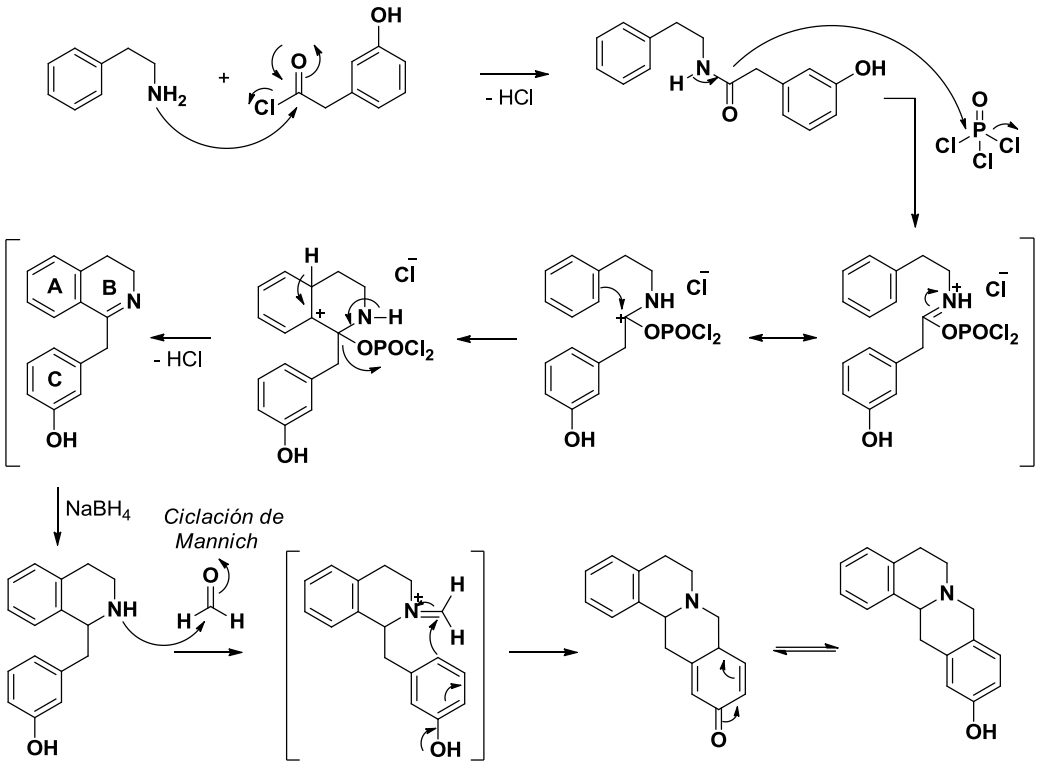

Esquema 11. Ciclación de Mannich

El método de síntesis que adoptamos en la presente Tesis Doctoral es el que utiliza como proceso de generación del anillo C de las THPB la ciclación de Mannich, debido a la similitud que tiene con el modelo biosintético, a la relativa facilidad de preparación a partir de las 1-bencil-THIQ precursoras y a la efectividad que presenta dicho método, teniendo en cuenta las limitaciones y posibles inconvenientes del mismo.

5.2.- Síntesis de 1,2,3,7,8,8a-Hexahidrociclopenta-[*ij*]-isoquinoleínas

Las rutas sintéticas desarrolladas para este tipo de moléculas isoquinoleínicas son escasas debido a la poca investigación que se ha realizado sobre ellas. No obstante, en la literatura se han encontrado dos tipos de desconexiones sintéticas que ilustran el método utilizado en cada caso para preparar moléculas con este esqueleto (**Figura 12**).

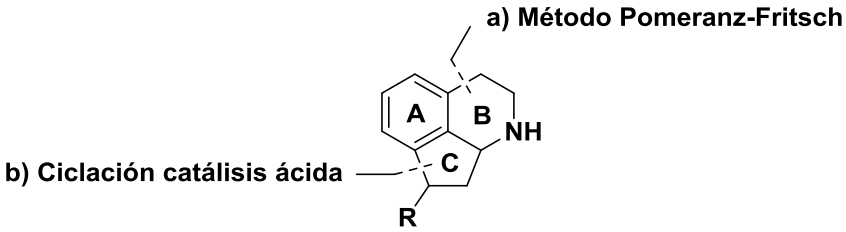

Figura 12. Aproximaciones sintéticas de HCPIQ

a) Ciclación mediante el Método de Pomeranz-Fritsch: Este método de síntesis de alcaloides IQ es uno de los más clásicos, en el que el anillo B o ciclo piperidínico del esqueleto es el último en formarse. Este método ha sido utilizado por diferentes grupos de investigación para la síntesis de proaporfinas.

Las proaporfinas tienen un elevado interés desde el punto de vista químico, porque son precursores, tanto naturales o biosintéticos como en síntesis orgánica, en la obtención de alcaloides IQ de tipo aporfínicos [57].

Como se ha comentado anteriormente, las aporfinas derivan biosintéticamente de la estructura 1-benzil-THIQ que a través de un acoplamiento oxidativo directo generará las proaporfinas y que mediante diferentes reagrupamientos conducirá a la obtención de moléculas con sustituciones en el anillo D (**Esquema 12**). Barton y colaboradores propusieron una variación de reagrupamiento dienona-fenol pasando por un intermediario proaporfinol, que seguido de un reagrupamiento dienol-benceno, se llega a los aporfinoides no sustituidos en el anillo D [58-60].

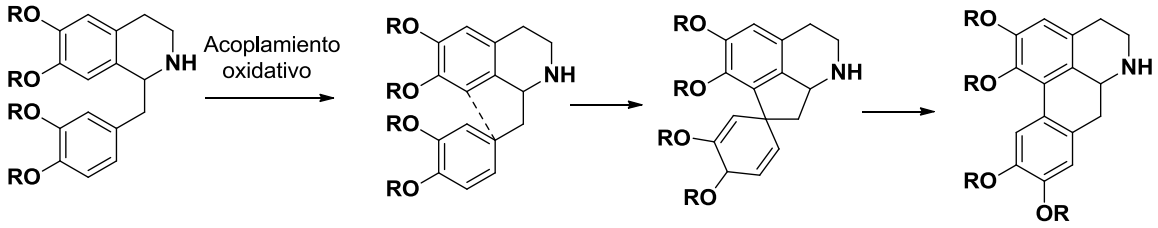

Esquema 12. Biosíntesis de Aporfinoides

Huffman y colaboradores sintetizaron la hexahidropronuciferina y derivados mediante las modificaciones de Bobbitt del método de Pomeranz-Fritsch. En esta ruta sintética partieron de 1-indanonas convenientemente sustituidas. Mediante la utilización de 2-etoxietanamina, que provoca un ataque nucleofílico de la amina a la cetona de la 1-indanona, y posterior pérdida de una molécula de agua, se produce la formación de la imina correspondiente. Posteriormente se produce la ciclación del anillo B o anillo piperidínico en medio ácido, generando el esqueleto IQ, y finalmente, la imina se reduce para generar la HCPIQ correspondiente (**Esquema 13**) [25].

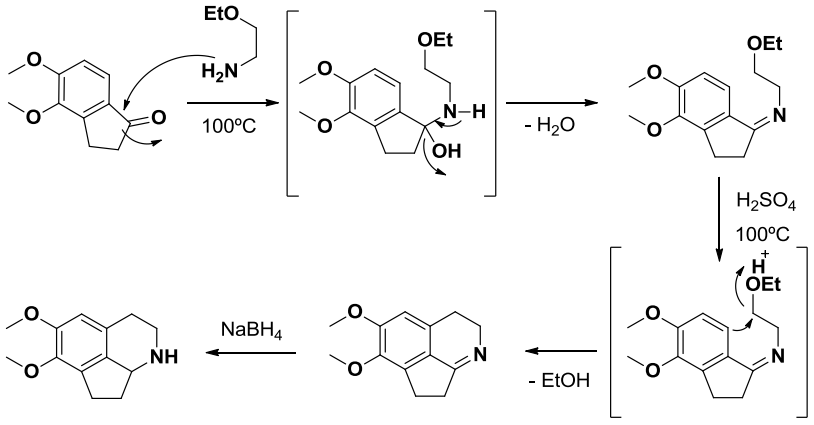

Esquema 13. Síntesis de HCPIQ propuesta por Huffman *et al*. [25]

La síntesis que propuso Huffman y colaboradores explicada anteriormente, pretendía obtener como productos finales proaporfinas como la pronuciferina. Por esta razón, las 1-indanonas que tuvo que utilizar para poder obtener este tipo de alcaloides IQs fueron del tipo espiro-[ciclohexan-1,1'-inden]-3'(2'H)-ona, y mediante una secuencia sintética similar a la ya descrita obtuvieron las proaporfinas deseadas (**Esquema 14**) [25].

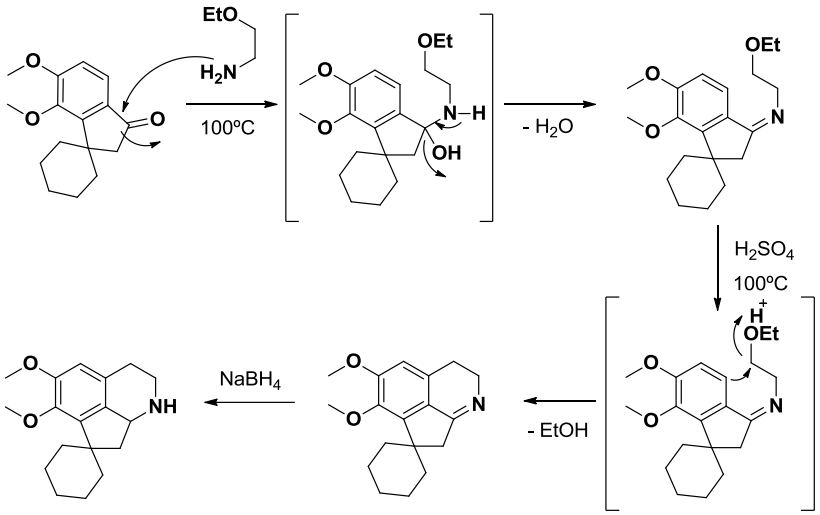

Esquema 14. Síntesis de proaporfinas propuesta por Huffman *et al*. [25]

b) Ciclación mediante Catálisis Ácida: Este método de obtención de HCPIQ tiene como característica principal que la reacción de cierre y formación del anillo C es una reacción catalítica mediada por un ácido, utilizándose principalmente el ácido polifosfórico (PPA) [26, 61 y 62]. Sin embargo, como veremos más adelante, Eaton y colaboradores encontraron un reactivo mejor, con la finalidad de mejorar esta reacción catalítica ácida mediante la que se forma el esqueleto HCPIQ [63].

Empleando el PPA, Casagrande y colaboradores utilizaron este método de obtención de HCPIQ para generar diferentes proaporfinas, al igual que ocurría en los casos anteriores ya descritos. En este caso, partieron de IQ convenientemente sustituidas en posición 1, preparadas previamente mediante reacciones clásicas de síntesis de THIQ. A través de una reacción catalítica ácida mediante PPA, obtuvieron la estructura HCPIQ. Este intermedio reaccionó con el metil 2-cloroacetato mediante una condensación de Darzens y se generó el epóxido correspondiente, el cual, tras la utilización de ácido metansulfónico (AMS), dará lugar al aldehído. A partir de dicho compuesto y gracias a la anelación de Robinson, en la que se utilizó como reactivo la 3-buten-2-ona, se formó el esqueleto proaporfinoide correspondiente. Como se puede observar en el siguiente esquema, la anelación de Robinson, consta de una adición de Michael, una adición aldólica intramolecular y una eliminación. En la última etapa, mediante la utilización de 2,3-dicloro-5,6-diciano-1,4-benzoquinona (DDQ) se obtuvo el compuesto oxidado (**Esquema 15**) [61].

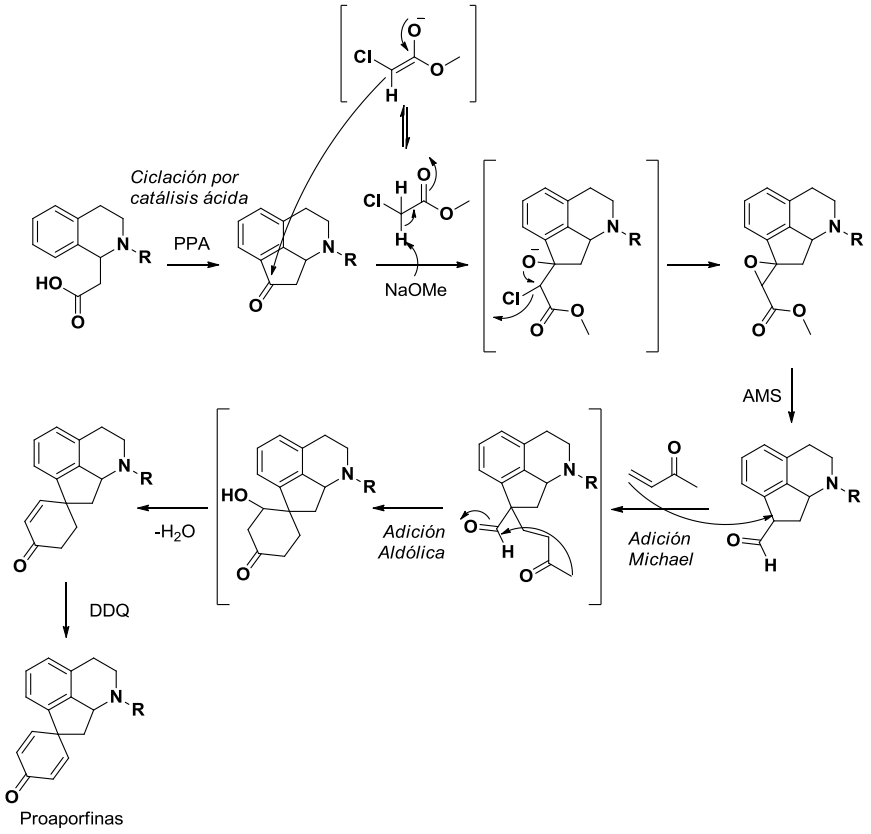

Esquema 15. Síntesis de proaporfinoides propuesta por Casagrande *et al*. [61]

Por otro lado, este grupo de investigación también desarrolló la síntesis de este mismo tipo de compuestos mediante una ruta similar. Partiendo de HCPIQ, obtenidas por catálisis ácida mediante PPA, se obtuvieron derivados HCPIQ 9-sustituidos utilizando una reacción de Wittig. A partir de estas se sintetizaron los compuestos proaporfínicos correspondientes siguiendo una síntesis idéntica a la descrita anteriormente (**Esquema 16**) [61].

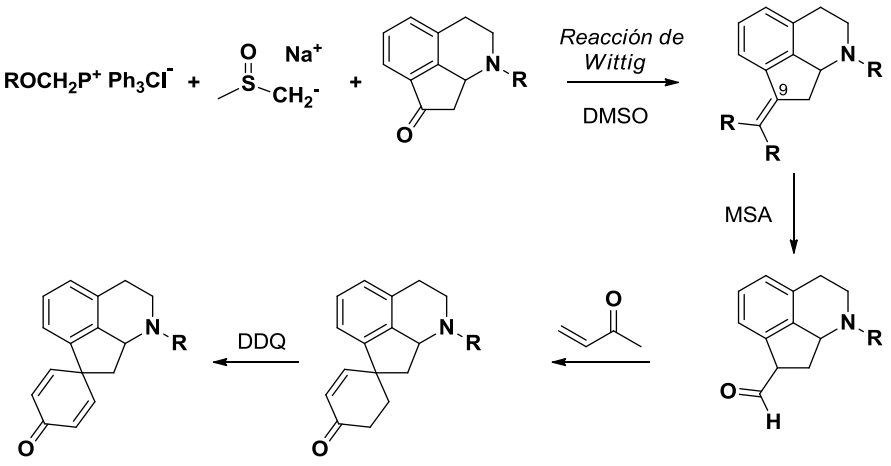

Esquema 16. Síntesis de proaporfinoides propuesta por Casagrande *et al*. [61]

Sakane y colaboradores prepararon una serie de derivados 3-aza-acenafteno. Como en el caso anterior, se parte de IQ 1 sustituida y mediante la utilización de anhídrido acético se produce la desprotección del éster para obtener el ácido carboxílico correspondiente. La protección de la amina secundaria se llevó a cabo mediante una acetilación. El esqueleto HCPIQ se generó por reacción catalítica ácida mediante la utilización de PPA. Por último, se producen reacciones de reducción para generar el 3-aza-acenafteno (**Esquema 17**) [62].

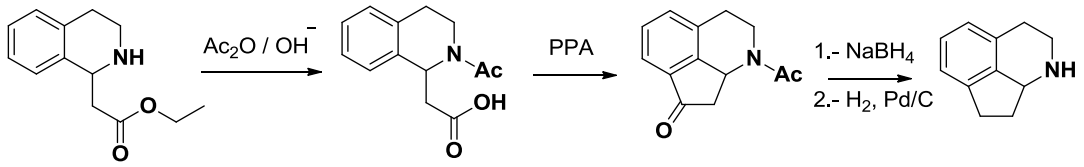

Esquema 17. Síntesis de 3-aza-acenafteno propuesta por Sakane *et al*. [62]

Pelletier y colaboradores sintetizaron una serie de alcaloides llamados aaptamina y derivados, que se observaron previamente en especies de esponjas marinas como *Aaptos aaptos*. En esta síntesis se obtuvieron HCPIQ como productos intermedios para la obtención de los alcaloides que se pretendía sintetizar. A partir de la 1,2,3,4-THIQ se obtuvo la correspondiente imina, que fue sustituida en posición 1 mediante la utilización de ácido malónico. En la siguiente etapa, a través del método de ciclación por catálisis ácida, se pudo obtener la HCPIQ correspondiente. Este será el producto de partida para la obtención de aaptamina y derivados. Mediante la utilización de azida sódica en medio ácido se producirá la integración de un átomo de nitrógeno en posición 9, creando una amida cíclica que, tras la reducción de la misma con éter de hidruro de aluminio y litio (LAH), conformará el esqueleto naftiridínico característico en este tipo de alcaloides. Una vez generado este, se oxidará el sistema mediante la utilización de paladio sobre carbono obteniendo la aaptamina y sus correspondientes derivados (**Esquema 18**) [26].

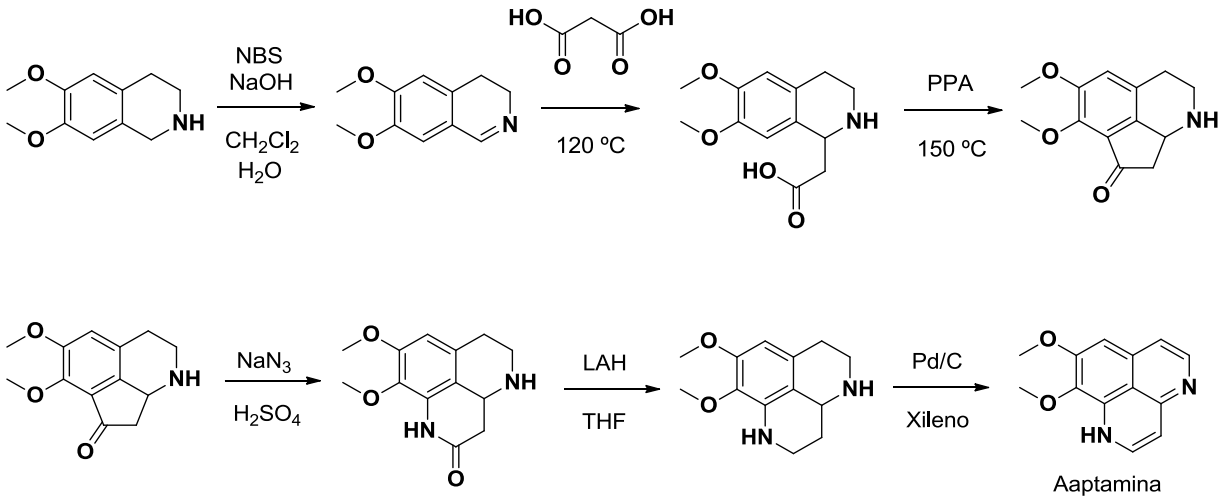

Esquema 18. Síntesis de aaptamina y derivados realizada por Pelletier *et al.* [26]

Eaton y colaboradores desarrollaron un reactivo compuesto por ácido metanosulfónico (AMS) y pentóxido de fósforo (P_2O_5) en una proporción 10:1, conocido como reactivo de Eaton, que mejoró este tipo de reacciones de alquilación y acilación en sistemas aromáticos y olefínicos. Mediante el uso de este reactivo, se prepararon toda una serie de ciclopentenonas (**Figura 13**) [63].

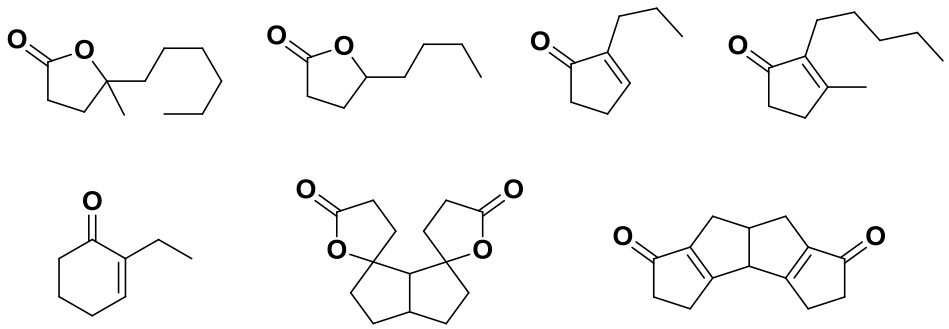

Figura 13. Ciclopentenonas sintetizadas por Eaton *et al.* [63]

En la presente Tesis Doctoral vamos a desarrollar la nueva alternativa propuesta por Eaton y colaboradores aplicada a la síntesis de compuestos HCPIQ, utilizando un producto de partida diferente al utilizado en los trabajos anteriores. La elección de este reactivo de Eaton se llevó cabo con la finalidad de mejorar los rendimientos y facilitar la sustitución en el esqueleto HCPIQ, para así obtener HCPIQ con elevada afinidad por los RD.

6.- Síntesis de Hexahidroindenopiridinas

Se han utilizado diversas rutas sintéticas a lo largo de los años para la preparación de HHIP, y en particular, de las clasificadas según su estructura dentro del **Grupo A** (*véase* **Figura 8**). Podemos agrupar estas síntesis en diversos tipos:

a) TIPO I: a partir de cianoalquil-indanona

Augstein y colaboradores abordaron la síntesis partiendo de la cianoalquil-indanona y mediante una ciclación reductiva con Ni llegaron a la hexahidro-1H-indeno-[1,2-*b*]-piridina, la cual fue tratada con KOH en *n*-BuOH a alta temperatura obteniendo el epímero correspondiente en posición 5, dando lugar al isómero *trans* (**Esquema 19**) [38].

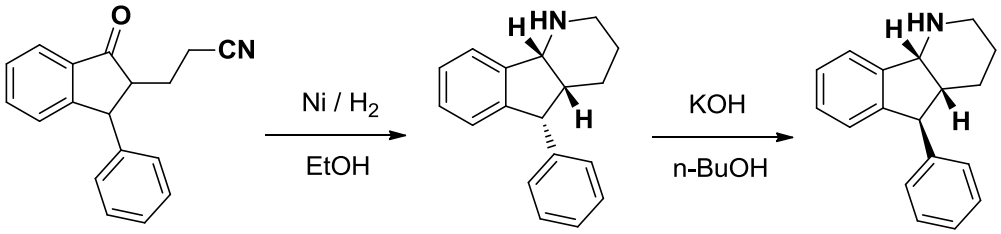

Esquema 19. Síntesis de HHIP propuesta por Augstein *et al*. [38]

b) TIPO II: a partir de 5-oxo-fenilvaleronitrilos

La carencia de una síntesis adecuada para hexahidro-1*H*-indeno-[1,2-*b*]-piridinas que permitiera conseguir una amplia variedad de sustituyentes, condujo a Kunstmann y colaboradores al diseño de una ruta sintética más versátil. Este método sintético parte de los compuestos 5-oxo-5-fenilvaleronitrilos, los cuales fácilmente ciclan obteniendo 6-fenil-3,4-dihidropiridin-2-onas, que condensan rápidamente con un aldehído apropiado y ácido polifosfórico obteniéndose hexahidro-1*H*-indeno-[1,2-*b*]-piridin-2-onas. Posteriormente, se produce una hidrogenación catalítica con Ni-Ra dando lugar a las hexahidro-1*H*-indeno-[1,2-*b*]-piridinas deseadas, las cuales reaccionan con KOH en n-BuOH a alta temperatura, dando lugar al epímero correspondiente, como hemos mencionado en el método sintético anterior (**Esquema 20**) [39].

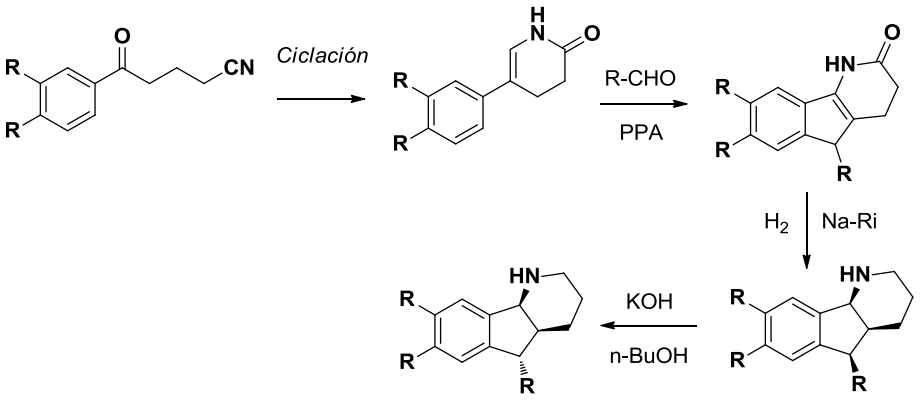

Esquema 20. Síntesis de HHIP propuesta por Kunstmann *et al*. [39]

c) TIPO III: a partir de indanonas

Van Emelen y colaboradores propusieron una síntesis diastereoselectiva de hexahidro-1*H*-indeno-[1,2-*b*]-piridinas. Una adición de Michael de 1-indanona *ß*-cetoéster y acrilonitrilo, seguida por una reacción de Grignard sobre el grupo ceto, permitía preparar un intermedio indanol, que mediante una reacción intramolecular de Ritter conducía al isómero *cis*-hexahidro-4a*H*-indeno-[1,2-*b*]-piridina, la cual podría considerarse como análogo tricíclico de los antagonistas piperidínicos de los receptores NK-1 y del ligando bicíclico de los RD, *trans*-2-amino-3-fenil-2,3-dihidro-1*H*-indeno-5-ol (**Esquema 21**) [36].

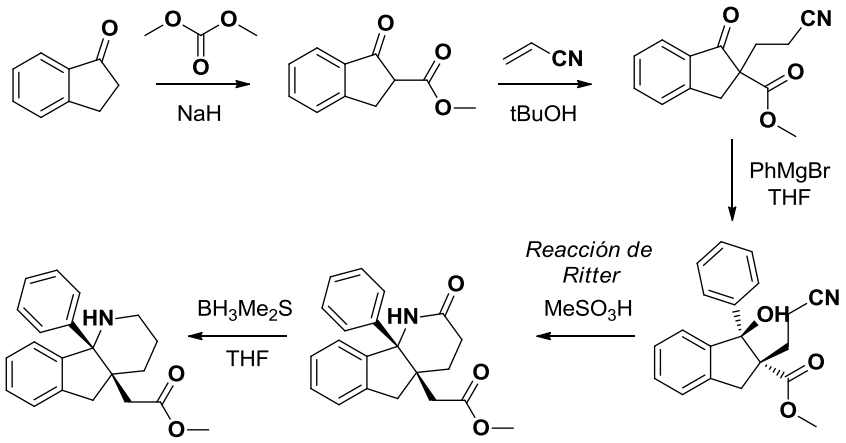

Esquema 21. Síntesis de HHIP propuesta por Van Emelen *et al*. [36]

d) TIPO IV: a partir de indenos (reacción de Diels-Alder)

Recientemente, Hong y colaboradores [40] han diseñado una ruta sintética para 5*H*-indeno-[1,2-*b*]-piridinas partiendo de un indeno con *N*-sulfonil-1-aza-1,3-butadieno vía cicloadición hetero Diels-Alder como etapa clave, consiguiendo una alta regio y estereoselectividad que mediante otros métodos sintéticos no era posible (**Esquema 22**). Con una posterior eliminación y reducción de la 5*H*-indeno-[1,2-*b*]-piridina, ofrecen una nueva ruta sintética de azafluorenonas para la preparación de onichina, alcaloide aislado por primera vez en 1976 de especies brasileñas de la familia Annonáceas (*Onychopetalum amazonicum* y *Guatteria dielsiana*) que mostró poseer actividad anti-candida [64].

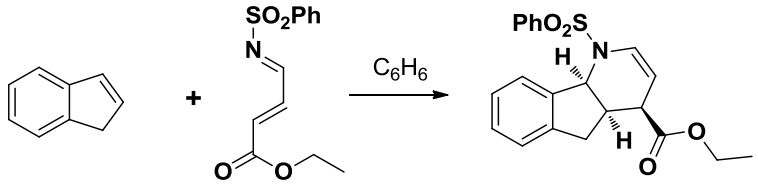

Esquema 22. Síntesis de HHIP propuesta por Hong *et al*. [64]

La ruta sintética que vamos a tratar en la presente Tesis Doctoral es una secuencia química nueva que utiliza como producto de partida indanonas. Este proceso de generación de las HHIP se ha desarrollado con el fin de reducir etapas para tratar de aumentar los rendimientos y facilitar el procedimiento de obtención de dichos compuestos.

7.- Actividades Biológicas

7.1.- Afinidad por los receptores de la dopamina

a) Dopamina

La dopamina (DA) o 3,4-dihidroxifeniletilamina, es una molécula de bajo peso molecular (153 g/mol), cuya fórmula molecular es $C_8H_{11}NO_2$. Se trata de un neurotransmisor que pertenece al grupo de las catecolaminas y se biosintetizada en las terminaciones neuronales dopaminérgicas. La DA se localiza fundamentalmente en cuerpo estriado y sistema límbico, almacenándose en vesículas sinápticas, y realiza sus funciones a nivel del sistema nervioso central (SNC) mediante la unión a familias de RD.

El precursor de la DA es el aminoácido tirosina y se obtiene a partir de una ruta metabólica de dos reacciones a nivel del SNC. La primera reacción está catalizada por la enzima tirosina hidroxilasa que transforma la tirosina en levodopa. La segunda reacción está catalizada por la L-aminoácido aromático descarboxilasa, obteniéndose DA (**Esquema 23**).

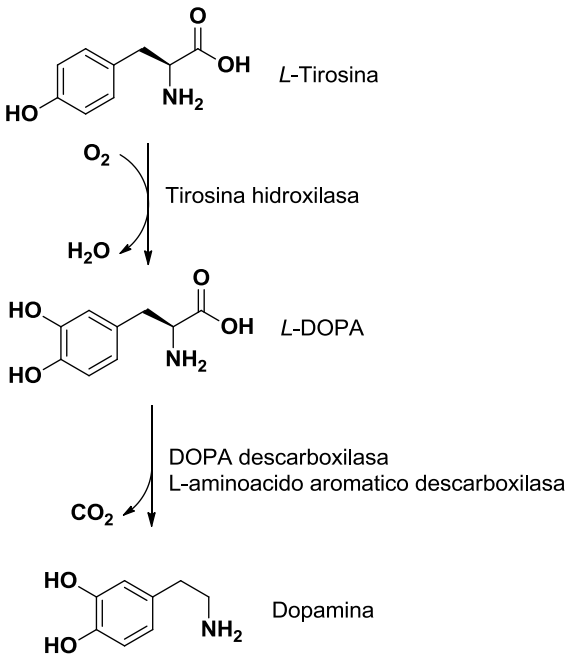

Esquema 23. Biosíntesis de la Dopamina

La neurotransmisión mediada por la DA juega un papel importante en diferentes trastornos neurológicos y psiquiátricos que afectan a varios millones de personas en todo el mundo. La DA se libera a la hendidura sináptica debido a variaciones en los potenciales de acción y en este espacio sináptico, la DA ejerce su función al unirse a los RD post y/o presinápticos. Además, la DA puede sufrir un proceso de recaptación por la neurona presináptica mediante el transportador de dopamina (DAT) o bien degradarse por las enzimas monoaminooxidasa (MAO) y catecol-*O*-metil-transferasa (COMT). Así pues, la actividad dopaminérgica se modula a través de los RD postsinápticos, y gran parte de la investigación destinada a tratar los trastornos neurológicos y/o psiquiátricos está orientada al descubrimiento de nuevos ligandos dopaminérgicos como posibles fármacos. Además, la biosíntesis de DA y su liberación de las neuronas pueden ser moduladas por dos mecanismos adicionales que afectan la neurotransmisión dopaminérgica (**Figura 14**) [65].

1. La estimulación de los autorreceptores presinápticos tipo D_2 por los agonistas dopaminérgicos [66-68].
2. El mecanismo de recaptación desde el espacio extraneuronal a las neuronas presinápticas por DAT [70, 71].

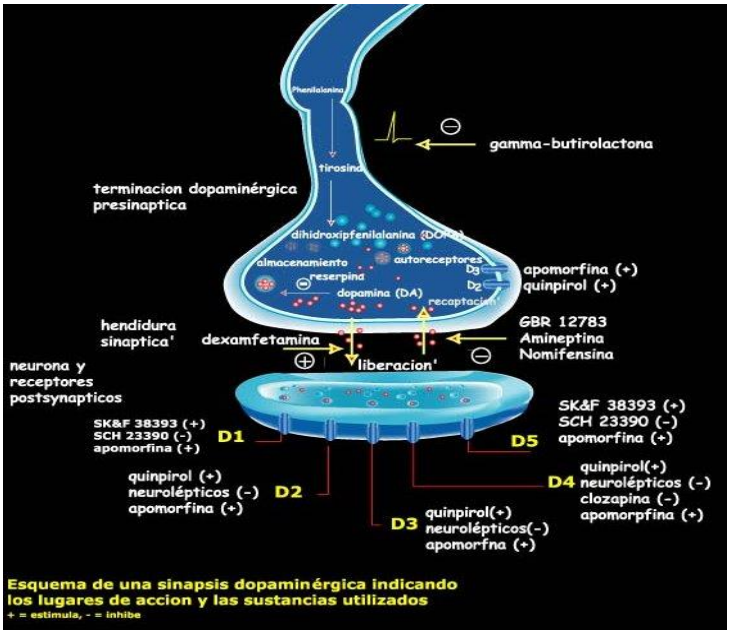

Figura 14. Terminación dopaminérgica

Importancia de la dopamina

Existen diversas funciones cerebrales en las que la DA tiene una importante función reguladora. Esta función se ve ejemplificada de manera significativa por algunos procesos patológicos relacionados con alteraciones en la transmisión dopaminérgica, desórdenes psiquiátricos y neurológicos que afectan a varios millones de personas en el mundo, como la enfermedad de Parkinson y la esquizofrenia. Las consecuencias de la activación o el bloqueo de la transmisión dopaminérgica pueden provocar síntomas neurológicos, psiquiátricos o fisiológicos. Por ello, existe un gran interés en el descubrimiento de nuevos ligandos dopaminérgicos como potenciales fármacos para el tratamiento de estas enfermedades [72].

La DA se sintetiza en distintas zonas del sistema nervioso central, principalmente en el sistema nigroestriado (75% de toda la DA del encéfalo), el cual participa en la regulación motora, de manera que un déficit biosintético de DA contribuye al desarrollo de la enfermedad de Parkinson. La DA también se sintetiza en los sistemas mesolímbico y mesocortical, que forman parte de los circuitos endógenos de recompensa de fenómenos psicótropos, y en el sistema tuberohipofisario, regulando la secreción de hormonas hipofisarias. Además, es la responsable de la afectividad y está implicada en los estados emocionales, las funciones cognitivas y los desórdenes de sustancias abusivas.

Así pués, las actividades dopaminérgicas están asociadas principalmente a cuatro vías principalmente: vía mesocortical, vía mesolímbica, vía nigroestriada y vía túberoinfundibular, de manera que una degeneración parcial de estas vías se manifiesta en el desarrollo de diversos tipos de desórdenes psicóticos y neurológicos, tales como desórdenes del comportamiento, la esquizofrenia, la enfermedad de Alzheimer y la ya mencionada Parkinson.

De tal manera que el tratamiento de la enfermedad de Parkinson está centrado en estimular los RD en el SNC, principalmente mediante el uso de L-DOPA y/o de agonistas dopaminérgicos, permitiendo una mejora sintomática de la enfermedad. Mientras que los fármacos capaces de bloquear los DR, fundamentalmente de tipo D_2, incluyen al grupo de los neurolépticos, que son eficaces en el tratamiento de enfermedades psicóticas, tales como la esquizofrenia.

b) Receptores Dopaminérgicos

Los RD son receptores de membrana, estructuralmente constituidos por siete dominios transmembrana hidrofóbicos acoplados a una proteína G. En función de su localización celular y de sus características farmacológicas, se pueden considerar varios aspectos relacionados con los RD. Fueron inicialmente clasificados en dos subtipos D_1 y D_2 basados en sus propiedades farmacológicas y en su diferente activación de la adenilciclasa [55]. Posteriormente, la aplicación de métodos de clonación usando técnicas de biología molecular, ha permitido reagruparlos en dos subfamilias, **tipo D_1** (D_1 y D_5) y **tipo D_2** (D_2, D_3 y D_4) con secuencias de aminoácidos y propiedades farmacológicas comunes. Aunque los RD se distribuyen en general por todas las áreas cerebrales, los subtipos D_1 y D_2 parecen localizarse principalmente en el caudado-putamen, núcleo accumbens, y tubérculo olfatorio, y en niveles más bajos en el área septal, hipotálamo y córtex. Además los RD D_2 se detectan en la sustancia negra, en el área tegmental ventral y el hipocampo mientras que los RD D_1 se encuentran en la amígdala. En el sistema periférico los RD D_1 se encontrarían en la glándula paratiroidea mientras que los DR D_2 en la glándula pituitaria [73].

Por lo tanto, se pueden distinguir dos tipos de familias de RD:

Familia D_1 (D_1 y D_5) que tiene efecto activador, se encuentran acoplados a un complejo proteína G_s Cuando un receptor de esta familia es estimulado por DA, la subunidad α_s de la proteína G_s se disocia del complejo y activa la adenilato-ciclasa, lo que causa un aumento en la formación de adenosín monofosfato cíclico (AMPc) intracelular en la neurona postsináptica a partir de ATP y la hidrólisis de fosfatidilinositol dando inositol trifosfato, que produce un aumento del calcio en plasma celular [74, 75]. Los receptores tipo D_1 presentan un 80% de similitud y propiedades fisiológicas similares, son receptores postsinápticos y se localizan en casi todas las áreas cerebrales con inervación dopaminérgica. Los receptores D_5 se diferencian de los D_1 en que son menos abundantes y están menos distribuidos, se localizan en el córtex frontal, cuerpo estriado, hipocampo e hipotálamo [76]. Estos receptores poseen alta afinidad por ligandos benzacepínicos, SCH 23390 y SKF 83566 (**Figura 15**) y una moderada afinidad por agonistas clásicos de DA (apomorfina) y por agonistas selectivos como SKF 38393.

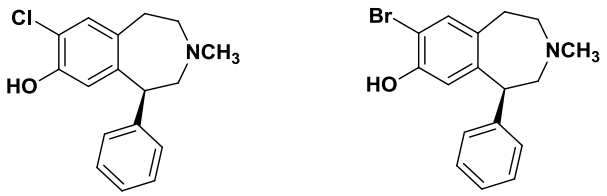

SCH 23390 SKF 83566

Figura 15. Ligandos específicos de receptores D_1

Familia D_2 (D_2, D_3 y D_4) que tiene efecto inhibidor, se encuentran acoplados a un complejo proteína G_i. Cuando la DA estimula un receptor de esta familia provoca la disociación del complejo proteína G_i, liberando la subunidad α_i que interacciona con la adenilato-ciclasa provocando su inhibición. Esto conduce a un descenso en la síntesis de AMPc y de la concentración de calcio en el plasma celular [74, 75]. Se sabe que D_2 y D_3 muestran un 75% de similitud, mientras que entre los receptores D_2 y D_4 sólo hay un 53% de similitud. Se encuentran mayoritariamente distribuidos en los sistema nigroestriado y mesolímbico y se localizan tanto a nivel presináptico (autorreceptores, regulan la liberación de DA), como postsináptico. Las butiferonas, como haloperidol, y las benzamidas sustituídas, como sulpirida y racloprida (antagonistas D_2) (**Figura 16**), poseen alta afinidad por dichos receptores, al igual que las fenotiazinas y los tioxantenos. Sin embargo, existen algunas diferencias entre las afinidades de estos tres receptores (D_2, D_3 y D_4) con algunos ligandos específicos. La benzamida racloprida, por ejemplo, presenta alta afinidad por los receptores D_2 y D_3 y baja por los receptores D_4. Dado que los receptores D_3 y D_4 se expresan fundamentalmente en las regiones corticales y límbicas, implicadas en el control del conocimiento y de las emociones, son el objetivo de nuevas generaciones de fármacos para muchos de los trastornos neurológicos y psiquiátricos con baja incidencia de efectos colaterales extrapiramidales [75-77].

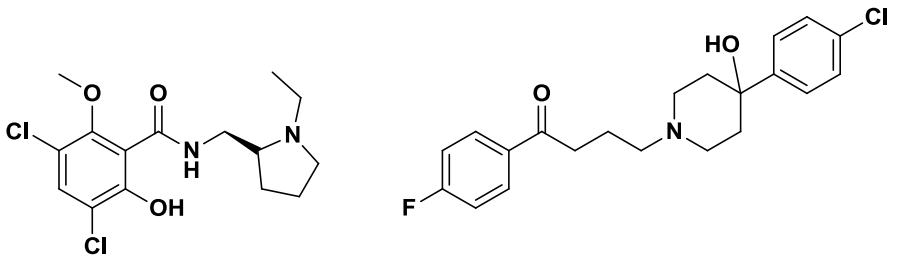

Racloprida Haloperidol

Figura 16. Antagonistas de receptores D_2

Farmacológicamente, los antagonistas dopaminérgicos son agentes importantes para el tratamiento clínico de la esquizofrenia, manía, delirios y la enfermedad de Huntington, mientras que los agonistas dopaminérgicos se utilizan en desórdenes neuroendocrinos y en la enfermedad de Parkinson [70]. Las drogas que actúan sobre los RD D_2 son de especial potencial terapéutico ya que los antagonistas son empleados en el tratamiento de la esquizofrenia (antipsicóticos) y los agonistas son empleados en la enfermedad del Parkinson [78, 79]. Muchos de los inhibidores del transportador de DA que inactivan el proceso de recaptación, actúan como antidepresivos puesto que aumentan la concentración de DA en la hendidura sináptica y por tanto activan la neurotransmisión dopaminérgica. Actualmente, los inhibidores del transportador de DA han sido prescritos para el tratamiento del déficit de atención en los casos de hiperactividad (ADHDs) [80] y han sido propuestos como fármacos potenciales en los tratamientos de abusos de cocaína [81]. Entre ellos destacan compuestos naturales y sintéticos, con esqueletos variados como tropánicos (tipo cocaína), núcleos IQs (tipo nomifensina), estructuras tricíclicas (tipo amineptina) o estructuras aril-piperacínicas (tipo GBR-12783).

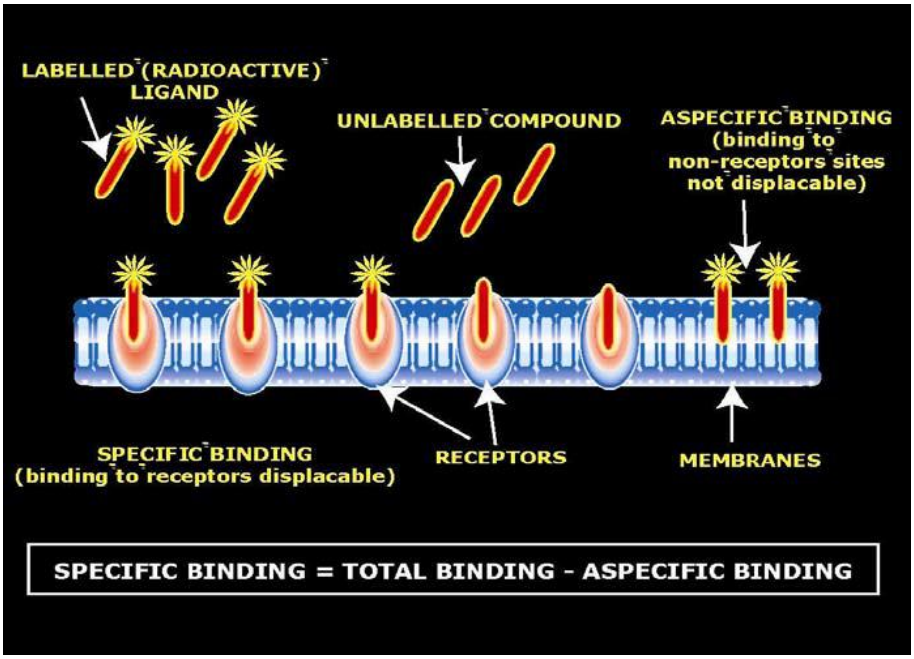

Figura 17. Técnica de fijación a receptores

Los estudios de afinidad por los receptores tipo D_1 y D_2 se llevan a cabo mediante ensayos *in vitro* utilizando técnicas de fijación con radioligandos específicos denominadas técnicas de binding (**Figura 17**), en cuerpo estriado de rata. Son experimentos de competición donde se evalúa la capacidad de los compuestos ensayados para desplazar los radioligandos, [^{3}H]-SCH 23390 (ligando selectivo de receptores tipo D_1) y [^{3}H]-racloprida (ligando selectivo de receptores tipo D_2) de sus lugares de unión al receptor [82]. En el caso de la recaptación de DA, los estudios *in vitro* de inhibición se realizan en los sinaptosomas de cuerpo estriado de rata y se utiliza [^{3}H]- dopamina como sustrato de los transportadores dopaminérgicos [83].

7.2.- Citotoxicidad Celular

La citotoxicidad celular se define como una alteración de las funciones celulares básicas que conlleva a un daño que puede ser detectado. Diferentes autores han desarrollado baterías de pruebas in vitro para predecir los efectos tóxicos de drogas y compuestos químicos, utilizando como modelos experimentales cultivos primarios y órganos aislados como líneas celulares establecidas.

Los ensayos de citotoxicidad, son capaces de detectar mediante diferentes mecanismos celulares conocidos, los efectos adversos de interferencia con estructura y/o propiedades esenciales para la supervivencia celular, proliferación y/o funciones. Dentro de estos se encuentran la integridad de la membrana y del citoesqueleto, metabolismo, síntesis y degradación, liberación de constituyentes celulares o productos, regulación iónica y división celular [84].

Diferentes autores han desarrollado baterías de pruebas *in vitro* para predecir los efectos tóxicos de las drogas y los compuestos químicos, utilizando como modelos experimentales cultivos primarios y órganos aislados como líneas celulares establecidas. Dentro de los ensayos más conocidos y validados se encuentran el ensayo de captación del rojo neutro, enlazamiento al azul de kenacid, ensayo de reducción del bromuro de 3-(4,5 dimetiltiazol-2-ilo)-2,5-difeniltetrazol (MTT) y la citometría de flujo [85].

A) Ensayo de MTT

Este ensayo fue desarrollado por Mosmann en 1983 y modificado en 1986 por Denizot y Lang [86, 87]. Se basa en la reducción metabólica del MTT realizada por la enzima mitocondrial succinato-deshidrogenasa (SDH) en un compuesto coloreado de color azul (formazan), permitiendo determinar la funcionalidad mitocondrial de las células tratadas. Este método ha sido muy utilizado para medir supervivencia y proliferación celular ya que la cantidad de células vivas es proporcional a la cantidad de formazán producido. Por lo tanto, se usa para determinar la viabilidad celular, dada por el número de células presentes en el cultivo, lo cual es capaz de medirse mediante la formación de un compuesto coloreado, debido a una reacción que tiene lugar en las mitocondrias de las células viables [88].

El MTT es captado por las células y reducido por la enzima succínico deshidrogenasa mitocondrial a su forma insoluble formazán. El producto de la reacción, el formazán queda retenido en las células y puede ser liberado mediante la solubilización de las mismas. De esta forma es cuantificada la cantidad de MTT reducido mediante un método colorimétrico, ya que se produce como consecuencia de la reacción un cambio de coloración, de amarillo a azul (**Esquema 24**) [89].

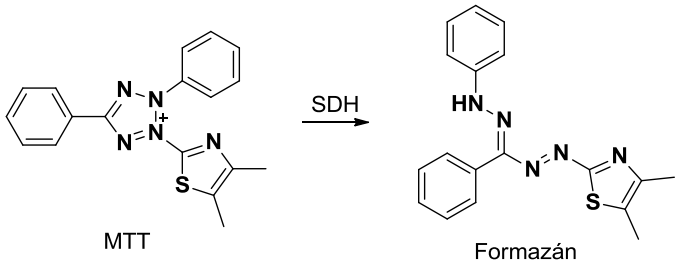

Esquema 24. Escisión del anillo tetrazólico de MTT

La capacidad de las células para reducir el MTT constituye un indicador de la integridad de las mitocondrias, y su actividad funcional es interpretada como una medida de la viabilidad celular. La determinación de la capacidad de las células de reducir al MTT a formazán después de su exposición a un compuesto permite obtener información acerca de la toxicidad del compuesto que se evalúa [90]. Las células deben ser conservadas en condiciones de esterilidad en N_2 líquido (-190 ºC). El período de exposición de la sustancia de ensayo varia, ya que puede ser durante períodos cortos (1-2 h de tratamiento), o largos (24 ó 72h). La densidad óptica (D.O) debe medirla al concluir el tiempo de incubación 550 nm utilizando un filtro de 620 nm

como referencia [91]. Por lo general se deben realizar al menos 8 réplicas de cada concentración que se evalúa. Se deben evaluar hasta 6 concentraciones del compuesto, alcanzando una concentración de 1000 µg/mL o hasta el límite máximo de solubilidad del producto en el medio. Si es alcanzada esta concentración y no se observa toxicidad, entonces resulta necesario aumentar el rango de concentraciones hasta 100 000 µg/mL o hasta la máxima concentración soluble del compuesto en el medio. Es necesario tener en cuenta que si el producto que se evalúa precipita en el medio de cultivo, estos resultados deben ser descartados. Debe utilizarse en el ensayo un control de medio, un control de disolvente y es recomendable un control positivo.

Los resultados se expresarán como porcentaje (%) de células vivas, según la siguiente relación: % = D.O de las células tratadas / D.O de las células controles x 100. La curva dosis respuesta debe ser calculada teniendo en cuenta el rango de concentración utilizado y el porcentaje de reducción del crecimiento celular correspondiente. A partir de ello se calcula la concentración que produce la reducción de la viabilidad celular en un 50 %.

B) Citometría de flujo

La citometría de flujo es un método analítico que permite la medición rápida de ciertas características físicas y químicas de células o partículas suspendidas en líquido que producen una señal de forma individual al interferir con una fuente de luz. La citometría de flujo representa un método rápido objetivo y cuantitativo de análisis de células, núcleos, cromosomas, mitocondrias u otras partículas en suspensión. Una de las características analíticas más importantes de los citómetros de flujo es su capacidad de medir múltiples parámetros celulares, como el tamaño, la forma y la complejidad y, por supuesto, cualquier componente celular o función que pueda ser marcada con un fluorocromo.

La información producida puede agruparse en dos tipos fundamentales: la generada por la dispersión de la luz y la relacionada con la emisión de luz por los fluorocromos presentes en la célula o partícula al ser excitados por el rayo luminoso. Las señales luminosas detectadas se transforman en impulsos eléctricos que se amplifican y se convierten en señales digitales que son procesadas por una computadora (**Figura 18**). Las aplicaciones de la citometría de flujo son numerosas, lo cual ha permitido el empleo de estos instrumentos de manera amplia en los campos, tanto de la investigación biológica como médica [92].

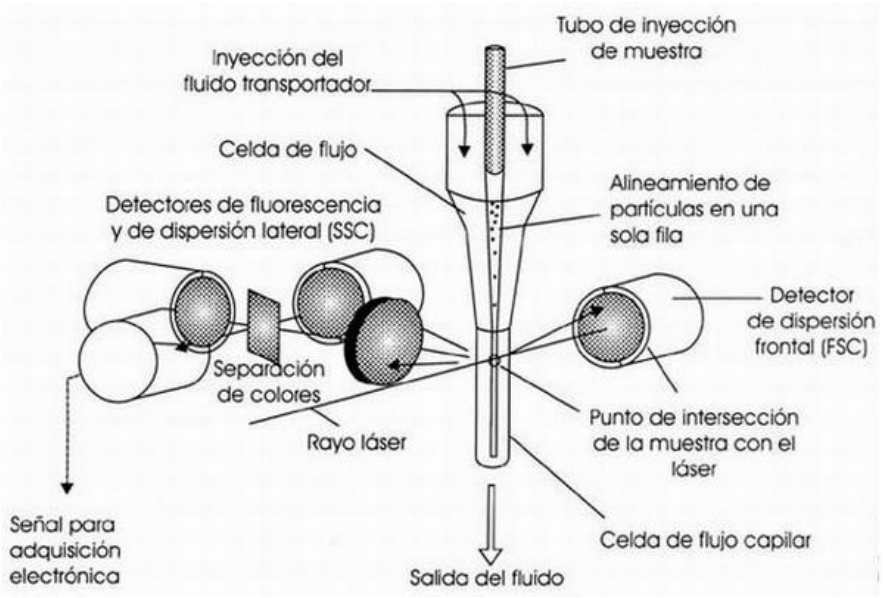

Figura 18. Esquema de un citómetro de flujo

La fluorescencia ha sido usada para visualizar ciertas moléculas y estructuras por medio de la microscopia óptica durante muchos años. Esta ha encontrado una extensa área de aplicación en la citometría de flujo. El objetivo del análisis por inmunofluorescencia en citometría de flujo es asignar a cada célula, un grupo específico de células que compartan propiedades comunes. El primer paso es identificar las células de interés. Una vez que las células de interés han sido distinguidas de los otros tipos celulares, se puede usar la inmunofluorescencia para determinar la proporción o el número de células que poseen un determinado marcador [93].

La citometría de flujo se ha convertido en un método de elección para el análisis de la muerte celular en una gran variedad de tipos celulares. Hay varios métodos que pueden ser utilizados para determinar cuantitativamente la viabilidad de las células. Estos métodos utilizan colorantes no permeantes, como por ejemplo yoduro de propidio o 7-amino actinomicina D. Las células que presentan la membrana plasmática dañada o el metabolismo celular alterado, no pueden evitar que el colorante entre en la ella. Una vez dentro de la célula, el colorante se une a estructuras intracelulares que producen aductos altamente fluorescentes y que identifican las células como "no viable". Por lo tanto, la viabilidad se expresará como porcentaje de células incoloras [94].

7.3. Afinidad por los receptores de la melatonina

a) Melatonina

La melatonina (MT), *N*-acetil-5-metoxitriptamina o metoxindol, es una hormona encontrada en animales superiores y en algunas algas, cuya concentración varía de acuerdo al ciclo diurno/nocturno. La MT se biosintetiza a partir del neurotransmisor serotonina (**Esquema 25**), principalmente en la glándula pineal [95], y participa en una gran variedad de procesos celulares, neuroendocrinos y neurofisiológicos. Una de las características más extraordinaria respecto a la biosíntesis pineal de MT, es su variabilidad a lo largo del ciclo diario, y su respuesta precisa a cambios en la iluminación ambiental. El patrón de secreción de MT consiste en un aumento gradual nocturno hasta alcanzar el pico de secreción y permite la información sobre el fotoperiodo y del ritmo circadiano a los órganos periféricos para la regulación fisiológica diaria y estacional [96, 97]. Por ello, la MT se considera una neurohormona producida por los pinealocitos en la glándula pineal (localizada en el diencéfalo), la cual produce la hormona bajo la influencia del núcleo supraquiasmático del hipotálamo, que recibe información de la retina acerca de los patrones diarios de luz y oscuridad. Se encuentra ocupando la depresión entre el colículo superior y la parte posterior del cuerpo calloso. A pesar de la existencia de conexiones entre la glándula pineal y el cerebro, aquella se encuentra fuera de la barrera hematoencefálica y está inervada principalmente por los nervios simpáticos que proceden de los ganglios cervicales superiores.

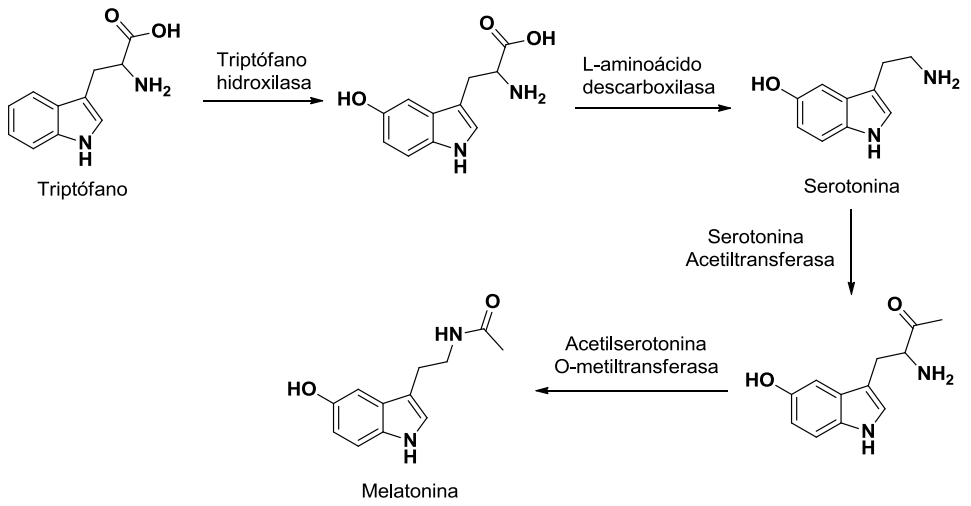

Esquema 25. Biosíntesis de Melatonina

Aunque durante mucho tiempo se consideró que la MT era de origen exclusivamente cerebral, se ha demostrado que su biosíntesis también se produce en otros tejidos como la retina, la glándula harderiana, el hígado, el intestino, los riñones, las adrenales, el timo, la glándula tiroides, las células inmunes, el páncreas, los ovarios, el cuerpo carotídeo, la placenta y el endometrio.

La síntesis de MT se produce constantemente, y disminuye abruptamente hacia los 30 años de edad. Después de la pubertad se produce una calcificación llamada "arenilla del cerebro", que recubre la glándula pineal, pero ésta sigue liberando melatonina. Estudios recientes observan que la MT tiene como funciones, además de la hipnoinductora, la de disminuir la oxidación; por esto los déficits de MT casi siempre van acompañados de alteraciones psíquicas como insomnio y depresión. Además, en la metabolización, el déficit de MT parece estar relacionado con una paulatina aceleración del envejecimiento. Esta indolamina se libera por un proceso de fototransducción, se estimula en la oscuridad ya que el ojo envía señales nerviosas a través del tracto retinohipotalámico, llega al núcleo supraquiasmático, sale por la médula al ganglio cervical superior, y de allí a la glándula pineal donde los pinealocitos secretaran MT. Por tanto, la glándula pineal es un transductor neuroendocrino [98].

Los factores que regulan la MT se pueden dividir en dos grupos, los ambientales (fotoperiodo, estaciones del año, temperatura, etc) y endógenos (estrés y la edad). La MT producida en la glándula pineal actúa como una hormona endocrina, ya que es liberada al torrente circulatorio, mientras que la producida en la retina y en el tracto gastrointestinal actúa como una hormona paracrina. Los lugares de acción de la MT pueden ser neurales: hipocampo, hipófisis, hipotálamo, retina, glándula pineal, etc; y no neurales: gónadas, intestino, vasos sanguíneos, células inmunes, etc.

b) Receptores melatoninérgicos

La MT ejerce sus efectos centrales y periféricos a través de un número aún no determinado de receptores o dianas moleculares [95]. Los receptores mejor conocidos son aquellos que se denominan receptores acoplados a proteína G y son MT_1 y MT_2 [99] que fueron clonados a mediados de la década de 1990 [100-103]. Estos receptores muestran un 55 % de identidad global en el nivel de aminoácidos y alrededor de un 70 % dentro de los dominios transmembrana. Están acoplados negativamente a la adenilato ciclasa y poseen una afinidad parecida por la MT (dentro del rango sub-nanomolar) [104 y 105].

Los receptores MT_1 se expresan en varias áreas del cerebro, en particular en el núcleo supraquiasmático (SCN) y los pares tuberalis. Los receptores MT_2 están localizados en el SNC y la retina. Otro receptor algo menos conocido es MT_3 que presenta una baja afinidad para el radioligando (RL) 2-[^{125}I]-yodomelatonina [106-109] y se ha caracterizado en hámster como el homólogo humano de la quinona reductasa 2 [110], aunque se había sugerido previamente que este receptor no estaba acoplado a proteína G [111, 112]. Existe un RL más específico, 2-[^{125}I]-yodo-5-metoxicarbonilamino-*N*-acetiltriptamina, y se ha demostrado que discrimina MT_3 de la proteína G acoplada a los receptores MT_1 y MT_2 [113-115]. Este sitio de unión de baja afinidad MT_3, parece estar involucrado en las respuestas inflamatorias agudas en la rata [116] y en la regulación de la presión intraocular en el conejo [117].

Debido a que los agonistas de MT sintéticos tienen considerables potenciales terapéuticos en la modulación del insomnio y trastornos relacionados con el ciclo circadiano del sueño, es deseable desarrollar compuestos melatoninérgicos selectivos de cada subtipo. Aunque hay algunos ligandos que muestran selectividad para MT_2 [118-123], se han encontrado muy pocos compuestos en la literatura selectivos para MT_1.

Referencias Bibliográficas

Referencias Bibliográficas

[1] Barbalho, S.M.; Alvares Goulart, R.; Vasques, F.M.; Soares, M.S.; Bueno, P.C.S.; Landgraf Guiguer, E.; Cressoni, A. y Groppo, M. *Annona sp*: Plants with multiple applications as alternative medicine – A review. *Curr. Bioact. Compd*. **2012**, *8*, 277.

[2] Bermejo, A.; Figadère, B.; Zafra-Polo, M.C.; Barrachina, I.; Estornell, E. y Cortes, D. Acetogenins from Annonaceae. Recent progress in isolation, synthesis and mechanism of action. *Nat. Prod. Rep*. **2005**, *22*, 269.

[3] Liaw, C.C.; Wu, T.Y.; Chang, F.R. y Wu, Y.C. Historic perspectives on Annonaceous Acetogenins from the chemical bench to preclinical trials. *Planta Med*. **2010**, *76*, 1390.

[4] Fatima, A.; Modolo, L.V.; Conegero, L.S.; Pilli, R.A.; Ferreira, C.V.; Kohn, L.K. y Carvalho, J.E. Styryl lactones and their derivatives: biological activities, mechanisms of action and potential leads for drug design. *Curr. Med. Chem*. **2006**, *13*, 3371.

[5] Popsavin, V.; Benedekovic, G.; Popsavin, M.; Kojic, V. y Bogdanovic, G. Divergent synthesis of cytotoxic styryl lactones isolated from *Polyalthia crassa*. The first total synthesis of crassalactone B. *Tetrahedron Lett*. **2010**, *51*, 3426.

[6] Hocquemiller, R.; Cortes, D.; Arango, G.; Myint, S.; Cavé, A.; Angelo, A.; Muñoz, V. y Fournet, A. Isolement et synthese de l'espintanol, nouveau monoterpene antiparasitaire. *J. Nat. Prod*. **1991**, *54*, 445.

[7] Soedeberg, B.C. y Fields, S.L. Expedient syntheses of espinatol, p-methoxycarvacrol, and thymoquinol dimethyl ether. *Org. Prep. Proced. Int.* **1996**, *10*, 1080.

[8] Zhang, J.; El-Shabrawy, A.R.; El-Shanawany, M.A.; Schiff, P.L. y Slatkin, D.J. New azafluorene alkaloids from *Oxandra xylopioides*. *J. Nat. Prod*. **1987**, *50*, 800.

[9] Arango, G.; Cortes, D. y Cavé, A. Three bisdehydroaporphines from *Oxandra* cf. *Major*. *Phytochemistry* **1987**, *26*, 1227.

[10] Arango, G.J.; Cortes, D.; Cassels, B.K.; Cavé, A. y Mérienne, C. Azafluorenones from *Oxandra cf. major* and Biogenetic considerations. *Phytochemistry* **1987**, *25*, 1691.

[11] Tinto, W.; Blair, L.; Reynolds, W. y McLean, S. Terpenoid constituents of *Oxandra asbeckii*. *J. Nat. Prod*. **1992**, *55*, 701.

[12] Hufford, C.D.; Sharma, A.S. y Oguntimein, B.O. Antibacterial and antifungal activity of liriodenina and related oxoaporfhine alkaloids. *J. Pharm. Sci*. **1980**, *69*, 1180.

[13] Cabedo, N.; Berenguer, I.; Figadère, B. y Cortes, D. An overview on benzylisoquinoline derivatives with dopaminergic and serotoninergic activities. *Curr. Med. Chem.* **2009**, *16*, 2441.

[14] Dewick, P.M. *Medicinal Natural Products, A Biosynthetic Approach*, John Wiley & Sons, Chichester, **1997**.

[15] Marco, J.A. *Química de los productos naturales*, Síntesis, Valencia, **2006**.

[16] Bentley, K.W. β-Phenylethylamines and the isokinoline alkaloids. *Nat. Prod. Rep*. **2006**, *23*, 444.

[17] Slobodníková, L.; KoSt'álová, D.; Labudová, D.; Kotulová, D. y Kettmann, V. Antimicrobial activity of *Mahonia aquifolium*. Crude extract and its major isolated alkaloids. *Phytother. Res*. **2004**, *18*, 674.

[18] Xiao, H.; Peng, J.; Liang, Y.; Yang, J.; Bai, X.; Hao, X.Y.; Yang, F.M. y Sun, Q.Y. Acetylcholinesterase inhibitors from *Corydalis yanhusuo. Nat. Prod. Res*. **2011**, *25*, 1418.

[19] Guinaudeau, H.; Leboeuf, M. y Cavé, A. Aporphinoid alkaloids. *J. Nat. Prod*. **1994**, *57*, 1033.

[20] Zhang, A.; Zhang, Y.; Branfman, A.R.; Baldessarini, R.J. y Neumeyer, J.L. Advances in Development of Dopaminergic Aporphinoids. *J. Med. Chem*. **2007**, *50*, 171.

[21] Campello, M.J.; Castedo, L.; Saa, J.M.; Suau, R. y Vidal, M.C. Cancentrine-type cularine alkaloids: sarcocapnine and oxosarcocapnine. *Tetrahedron Lett*. **1982**, *23*, 239.

[22] Guineudeau, H. y Allais, P. New isoquinoline alkaloids from *Corydalis claviculata*. *Heterocycles* **1984**, *22*, 107.

[23] Blanco, O.; Castedo, L.; Cortes, D. y Villaverde, M.C. Alkaloids from *Sarcocapnos saetabensis*. *Phytochemistry* **1991**, *30*, 2071.

[24] Valpuesta, M.; Posadas, N.; Ruis, I.; Silva, M.V.; Gómez, A.I.; Suau, R.; Pérez, B.; Pliego, F. y Cabezudo, B. Alkaloids from *Ceratocapnos heterocarpa* plants and in vitro cultures. *Phytochemistry* **1995**, *38*, 113.

[25] Huffman, J.W. y Opliger, E. The Synthesis of (±)-Hexahydropronuciferine and Related Compounds. *J. Org. Chem*. **1971**, *6*, 111.

[26] Pelletier, J.C. y Cava, M.P. Synthesis of the Marine Alkaloids Aaptamine and Demethyloxyaaptamine and of the Parent Structure Didemethoxyaaptamine. *J. Org. Chem.* **1987**, *52***,** 616.

[27] Wang, S. y Seto, C.T. Enantioselective Addition of Vinylzinc Reagents to 3,4-Dihydroisoquinoline N-Oxide. *Org. Lett*. **2006**, *8*, 3979.

[28] Toth, J.; Dancsó, A.; Blaskó, G.; Töke, L.; Groundwater, P.W. y Nyerges, M. 1,7-Electrocyclization reactions of stabilized α,β:ɣ,ɗ-unsaturated azomethine ylides. *Tetrahedron* **2006**, *62*, 5725.

[29] Abate, C.; Selivanova, S.V.; Müller, A.; Krämer, S.D.; Schibli, R.; Marotolli, R.; Peronne, R.; Berardi, F.; Niso M. y Ametamey, S.M. Development of 3,4-dihydroisoquinolin-1(2H)-one derivatives for the Positron Emission Tomography (PET) imaging of σ2 receptors. *Eur. J. Med. Chem*. **2013**, *69*, 920.

[30] Ponnala, S. y Harding, W.W. A new route to azafluoranthene natural products via direct arylation. *Eur. J. Org. Chem*. **2013**, 1107.

[31] Grunewald, G.L.; Sall, D.J. y Monn, J.A. Conformational and steric aspects of the inhibition of phenylethanolamine *N*-methyltransferase by benzylamines. *J. Med. Chem*. **1988**, *31*, 433.

[32] Ye, N.; Chen, C.H.; Chen, T.T.; Song, Z.; He, J.X.; Huan, X.J.; Song, S.S.; Liu, Q.; Chen, Y.; Ding, J.; Xu, Y.; Miao, Z.H. y Zhang, A. Design, synthesis, and biological evaluation of a series of benzo[*de*][1,7]naphthyridin-7-(8H)-ones bearing a functionalized longer chain appendage as novel PARP1 inhibitors. *J. Med. Chem*. **2013**, *56*, 2885.

[33] Fournet, A.; Ferreira, M.E.; Rojas de Arias, A.; Guy I.; Guinaudeau, H. y Heinzen, H. Phytochemical and antiprotozoal activity of *Ocotea lancifolia*. *Fitoterapia* **2007**, *78*, 382.

[34] Van Emelen, K.; De Wit, T.; Hoornaert, G.J. y Compernolle, F. Diastereoselective intramolecular Ritter reaction: generation of a *cis*-fused hexahydro-4a*H*-indeno[1,2-*b*]pyridine ring system with 4a,9b-diangular substituents. *Org. Lett.* **2000**, *2*, 4225.

[35] De Wit, T.; Van Emelen, K.; Maertens, F.; Hoornaert, G.J. y Compernolle, F. *Cis*-fused hexahydro-4a*H*-indeno[1,2-*b*]pyridine: transformation of bridgehead ester group and conversion to tricyclic analogues of NK-1 and dopamine receptor ligands. *Tetrahedron Lett.* **2001**, *42*, 4919.

[36] Van Emelen, K.; De Wit, T.; Hoornaert, G.J. y Compernolle, F. Synthesis of *cis*-fused hexahydro-4a*H*-indeno[1,2-*b*]pyridine via intramolecular Ritter reaction and their conversion into tricyclic analogues of NK-1 and dopamine receptor ligands. *Tetrahedron* **2002**, *58*, 4225.

[37] Sterling, J.; Herzig, Y.; Goren, T.; Finkelstein, N.; Lerner, D.; Goldenberg, W.; Miskolczi, I.; Molnar, S.; Rantal, F.; Tamas, T.; Toth, G.; Zagyva, A.; Zekany, A.; Lavian, G.; Gross, A.; Friedman, R.; Razin, M.; Huang, W.; Krais, B.; Chorev, M.; Youdin, M.B. y Weinstock, M. Novel dual inhibitors of AChE and MAO derived from hydroxy aminoindan and phenethylamine as potential treatment for Alzehimer´s disease. *J. Med. Chem*. **2002**, *45*, 5260.

[38] Augstein, J.; Ham, A.L. y Leeming, P.R. Relationship between antihistamine and antidepressant activity in hexahydroindenopyridines. *J. Med. Chem.* **1972**, *15*, 466.

[39] Kunstmann, R.; Lerch, U.; Gerhards, H.; Leven, M. y Schacht, U. 2,3,4,4a,5,9b-Hexahydro-1*H*-indeno[1,2-*b*]pyridines: potential antidepressants. *J. Med. Chem.* **1984**, *27*, 432.

[40] Hong, B-C.; Hallur, M.S. y Liao, J-H. Hetero Diels-Alder cycloaddition of indene for the formal synthesis of onychnine. *Synth. Commun*. **2006**, *36*, 1521.

[41] Chen, W. y Lee, T. Substituted tricyclic heterocycles as serotonin receptor agonists and antagonists, US20070049613.

[42] Eckhardt, M. Martin, H. J.; Schuehle, M.; Sick, S. y Yang, B. S. Aryl and heteroarylcarbonyl derivatives of hexahydroindenopyridine and octahydrobenzoquinoline, US20120157488.

[43] Protais, P.; Arbaoui, J.; Bakkali, E-H.; Bermejo, A. y Cortes, D. Effects of various isoquinoline alkaloids on in vitro ^{3}H-Dopamine uptake by rat striatal synaptosomes. *J. Nat. Prod*. **1995**, *58*, 1475.

[44] Cabedo, N.; Protais, P.; Cassels, B.K. y Cortes, D. Synthesis and Dopamine Receptor Selectivity of the Benzyl-Tetrahydroisoquinoline, (*R*)-(+)-nor-Roefractine. *J. Nat. Prod*. **1998**, *61*, 709.

[45] Andreu, I.; Cortes, D.; Protais, P.; Cassels, B.K.; Chagraoui, A. y Cabedo, N. Preparation of dopaminergic *N*-alkyl-benzyltetrahydroisoquinolines using a One pot procedure in acid medium. *Bioorg. Med. Chem*. **2000**, *8*, 889.

[46] Cabedo, N.; Andreu, I.; Ramírez de Arellano, M.C.; Chagraoui, A.; Serrano, A.; Bermejo, A.; Protais, P. y Cortes, D. Enantioselective syntheses of dopaminergic (*R*)- and (*S*)-benzyltetrahydroisoquinolines. *J. Med. Chem*. **2001**, *44*, 1794.

[47] Andreu, I.; Cabedo, N.; Torres, G.; Chagraoui, A.; Ramírez de Arellano, M.C.; Gil, S.; Bermejo, A.; Valpuesta, M.; Protais, P. y Cortes, D. Syntheses of dopaminergic 1-cyclohexylmethyl-7,8-dioxygenated tetra-hydroisoquinolines by selective heterogenous tandem hydrogenation. *Tetrahedron* **2002**, *58*, 10173.

[48] Suvire, F.D.; Andreu, I.; Bermejo, A.; Zamora, M.A.; Cortes, D. y Enriz, R.D. Conformational study of *N*-alkyl-benzyltetrahydroisoquinoline alkaloids. *J. Mol. Struc. (Teochem)* **2003**, *666-667*, 109.

[49] Suvire, F.D.; Cabedo, N.; Chagraoui, A.; Zamora, M.A.; Cortes, D. y Enriz, R.D. Molecular recognition and Binding mechanism of N-alkyl-benzyltetrahydroisoquinolines to the D_1 dopamine receptor. A computational approach. *J. Mol. Struc. (Teochem)* **2003**, *666-667*, 455.

[50] Berenguer, I.; El Aouad, N.; Andújar, S.; Romero, V.; Suvire, F.; Freret, T.; Bermejo, A.; Ivorra, M.D.; Enriz, R.D.; Boulouard, M.; Cabedo, N. y Cortes, D. Tetrahydroisoquinolines as dopaminergic ligands: 1-Butyl-7-chloro-6-hydroxi-tetrahydroisoquinoline, a new compound with antidepressant like activity in mice. *Bioorg. Med. Chem*. **2009**, *17*, 4968.

[51] El Aouad, N.; Berenguer, I.; Romero, V.; Marin, P.; Serrano, A.; Andújar, S.; Suvire, F.; Bermejo, A.; Ivorra, M.D.; Enriz, R.D.; Cabedo, N. y Cortes, D. Structure-activity relationship of dopaminergic halogenated 1-benzyl-tetrahydroisoquinoline derivatives. *Eur. J. Med. Chem*. **2009**, *44*, 4616.

[52] Mali, R.S.; Patil, S.D. y Patil, S.L. Novel syntheses of 1-substituted 7,8-dialkoxyisochroman-3-ones and 8-substituted 2,3,9,10-tetramethoxyberbines. *Tetrahedron* **1986**, *42*, 2075.

[53] Dean, R.T. y Rapoport, H. Stereospecific Cyclizations of Iminium Salts from a-Amino Acid Decarbonylation. Synthesis of 8- and 13-Methylberbines. *J. Org Chem*. **1978**, *43*, 4183.

[54] Kametani, T.; Ujiie, A.; Ihara, M.; Fukumoto, K. y Lu, S.T. Studies on the syntheses of heterocyclic compounds. Synthesis of Corytenchirine. *J. Chem. Soc., Perkin Trans. 1,* **1976**, 1218.

[55] Suau, R.; Silva, M.V. y Valpuesta, M. Structure and total synthesis of (-)-malacitanine. An unusual protoberberine alkaloid from *Ceratocapnos heterocarpa*. *Tetrahedron* **1990**, *46*, 4421.

[56] Sun, H.; Zhu, L.; Yang, H.; Qian, W.; Guo, L.; Zhou, S.; Gao, B.; Li, Z.; Zhou, Y.; Jiang, H.; Chen, K.; Zhen, X.; Liu, H. Asymmetric total synthesis and identification of tetrahydroprotoberberine derivatives as new antipsychotic agents possessing a dopamine D_1, D_2 and serotonin 5-HT_{1A} multi-action profile. *Bioorg. Med. Chem.* **2013**, *21*, 856.

[57] Baldwin, M.; Loudon, A.G. y Maccoll, A. Alkaloids from *Croton* Species. Part VI. Mass Spectrometric Studies of the Crotonosine Alkaloids. *J. Chem. Soc. C*. **1967**, 154.

[58] Barton, D.H.R.; Bhakuni, D.S.; Chapma, G.M. y Kirby, G.W. The biosynthesis of Roemerine, Anonaine and Mecambine. *J. Chem. Soc. C*. **1966**, 259.

[59] Shamma, M. y Guinaudeau, H. Biogenetic pathways for the aporphinoid alkaloids. *Tetrahedron* **1984**, *40*, 4795.

[60] Dewick, P.M. *Medicinal Natural Products, A Biosynthetic Approach*, 2ed. Jonh Wiley & Sons, Chichester, **2002**.

[61] Casagrande, C.; Canonica, L. y Severini-Ricca, G. Studies on Proaporphine and Aporphine Alkaloids. Part VI. Synthesis of (±)-Glaziovine by Spiran Ring Construction on a Cyclopent[ij]isoquinoline, Stereochemistry of Reduced Proaporphines. *J. Chem. Soc., Perkin Trans. 1*, **1975**, 1652.

[62] Sakane, K.; Terayama, K.; Haruki, E.; Otsuji, Y. e Imoto, E. Syntheses of 3-Azaacenaphtene and Its derivatives. *Nippon Kagaku Kaishi.* **1974**, *8*, 1535.

[63] Eaton, E.P.; Carlson, G.R. y Lee, J.T. Phosphorus pentoxide-methanesulfonic acid. Convenient alternative to polyphosphoric acid. *J. Org. Chem.* **1972**, *38*, 4071.

[64] De Almeida, M.E.I.; Braz, F.R.; von Bulow, M.V.; Gottleib, O.R. y Maia, J.G.S. The chemistry of Brazilian Annonaceae. Part 1. Onychine, an alkaloid from *Onychopetalum amazonicum*. *Phytochemistry*. **1976**, *15*, 1186.

[65] Zhang, A.; Neumeyer, J.L. y Baldessarini, R.J. Recent progress in development of dopamine receptor subtype-selective agents: potential therapeutics for neurological and psychiatric disorders. *Chem. Rev*. **2007**, *107*, 274.

[66] Carlsson, A. Dopamine receptor agonists: intrinsic activity vs state of receptor. *J. Neural. Transm.* **1983**, *57*, 309.

[67] Clarck, D.; Hjorth, S. y Carlsson, A. Dopamine-receptor agonists: mechanisms underlying autoreceptor selectivity. I. Review of the evidence. *J. Neural. Transm.* **1985**, *62*, 151.

[68] Clarck, D.; Hjorth, S. y Carlsson, A. Dopamine receptor agonists: mechanisms underlying autoreceptor selectivity. II. Theoretical considerations. *J. Neural. Transm*. **1985**, *62*, 171.

[69] Tamminga, C.A. Partial dopamine agonist and the treatment of psychosis. *Curr. Neuropharmacol*. **2005**, *3*, 3.

[70] Gainetdinov, R.R. y Caron, M.G. Monoamine transporters: from genes to behaviour. *Annu. Rev. Pharmacol. Toxicol*. **2003**, *43*, 261.

[71] Marsden, C.A. Dopamine: the rewarding years. *Br. J. Pharmacol*. **2006**, *147*, 136.

[72] Oloff, S.; Mailman, R.B. y Trophsa, A. Application of valided QSAR models of D_1 dopaminergic antagonist for database mining. *J. Med. Chem*. **2005**, *48*, 7322.

[73] Civelli, O.; Bunzow, J.R.; Grandy, D.K.; Zhou, Q.Y. y Van Tol, H.H.M. Molecular biology of the dopamine receptors. A review. *Eur. J. Pharmacol*. **1991**, *207*, 277.

[74] Kebabian, J.W. y Calne, D.B. Multiple receptors for dopamine. *Nature* **1979**, *277*, 93.

[75] Missale, C.; Nash, S.R.; Robinson, S.W.; Jaber, M. y Caron, M.G. Dopamine receptors: from structure to function. *Physiol. Rev*. **1998**, *78*, 189.

[76] Sunahara, R.K.; Guan, H.C.; O´Dowd, B.F.; Seemann, P.; Laurier, L.G.; Ng, G.; George, S. R.; Torchia, J.; Van yol, H.H. y Niznik, H.B. Cloning for a gene for human dopamine D_5 receptor with higher affinity for dopamine than D_1. *Nature* **1991**, *350*, 614.

[77] Levant, B. The D_3 dopamine receptor: neurobiology and potential clinical relevance. *Pharmacol. Rev*. **1997**, *49*, 231.

[78] Poewe, W. Treatments for Parkinson disease-past achievements and current clinical needs. *Neurology* **2009**, *72*, S65.

[79] Luthra, P.M. y Kumar, J.B.S. Plausible improvements for selective targeting of dopamine receptors in therapy of Parkinson's disease. *Mini-reviews in Med. Chem.* **2012**, *14*, 1556.

[80] Bobb, A.J.; Castellanos, F.X.; Addington, A.M. y Rapport, J.L. Molecular genetic studies of ADHD: 1991 to 2004. *Am. J. Med. Genet. B (Neuropsychiatr. Genet.)* **2006**, *141B*, 551.

[81] Howell, L.L. y Wilcox, K.M. The dopamine transporter and cocaine medication development: drug selfadministration in nonhuman primates. *J. Pharmacol. Exp. Ther*. **2001**, *298*, 1.

[82] Protais, P.; Cortes, D.; Pons, J.L.; López, S.; Villaverde, M.C. y Castedo, L. Displacement activity of some natural cularine alkaloid at striatal [3H]-SCH 23390 and [3H]-raclopride binding sites. *Experentia* **1992**, *48*, 27.

[83] Neumeyer, J.L.; Gao, Y.; Kula, N.S. y Baldessarini, R.J. *R* and *S* enantiomers of 11-hydroxy-N-allynoraporphine and 10,11-dihydroxy-N- allynoraporphine. Synthesis and affinity for dopamine receptors in rat brain tissue. *J. Med. Chem*. **1991**, *34*, 24.

[84] Repetto, M. *Toxicología Fundamental. Métodos alternativos, Toxicidad in vitro*, Enpses-Mercie Group .3ª ed. Sevilla, **2002**.

[85] Fentem, J.H. The use of human tissues in in vitro toxicology, Summary of general discussions. *Human Experimental Toxicology* **1994,** *13*, 445.

[86] Mosmann, T. Rapid colorimetric assay for cellular growth and survival: Application to proliferation and cytotoxicity assay. *J. Inmunol. Methods* **1983**, *65*, 55.

[87] Denizot, F. y Lang, R. Rapid colorimetric assay for cell growth and survival, Modifications to the tetrazolium dye procedure giving improved sensitivity and reliability. *J. Immunol. Methods* **1986**, *89*, 271.

[88] Shayne, G.C. *Alternatives to in vivo studies in toxicology, General and applied toxicology, vol 1, Grove's dictionaries Inc*, **1999**.

[89] Eisenbrand, G.; Pool-Zobel, B.; Baker, V.; Balls, M.; Blaauboer, B.J. y Boobis, A. Methods of in vitro toxicology. *Food Chem. Toxicol* **2002**, *40*, 193.

[90] Jiménez, N.; González, M.; Fernández, C. y López, J. Estudio de la biocompatibilidad in vitro de polímeros metacrílicos derivados de pirrolidona/ina. *Biomecánica* **2007**, *15*, 63.

[91] Pareja, A.; García, C.; Abad, P.J. y Márquez, M.E. Estudio in vitro de la citotoxicidad y genotoxicidad de los productos liberados del acero inoxidable 316L con recubrimientos cerámicos bioactivos. *IATREIA* **2007,** *20*, 12.

[92] Shapiro, H.M. *Practical Flow Cytometry,* Wiley-Liss, 4ª ed. New Jersey, **2003**.

[93] Longobardi, G.A. *Flow Cytometry, First Principles,* Willey-Liss, New York, **1992**.

[94] Cheddadia, M.; López-Cabarcos, E.; Slowingc, K.; Barcia, E. y Fernández-Carballido, A. Cytotoxicity and biocompatibility evaluation of a poly(magnesium acrylate)hydrogel synthesized for drug delivery. *Int. J. Pharm*. **2011**, *413*, 126.

[95] Arendt, J.; Deacon, S.K; English, J.; Hampton, S. y Morgan, L. Melatonin and adjustment to phase shift. *J. Sleep. Res*. **1995**, *4,* 74.

[96] Delagrange, P.; Atkinson, J.; Boutin, J.A.; Casteilla, L.; Lesieur, D.; Misslin, R.; Pellissier, S.; Pénicaud, L. y Renard, P. Therapeutic perspectives for melatonin agonists and antagonists. *J. Neuroendocrinol*. **2003**, *15*, 442.

[97] Boutin, J.A.; Audinot, V.; Ferry, G. y Delagrange, P. Molecular tools to study melatonin pathways and actions. *Trends Pharmacol. Sci*. **2005**, *26*, 412.

[98] Florez, J. Farmacología humana. *Tocris Cookson* **2003**, 501.

[99] Sugden, D. Melatonin receptors. *Tocris Cookson* **2000**, 1.

[100] Reiter, R.J. The melatonin rhythm: Both a clock and a calendar. *Experientia* **1993**, *49*, 654.

[101] Dubocovich, M.L.; Mansana, M.I. y Benloucif, S. Molecular pharmacology and function of melatonin receptor subtype. *Adv.Exp. Med. Biol.* **1999**, *460*, 181.

[102] Malpaux, B.; Migaud, M.; Tricoire, H. y Chemineau, P. Biology of mammalian photoperiodism and the critical role of the pineal gland and melatonin. *J. Biol. Rhythms*. **2001**, *16*, 336.

[103] Guerrero, J.M. y Reiter, R.J. Melatonin-immune system relationships. *Curr. Top. Med. Chem*. **2002**, *2*, 167.

[104] Reppert, S.M.; Weaver, D.R. y Ebisawa T. Cloning and characterization of a mammalian melatonin receptor that mediates reproductive and circadian responses. *Neuron*. **1994**, *13*, 1177.

[105] Reppert, S.M.; Godson, C.; Mahle, C.D.; Weave, D.R.; Slaugenhaupt, S.A. y Gusella, J.F. Molecular characterization of a second melatonin receptor expressed in human retina and brain: The Mel1b melatonin receptor. *Proc. Natl. Acad. Sci. USA*, **1995**, *92*, 734.

[106] Duncan, M.J.; Takahashi, J.S. y Dubocovich, M.L. 2-[125I]-iodomelatonin binding sites in hamster brain membranes: pharmacological characteristics and regional distribution. *Endocrinology* **1988**, *122*, 1825.

[107] Duncan, M.J.; Takahashi, J.S. y Dubocovich, M.L. Characteristics and autoradiographic localization of 2-[125I]-iodomelatonin binding sites in Djungarian hamster brain. *Endocrinology* **1989**, *125*, 1011.

[108] Pickering, D.S. y Niles, L.P. Pharmacological characterization of melatonin binding sites in Syrian hamster hypothalamus. *Eur. J. Pharmacol.* **1990**, *175,* 71.

[109] Paul, P.; Lahaye, C.; Delagrange, P.; Nicolas, J.P.; Canet, E. y Boutin, J.A. Characterization of 2-[125I]-iodomelatonin binding sites in Syrian hamster peripheral organs. *J. Pharmacol. Exp. Ther*. **1999**, *290*, 334.

[110] Prendergast B.J. MT_1 melatonin receptors mediate somatic, behavioral, and reproductive neuroendocrine responses to photoperiod and melatonin in Siberian hamsters. *J. Biol. Chem*. **2010**, *151*, 714.

[111] Dubocovich, M.L. Pharmacology and function of melatonin receptors. *FASEB J*. **1988**, *2*, 2765.

[112] Dubocovich, M.L. Melatonin receptors: are there multiple subtypes? *Trends Pharmacol. Sci*. **1995**, *16*, 50.

[113] Molinari, E.J.; North, P.C. y Dubocovich, M.L. 2-[125I]-iodo-5-methoxycarbonylamino-*N*-acetyltryptamine: a selective radioligand for the characterization of melatonin ML2 binding sites. *Eur. J. Pharmacol*. **1996**, *301*, 159.

[114] Nosjean, O.; Ferro, M.; Coge, F.; Beauverger, P.; Henlin, J.M.; Lefoulon, F.; Fauchère, J.L.; Delagrange, P.; Canet, E. y Boutin, J.A. Identification of the melatonin-binding site MT_3 as the quinone reductase 2. *J. Biol. Chem*. **2000**, *275*, 31311.

[115] Nosjean, O.; Nicolas, J.P.; Klupsch, F.; Delagrange, P.; Canet, E. y Boutin, J.A. Comparative pharmacological studies of melatonin receptors: MT_1, MT_2 and MT_3/QR_2. Tissue distribution of MT_3/QR_2. *Biochem. Pharmacol.* **2001**, *61*, 1369.

[116] Lotufo, C.M.C.; Lopes, C.; Dubocovich, M.L.; Farsky, S.H.P. y Markus, R.P. Melatonin and *N*-acetylserotonin inhibit leukocyte rolling and adhesion to rat microcirculation. *Eur. J. Pharmacol*. **2001**, *430*, 351.

[117] Pintor, J.; Martin, L.; Pelaez, T.; Hoyle, C.H.V. y Peral, A. Involvement of melatonin *MT3* receptors in the regulation of intraocular pressure in rabbits. *Eur. J. Pharmacol.* **2001**, *416*, 251.

[118] Dubocovich, M.L.; Masana, M.I.; Iacob, S. y Sauri, D.M. Melatonin receptor antagonists that differentiate between the human Mel1a and Mel1b recombinant subtypes are used to assess the pharmacological profile of the rabbit retina ML1 presynaptic heteroreceptor. *Naunyn-Schmiedebergs Arch. Pharmacol*. **1997**, *355*, 365.

[119] Teh, M.T. y Sugden, D. Comparison of the structure-activity relationships of melatonin receptor agonists and antagonists: lengthening the N-acyl side-chain has differing effects on potency on Xenopus melanophores. *Naunyn-Schmiedebergs Arch. Pharmacol*. **1998**, *358*, 522.

[120] Sugden, D.; Yeh, L.K. y Teh, M.T. Design of subtype selective melatonin receptor agonists and antagonists. *Reprod. Nutr. Dev*. **1999**, *39*, 335.

[121] Faust, R.; Garratt, P.J.; Jones, R. y Yeh, L.K. Mapping the melatonin receptor. 6.Melatonin agonists and antagonists derived from 6*H*-isoindolo[2,1-α]indoles, 5,6-dihydroindolo[2,1-α]isoquinolines, and 6,7-dihydro-5H-benzo[c]azepino[2,1-α]indoles. *J. Med. Chem*. **2000**, *43*, 1050.

[122] Spadoni, G.; Balsamini, C.; Diamantini, G.; Tontini, A. y Tarzia G. 2-*N*-Acylaminoalkylindoles: design and quantitative structure-activity relationship studies leading to MT2-selective melatonin antagonists. *J. Med. Chem.* **2001**, *44*, 2900.

[123] Wallez, V.; Durieux-Poissonnier, S.; Chavatte, P.; Boutin, J.A.; Audinot, V.; Nicolas, J.P.; Bennejean, C.; Delagrange, P.; Renard, P. y Lesieur, D. Synthesis and structure-activity relationships of novel benzofuran derivatives as MT(2) melatonin receptor selective ligands. *J. Med. Chem*. **2002**, *45*, 2788.

Capítulo 1

Síntesis y estudios de afinidad por los receptores dopaminérgicos de Isoquinoleínas:

- Tetrahidroprotoberberinas (THPB)

-7-Fenil-hexahidrociclopenta-[*ij*]-isoquinoleínas (HCPIQ)

Artículo 1: "2,3,9- and 2,3,11- Trisubstituted tetrahydroprotoberberines as D_2 dopaminergic ligands" (En: *European Journal of Medicinal Chemistry*, **2013**, *68*, 150)

Artículo 2: "Synthesis of hexahydrocyclopenta[*ij*]isoquinolines as a new class of a dopaminergic agents" (En: *European Journal of Medicinal Chemistry*, **2015**, *90*, 101)

Artículo 3: "3-Chlorotyramine Acting as Ligand of the D_2 Dopamine Receptor. Molecular Modeling, Synthesis and D_2 Receptor Affinity" (En: *Molecular informatics*, **2014,** *in press*)

European Journal of Medicinal Chemistry 68 (2013) 150–166

Contents lists available at ScienceDirect

European Journal of Medicinal Chemistry

journal homepage: http://www.elsevier.com/locate/ejmech

Original article

2,3,9- and 2,3,11-Trisubstituted tetrahydroprotoberberines as D_2 dopaminergic ligands

Javier Párraga [a], Nuria Cabedo [b], Sebastián Andujar [c], Laura Piqueras [d], Laura Moreno [a], Abraham Galán [a], Emilio Angelina [c], Ricardo D. Enriz [c], María Dolores Ivorra [a], María Jesús Sanz [d,e], Diego Cortes [a,*]

[a] Departamento de Farmacología, Laboratorio de Farmacoquímica, Facultad de Farmacia, Universidad de Valencia, Burjassot, 46100 Valencia, Spain
[b] Centro de Ecología Química Agrícola – Instituto Agroforestal Mediterráneo, Universidad Politécnica de Valencia, Campus de Vera, Edificio 6C, 46022 Valencia, Spain
[c] Departamento de Química, Universidad Nacional de San Luís, Argentina
[d] Departamento de Farmacología, Facultad de Medicina, Universidad de Valencia, 46010 Valencia, Spain
[e] Institute of Health Research – INCLIVA, University Clinic Hospital of Valencia, Valencia, Spain

ARTICLE INFO

Article history:
Received 13 May 2013
Received in revised form
23 July 2013
Accepted 25 July 2013
Available online 11 August 2013

Keywords:
Tetrahydroprotoberberines
Dopamine receptors
Structure–activity relationships cytotoxicity
MTT and cytofluorometric analysis
Theoretical calculations

ABSTRACT

Dopamine-mediated neurotransmission plays an important role in relevant psychiatric and neurological disorders. Nowadays, there is an enormous interest in the development of new dopamine receptors (DR) acting drugs as potential new targets for the treatment of schizophrenia or Parkinson's disease. Previous studies have revealed that isoquinoline compounds such as tetrahydroisoquinolines (THIQs) and tetrahydroprotoberberines (THPBs) can behave as selective D_2 dopaminergic alkaloids since they share structural similarities with dopamine. In the present study we have synthesized eleven 2,3,9- and 2,3,11-trisubstituted THPB compounds (six of them are described for the first time) and evaluated their potential dopaminergic activity. Binding studies on rat striatal membranes were used to evaluate their affinity and selectivity towards D_1 and D_2 DR and establish the structure–activity relationship (SAR) as dopaminergic agents. In general, all the tested THPBs with protected phenolic hydroxyls showed a lower affinity for D_1 and D_2 DR than their corresponding homologues with free hydroxyl groups. In previous studies in which dopaminergic affinity of 1-benzyl-THIQs (BTHIQs) was evaluated, the presence of a Cl into the A-ring resulted in increased affinity and selectivity towards D_2 DR. This is in contrast with the current study since the existence of a chlorine atom into the A-ring of the THPBs caused increased affinity for D_1 DR but dramatically reduced the selectivity for D_2 DR. An OH group in position 9 of the THPB (**9f**) resulted in a higher affinity for DR than its homologue with an OH group in position 11 (**9e**) (250 fold for D_2 DR). None of the compounds showed any cytotoxicity in freshly isolated human neutrophils. A molecular modelling study of three representative THPBs was carried out. The combination of MD simulations with DFT calculations provided a clear picture of the ligand binding interactions from a structural and energetic point of view. Therefore, it is likely that compound **9d** (2,3,9-trihydroxy-THPB) behave as D_2 DR agonist since serine residues cluster are crucial for agonist binding and receptor activation.

1. Introduction

Dopamine-mediated neurotransmission plays an important role in several psychiatric and neurological disorders affecting several million people worldwide. Researchers have focused their efforts in investigating the modulation of dopaminergic activity via the dopamine receptors (DR) as potential targets for treating schizophrenia or Parkinson's disease. Therefore, there is an increased interest in the discovery of novel dopaminergic ligands as potential drug candidates in the therapy of these neurological disorders [1]. DR can be classified into two pharmacologic families (D_1 and D_2-like) that are encoded by at least five genes. From a therapeutical point of view, drugs acting at D_2-like DR are more relevant than those interacting with D_1-like DR [2]. In this context, whereas the D_2-like DR antagonists are used in the treatment of schizophrenia (antipsychotics), the agonists are used in the treatment of

* Corresponding author. Tel.: +34 963 54 49 75; fax: +34 963 54 49 43.
E-mail addresses: dcortes@uv.es, Diego.M.Cortes@uv.es (D. Cortes).
URL: http://www.farmacoquimicavalencia.es//

0223-5234/$ – see front matter © 2013 Elsevier Masson SAS. All rights reserved.
http://dx.doi.org/10.1016/j.ejmech.2013.07.036

Parkinson's disease [1,3]. In addition, other studies have revealed the potential role of D_2 agonist in the treatment of depression. The pathophysiology of depression has been classically assigned to the noradrenaline and serotonine systems however, nowadays, published reports also support a role of the dopaminergic system in this disorder [2]. In regard to this, different selective D_2-type DR agonists were found to display antidepressant-like actions in several rodent models, suggesting a specific role of this receptor subtype in their antidepressant efficacy [4–8].

Previous studies from our group have revealed that isoquinoline compounds such as tetrahydroisoquinolines (THIQs) have affinity for DR in striate membranes of rat brain tissue which was likely due to their structural similarities to dopamine [8–18]. Likewise, tetrahydroprotoberberines (THPBs) are another group of natural and synthetic isoquinoline alkaloids with a variety of powerful biological activities, including dopaminergic activity [19–21]. Indeed, coreximine, a natural tetrasubstituted THPB, and other analogues were reported as selective D_2 dopaminergic alkaloids [22]. Recently, L-stepholidine analogues have been synthetized displaying a dual dopaminergic activity, partial agonism at the D_1 DR and antagonism at D_2 DR [23].

Since THPBs, THIQs and dopamine share structural similarities, in the present study we have synthesized eleven 2,3,9- and 2,3,11-trisubstituted THPB compounds (six of them are here described for the first time) and evaluated their potential dopaminergic activity. Their structures were determined on the basis of their NMR spectral data and mass spectrometry analysis. The structural features that define the affinity and selectivity of the three series of THPBs synthesized for D_1/D_2 receptors was determined analyzing the influence of the substitution at the 2,3- and 9 or 11 positions, in order to obtain dopaminergic ligands with increased specificity. Therefore, all the synthesized compounds were tested for their ability to displace the selective radioligands of D_1 and D_2-like DR from their specific binding sites in striatal membranes in order to establish the structure–activity relationship (SAR) as dopaminergic agents. In addition, cytotoxicity studies in human cells were carried out. For this purpose, we used the MTT ((3-(4,5-Dimethylthiazol-2-yl)-2,5-diphenyltetrazolium bromide) assay and a cytofluorometric analysis to determine their impact on human neutrophil apoptosis and survival [24–26]. All of them were devoid of any toxic effect in these in vitro assays.

In order to better understand the molecular interactions stabilizing and destabilizing the different THPBs/D_2DR complexes, a molecular modelling study using molecular dynamic simulations and quantum mechanic calculations was carried out for the most representative compounds of this series. Thus, the possible stereo-electronic requirements of the THPBs/D_2DR interactions have been discussed based on their different affinities.

2. Results and discussion

In the present study, the impact of different substituents into the A- and D-ring of synthesized THPBs on dopaminergic affinity was evaluated. In previous reports, we determined the relevance of different substitutions into the A-ring in natural and synthetic isoquinoline alkaloids. We observed that the presence of hydroxyls groups in this ring caused increased affinity for the D_1-like and D_2-like DR families, while blockade of these hydroxyls groups resulted in decreased affinity [8,12–15]. Moreover, the presence of a halogen in the A-ring led to a selective binding at least to one of the two DR subtypes investigated [8,16,17]. Therefore, we have prepared three series of THPBs: 2,11-dihydroxy-3-chloro-THPB (series 1), 2,3-dihydroxy-11-methoxy-THPB (series 2) and 2,3,11-trihydroxy-THPB and 2,3,9-trihydroxy-THPB (series 3) and differently substituted analogues (Fig. 1).

Inasmuch, at the concentrations tested none of the synthesized THPBs affected human neutrophil apoptosis or survival, indicating the absence of cytotoxicity for human cells in these in vitro approaches. Molecular modelling of the possible stereo-electronic requirements for dopamine D_2 receptor ligands of the THPBs synthesized has been discussed based on the different affinities displayed.

2.1. Chemistry

The synthesis of the THPBs has been performed as outlined in the Schemes 1–3. The THPBs of the series 1 (Scheme 1) have been synthesized from 3-chloro-4-methoxybenzaldehyde as starting material. 3-Chloro-4-methoxy-β-nitroestyrene was obtained from 3-chloro-4-methoxybenzaldehyde by a Henry's reaction using nitromethane, ammonium acetate and acetic acid as solvent [27], and then, 3-chloro-4-methoxyphenylethylamine (**1**) was obtained by reduction with lithium aluminium hydride [28]. This phenylethylamine (**1**), was treated with 3-methoxyphenylacetyl chloride under Schotten–Baumann conditions to generate the *N*-(3-cloro-4-methoxyphenylethyl)-β-(3′-methoxyphenyl)acetamide (**2**) [29,30].

Next, the phenylacetamide (**2**) was converted into the corresponding 1-benzyltetrahydroisoquinoline (BTHIQ) (**3**) using the Bischler–Napieralski cyclodehydration reaction. The use of a $POCl_3$ and P_2O_5 mixture in dry toluene followed by $NaBH_4$ reduction was required since the presence of a halogen in position 3 of the phenylacetamide can inactivate the Bischler–Napieralski cyclodehydration reaction due to the electro-attractive properties of the halogen [8,31–33]. Once obtained, the BTHIQ 6-chloro-7-methoxy-1-(3′-methoxybenzyl)-1,2,3,4-THIQ hydrochloride (**3**) was subjected to Mannich cyclization conditions using 37% aqueous formaldehyde [34] to generate the corresponding 2,11-dimethoxy-3-chloro-THPB (**3a**) with high yield (86%). Finally, the *O*-demethylation was performed by adding of 4 equivalents of BBr_3 reagent for 2 h at room temperature [8] to obtain the 2,11-dihydroxy-3-chloro-THPB (**3b**) (Scheme 1).

The THPBs of the series 2 (Scheme 2) have been synthesized using similar approaches to those previously described. A protective reaction of the hydroxyl groups was performed in 3,4-dihydroxybenzaldehyde through dibenzylation [28]. Once prepared the protected 3,4-dibenzyloxybenzaldehyde, a similar sequence of synthesis steps were carried out to obtain the phenylethylamine (**4**), the phenylacetamide (**5**), the BTHIQ (**6**) and

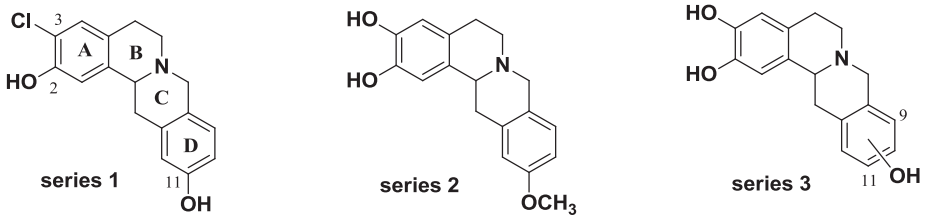

Fig. 1. THPBs series.

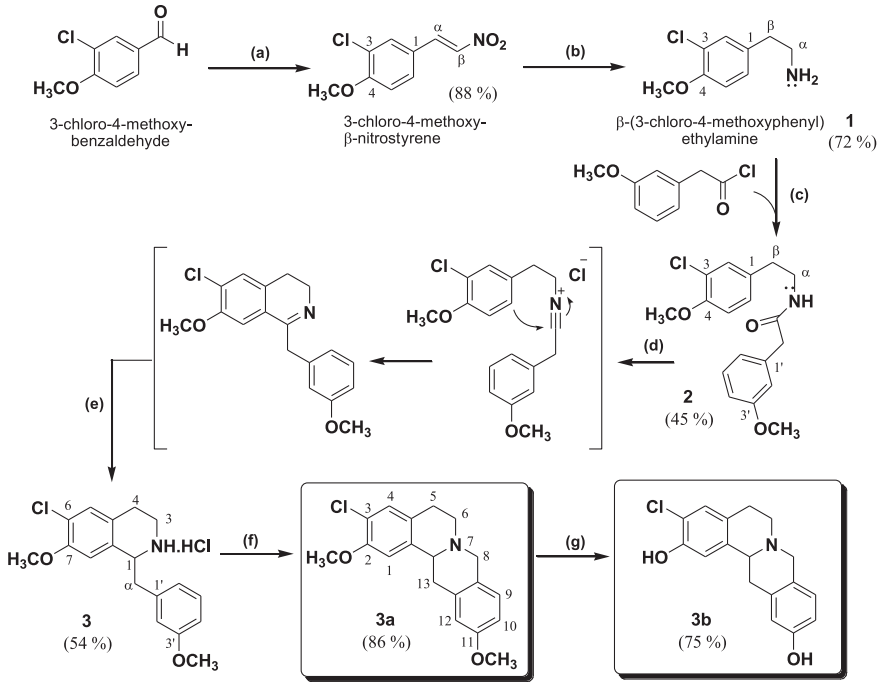

Scheme 1. Synthesis of THPBs **3a** and **3b** (Series 1). Reagents and conditions: (a) Nitromethane, NH_4OAc, AcOH, reflux, 4 h; (b) $LiAlH_4$, THF/Et_2O, N_2, reflux, 2 h; (c) CH_2Cl_2, 3-methoxyphenylacetyl chloride, 5% NaOH, rt, 3 h; (d) P_2O_5, $POCl_3$, Toluene, N_2, reflux, 8 h; (e) $NaBH_4$; MeOH, rt, 2 h; (f) HCHO, EtOH, H_2O, reflux, 5 h; (g) CH_2Cl_2, BBr_3, rt, 2 h.

finally, the corresponding 2,3-dibenzyloxy-11-methoxy-THPB (**6a**) with good yields (63–93%). In this series, the Bischler–Napieralski cyclodehydration was performed using only $POCl_3$ in dry acetonitrile since the presence of an alkoxy group in position 3 of the phenylacetamide can activate the Bischler–Napieralski cyclodehydration reaction due to the electro-donor ability of the oxygenated group. Then, this THPB was subjected to acidic conditions in absolute ethanol [12–35] in order to deprotect the phenolic hydroxyls groups yielding 2,3-dihydroxy-11-methoxy-THPB (**6b**). A methylendioxy group was generated by CsF and dichloromethane [13] from **6b** to obtain the 2,3-methylendioxy-11-methoxy-THPB (**6c**).

The THPBs of the series 3 (Scheme 3) have been synthesized employing similar procedures to those followed in series 1 and 2. The corresponding trisubstituted THPBs: 2,3,11-trimethoxy-THPB (**9a**) and 2,3,9-trimethoxy-THPB (**9b**) were obtained from 3,4-

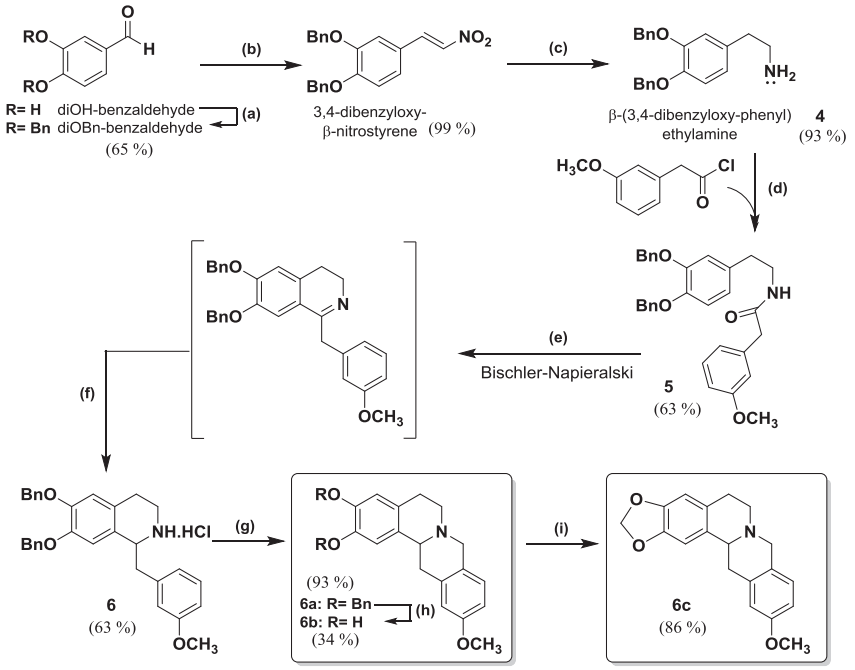

Scheme 2. Synthesis of THPBs **6a**–**6c** (Series 2). Reagents and conditions: (a) Benzyl chloride, K_2CO_3, EtOH, reflux, 6 h; (b) Nitromethane, NH_4OAc, AcOH, reflux, 4 h; (c) $LiAlH_4$, THF/Et_2O, N_2, reflux, 2 h; (d) CH_2Cl_2, 3-methoxyphenylacetyl chloride, 5% NaOH, rt, 3 h; (e) $POCl_3$, CH_3CN, N_2, reflux, 5 h; (f) $NaBH_4$; MeOH, rt, 2 h; (g) 37% HCHO, EtOH, H_2O, reflux, 5 h; (h) EtOH–HCl, reflux, 3 h; (i) DMF, CH_2Cl_2, CsF, reflux, 3 h.

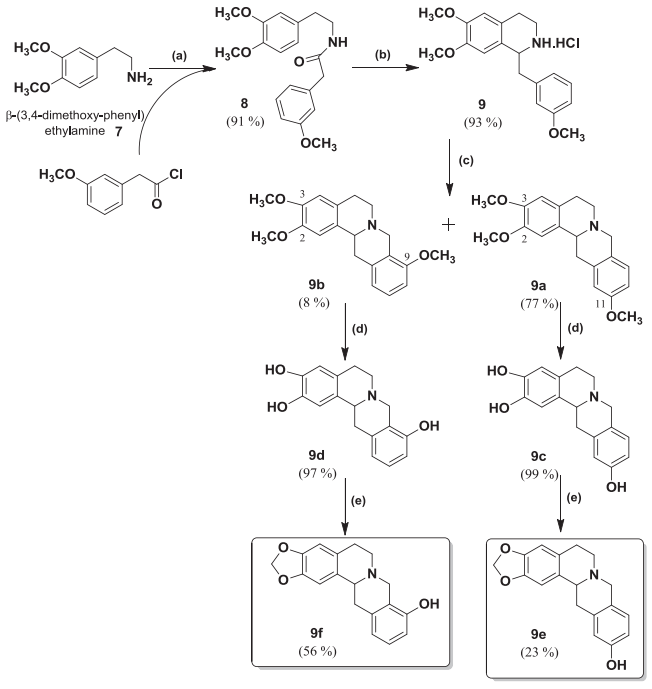

Scheme 3. Synthesis of THPBs **9a**–**9f** (Series 3). Reagents and conditions: (a) CH_2Cl_2, 3-methoxyphenylacetyl chloride, 5% NaOH, rt, 3 h; (b) $POCl_3$, CH_3CN, N_2, reflux, 5 h; and, $NaBH_4$, MeOH, rt, 2 h; (c) HCHO, EtOH, H_2O, reflux, 5 h; (d) CH_2Cl_2, BBr_3, rt, 2 h; (e) DMF, CH_2Cl_2, CsF, reflux, 3 h.

dimethoxyphenylethylamine (**7**). In this series, two different compounds were obtained based on the two possible positions of the Mannich cyclization. When cyclization was in *para* to the benzylic methoxy group, the 2,3,11-trimethoxy-THPB (**9a**) was the major product generated (77% yield). In contrast, when cyclization occurred in *ortho* to the benzylic methoxy group then 2,3,9-trimethoxy-THPB (**9b**) was produced (8% yield). The phenolic hydroxyl groups were deprotected through *O*-demethylation conditions to obtain the corresponding 2,3,11-trihydroxy-THPB (**9c**) and 2,3,9-trihydroxy-THPB (**9d**) respectively. Finally, the THPBs with methylendioxy group were prepared as above described to generate 2,3-methylendioxy-11-hydroxy-THPB (**9e**) and 2,3-methylendioxy-9-hydroxy-THPB (**9f**) respectively.

2.2. Binding affinities for dopamine receptors: structure–activity relationship

All the synthesized THPB compounds were assayed in vitro for their ability to displace the selective ligands of D_1 and D_2 DR from their respective specific binding sites in the striatal membranes. All the compounds except **6a**, were able to displace [^{3}H]-SCH 23390 and [^{3}H]-raclopride from their specific binding sites at micromolar (μM) or nanomolar (nM) concentrations. This was not surprising given the bulky substituents (Bn) at C3 and C4 in compound **6a**. The binding affinities for D_1 and D_2 DR are summarized in Table 1 illustrating some general trends of the structure–activity relationship.

2.2.1. Effect of the substituents into the A-ring of THPB

a) In general, all the tested THPBs with protected phenolic hydroxyls showed a lower affinity for D_1 and D_2 DR than their corresponding homologues with free hydroxyl groups (see **3a** vs **3b**, **6a** vs **6b**, **9a** vs **9c**, **9b** vs **9d** in Table 1). The higher affinity for D_1 and D_2 DR of compounds with free phenolic group than those without was previously described albeit in several isoquinolines [8,12,16,21].
b) In previous studies in which dopaminergic affinity of BTHIQs was evaluated, the presence of a chlorine atom into the A-ring (*ortho* of oxygenated group) resulted in increased affinity and selectivity towards D_2 DR [8,16–18]. This is in contrast with the current study since the existence of a chlorine atom into the A-

Table 1
Values of affinity (K_i, pK_i) and selectivity (ratio K_i D_1/K_i D_2) determined in binding experiments to D_1 and D_2 DR of series **1**–**3**.

THPB		Specific ligand D_1 [^{3}H]-SCH 23390		Specific ligand D_2 [^{3}H]-raclopride		K_i D_1/D_2
		K_i (μM)[m]	pK_i[m]	K_i (μM)[m]	pK_i[m]	
3a	3-Cl-2,11-diMeO	1.813 ± 0.146	5.76 ± 0.09	2.046 ± 0.347	5.70 ± 0.07	0.9
3b	3-Cl-2,11-diOH	**0.107 ± 0.004**	**6.97 ± 0.02**[d,i]	0.188 ± 0.021	6.73 ± 0.05[b,i]	**0.6**
6a	2,3-diBnO-11-MeO	40.607 ± 4.215	4.39 ± 0.04[j]	40.866 ± 1.461	4.38 ± 0.02[j]	1.0
6b	2,3-diOH-11-MeO	1.108 ± 0.411	6.02 ± 0.17[e,h]	**0.078 ± 0.017**	**7.13 ± 0.09**[b,d,h]	**14.2**
6c	2,3-OCH_2O-11-MeO	2.373 ± 1.208	5.77 ± 0.27[f]	1.331 ± 0.536	5.94 ± 0.17[l]	1.8
9a	2,3,11-triMeO	4.314 ± 0.703	5. 38 ± 0.07	8.543 ± 4.709	5.29 ± 0.36	0.5
9b	2,3,9-triMeO	3.927 ± 0.908	5.44 ± 0.11	0.393 ± 0.115	6.44 ± 0.12[b,c,k]	**10**
9c	2,3,11-triOH	2.962 ± 1.042	5.58 ± 0.15	0.396 ± 0.028	6.41 ± 0.03[a]	7.5
9d	2,3,9-triOH	3.775 ± 0.992	5.46 ± 0.14	**0.093 ± 0.024**	**7.07 ± 0.14**[b,d]	**40.6**
9e	2,3-OCH_2O-11-OH	32.999 ± 5.009	4.49 ± 0.07[d]	7.506±1.591	5.16 ± 0.09[d]	4.4
9f	2,3-OCH_2O-9-OH	0.344 ± 0.027	6.47 ± 0.03[f,g]	**0.035 ± 0.012**	**7.55 ± 0.16**[a,f]	**10.0**

ANOVA, post Newmann-Keuls multiple comparison tests.
[a] $p < 0.05$.
[b] $p < 0.01$, vs D_1-like DR.
[c] $p < 0.001$ vs **9a**.
[d] $p < 0.001$ vs **9c**.
[e] $p < 0.05$ vs **9c**.
[f] $p < 0.001$ vs **9e**.
[g] $p < 0.001$ vs **9d**.
[h] $p < 0.001$ vs **6a**, **6c**, **9a**.
[i] $p < 0.001$ vs **3a**.
[j] $p < 0.001$ vs **6b**.
[k] $p < 0.05$ vs **9d**.
[l] $p < 0.01$ vs **9e.**
[m] Data were displayed as mean ± SEM for 3–5 experiments.

ring of the THPBs caused increased affinity for D_1 DR but dramatically reduced the selectivity for D_2 DR (see **3b** vs **9c** in Table 1).

c) Our results also showed that the presence of a methylenedioxy group in 2,3 position decreased the selectivity for D_2 DR (see **6c** vs **6b** and **9e** vs **9c** in Table 1). This effect was also observed when the substituent into the D-ring was in position 9. In fact, when the dopaminergic affinities of THPB **9d** (2,3,9-triOH) and **9f** (2,3-OCH_2O-, 9-OH) were compared, **9d** exerted higher selectivity for D_2 DR (K_i $D_1/D_2 = 40.6$) than **9f** (K_i $D_1/D_2 = 10$). Moreover, the latter compound (**9f**) is the THPB displaying the highest affinity for both DR types ($K_i = 344$ nM for D_1 and $K_i = 35$ nM for D_2) (see Table 1 and Fig. 2).

*2.2.2. Effect of the **9** or **11** substituent into the D-ring of THPB*

The present study demonstrated that the affinity and the selectivity for DR depended on the position of the oxygenated substituents in positions 9 or 11 and on their protection or deprotection. In regard to this:

a) A hydroxyl group in position 9 of the THPB (**9f**) resulted in a higher affinity for D_1 and D_2 DR than its homologue with a hydroxyl group in position 11 (**9e**). In this context, the affinity for D_2 DR displayed by **9f** was 214 fold higher than **9e** (Table 1 and Fig. 3).

b) Surprisingly, either when this 2,3-methylenedioxy-11-OH-THPB (**9e**) was compared with the protected 2,3-methylenedioxy-11-OMe-THPB (**6c**), or when the 2,3,11-triOH-THPB (**9c**) was compared with the protected 2,3-diOH-11-OMe-THPB (**6b**), an increased affinity for D_1 and D_2 DR was observed with the 11-O-protected derivatives (**6c** and **6b,** see Table 1 and Fig. 4).

2.3. Cytotoxicity studies

After determining the affinity for DRs of the synthesized THPBs, the potential cytotoxicity of these compounds was determined by the use of the MTT assay. The concentrations tested were selected based on their respective Ki value for D_2 DR. None of the THPBs evaluated displayed any cytotoxicity on freshly isolated human neutrophils (Fig. 5).

To confirm the absence of toxicity, we next investigated the effect on neutrophil apoptosis and survival of the most active THPBs on D_2 DRs (**6b**, **9d** and **9f**). For this purpose a cytofluorimetric method was employed. As depicted in Fig. 6 none of the THPBs at the concentrations assayed affected neutrophil apoptosis or survival indicating the lack of human cell toxicity of these compounds in this in vitro approach.

2.4. Molecular modelling

A molecular modelling study of three representative compounds of these series was performed to add further support to the results described in Section 2.2. Special attention was paid to the effects exerted by the substituents into the D-ring of THPBs as well as to the increased affinity for the D_2 DR detected by the 11-O-protected derivatives. Therefore, compounds **9d**, **9c** and **6b** were selected for this comparative analysis due to their structural differences.

First, MD calculations were carried out simulating the molecular interactions between compounds **9d**, **9c** and **6b** with the human D_2 DR (Fig. 7). In general, the three compounds displayed their pharmacophoric portions in a closely related spatial form to that reported for dopamine [17,18]. Consistent with previous experimental [36] and theoretical [37] data, the simulation indicated the relevance of the negatively charged aspartate 114 (D114) for ligand binding. In this context, the highly conserved D114 in *trans*-membrane helix 3 (TM3) is important for both D_2 DR agonists and antagonists binding [36,38], and its terminal carboxyl group may function as an anchoring point for ligands with protonated amino groups [39–41]. In the current study, all the compounds simulated were docked into the receptor with the protonated amino group close to D114. Although after 5 ns of MD simulations the ligands slightly moved in a way different from the initial position, the strong interaction with D114 was maintained for all the complexes (see Fig. 7), reinforcing the role of the amino acid as an anchoring point for ligands with protonated amino groups.

Next, the relative energies ($\Delta\Delta G$ values) obtained for the different complexes were analysed. A 0.00, 12.14 and 2.58 kcal/mol for complexes **9d**/D_2DR, **9c**/D_2DR and **6b**/D_2DR, respectively were obtained. These binding energies (BE) were in agreement with the experimental data (see K_i values in Table 1). However, although BE allowed to differentiate between very good and weak binders

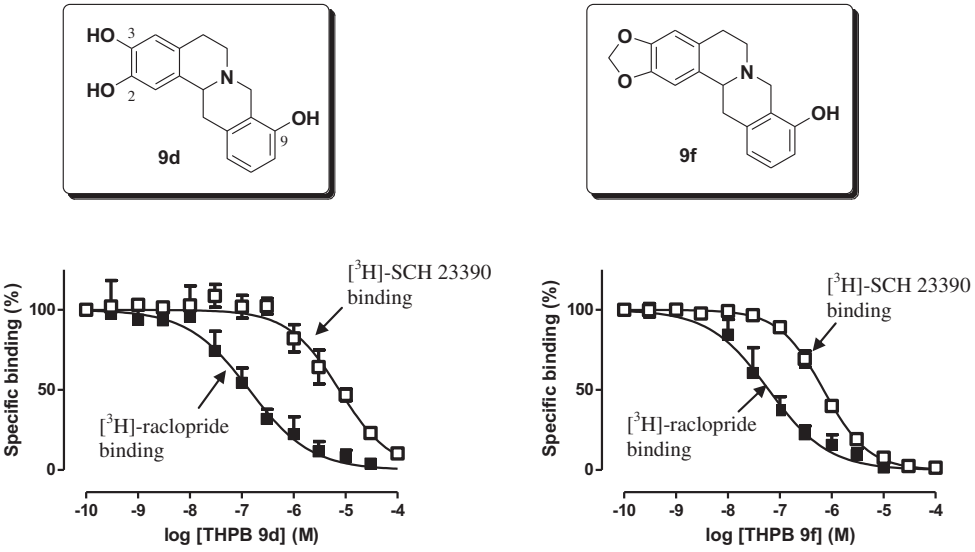

Fig. 2. Displacement curves of [^{3}H]-SCH 23390 (D_1) and [^{3}H] raclopride (D_2) specific binding by compounds **9d** and **9f**. Data were displayed as mean ± SEM for 3–5 experiments.

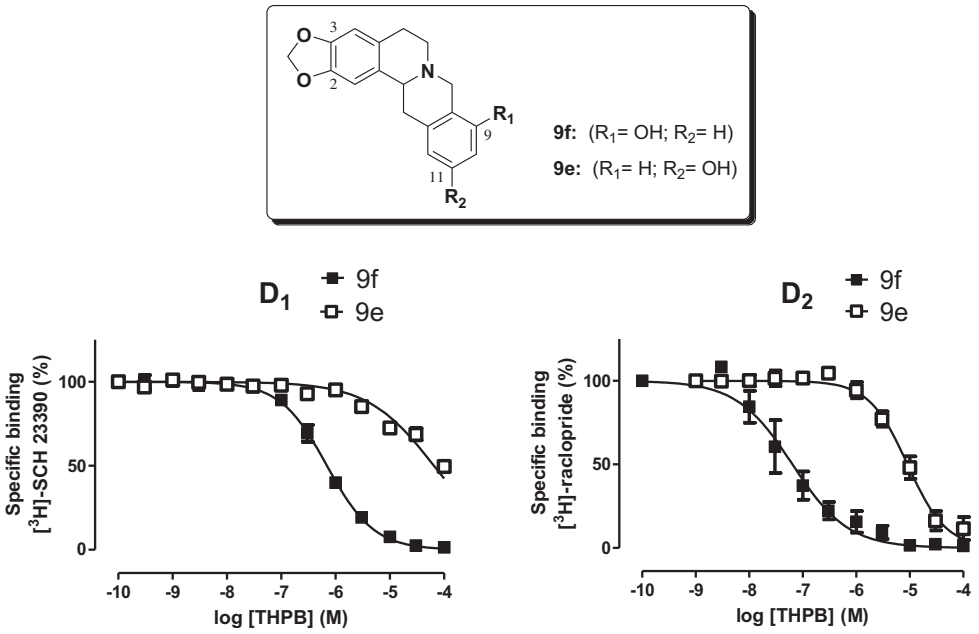

Fig. 3. Displacement curves of the specific binding of D_1 and D_2 DR ligands by the compounds **9e** and **9f**. Data were displayed as mean ± SEM for 3–5 experiments.

(0.00 kcal/mol for compound **9d** vs 12.14 kcal/mol for compound **9c**), those with similar binding affinities did not (0.0 kcal/mol for compound **9d** vs 2.58 kcal/mol for compound **6b**). This was not surprising since MD simulations poorly approximate features that might be playing determinant roles such as lone pair directionality in hydrogen bonds, explicit π···π stacking polarization effects, hydrogen bonding networks, induced fit, and conformational entropy. Collectively, the information obtained from MD simulations might explain in part the differential D_2 DR affinity displayed by compounds **9d** and **9c**.

To acquire more detailed insights into the mechanisms driving the binding of the THPBs to the D_2 DR active site, the structure–affinity relationship was further analysed. The THPB-residue interaction spectra calculated by the free energy decomposition suggested that the interaction spectra of compounds **9d, 9c** and **6b** with D_2 DR was closely related. Nevertheless, some subtle but significant differences were detected reflecting differential binding features (Fig. 8).

In this regard, it is interesting to note that the only structural difference between compounds **9d** and **9c** is the position of the OH groups in the D ring (see Scheme 3). Despite of it, a significant difference was obtained for their respective calculated BE, indicating that **9d**/D_2DR complex was markedly more stable than **9c**/D_2DR. The comparison of both spectra (Fig. 8a and b) revealed that

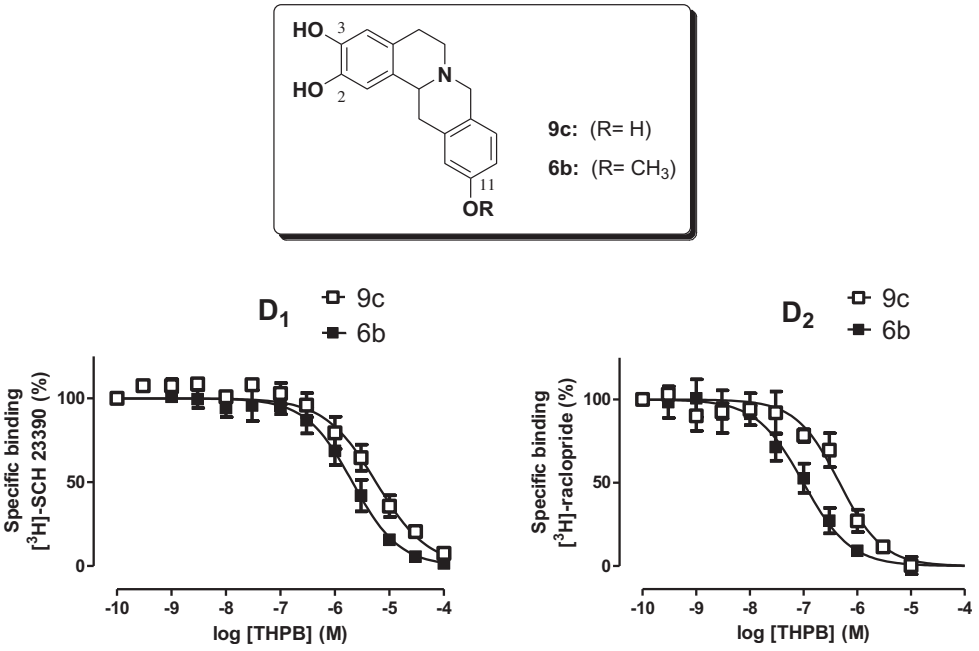

Fig. 4. Displacement curves of the specific binding of D_1 and D_2 DR ligands by the compounds **6b** and **9c**. Data were displayed as mean ± SEM for 3–5 experiments.

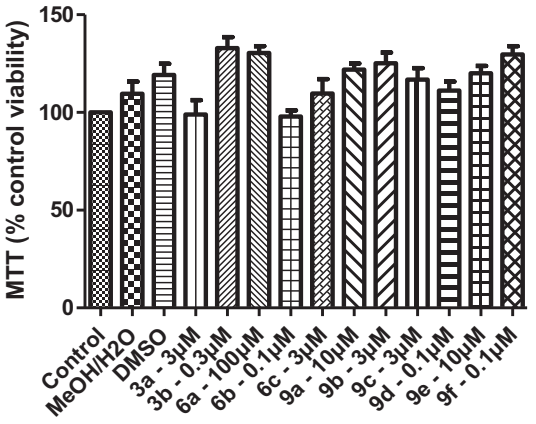

Fig. 5. Effect of the synthesized THPBs on viability of human neutrophils. Data are presented as mean ± SEM of $n = 3$ independent experiments.

the OH group of compound **9d** at position 9 (Fig. 8a) was forming a strong hydrogen bond interaction with Y416. This is a particularly strong stabilizing interaction which is due to the acidic character of the oxygen atom of the Tyr residue. In contrast, the OH group of **9c**/D_2DR complex (Fig. 8b), was located within a hydrophobic pocket where only weak hydrogen bonds (O···H–C with the side chains of the amino acids) can take place (see the weak stabilizing interaction with Y416, Fig. 8b). In addition, although the complex of compound **9c** displayed a moderated interaction with S193, there was not a stabilizing interaction with S197. This is in sharp contrast with **9d** spectra since two strong interactions with S193 and Ser197 were encountered (Fig. 8a).

The remainder of the amino acids stabilizing these complexes (D114, V111 V115, C118, C182, I183, I184 W382, H393, F389, F390 and T412) exerted closely related interactions. In light of these observations, it is tempting to speculate that the different stabilizing interactions of complexes **9d**/D_2DR and **9c**/D_2DR could

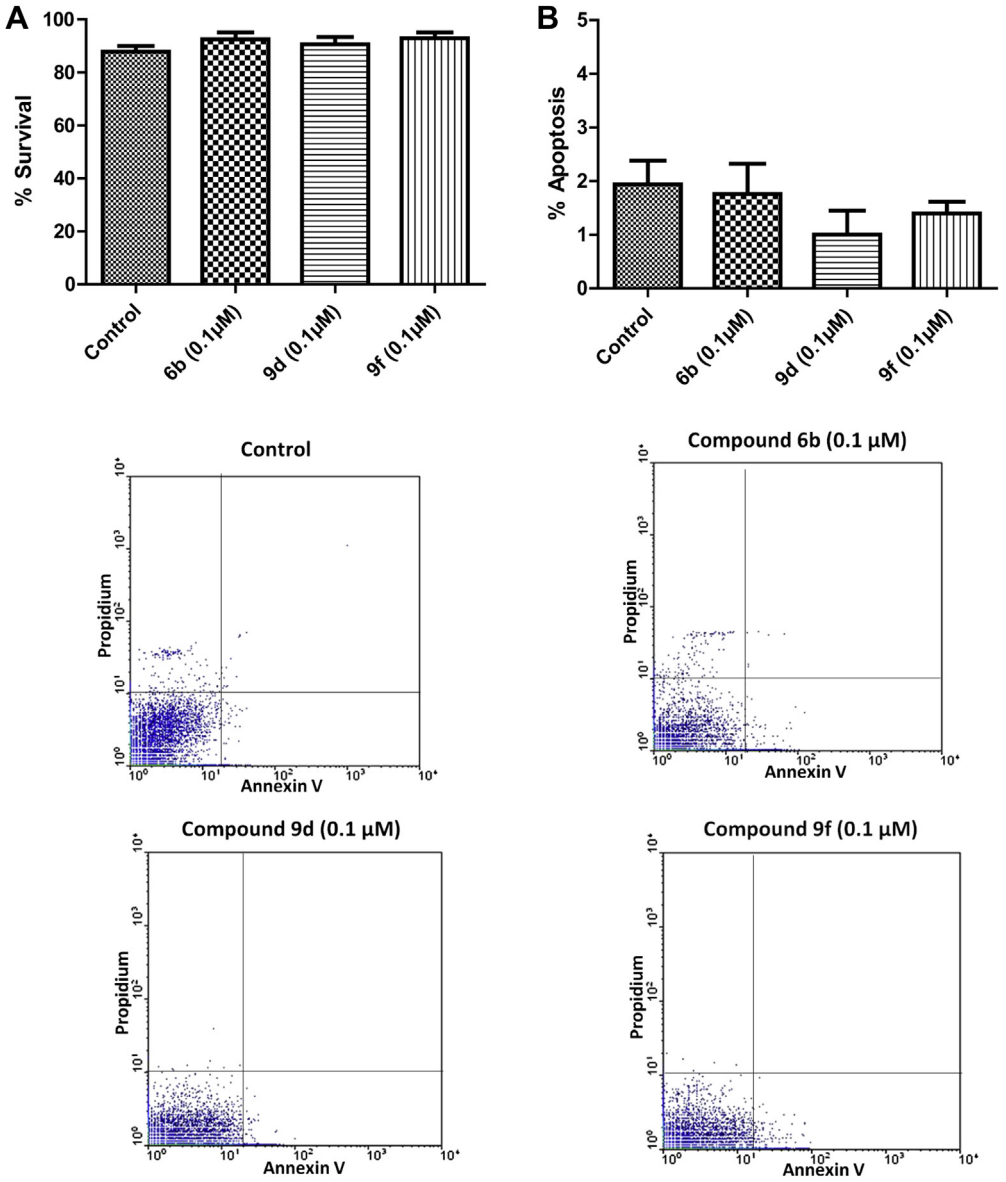

Fig. 6. Percentage of apoptotic (A) and survival cells (B) after incubation with THPBs **6b**, **9d** and **9f**. Early apoptotic cells were quantified as the percentage of total population of annexin V^+, PI^- cells, late apoptotic, and/or necrotic cells as annexin V^+ and PI^+, and viable nonapoptotic cells as annexin V^- and PI^- at 24 h of culture of human neutrophils. The columns are the means ± SEM of $n = 3$ independent experiments. Representative flow cytometry panels showing the effects of compounds **6b**, **9d** and **9f** on human neutrophil apoptosis have been included.

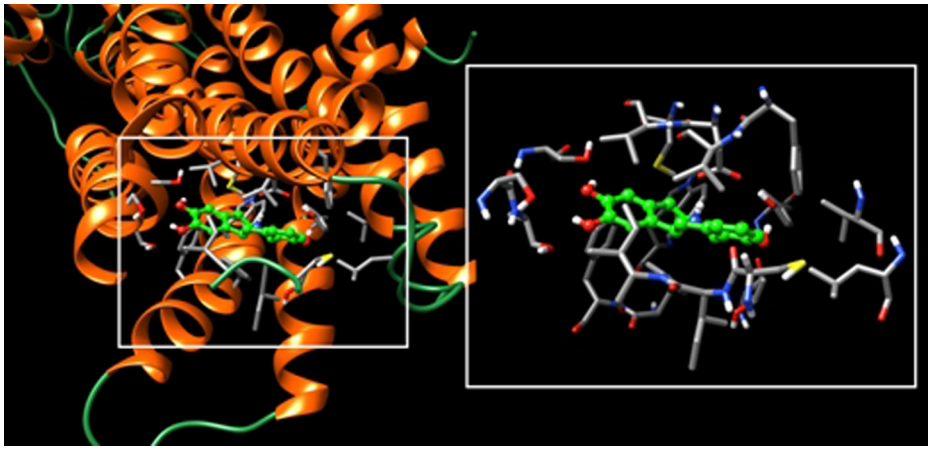

Fig. 7. Spatial view of compound **9d** (green)/D_2DR interaction. Magnification of the receptor active site at the right. (For interpretation of the references to colour in this figure legend, the reader is referred to the web version of this article.)

explain both the different $\Delta\Delta G$ values and the experimental affinities (Table 1).

On the other hand, when the activities of the 2,3,11-triOH-THPB (**9c**) and the protected 2,3-diOH-11-OMe-THPB (**6b**) were compared, an increased affinity for D_2 DR was exerted by the 11-O-protected derivative (Table 1). The analysis of the two spectra (Fig. 8b and c) showed that compound **6b** can establish two strong molecular interactions with two serine residues (S193 and S197). The average structures obtained for the complexes **9d**/D_2DR, **9c**/D_2DR, and **6b**/D_2DR from the last ns of simulation are shown in Fig. 9a, b and c, respectively. The salt bridge between the protonated N–H group of BTHPs and the carboxyl group of D114 as well as the rest of the interactions previously discussed can be appreciated in this figure.

At this stage, the trend predicted for the MD simulations can be considered as certainly significant. However, it should be noted that we were dealing with relatively weak interactions and therefore MD simulations might underestimate such interactions. Therefore, reduced models were constructed to perform more accurate DFT calculations (B3LYP/6-1G(d)). These calculations allowed to perform a QTAIM analysis for a further characterization of the most critical interactions for these ligands.

The main interactions of compound **9d** at the binding pocket and the interactions net obtained are illustrated in Fig. 10. The OH-2 in the catecholic ring is acting as a proton donor with S193 (ρ(rb) = 0.0207 au) and as a proton acceptor with two amino acids, H393 (0.0187 au) and S194 (0.0012 au). The OH-3 behaves as a proton donor with S197 (0.0238 au) and is also involved in three weak C–H hydrogen bonds with S193, S194 and V115. The OH-9 possesses only one strong hydrogen bond with Y416 (0.0370 au). It is noteworthy that the hydrogen bonds between the catecholic hydroxyls (OH-2 and OH-3) with the serine residues (S193 and S194) are facilitated by the adequate spatial orientation of the molecule in which the atoms of rings A, B, C and D are making further interactions with other residues (Fig. 10). These stabilizing interactions include the strong salt bridge between the ammonium group of **9d** with the carboxyl group of D114, the weaker C–H–S interaction with S118 and the C–H–π interactions with F389 and V115. These interactions are present with varying intensity in the three compounds here analyzed.

The main interactions of compound **9c** at the binding pocket are shown in Fig. 11. To facilitate the description of the molecule interactions, this figure was divided in two and the interactions of the catecholic ring are illustrated in Fig. 11a. The OH-2 establishes a hydrogen bond with the carbonyl oxygen of the backbone of S193 (0.0246 au) but not with the side chain oxygen as found for **9d**/D_2DR. It also acts as a proton acceptor with H393 (0.0147 au) and with a C–H bond of the side chain of S193 (0.0067 au). The OH-3 behaves as a proton acceptor for C–H interactions with F390 and V115 without proton donor activity with any residue except a very weak H–H contact with S197 (0.0016 au). In addition, this OH can establish two O–O interactions with the carbonyl oxygen at S193 and the hydroxyl at S197. Such interactions suggest that this hydroxyl group is weakly bond at the binding site compared with **9d**/D_2DR complex. In fact, while the sum of electronic density of all OH-3 interactions in the binding site ($\sum\rho$ (rb)) is 0.0247 for compound **9c**, the value for compound **9d** was 0.0391 au. The OH-11 is forming C–H–O type interactions with C182 (0.0031 au), I183 (0.0037 au) and F110 (0.0022 au), O––O type interactions with the carbonyl oxygen of backbone C182 (0.0044 au) and a weak H–H interaction with V91 (0.0019 au) (Fig. 11b).

Fig. 12 shows the main interactions of compound **6b** at the binding pocket. The interaction pattern of this compound shares similarities with those observed for compound **9d**. In fact, OH-2 and OH-3 are acting as proton donors with S193 (0.0340 au) and S197 (0.0308 au) and as proton acceptors with H393 (0.0064 au), I184 (0.0048 au), S193 (0.0114 au) and V115 (0.0065 au) (Fig. 12a). OMe-11 is only forming two very weak hydrogen bonds with the C–H bonds of the side chain (ρ(rb) = 0.0015) and the backbone (0.0011au) of I183 (Fig. 12b). The CH_3 group is interacting with C182 (C–H–S interaction (0.0039 au)), V91 (C–H interaction (0.0085 au)) as well as with F110 (H–H interaction (ρ(rb) = 0.0184 au). Taken together all these observations and the sum of the electronic density of all the interactions (0.0150 au), it can be concluded that the binding strength of OMe-11 to D_2DR is not relevant. In contrast, compound **6b** interactions seemed to be stronger when they are established between the catecholic hydroxyls and the serine residues. As oppose to the OH-11 of **9c** who remained almost fixed with the same orientation (Fig. 11b), the OMe-11 group in **6b** is rotating almost freely during the simulation for MD calculations. This is a striking observation which may account for **9c** and **6b** differential D_2DR affinities. Finally, the QTAIM analysis seem to indicate that the increased affinities of compounds **9d** and **6b** compared with those of **9c** may rely on the stronger interactions established between the catecholic hydroxyls and the serine residues.

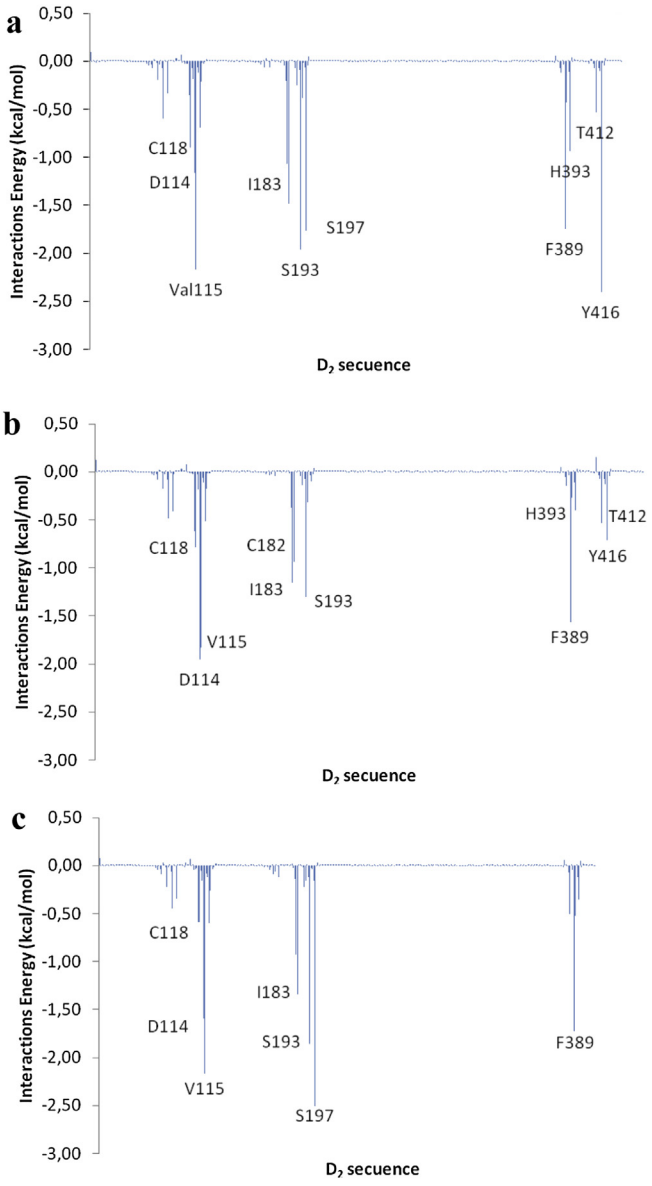

Fig. 8. Histograms of interaction energies partitioned for D_2DR amino acids when complexed with compound **9d** (a), compound **9c** (b) and compound **6b** (c). The *x-axis* denotes the residue number of D_2DR, and the *y-axis* shows the interaction energy between the compound and the specific residue. Negative and positive values represent favourable or unfavourable binding, respectively.

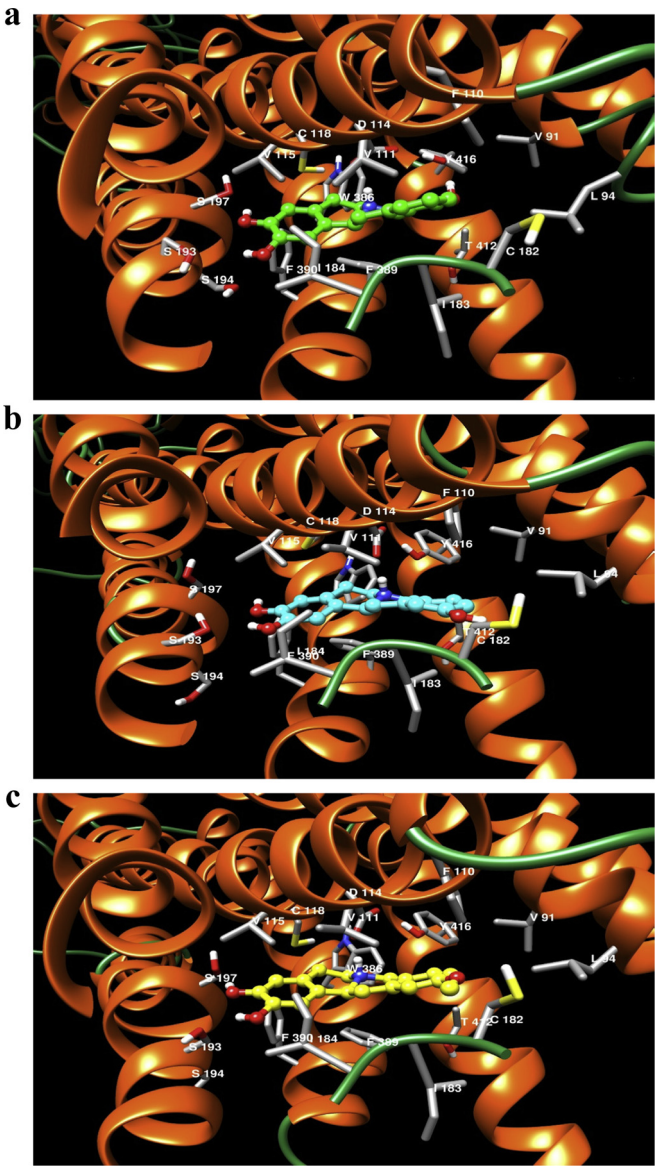

Fig. 9. Spatial view of the active D_2 DR site for compounds **9d** (a), **9c** (b) and **6b** (c). The names of the residues involved in the main interactions are written in the figure.

3. Conclusions

In summary, we have synthesized several THPBs with different substituents into their A- and D- rings and evaluated the SAR for their potential dopaminergic affinity. Three series of THPBs were obtained: 2,11-dihydroxy-3-chloro-THPBs (series 1), 2,3-dihydroxy-11-methoxy-THPBs (series 2) and 2,3,11-trihydroxy-THPBs and 2,3,9-trihydroxy-THPBs (series 3). Concerning to their affinity for DR: first, the presence of hydroxyls groups into the A-ring resulted in increased the DR affinity and, blockade of these groups blunted these responses; second, a halogen in the A-ring shifted the selectivity of the compound towards one of the DR investigated; third, while the presence of an OH at position 9 resulted in a positive effect on DR affinities, its localization at position 11 was surprisingly detrimental, and the blockade of this hydroxyl group at position 11 (MeO) reversed their DR affinity.

In addition, none of the compounds evaluated showed any cytotoxicity in freshly isolated human neutrophils. Finally, a molecular modelling study of three representative THPBs was carried out. The QTAIM analysis allowed a further understanding of the different experimental affinities obtained for compounds **9d**, **9c** and **6b**. Since serine residues cluster seemed to be crucial for agonist binding and receptor activation, it is likely that compounds **9d** and **6b** displayed such capability.

4. Experimental section

4.1. General instrumentation

EIMS and FAB mass were recorded on a VG Auto Spec Fisons spectrometer instruments (Fisons, Manchester, United Kingdom). ^{1}H NMR and ^{13}C NMR spectra were recorded with $CDCl_3$ or C_5D_5N as a solvent on a Bruker AC-300, AC-400 or AC-500. Multiplicities of ^{13}C NMR resonances were assigned by DEPT experiments. COSY, HSQC and HMBC correlations were recorded at 400 MHz and

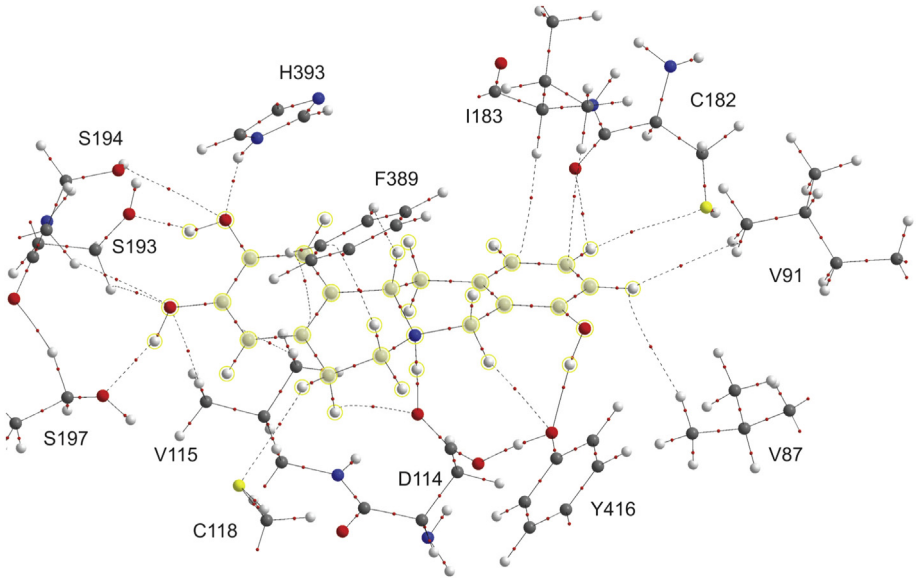

Fig. 10. Molecular graph of compound **9d** interaction with the binding site. Large spheres represent attractors or nuclear critical points (3, −3) attributed to the atomic nuclei. The connecting nuclei lines are bond paths and small spheres on them are bond critical points (3, −1).

500 MHz (Bruker AC-400° AC-500). The assignments of all compounds were made by COSY, DEPT, HSQC and HMBC. All the reactions were monitored by analytical TLC by silica gel 60 F_{254} (Merck 5554). Residues were purified by sílica gel 60 (40–63 μm, Merck 9385) column chromatography. Solvents and reagents used were purchased from commercial sources. Quoted yields are of purified material. The HCl salts of the synthesized compounds were prepared from the corresponding base with 5% HCl in MeOH.

4.2. Chemistry

4.2.1. General procedure for the synthesis of phenyethylamines (*1* and *4*)

4.2.1.1. 3,4-Dibenzyloxybenzaldehyde. A mixture of 3,4-dihydroxybenzaldehyde (1 g, 7.24 mmol), benzyl chloride (3 mL, 24.51 mmol) and anhydrous K_2CO_3 (2.1 g, 14.3 mmol) in absolute EtOH (15 mL) was refluxed for 6 h. After being stirred, the reaction mixture was concentrated to dryness, redissolved in 10 mL of CH_2Cl_2, and then 5% aqueous NaOH (3 × 10 mL) was added. The combined organic layers were dried over with anhydrous Na_2SO_4 and evaporated to dryness. The residue obtained was purified by silica gel column chromatography (Hexane/EtOAc, 8:2) to obtain the 3,4-dibenzyloxybenzaldehyde (1.5 g, 65%) as a white solid. ^{1}H NMR (500 MHz, $CDCl_3$): δ = 9.83 (s, 1H, CHO), 7.56 (m, 2H, H-2, H-6), 7.48–7.27 (m, 10H, 2 × Ph), 7.02 (d, J = 13.7 Hz, 1H, H-5), 5.22 (s, 2H, $PhCH_2O$-3), 5.17 (s, 2H, $PhCH_2O$-4); ^{13}C NMR (125 MHz, $CDCl_3$) δ = 191.2 (CHO), 155.7 (C-4), 150.6 (C-3), 136.5 (C-1′), 136.3 (C-1″), 130.5 (C-1), 129–127 (6C, C-2′-4′ y C-2″-4″), 124.6 (CH-6), 116.9 (CH-5), 115.7 (CH-2), 71.3 ($PhCH_2O$-3), 71.1 ($PhCH_2O$-4); ESMS m/z (%): 341 $[M + Na]^+$, 313 (100).

4.2.1.2. 3-Chloro-4-methoxy-β-nitrostyrene. A mixture of 3-chloro-4-methoxy-benzaldehyde (1 g, 5.87 mmol), nitromethane (1 mL, 18.41 mmol) and NH_4OAc (1.2 g, 15.57 mmol) in AcOH (15 mL) was refluxed for 4 h. After this time, the reaction mixture was cooled to room temperature, diluted with H_2O (10 mL), and extracted with CH_2Cl_2 (3 × 10 mL). The combined organic layer were washed with brine (2 × 10 mL) and H_2O (2 × 10 mL), dried over with anhydrous Na_2SO_4, and evaporated to dryness to obtain the 3-chloro-4-methoxy-β-nitrostyrene (1.1 g, 88%) as yellow needles, which was used in the following step with no further purification. ^{1}H NMR (400 MHz, $CDCl_3$): δ = 7.91 (d, J = 13.7 Hz, 1H, H-β), 7.59 (d, J = 2.2 Hz, 1H, H-2), 7.52 (d, J = 13.7 Hz, 1H, H-α), 7.44 (dd, J = 8.6, 2.2 Hz, 1H, H-6), 6.97 (d, J = 8.6 Hz, 1H, H-5), 3.90 (s, 3H, OCH_3-4); ^{13}C NMR (100 MHz, $CDCl_3$) δ 158.4 (C-4), 138.4 (CH-β), 136.4 (CH-α), 130.9 (CH-2), 130.1 (CH-6), 124.2 (C-1), 123.7 (C-3), 112.7 (CH-5), 56.8 (OCH_3-4); MS (EI) m/z (%): 213 (55) $[M]^+$, 185 (100).

4.2.1.3. 3,4-Dibenzyloxy-β-nitrostyrene. 3,4-dibenzyloxybenzaldehyde (1 g, 3.15 mmol) was subjected to similar conditions to those above described to obtain the 3,4-dibenzyloxy-β-nitrostyrene (1.70 g, 99%) as yellow needles, which was used in the following step with no further purification. ^{1}H NMR (500 MHz, $CDCl_3$): δ = 7.81 (d, J = 13.6 Hz, 1H, H-β), 7.36 (d, J = 13.6 Hz, 1H, H-α), 7.38–7.23 (m, 10H, 2 × Ph), 7.01 (dd, J = 8.3, 2.1 Hz, 1H, H-6), 6.99 (d, J = 2.1 Hz, 1H, H-2), 6.87 (d, J = 8.3 Hz, 1H, H-5), 5.15 (s, 2H, $PhCH_2O$-3), 5.10 (s, 2H, $PhCH_2O$-4); ^{13}C NMR (125 MHz, $CDCl_3$) δ = 152.7 (C-4), 149.1 (C-3), 139.1 (CH-β), 136.4 (C-1′), 136.2 (C-1″), 135.3 (CH-α), 129–127 (6C, C-2′-4′ y C-2″-4″), 124.7 (CH-6), 123.1 (C-1), 114.3 (CH-2), 114.2 (CH-5), 71.4 ($PhCH_2O$-4), 70.8 ($PhCH_2O$-3); ESMS m/z (%): 362 (100) $[M + H]^+$.

*4.2.1.4. β-(3-Chloro-4-methoxyphenyl)ethylamine (**1**).* A solution of 3-chloro-4-methoxy-β-nitrostyrene (1 g, 4.7 mmol) in anhydrous THF (14 mL) was added dropwise to a well-stirred suspension of $LiAlH_4$ (0.7 g, 18.5 mmol) in anhydrous Et_2O (20 mL) under nitrogen atmosphere, and refluxed for 2 h. Then the reaction mixture was cooled and the excess reagent was destroyed by a dropwise addition of H_2O (2 mL) and 15% aqueous NaOH (5 mL). After a partial evaporation of the filtered portion, the aqueous solution was extracted with CH_2Cl_2 (3 × 10 mL) and the organic layer was extracted with 5% aqueous HCl (3 × 10 mL). The resulting aqueous acid layer was made basic (5% aqueous NH_4OH to achieve pH ≈ 9) and extracted with CH_2Cl_2 (3 × 10 mL). The organic layers were washed with brine (2 × 10 mL) and H_2O (2 × 10 mL), dried over with anhydrous Na_2SO_4 and concentrated to dryness to obtain the β-(3-chloro-4-methoxyphenyl)ethylamine (**1**) (630 mg, 72%) as a yellow oil. ^{1}H NMR (500 MHz, $CDCl_3$): δ = 7.33 (d, J = 2.2 Hz, 1H, H-2), 7.21 (dd, J = 8.5, 2.2 Hz, 1H, H-6), 6.88 (d, J = 8.5 Hz, 1H, H-5),

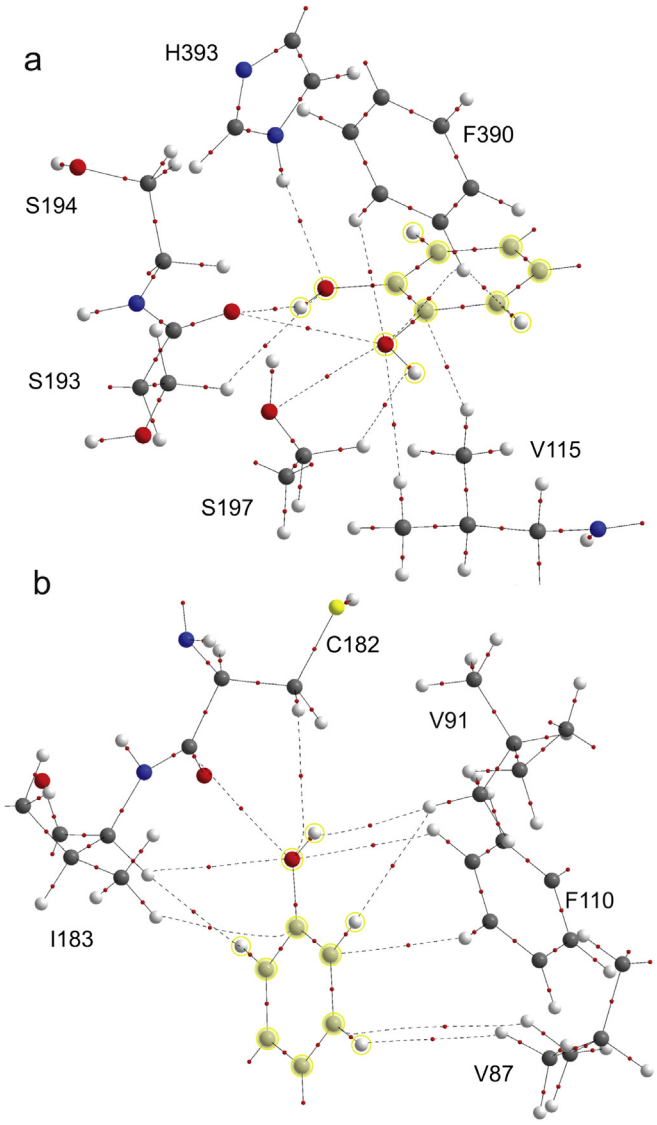

Fig. 11. Molecular graph of compound **9c** interaction with the binding site. The interactions for the catecholic hydroxyls are shown in (a) and the interactions of OH-11 are shown in (b).

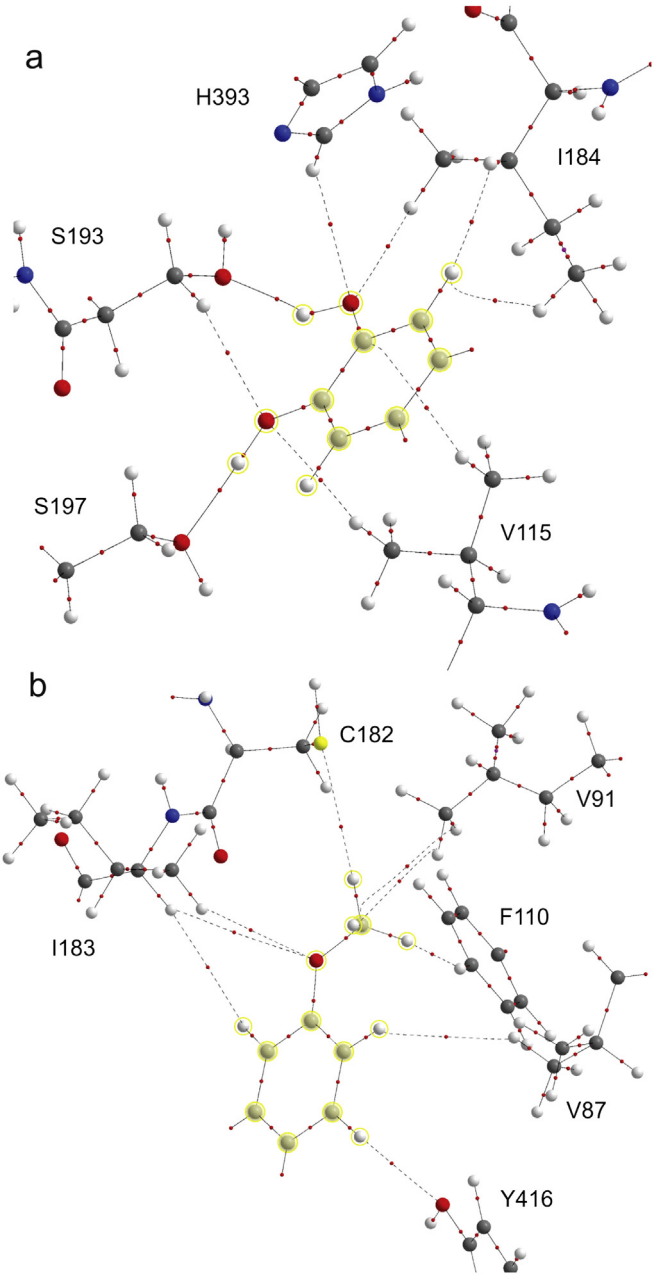

Fig. 12. Molecular graph for compound **6b** interaction at the binding site. The interactions for the catecholic hydroxyls are shown in (a) and the interactions of OMe-11 are shown in (b).

3.89 (s, 3H, OCH_3-4), 2.96 (m, 2H, H-β), 2.67 (m, 2H, H-α); ^{13}C NMR (125 MHz, $CDCl_3$): δ = 153.8 (C-4), 133.3 (C-1), 130.8 (CH-2), 128.4 (CH-6), 122.6 (C-3), 112.5 (CH-5), 56.5 (OCH_3-4), 43.8 (CH_2-β), 39.1 (CH_2-α); MS (EI) *m/z* (%): 185 (45) $[M]^+$.

*4.2.1.5. β-(3,4-Dibenzyloxy-phenyl)ethylamine (**4**).* 3,4-dibenzyloxy-β-nitrostyrene (1.70 g, 4.7 mmol) was subjected to similar conditions to those above described to obtain the β-(3,4-dibenzyloxyphenyl)ethylamine (**4**) (1.44 g, 93%) as a yellow oil. ^1H NMR (500 MHz, $CDCl_3$): δ = 7.47 (m, 4H, H-2′, H-6′ y H-2″, H-6″), 7.38 (m, 6H, H-3′, H-5′ y H-3″, H-5″), 6.83–6.76 (m, 3H, H-2, H-5, H-6), 5.16 (s, 2H, $PhCH_2O$-3), 5.15 (s, 2H, $PhCH_2O$-4), 2.98 (m, 2H, CH_2-β), 2.83 (m, 2H, CH_2-α); ^{13}C NMR (125 MHz, $CDCl_3$): δ = 149.7 (C-3), 147.0 (C-4), 136.7 (C-1′), 136.6 (C-1″), 130.8 (C-1), 128.9–127.1 (6C, C-2′, C-4′ y C-2″,C-4″), 122.1 (CH-6), 112.8 (CH-2), 112.3 (CH-5), 121.9 (CH-6), 116.0 (CH-2), 112.8 (CH-4), 71.3 ($PhCH_2O$-4), 71.2 ($PhCH_2O$-3), 41.9 (CH_2-β), 39.3 (CH_2-α); ESMS *m/z* (%): 333 (100) $[M + H]^+$.

*4.2.2. General procedure for the synthesis of acetamides (**2**, **5** and **8**) under Schotten–Baumann conditions*

Formation of acetamides was carried out under Schotten–Baumann conditions using the appropriate phenylethylamine and the corresponding acid chloride.

*4.2.2.1. N-(3-chloro-4-methoxyphenylethyl)-β-(3′-methoxyphenyl) acetamide (**2**).* An amount of 0.3 mL of 2-(3-methoxyphenyl)acetyl chloride (2.55 mmol) was added dropwise at 0 °C to a solution of β-(3-chloro-4-methoxyphenyl)ethylamine (**1**) (500 mg, 2.69 mmol) in CH_2Cl_2 (20 mL) and 5% aqueous NaOH (4.4 mL) with stirring at room temperature for 3 h. After the mixture was stirred, 2.5% aqueous HCl was added and the organic solution was washed with brine (2 × 10 mL) and H_2O (2 × 10 mL), dried over with anhydrous

Na_2SO_4 and evaporated to dryness. The residue obtained was purified by sílica gel column chromatography (Hexane/CH_2Cl_2/EtOAc, 20:70:10) to afford the acetamide (**2**) (378 mg, 45%) as a white oil. ^{1}H NMR (500 MHz, $CDCl_3$): δ = 7.15 (t, J = 9.5 Hz, 1H, H-5′), 6.98 (d, J = 2.1 Hz, 1H, H-2), 6.74 (dd, J = 8.4, 2.1 Hz, 1H, H-6), 6.70 (dd, J = 9.5, 3.3 Hz, 1H, H-4′), 6.68 (m, 1H, H-5), 6.65 (m, 1H, H-6′), 6.62 (t, J = 3.3 Hz, 1H, H-2′), 5.50 (m, 1H, NH), 3.77 (s, 3H, OCH_3-4), 3.68 (s, 3H, OCH_3-3′), 3.33 (s, 2H, CH_2—CO), 3.31 (dd, J = 12.9, 6.8 Hz, 2H, H-α), 2.55 (t, J = 6.8 Hz, 2H, H-β); ^{13}C NMR (125 MHz, $CDCl_3$): δ = 170.7 (CO), 159.9 (C-3′), 153.5 (C-4), 136.1 (C-1′), 131.7 (C-1), 130.4 (CH-2), 130.0 (CH-5′), 127.9 (CH-6), 122.2 (C-3), 121.6 (CH-6′), 114.9 (CH-2′), 112.8 (CH-4′), 112.1 (CH-5), 56.1 (OCH_3-4), 55.1 (OCH_3-3′), 43.8 (CH_2—CO), 40.6 (CH_2-α), 34.3 (CH_2-β); MS (FAB) *m/z* (%): 356 $[M + Na]^+$, 186 (85), 169 (100).

*4.2.2.2. N-(3,4-Dibenzyloxyphenylethyl)-β-(3′-methoxyphenyl) acetamide (**5**).* β-(3,4-dibenzyloxyphenyl)ethylamine (500 mg, 1.5 mmol) was subjected to similar conditions to those above described to obtain the *N*-(3,4-dibenzyloxyphenylethyl)-β-(3′-methoxyphenyl)acetamide (**5**). The residue was purified by silica gel column chromatography (Hexane/CH_2Cl_2/EtOAc, 20:70:10), to obtain the acetamide **5** (450 mg, 63%) as a white oil. ^{1}H NMR (500 MHz, $CDCl_3$): δ = 7.45–7.30 (m, 10H, Ph-3 y Ph-4), 7.20 (t, J = 8.0 Hz, 1H, H-5′), 6.80 (m, 1H, H-5), 6.80 (m, 1H, H-6′), 6.78 (m, 1H, H-2′), 6.72 (m, 1H, H-2), 6.72 (m, 1H, H-4′), 6.52 (dd, J = 8.1, 1.9 Hz, 1H, H-6), 5.43 (m, 1H, NH), 5.13 (s, 2H, $PhCH_2O$-4), 5.10 (s, 2H, $PhCH_2O$-3), 3.75 (s, 3H, OCH_3-3′), 3.47 (s, 2H, $NHCOCH_2$), 3.39 (q, J = 6.7 Hz, 2H, H-α), 2.63 (t, J = 6.7 Hz, 2H, H-β); ^{13}C NMR (125 MHz, $CDCl_3$): δ = 170.6 (CO), 159.9 (C-3′), 149.0 (C-3), 147.6 (C-4), 137.4 (C-1‴), 137.2 (C-1″), 136.2 (C-1′), 132.0 (C-1), 129.9 (CH-5′), 128.5–127.3 (10CH, Ph-3 y Ph-4), 121.6 (CH-6), 121.5 (CH-2′), 114.9 (CH-2), 114.9 (CH-4′), 112.8 (CH-5), 112.8 (CH-6′), 71.4 ($PhCH_2O$-4), 71.3 ($PhCH_2O$-3), 55.1 (OCH_3-3′), 43.8 ($NHCOCH_2$), 40.6 (CH_2-α), 34.8 (CH_2-β); MS (FAB) *m/z* (%): 504 $[M + Na]^+$, 413 (55), 322 (100).

*4.2.2.3. N-(3,4-Dimethoxyphenylethyl)-β-(3′-methoxyphenyl)acetamide (**8**).* 3,4-dimethoxy-phenylethylamine (500 mg, 2.79 mmol) was subjected to similar conditions to those above described to obtain the *N*-(3,4-dimethoxyphenylethyl)-β-(3′-methoxyphenyl) acetamide (**8**). The residue was purified by silica gel column chromatography (Hexane/CH_2Cl_2/EtOAc, 20:70:10), to obtain the acetamide **8** (2 g, 91%) as a white oil. ^{1}H NMR (500 MHz, $CDCl_3$): δ = 7.21 (dd, J = 8.3, 7.9 Hz, 1H, H-5′), 6.80 (dd, J = 8.3, 1.9 Hz, 1H, H-4′), 6.73 (d, J = 7.9 Hz, 1H, H-6′), 6.72 (m, 1H, H-2′), 6.70 (d, J = 8.1 Hz, 1H, H-2), 6.60 (d, J = 1.9 Hz, 1H, H-5), 6.53 (dd, J = 8.1, 1.9 Hz, 1H, H-6), 5.44 (m, 1H, NH), 3.85 (s, 3H, OCH_3-4), 3.81 (s, 3H, OCH_3-3), 3.76 (s, 3H, OCH_3-3′), 3.49 (s, 2H, $NHCOCH_2$), 3.43 (dd, J = 12.8, 6.8 Hz, 2H, H-α), 2.67 (t, J = 6.8 Hz, 2H, H-β); ^{13}C NMR (125 MHz, $CDCl_3$): δ = 170.7 (CO), 159.9 (C-3′), 148.9 (C-3), 147.6 (C-4), 136.2 (C-1′), 131.1 (C-1), 129.9 (CH-5′), 121.6 (CH-6′), 120.5 (CH-6), 114.9 (CH-2), 112.8 (CH-2′), 111.7 (C-4′), 111.2 (CH-5), 55.8 (OCH_3-4), 55.7 (OCH_3-3), 55.1 (OCH_3-3′), 43.9 ($COCH_2$), 40.7 (CH_2-α), 34.9 (CH_2-β); MS (FAB) *m/z* (%): 330 $[M + H]^+$, 182 (45), 165 (100).

*4.2.3. Synthesis of 1,2,3,4-tetrahydroisoquinoleines (**3**, **6** and **9**) by Bischler–Napieralski cyclisation*

*4.2.3.1. 6-Chloro-7-methoxy-1-(3′-methoxybenzyl)-1,2,3,4-THIQ (**3**).* The acetamide **2** (300 mg, 0.93 mmol) was added in dry toluene (10 mL) to a 100 mL three-neck round-bottom flask at 0 °C under N_2 and treated with P_2O_5 (4.2 g, 15.02 mmol), which was added in portions and followed by the dropwise addition of $POCl_3$ (1.37 mL, 15.02 mmol). The mixture was stirred and refluxed under N_2 for 6 h, and then cooled to room temperature. Toluene was concentrated under reduced pressure and the reaction mixture was slowly poured into a mixture of crushed ice. The solid residue was triturated with 20% aqueous NaOH to obtain a suspension (pH ≈ 8–9) and then extracted with CH_2Cl_2 (3 × 15 mL). The combined CH_2Cl_2 extracts were dried over Na_2SO_4 and the solvent was evaporated *in vacuo* obtaining a reddish oil. The residue was dissolved in MeOH (10 mL), cooled to −78 °C and then treated with $NaBH_4$ (76 mg, 2 mmol). The reaction mixture was stirred for 2 h. Thereafter, H_2O (15 mL) was added and volatiles were evaporated under reduced pressure. The aqueous phase was extracted with CH_2Cl_2 (3 × 15 mL), and the combined organic layers were dried over with anhydrous Na_2SO_4 and evaporated to dryness. The crude product was purified by silica gel column chromatography (CH_2Cl_2/MeOH, 95:5) to furnish 6-chloro-7-methoxy-1-(3′-methoxybenzyl)-1,2,3,4-THIQ (**3**) (155 mg, 54%) as a yellow oil. Then, the **3** hydrochloride salt was prepared for use in the next reaction. ^{1}H NMR (500 MHz, $CDCl_3$) for the free base form: δ = 7.25 (t, J = 7.5 Hz, 1H, H-5′), 7.10 (s, 1H, H-5), 6.83 (d, J = 7.5 Hz, 1H, H-6′), 6.80 (m, 1H, H-4′), 6.79 (m, 1H, H-2′), 6.64 (s, 1H, H-8), 4.18 (dd, J = 9.2, 4.7 Hz, 1H, H-1), 3.80 (s, 3H, OCH_3-7), 3.77 (s, 3H, OCH_3-3′), 3.17–2.92 (m, 4H, H-3 y CH_2-α), 2.71 (m, 2H, H-4); ^{13}C NMR (125 MHz, $CDCl_3$): δ = 159.8 (C-3′), 152.7 (C-7), 140.2 (C-1′), 137.8 (C-8a), 130.5 (CH-5), 129.6 (CH-5′), 128.2 (C-4a), 121.7 (CH-6′), 120.3 (C-6), 115.1 (CH-2′), 111.9 (CH-4′), 110.1 (CH-8), 56.9 (CH-1), 56.1 (OCH_3-7), 55.1 (OCH_3-3′), 42.6 (CH_2-α), 40.2 (CH_2-3), 28.7 (CH_2-4); MS (FAB) *m/z* (%): 318 $[M + H]^+$, 196 (100).

*4.2.4. General procedure for the synthesis of 1,2,3,4-tetrahydroisoquinoleines (**6** and **9**) by Bischler–Napieralski cyclisation*

*4.2.4.1. 6,7-Dibenzyloxy-1-(3′-methoxybenzyl)-1,2,3,4-THIQ (**6**).* The corresponding acetamide **5** (300 mg, 0.645 mmol) was added in dry acetonitrile (20 mL) to a 100 mL three-neck round-bottom flask at 0 °C under N_2, and treated with $POCl_3$ (0.45 mL, 4.5 mmol). The mixture was stirred and refluxed under N_2 for 5 h and then cooled to room temperature. Acetonitrile was concentrated under reduced pressure and the reaction mixture was slowly poured into a mixture of crushed ice. The solid residue was triturated with 10% aqueous NaOH to obtain a suspension (pH ≈ 8–9) which was then extracted with CH_2Cl_2 (3 × 15 mL). The combined CH_2Cl_2 extracts were dried over Na_2SO_4 and the solvent was evaporated *in vacuo* obtaining a reddish oil. The residue was dissolved in MeOH (10 mL), cooled to −78 °C and then treated with $NaBH_4$ (76 mg, 2 mmol). The reaction mixture was stirred for 2 h. Next, H_2O (15 mL) was added and volatiles were evaporated under reduced pressure. The aqueous phase was extracted with CH_2Cl_2 (3 × 15 mL), and the combined organic layers were dried over Na_2SO_4 and evaporated to dryness. The crude product was purified by silica gel column chromatography (CH_2Cl_2/MeOH, 95:5) to furnish THIQ (**6**) (180 mg, 63%) as a yellow oil. Then, the **6** hydrochloride salt was prepared for use in the next reaction. ^{1}H NMR (500 MHz, $CDCl_3$) for the free base form: δ = 7.45–7.30 (m, 10H, Ph-4 y Ph-3), 7.26 (m, 1H, H-5′), 6.81 (m, 1H, H-6′), 6.83 (m, 2H, H-2′, H-4′), 6.77 (s, 1H, H-5), 6.71 (s, 1H, H-8), 5.15 (s, 2H, $PhCH_2O$-4), 5.11 (s, 2H, $PhCH_2O$-3), 4.11 (dd, J = 9.5, 4.2 Hz, 1H, H-1), 3.81 (s, 3H, OCH_3-3′), 3.18 (m, 1H, H-3α), 3.10 (dd, J = 13.6, 4.2 Hz, 1H, H-α′), 2.91 (m, 1H, H-3β), 2.85 (dd, J = 13.6, 9.5 Hz, 1H, H-α″), 2.73 (m, 1H, H-4α), 2.69 (m, 1H, H-4β); ^{13}C NMR (125 MHz, $CDCl_3$): δ = 159.7 (C-3′), 147.6 (C-7), 146.8 (C-6), 140.6 (C-1′), 137.5 (C-1″), 137.4 (C-1‴), 131.4 (C-8a), 129.6 (CH-5′), 128.4–127.3 (10CH, Ph-6 y Ph-7), 127.9 (C-4a), 121.7 (CH-6′), 115.5 (CH-4′), 115.0 (CH-5), 113.9 (CH-2′), 111.8 (CH-8), 71.8 ($PhCH_2O$-7), 71.3 ($PhCH_2O$-6), 56.7 (CH-1), 55.1 (OCH_3-3′), 42.6 (CH_2-α), 40.7 (CH_2-3), 34.8 (CH_2-4); MS (FAB) *m/z* (%): 466 $[M + H]^+$, 344 (100).

*4.2.4.2. 6,7-Dimethoxy-1-(3′-methoxybenzyl)-1,2,3,4-THIQ (**9**).* *N*-(3,4-dimethoxy-phenyl-ethyl)-β-(3′-methoxyphenyl)acetamide

(300 mg, 0.91 mmol) was subjected to similar conditions to those above described to obtain the 6,7-dimethoxy-1-(3′-methoxybenzyl)-1,2,3,4-THIQ (**9**). The residue was purified by silica gel column chromatography (CH_2Cl_2/MeOH, 95:5), to afford the THIQ (**9**) (264 mg, 93%), as a yellow oil. Then, the **9** hydrochloride salt was prepared for use in the next reaction. ^{1}H NMR (500 MHz, $CDCl_3$) for the free base form: δ = 7.23 (dd, J = 7.6 Hz, 1H, H-5′), 6.83 (d, J = 7.6 Hz 1H, H-6′), 6.79 (m, 1H, H-2′), 6.77 (m, 1H, H-4′), 6.58 (s, 1H, H-5), 6.53 (s, 1H, H-8), 4.22 (dd, J = 8.5, 5.2 Hz, 1H, H-1), 3.84 (s, 3H, OCH_3-6), 3.77 (s, 3H, OCH_3-3′), 3.76 (s, 3H, OCH_3-7), 3.18 (dt, J = 12.0, 5.9 Hz 1H, H-3α), 3.16 (dd, J = 12.7, 5.2 Hz, 1H, H-α′), 2.99 (dd, J = 12.7, 8.5 Hz 1H, H-3β), 2.96 (m, 1H, H-α″), 2.78 (m, 2H, H-4); ^{13}C NMR (125 MHz, $CDCl_3$): δ = 159.7 (C-3′), 147.6 (C-6), 147.0 (C-7), 140.1 (C-1′), 129.6 (CH-5′), 129.2 (C-8a), 126.6 (C-4a), 121.7 (CH-6′), 115.1 (CH-2′), 111.9 (CH-5), 111.7 (CH-4′), 109.5 (CH-8), 56.5 (CH-1), 55.8 (OCH_3-3′), 55.8 (OCH_3-7), 55.1 (OCH_3-6), 42.5 (CH_2-α), 40.3 (CH_2-3), 28.7 (CH_2-4); MS (FAB) m/z (%): 314 $[M + H]^+$, 192 (100).

4.2.5. General procedure for the synthesis of tetrahydroprotoberberines (*3a*, *6a*, *9a* and *9b*) by Mannich cyclisation

*4.2.5.1. 2,11-Dimethoxy-3-chlorotetrahydroprotoberberine (**3a**).* The corresponding THIQ **3** (100 mg, 0.313 mmol) hydrochloride was added to a MeOH/HCl 37% (20:1) (pH 1–4) solution placed in a 100 mL round-bottom flask and then evaporated to dryness. The compound was then dissolved in absolute ethanol (2 mL), H_2O (3 mL) and 37% aqueous formaldehyde (3 mL) and stirred and refluxed for 5 h. Thereafter, the reaction mixture was concentrated to dryness. The residue was basified with a 5% aqueous NaOH and the aqueous layer was extracted with CH_2Cl_2 (3 × 15 mL). The combined organic layers were dried over with anhydrous Na_2SO_4 and concentrated to dryness. The crude product was purified by silica gel column chromatography (Hexane/CH_2Cl_2/EtOAc, 20:70:10) to obtain THPB (**3a**) (85.4 mg, 0.26 mmol, 86%). ^{1}H NMR (500 MHz, $CDCl_3$): δ = 7.14 (s, 1H, H-4), 7.00 (d, J = 8.4 Hz, 1H, H-9), 6.75 (s, 1H, H-1), 6.73 (dd, J = 8.4, 2.5 Hz, 1H, H-10), 6.70 (d, J = 2.5 Hz, 1H, H-12), 3.98 (d, J = 14.5 Hz, 1H, H-8α), 3.91 (s, 3H, OCH_3-2), 3.79 (s, 3H, OCH_3-11), 3.70 (d, J = 14.5 Hz, 1H, H-8β), 3.64 (dd, J = 11.4, 3.6 Hz, 1H, H-14), 3.29 (dd, J = 16.2, 3.6 Hz, 1H, H-13α), 3.15 (m, 1H, H-6α), 3.10 (m, 1H, H-5α), 2.93 (dd, J = 16.2, 11.4 Hz, 1H, H-13β), 2.67 (m, 1H, H-5β), 2.60 (m, 1H, H-6β); ^{13}C NMR (125 MHz, $CDCl_3$): δ = 158.1 (C-11), 153.2 (C-2), 137.2 (C-14a), 135.1 (C-12a), 130.1 (CH-4), 127.7 (C-4a), 127.1 (CH-9), 126.3 (C-8a), 120.5 (C-3), 113.2 (CH-12), 112.4 (CH-10), 109.2 (CH-1), 59.5 (CH-14), 57.8 (CH_2-8), 56.3 (OCH_3-2), 55.2 (OCH_3-11), 50.9 (CH_2-6), 36.7 (CH_2-13), 28.3 (CH_2-5); MS (FAB) m/z (%): 330 $[M + H]^+$, 196 (100); HRMS-FAB $[M + H]^+$ calcd for $C_{19}H_{21}NO_2Cl$: 330.1255, found: 330.1262.

*4.2.5.2. 2,3-Dibenzyloxy-11-methoxytetrahydroprotoberberine (**6a**).* 6,7-dibenzyloxy-1-(3′-methoxybenzyl)-1,2,3,4-THIQ (**6**) (100 mg, 0.215 mmol) hydrochloride was subjected to similar conditions to those above described to obtain the 2,3-dibenzyloxy-11-methoxy-THPB (**6a**). The residue was purified by silica gel column chromatography (CH_2Cl_2/MeOH, 99:1), to obtain THPB **6a** (93 mg, 93%) as a yellow oil. ^{1}H NMR (500 MHz, $CDCl_3$): δ = 7.45–7.30 (m, 10H, Ph-2 y Ph-3), 6.99 (d, J = 8.4 Hz, 1H, H-9), 6.83 (s, 1H, H-1), 6.75 (m, 1H, H-10), 6.72 (s, 1H, H-4), 6.68 (m, 1H, H-12), 5.16 (s, 2H, $PhCH_2O$-2), 5.12 (s, 2H, $PhCH_2O$-3), 3.95 (d, J = 14.4 Hz, 1H, H-8α), 3.79 (s, 3H, OCH_3-11), 3.63 (d, J = 14.4 Hz, 1H, H-8β), 3.53 (dd, J = 11.2, 3.5 Hz, 1H, H-14), 3.17 (dd, J = 16.3, 3.5 Hz, 1H, H-13α), 3.13 (m, 1H, H-6α), 3.10 (m, 1H, H-5α), 2.82 (dd, J = 16.3, 11.2 Hz, 1H, H-13β), 2.60 (m, 1H, H-5β), 2.58 (m, 1H, H-6β); ^{13}C NMR (125 MHz, $CDCl_3$): δ = 157.9 (C-11), 147.7 (C-2), 147.2 (C-3), 137.4 (C-1‴), 137.2 (C-1″), 135.5 (C-12a), 130.6 (C-14a), 128.4–127.3 (8 × CH-Ph, CH-9), 127.0 (C-4a), 126.7 (C-8a), 114.9 (CH-4), 113.4 (CH-10), 113.2 (CH-1), 112.1 (CH-12), 72.2 ($PhCH_2O$-3), 71.1 ($PhCH_2O$-2), 59.4 (CH-14), 58.1 (CH_2-8), 55.2 (OCH_3-11), 51.4 (CH_2-6), 36.9 (CH_2-13), 28.9 (CH_2-5); MS (FAB) m/z (%): 478 $[M + H]^+$, 344 (100). HRMS-FAB $[M + H]^+$ calcd for $C_{32}H_{32}NO_3$: 478.2377, found: 478.2389.

*4.2.5.3. 2,3,11-Trimethoxytetrahydroprotoberberine (**9a**) and 2,3,9-trimethoxy-tetrahydroprotoberberine (**9b**) by Mannich cyclisation.* 6,7-dimethoxy-1-(3′-methoxybenzyl)-1,2,3,4-THIQ (**9**) (100 mg, 0.32 mmol) hydrochloride was subjected to similar conditions to those above described to obtain the 2,3,11-trimethoxy-THPB (**9a**) and 2,3,9-trimethoxy-THPB (**9b**). In this case, both compounds were obtained as a consequence the two possible cyclization positions: in *para* position to the methoxyl group (THPB **9a**, major product) or in *ortho* position (THPB **9b**, minor product).

*4.2.5.4. 2,3,11-Trimethoxytetrahydroprotoberberine (**9a**).* was purified by silica gel column chromatography (Hexane/EtOAc, 50:50, to obtain **9a** as a white oil (76 mg, 77%). ^{1}H NMR (500 MHz, $CDCl_3$): δ = 7.00 (d, J = 8.3 Hz, 1H, H-9), 6.74 (s, 1H, H-1), 6.72 (m, 1H, H-10), 6.70 (m, 1H, H-12), 6.62 (s, 1H, H-4), 3.97 (d, J = 14.5 Hz, 1H, H-8α), 3.89 (s, 3H, OCH_3-2), 3.86 (s, 3H, OCH_3-3), 3.78 (s, 3H, OCH_3-11), 3.66 (d, J = 14.5 Hz, 1H, H-8β), 3.58 (dd, J = 11.3, 3.5 Hz, 1H, H-14), 3.29 (dd, J = 16.2, 3.4 Hz, 1H, H-13α), 3.15 (m, 1H, H-6α), 3.15 (m, 1H, H-5α), 2.88 (dd, J = 16.2, 11.3 Hz, 1H, H-13β), 2.65 (m, 1H, H-5β), 2.60 (m, 1H, H-6β); ^{13}C NMR (125 MHz, $CDCl_3$): δ = 157.9 (C-11), 147.4 (C-2), 147.4 (C-3), 135.5 (C-12a), 129.6 (C-14a), 127.1 (CH-9), 126.7 (C-4a), 126.6 (C-8a), 113.2 (CH-12), 112.3 (CH-10), 111.3 (CH-4), 108.6 (CH-1), 59.5 (CH-14), 58.1 (CH_2-8), 56.0 (OCH_3-2), 55.8 (OCH_3-3), 55.2 (OCH_3-11), 51.4 (CH_2-6), 37.1 (CH_2-13), 29.0 (CH_2-5); MS (FAB) m/z (%): 326 $[M + H]^+$, 192 (100). HRMS-FAB $[M + H]^+$ calcd for $C_{20}H_{24}NO_3$: 326.1751, found: 326.1750.

*4.2.5.5. 2,3,9-Trimethoxytetrahydroprotoberberine (**9b**).* was purified by silica gel column chromatography (Hexane/EtOAc, 50:50), to obtain **9b** as a yellow oil (8 mg, 0.0246 mmol, 8%). ^{1}H NMR (500 MHz, $CDCl_3$): δ = 7.15 (t, J = 7.9 Hz, 1H, H-11), 6.79 (d, J = 7.9 Hz, 1H, H-12), 6.75 (s, 1H, H-1), 6.70 (d, J = 7.9 Hz, 1H, H-10), 6.62 (s, 1H, H-4), 4.20 (d, J = 15.8 Hz, 1H, H-8α), 3.89 (s, 3H, OCH_3-2), 3.87 (s, 3H, OCH_3-3), 3.83 (s, 3H, OCH_3-9), 3.60 (dd, J = 11.1, 3.1 Hz, 1H, H-14), 3.46 (d, J = 15.8 Hz, 1H, H-8β), 3.30 (dd, J = 16.1, 3.1 Hz, 1H, H-13α), 3.20 (m, 1H, H-6α), 3.15 (m, 1H, H-5α), 2.90 (dd, J = 16.1, 11.1 Hz, 1H, H-13β), 2.65 (m, 1H, H-5β), 2.65 (m, 1H, H-6β); ^{13}C NMR (125 MHz, $CDCl_3$): δ = 155.8 (C-9), 147.4 (C-2), 147.4 (C-3), 135.8 (C-12a), 129.7 (C-14a), 126.8 (C-4a), 126.7 (CH-11), 123.4 (C-8a), 120.8 (CH-12), 111.4 (CH-4), 108.6 (CH-1), 107.1 (CH-10), 58.9 (CH-14), 56.0 (OCH_3-2), 55.8 (OCH_3-3), 55.2 (OCH_3-9), 53.7 (CH_2-8), 51.4 (CH_2-6), 36.9 (CH_2-13), 29.1 (CH_2-5); MS (FAB) m/z (%): 326 $[M + H]^+$, 192 (100); HRMS-FAB $[M + H]^+$ calcd for $C_{20}H_{24}NO_3$: 326.1751, found: 326.1754.

4.2.6. General procedure for the synthesis of THP *3b*, *9c* and *9d* by O-demethylation

*4.2.6.1. 2,11-Dihydroxy-3-chloro-tetrahydroprotoberberine (**3b**).* A solution of the appropriate THPB (**3a**) (50 mg, 0.15 mmol) in dry CH_2Cl_2 (5 mL) was cooled to −78 °C. Then, BBr_3 (0.4 mL, 1.02 mmol) was dropwise added to the stirring solution. After 15 min, the reaction mixture was left to warm up to room temperature and stirred for 2 h. The reaction was terminated by the dropwise addition of MeOH (1 mL) and the mixture was further stirred for another 30 min. The solvent was concentrated to dryness. The crude product was purified by silica gel column chromatography (CH_2Cl_2:MeOH, 90:10), to obtain THPB (**3b**) (37 mg, 75%) as a yellow oil. ^{1}H NMR (500 MHz, C_5D_5N) δ = 7.22 (s, 1H, H-1), 7.18 (s, 1H, H-4), 7.05 (m, 1H, H-10), 7.03 (m, 1H, H-9), 6.96 (m, 1H, H-12), 3.99 (d, J = 14.3 Hz, 1H, H-8α), 3.61 (m, 1H, H-8β), 3.56 (m, 1H, H-14), 3.26

(dd, J = 16.1, 3.5 Hz, 1H, H-13α), 3.12 (m, 1H, H-5α), 3.06 (m, 1H, H-6α), 2.98 (dd, J = 16.1, 11.6 Hz, 1H, H-13β), 2.60 (m, 1H, H-5β), 2.52 (m, 1H, H-6β); ^{13}C NMR (125 MHz, C_5D_5N): δ = 157.1 (C-11), 152.6 (C-2), 138.1 (CH-14a), 135.9 (C-12a 8a), 130.0 (CH-4), 127.3 (CH-9), 126.7 (C-4a), 125.1 (C-12a), 119.6 (C-3), 115.7 (CH-12), 114.8 (CH-1), 114.4 (CH-10), 59.5 (CH-14), 57.9 (CH_2-8), 51.4 (CH_2-6), 36.9 (CH_2-13), 28.3 (CH_2-5); MS (FAB) *m/z* (%): 302 [M + H]$^+$, 182 (100); HRMS-FAB [M + H]$^+$ calcd for $C_{17}H_{17}NO_2Cl$: 302.0942, found: 302.0946.

*4.2.6.2. 2,3,11-Trihydroxy-tetrahydroprotoberberine (**9c**).* 2,3,11-trimethoxy-THPB (**9a**) (50 mg, 0.15 mmol) was subjected to similar conditions to those above described to obtain the 2,3,11-trihydroxy-THPB (**9c**). The same equivalents of BBr_3 were employed despite the presence of increased methoxyl group numbers. The residue was purified by silica gel column chromatography (CH_2Cl_2/MeOH, 90:10), to obtain the THPB **9c** (43 mg, 99%) as a white oil. ^{1}H NMR (500 MHz, C_5D_5N): δ = 7.15 (s, 1H, H-1), 7.01 (m, 1H, H-9), 7.00 (s, 3H, OH), 6.99 (m, 1H, H-12), 6.96 (s, 1H, H-4), 6.92 (m, 1H, H-10), 4.26 (d, J = 14.5 Hz, 1H, H-8α), 3.99 (d, J = 10.8 Hz, 1H, H-14), 3.91 (d, J = 14.5 Hz, 1H, H-8β), 3.37 (m, 1H, H-13α), 3.33 (m, 1H, H-5α), 3.32 (m, 1H, H-6α), 3.14 (m, 1H, H-13β), 2.89 (m, 1H, H-6β), 2.71 (m, 1H, H-5β); ^{13}C NMR (125 MHz, C_5D_5N): δ = 157.6 (C-11), 146.2 (C-2), 145.9 (C-3), 135.1 (C-12a), 127.5 (C-14a), 127.5 (CH-9), 124.5 (C-8a), 122.9 (C-4a), 116.1 (CH-4), 115.7 (CH-10), 114.7 (CH-12), 113.5 (CH-1), 59.7 (CH-14), 57.2 (CH-8), 51.4 (CH_2-6), 36.1 (CH_2-13), 27.8 (CH_2-5); MS (FAB) *m/z* (%): 284 [M + H]$^+$, 164 (100); HRMS-FAB [M + H]$^+$ calcd for $C_{17}H_{18}NO_3$: 284.1281, found: 284.1284.

*4.2.6.3. 2,3,9-Trihydroxytetrahydroprotoberberine (**9d**).* 2,3,9-trimethoxy-THPB (**9b**) (50 mg, 0.15 mmol) was subjected to similar conditions to those above described to obtain the 2,3,9-trihydroxy-THPB (**9d**). The residue was purified by silica gel column chromatography (CH_2Cl_2/MeOH, 90:10), to obtain the THPB **9d** (42 mg, 97%) as a grey oil. ^{1}H NMR (500 MHz, C_5D_5N): δ = 7.21 (s, 1H, H-1), 7.11 (t, J = 7.8 Hz, 1H, H-11), 6.97 (s, 1H, H-4), 6.94 (d, J = 7.8 Hz, 1H, H-10), 6.71 (d, J = 7.8 Hz, 1H, H-12), 6.00 (s, 3H, OH), 4.71 (d, J = 15.7 Hz, 1H, H-8α), 3.97 (dd, J = 11.3, 3.4 Hz, 1H, H-14), 3.92 (d, J = 15.7 Hz, 1H, H-8β), 3.42 (dd, J = 16.4, 3.4 Hz, 1H, H-13α), 3.38 (m, 1H, H-5α), 3.36 (m, 1H, H-6α), 3.28 (dd, J = 16.4, 11.3 Hz, 1H, H-13β), 2.87 (m, 1H, H-6β), 2.68 (m, 1H, H-5β); ^{13}C NMR (125 MHz, C_5D_5N): δ = 154.9 (C-9), 146.1 (C-2), 145.9 (C-3), 135.9 (C-12a), 127.5 (CH-11), 124.9 (C-14a), 123.7 (C-8a), 122.9 (C-4a), 119.6 (CH-12), 116.1 (CH-4), 113.6 (CH-1), 112.6 (CH-10), 59.6 (CH-14), 54.0 (CH-8), 51.8 (CH_2-6), 36.4 (CH_2-13), 28.2 (CH_2-5); MS (FAB) *m/z* (%): 284 [M + H]$^+$, 164 (100); HRMS-FAB [M + H]$^+$ calcd for $C_{17}H_{18}NO_3$: 284.1281, found: 284.1282.

*4.2.6.4. Synthesis of THP **6b** by O-debenzylation.* A solution of 2,3-dibenzyloxy-11-methoxy-THPB (**6a**) (200 mg, 0.419 mmol) was refluxed for 3 h in absolute EtOH (25 mL) and concentrated HCl (25 mL). The reaction mixture was evaporated to dryness, redissolved in CH_2Cl_2 (10 mL) and made basic (15% aqueous NH_4OH). The organic solution was washed with brine (2 × 5 mL) and H_2O (2 × 5 mL), dried with anhydrous Na_2SO_4, and evaporated to dryness. The crude product was purified by silica gel column chromatography (CH_2Cl_2/MeOH 95:5) to obtain the 2,3-dihydroxy-11-methoxy-THPB (**6b**) (67 mg, 33%) as a yellow oil. ^{1}H NMR (500 MHz, $CDCl_3$): δ = 6.95 (d, J = 8.5 Hz, 1H, H-9), 6.70 (dd, J = 8.5, 2.4 Hz, 1H, H-10), 6.61 (d, J = 2.4 Hz, 1H, H-12), 6.51 (s, 1H, H-1), 6.20 (s, 3H, H-4, 2 × OH), 3.93 (d, J = 14.8 Hz, 1H, H-8α), 3.73 (s, 3H, OCH_3-11), 3.67 (d, J = 14.8 Hz, 1H, H-8β), 3.53 (dd, J = 11.2, 3.4 Hz, 1H, H-14), 3.08 (dd, J = 16.7, 3.4 Hz, 1H, H-13α), 3.03 (m, 1H, H-6α), 2.90 (m, 1H, H-5α), 2.76 (dd, J = 16.7, 11.2 Hz, 1H, H-13β), 2.57 (m, 1H, H-6β), 2.40 (m, 1H, H-5β); ^{13}C NMR (125 MHz, $CDCl_3$): δ = 158.3 (C-11), 143.6 (C-3), 143.5 (C-2), 134.9 (C-12a), 127.9 (C-14a), 127.1 (CH-9), 125.1 (C-4a), 124.9 (C-8a), 114.9 (CH-4), 113.5 (CH-12), 112.5 (CH-10), 111.9 (CH-1), 59.0 (CH-14), 57.4 (CH_2-8), 55.2 (OCH_3-11), 51.1 (CH_2-6), 35.4 (CH_2-13), 27.5 (CH_2-5); MS (FAB) *m/z* (%): 298 [M + H]$^+$, 164 (100); HRMS-FAB [M + H] $^+$ calcd for $C_{18}H_{20}NO_3$: 298.1438, found: 298.1439.

*4.2.7. General procedure for the synthesis of THP **6c**, **9e** and **9f** by formation of methylenedioxy group*

*4.2.7.1. 2,3-Methylenedioxy-11-methoxytetrahydroprotoberberine (**6c**).* A solution of 2,3-dihydroxy-11-methoxy-THPB (**6b**) (100 mg, 0.34 mmol) in anhydrous DMF (3 mL) was treated with dichloromethane (10 mL, 155.6 mmol) and CsF (250 mg, 1.64 mmol). The mixture was refluxed for 3 h with stirring. After cooling, the reaction mixture was extracted with CH_2Cl_2 and the organic layer was washed with 5% aqueous $NaHCO_3$ and H_2O, dried over with anhydrous Na_2SO_4 and concentrated *in vacuo* to dryness. The residue was purified by silica gel column chromatography (CH_2Cl_2/MeOH 95:5) to obtain the 2,3-methylendioxy-11-methoxy-THPB (**6c**) (90 mg, 86%) as a yellow oil. ^{1}H NMR (500 MHz, $CDCl_3$): δ = 6.99 (d, J = 8.4 Hz, 1H, H-9), 6.74 (s, 1H, H-1), 6.72 (dd, J = 8.4, 2.5 Hz, 1H, H-10), 6.68 (d, J = 2.5 Hz, 1H, H-12), 6.59 (s, 1H, H-4), 5.92 (s, 2H, OCH_2O), 3.95 (d, J = 14.4 Hz, 1H, H-8α), 3.79 (s, 3H, OCH_3-11), 3.65 (d, J = 14.4 Hz, 1H, H-8β), 3.57 (dd, J = 11.2, 3.5 Hz, 1H, H-14), 3.25 (dd, J = 16.3, 3.5 Hz, 1H, H-13α), 3.12 (m, 1H, H-6α), 3.09 (m, 1H, H-5α), 2.87 (dd, J = 16.3, 11.2 Hz, 1H, H-13β), 2.63 (m, 1H, H-5β), 2.60 (m, 1H, H-6β); ^{13}C NMR (125 MHz, $CDCl_3$): δ = 158.0 (C-11), 146.1 (C-2), 145.9 (C-3), 135.5 (C-12a), 130.8 (C-14a), 127.8 (C-4a), 127.1 (CH-9), 126.6 (C-8a), 113.2 (CH-12), 112.3 (CH-10), 108.4 (CH-4), 105.5 (CH-1), 100.7 (OCH_2O), 59.8 (CH-14), 58.0 (CH_2-8), 55.2 (OCH_3-11), 51.3 (CH_2-6), 37.2 (CH_2-13), 29.5 (CH_2-5); MS (FAB) *m/z* (%): 310 [M + H]$^+$, 176 (100); HRMS-FAB [M + H]$^+$ calcd for $C_{19}H_{20}NO_3$: 310.1438, found: 310.1440.

*4.2.7.2. 2,3-Methylenedioxy-11-hydroxytetrahydroprotoberberine (**9e**).* 2,3,11-trihydroxy-THPB (**9c**) (100 mg, 0.353 mmol) was subjected to similar conditions to those above described to obtain the 2,3-methylenedioxy-11-hydroxy-THPB (**9e**). The residue was purified by silica gel column chromatography (CH_2Cl_2/MeOH, 98:2), to obtain the THPB **9e** (23 mg, 23%) as a white oil. ^{1}H NMR (500 MHz, C_5D_5N): δ = 7.06 (m, 3H, H-9, H-10, H-12), 6.90 (s, 1H, H-1), 6.63 (s, 1H, H-4), 5.96 (dd, J = 4.1, 1.2 Hz, 2H, OCH_2O), 4.00 (d, J = 14.3 Hz, 1H, H-8α), 3.62 (d, J = 14.3 Hz, 1H, H-8β), 3.57 (d, J = 11.4, 3.8 Hz, 1H, H-14), 3.33 (dd, J = 16.1, 3.8 Hz, 1H, H-13α), 3.12 (m, 1H, H-5α), 3.04 (m, 1H, H-6α), 2.99 (dd, J = 16.1, 11.4 Hz, 1H, H-13β), 2.58 (m, 1H, H-5β), 2.54 (m, 1H, H-6β); ^{13}C NMR (125 MHz, C_5D_5N): δ = 157.4 (C-11), 146.7 (C-2), 146.5 (C-3), 136.1 (C-12a), 131.3 (C-14a), 128.1 (C-4a), 127.5 (CH-9), 125.3 (C-8a), 115.8 (CH-12), 114.6 (CH-10), 108.7 (CH-4), 106.5 (CH-1), 101.3 (OCH_2O), 60.2 (CH-14), 58.1 (CH_2-8), 51.5 (CH_2-6), 37.3 (CH_2-13), 29.6 (CH_2-5); MS (FAB) *m/z* (%): 296 [M + H]$^+$, 176 (100); HRMS-FAB [M + H]$^+$ calcd for $C_{18}H_{18}NO_3$: 296.1281, found: 296.1282.

*4.2.7.3. 2,3-Methylenedioxy-9-hydroxytetrahydroprotoberberine (**9f**).* 2,3,9-trihydroxy-THPB (**9d**) (100 mg, 0.353 mmol) was submitted to the same conditions depicted above to obtain the 2,3-methylenedioxy-9-hydroxy-THPB (**9f**). The residue was purified by silica gel column chromatography (CH_2Cl_2/MeOH, 98:2), to obtain the THPB **9f** (58 mg, 56%) as a white oil. ^{1}H NMR (500 MHz, C_5D_5N): δ = 7.16 (t, J = 7.8 Hz, 1H, H-11), 6.99 (d, J = 7.8 Hz, 1H, H-10), 6.95 (s, 1H, H-1), 6.84 (d, J = 7.8 Hz, 1H, H-12), 6.64 (s, 1H, H-4), 5.97 (dd, J = 4.9, 1.2 Hz, 1H, OCH_2O), 4.55 (d, J = 15.6 Hz, 1H, H-8α), 3.70 (d, J = 15.6 Hz, 1H, H-8β), 3.57 (dd, J = 11.1, 3.0 Hz, 1H, H-14), 3.38 (dd, J = 15.9, 3.0 Hz, 1H, H-13α), 3.12 (m, 1H, H-6α), 3.06 (m, 1H, H-5α),

3.01 (dd, $J = 15.9, 11.1$ Hz, 1H, H-13β), 2.54 (m, 1H, H-5β), 2.48 (m, 1H, H-6β); ^{13}C NMR (125 MHz, C_5D_5N): $\delta = 155.0$ (C-9), 146.7 (C-2), 146.4 (C-3), 136.8 (C-12a), 131.8 (C-14a), 128.4 (C-4a), 127.1 (CH-11), 123.1 (C-8a), 119.8 (CH-12), 112.5 (CH-10), 108.7 (CH-4), 106.3 (CH-1), 101.2 (OCH_2O), 59.9 (CH-14), 54.8 (CH_2-8), 51.8 (CH_2-6), 37.7 (CH_2-13), 29.9 (CH_2-5); MS (FAB) *m/z* (%): 296 $[M + H]^+$, 176 (100); HRMS-FAB $[M + H]^+$ calcd for $C_{18}H_{18}NO_3$: 296.1281, found: 296.1280.

4.3. Bioassays

4.3.1. Binding experiments

These experiments were performed on striatal membranes. Each striatum was homogenized in 2 mL ice-cold Tris–HCl buffer (50 mM, pH = 7.4 at 22 °C) with a Polytron (4s, maximal scale) and immediately diluted with Tris buffer. The homogenate was centrifuged either twice ([^{3}H] SCH 23390 binding experiments) on four times ([^{3}H] raclopride binding experiments) at 20,000 g for 10 min at 4 °C with resuspension in the same volume of Tris buffer between centrifugations. For [^{3}H] SCH 23390 binding experiments, the final pellet was resuspended in Tris buffer containing 5 mM $MgSO_4$, 0.5 mM EDTA and 0.02% ascorbic acid (Tris-Mg buffer), and the suspension was briefly sonicated and diluted to a protein concentration of 1 mg/mL. A 100 μL aliquot of freshly prepared membrane suspension (100 μg of striatal protein) was incubated for 1 h at 25 °C with 100 μL Tris buffer containing [^{3}H] SCH 23390 (0.25 nM final concentration) and 800 μL of Tris-Mg buffer containing the required drugs. Non-specific binding was determined in the presence of 30 μM SK&F 38393 and represented around 2–3% of total binding. For [^{3}H] raclopride binding experiments, the final pellet was resuspended in Tris buffer containing 120 mM NaCl, 5 mM KCl, 1 mM $CaCl_2$, 1 mM $MgCl_2$ and 0.1% ascorbic acid (Tris-ions buffer), and the suspension was treated as described above. A 200 μL aliquot of freshly prepared membrane suspension (200 μg of striatal protein) was incubated for 1 h at 25 °C with 200 μL of Tris buffer containing [^{3}H] raclopride (0.5 nM, final concentration) and 400 μL of Tris-ions buffer containing the drug under investigation. Non-specific binding was determined in the presence of 50 μM apomorphine and represented around 5–7% of the total binding. In both cases, incubations were stopped by addition of 3 mL of ice-cold buffer (Tris-Mg buffer or Tris-ions buffer, as appropriate) followed by rapid filtration through Whatman GF/B filters. Tubes were rinsed with 3 mL of ice-cold buffer, and filters were washed with 3 × 3 mL ice-cold buffer. After the filters had been dried, radioactivity was counted in 4 mL BCS scintillation liquid at an efficiency of 45%. Filter blanks corresponded to approximately 0.5% of total binding and were not modified by drugs.

4.3.2. In vitro cytotoxicity studies

Cytotoxicity of the THPBs was studied by the use of two different in vitro approaches (MTT colorimetric assay and flow cytometry analysis) [42]. Cytotoxicity was evaluated on freshly isolated human peripheral blood neutrophils. Human neutrophils were obtained from buffy coats of healthy donors by Ficoll-Hypaque density gradient centrifugation, as previously described [43]. Cultures were maintained at 37 °C under 5% CO_2 and 95% air atmosphere in RPMI-1640 medium (Sigma–Aldrich Chemical, USA).

4.3.2.1. MTT assay. The viability of neutrophils was determined using the previously described MTT (3-(4,5-dimethylthiazol-2-yl)-2,5-diphenyltetrazolium bromide) colorimetric assay [44]. In this assay, the yellow MTT is reduced to a blue formazan product by the mitochondria of viable cells. MTT (Sigma–Aldrich) was prepared at 1 mg/mL in RPMI and stored at 4 °C in the dark. 100 μl of neutrophils suspension (2×10^5 cells/mL) was added to each well of a 96-well microtiter plate followed by 20 μl of the appropriate concentration of the THPBs tested. The mixture was incubated at 37 °C for 24 h. Then, 100 μl aliquot of MTT solution was added to each well and incubated at 37 °C for another 60 min. The supernatants were discarded and 100 μl of DMSO was added to each well to dissolve the precipitated formazan. The optical densities at dual wavelengths (570 and 630 nm) were determined in a spectrophotometer (Infinite M200, Tecan, Mannedorf, Switzerland).

4.3.2.2. Cytofluorometric analysis of neutrophil apoptosis and survival. Freshly isolated neutrophils were resuspended in supplemented RPMI medium at 2×10^6 cells/mL. 25 μl were cultured in a 24-well plate containing 200 μl of supplemented RPMI medium for 24 h in the absence or presence of the most active THPBs on D_2 DR (**6b**, **9d** and **9f**). Assessment of apoptosis was performed by flow cytometry using annexin V- FITC and propidium iodide (PI). The protocol indicated by the manufacturer (Annexin-Fluos; Roche Applied Science) was used as outlined previously [45]. Cells (1×10^4) were analyzed in a Beckman Coulter Epics XL (Fullerton, CA) and differentiated as early or viable apoptotic (annexin V^+ and PI^-), late apoptotic and/or necrotic (annexin V^+ and PI^+), and viable nonapoptotic (annexin V^- and PI^-) cells.

4.4. Molecular modelling

4.4.1. Molecular dynamics simulations of complexes

A 3D model of the human D_2 DR was used for the MD simulations. This model is based on the homology model from the crystallized D_3 DR, β2 adrenoceptor and A2α adenosine receptor as templates [46]. (PMDB: http://mi.caspur.it/PMDB/codes: PM0077430).

The complex geometries from docking were soaked in boxes of explicit water using the TIP3P model [47] and subjected to MD simulation. All MD simulations were performed with the Amber software package using periodic boundary conditions and cubic simulation cells. The particle mesh Ewald method (PME) [48] was applied using a grid spacing of 1.2 Å, a spline interpolation order of 4 and a real space direct sum cutoff of 10 Å. The SHAKE algorithm was applied allowing for an integration time step of 2 fs. MD simulations were carried out at 300 K target temperature and extended to 10 ns overall simulation time. The NPT ensemble was employed using Berendsen coupling to a baro/thermostat (target pressure 1 atm, relaxation time 0.1 ps). Post MD analysis was carried out with program PTRAJ.

4.4.2. MM-GBSA free energy decomposition

In order to determine the residues of the D_2 DR active site involved in the interactions, the residues proposed by Andujar et al. [17] and Soriano-Ursua et al. were first identified. Then MM-GBSA free energy decomposition using the *mm_pbsa* program in AMBER12 was employed to corroborate the amino acids interacting with the ligands. This calculation can decompose the interaction energies of each residue considering molecular mechanics and solvation energies [49,50]. Each ligand–residue pair includes four energy terms: van der Waals contribution (E_{vdw}), electrostatic contribution (E_{ele}), polar desolvation term (G_{GB}) and nonpolar desolvation term (G_{SA}), which are summarized in the following equation: $\Delta G_{inhibitor-residue} = \Delta E_{vdW} + \Delta E_{ele} + \Delta G_{GB} + \Delta G_{SA}$

For MM-GBSA methodology, snapshots were taken at 10 ps time intervals from the corresponding last 1000 ps MD trajectories and the explicit water molecules were removed from the snapshots.

4.4.3. Quantum mechanics calculations and topological study of the electron charge density distribution

19 amino acids were included in this reduced model based on the generated data. Three molecular complexes, **9d**/D_2DR, **9c**/D_2DR and **6b**/D_2DR, obtained for our "reduced model system", were

selected due to their representative chemical features for the calculation of the charge density. Single point calculations were performed with Gaussian 03 and employing a hybrid B3LYP functional and 6-31G(d) as basis set. This type of calculation has been recently used in studies on the topology of (r) because it ensures a reasonable compromise between the wave function quality required to obtain reliable values of the derivatives of (r) and the computer power available, due to the extension of the system in study [17,18]. The topological properties of a scalar field such as (r) are summarized in terms of their critical points, i.e., the points r_c where $(r) = 0$. Critical points are classified according to their type (,) by stating their rank, and signature. The rank is equal to the number of nonzero eigenvalues of the Hessian matrix of (r) at r_c, while the signature is the algebraic sum of the signs of the eigenvalues of this matrix. Critical points of (3, −1) and (3, +1) type describe saddle points, where the (3, −3) is the maximum and (3, +3) is the minimum in the field. Among these critical points, the (3, −1) or bond critical points are the most relevant ones since they are found between any two atoms linked by a chemical bond. The determination of all the bond critical points and the corresponding bond paths connecting these point with bonded nuclei, were performed with the AIMAll software. The molecular graphs were drafted using the same program. Spatial views shown in Figs. 10 and 11 were constructed using the UCSF Chimera program as graphic interface.

It should be noted that the THPBs here reported were enantiomeric, they possessed one chiral centre and they could raise two isomers (*S* and *R*). However, although an enantiomeric resolution for the biological assays was not carried out, only one isomer of each compound was evaluated in the calculations. The isomeric forms selected were first chosen on the basis of previously reported results [8–14] and on the exploratory simulations in which the spatially preferred form for these compounds was determined (results not shown). In this context, Sun et al. [23] showed that when a substitution was performed at the D ring, the S-isomers of THPBs displayed stronger affinities for the D_2 DR than their corresponding R-isomer. In addition, previous experimental findings with BTHIQs also supported this hypothesis since *S* forms were the preferred conformation of these compounds [13]. Finally, the preliminary and exploratory MD simulations performed for the THPBs here synthesized revealed that the $\Delta\Delta G$ values obtained for the *R*-isomers are at least 10 kcal/mol higher than their respective *S*-isomers. Therefore, the spatial conformation adopted by the *S* forms seemed to provide the adequate orientation of the molecules for their interaction with the active site at the D_2 DR.

Acknowledgements

This study was supported by grants SAF2011-23777, Spanish Ministry of Economy and Competitiveness, RIER RD08/0075/0016, Carlos III Health Institute, Spanish Ministry of Health and the European Regional Development Fund (FEDER). R.D.E. and S.A.A. are staff members of the National Research Council of Argentina (CONICET-Argentina).

Appendix A. Supplementary data

Supplementary data related to this article can be found at http://dx.doi.org/10.1016/j.ejmech.2013.07.036.

References

[1] P.M. Luthra, J.B. Kumar, Plausible improvements for selective targeting of dopamine receptors in therapy of Parkinson's disease, J. Med. Chem. 14 (2012) 1556–1564.
[2] J.M. Beaulieu, R.R. Gainetdinov, The physiology, signaling, and pharmacology of dopamine receptors, Pharmacol. Rev. 63 (2011) 182–217.
[3] W. Poewe, Treatments for Parkinson disease-past achievements and current clinical needs, Neurology 72 (2009) S65–S73.
[4] N. Clausius, C. Born, H. Grunze, The relevance of dopamine agonists in the treatment of depression, Neuropsychiatry 23 (2009) 15–25.
[5] A.M. Basso, K.B. Gallagher, N.A. Bratcher, J.D. Brioni, R.B. Moreland, G.C. Hsieh, K. Drescher, G.B. Fox, M.W. Decker, L.E. Rueter, Antidepressant-like effect of D(2/3) receptor-, but not D(4) receptor-activation in the rat forced swim test, Neuropsychopharmacology 30 (2005) 1257–1268.
[6] M. Brocco, A. Dekeyne, M. Papp, M.J. Millan, Antidepressant-like properties of the anti-Parkinson agent, piribedil, in rodents: mediation by dopamine D2 receptors, Behav. Pharmacol. 17 (2006) 559–572.
[7] K. Kitagawa, Y. Kitamura, T. Miyazaki, J. Miyaoka, H. Kawasaki, M. Asanuma, T. Sendo, Effects of pramipexole on the duration of immobility during the forced swim test in normal and ACTH-treated rats, Naunyn Schmiedebergs Arch. Pharmacol. 380 (2009) 59–66.
[8] I. Berenguer, N. El Aouad, S. Andujar, V. Romero, F. Surive, T. Freret, A. Bermejo, M.D. Ivorra, R.D. Enriz, M. Boulouard, N. Cabedo, D. Cortes, Tetrahydroisoquinolines as dopaminergic ligands: 1-butyl-7-chloro-6-hydroxy-tetrahydroisoquinoline, a new compound with antidepressant-like activity in mice, Bioorg. Med. Chem. 17 (2009) 4968–4980.
[9] P. Protais, J. Arbaoui, E.H. Bakkali, A. Bermejo, D. Cortes, Effects of various isoquinoline alkaloids on in vitro 3H-dopamine uptake, J. Nat. Prod. 58 (1995) 1475–1484.
[10] A. Bermejo, P. Protais, M.A. Blázquez, K.S. Rao, M.C. Zafra-Polo, D. Cortes, Dopaminergic isoquinoline alkaloids from roots of *Xylopia papuana*, Nat. Prod. Lett. 6 (1995) 57–62.
[11] N. Cabedo, P. Protais, B.K. Cassels, D. Cortes, Synthesis and dopamine receptor selectivity of the benzyltetrahydroisoquinoline, (R)-(+)-nor-roefractine, J. Nat. Prod. 61 (1998) 709–712.
[12] I. Andreu, D. Cortes, P. Protais, B.K. Cassels, A. Chagraoui, N. Cabedo, Preparation of dopaminergic N-alkyl-benzyltetrahydroisoquinolines using a 'one-pot' procedure in acid medium, Bioorg. Med. Chem. 8 (2000) 889–895.
[13] N. Cabedo, I. Andreu, M.C. Ramírez de Arellano, A. Chagraoui, A. Serrano, B. Bermejo, P. Protais, D. Cortes, Enantioselective syntheses of dopaminergic (R)- and (S)-benzyltetrahydroisoquinolines, J. Med. Chem. 44 (2001) 1794–1801.
[14] I. Andreu, N. Cabedo, G. Torres, A. Chagraoui, M.C. Ramirez de Arellano, S. Gil, A. Bermejo, M. Valpuesta, P. Portais, D. Cortes, Syntheses of dopaminergic 1-cyclohexylmethyl-7,8-dioxygenated tetrahydroisoquinolines by selective heterogeneous tandem hydrogenation, Tetrahedron 58 (2002) 10173–10179.
[15] F.D. Suvire, N. Cabedo, A. Chagraoui, M.A. Zamora, D. Cortes, R.D. Enriz, Molecular recognition and binding mechanism of N-alkyl-benzyltetrahydroisoquinolines to the D_1 dopamine receptor. A computational approach, J. Mol. Struct. (Theochem) 666–667 (2003) 455–467.
[16] N. El Aouad, I. Berenguer, V. Romero, P. Marín, A. Serrano, S. Andujar, F. Suvire, A. Bermejo, M.D. Ivorra, R.D. Enriz, N. Cabedo, D. Cortes, Structure-activity relationship of dopaminergic halogenated 1-benzyl-tetrahydroisoquinoline derivatives, Eur. J. Med. Chem. 44 (2009) 4616–4621.
[17] S. Andujar, F. Suvire, I. Berenguer, N. Cabedo, P. Marín, L. Moreno, M.D. Ivorra, D. Cortes, R.D. Enriz, Tetrahydroisoquinolines acting as dopaminergic ligands. A molecular modeling study using MD simulations and QM calculations, J. Mol. Model 18 (2012) 419–431.
[18] S.A. Andujar, R.D. Tosso, F.D. Suvire, E. Angelina, N. Peruchena, N. Cabedo, D. Cortes, R.D. Enriz, Searching the biologically relevant conformation of dopamine: a computational approach, J. Chem. Inf. Model 52 (2012) 99–112.
[19] H. Xiao, J. Peng, Y. Liang, J. Yang, X. Bai, X.Y. Hao, F.M. Yang, Q.Y. Sun, Acetylcholinesterase inhibitors from *Corydalis yanhusuo*, Nat. Prod. Res. 25 (2011) 1418–1422.
[20] L. Slobodníková, D. Kostálová, D. Labudová, D. Kotulová, V. Kettmann, Antimicrobial activity of *Mahonia aquifolium* crude extract and its major isolated alkaloids, Phytother. Res. 18 (2004) 674–676.
[21] N. Cabedo, I. Berenguer, B. Figadère, D. Cortes, An overview on benzylisoquinoline derivatives with dopaminergic and serotonergic activities, Curr. Med. Chem. 16 (2009) 2441–2467.
[22] D. Cortes, J. Arbaoui, P. Protais, High affinity and selectivity of some tetrahydroprotoberberine alkaloids for rat striatal ^{3}H-raclopride binding sites, Nat. Prod. Lett. 3 (1993) 233–238.
[23] H. Sun, L. Zhu, H. Yang, W. Qian, L. Guo, S. Zhou, B. Gao, Z. Li, Y. Zhou, H. Jiang, K. Chen, X. Zhen, H. Liu, Asymmetric total synthesis and identification of tetrahydroprotoberberine derivatives as new antipsychotic agents possessing a dopamine D_1, D_2 and serotonin 5-HT_{1A} multi-action profile, Bioorg. Med. Chem. 21 (2013) 856–868.
[24] J. Dou, C. Tan, Y. Du, X. Bai, K. Wang, X. Ma, Effects of chitooligosaccharides on rabbit neutrophils in vitro, Carbohydr. Polym. 69 (2007) 209–213.
[25] M. Cheddadi, E. López-Cabarcos, K. Slowing, E. Barcia, A. Fernández-Carballido, Cytotoxicity and biocompatibility evaluation of a poly(magnesium acrylate) hydrogel synthesized for drug delivery, Int. J. Pharm. 413 (2011) 126–133.
[26] M.T. García, M.A. Blázquez, M.J. Ferrándiz, M.J. Sanz, N. Silva-Martín, J.A. Hermoso, A.G. de la Campa, New alkaloid antibiotics that target the DNA topoisomerase I of *Streptococcus pneumoniae*, J. Biol. Chem. 286 (2011) 6402–6413.
[27] G.W. Kabalka, R.S. Varma, Syntheses and selected reductions of conjugated nitroalkenes, Org. Prep. Proced. Int. 19 (1987) 283–328.
[28] C.M. Chen, Y.F. Fu, T.H. Yang, Synthesis of (±)-annonelliptine and (±)-anomoline, J. Nat. Prod. 58 (1995) 1767–1771.
[29] M. Shamma, The Isoquinoline Alkaloids: Chemistry and Pharmacology, Academic Press, New York, 1972.

[30] H.A. Ammar, P.L. Schiff Jr., D.J. Slatkin, Synthesis of 7,7-dimethylaporphine alkaloids, Heterocycles 20 (1983) 451–454.
[31] T. Kametani, T. Kobari, K. Fukimoto, M. Fujihara, Studies on the synthesis of heterocycle compounds. Part CCCXCII. An alternative total synthesis of pet-aline, J. Chem. Soc. C (1971) 1796–1800.
[32] B.C. Uff, J.R. Kershaw, S.R. Chhabra, Reissert compound chemistry. Some rearrangement and substitution reactions, J. Chem. Soc. Perkin Trans. (1972) 479–484.
[33] S. Doi, N. Shirai, Y. Sato, Abnormal products in the Bischler–Napieralski isoquinoline synthesis, J. Chem. Soc. Perkin Trans. (1997) 2217–2221.
[34] R. Suau, M.V. Silva, M. Valpuesta, Structure and total synthesis of (−)-malacitanine. An unusual protoberberine alkaloid from *Ceratocapnos heterocarpa*, Tetrahedron 46 (1990) 4421–4428.
[35] M. Shamma, D.Y. Hwang, The synthesis of (±)-thalphenine, thaliglucine and thaliglucinona, Tetrahedron 30 (1974) 2279–2282.
[36] A. Manzour, F. Meng, J.H. Meador-Woodruff, L.P. Taylor, O. Civelli, H. Akil, Site directed mutagenesis of the human dopamine D_2 receptor, Eur. J. Pharmacol. Mol. Pharmacol. 227 (1992) 205–214.
[37] E. Hjerde, S.G. Dahl, I. Sylte, Atypical and typical antipsychotic drug interactions with the dopamine D_2 receptor, Eur. J. Med. Chem. 40 (2005) 185–194.
[38] W. Cho, L.P. Taylor, A. Mansour, A. Akil, Hydrophobic residues of the D_2 dopamine receptor are important for binding and signal transduction, J. Neurochem. 65 (1995) 2105–2115.
[39] D.A. Case, T.E. Cheatham, T. Darden, H. Gohlke, R. Luo, K.M. Merz, A. Onufriev, C. Simmerling, B. Wang, R.J. Woods, The amber biomolecular simulation programs, J. Comput. Chem. 26 (2005) 1668–1688.
[40] K.A. Neve, M.G. Cumbay, K.R. Thompson, R. Yang, D.C. Buck, V.J. Watts, C.J. Durand, M.M. Teeter, Modeling and mutational analysis of a putative sodium-binding pocket on the dopamine D_2 receptor, Mol. Pharmacol. 60 (2001) 373–381.
[41] R.E. Wilcox, W.H. Huang, M.Y.K. Brusniak, D.M. Wilcox, R.S. Pearlman, M.M. Teeter, C.J. Durand, B.L. Wiens, K.A. Neve, CoMFA-based prediction of agonist affinities at recombinant wild type versus serine to alanine point mutated D_2 dopamine receptors, J. Med. Chem. 43 (2000) 3005–3019.
[42] L.E. Smith, S. Rimmer, S. MacNeil, Examination of the effects of poly(N-vinyl pyrrolidinone) hydrogels in direct and indirect contact with cells, Biomaterials 27 (2006) 2806–2812.
[43] C. Rius, M. Abu-Taha, C. Hermenegildo, L. Piqueras, J.M. Cerda-Nicolas, A.C. Issekutz, L. Estañ, J. Cortijo, E.J. Morcillo, F. Orallo, M.J. Sanz, Trans- but not cis-resveratrol impairs angiotensin-II-mediated vascular inflammation through inhibition of NF-κB activation and peroxisome proliferator-activated receptor-gamma upregulation, J. Immunol. 185 (2010) 3718–3727.
[44] M. Iacobini, A. Menichelli, G. Palumbo, G. Multari, B. Werner, D. Del Principe, Involvement of oxygen radicals in cytarabine induced apoptosis in human polymorphonuclear cells, Biochem. Pharmacol. 61 (2001) 1033–1040.
[45] M.C. Martin, I. Dransfield, C. Haslett, A.G. Rossi, Cyclic AMP regulation of neutrophil apoptosis occurs via a novel protein kinase A-independent signaling pathway, J. Biol. Chem. 276 (2001) 45041–45050.
[46] M.A. Soriano-Ursua, J.O. Ocampo-Lopez, K. Ocampo-Mendoza, J.G. Trujillo-Ferrara, J. Correa-Basurto, Theoretical study of 3-D molecular similarity and ligand binding modes of orthologous human and rat D_2 dopamine receptors, Comput. Biol. Med. 41 (2011) 537–545.
[47] W.L. Jorgensen, J. Chandrasekhar, J.D. Madura, R.W. Impey, M.L. Klein, Comparison of simple potential functions for simulating liquid water, J. Chem. Phys. 79 (1983) 926–935.
[48] T. Darden, D. York, L. Pedersen, Particle mesh Ewald: an N·log(N) method for Ewald sums in large systems, J. Chem. Phys. 98 (1993) 10089–10092.
[49] T. Hou, N. Li, Y. Li, W. Wang, Characterization of domain-peptide interaction interface: prediction of SH3 domain-mediated protein-protein interaction network in yeast by generic structure-based models, J. Proteome Res. 11 (2012) 2982–2995.
[50] H. Gohlke, C. Kiel, D.A. Case, Insights into protein-protein binding by binding free energy calculation and free energy decomposition for the Ras–Raf and Ras–RalGDS complexes, J. Mol. Biol. 330 (2003) 891–913.

European Journal of Medicinal Chemistry 90 (2015) 101–106

Contents lists available at ScienceDirect

European Journal of Medicinal Chemistry

journal homepage: http://www.elsevier.com/locate/ejmech

Short communication

Synthesis of hexahydrocyclopenta[*ij*]isoquinolines as a new class of dopaminergic agents

Javier Párraga [a], Abraham Galán [a], Maria Jesús Sanz [b, c], Nuria Cabedo [a, d, *], Diego Cortes [a, **]

[a] Departamento de Farmacología, Facultad de Farmacia, Laboratorio de Farmacoquímica, Universidad de Valencia, 46100, Vicent Andres Estellés s/n, Burjassot, Valencia, Spain
[b] Departamento de Farmacología, Facultad de Medicina, Universidad de Valencia, 46013, Valencia, Spain
[c] Institute of Health Research-INCLIVA, University Clinic Hospital of Valencia, Valencia, Spain
[d] Centro de Ecología Química Agrícola-Instituto Agroforestal Mediterraneo, Universidad Politécnica de Valencia (UPV), Campus de Vera s/n, Edificio 6C, 46022, Valencia, Spain

ARTICLE INFO

Article history:
Received 18 September 2014
Received in revised form
29 October 2014
Accepted 5 November 2014
Available online 5 November 2014

Keywords:
Tetrahydroisoquinolines
Hexahydrocyclopenta[*ij*]isoquinolines
Bischler–Napieralski cyclodehydration
Friedel–Crafts cyclization
Dopamine receptors
Binding assays

ABSTRACT

In this study, we have described the synthesis of the tricyclic 1,2,3,7,8,8a-hexahydrocyclopenta [*ij*]isoquinoline (HCPIQ). Herein, six differently substituted 5,6-dioxygenated-7-phenyl-HCPIQs have been synthesized using a new methodology via (*E*)-1-styryl-THIQ by Friedel–Crafts cyclization with Eaton's reagent. Results showed that HCPIQs (**3**, **3a**–**e**) displayed a moderate affinity for D_1 dopamine receptors (DR) in the micromolar range, furthermore the catecholic HCPIQs **3a** (*N*H), **3c** (*N*CH_3) and **3e** (*N*$CH_2CH{=}CH_2$) exhibited outstanding affinity and high selectivity towards D_2 DR. Indeed, **3a**, **3c** and **3e** showed Ki values of 29 nM, 13 nM and 18 nM, respectively, and HCPIQs **3a** (*N*H) and **3c** (*N*CH_3) displayed a remarkable selectivity (Ki D_1/D_2 ratio ~ 1000–2500). In addition, none of the catecholic compounds showed any cytotoxicity in freshly isolated human neutrophils. Although further studies are needed, these compounds and particularly catecholic HCPIQs, show high potential in the treatment of Parkinson's disease, psychosis or depression.

1. Introduction

Tetrahydroisoquinoline (THIQ) alkaloids are biosynthetically dopamine-derived metabolites which are present in many vegetal species belonging to different families such as Papaveraceae, Berberidaceae, Ranunculaceae and Aristolochiaceae [1–3]. This class of alkaloids is relevant due to their diverse pharmacological activities that include β-adrenergic [4], inhibitor of α-glucosidase enzyme [5], as well as NMDA (N-methyl D-aspartate) [6], serotoninergic [7] and D_1 and D_2 dopaminergic receptor (DR) activities [7–20]. From a therapeutical point of view, drugs acting at D_2-like DR are more important than those interacting with D_1-like DR. In this context, the D_2-like DR antagonists are included in the therapy of schizophrenia (antipsychotics), and the agonists are used in the treatment of Parkinson's disease [21–25]. In the last two decades, our research group has been studying dopaminergic activity of natural and synthetic THIQs, including 1-benzy-IQ, bisbenzylisoquinolines, aporphines, tetrahydroprotoberberines and phenanthrenes [7–20]. We previously reported the synthesis of 1-butyl-7-chloro-6-hydroxy-THIQ. At that time, it displayed the highest affinity towards D_2-like DR (Ki value of 66 nM) and the highest selectivity (49-fold D_2 *vs* D_1) by *in vitro* binding experiments [9]. Afterwards, its evaluation in behavioural assays (spontaneous activity and forced swimming test) in mice, showed an increased locomotor activity in a large dose range (0.04–25 mg/kg). Furthermore, this lead compound produced reduction in immobility time in the forced swimming test at a dose of 0.01 mg/kg that did not modify locomotor activity. Haloperidol (0.03 mg/kg), a D_2 DR preferred antagonist, blocked the antidepressant-like effect of this compound [9].

In the present study, we have considered the synthesis of a series of tricyclic alkaloids with 1,2,3,7,8,8a-hexahydrocyclopenta [*ij*] isoquinoline (HCPIQ) skeleton. The HCPIQ system constitutes the nucleus of the naturally occurring proaporphines (pronuciferin type) [26,27], and besides, this system is structurally related to the azafluoranthene alkaloids (Fig. 1) [28]. Although HCPIQs constitute a small group into the IQ alkaloids, several synthesis have been

* Corresponding author. Centro de Ecología Química Agrícola-Instituto Agroforestal Mediterraneo, Universidad Politécnica de Valencia (UPV), Campus de Vera s/n, Edificio 6C, Valencia 46022, Spain.
** Corresponding author.
E-mail addresses: ncabedo@ceqa.upv.es (N. Cabedo), dcortes@uv.es (D. Cortes).

http://dx.doi.org/10.1016/j.ejmech.2014.11.009
0223-5234/

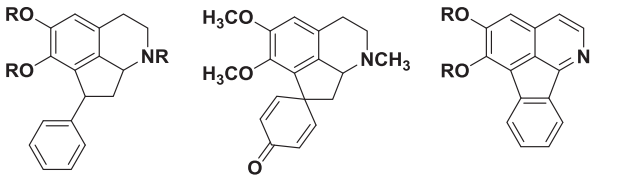

Fig. 1. THIQs skeletons: hexahydrocyclopenta [*ij*]isoquinoline (HCPIQ), proaporphine and azafluoranthene.

reported [29–34] given their potential and useful biological properties, including the inhibition of phenylethanolamine *N*-methyltransferase (PNMT) [29] and poly(ADP-ribose) polymerases (PARPs) [30] enzymes, as well as their antiprotozoal [35] activities.

Herein, we have synthesized six differently substituted 5,6-dioxygenated-7-phenyl-HCPIQs in order to evaluate the ability of this HCPIQ skeleton to bind to D_1 and D_2-like DR from rat striatal membranes (Scheme 1). Substituents have been chosen on the basis of previous reports with natural and synthetic IQ alkaloids, which included computational analysis [11–20]. Therefore, we have taken into account the relevance of the di-oxygenated IQ nucleus, the nature of the N-substituents and the presence of a hydrophobic part in the molecule to reach the dopaminergic activity. These 7-phenyl-HCPIQs have been obtained using a new methodology via (*E*)-1-styryl-THIQ intermediate by acid-catalysed cyclization with Eaton's reagent [36]. Their structures were determined by NMR spectroscopy and HRESIMS spectrometry.

2. Results and discussion

2.1. Chemistry

The synthesis starts from the available 2-(3,4-dimethoxyphenyl) ethylamine that reacts with cinnamoyl chloride under Schotten–Baumann conditions to generate the *N*-(3,4-dimethoxyphenethyl)cinnamamide (**1**) in 91% yield [9,16]. Next, the cinnamamide **1** was treated with $POCl_3$ in dry acetonitrile to perform the Bischler–Napieralski cyclodehydration [11–13]. The corresponding 1-styryl-dihydroisoquinoline was obtained and the imine function reduced by using $NaBH_4$ reagent to give the (*E*)-6,7-dimethoxy-1-styryl-1,2,3,4-THIQ (**2**) in 81% yield. Compound **2** was subjected to an intramolecular cyclization under mild Friedel–Crafts conditions using Eaton's reagent [36] (1:10 w/w P_2O_5 in CH_3SO_3H) to generate the 5,6-dimethoxy-7-phenyl-1,2,3,7,8,8a-hexahydrocyclopenta[*ij*] isoquinoline (**3**), containing the cyclopentane ring, in 68% yield. Once synthesized the HCPIQ **3**, we have introduced different substituents on the nitrogen atom like methyl or allyl groups. Therefore, we have obtained the corresponding *N*-methyl-HCPIQ **3b** (82%) using formaldehyde and formic acid in methanol followed by reduction with $NaBH_4$, besides the corresponding *N*-allyl- HCPIQ **3d** (89%) using allyl chloride and K_2CO_3 in acetonitrile. Finally, these HCPIQs **3** (*NH*), **3b** (*NCH*$_3$) and **3d** (*NCH*$_2$*CH*=*CH*$_2$) were subjected to *O*-demethylation by addition of 4 equivalents of BBr_3 for 2 h at room temperature [9] to obtain the catecholic HCPIQs **3a** (88%), **3c** (94%), and **3e** (90%), respectively (Scheme 1).

A single isomer has been produced during cyclization step given that the ^{1}H and ^{13}C NMR spectrum of HCPIQ **3** showed only one set of proton or carbon resonances. The relative stereochemistry of H-8a and Ph was assigned by coupling constants values of H-8a, H-8 and H-7. The vicinal coupling constant values of H-8a at 4.24 ppm (dd, J = 11.8 and 6.4 Hz) imply that H-8β at 2.50 ppm is located in pseudoequatorial disposition ($J_{8a,8\beta}$ = 6.4 Hz) and H-8α at 2.35 ppm is in pseudoaxial disposition ($J_{8a,8\alpha}$ = 11.8 Hz). In addition, the H-7 at 4.59 ppm must be pseudoaxial since its coupling constant value is $J_{7,8\alpha}$ = 8.3 Hz, which was corroborated by NOE experiment between H-8α and H-7. Therefore, the phenyl group (pseudoequatorial) is *cis* to H-8a (pseudoaxial) (Fig. 2).

2.2. Dopaminergic receptors activity

In general, the HCPIQs with protected phenolic groups displayed a lower affinity for D_1 and principally D_2 DR than their corresponding homologues with free hydroxyl groups (see in Table 1, **3b** vs **3c**, and **3d** vs **3e**). Indeed, the higher affinity for D_1 and D_2 DR of catecholic THIQs in comparison with those with blocked hydroxyl groups was previously described in several isoquinolines [7,9,12,16,19]. All synthesized HCPIQs (**3**, **3a**–**e**) were able to displace [^{3}H]SCH 23390 (selective D_1 DR ligand) and [^{3}H] raclopride (selective D_2 DR ligand) from its binding sites in micromolar and nanomolar ranges, respectively. Furthermore and surprisingly the catecholic HCPIQs **3a** (*NH*), **3c** (*NCH*$_3$) and **3e** (*NCH*$_2$*CH*=*CH*$_2$) exhibited outstanding affinity and high selectivity towards D_2 DR. Therefore, **3a**, **3c** and **3e** showed Ki values of 29, 13 and 18 nM, respectively. In addition, HCPIQs **3a** (*NH*) and **3c** (*NCH*$_3$) displayed a remarkable selectivity with a Ki D_1/D_2 ratio of 2465 and 1010, respectively. For instance, the huge selectivity of **3a** and **3c** is graphically represented in Fig. 3. Regarding the N-substituent, we observed that in *O*-methylated HCPIQs the affinity for DR did not change when a substituent like methyl or allyl was located on the *N* atom (see in Table 1, **3** vs **3b** and **3d**), however in catecholic HCPIQs an increase of the affinity towards D_1 DR was observed (see in Table 1, **3a** vs **3c** and **3e**). Moreover, the potential cytotoxicity of these catecholic HCPIQs was determined by the use of the MTT assay on freshly isolated human neutrophils [19]. The concentrations tested were selected based on their respective Ki value for D_2 DR. Results showed that none of the evaluated HCPIQs displayed any cytotoxicity.

3. Conclusions

We have synthesized a new molecular skeleton HCPIQ via (*E*)-1-styryl-THIQ by intramolecular Friedel–Crafts cyclization using Eaton's reagent. The six differently substituted 5,6-dioxygenated-7-phenyl-HCPIQ displayed affinity towards both D_1 and D_2 DR receptors. Moreover, the three catecholic HCPIQs **3a** (*NH*), **3c** (*NCH*$_3$) and **3e** (*NCH*$_2$*CH*=*CH*$_2$) showed D_2 DR affinity in the nanomolar range. Indeed, they exhibited higher affinity (2.3–5-fold) and selectivity (Ki D_1/D_2 ratios ~1000–2500) for D_2 DR than the 1-butyl-7-chloro-6-hydroxy-THIQ, which is one of the most active antidepressant THIQ synthesized by our group [9]. The major goal of this study is the discovery of a new skeleton HCPIQs with both high affinity and selectivity towards D_2 DR in *in vitro* assays. Although further studies are needed, these compounds and particularly catecholic HCPIQs, which did not show cytotoxicity, present high potential application in the treatment of Parkinson's disease, psychosis or depression.

4. Experimental section

4.1. General instrumentation

High resolution (HRESIMS) data were recorded on a Waters Xevo quadrupole time-of-flight (Q-TOF) spectrometer (Waters Corp., Milford, MA, USA) coupled to an Acquity UPLC system (Waters Corp., Milford, MA, USA) via an electrospray ionization (ESI) interface operating in positive mode and using a Waters Acquity BEH C18 column (50 × 2.1 mm i.d., 1.7 μm); ^{1}H NMR spectra were recorded with $CDCl_3$ or Methanol-d_4 as a solvent on a Bruker AC-

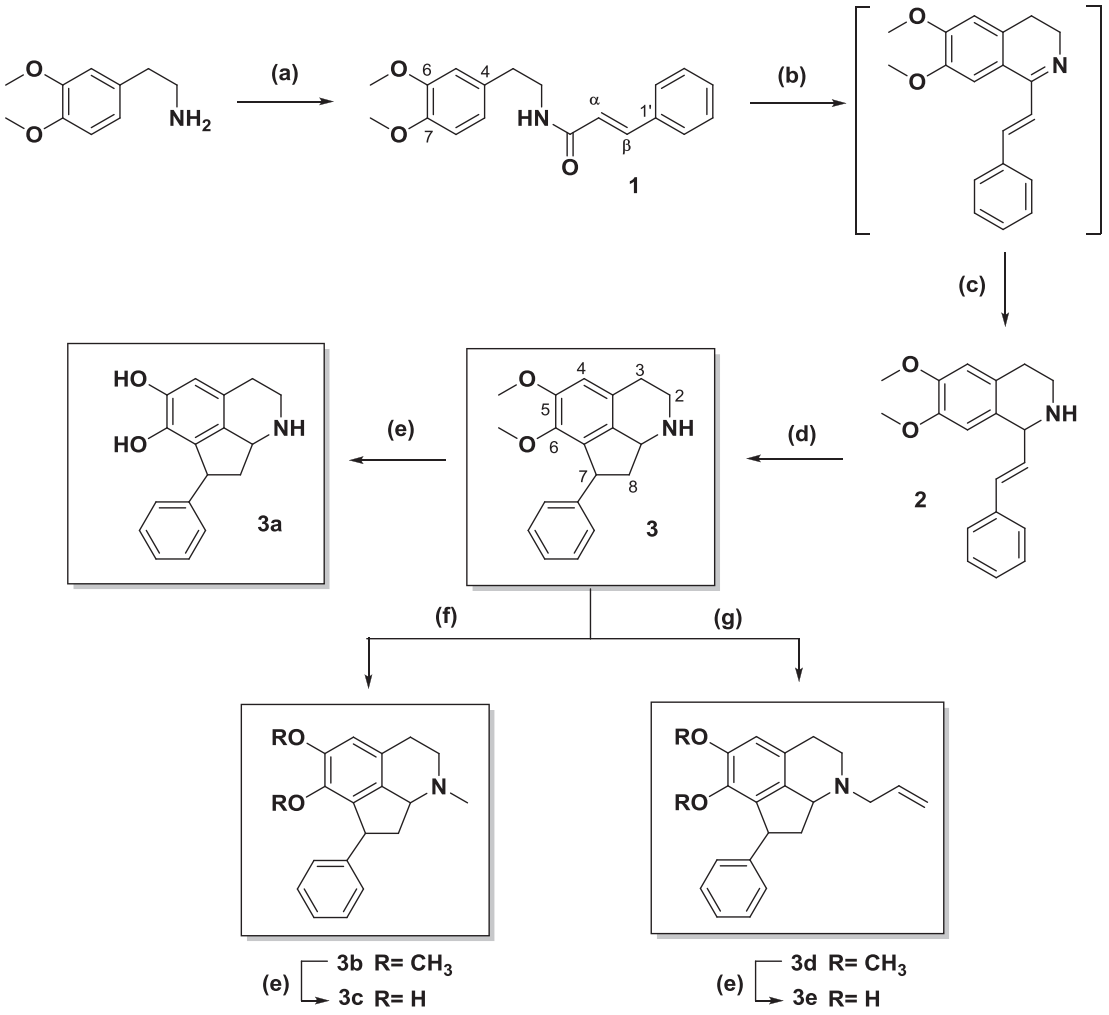

Scheme 1. Synthesis of HCPIQs (**3**, **3a**–**e**). Reagents and Conditions: (a) cinnamoyl chloride, NaOH 5%, CH_2Cl_2, rt, 3 h; (b) $POCl_3$, CH_3CN, N_2, reflux, 5 h; (c) $NaBH_4$; MeOH, rt, 2 h; (d) Eaton's reagent (P_2O_5–CH_3SO_3H, 1:10 w/w), 45 °C, 15 h; (e) BBr_3, CH_2Cl_2, rt, 2 h; (f) HCHO, HCO_2H, MeOH, reflux, 1 h, followed by $NaBH_4$, reflux, 1 h; (g) K_2CO_3, allyl chloride, CH_3CN, reflux, 10 h.

500. The assignments were made by COSY, DEPT, HSQC and HMBC. All the reactions were monitored by analytical TLC by silica gel 60 F_{254} (Merck 5554). Residues were purified by silica gel 60 (40–63 μm, Merck 9385) column chromatography. Solvents and reagents used were purchased from commercial sources. Quoted yields are of purified material.

4.2. Friedel–Crafts cyclization of (E)-6,7-dimethoxy-1-styryl-1,2,3,4-tetrahydroisoquinoline (*2*) to obtain 5,6-dimethoxy-7-phenyl-1,2,3,7,8,8a-hexahydrocyclopenta[ij]isoquinoline (*3*)

An amount of 500 mg of (*E*)-6,7-dimethoxy-1-styryl-1,2,3,4-tetrahydroisoquinoline (**2**) (1.69 mmol) was dissolved in 5 ml of Eaton's reagent (P_2O_5–CH_3SO_3H, 1:10 w/w) at room temperature and the solution was stirred for 15 h at 45 °C. After, 5% aqueous NaOH was added and the mixture was then extracted with CH_2Cl_2 (3 × 15 mL). The combined CH_2Cl_2 extracts were dried over Na_2SO_4 and the solvent evaporated in a *vacuum* to obtain a reddish oil. The residue obtained was purified by silica gel column chromatography (CH_2Cl_2/MeOH, 95:5) to obtain HCPIQ **3** as a brown oil (68% yield). ^{1}H NMR (500 MHz, $CDCl_3$): δ = 7.27 (m, 2H, CH-3′ and CH-5′), 7.19 (m, 2H, CH-2′ and CH-6′), 7.18 (m, 1H, CH-4′), 6.64 (s, 1H, CH-4), 4.59 (d, J = 8.3 Hz, 1H, CH-7), 4.24 (dd, J = 11.8, 6.4 Hz, 1H, CH-8a), 3.84 (s, 3H, OCH_3-5), 3.59 (s, 3H, OCH_3-6), 3.49 (dd, J = 12.6, 6.7 Hz, 1H, CH_2-2α), 3.14 (dd, J = 12.6, 10.5 Hz, 1H, CH_2-2β), 2.81 (m, 1H, CH_2-3α), 2.72 (m, 1H, CH_2-3β), 2.50 (dd, J = 11.8, 6.4 Hz, 1H, CH_2-8α), 2.35 (dd, J = 11.8, 8.3 Hz, 1H, CH_2-8β); HRESIMS *m/z* 296.1637 $[M + H]^+$ (296.1651, calc for $C_{19}H_{22}NO_2$).

4.3. 7-Phenyl-1,2,3,7,8,8a-hexahydrocyclopenta[ij]isoquinoline-5,6-diol (*3a*)

Brown oil (88% yield). ^{1}H NMR (500 MHz, CD_3OD): δ = 7.25 (t, J = 7.7 Hz, 2H, CH-3′ and CH-5′), 7.19 (d, J = 7.7 Hz, 2H, CH-2′ and

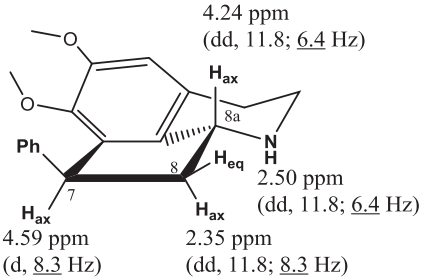

HCPIQ **3**

Fig. 2. Relative stereochemistry of HCPIQ **3**.

Table 1
Values of affinity (Ki, pK_i) and selectivity (ratio Ki D_1/Ki D_2) determined in binding experiments to D_1 and D_2 DR.

Cmpd	[^{3}H]-SCH 23390[a]		[^{3}H]-raclopride[a]		Ki ratio
	Ki (μM)[b]	pKi[b]	Ki (μM)[b]	pKi[b]	D_1/D_2
3	33.373 ± 6.891	4.499 ± 0.104	10.977 ± 1.933	4.972 ± 0.071	3.0[c]
3a	71.493 ± 16.281	4.174 ± 0.117	0.029 ± 0.009	7.593 ± 0.184[f]	2465.3[e]
3b	23.780 ± 4.549	4.640 ± 0.084	4.188 ± 1.348	5.422 ± 0.137[g]	5.7[d]
3c	13.136 ± 2.452	4.895 ± 0.076[h]	0.013 ± 0.002	7.890 ± 0.083[i]	1010.5[e]
3d	18.620 ± 4.822	4.758 ± 0.109	3.514 ± 0.654	5.472 ± 0.092[g]	5.29[d]
3e	6.873 ± 1.391	5.179 ± 0.085[h]	0.018 ± 0.007	7.800 ± 0.160[j]	381.8[e]

[a] Specific radioligands are [^{3}H]-SCH 23390 and [^{3}H]-raclopride for D_1 and D_2 dopamine receptors, respectively.
[b] Data were displayed as mean ± SEM of $n = 3$ independent experiments. ANOVA, post Newmann–Keuls multiple comparison tests.
[c] $p < 0.05$ vs D_1-like dopaminergic receptor.
[d] $p < 0.01$ vs D_1-like dopaminergic receptor.
[e] $p < 0.001$ vs D_1-like dopaminergic receptor.
[f] $p < 0.001$ vs **3**.
[g] $p < 0.05$ vs **3**.
[h] $p < 0.001$ vs **3a**.
[i] $p < 0.001$ vs **3b**.
[j] $p < 0.001$ vs **3d**.

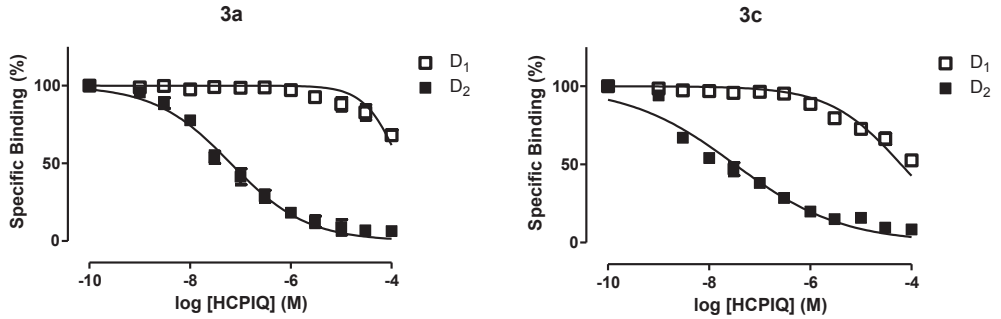

Fig. 3. Displacement curves of [^{3}H]-SCH 23390 (D_1) and [^{3}H] raclopride (D_2) specific binding by compounds **3a** vs **3c**. Data were displayed as mean ± SEM for 3 experiments.

CH-6′), 7.17 (m, 1H, CH-4′), 6.70 (s, 1H, CH-4), 4.66 (dd, $J = 9.0$, 6.6 Hz, 1H, CH-8a), 4.63 (d, $J = 8.1$ Hz, 1H, CH-7), 3.78 (dd, $J = 13.1$, 6.8 Hz, 1H, CH_2-2α), 3.51 (ddd, $J = 13.1$, 11.4, 6.8 Hz, 1H, CH_2-2β), 3.05 (dd, $J = 11.4$, 6.8 Hz, 1H, CH_2-3α), 2.97 (dd, $J = 13.1$, 6.8 Hz, 1H, CH_2-3β), 2.69 (dd, $J = 12.1$, 8.1 Hz, 1H, CH_2-8α), 2.62 (d, $J = 12.1$, 6.6 Hz, 1H, CH_2-8β); HRESIMS *m/z* 268.1331 $[M + H]^+$ (268.1338, calc for $C_{17}H_{18}NO_2$).

4.4. 1-Methyl-7-phenyl-1,2,3,7,8,8a-hexahydrocyclopenta[ij] isoquinoline-5,6-diol (**3c**)

Green oil (94% yield). ^{1}H NMR (500 MHz, CD_3OD): $\delta = 7.26$ (t, $J = 7.5$ Hz, 2H, CH-3′ and CH-5′), 7.16 (m, 2H, CH-2′ and CH-6′), 7.14 (m, 1H, CH-4′), 6.48 (s, 1H, CH-4), 4.42 (d, $J = 8.4$ Hz, 1H, CH-7), 3.38 (m, 1H, CH-8a), 3.07 (m, 1H, CH_2-2α), 2.72 (m, 1H, CH_2-3α), 2.63 (m, 1H, CH_2-3β), 2.49 (m, 1H, CH_2-2β), 2.36 (m, 1H, CH_2-8α), 2.20 (s, 3H, NCH_3), 2.14 (m, 1H, CH_2-8β); HRESIMS *m/z* 282.1495 $[M + H]^+$ (282.1494, calc for $C_{18}H_{20}NO_2$).

4.5. 1-Allyl-7-phenyl-1,2,3,7,8,8a-hexahydrocyclopenta[ij] isoquinoline-5,6-diol (**3e**)

Brown oil (90% yield). ^{1}H NMR (500 MHz, CD_3OD): $\delta = 7.24$ (t, $J = 7.2$ Hz, 2H, CH-3′ and CH-5′), 7.18 (d, $J = 7.2$ Hz, 2H, CH-2′ and CH-6′), 7.14 (m, 1H, CH-4′), 6.52 (s, 1H, CH-4), 5.87 (dddd, $J = 17.3$, 10.2, 8.0, 4.8 Hz, 1H, CH-2″), 5.18 (d, $J = 17.3$ Hz, 1H, CH_2-3″α), 5.09 (d, $J = 10.2$ Hz, 1H, CH_2-3″β), 4.49 (d, $J = 8.5$ Hz, 1H, CH-7), 3.45 (dd, $J = 10.4$, 6.0 Hz, 1H, CH-8a), 3.39 (dd, $J = 13.8$, 4.8 Hz, 1H, CH_2-1″α), 3.16 (dd, $J = 11.8$, 6.4 Hz, 1H, CH_2-2α), 2.72 (m, 1H, CH_2-3α), 2.68 (dd, $J = 13.8$, 8.2 Hz, 1H, CH_2-1″β), 2.65 (dd, $J = 16.4$, 6.0 Hz, 1H, CH_2-8α), 2.64 (dd, $J = 11.8$, 6.4 Hz, 1H, CH_2-3β), 2.41 (dd, $J = 11.8$, 5.9 Hz, 1H, CH_2-2β), 2.22 (m, 1H, CH_2-8β); HRESIMS *m/z* 308.1641 $[M + H]^+$ (308.1651, calc for $C_{20}H_{22}NO_2$).

4.6. 5,6-Dimethoxy-1-methyl-7-phenyl-1,2,3,7,8,8a-hexahydrocyclopenta-[ij]-isoquinoline (**3b**)

White oil. (82% yield). HRESIMS *m/z* 310.1797 $[M + H]^+$ (310.1807, calc for $C_{20}H_{24}NO_2$).

4.7. 1-Allyl-5,6-dimethoxy-7-phenyl-1,2,3,7,8,8a-hexahydrocyclopenta[ij]-isoquinoline (**3d**)

Brown oil (89% yield). HRESIMS *m/z* 336.1956 $[M + H]^+$ (336.1964, calc for $C_{22}H_{26}NO_2$).

4.8. Binding experiments

These experiments were performed on striatal membranes. Each striatum was homogenized in 2 mL ice-cold Tris–HCl buffer (50 mM, pH = 7.4 at 22 °C) with a Polytron (4s, maximal scale) and immediately diluted with Tris buffer. The homogenate was centrifuged either twice ([^{3}H] SCH 23390 binding experiments) on four times ([^{3}H] raclopride binding experiments) at 20000 g for 10 min at 4 °C with resuspension in the same volume of Tris buffer between centrifugations. For [^{3}H] SCH 23390 binding experiments, the final pellet was resuspended in Tris buffer containing 5 mM $MgSO_4$, 0.5 mM EDTA and 0.02% ascorbic acid (Tris-Mg buffer), and the suspension was briefly sonicated and diluted to a protein concentration of 1 mg/mL. A 100 μL aliquot of freshly prepared

membrane suspension (100 μg of striatal protein) was incubated for 1 h at 25 °C with 100 μL Tris buffer containing [^{3}H] SCH 23390 (0.25 nM final concentration) and 800 μL of Tris-Mg buffer containing the required drugs. Non-specific binding was determined in the presence of 30 μM SK&F 38393 and represented around 2–3% of total binding. For [^{3}H] raclopride binding experiments, the final pellet was resuspended in Tris buffer containing 120 mM NaCl, 5 mM KCl, 1 mM $CaCl_2$, 1 mM $MgCl_2$ and 0.1% ascorbic acid (Tris-ions buffer), and the suspension was treated as described above. A 200 μL aliquot of freshly prepared membrane suspension (200 μg of striatal protein) was incubated for 1 h at 25 °C with 200 μL of Tris buffer containing [^{3}H] raclopride (0.5 nM, final concentration) and 400 μL of Tris-ions buffer containing the drug under investigation. Non-specific binding was determined in the presence of 50 μM apomorphine and represented around 5–7% of the total binding. In both cases, incubations were stopped by addition of 3 mL of ice-cold buffer (Tris-Mg buffer or Tris-ions buffer, as appropriate) followed by rapid filtration through Whatman GF/B filters. Tubes were rinsed with 3 mL of ice-cold buffer, and filters were washed with 3 × 3 mL ice-cold buffer. After the filters had been dried, radioactivity was counted in 4 mL BCS scintillation liquid at an efficiency of 45%. Filter blanks corresponded to approximately 0.5% of total binding and were not modified by drugs.

4.9. MTT assay

The viability of neutrophils was determined using the previously described MTT (3-(4,5-dimethylthiazol-2-yl)-2,5-diphenyltetrazolium bromide) colorimetric assay. In this assay, the yellow MTT is reduced to a blue formazan product by the mitochondria of viable cells. MTT (Sigma–Aldrich) was prepared at 1 mg/mL in RPMI and stored at 4 °C in the dark. 100 μl of neutrophils suspension (2×10^5 cells/mL) was added to each well of a 96-well microtiter plate followed by 20 μl of the appropriate concentration of the THPBs tested. The mixture was incubated at 37 °C for 24 h. Then, 100 μl aliquot of MTT solution was added to each well and incubated at 37 °C for another 60 min. The supernatants were discarded and 100 μl of DMSO was added to each well to dissolve the precipitated formazan. The optical densities at dual wavelengths (570 and 630 nm) were determined in a spectrophotometer (Infinite M200, Tecan, Mannedorf, Switzerland).

Acknowledgements

This work was supported by the Spanish Ministry of Education, Culture and Sport, SAF2011-23777, Spanish Ministry of Economy and Competitiveness, the European Regional Development Fund (FEDER) and research grants from Generalitat Valenciana (GVA-COMP2014-006). A.G. (FPU12/00744) is thankful to the Spanish Ministry of Education, Culture and Sport for a fellowship from FPU program.

Appendix A. Supplementary data

Supplementary data related to this article can be found at http://dx.doi.org/10.1016/j.ejmech.2014.11.009.

References

[1] K.W. Bentley, β-Phenylethylamines and the isoquinoline alkaloids, Nat. Prod. Rep. 23 (2006) 444.
[2] K.W. Bentley, β-Phenylethylamines and the isoquinoline alkaloids, Nat. Prod. Rep. 22 (2005) 249.
[3] K.W. Bentley, β-Phenylethylamines and the isoquinoline alkaloids, Nat. Prod. Rep. 21 (2004) 395.
[4] V.I. Nikulin, I.M. Rakov, J.E. De Los Angeles, R.C. Metha, L.Y. Boyd, D.R. Feller, D.D. Miller, Bioorg. Med. Chem. 14 (2006) 1684.
[5] K. Takada, T. Uehara, Y. Nakao, S. Matsunaga, R.W. van Soest, N.J. Fusetani, Schulzeines A–C, new α-glucosidase inhibitors from the marine sponge *Penares schulzei*, J. Am. Chem. Soc. 126 (2004) 187.
[6] K.T. Warner, H. Beer, G. Höfner, M. Ludwig, Asymmetric synthesis and enantioselectivity of binding of 1-aryl-1,2,3,4-tetrahydroisoquinolines at the *PCP* site of the *NMDA* receptor complex, Eur. J. Org. Chem. (1998) 2019.
[7] N. Cabedo, I. Berenguer, B. Figadère, D. Cortes, An overview on benzylisoquinoline derivatives with dopaminergic and serotonergic activities, Curr. Med. Chem. 16 (2009) 2441.
[8] A. Bermejo, P. Protais, M.A. Blázquez, K.S. Rao, M.C. Zafra-Polo, D. Cortes, Dopaminergic isoquinoline alkaloids from roots of *Xylopia papuana*, Nat. Prod. Lett. 6 (1995) 57.
[9] I. Berenguer, N. El Aouad, S. Andujar, V. Romero, F. Surive, T. Freret, A. Bermejo, M.D. Ivorra, R.D. Enriz, M. Boulouard, N. Cabedo, D. Cortes, Tetrahydroisoquinolines as dopaminergic ligands: 1-Butyl-7-chloro-6-hydroxy-tetrahydroisoquinoline, a new compound with antidepressant-like activity in mice, Bioorg. Med. Chem. 17 (2009) 4968.
[10] P. Protais, J. Arbaoui, E.H. Bakkali, A. Bermejo, D. Cortes, Effects of various isoquinoline alkaloids on in vitro ^{3}H-dopamine uptake, J. Nat. Prod. 58 (1995) 1475.
[11] N. Cabedo, P. Protais, B.K. Cassels, D. Cortes, Synthesis and dopamine receptor selectivity of the benzyltetrahydroisoquinoline, (*R*)-(+)-*nor*-roefractine, J. Nat. Prod. 61 (1998) 709.
[12] I. Andreu, D. Cortes, P. Protais, B.K. Cassels, A. Chagraoui, N. Cabedo, Preparation of dopaminergic *N*-alkyl-benzyltetrahydroisoquinolines using a 'One-Pot' procedure in acid medium, Bioorg. Med. Chem. 8 (2000) 889.
[13] N. Cabedo, I. Andreu, M.C. Ramírez de Arellano, A. Chagraoui, A. Serrano, A. Bermejo, P. Protais, D. Cortes, Enantioselective syntheses of dopaminergic (*R*)- and (*S*)-benzyltetrahydroisoquinolines, J. Med. Chem. 44 (2001) 1794.
[14] I. Andreu, N. Cabedo, G. Torres, A. Chagraoui, M.C. Ramirez de Arellano, S. Gil, A. Bermejo, M. Valpuesta, P. Protais, D. Cortes, Syntheses of dopaminergic 1-cyclohexylmethyl-7,8-dioxygenated tetrahydroisoquinolines by selective heterogeneous tandem hydrogenation, Tetrahedron 58 (2002) 10173.
[15] F.D. Suvire, N. Cabedo, A. Chagraoui, M.A. Zamora, D. Cortes, R.D. Enriz, Molecular recognition and binding mechanism of *N*-alkyl-benzyltetrahydroisoquinolines to the D_1 dopamine receptor. A computational approach, J. Mol. Struct. (Teochem.) 666–667 (2003) 455.
[16] N. El Aouad, I. Berenguer, V. Romero, P. Marín, A. Serrano, S. Andujar, F. Suvire, A. Bermejo, M.D. Ivorra, R.D. Enriz, N. Cabedo, D. Cortes, Structure-activity relationship of dopaminergic halogenated 1-benzyl-tetrahydroisoquinoline derivatives, Eur. J. Med. Chem. 44 (2009) 4616.
[17] S. Andujar, F. Suvire, I. Berenguer, N. Cabedo, P. Marín, L. Moreno, M.D. Ivorra, D. Cortes, R.D. Enriz, Tetrahydroisoquinolines acting as dopaminergic ligands. A molecular modeling study using MD simulations and QM calculations, J. Mol. Model. 18 (2012) 419.
[18] S.A. Andujar, R.D. Tosso, F.D. Suvire, E. Angelina, N. Peruchena, N. Cabedo, D. Cortes, R.D. Enriz, Searching the biologically relevant conformation of dopamine: a computational approach, J. Chem. Inf. Model. 52 (2012) 99.
[19] J. Párraga, N. Cabedo, S. Andújar, L. Piqueras, L. Moreno, A. Galán, E. Angelina, R.D. Enriz, M.D. Ivorra, M.J. Sanz, D. Cortes, 2,3,9- and 2,3,11-Trisubstituted tetrahydroprotoberberines as D_2 dopaminergic ligands, Eur. J. Med. Chem. 68 (2013) 150.
[20] L. Moreno, N. Cabedo, M.D. Ivorra, M.J. Sanz, A. López-Castel, M.C. Alvarez, D. Cortes, 3,4-Dihydroxy- and 3,4-methylenedioxy phenanthrene-type alkaloids with high selectivity for D_2 dopamine receptor, Bioorg. Med. Chem. Lett. 23 (2013) 4824.
[21] P.M. Luthra, J.B. Kumar, Plausible improvements for selective targeting of dopamine receptors in therapy of Parkinson's disease, Mini Rev. Med. Chem. 14 (2012) 1556.
[22] A. Zhang, J.L. Neumeyer, R.J. Baldessarini, Recent progress in development of dopamine receptor subtype-selective agents: potential therapeutics for neurological and psychiatric disorders, Chem. Rev. 107 (2007) 274.
[23] P.J. Conn, A. Christopoulos, C.W. Lindsley, Allosteric modulators of GPCRs: a novel approach for the treatment of CNS disorders, Nat. Rev. Drug Discov. 8 (2009) 41.
[24] J.M. Beaulieu, R.R. Gainetdinov, The physiology, signaling, and pharmacology of dopamine receptors, Pharmacol. Rev. 63 (2011) 182.
[25] W. Poewe, Treatments for Parkinson disease-past achievements and current clinical needs, Neurology 72 (2009) S65.
[26] K. Bernauer, Über die synthese des pronuciferins und einiger weiterer proaporphin-alkaloid. 6. Mitteilung über natürliche und synthetische isochinolinderivate, Helv. Chim. Acta 51 (1968) 1119.
[27] C. Casagrande, L. Canonica, G. Severini-Ricca, Studies on proaporphine and aporphine alkaloids. Part VII. Stereoselectivity of reduced proaporphines of *Croton sparsiflorus* and *C. linearis*, J. Chem. Soc. Perkin Trans. 1 (1975) 1659.
[28] S. Ponnala, W.W. Harding, A new route to azafluoranthene natural products via direct arylation, Eur. J. Org. Chem. (2013) 1107.
[29] G.L. Grunewald, D.J. Sall, J.A. Monn, Conformational and steric aspects of the inhibition of phenylethanolamine *N*-methyltransferase by benzylamines, J. Med. Chem. 31 (1988) 433.
[30] N. Ye, C.-H. Chen, T.T. Chen, Z. Song, J.-X. He, X.-J. Huan, S.-S. Song, Q. Liu, Y. Chen, J. Ding, Y. Xu, Z.-H. Miao, A. Zhang, Design, synthesis, and biological evaluation of a series of benzo[*de*][1,7]naphthyridin-7(8H)-ones bearing a

functionalized longer chain appendage as novel PARP1 inhibitors, J. Med. Chem. 56 (2013) 2885.
[31] J.W. Huffman, E. Opliger, The synthesis of (±)-hexahydropronuciferine and related compounds, J. Org. Chem. 6 (1971) 111.
[32] H.A. Patel, D.B. McLean, Synthesis of indeno[l,2,3-ijlisoquinolines, Can. J. Chem. 61 (1983) 7.
[33] J.C. Pelletier, M.P. Cava, Synthesis of the marine alkaloids aaptamine and demethyloxyaaptamine and of the parent structure didemethoxyaaptamine, J. Org. Chem. 52 (1987) 616.
[34] J.-S. Ryu, G.Y. Li, T.J. Marks, Organolathanide-catalyzed regioselective intermolecular hydroamination of alkenes, alkynes, vinylarenes, di- and trivinylarenes, and methylenecyclopropanes. Scope and mechanistic comparison to intramolecular cyclohydroaminations, J. Am. Chem. Soc. 125 (2003) 12584.
[35] A. Fournet, M.E. Ferreira, A. Rojas de Arias, I. Guy, H. Guinaudeau, H. Heinzen, Phytochemical and antiprotozoal activity of *Ocotea lancifolia*, Fitoterapia 78 (2007) 382.
[36] E.P. Eaton, G.R. Carlson, J.T. Lee, Phosphorus pentoxide-methanesulfonic acid. Convenient alternative to polyphosphoric acid, J. Org. Chem. 38 (1972) 4071.

DOI: 10.1002/minf.201400093

3-Chlorotyramine Acting as Ligand of the D_2 Dopamine Receptor. Molecular Modeling, Synthesis and D_2 Receptor Affinity

Emilio Angelina,[a, d] Sebastian Andujar,*[a, b] Laura Moreno,[c] Francisco Garibotto,[a, b] Javier Párraga,[c] Nelida Peruchena,[d] Nuria Cabedo,[e] Margarita Villecco,[f] Diego Cortes,[c] and Ricardo D. Enriz[a, b]

Abstract: We synthesized and tested 3-chlorotyramine as a ligand of the D_2 dopamine receptor. This compound displayed a similar affinity by this receptor to that previously reported for dopamine. In order to understand further the experimental results we performed a molecular modeling study of 3-chlorotyramine and structurally related compounds. By combining molecular dynamics simulations with semiempirical (PM6), ab initio and density functional theory calculations, a simple and generally applicable procedure to evaluate the binding energies of these ligands interacting with the D_2 dopamine receptors is reported here. These results provided a clear picture of the binding interactions of these compounds from both structural and energetic view points. A reduced model for the binding pocket was used. This approach allowed us to perform more accurate quantum mechanical calculations as well as to obtain a detailed electronic analysis using the Quantum Theory of Atoms in Molecules (QTAIM) technique. Molecular aspects of the binding interactions between ligands and the D_2 dopamine receptor are discussed in detail. A good correlation between the relative binding energies obtained from theoretical calculations and experimental IC50 values was obtained. These results allowed us to predict that 3-chlorotyramine possesses a significant affinity by the D_2-DR. Our theoretical predictions were experimentally corroborated when we synthesized and tested 3-chlorotyramine which displayed a similar affinity by the D_2-DR to that reported for DA.

Keywords: 3-Chlorotyramine · MD simulations · QTAIM analysis · D_2 dopamine receptor

1 Introduction

In the past the potential clinical usefulness of centrally acting dopamine receptor (DR) agonists has stimulated intense research on new dopaminergic agents. Thus, in general, different efforts in medicinal chemistry and neuropharmacology have yield substantial numbers of compounds with activity and selectivity at each of the major DRs.[1–6] Particularly noteworthy is the work of Reutlinger, et al. who have recently reported the development and application of a computational molecular design method for obtaining bioactive compounds with desired on- and off target binding.[7] The authors used the molecular algorithm (MAntA)[8] which effectively transfers a nature-inspired optimization

[a] *E. Angelina, S. Andujar, F. Garibotto, R. D. Enriz*
Instituto Multidisciplinario de Investigaciones Biologicas (IMIBIO-SL -CONICET)
Chacabuco 915, 5700 San Luis, Argentina
phone: (54) 2652.423789
**e-mail: saanduja@unsl.edu.ar*

[b] *S. Andujar, F. Garibotto, R. D. Enriz*
Facultad de Química, Bioquímica y Farmacia, Universidad Nacional de San Luis
Chacabuco 915, 5700 San Luis, Argentina

[c] *L. Moreno, J. Párraga, D. Cortes*
Departamento de Farmacología, Laboratorio de Fármacoquímica, Facultad de Farmacia, Universidad de Valencia
46100 Burjassot, Valencia, España

[d] *E. Angelina, N. Peruchena*
Laboratorio de Estructura Molecular y Propiedades, Área de Química Física, Departamento de Química, Facultad de Ciencias Exactas y Naturales y Agrimensura, Universidad Nacional del Nordeste
Avda. Libertad 5460, (3400) Corrientes, Argentina

[e] *N. Cabedo*
Centro de Ecología Química Agrícola-Instituto Agroforestal Mediterráneo, Universidad Politécnica de Valencia, Campus de Vera
Edificio 6C, 46022 Valencia, España,

[f] *M. Villecco*
Instituto de Química Orgánica, Facultad de Bioquímica Química y Farmacia, Universidad Nacional de Tucumán
Ayacucho 471, S. M. de Tucumán, T4000INI. Argentina

Supporting Information for this article is available on the WWW under http://dx.doi.org/10.1002/minf.201400093.

principle to chemistry-driven molecular design; and they successfully designed antagonist compounds for the dopamine D4 receptor demonstrating the successful application of MAntA to dopamine receptors. However, despite the efforts of these authors, in general the design and development of DR-selective ligands remains largely empirical, quite conservative in following molecular precedents, somewhat unpredictable and not ready for routine applications of computer-aided drug design techniques. The computational limitations and/or errors can arise in many ways depending on the methodology: some possibilities include errors in the structure of the host, choice of ionization state, structure of the complex, inadequate sampling of internal degrees of freedom and the so called "ligand-receptor stereo-electronic problem.

In order to obtain new dopaminergic agonists, The dopamine molecule (compound **1** in Figure 1) has been modified on the amino group, on the ethylamine chain, and on the catechol moiety as well.[9–17] Claudi et al. reported the synthesis and binding affinity for D_1 and D_2 subtypes of DRs of 2-(4-fluoro-3-hydroxyphenyl)ethylamine (compound **7**, Figure 1).[16] This compound showed about two-fold lower affinity than dopamine for both binding sites. Previously Cardinelli et al reported low activity for other fluorine derivatives of dopamine including 2-(3-fluoro-4-hydroxyphenyl)ethylamine (compound **6**).[15] Studies on aminotetralins showed that 2-amino-6-chloro-7-hydroxytetralins (compound **8**) are weakly effective in the binding assays.[18] In addition Claudi et al. reported that 2-chlorothyramine (compound **2**) is not able to discriminate between the two subtypes of dopamine receptors (D_1 and D_2), and has sevenfold lower affinity than dopamine for both sites.[17]

It must be pointed out that although 3-chlorotyramine (2-(3-chloro-4-hydroxyphenyl)ethanaminium chloride) (compound **3**) has been previously reported by Fuller[19] in 1971 and Stark and Fuller[20] in 1972; however, according to our bibliographic information, the dopaminergic effect of compound **3** has not been analyzed yet as a D_2-DR ligand. One possible explanation for this is that due to the low activity obtained for the analogues of this compound, compound **3** has been directly discarded as a potential ligand of interest for the D_2-DR.

The replacement of OH group by halogen introduces significant changes in the biological response of these ligands. For example it is interesting to note that in the series of benzazepines the 2,3,4,5-tetrahydro-7,8-dihidro-3-methyl-1-phenyl-1*H*-3-benzazepine (compound **9**) had only micromolar affinity at D_1 and D_2 receptors.[21] However 2,3,4,5-tetrahydro-7-chloro-8-hydroxy-3-methyl-1-phenyl-1*H*-3-benzazepine (compound **10**), obtained by replacing the 7-OH of **9** with a chlorine, has nanomolar affinity possessing a high selectivity by D1 receptors. In the same way our own studies performed on a series of benzyl-tetrahydroisoquinolines (BTHIQs) indicated that the presence of a chlorine group at C7 is very important for the adrenergic effect of such derivatives (compounds **11**–**14**).[22–24] In fact such BTHIQs possessing a chlorine group at C7 displayed the strongest affinity for both D_1 and D_2 DRs in this series.[23] It should be noted that the inductive effect of chlorine could influence the acidity of the phenolic group and produce different interactions at the binding pocket altering the affinity for D_2-DR. One question which arises is if compound **3**, which has not been previously studied as a D_2-DR ligand, have low or high affinity for this receptor and in either case try to find an explanation at sub-molecular level for such behavior. Another question which might arise is why to evaluate compound **3** and why now? There are different reasons to analyze this molecule with the computational approaches now available. On one hand it is possible to exploit recent information obtained for dopamine with respect to its biologically relevant conformation.[25] On the other hand is also now possible to study with some accuracy the electronic effects introduced to the ligand when replacing an OH by Cl and the effects of such change when the ligand is interacting with its biological receptor. Recently we reported a comprehensive conformational study of dopamine interacting with the D_2-DR, using a combination of molecular dynamics (MD) simulations, semiempirical and DFT calculations.[25] In addition, a detailed electronic analysis using Quantum Theory of Atoms in Molecules (QTAIM)[26–28] technique was also carried out. By using this approach it is possible to evaluate with some details the conformational and electronic behaviours of dopamine and its halogenated derivatives.

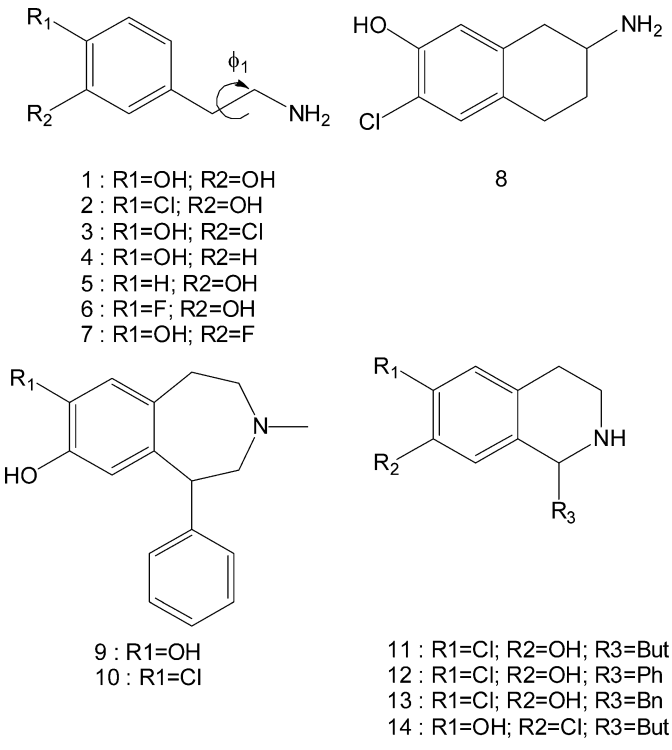

Figure 1. Structural feature of dopamine and derivatives.

Halogens, especially the lighter fluorine and chlorine, are widely used substituents in medicinal chemistry. Until recently, they were merely perceived as hydrophobic moieties and Lewis bases in accordance with their electronegativities. Much in contrast to this perception, compounds containing chlorine can also form directed close contacts of the type R–X·Y–R′, where the halogen X acts as a Lewis acid and Y can be any electron donor moiety. This interaction, referred to as "halogen bonding" since 1978[29] is driven by the σ-hole, a positively charged region on the hind side of X along the R–X bond axis that is caused by an anisotropy of electron density on the halogen.[30,31] The intriguing formal similarity between halogen bonding, R–X—B, and hydrogen bonding, R–H—B, has been noted and discussed in detail by Legon.[32,33] However, he also does point out that the hydrogen bond is more likely to be non-linear. In turn a halogen bond is a highly directional, electrostatically-driven non-covalent interaction between a region of positive electrostatic potential on the outer side of the halogen X in a molecule R–X and a negative site B, such as a lone pair of a Lewis base or the p-electrons of an unsaturated system. In a very elegant paper Politzer et al. have introduced the "σ-hole concept" allowing to explain the empirically-observed characteristics of halogen bonding: its marked directionality, its dependence upon the polarizability and electronegativity of the halogen atom, and the role of the electron-withdrawing power of the R portion of any molecule.[34]

In a recent review on different types of protein–ligand interactions relevant to medicinal chemistry,[35] the authors conclude that halogen bonds are a useful addition to the arsenal of favorable interactions in molecular recognition and can lead to significant affinity gains in some cases. There are a number of experimental studies where the effect of halogen substitution on binding affinity has been systematically evaluated.[36–38] The strengths of halogen bonds can be evaluated theoretically through quantum chemical model calculations. It is evident that halogen bonding is best described theoretically using high-level quantum chemical methods such as coupled cluster[39] (CCSD-(T)) and perturbation theory[40,41] (MP2) calculations; yet using these methods greatly limits the size of the model systems amenable to computational studies. Thus, much larger systems (like those studied here) can be treated using QM/MM calculations,[42,43] semiempirical studies[44] or using reduced model systems.[25]

Regarding the structural aspects of the D_2-DR it is well known that the binding of DA to the receptor is substantially affected by multiple serine/alanine mutations. The multiple mutations including a S193 susbstitution produce the greatest effect.[45,46] It has been previously reported that the effects of the multiple mutations were not additive, with the single serine mutation having relatively larger effects, which is indicative of a very precise network of hydrogen bonds between the TMV (transmembrane spanning region) serine residues and the catechol hydroxyls of the DA molecule.[47] A further interesting finding was that addition of a 4-hydroxyl group (p-tyramine) to beta-phenylethylamine (compound **4**) does not enhance affinity, but addition of a 3-hydroxyl group (*m*-tyramine) (compound **5**) is favorable. When the 3-and 4- hydroxyls are present (the case of dopamine), the affinity is enhanced over the effects of the individual hydroxyl groups. These results are consistent with a productive and specific interaction of the two hydroxyl groups of DA with a network of serine residues. Our previous results[25] suggested that the region near these serine residues may be rather mobile which is consistent with a model of receptor function where the binding of DA locks the receptor into a relatively rigid conformation with precise interactions between ligand and receptor.

On the other hand it is well-known that the non covalent interactions generally are weaker than the covalent ones; such interactions are more difficult to describe properly. However, recent advances in computational calculation of the electron charge density make possible the proper description of the three-dimensional network of bonding and non bonding interactions in biological systems[27,48–50] in the context of the quantum theory of atoms in molecules (QTAIM).[51] Starting with strong and moderated hydrogen bonds or halogen bonds, moving on to weaker polar interactions and ending with stacking and T-shape interactions between aromatic rings, all of them can be evaluated by QTAIM analysis.[52] In fact, nowadays it is well know that the stacking amino acids aromatic rings in proteins is evidently much more important than it has been previously believed and, indeed, can form one of the dominant stabilizing contributions.[28] Our previous results show that the interactions of the catechol OH groups of the ligand, in the different conformations of the dopamine/D_2-DR complex, determine the decrease or increase of the electron density on the aromatic ring of dopamine. In turn, the electronic population of the aromatic ring of dopamine defines its orientation within the binding site and the type of interactions that are established with the aromatic rings of the receptor. It is evident that a description non quantum mechanical of the problem would overlook these electronic effects that are crucial to understand the binding modes of the ligand within the receptor binding site.

We were particularly intrigued to know which is the affinity of compound **3** by the D_2-DR and whether it was possible to explain such behavior through computational simulations. Thus, first we synthesized and tested compound **3** as a D_2-DR ligand. Whereas this compound showed an affinity comparable to that reported for dopamine in a second stage of our study we performed MD simulations for the complexes of compounds **1–5** with the D_2-DR. It should be noted that these compounds were carefully selected in function of their substituents at the catecholic portion. The selected compounds were: compounds **4** and **5** possessing only one hydroxyl group at *para* and *meta* position, respectively and compounds **2** and **3** possessing chlorine and hydroxyl groups at *para* and *meta* positions,

respectively. We also include in our comparative study dopamine (compound **1**), possessing the catecholic ring. The next step was to construct a reduced model for the binding site which allowed us to perform more accurate quantum mechanical calculations. The fourth step was to simulate the molecular interactions between the different ligands and the D_2-DR using a QTAIM analysis; being the principal goal of such calculations try to obtain a detailed description of the molecular interactions which stabilize and destabilize the different complexes. It is clear that a detailed analysis of the such interactions would be of paramount importance to determine the intricacies of the network of serine residues located at the binding pocket of the D_2-DR. Finally, we performed a comparative analysis among the different complexes and the conclusions are put forward in the last section.

2 Methods

2.1 Chromatographic and Spectroscopic Analysis

The reaction was monitored by analytical TLC with silicagel 60 F_{254} (Merck 5554). The residue was purified through silica gel C–18 (SPE, Alltech, 100 mg/1.5 mL) column chromatography. Isolation and purification was carried out by a Waters HPLC system with a 600 pump and both a 2996 Photodiode Array Detector (PDA) and ELSD 2420 Detector (Milford, MA). ^{1}H, NMR spectra was recorded on a Bruker AV 300 MHz instrument (Rheinstetten, Germany). Chemical shifts (δ) are reported in ppm for a solution of the compound in $CDCl_3$ and the coupling constants (J) values are given in Hz. High resolution ESIMS (electrospray) data were carried out on a Micromass Q-TOF Micro coupled with a HPLC Waters Alliance 2695 (Milford, MA). The instrument was calibrated by using a PEG mixture from 200 to 1000 MW (resolution specification 5000 FWHM, deviation $<$5 ppm RMS in the presence of a known lock mass). The HCl salts of the synthesized compounds were prepared from the corresponding base with 5% HCl in MeOH. *N*-(4-benzyloxy)-3-chlorophenethyl)benzamide was prepared by standard methods from 3-chloro-4-methoxybenzaldehyde and benzoyl chloride.[22]

2.2 Synthesis of 3-Chlorothyramine (3)

A solution of the *N*-(4-benzyloxy)-3-chlorophenethyl)benzamide (1, 20 mg, 0.055 mmol) in a mixture of 2.5 N HCl/HOAc (4:1 mL) was heated for 42 h at 100 °C. Then, the solvent was removed under reduced pressure and the residue partitioned between H_2O/EtOAc. The phases were separated and the acid aqueous layer evaporated under reduced pressure to give a residue which was purified by column chromatography C–18 (SPE, Alltech, 100 mg/1.5 mL) and eluted in a gradient from 100% H_2O to 100% MeOH. The first fraction eluted with H_2O/MeOH (9:1) was evaporated and purified by semi-preparative HPLC using a Tracer Excel 120 ODS-B C18 column, 5 μm (25.0×1 cm), and MeOH/H_2O in 1% HOAc (20:80) as mobile phase with a flow of 2 mL/min. The 3-chloro-4-hydroxy-β-fenilethylamine (7 mg, 0.041 mmol, 75% yield) was isolated with a retention time (*Rt*) of 14.5 min as a white solid. ^{1}H NMR* (300 MHz, $CDCl_3$) δ 7.20 (s, 1H, H-2), 6.9 (s, 1H, H-6), 6.8 (s, 1H, H-5), 3.2 (m, 2H, CH_2-α), 2.8 (m, 2H, CH_2-β); ESMS *m/z* (%) 172 $[M+1]^+$ (39), 155 (100).

2.3 Binding Experiments

These experiments were performed on striatal membranes. Each striatum was homogenized in 2 mL ice-cold Tris-HCl buffer (50 mM, pH 7.4 at 22 °C) with a Polytron (4 s, maximal scale) and immediately diluted with Tris buffer. The homogenate was centrifuged on four times at 20000g for 10 min at 4 °C with resuspension in the same volume of Tris buffer between centrifugations. The final pellet was resuspended in Tris buffer containing 120 mM NaCl, 5 mM KCl, 1 mM CaCl2, 1 mM MgCl2 and 0.1% ascorbic acid (Tris-ions buffer), and the suspension was treated as described above. A 200 μL aliquot of freshly prepared membrane suspension (200 μg of striatal protein) was incubated for 1 h at 25 °C with 200 μL of Tris buffer containing [3H] raclopride (0.5 nM, final concentration) and 400 μL of Tris-ions buffer containing the drug under investigation. Non-specific binding was determined in the presence of 50 μM apomorphine and represented around 5–7% of the total binding. In both cases, incubations were stopped by addition of 3 mL of ice-cold buffer (Tris-Mg buffer or Tris-ions buffer, as appropriate) followed by rapid filtration through Whatman GF/B filters. Tubes were rinsed with 3 mL of ice-cold buffer, and filters were washed with 3×3 mL ice-cold buffer. After the filters had been dried, radioactivity was counted in 4 mL BCS scintillation liquid at an efficiency of 45%. Filter blanks corresponded to approximately 0.5% of total binding and were not modified by drugs.

2.4 Molecular Modeling

A 3D model of the human D_2-DR was used for the MD simulations. This model is based on the homology model from the crystallized D_3-DR, β_2 adrenoreceptor and A2α adenosine receptor as templates.[49,53,54]

Molecular docking simulations were performed with AutoDock4 program[55] using rotatable bonds in the ligands and flexible side chains in selected amino acids of the fifth transmembrane domain due to its implication in the formation of binding pocket.[47] Assignation of atomic partial charges (Gasteiger), rotable bonds as well as merging of non-polar hydrogens were performed with AutoDock Tools 1.5.2.[55] The ligands were then docked inside a cubic GRID box (70×70×70 Å, grid points separated by 0.375 Å) centered at the midpoint between the D114 and S194 alfa carbons (both residues conserved at the D_2-DR putative bind-

ing site). This docking simulation was achieved under the hybrid Lamarckian genetic algorithm with an initial population of 100 randomly placed individuals and a maximum number of energy evaluations set at 1×10^7. All of the other parameters were maintained at their default settings.[55] The resulting docked orientations within a root mean square deviation (*RMSD*) of 0.5 Å were clustered together. From the lowest energy cluster, the best ranked conformation for each compound was then soaked in boxes of explicit water using the TIP3P model[56] and subjected to MD simulation. All MD simulations were performed with the Amber software package (All-atoms force field FF99SB)[57,58] using periodic boundary conditions and cubic simulation cells. The particle mesh Ewald method (PME)[59,60] was applied using a grid spacing of 1.2 Å , a spline interpolation order of 4 and a real space direct sum cutoff of 10 Å. The SHAKE algorithm was applied allowing for an integration time step of 2 fs. MD simulations were carried out at 300 K target temperature and extended to 10 ns overall simulation time. Positional restraints were applied to all the backbone alpha carbons of the receptor except those of the transmembrane 5 (TM5) domain that were left free. The NPT ensemble was employed using Berendsen coupling to a baro/thermostat (target pressure 1 atm, relaxation time 0.1 ps). Post MD analysis was carried out with program PTRAJ.[57]

2.5 MM-GBSA Free Energy and Per-Reside Decomposition Analysis

The MM-GBSA protocol was applied to calculate the relative binding energies of the complexes by taking snapshots at 10 ps time intervals from the last 1000 ps of the MD trajectory.

In order to determine the residues involved in the complexes intermolecular interactions, a per-reside free energy decomposition analysis using the mm_pbsa program in AMBER[61,62] was performed.

2.6 Quantum Mechanics Calculations and Topological Study of the Electron Charge Density Distribution

Reduced 3D models systems representing the D_2-DR binding pocket in the five molecular complexes **1**/D_2-DR, **2**/D_2-DR, **3**/D_2-DR, **4**/D_2-DR and **5**/D_2-DR were constructed from the coordinates of the potential energy minimum during the molecular dynamics simulation trajectory. Then, geometrical optimizations of the reduced model systems were carried out at semiempirical level employing a PM6 method with halogen bonding correction (PM6-D2X)[63] included in the MOPAC program.[64] The optimized models were then used as input for the calculation of the electron charge density topological analysis. Single point calculations were computed with Gaussian 03[65] employing a hybrid PBE functional and 6-31G(d) as basis set.

The topological properties of a scalar field such as ρ(r) are summarized in terms of their critical points, i.e., the points r_c where $\Delta\rho(r)=0$. Critical points are classified according to their type (ω,σ) by stating their rank, ω, and signature, σ. The rank is equal to the number of nonzero eigenvalues of the Hessian matrix of $\rho(r)$ at r_c, while the signature is the algebraic sum of the signs of the eigenvalues of this matrix. Critical points of (3, −1) and (3, +1) type describe saddle points, while the (3, −3) is a maximum and (3, +3) is a minimum in the field. Among these critical points, the (3, −1) or bond critical points are the most relevant ones since they are found between any two atoms linked by a chemical bond. The determination of all the bond critical points and the corresponding bond paths connecting these point with bonded nuclei, were performed with the AIMAll software.[66]

3 Results and Discussion

As was pointed out in the introduction it is curious that until now it has not been reported the affinity for the D_2-DR of compound **3** which is relatively a simple molecule, at least from a structural point of view. One possible reason is that in that moment when the structurally related compounds were studied, this compound was discarded without an exhaustive analysis. It is also fair to note that at the time in which the analogues of compound **3** were reported it was not possible to perform theoretical calculations with a relatively detailed electronic analysis as has been done in this work. Anyway, the first thing we did was to synthesize compound 3 and then test its affinity for the D_2-DR.

3.1 Synthesis and Binding Affinity of 3-Chlorotyramine (Compound 3)

Compound **3** has been previously obtained by the Chung's method,[67] which consists in the oxidative chlorination of phenols with HCl and *m*-chloro perbenzoic acid (*m*-CPBA) in *N*,*N*-dimethyl formamide, and also using an enzymatic procedure.[68] In the course of our work on the synthesis of 1-substituted-1,2,3,4-tetrahydroisoquinolines,[22] the availability of the *N*-(4-(benzyloxy)-3-chlorophenethyl)benzamide (**1**) allowed us to obtain compound **3** by hydrolysis of the benzamide bond. Initially and unsuccessfully, various basic and acid conditions excessively strong for the hydrolysis of the benzamide (**1**) were assayed. Finally, we used a hydrolysis reaction in milder conditions,[69] a mixture of 2.5 N HCl/HOAc (4 : 1) at reflux for 42 h, which afforded the 3-chlorinated dopamine analogue (compound **3**) in good yield (Scheme 1).

In order to minimize the experimental errors due to the methodology employed we used a very similar experimental protocol to that reported in reference.[70] Our experimental measurements indicated that compounds **3** possess a *Ki* value of 0.146 μM. It should be noted that this compound displayed a significant affinity by the D_2-DR; In fact this compound displayed an affinity very similar to that re-

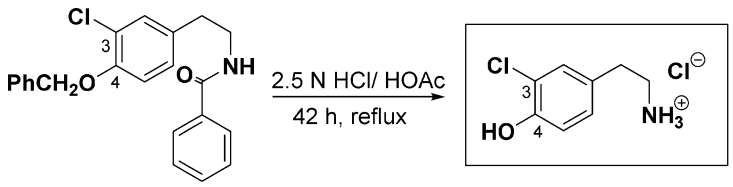

benzamide

3-chlorotyramine hydrochloride (compound **3**)

Scheme 1. Scheme of synthesis of compound **3.**

ported for the endogen ligand DA ($Ki = 0.52$ μM).[70] This result was somewhat surprising to us since we expected a lower affinity for compound **3** relative to dopamine. After all the affinity reported for compound **2** is significantly lower than that of dopamine.[17] From these results we performed a molecular modeling study in which we analyzed exhaustively the molecular interactions in order to better understand these experimental results.

3.2 Molecular Dynamic Simulations

Comparing the MD trajectories obtained for the different complexes, interesting general conclusions might be obtained. Consistent with previous experimental[45–47] and theoretical[24,25] results, our simulations indicate the importance of the negatively charged aspartate 114 for the binding of these ligands. It is well-known that a highly conserved aspartic acid (D114) in transmembrane 3 (TM3) is important for the binding of both agonists and antagonists to the D_2-DR.[24,71,72] In the present study, all the compounds simulated were docked into the receptor with the protonated amino group near D114. After 10 ns of MD simulations, the ligands had moved slightly but in a different form compared with the initial position. However, the strong interaction with D114 was maintained for all the complexes (see figures 2–5) which support that D114 is the anchoring point for ligands with a protonated amino group.

In the next step of our study we evaluated the relative free energy ($\Delta(\Delta G_{bind})$) obtained for the different complexes (table 1, second column). The results obtained for compounds **4** and **5** were as expected since both compounds showed a lower affinity for the D_2-DR than compound **1**. Regarding compounds **2** and **3** and from the relative binding energies obtained in our MD simulations, one can appreciate that replacing the OH in *meta* (*m*-OH) by a chlorine atom increases the affinity for the D_2-DR in comparison to compound **1**, indicated by the lowest value of the relative free energy obtained for compound **3**. In contrast replacing the OH in *para* position (*p*-OH) displays the opposite effect, ie decreases the affinity for the receptor (5.57 kcal/mol above the value obtained for **3**). These results are at least qualitatively in agreement with the experimental results previously reported for compounds **1**, **2**, **4** and **5**[17,70,73] as well as with the experimental results reported here for compound **3**. To try to better understand these results we compared the results obtained for **1**/D_2-DR complex with those complexes obtained for compounds **2**–**5**.

Figures 2 and 3 show the complexes obtained for compounds **3** and **2**, respectively, superimposed to complex **1**/D_2-DR for comparison. Figures 1S and 2S (electronic supporting material) show complexes **5**/D_2-DR and **4**/D_2-DR, respectively.

The superposition of the complexes **1**/D_2-DR and **3**/D_2-DR (see Figure 2) shows that both structures are very similar of the orientation of the ligand in the receptor binding site. In both complexes the ligand adopts extended conformation (torsional angle $\phi 1 = 171^\circ$ and 177° respectively; see Figure 1 for $\phi 1$ definition) and the aromatic ring of compound **3** overlaps almost perfectly with the catecholic ring of **1**, with the difference that the first one is rotated 180° with respect to dopamine ring. In contrast, the superimposition of complexes **2**/D_2-DR and **1**/D_2-DR (see Figure 3) reveals a marked deviation of compound **2** orientation with respect to DA, with the first one displaying a smaller value of the $\phi 1$ torsional angle ($\phi 1 = 97^\circ$).

Moreover, by comparison of chlorine atom binding mode in both chlorinated analogues one can see that in complex of compound **2** the chlorine atom is located in an hydrophobic environment composed of residues I184, F389, V190 and C–H bonds from H393 whereas in complex of compound **3** the same atom establishes interactions with the more polar residues S193 and S194.

3.3 Conformational Change in the Transmembrane 5 (TM5) Domain

Figures 4A and 4B give a different spatial view of the same complexes shown in Figures 2 and 3. One can see in these figures that in complexes **1**/D_2-DR and **3**/D_2-DR (see Figure 4A) the side-chain of S197 from transmembrane 5 (TM5) domain interacts with T119 from transmembrane 3 (TM3) domain. In contrast, in **2**/D_2-DR complex (see Figure 4B) this interaction has been disrupted during the MD simulation and the side chain of S197 associates with the backbone of residue S193 from the same TM5, causing distortion of the backbone interactions of TM5 and therefore the change in the structure of this transmembrane domain. It is worth noting that the change experienced by TM5

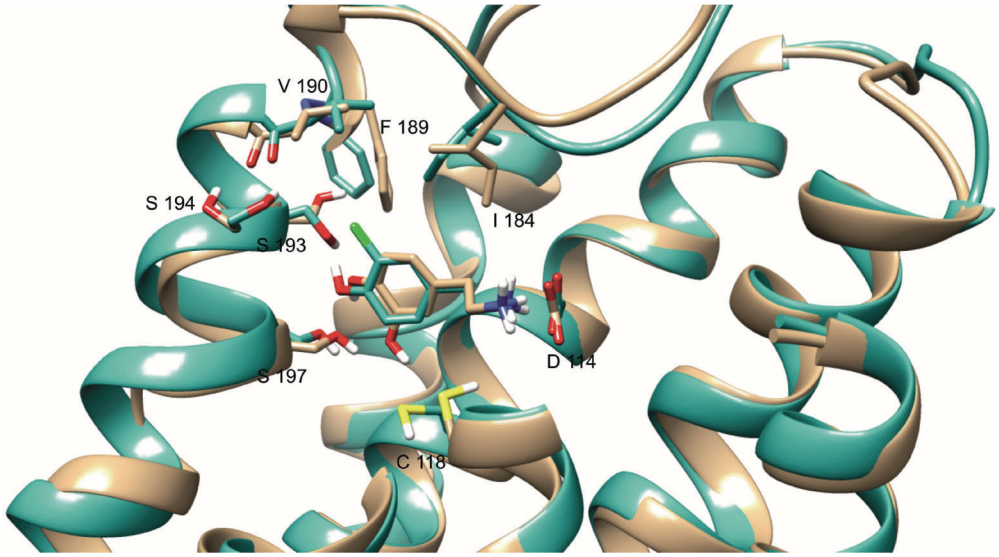

Figure 2. Spatial view of complex **3**/D_2-DR (cyan). Complex **1**/D_2-DR (in gray) is overimposed for comparison.

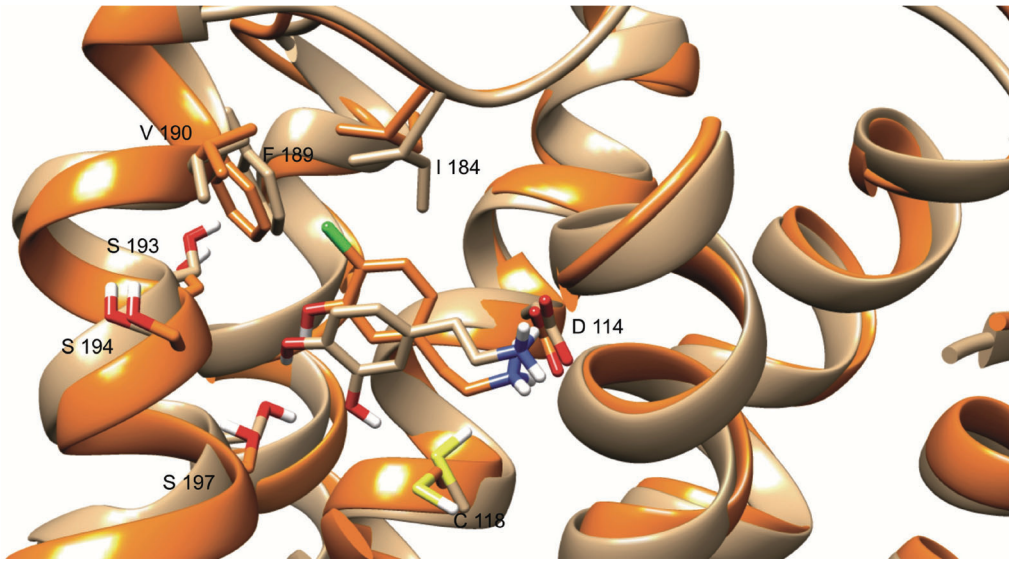

Figure 3. Spatial view of complex **2**/D_2-DR (orange). Complex **1**/D_2-DR (in gray) is overimposed for comparison.

domain the complex **2**/D_2-DR reflects the importance of preserving the flexibility of the backbone of TM5 during the simulation, as suggested by other authors.[53,74]

3.4 Possible Role of the Aromatic Residues of the Binding Site

From Figures 4A and 4B one also can see how the spatial distribution of the aromatic residues of the binding pocket of complexes **2**/D_2-DR and **3**/D_2-DR differs from that of complex **1**/D_2-DR. Figure 4A shows that the side chains of F389, F390 and F198 overlap almost perfectly in complexes **1**/D_2-DR and **3**/D_2-DR. These three residues are linked together by C–H·π interaction type (some of these interactions are shown in the molecular graphs later) forming a conserved structure that has been observed also in D_2-DR complexes with alkaloids possessing a tetrahidroprotoberberine structure.[49] This conserved structure forms specific interactions with the ligand, contributing, together with the principal interaction D114 to its anchoring in the proper orientation within the binding site. On the other hand, in complex **2**/D_2-DR the side chains of the phenylalanine triad show a marked deviation in its rings spatial distribution relative to **1**/D_2-DR (see Figure 4B). This alteration in the phenylalanine triad structure is a consequence of the distortion that TM5 undergoes in the **2**/D_2-DR complex,

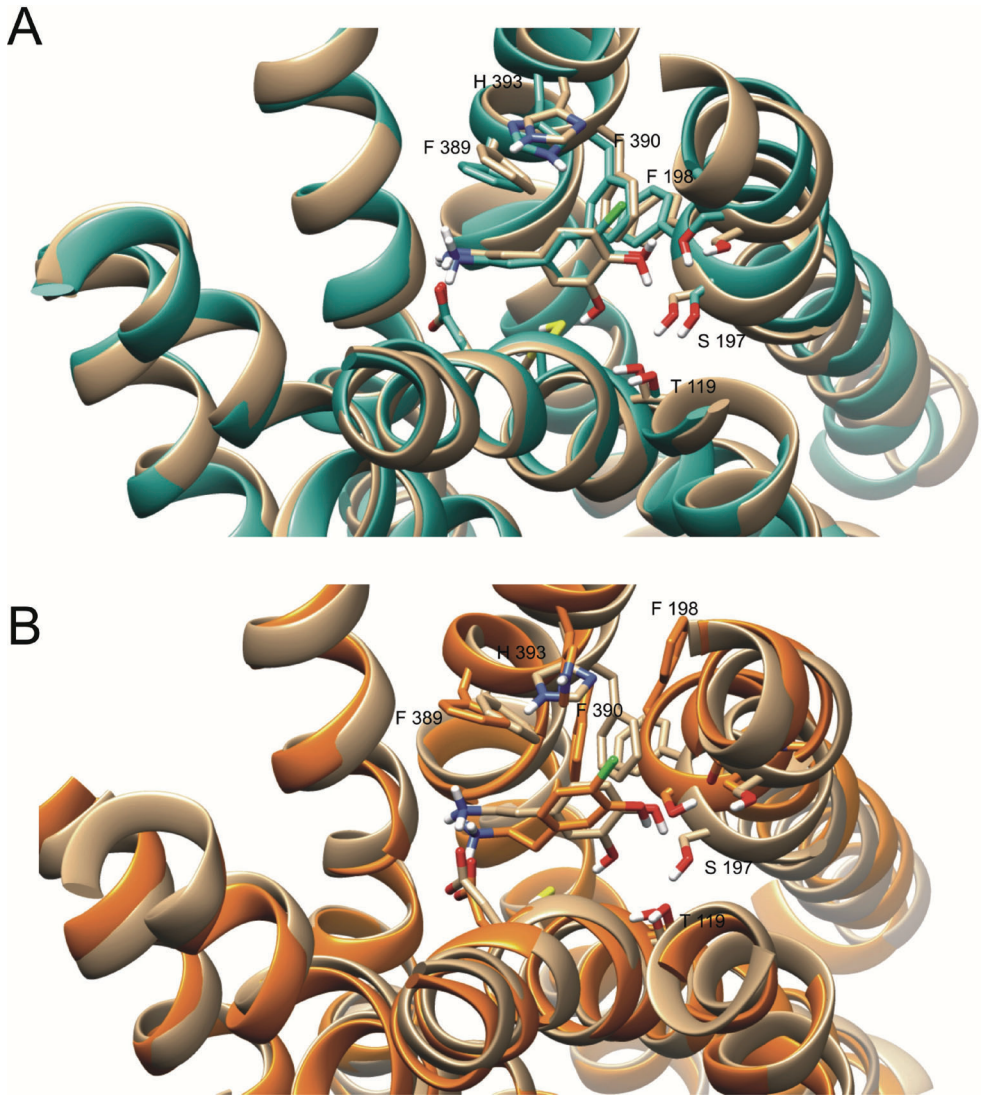

Figure 4. Similar spatial view to that shown in Figure 2 (4A) and 3 (4B) but in this case displaying the spatial distribution of the aromatic residues of the binding site.

which produces a displacement of the F198 (residue that belongs to TM5) so that it can no longer be associated with F190. Since phenylalanine triad produces specific interactions with the ligand, the alteration of its structure necessarily affects the binding mode of the ligand into the binding site, being this another factor that helps to explain the change in orientation of compound **2** within the binding site with respect to compounds **1** and **3**.

At this stage of our work we consider the trend predicted for the MD simulations as certainly significant but, on the other hand the approximations involved in this approach compels us to go beyond the classical treatment of the interactions to confirm our results. It should be noted that we are dealing with relatively weak interactions and therefore MD simulations might underestimate such interactions. Thus, in the next step of our study we constructed reduced model systems using combined semiempirical and DFT calculations.

3.5 Constructing the Reduced Models for the Binding Site

Figure 5 shows the ligand-residue interaction spectra calculated by the per residue free energy decomposition, which suggests that the interaction spectra of compounds **1**–**5** with D_2-DR are closely related and reflects their similar binding modes. As shown in Figure 5, the residues D114 and V115 are those with the greatest contribution to the interaction energy, this is true not only for compounds **1**–**5**, but also for other compounds with dopaminergic activity previously reported.[49]

Since the salt bridge with D114 is the strongest interaction established in the binding site it is considered a guide-

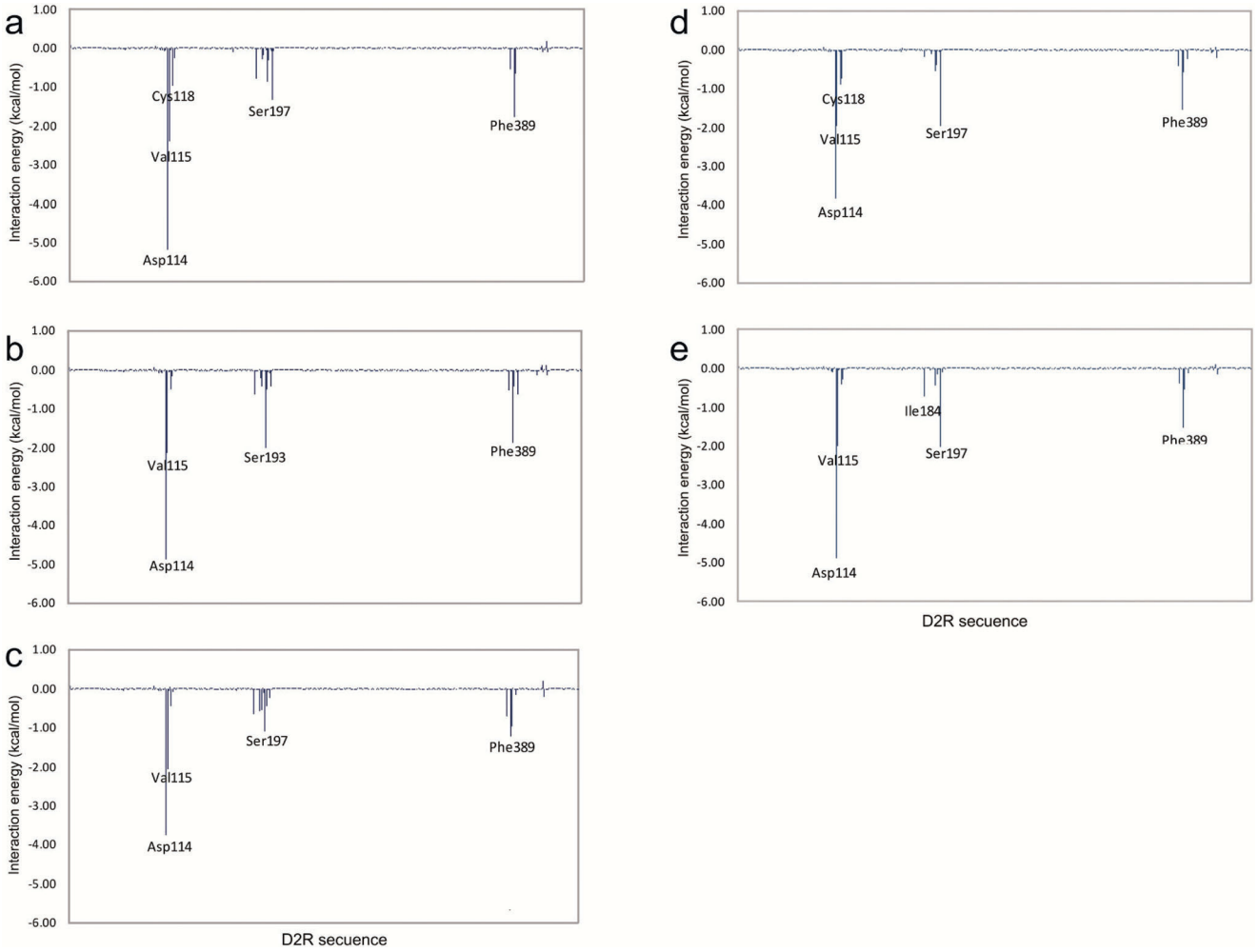

Figure 5. Histograms of interaction energies partitioned for D_2-DR amino acids when complexed with compound 1 (a), compound **3** (b), compound **2** (c), compound **5** (d) and compound **4** (e). The *x*-axis denotes the residue number of D_2-DR, and the y-axis shows the interaction energy between the compound and the specific residue. Negative and positive values represent favorable or unfavorable binding, respectively.

line interaction for ligand anchoring into the D_2-DR binding site. With respect to V115, this amino acid forms several C–H·π interactions with the aromatic ring of dopamine. These interactions are not shown in the molecular graphs displayed below for easy viewing of the molecular interactions of *meta*-OH/Cl and *para*-OH/Cl. Moreover, among the serine residues of the binding site, S197 is the residue that has the largest contribution to the interaction energy in complexes **1**/D_2-DR and **2**/D_2-DR, being higher in the first one, while S193 presents the most important contribution in the complex **3**/D_2-DR. Finally, the residue decomposition analysis also shows a significant contribution of one of the residues of the phenylalanine triad, F389, its contribution being greater in **1**/D_2-DR and **3**/D_2-DR than in **2**/D_2-DR.

From these results we considered prudent to include in the reduced model not just those amino acids involved in the most relevant molecular interactions displayed in the different spectra, but also all the residues involved in stabilizing and destabilizing interactions showing non negligible contribution in the per residue energy decomposition spectra. Thus, residues D114, V115, M116, C118, T119, I184, F189, V190, V191, Y192, S193, S194, I195, V196, S197, F198, W386, F389, F390, H393, Y408, T412 and Y416 were included in the reduced model for the binding pocket of D_2-DR and therefore a final number of 23 amino acids were included in our model. A spatial view of this reduced model is shown in Figure 6.

3.6 Quantum Mechanics Calculations and Topological Analysis of the Electron Density

The starting geometries for each complex were obtained from the coordinates of the potential energy minimum during the simulation time. PM6-D2X optimizations were performed by considering the mentioned 23 residues from the receptor binding pocket. Next, DFT (PBE/6-31G(d)

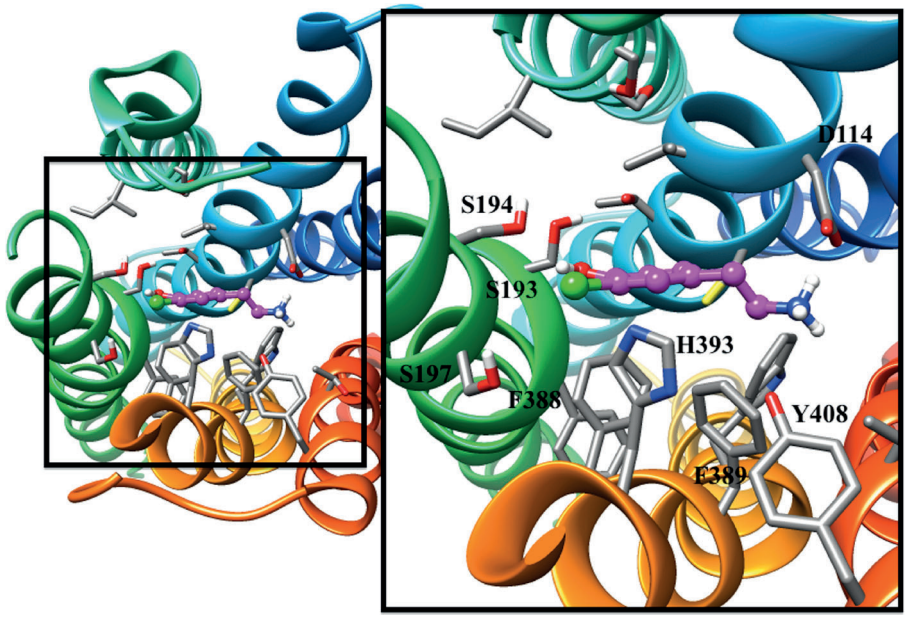

Figure 6. Spatial view of compound **3** (magenta)/D_2-DR interaction. Magnification of the receptor active site at the right. The names of the residues involved in the main interactions are written in the figure.

single point calculations were carried out for each of the PM6-D2X optimized complexes.

3.7 Evaluating the Molecular Interactions for the Different Complexes

On the basis of the results obtained from the MD simulations we focused the quantum mechanical analysis on dopamine (compound **1**) and its two chlorinated analogues (compounds **2** and **3**).

Figure 7 gives the values of ρ_b summation ($\Sigma\rho_b$) corresponding to all the intermolecular interactions (Figure 7A) and only those interactions involving substituent in the *meta* (*m*-OH/Cl) and *para* positions (*p*-OH/Cl) (Figure 7B) of compounds **1**–3 at the D_2-DR binding site.

In accordance with the relative free energy data (see Table 1) the $\Sigma\rho_b$ values corresponding to all the intermolecular interactions (Figure 7A) shows that compounds **3** and **2** are more strongly and more weakly anchored to the D_2-DR binding site than compound **1**, respectively.

Table 1. Relative free energy ($\Delta(\Delta G_{bind})$) obtained in kcal/mol for the five complexes studied here. IC_{50} experimental values are given in the second column.

Complex	$\Delta(\Delta G_{bind})$	IC_{50} (μM)	Reference
1/D_2-DR	3.10	0.52	[41]
2/D_2-DR	5.57	26.31	[9]
3/D_2-DR	0.00	0.15	This work
4/D_2-DR	4.84	>300	[42]
5/D_2-DR	4.00	26.5	[42]

Figures 8, 9 and 10 show the molecular graph of electron density obtained for compounds **1**, **3** and **2** in the D_2-DR binding site, respectively.

3.8 Catechol Interactions

The molecular graph of Figure 8 shows the most important interactions of compound **1** with the residues of the binding site. In particular, it is observed that OH in the *meta* position (*m*-OH) establishes a strong O–H·S hydrogen bond (HB) with C118 ($\rho_b = 0.0202$ au), other weaker HBs of the type C–H·O with F390 ($\rho_b = 0.0023$ au), S197 ($\rho_b = 0.0065$ au) and V115 ($\rho_b = 0.0032$ au) and two O·O contacts with T119 ($\rho_b = 0.0061$ au) and S197 ($\rho_b = 0.0072$ au). While in position *para* the OH behaves as a proton donor against S197 ($\rho_b = 0.0212$ au), and as proton acceptor against C–H bonds of F390 ($\rho_b = 0.0034$ au). Furthermore, like *m*-OH, *p*-OH also establishes a contact of the type O·O with backbone of S193 ($\rho_b = 0.0027$ au).

It is important to highlight the three O·O interactions in the **1**/D_2-DR complex. Even more interesting, the oxygen atoms of S197 and T119 that are engaged to the oxygen in *meta* position (*m*-O) are connected each other through a strong OH·O hydrogen bond. Thus, the three oxygen atoms are connected directly or indirectly by bond paths to give a topological ring (see Figure 7). This kind of O·O contacts has been already described in previous reports[25,49] and in such sense we believe they could be involved in the ligand/receptor recognition process.

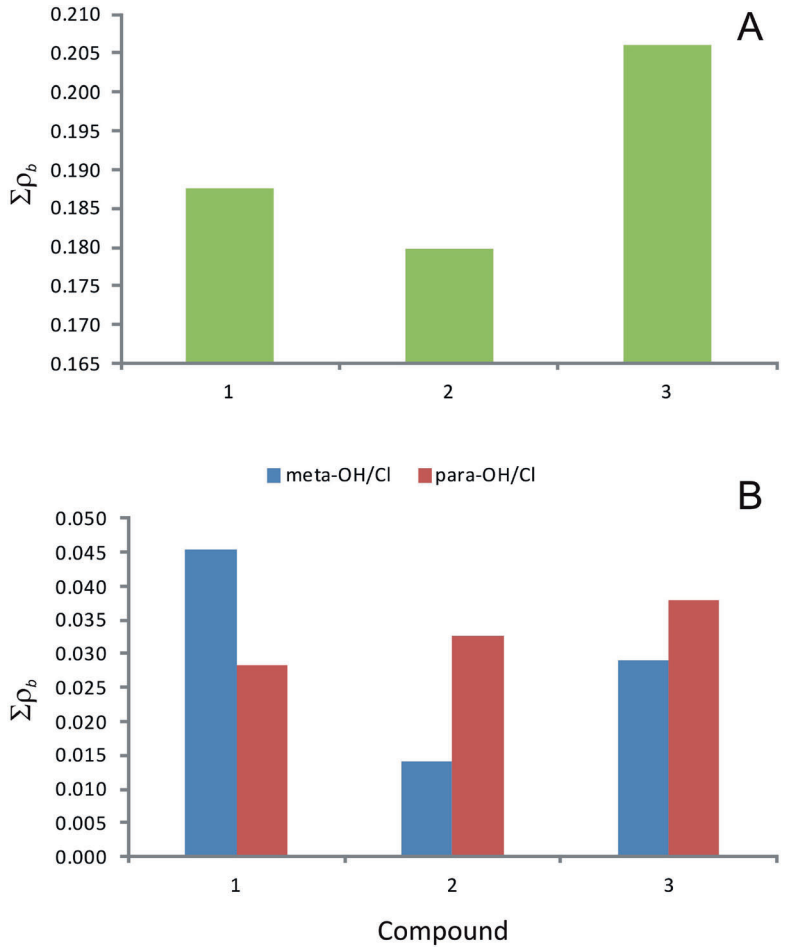

Figure 7. $\Sigma\rho_b$ values obtained for all the intermolecular interactions (7A) and only those involving substituents in meta (*m*-OH/Cl) and position (p-OH/Cl) (7B) of compounds **1**–**3** at the D_2-DR binding site.

3.9 Interactions of the Chlorine Atom

As can be seen in Figure 9, the chlorine atom of compound **3** (in *meta* position, *m*-Cl) establishes six interactions with the binding site of D_2-DR. Three C–H·Cl interactions with residues I184, V190 and H393 ($\Sigma\rho_b = 0.0149$ au), two interactions of the O·Cl type with S193 ($\rho_b = 0.0128$ au) and S194 ($\rho_b = 0.0013$ au) and a strong intramolecular (O–)H·Cl HB interaction with the OH in *para* position ($\rho_b = 0.0240$ au).

Moreover, in complex of compound **2**, the chlorine atom is more "buried" in the hydrophobic region (see Figure 10) forming only C–H·Cl interactions (a total of six interactions with residues I184, F189, V190 and H393 ($\Sigma\rho_b = 0.0326$ au)). Note that in this complex the chlorine atom is not forming an intramolecular HB with *m*-OH as in the case of compound **3**.

The two Cl·O interactions that are only established in complex **3**/D_2-DR could explain the favorable binding behavior observed for compound **3**. In other words, the Cl·O in complex **3**/D_2-DR might be mimicking the behavior of the dopamine O·O interactions with carbonyl and hydroxyl groups of the biological receptor.

Going back to Figure 7B, the ρ_b summation ($\Sigma\rho_b$) corresponding to interactions of *m*-Cl and *p*-Cl shows that the chlorine atom in compound **2** is more strongly anchored to the D_2-DR binding pocket than the same atom in compound **3**. Thus, based in these results, it is fair to say that the chlorine atom prefers to be in an hydrophobic environment as in complex **2**/D_2-DR where only C–H·Cl interactions are formed rather than a more polar one, as in complex **3**/D_2-DR where two Cl·O interactions are established.

On the basis of this results, the next question one might ask is what then makes compound **3** be more strongly anchored to the D_2-DR binding site than compound **2**? This issue is explored in the next section.

3.10 Effects of the Chlorine Substitutions on the Interactions of the OH Groups

Figure 7B shows that when the OH in *meta* position of compound **1** is replaced by a chlorine atom as in com-

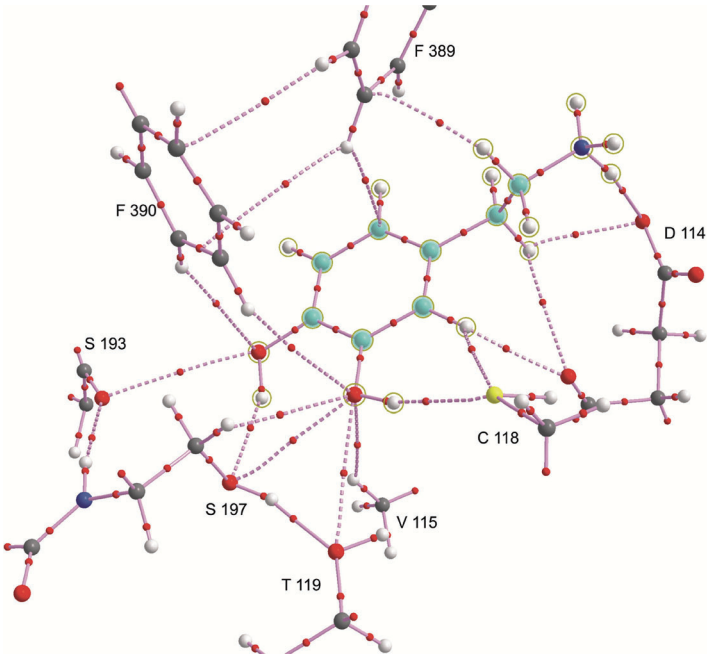

Figure 8. Molecular graph of compound **1** at the D_2-DR binding site. Large spheres represent attractors or nuclear critical points (3, −3) attributed to the atomic nuclei. Lines connecting the nuclei are bond paths and small spheres on them are bond critical points (3, −1).

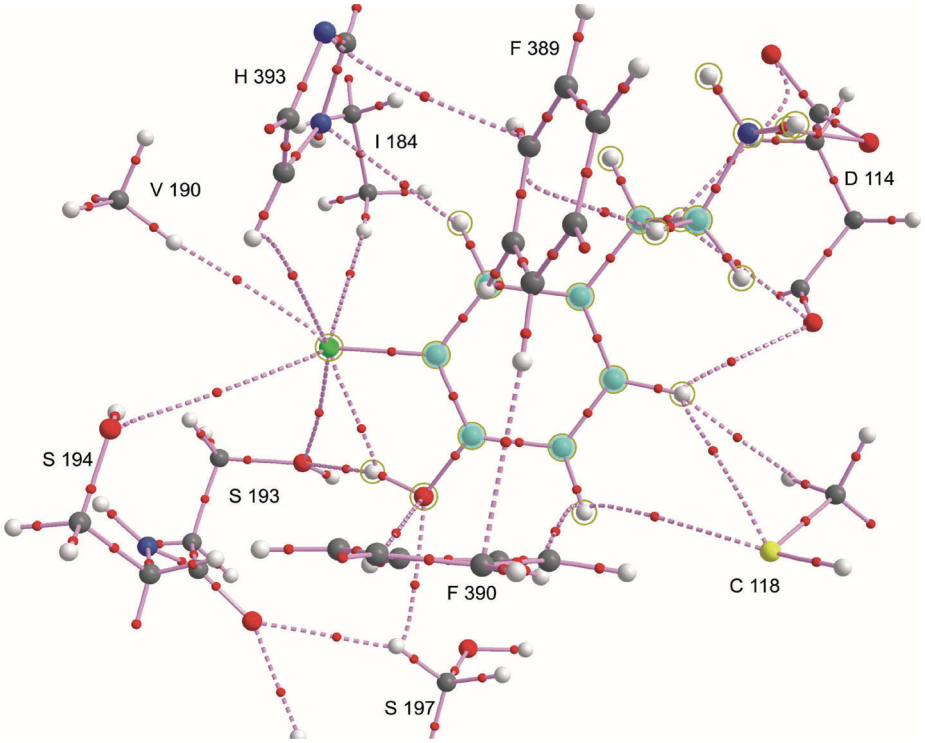

Figure 9. Molecular graph of compound **3** at the D_2-DR binding site. Large spheres represent attractors or nuclear critical points (3, −3) attributed to the atomic nuclei. Lines connecting the nuclei are bond paths and small spheres on them are bond critical points (3, −1).

pound **3**, it cannot be anchored to the binding site with the same force as the *m*-OH of compound **1**. However, the introduction of Cl at *meta* position improves the interactions of p-OH with respect to the same group in **1**. Thus, both groups together, *m*-Cl and *p*-OH are anchored to the binding site with almost the same strength as the corre-

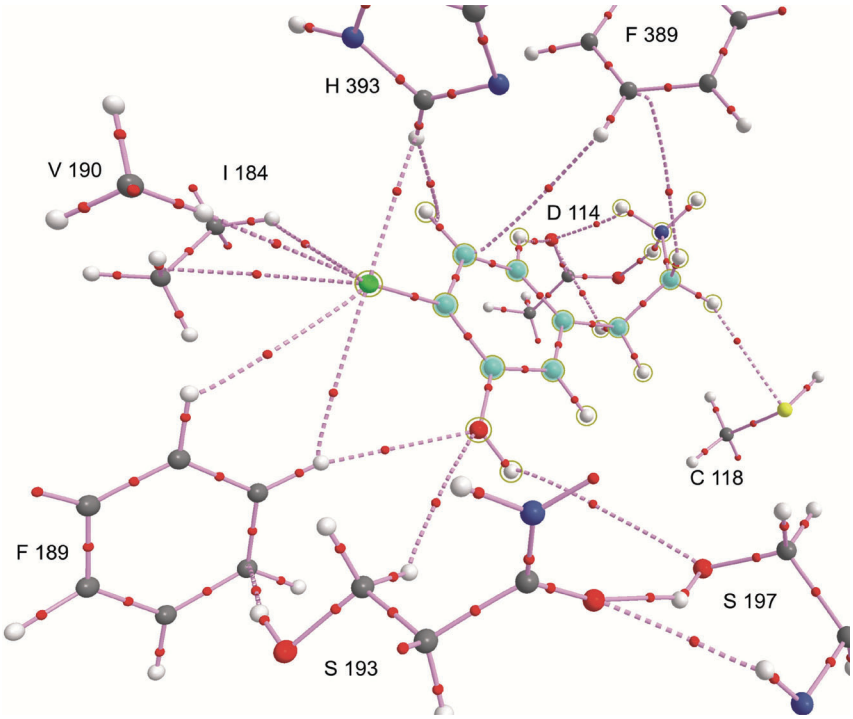

Figure 10. Molecular graph of compound **2** at the D_2-DR binding site. Large spheres represent attractors or nuclear critical points (3, −3) attributed to the atomic nuclei. Lines connecting the nuclei are bond paths and small spheres on them are bond critical points (3, −1).

sponding catecholic hydroxyls of **1**. Thus, the presence of the chlorine atom in the *meta* position modifies the binding site (throught the Cl·O interactions with serine residues) in order to strengthen interaction of *p*-OH.

On the other hand, when *p*-OH of compound **1** is replaced by chlorine as in compound **2**, the halogen provides stronger interactions than the corresponding OH group. However, the introduction of chlorine significantly weakens the interactions of *m*-OH in comparison to the same group in **1**/D_2-DR complex, so that both groups together bind much more weakly to the binding site that the corresponding OH groups of compound **1**.

As discussed above, in complex **2**/D_2-DR the chlorine atom is more "buried" in the hydrophobic pocket formed by residues I48, F154 and V190 that in the **3**/D_2-DR complex. This determines that *m*-OH be poorly positioned to interact with the serines of the binding site.

Summarizing the results of the molecular modeling section, it was shown that the binding mode of compound **3** in the D_2-DR binding pocket resemble the DA binding mode (see Figure 2) whereas in compound **2**, the anchoring of the chorine atom in an hydrophobic pocket determines a different binding mode for this compound (see Figure 3). While the chlorine atom in compound **2** is more strongly anchored in the D_2-DR binding pocket than the same atom in compound **3** (Figure 7B), the overall binding of the last compound is stronger than the first one (Table 1 and Figure 7A) in part due to the better placement of the hydroxyl group to interact with the serine residues from the receptor binding pocket. Furthermore, it was shown that the binding mode of compound **2** to D_2-DR determines a distortion of TM5 that in turn disturbs specific interactions between phenylalanine resides of the binding pocket and the ligand (Figures 4A,B).

3.11 Scope and Limitations of the Methodology Used Here

Let us now make some comments on the scope and limitations that might have the application of calculations used in this work.

With respect to the applicability to other biological systems, It is important to note that studies using molecular techniques QTAIM applied to large systems of biological interest are relatively new and therefore there are few studies previously reported in the literature. However, it is important to note that these simulations have been used successfully in inhibitors of dihydrofolate reductase (DHFR)[48] as well as with BACE 1 inhibitors.[75,76] Although the types of receptors studied so far are very few, at least it is interesting to note that it is possible to do this kind of simulations successfully in different types of receptors. Now we are doing studies on different types of ligand-receptor complexes with different types of interactions (from very strong to very weak ones). It is clear that the results obtained in such study will give us a better picture about the scope of applicability of the simulations used here.

With respect to the applicability of these simulations to structurally unrelated chemotypes. We have recently reported some works in which we have studied compounds structurally different with this type of approach.[25,49,50] In a study of DHFR inhibitors it was possible to include in the correlation two new series of compounds possessing significant structural differences with respect to the known classical and non-classical inhibitors.[48] In the particular case of D_2-DR in previous works we have reported the analysis of BTHIQs compounds[24] as well as of protoberberine derivatives[49] by using this type of simulations. While the structural variability is still very meager, the results obtained so far are very promising for this kind of approach using reduced models and QTAIM calculations. Thus, it appears very reasonable that these simulations might be successfully applied to compounds with different structural chemotypes. Importantly, in all the above cases, these studies including quantum mechanical calculations and QTAIM studies have significantly improved correlations between experimental and theoretical results in a quantitative mode which indicates how valuable is this protocol for prioritizing certain chemotypes.

A somewhat negative aspect also needs to be highlighted. The protocol used is far from to be considered a post-docking routine method in its current form. However, considering that the type of calculations performed are not particularly sophisticated, it would be possible to design a protocol developing the various steps in a more systematic and friendly way. We are working on it.

4 Conclusions

In this paper we performed a molecular modeling study of 3-chlorotyramine and analogues. The theoretical and experimental results reported here allowed us to reach at least two interesting conclusions. On one side we are reporting that 3-chlorotyramine has a D_2 receptor affinity that it is comparable to that of the endogenous ligand (dopamine). This result is very interesting because until now it has been reported that all halogenated dopamine derivatives have a significantly lower affinity for both D_1 and D_2 receptors. On the other hand it should be noted that our theoretical study (including a comprehensive analysis of the molecular interactions) has been able to explain such a significant affinity of 3-chlorotyramine for the D_2 receptor. However, it is important to note that in order to evaluate in detail the various molecular interactions of ligands at its site of action, it is necessary to use reduced models systems which allow to perform quantum mechanical calculations and QTAIM type studies. While these calculations require more time than traditional or standard simulations, apparently this effort is justified because it allows a deeper and more appropriate description of the ligand-receptor interactions.

By combining MD simulations with semiempirical and DFT calculations, a simple and generally applicable procedure to evaluate the binding energies of ligands interacting with the D_2-DR has been reported here. Thus, our theoretical and experimental results contribute to the understanding of the non covalent interactions in the context of the ligand - receptor binding event in a two-way manner, by providing a detailed topological description of the interaction network of the ligand in the receptor binding pocket and by showing the convenience of going beyond the concept of pair-wise interactions in order to "see" the electronic effects within the intricate biological environment. Undoubtedly the results presented here show the importance of performing these studies as comprehensive as possible when hydrogen bonds are involved and even more if there are halogen atoms involved in these interactions. Thus, we believe our results may be helpful in the structural identification and understanding of the minimum structural requirements for these molecules and can provide a guide in the design of new ligands for the D_2 receptor of dopamine.

List of the Abbreviations

QTAIM	Quantum theory of atoms in molecules
DR	Dopamine receptor
DA	Dopamine
MD	Molecular dynamics
BTHIQs	Benzyl-tetrahydroisoquinolines

Acknowledgements

Grants from *Universidad Nacional de San Luis* (*UNSL*), partially supported this work. This research was also supported by PIP 095 CONICET. R. D. Enriz; N. M. Peruchena, F. M. Garibotto, E. L. Angelina and S. A. Andujar are members of the *Consejo Nacional de Investigaciones Científicas y Técnicas* (*CONICET-Argentina*) staff.

References

[1] L. Bettinetti, S. Löber, S. Hübner, P. Gmeiner, *J. Comb. Chem.* **2005**, *7*, 309 – 316.
[2] J. W. Kebabian, F. I. Tarazi, N. S. Kula, R. J. Baldessarini, *Drug Discov. Today* **1997**, *2*, 333 – 340.
[3] R. J. Baldessarini, in *The Dopamine Receptors* (Eds: K. A. Neve, R. L. Neve), Humana Press, Totowa, NJ, **1997**, 457 – 498.
[4] R. B. Mailman, D. E. Nichols, A. Tropsha, in *The Dopamine Receptors* (Eds: K. A. Neve, R. L. Neve), Humana Press, Totowa, NJ, **1997,** 105 – 133.
[5] J. P. Kelleher, F. Centorrino, M. J. Albert, R. J. Baldessarini, *CNS Drugs.* **2002**, *16*, 249 – 261.
[6] M. Rowley, L. J. Bristow, P. H. Hutson, *J. Med. Chem.* **2001**, *44*, 477 – 501.
[7] M. Reutlinger, T. Rodrigues, P. Schneider, G. Schneider, *Angew. Chem. Int. Ed.* **2014**, *53*, 1 – 6.

[8] a) J. A. Hiss, M. Hartenfeller, G. Schneider, *Curr. Pharm. Des.* **2010**, *16*, 1656 – 1665; b) J. A. Hiss, M. Reutlinger, C. P. Koch, A. M. Perna, P. Schneider, T. Rodrigues, S. Haller, G. Folkers, L. Weber, R. B. Baleeiro, P. Walden, P. Wrede, G. Schneider, *Future Med. Chem.* **2014**, *6*, 267 – 280.

[9] G. Gallagher, P. J. Lavanchy, J. W. Wilson, J. P. Hieble, R. M. Marinis, *J. Med. Chem.* **1985**, *28*, 1533 – 1536.

[10] K. L. Kirk, C. R. Creveling, *Med. Res. Reu.* **1984**, *4*, 189 – 220.

[11] R. M. De Marinis, G. Gallagher, R. F. Hall, R. G. Franz, C. Webster, W. F. Huffmann, M. S. Schwartz, C. Kaiser, S. T. Ross, J. W. Wilson, P. Hieble, *J. Med. Chem.* **1986**, *29*, 939 – 947.

[12] J. R. McCarthy, J. McCowan, M. B. Zimmerman, M. A. Wenger, L. W. Emmert, *J. Med. Chem.* **1986**, *29*, 1586 – 1590.

[13] J. Weinstock, D. E. Gaitanopouloe, O. D. Stringer, R. G. Franz, J. P. Hieble, L. B. Kinter, W. A. Maan, K. E. Flaim, G. Gessner, *J. Med. Chem.* **1987**, *30*, 1166 – 1176.

[14] L. Nedelec, C. Dumont, C. Obrlander, D. Frechet, J. Laurent, J. R. Bohier, *Eur. J. Med. Chem.* **1978**, *13*, 553 – 563.

[15] M. Cardellini, G. M. Cingolani, F. Claudi, V. Perlini, W. Balduini, F. Cattabeni, *Farmaco Ed. Sci.* **1988**, *43*, 49 – 59.

[16] F. Claudi, M. Cardelhi, G. M. Ciolani, A. Piergentili, G. Peruzzi, W. Balduini, SynWi, *J. Med. Chem.* **1990**, *33*, 2408 – 2412.

[17] F. Claudi, G. Giorgioni, A. Di Stefano, M. P. Abbracchio, A. M. Paoletti, W. Balduinio, *J. Med. Chem.* **1992**, *35*, 4408 – 4414.

[18] J. Weinstock, D. E. Gaitanopoulos, O. Hye-Ja, F. R. Pfeiffer, C. B. Karaeh, J. W. Venslavsky, H. M. Sarau, K. E. Flaim, J. P. Hieble, C. Kaiser, *J. Med. Chem.* **1986**, *29*, 1613 – 1627.

[19] R. W. Fuller, J. Mills, M. M. Marsh, *J. Med. Chem.* **1971**, *14*, 322 – 325.

[20] P. Stark, W. Fuller, *Neurophormacology* **1972**, *11*, 261 – 272.

[21] K. M. O'Boyle, J. L. Waddington, *Eur. J. Pharmacol.* **1985**, *115*, 291 – 295.

[22] I. Berenguer, N. El Aouad, S. Andujar, V. Romero, F. Suvire, T. Freret, A. Bermejo, M. D. Ivorra, R. D. Enriz, M. Boulouard, N. Cabedo, D. Cortes, *Bioorg. Med. Chem.* **2009**, *17*, 4968 – 4980.

[23] N. El Aouad, I. Berenguer, V. Romero, P. Marín, A. Serrano, S. Andujar, F. Suvire, A. Bermejo, M. D. Ivorra, R. D. Enriz, N. Cabedo, D. Cortes, *Eur. J. Med. Chem*, **2009**, *44*, 4616 – 4621.

[24] S. Andujar, F. Suvire, I. Berenguer, N. Cabedo, P. Marín, L. Moreno, M. D. Ivorra, D. Cortes, R. D. Enriz, *J. Mol. Model.* **2012**, *18*, 419 – 431.

[25] S. A. Andujar, R. D. Tosso, F. D. Suvire, E. Angelina, N. Peruchena, N. Cabedo, D. Cortes, R. D. Enriz, *J. Chem. Inf. Model.* **2012**, *52(1)*, 99 – 112.

[26] U. Koch, P. L. Popelier, *J. Phys. Chem.* **1995**, *99*, 9747 – 9754.

[27] C. F. Matta, N. Castillo, R. J. Boyd, *J. Phys. Chem. B.* **2005**, *110*, 563 – 578.

[28] R. A. Mosquera, M. J. G. Moa, L. Estévez, M. Mandado, A. M. Graña, in *Quantum Biochemistry* (Ed: C. F. Matta), Wiley-VCH, Weinheim, Germany, **2010**.

[29] J. M. Dumas, H. Peurichard, M. Gomel, *J. Chem. Res.* **1978**, *2*, 54 – 55.

[30] T. Clark, M. Hennemann, J. S. Murray, P. Politzer, *J. Mol. Model.* **2007**, *13(2)*, 291 – 296.

[31] T. Clark, *σ-Holes*, *Comput. Mol. Sci.* **2012**, DOI: 10.1002/wcms.1113.

[32] A. Legon, *Phys. Chem. Chem. Phys.* **2010**, *12*, 7736 – 7747.

[33] A. C. Legon, *Angew. Chem., Int. Ed.* **1999**, *38*, 2686 – 2714.

[34] P. Politzer, J. S. Murray, T. Clark, *Phys. Chem. Chem. Phys.* **2010**, *12*, 7748 – 7757.

[35] C. Bissantz, B. Kuhn, M. Stahl, *J. Med. Chem.* **2010**, *53(14)*, 5061 – 5084.

[36] L. A. Hardegger, B. Kuhn, B. Spinnler, L. Anselm, R. Ecabert, M. Stihle, B. Gsell, R. Thoma, J. Diez, J. Benz, J. M. Plancher, G. Hartmann, D. W. Banner, W. Haap, F. Diederich, *Angew. Chem., Int. Ed.* **2011**, *50(1)*, 314 – 318.

[37] L. A. Hardegger, B. Kuhn, B. Spinnler, L. Anselm, R. Ecabert, M. Stihle, B. Gsell, R. Thoma, J. Diez, J. Benz, J. M. Plancher, G. Hartmann, Y. Isshiki, K. Morikami, N. Shimma, W. Haap, D. W. Banner, F. Diederich, *ChemMedChem.* **2011**, *6(11)*, 2048 – 2054.

[38] R. Wilcken, X. Liu, M. O. Zimmermann, T. J. Rutherford, A. R. Fersht, A. C. Joerger, F. M. Boeckler, *J. Am. Chem. Soc.* **2012**, *134(15)*, 6810 – 6818.

[39] H. G. Kümmel, *Biography of the Coupled Cluster Method*; World Scientific, Singapore. **2002**.

[40] C. Møller, M. S. Plesset, *Phys. Rev.* **1934**, *46(7)*, 618.

[41] J. A. Pople, J. S. Binkley, R. Seeger, *Int. J. Quantum Chem.* **1976**, 1 – 19.

[42] Y. Lu, Y. Wang, W. Zhu, *Phys. Chem. Chem. Phys.* **2010**, *12(18)*, 4543 – 4551.

[43] Y. Lu, T. Shi, Y. Wang, H. Yang, X. Yan, X. Luo, H. Jiang, W. Zhu, *J. Med. Chem.* **2009**, *52(9)*, 2854 – 2862.

[44] P. Dobes, J. Rezáč, J. Fanfrlík, M. Otyepka, P. Hobza, *J. Phys. Chem. B* **2011**, *115(26)*, 8581 – 8589.

[45] C. Coley, R. Woodward, A. M. Johansson, P. G. Strange, L. H. Naylor, *J. Neurochem.* **2000**, *74(1)*, 358 – 366.

[46] R. Woodward, C. Coley, S. Daniell, L. H. Naylor, P. G. Strange, *J. Neurochem.* **1996**, *66(1)*, 394 – 402.

[47] B. A. Cox, R. A. Henningsen, A. Spanoyannis, R. L. Neve, K. A. Neve, *J. Neurochem.* **1992**, *59*, 627 – 635.

[48] R. D. Tosso, S. A. Andujar, L. Gutierrez, E. Angelina, R. Rodríguez, M. Nogueras, H. Baldoni, F. D. Suvire, J. Cobo, R. D. Enriz, *J. Chem. Inf. Model.* **2013**, *53*(8), 2018 – 2032.

[49] J. Párraga, N. Cabedo, S. Andujar, L. Piqueras, L. Moreno, A. Galán, E. Angelina, R. D. Enriz, M. D. Ivorra, M. J. Sanz, D. Cortes, *Eur. J. Med. Chem.* **2013**, *68*, 150 – 166.

[50] E. Angelina, S. A. Andujar, R. D. Tosso, R. D. Enriz, N. Peruchena, *Non-covalent interactions in receptor-ligand complexes. A study based on the electron charge density.* CLAFCO Congress, Foz Iguazu (Brasil), **2013**.

[51] R. Bader, *Atoms in Molecules: A Quantum Theory*, Oxford University Press, New York, **1990**.

[52] S. J. Grabowski, *J. Phys. Chem. A* **2012**, *116*, 1838 – 1846.

[53] M. A. Soriano-Ursúa, J. O. Ocampo-López, K. Ocampo-Mendoza, J. G. Trujillo-Ferrara, J. Correa-Basurto, *Comput. Biol. Med.* **2011**, *41*, 537 – 445.

[54] M. Y. Kalani, N. Vaidehi, S. E. Hall, R. J. Trabanino, P. L. Freddolino, M. A. Kalani, W. B. Floriano, V. W. Kam, W. A. Goddard 3rd, *Proc. Natl. Acad. Sci.* **2004**, *101*, 3815–3820.

[55] G. M. Morris, D. S. Goodsell, R. S. Halliday, R. Huey, E. Hart, R. K. Belew, A. J. Olson, *J. Comp. Chem.* **1998**, *19*, 1639 – 1662.

[56] W. L. Jorgensen, J. Chandrasekhar, J. D. Madura, R. W. Impey, M. L. Klein, *J. Chem. Phys.* **1983**, *79*, 926 – 935.

[57] D. A. Case, T. E. Cheatham, T. Darden, H. Gohlke, R. Luo, K. M. Merz Jr., A. Onufriev, C. Simmerling, B. Wang, R. J. Woods, *J. Comput. Chem.* **2005**, *26*, 1668 – 1688.

[58] D. A. Case, T. A. Darden, T. E. Cheatham III, C. L. Simmerling, J. Wang, R. A. Duke, R. Luo, R. C. Walker, W. Zhang, K. M. Merz, *AMBER12*, University of California, San Francisco. **2012**.

[59] T. Darden, D. York, L. Pedersen, *J. Chem. Phys.* **1993**, *98*, 10089 – 10092.

[60] U. Essmann, L. Perera, M. L. Berkowitz, T. Darden, H. Lee, L. G. Pedersen, *J. Chem. Phys.* **1995**, *103*, 8577 – 8593.

[61] T. Hou, N. Li, Y. Li, W. Wang, *J. Proteome Res.* **2012**, *11*, 2982 – 95.

[62] H. Gohlke, C. Kiel, D. A. Case, *J. Mol. Biol.* **2003**, *330*, 891 – 913.

[63] J. Řezáč, P. Hobza, *Chem. Phys. Lett.* **2011**, *506*, 286 – 289.

[64] J. J. P. Stewart, MOPAC2009 Stewart Computational Chemistry, Colorado Springs, CO, USA, **2008**.
[65] M. J. Frisch, G. W. Trucks, H. B. Schlegel, G. E. Scuseria, M. A. Robb, J. R. Cheeseman, J. A. Montgomery Jr., T. Vreven, K. N. Kudin, J. C. Burant, *Gaussian 03, Revision C05,*Gaussian, Inc., Wallingford, CT, **2004**.
[66] T. Keith, *AIMA11, 12.11.09*, Gristmill Software, Overland Park, KS, USA, **2012**.
[67] K. H. Chung, H. J. Kim, H. R. Kim, E. K. Ryu, *Synth. Commun.* **1990**, *20*, 2991 – 2997.
[68] H. Nakazawa, K. Sano, K. Matsuda, K. Mitsugi, *Biosci. Biotech. Biochem.* **1993**, *57*, 1210 – 1211.
[69] M. Alías, M. P. López, C. Cativiela, *Tetrahedron* **2004**, *60*, 885 – 891.
[70] L. B. Kozell, K. A. Neve, *Mol. Pharmacol.* **1997**, *52(6)*, 1137 – 1149.
[71] M. M. Teeter, M. F. Froimowitz, B. Stec, C. J. Durand, *J. Med. Chem.* **1994**, *37*, 2874 – 2888.
[72] A. Mansour, F. Meng, J. H. Meador-Woodruff, L. P. Taylor, O. Civelli, H. Akil, *Eur J Pharmacol.* **1992**, *227*, 205 – 214.
[73] S. L. Payne, A. M. Johansson, P. G. Strange, *J. Neurochem.* **2002**, *82(5)*, 1106 – 1117.
[74] V. Katritch, K. A. Reynolds, V. Cherezov, M. A. Hanson, C. B. Roth, M. Yeager, R. Abagyan, *J. Mol. Recognit.* **2009**, *22*, 307 – 318.
[75] L. J. Gutierrez, E. Angelina, N. Peruchena, H. A. Baldóni, R. D. Enriz, *Small-size peptides acting as inhibitors of the BACE1-exosite. A molecular modeling study using MD simulations and QM calculations*, *10th Congress of the World Association of Theoretical and Computational Chemists (WATOC), Santiago, Chile*, **2014**. http://watoc2014.com/
[76] L. J. Gutierrez, *Search and molecular modeling study of the exosite of BACE1*, PhD Thesis, National University of San Luis (Argentina), **2013**.

Received: July 2, 2014
Accepted: September 4, 2014
Published online: ■■ ▮▮, 0000

FULL PAPERS

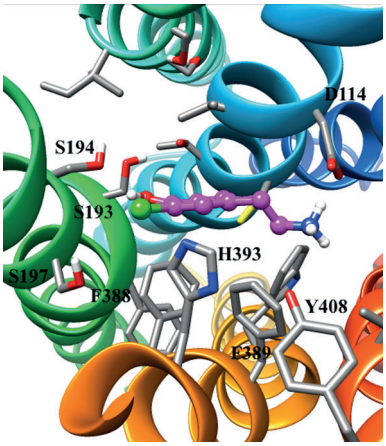

E. Angelina, S. Andujar, L. Moreno, F. Garibotto, J. Párraga, N. Peruchena, N. Cabedo, M. Villecco, D. Cortes, R. D. Enriz*

■■ – ■■

3-Chlorotyramine Acting as Ligand of the D_2 Dopamine Receptor. Molecular Modeling, Synthesis and D_2 Receptor Affinity

Capítulo 2

Síntesis y estudios de afinidad por los receptores melatoninérgicos de HHIP

Artículo 4: "Synthesis of new melatoninergic hexahydroindenopyridines"
(En: *Bioorganic & Medicinal Chemistry Letters*, **2014**, *24*, 3534)

Artículo 5:"Efficient synthesis of hexahydroindenopyridines and their potencial as melatoninergic ligands" (En: *European Journal of Medicinal Chemistry*, **2014**, *86*, 700)

Bioorganic & Medicinal Chemistry Letters 24 (2014) 3534–3536

Contents lists available at ScienceDirect

Bioorganic & Medicinal Chemistry Letters

journal homepage: www.elsevier.com/locate/bmcl

Synthesis of new melatoninergic hexahydroindenopyridines

Laura Moreno [a,*], Inmaculada Berenguer [a], Amelia Diaz [b], Paloma Marín [a], Javier Párraga [a], Daniel-Henri Caignard [c], Bruno Figadère [d], Nuria Cabedo [e,*], Diego Cortes [a]

[a] Departamento de Farmacología, Laboratorio de Farmacoquímica, Facultad de Farmacia, Universidad de Valencia, 46100 Burjassot, Valencia, Spain
[b] Departamento de Química Orgánica, Facultad de Ciencias, Universidad de Málaga, 29071 Málaga, Spain
[c] Département des Sciences Expérimentales, Institut de Recherches Servier, 92150 Suresnes, France
[d] UMR CNRS 8076, LERMIT, Université Paris-Sud, Laboratoire de Pharmacognosie, UFR de Pharmacie, Châtenay-Malabry F-92296, France
[e] Centro de Ecología Química Agrícola-Instituto Agroforestal Mediterraneo, UPV, Campus de Vera, Edificio 6C, 46022 Valencia, Spain

ARTICLE INFO

Article history:
Received 16 April 2014
Revised 13 May 2014
Accepted 15 May 2014
Available online 2 June 2014

Keywords:
Hexahydroindenopyridines
Melatonin
Receptor binding
Synthesis

ABSTRACT

Hexahydroindenopyridine (HHIP) is an interesting heterocyclic framework that contains an indene core similar to ramelteon. This type of tricyclic piperidines aroused our interest as potential melatoninergic ligands. Melatonin receptor ligands have applications in insomnia and depression. We report herein an efficient two-step method to prepare new HHIP by the reaction of an enamine with 3-bromopropylamine hydrobromide. Some synthesized compounds showed moderate affinity for melatonin receptors in the nanomolar or low micromolar range. Furthermore, the methylenedioxy HHIPs **2d** (*N*-phenylacetamide) and **2f** (*N*,*N*-diethylacetamide), exhibited high selectivity at MT_1 or MT_2 receptors, respectively, when compared with melatonin. It seems that the methylenedioxy group on the indene ring system and the *N*-acetamide substituent are important structural features to bind selectively MT_1 or MT_2 subtypes.

Melatonin (*N*-acetyl-5-methoxytryptamine, MLT) is a serotonin-derived neurohormone of long standing interest which is produced in the pineal gland (Fig. 1).[1] Due to its nocturnal synthesis, melatonin is suspected to relay the circadian rhythm and the information on the photoperiod to the peripheral organs for daily and seasonal physiological regulations.[2,3] In recent years, considerable attention has been paid to melatonin receptor ligands because of their applications in insomnia and depression. Among the melatoninergic drugs, the commercialized antidepressant agomelatine (Valdoxan®, by Servier Pharmaceutical Company) and the hypnotic ramelteon (Rozerem®, by Takeda Pharmaceuticals) stand out for its interesting properties as potent agonists of melatonin receptors (MT_1 and MT_2).[4,5]

Hexahydroindenopyridine (HHIP) is an intriguing heterocyclic framework that provides a new class of compounds with potential usefulness as therapeutical agents. HHIPs have been reported to display several biological activities, including antidepressant,[6,7] serotoninergic,[8] antispermatogenic,[9] inhibition of the 11β-hydroxysteroid dehydrogenase enzyme[10] or affinity for opioid receptors.[11] In our search for the synthesis of bioactive piperidines and given that likewise to ramelteon, HHIPs are provided with an indene core, we have envisaged the synthesis of this type of tricyclic piperidines which aroused our interest as potential melatoninergic ligands (Fig. 1). In addition, considering the structural features of melatonin, agomelatin and ramelteon, a methoxy or methylenedioxy substituent at 8-position on the benzene ring as well as an *N*-amide group were incorporated into the tricyclic ring system. Although some synthetic approaches have been described in the literature,[6,7,12,13] we decided to explore a method that allowed us to easily obtain the HHIP framework in a very steps with good yields.

The first step of our method for the synthesis of the HHIP structure consisted in preparing the appropriate enamine (**1a** or **2a**) from a commercially available 1-indanone and piperidine, using $TiCl_4$ as a Lewis acid catalyst and a water scavenger.[14–16] As the starting material, we employed either 5-chloro-6-methoxy-1-indanone (**1**) or 5,6-methylenedioxy-1-indanone (**2**). Enamine formation takes place at room temperature in toluene after stirring for 3 days. Next, the enamine was subjected to cyclization, which consisted in a reaction with 3-bromopropylamine hydrobromide in dry DMF under reflux. This reaction successfully led to the desired imine, which was reduced with $NaBH_4$ in ethanol to obtain the expected HHIP skeleton (Scheme 1). Therefore, we prepared 7-chloro-8-methoxy HHIP **1b** and 7,8-methylenedioxy HHIP **2b** by an efficient two-step procedure, depending on the indanone (**1** or **2**) used as the starting material.[17] The synthesis produces the *trans* ring fused-HHIPs **1b** and **2b** due to the presence of a sole diastereomer by ^1H NMR analysis. The vicinal coupling constant

* Corresponding authors. Tel.: +34 963 544 975; fax: +34 963 544 943.
E-mail addresses: laura.moreno@uv.es (L. Moreno), ncabedo@ceqa.upv.es (N. Cabedo).

http://dx.doi.org/10.1016/j.bmcl.2014.05.053
0960-894X/

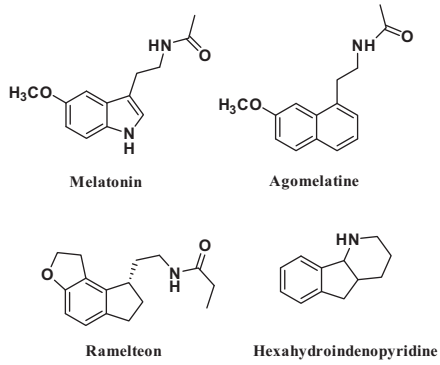

Figure 1. Melatonin, agomelatine, ramelteon and hexahydroindenopyridine.

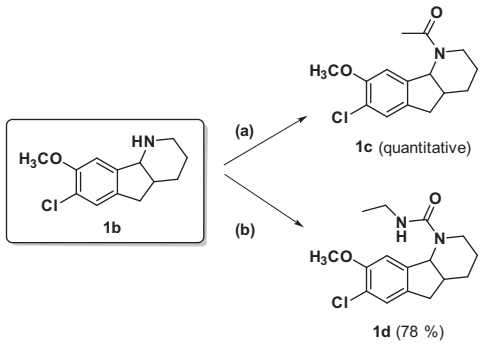

Scheme 2. Synthesis of HHIP **1c** and **1d**. Reagents and conditions: (a) Ac_2O/pyr, rt, 2 h; (b) ethylisocyanate, CH_2Cl_2, reflux, 2 h.

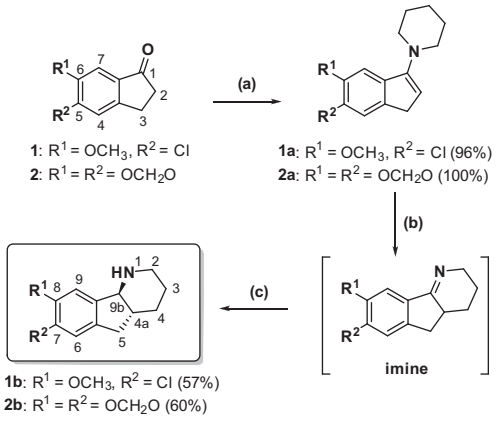

1: $R^1 = OCH_3$, $R^2 = Cl$
2: $R^1 = R^2 = OCH_2O$
1a: $R^1 = OCH_3$, $R^2 = Cl$ (96%)
2a: $R^1 = R^2 = OCH_2O$ (100%)
1b: $R^1 = OCH_3$, $R^2 = Cl$ (57%)
2b: $R^1 = R^2 = OCH_2O$ (60%)

Scheme 1. Synthesis of HHIP **1b** and **2b**. Reagents and conditions: (a) piperidine, $TiCl_4$, dry toluene, N_2 atmosphere, rt, 3 days; (b) 3-bromopropylamine hydrobromide, dry DMF, N_2 atmosphere, 110 °C, 8 h; (c) $NaBH_4$, EtOH, rt, 16 h.

value of H-9b ($^3J_{H9b,4a} \sim 10$ Hz) implies that both H-9b and H-4a are located in axial positions.

Furthermore, in order to explore the ability of the HHIP structure to bind to melatonin receptors, we decided to synthesize several amide and carbamate derivatives of HHIP. Chloro-8-methoxy HHIP **1b** was subjected to Ac_2O/pyridine to obtain *N*-acetyl **1c**, and urea derivative **1d** was obtained in good yield when **1b** was treated with ethyl isocyanate[18] (Scheme 2). 7,8-Methylenedioxy HHIP **2b** was treated with *p*-fluorophenyl isocyanate to obtain the urea derivative **2c** in good yield. When **2b** was *N*-alkylated using the corresponding amide alkyl bromides,[19] compounds **2d**, **2e** and **2f** were prepared (Scheme 3).

The key step in our synthetic route was the alkylation–cyclization from the corresponding enamine to obtain the indenopyridine skeleton. The enamine is first alkylated by 3-bromopropylamine, resulting on the addition of the alkyl chain in β position and formation of an iminium salt. Then, primary amine rapidly attacks the iminium and piperidine is released, through an intramolecular condensation, which generates the imine indenopyridine (Scheme 4).

All synthesized HHIP compounds were evaluated for their binding affinity for human MT_1 and MT_2 receptors stably transfected in human embryonic kidney (HEK 293) cells using 2-[^{125}I]iodomelatonin as radioligand (Table 1).[20] Results showed that 7-chloro-8-methoxy HHIP **1d**[21] with an urea motif was able to bind to both receptors in the nanomolar or low micromolar range (MT_1 K_i = 670 nM and MT_2 K_i = 190 nM), with a MT_1/MT_2 affinity ratio of about 3.5, whereas its analogue **1c** with *N*-acetyl substituent showed no binding affinity at the highest concentration tested. Moreover, the *N*-acetamide function on the piperidine is also important to bind MT receptors. Indeed, the methylenedioxy HHIP **2d**[22] with *N*-phenylacetamide motif displayed selectivity towards MT_1 receptors, and **2f**[23] with *N*-alkylacetamide substituent showed selectivity for MT_2 subtypes. It seems that the methylenedioxy group on the indene ring system and the *N*-phenylacetamide or *N*,*N*-diethylacetamide side-chain hold the suitable configuration to bind selectively MT_1 or MT_2 receptors, respectively. However, no binding affinity was found for both the acetamide derivative **2e** with a cyclohexyl substituent, which is provided of a non-planar conformation, and the analogue with phenylurea function **2c**.

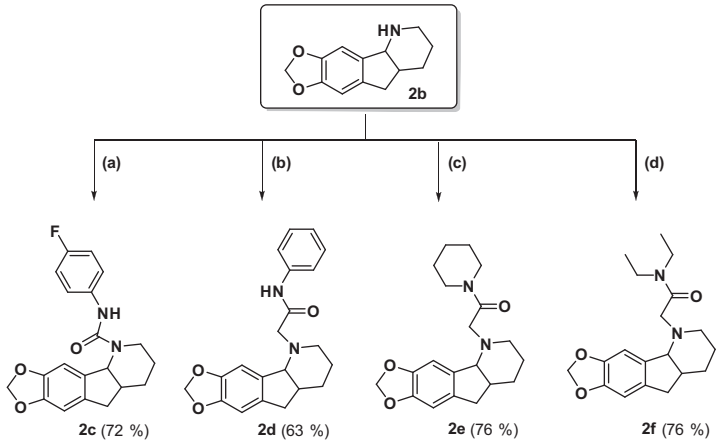

Scheme 3. Synthesis of HHIP **2c**–**2f**. Reagents and conditions: (a) *p*-fluorophenyl isocyanate, CH_2Cl_2, reflux, 2 h; (b) 2-bromo-*N*-phenylacetamide, Et_3N, dry CH_3CN, reflux, 2 h; (c) 2-bromo-1-(piperidin-1-yl)ethanone, Et_3N, dry CH_3CN, reflux, 2 h; (d) 2-bromo-*N*,*N*-diethylacetamide, Et_3N, dry CH_3CN, reflux, 2 h.

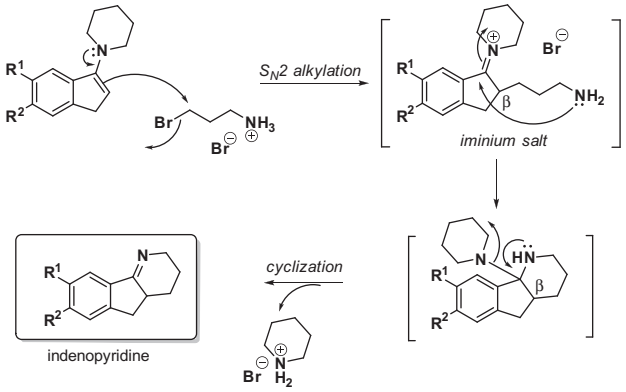

Scheme 4. Alkylation and cyclization through *trans*-imine formation.

Table 1
MT_1 and MT_2 receptor-binding affinities of hexahydroindenopyridines

Compounds	MT_1 K_i[a] (nM)	MT_2 K_i[a] (nM)
1b	>10,000	>10,000
1c	>10,000	>10,000
1d	670 ± 62	190 ± 35
2b	>10,000	>10,000
2c	>10,000	>10,000
2d	500 ± 34	>10,000
2e	>10,000	>10,000
2f	>10,000	380 ± 42
MLT	0.14 ± 0.03	0.41 ± 0.04

[a] Data are expressed as mean ± SEM of at least three independent experiments.

Although these HHIPs showed lower binding affinities than melatonin and commercialized reference compounds, **2d** and **2f** exhibited a much higher selectivity for MT_1 or MT_2 receptors, respectively. These preliminary results indicate for the first time the potential of HHIP nucleus in the search of melatonin receptors ligands, and the important role played by the *N*-substituent (Table 1).

In conclusion, we reported an efficient, high yielding formation of new HHIPs from the corresponding indanone via enamine alkylation–cyclization with 3-bromopropyl amine, followed by a reduction in imine intermediates. Some HHIPs show interesting melatoninergic properties at nanomolar or low micromolar concentrations with selectivity for either MT_1 or MT_2 receptors. It seems that the methylenedioxy group on the indene ring system and the *N*-acetamide substituent are important structural features for selectivity. These preliminary results show that it should be possible to obtain more potent MT_1 and/or MT_2 receptor ligands by means of further structural development which qualify them as promising new leads for more structure–activity relationship studies in order to find new therapeutic agents for depression and/or insomnia.

Acknowledgments

This study was supported by the Grant SAF2011-23777, Spanish Ministry of Economy and Competitiveness.

References and notes

1. Arendt, J.; Deacon, S.; English, J.; Morgan, L. *J. Sleep Res.* **1995**, *4*, 74.
2. Delagrange, P.; Arkinson, J.; Boutin, J. A.; Casteilla, L.; Lesieur, D.; Misslin, R.; Pelissier, S.; Renard, P. *J. Neuroendocrinol.* **2003**, *15*, 442.
3. Boutin, J. A.; Audinot, V.; Ferry, G.; Delagrange, P. *Trends Pharmacol. Sci.* **2005**, *26*, 412.
4. Corruble, E.; De Bodinat, C.; Belaidi, C.; Goodwin, G. M. *Int. J. Neuropsychop.* **2013**, *16*, 2219.
5. Zlotos, D. P.; Jockers, R.; Cecon, E.; Rivara, S.; Witt-Enderby, P. A. *J. Med. Chem.* **2014**, *57*, 3161.
6. Augstein, J.; Ham, A. L.; Leeming, P. R. *J. Med. Chem.* **1972**, *15*, 466.
7. Kunstmann, R.; Lerch, U.; Gerhards, H.; Leven, M.; Schacht, U. *J. Med. Chem.* **1984**, *27*, 432.
8. Meyer, M. D.; DeBernardis, J. F.; Hancock, A. A. *J. Med. Chem.* **1994**, *37*, 105.
9. Cook, C. E.; Wani, M. C.; Jump, J. M.; Lee, Y.-W.; Fail, P. A.; Anderson, S. A.; Gu, Y.-Q.; Petrow, V. *J. Med. Chem.* **1995**, *38*, 753.
10. Eckhardt, M.; Peters, S.; Nar, H.; Himmelsbach, F.; Zhuang, L. *PCT Int. Appl.* **2011**, WO 2011057054, A1 20110512.
11. Kiwata, S.; Izumoto, N.; Nagase, H. *Jpn. Kokai Tokkyo Koho* **2008**. JP 2008179556A 20080807.
12. Van Emelen, K.; De Wit, T.; Hoornaert, G. J.; Compernolle, F. *Tetrahedron* **2002**, *58*, 4225.
13. Hong, B.-C.; Hallur, M. S.; Liao, J.-H. *Synth. Commun.* **2006**, *36*, 1521.
14. White, W. A.; Weingarten, H. *J. Org. Chem.* **1967**, *32*, 213.
15. Carlson, R.; Nilsson, A.; Strömqvist, M. *Acta Chem. Scand. Ser. B* **1983**, *37*, 7.
16. Guinot, S. G. R.; Hepworth, J. D.; Wainwright, M. *Dyes Pigments* **1998**, *36*, 387.
17. *General procedure for the synthesis of hexahydroindenopyridines (**1b**,**2b**):* A solution of indanone **1** or **2** (2.55 mmol) in dry toluene (10 mL) was treated with piperidine (15.17 mmol), and the mixture and cooled to −10 °C. Then, $TiCl_4$ (0.17 mL, 1.53 mmol) was added and stirred at −10 °C for one additional hour. The reaction mixture was stirred at room temperature for 3 days. The resulting suspension was filtered through Celite, washed with AcOEt, dried over Na_2SO_4 and concentrated to dryness to give **1a** (96%) or **2a** (100%) that was used in the following step with no further purification. Thus, **1a** or **2a** was added to a well-stirred solution of 3-bromopropylamine hydrobromide (2.51 mmol) in dry DMF (5 mL). The mixture was heated at 110 °C under N_2 atmosphere for 8 h. Afterwards, the reaction mixture was evaporated to dryness, dissolved in EtOH (15 mL) and treated with $NaBH_4$ (11.08 mmol). The mixture was stirred overnight at room temperature. Afterwards, water (2 mL) was added and the solvent partially removed and the resulting suspension was extracted with AcOEt (3 × 10 mL). The combined organic layers were dried over Na_2SO_4 and concentrated to dryness to give **1b** (57%) or **2b** (60%) after purification by silica gel column chromatography. ^{1}H NMR for **1b** (500 MHz, CDCl3) δ 7.06 (s, 1H, CH-6), 6.78 (s, 1H, CH-9), 3.74 (s, 3H, OCH_3), 3.38 (d, 1H, J = 10.0 Hz, CH-9b), 3.14 (m, 1H, CH_2-2α), 2.73 (td, 1H, J = 3.2, 13.0 Hz, CH_2-2β), 2.62 (dd, 1H, J = 6.5, 14.5 Hz, CH_2-5α), 2.26 (m, 1H, CH_2-5β), 1.94 (m, 1H, CH_2-4α), 1.64 (m, 2H, CH_2-3α and CH-4a), 1.50 (m, 1H, CH_2-4β), 1.40 (m, 1H, CH_2-3β); EIMS m/z (%) 236 $[M-H]^+$ (100), 194 (75), 145 (40), 115 (40), 102 (40). ^{1}H NMR for **2b**: (500 MHz, $CDCl_3$) δ 6.59 (s, 1H, CH-9), 6.56 (s, 1H, CH-6), 5.77 (s, 1H, OCH_2O-α), 5.74 (s, 1H, OCH_2O-β), 3.27 (d, 1H, J = 10.0 Hz, CH-9b), 3.10 (m, 1H, CH_2-2α), 2.67 (td, 1H, J = 3.2, 13.0 Hz, CH_2-2β), 2.55 (dd, 1H, J = 6.5, 14.5 Hz, CH_2-5α), 2.20 (m, 1H, CH_2-5β), 1.86 (m, 1H, CH_2-4α), 1.60 (m, 2H, CH_2-3α and CH-4a), 1.47 (m, 1H, CH_2-4β), 1.37 (m, 1H, CH_2-3β); EIMS m/z (%) 216 $[M-H]^+$ (100), 174 (25), 102 (40).
18. Mistry, S. N.; Baker, J. G.; Fischer, P. M.; Hill, S. J.; Gardiner, S. M.; Kellam, B. *J. Med. Chem.* **2013**, *56*, 3852.
19. Salvatore, R. N.; Yoon, C. H.; Jung, K. W. *Tetrahedron* **2001**, *57*, 7785.
20. Nosjean, O.; Nicolas, J.-P.; Klupsch, F.; Delagrange, P.; Canet, E.; Boutin, J. A. *Biochem. Pharmacol.* **2001**, *61*, 1369.
21. ^{1}H NMR for **1d** (500 MHz, $CDCl_3$) δ 7.26 (s, 1H, CH-6), 6.94 (s, 1H, CH-9), 4.57 (s, 1H, NH), 4.45 (m, 1H, CH_2-2α), 4.20 (d, 1H, J = 10.7 Hz, CH-9b), 3.84 (s, 3H, OCH_3), 3.28 (m, 1H, CH_2-2′α), 3.04 (m, 1H, CH_2-2′β), 2.90 (m, 2H, CH_2-2β and CH_2-5α), 2.41 (m, 1H, CH_2-5β), 2.35 (m, 1H, CH-4a), 2.14 (m, 1H, CH_2-4α), 1.64 (m, 3H, CH_2-4β and CH_2-3), 0.96 (t, 3H, J = 7.0 Hz, CH_3-3′); HRESIMS m/z 309.1372 $[M+H]^+$ (309.1370, calcd for $C_{16}H_{22}N_2O_2Cl$).
22. ^{1}H NMR for **2d** (500 MHz, $CDCl_3$) δ 9.66 (s, 1H, NH), 7.65 (m, 2H, CH-2′ and CH-6′), 7.36 (m, 2H, CH-3′ and CH-5′), 7.12 (m, 1H, CH-4′), 6.70 (s, 1H, CH-6), 6.60 (s, 1H, CH-9), 5.89 (s, 2H, OCH_2O), 3.80 (d, 1H, J = 8.7 Hz, CH-9b), 3.32 (m, 2H, CH_2CO), 3.01 (m, 2H, CH_2-2), 2.75 (dd, 1H, J = 6.1, 14.2 Hz, CH_2-5α), 2.32 (m, 1H, CH_2-5β), 2.05 (m, 1H, CH_2-4α) 1.78 (m, 1H, CH-4a), 1.60 (m, 1H, CH_2-3α), 1.52 (m, 1H, CH_2-4β), 1.37 (m, 1H, CH_2-3β); HRESIMS m/z 351.1707 $[M+H]^+$ (351.1709, calcd for $C_{21}H_{23}N_2O_3$).
23. ^{1}H NMR for **2f** (500 MHz, $CDCl_3$) δ 6.76 (s, 1H, CH-9), 6.69 (s, 1H, CH-6), 5.92 (s, 1H, OCH_2O-α), 5.88 (s, 1H, OCH_2O-β), 3.80 (d, 1H, J = 9.4 Hz, CH-9b), 3.54 (d, 1H, J = 13.2 Hz, CH_2CO-α), 3.43 (m, 1H, CH_2CO-β), 3.36 (m, 4H, CH_2-2′ and CH_2-4′), 3.17 (m, 1H, CH_2-2α), 2.92 (td, 1H, J = 2.1, 12.1 Hz, CH_2-2β), 2.73 (dd, 1H, J = 6.2, 12.6 Hz, CH_2-5α), 2.28 (m, 1H, CH_2-5β), 2.12 (m, 1H, H-4a), 2.03 (m, 1H, CH_2-4α), 1.82 (m, 1H, CH_2-3α), 1.55 (m, 1H, CH_2-4β), 1.46 (m, 1H, CH_2-3β), 1.14 (m, 6H, CH_3-3′ and CH_3-5′); EIMS m/z (%) m/z (%) 330 $[M]^+$ (90), 282 (35). HRESIMS m/z 331.2033 $[M+H]^+$ (331.2022, calcd for $C_{19}H_{27}N_2O_3$).

European Journal of Medicinal Chemistry 86 (2014) 700–709

Contents lists available at ScienceDirect

European Journal of Medicinal Chemistry

journal homepage: http://www.elsevier.com/locate/ejmech

Original article

Efficient synthesis of hexahydroindenopyridines and their potential as melatoninergic ligands

Javier Párraga [a], Laura Moreno [a], Amelia Diaz [b], Noureddine El Aouad [a], Abraham Galán [a], María Jesús Sanz [c, d], Daniel-Henri Caignard [e], Bruno Figadère [f], Nuria Cabedo [a, g, *], Diego Cortes [a]

[a] Departamento de Farmacología, Laboratorio de Farmacoquímica, Facultad de Farmacia, Universidad de Valencia, Burjassot, 46100 Valencia, Spain
[b] Departamento de Química Orgánica, Facultad de Ciencias, Universidad de Málaga, 29071 Málaga, Spain
[c] Departamento de Farmacología, Facultad de Medicina, Universidad de Valencia, 46010 Valencia, Spain
[d] Institute of Health Research-INCLIVA, University Clinic Hospital of Valencia, Valencia, Spain
[e] Département des Sciences Expérimentales, Institut de Recherches Servier, 92150 Suresnes, France
[f] UMR CNRS 8076, LERMIT, Université Paris-Sud, Laboratoire de Pharmacognosie, UFR de Pharmacie, Châtenay-Malabry F-92296, France
[g] Centro de Ecología Química Agrícola-Instituto Agroforestal Mediterraneo, UPV, Campus de Vera, Edificio 6C, 46022 Valencia, Spain

ARTICLE INFO

Article history:
Received 27 February 2014
Received in revised form
4 September 2014
Accepted 11 September 2014
Available online 16 September 2014

Keywords:
Hexahydroindenopyridines
Melatonin
MT_1 and MT_2 receptor binding
Synthesis

ABSTRACT

Hexahydroindenopyridine (HHIP) is an interesting tricyclic piperidine nucleus that is structurally related to melatonin, a serotonin-derived neurohormone. Melatonin receptor ligands have applications in several cellular, neuroendocrine and neurophysiological disorders, including depression and/or insomnia. We report herein an efficient two-step method to prepare new HHIP via enamine *C*-alkylation-cyclization. The influence of substituents on the benzene ring and the nitrogen atom on melatoninergic receptors has been studied. Among the 25 synthesized HHIPs, some of them containing methylenedioxy (series 2) and 8-chloro-7-methoxy substituents (series 4) on the benzene ring revealed affinity for the MT_1 and/or the MT_2 receptors within the nanomolar range or low micromolar. Similar activities were also encountered for those presenting urea (**4g**), *N*-aryl (**2e**) and *N*-alkyl (**2f**) acetamide functions. Therefore, new synthesized compounds with a HHIP nucleus have emerged as new promising leads towards the discovery of melatoninergic ligands which could provide new therapeutic agents.

1. Introduction

Melatonin (*N*-acetyl-5-methoxytryptamine) is a serotonin-derived neurohormone of long-standing interest found in some algae and higher animals, including humans. The pineal gland produces melatonin under the influence of the suprachiasmatic nucleus of the hypothalamus by a circadian rhythm of secretion, with peak levels occurring during darkness [1]. Melatonin (MLT) participates in a variety of cellular, neuroendocrine and neurophysiological processes. It is involved in the modulation of the cardiovascular and immune systems, as well as in the glucose metabolism and hormone secretion. For this reason, a disturbance in melatonin rhythm and secretion is involved in the development of neurodegenerative diseases, cancer, stroke, thermoregulation and sleep disorders [2–7]. Melatonin exerts its effects by several molecular mechanisms, including via high-affinity G-protein-coupled receptors. Indeed, it activates MT_1 and MT_2 receptors, at nanomolar concentrations, and also binds with a lower affinity to the third putative isoform MT_3 receptor, which is the intracellular protein quinone reductase 2 [8,9].

Since both MT_1 and MT_2 receptors are widely distributed in different areas of the brain and extracerebral organs, multiple functional roles for melatonin have been suggested. However, considerable attention has been paid to melatonin receptor ligands in recent years given their applications in insomnia and depression. Among the melatoninergic drugs, agomelatine is a commercialized antidepressant (Laboratoires Servier, valdoxan® and thymanax®) that stands out for its interesting properties as a potent agonist of MT_1 and MT_2 receptors (Fig. 1) [10,11].

Hexahydroindenopyridine (HHIP) is an intriguing heterocyclic framework that provides a new class of compounds with potential use as therapeutic agents. HHIPs possess a tricyclic ring system that contains a constrained indeno-piperidine pharmacophoric nucleus. This class of compounds displays several biological activities, including antidepressant [12–14], serotoninergic [15,16],

* Corresponding author. Centro de Ecología Química Agrícola-Instituto Agroforestal Mediterraneo, UPV, Campus de Vera, Edificio 6C, 46022 Valencia, Spain.
E-mail addresses: ncabedo@ceqa.upv.es, ncabedo@uv.es (N. Cabedo).

http://dx.doi.org/10.1016/j.ejmech.2014.09.038
0223-5234/

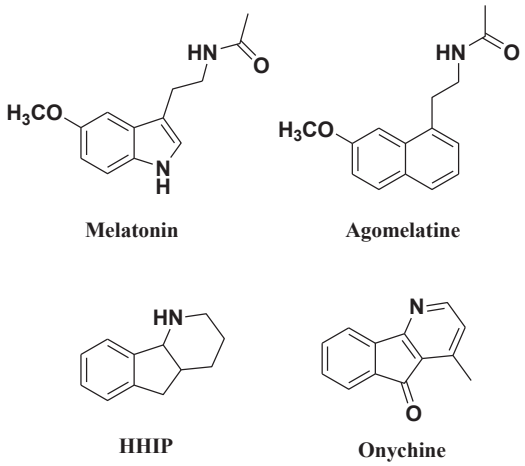

Fig. 1. Melatonin, agomelatine, HHIP and onychine.

antipsychotic [17], antispermatogenic [18] and inhibition of the 11β-hydroxysteroid dehydrogenase enzyme [19]. Furthermore, HHIPs have attracted our interest as potential melatoninergic ligands thanks to their original melatonin-related structure (Fig. 1).

The literature has described different synthetic methods to obtain this type of molecules. In this regard, Augstein et al. prepared 5-phenyl-HHIPs from a cyanoethyl phenylindanone in two steps, but obtained low yields [12]. Some authors achieved the synthesis of HHIPs via a tricyclic lactam intermediate. Kunstmann et al. carried out the synthesis through the condensation of aldehydes and 6-phenyl-3,4-dihydropyridin-2-ones which were prepared from 5-oxo-5-phenylvaleronitriles [13]. Van Emelen et al. did so by an intramolecular Ritter reaction of a hydroxynitrile [20] whereas Hong et al. obtained 4-azafluorenes, onychine-type (Fig. 1), through a hetero Diels–Alder cycloaddition of indenes with 1,3-azabutadienes [21].

In this work, we decided to use a new method which allowed us to easily obtain the HHIP framework in very few steps and with good yields [22]. We evaluated the influence of different substituents in the nitrogen atom and at the C-7 and C-8 positions of the benzene ring of the synthesized HHIPs on their affinity towards melatoninergic receptors. To this end, we have prepared four sets of differently substituted HHIPs (series 1–4) and their affinity towards MT_1 and MT_2 receptors was tested to establish a chemical structure-activity relationship (SAR).

2. Results and discussion

2.1. Chemistry

The synthesis of HHIP has been accomplished as outlined in Schemes 1–6. We have prepared four series of compounds (series 1–4) in accordance with the starting material. Therefore, we synthesized the following parent compounds: 7,8-dimethoxy-2,3,4,4a,5,9b-hexahydro-1*H*-indeno[1,2-*b*]pyridine (series 1) (Schemes 1 and 3); 7,8-methylenedioxy-2,3,4,4a,5,9b-hexahydro-1*H*-indeno[1,2-*b*]pyridine (series 2) (Schemes 1 and 4); 8-methoxy-2,3,4,4a,5,9b-hexahydro-1*H*-indeno[1,2-*b*]pyridine (series 3) (Schemes 1 and 5); and 7-chloro-8-methoxy-2,3,4,4a,5,9b-hexahydro-1*H*-indeno[1,2-*b*]pyridine (series 4) (Schemes 1 and 6).

The first step consisted in preparing the appropriate enamine (**1a**–**4a**) from a commercially available 1-indanone (**1**–**4**), using piperidine in the presence of $TiCl_4$ which acts as both Lewis acid catalyst and water scavenger. As starting materials, we employed: 5,6-dimethoxy-1-indanone (**1**, series 1), 5,6-methylenedioxy-1-indanone (**2**, series 2), 6-methoxy-1-indanone (**3**, series 3) and 5-chloro-6-methoxy-1-indanone (**4**, series 4). This reaction took place at room temperature in toluene for 3 days. Next, and with no further purification, the enamine (**1a**-**4a**) was treated with 3-bromopropylamine hydrobromide in DMF under reflux to give the tricyclic ring system with an imine function, which was reduced with $NaBH_4$ in ethanol to obtain the expected HHIP nucleus (Scheme 1) [22–25].

Parcell and Hauck [25] proposed that this reaction worked via an iminium ion in which, firstly the 3-bromopropylamine would attack the iminium tautomeric form of the enamine, followed by the piperidine elimination to give a new imine. This imine would be in equilibrium with an enamine form, and its double bond could react with the bromopropylamine chain (SN2) to displace the bromine anion with intramolecular cyclization. However, this mechanism shows some inconsistencies and the more feasible reaction mechanism would be the well-known C-alkylation reaction

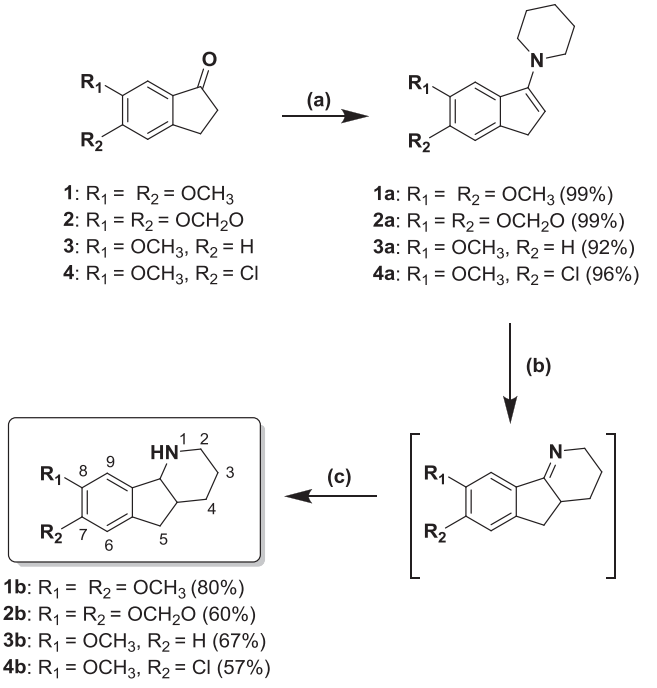

Scheme 1. Synthesis of HHIPs **1b**–**4b** (series 1–4). Reagents and conditions: (a) piperidine, $TiCl_4$, toluene, N_2 atmosphere, r.t., 3 days; (b) 3-bromopropylamine hydrobromide, DMF, N_2 atmosphere, reflux, 8 h; (c) $NaBH_4$, EtOH, rt, 16 h.

of enamines with alkyl halides (Scheme 2) [22].

Synthesis of compounds of the series 1 (Scheme 3): 7,8-dimethoxy-2,3,4,4a,5,9b-hexahydro-1*H*-indeno[1,2-*b*]pyridine (**1b**) was *N*-methylated with formaldehyde and formic acid, followed by reduction with $NaBH_4$ to obtain **1c**. When **1b** and **1c** were O-demethylated after the treatment with BBr_3, catecholic HHIPs **1d** and **1e**, were respectively prepared. The N-acetylation of **1b** with Ac_2O and pyridine allowed us to attain **1f**. When **1b** was treated with an isothiocyanate reagent, such as 1-(2-isothiocyanatoethyl) piperidine and 1,2,3-trifluoro-4-isothiocyanatobenzene, the corresponding thiourea derivatives **1g** and **1h**, were respectively obtained.

Synthesis of compounds of the series 2 (Scheme 4): 7,8-methylenedioxy-2,3,4,4a,5,9b-hexahydro-1*H*-indeno[1,2-*b*]

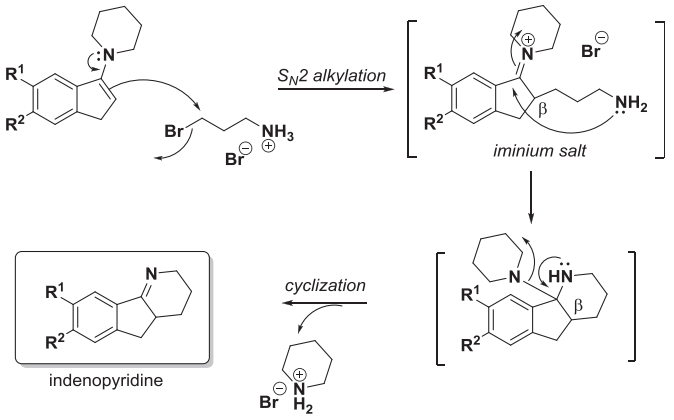

Scheme 2. Mechanism of *C*-alkylation-cyclization.

also treated with an isocyanate (ethyl isocyanate), to produce the urea derivative **4g**.

2.2. Binding affinities for melatonin receptors: SAR study

All the synthesized HHIPs of the four series (**1**–**4**) were evaluated as melatoninergic MT_1 and MT_2 ligands by binding assays [26,27] and the influence of the substituents in the nitrogen atom and at C-8 and C-9 positions in the benzene ring were explored. Neither the 7,8-dimethoxy (series 1: **1b**, **1c**, **1f**, **1g** and **1h**) nor the 8-methoxy (series 3: **3b**, **3c**, **3f** and **3g**) substituents on the benzene ring, including their catecholic (**1e** and **1d**) or phenolic (**3e** and **3d**) analogs, were favorable for melatoninergic activity. However, some derivatives with 7,8-methylenedioxy (series 2) and 7-chloro-8-methoxy (series 4) substituents in the benzene ring were able to displace MT_1 and MT_2 radioligand, 2-[^{125}I]iodomelatonin, from the

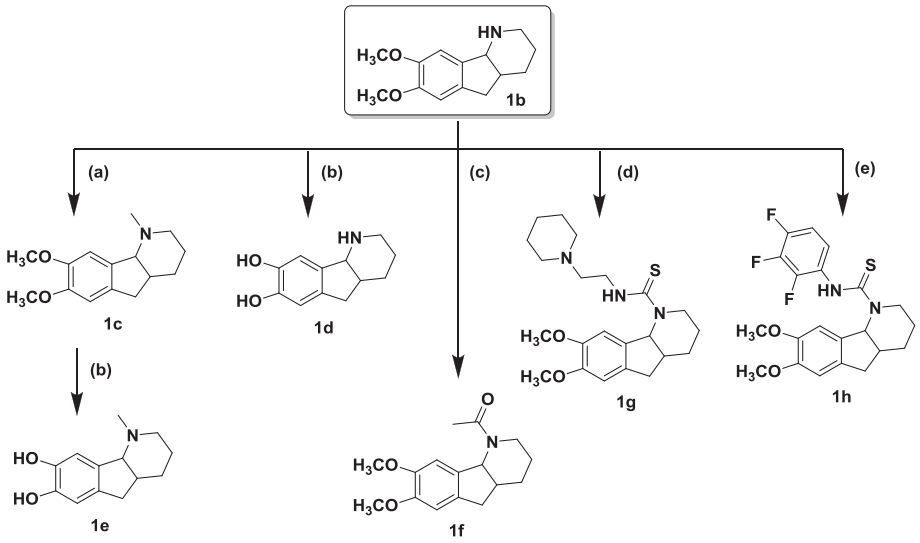

Scheme 3. Synthesis of HHIP **1c**–**1h**. Reagents and conditions: (a) 37% formaldehyde, formic acid, MeOH, reflux, 1 h; $NaBH_4$, reflux, 1 h; (b) BBr_3, CH_2Cl_2, −78 °C, 2 h; (c) Ac_2O, pyr, rt, 2 h; (d) 1-(2-isothiocyanatoethyl)piperidine, CH_2Cl_2, reflux, N_2 atmosphere, 2 h; (e) 1,2,3-trifluoro-4-isothiocyanatobenzene, CH_2Cl_2, reflux, N_2 atmosphere, 2 h.

pyridine (**2b**) was *N*-methylated with formaldehyde and formic acid, followed by reduction with $NaBH_4$ to obtain **2c**. When **2b** was treated with 1-fluoro-4-isocyanatobenzene, urea derivative **2d** was attained. The alkylation of **2b** with alkyl bromides, such as 2-bromo-*N*-phenylacetamide, 2-bromo-*N*,*N*-diethylacetamide or 2-bromo-1-(piperidin-1-yl)ethanone under basic conditions (Et_3N), gave the corresponding acetamides **2e**, **2f** and **2g**, respectively.

Synthesis of compounds of the series 3 (Scheme 5): 8-methoxy-2,3,4,4a,5,9b-hexahydro-1*H*-indeno[1,2-*b*]pyridine (**3b**) was *N*-methylated with formaldehyde and formic acid, followed by reduction with $NaBH_4$ to obtain **3c**. When **3b** and **3c** were O-demethylated with BBr_3, **3d** and **3e**, were respectively obtained. HHIP **3b** was also subjected to the reactions of *N*-acylation. Hence, **3b** was treated with Ac_2O and pyridine, or with ethyl 4-chloro-4-oxobutanoate, under basic conditions (5% NaOH) to attain *N*-acylated **3f** and amide **3g**, respectively.

Synthesis of compounds of the series 4 (Scheme 6): 7-chloro-8-methoxy-2,3,4,4a,5,9b-hexahydro-1*H*-indeno[1,2-*b*]pyridine (**4b**) was *N*-alkylated with formaldehyde and formic acid, followed by reduction with $NaBH_4$ to give **4c**. When **4b** and **4c** were *O*-demethylated with BBr_3, **4d** and **4e**, were respectively obtained. HHIP **4b** was *N*-acetylated with Ac_2O and pyridine to form **4f**. HHIP **4b** was

binding sites. Indeed, the 7-chloro-8-methoxy HHIP **4g** (series 4) which bears an urea function was able to bind to both receptors at namomolar or low micromolar concentrations: Ki MT_1 670 nM and Ki MT_2 190 nM. Of note, both methylenedioxy HHIPs (series 2) **2e** with a *N*-aryl acetamide motif and **2f** bearing a *N*-alkyl acetamide on the nitrogen atom, displayed selectivity towards the MT_1 or MT_2 receptors, respectively, at nanomolar or low micromolar concentrations: Ki MT_1 500 nM and Ki MT_2 380 nM (Table 1).

3. Conclusions

Twenty-five compounds containing an HHIP nucleus were synthesized from the corresponding indanones (**1**–**4**) via enamine *C*-alkylation-cyclization in a two-step procedure with good yields. Sets of four series (series 1–4) were prepared depending on the starting materials to give parents HHIPs with different substituents in the benzene ring: 7,8-dimethoxy-2,3,4,4a,5,9b-hexahydro-1*H*-indeno[1,2-*b*]pyridine (**1b**, series 1), 7,8-methylenedioxy-2,3,4,4a,5,9b-hexahydro-1*H*-indeno[1,2-*b*]pyridine (**2b**, series 2), 8-methoxy-2,3,4,4a,5,9b-hexahydro-1*H*-indeno[1,2-*b*]pyridine (**3b**, series 3) and 7-chloro-8-methoxy-2,3,4,4a,5,9b-hexahydro-1*H*-indeno[1,2-*b*]pyridine (**4b**, series 4). All the synthesized HHIPs were evaluated for their ability to displace radioligand 2-[^{125}I]

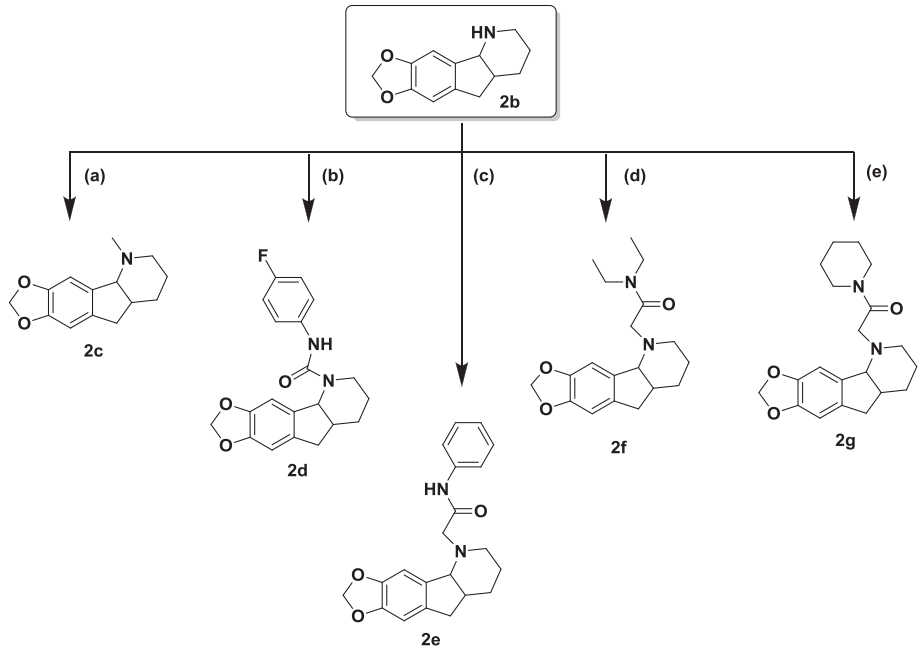

Scheme 4. Synthesis of HHIP **2c**–**2g**. Reagents and conditions: (a) 37% formaldehyde, formic acid, MeOH, reflux, 1 h; $NaBH_4$, reflux, 1 h; (b) 1-fluoro-4-isocyanatobenzene, CH_2Cl_2, reflux, N_2 atmosphere, 2 h; (c) 2-bromo-*N*-phenylacetamide, CH_3CN, Et_3N, reflux, N_2 atmosphere, 4 h; (d) 2-bromo-*N*,*N*-diethylacetamide, CH_3CN, Et_3N, reflux, N_2 atmosphere, 4 h; (e) 2-bromo-1-(piperidin-1-yl)ethanone, CH_3CN, Et_3N, reflux, N_2 atmosphere, 4 h.

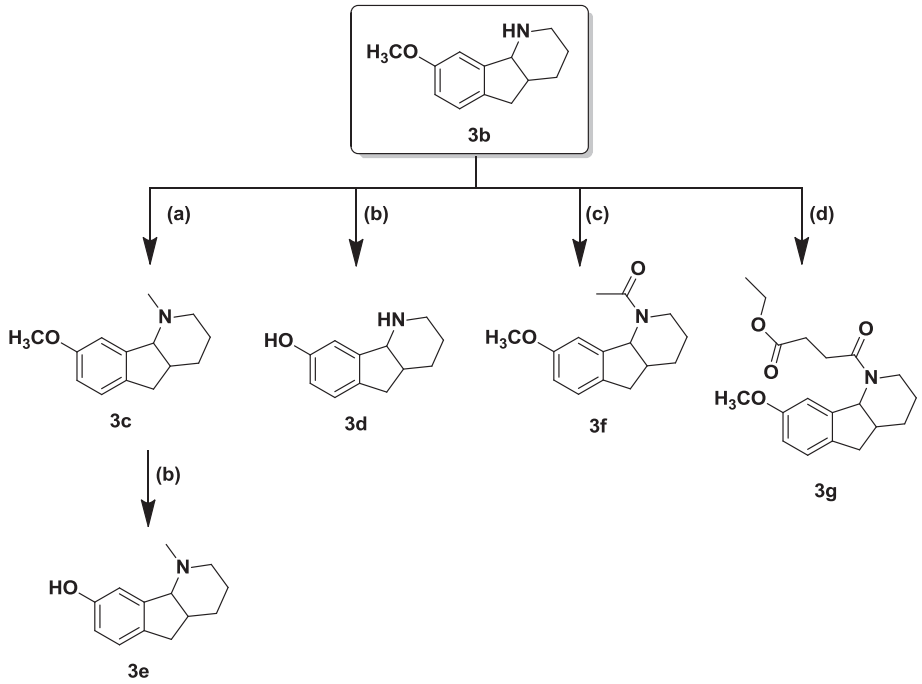

Scheme 5. Synthesis of HHIP **3c**–**3g**. Reagents and conditions: (a) 37% formaldehyde, formic acid, MeOH, reflux, 1 h; $NaBH_4$, reflux, 1 h; (b) BBr_3, CH_2Cl_2, −78 °C, 2 h; (c) Ac_2O, pyr, rt, 2 h; (d) ethyl 4-chloro-4-oxobutanoate, CH_2Cl_2, 5% NaOH, rt, 2 h.

iodomelatonin from its melatoninergic MT_1 and MT_2 receptor-binding sites. Of these, only few derivatives bearing 7,8-methylenedioxy (series 2) and 7-chloro-8-methoxy (series 4) substituents in the HHIP nucleus were able to bind melatoninergic receptors at nanomolar concentrations. In particular, **4g** from series 4 with an urea function was able to bind to both MT_1 and MT_2 receptors, whereas **2e** and **2f** from series 2 with *N*-aryl and *N*-alkyl acetamide functions, respectively, displayed high selectivity for receptors MT_1 or MT_2. In this work, new feasible synthesized compounds with an HHIP nucleus have emerged as new promising leads for the discovery of melatoninergic ligands. These new therapeutic agents may turn into potential candidates for clinical application in the control of several cellular, neuroendocrine and

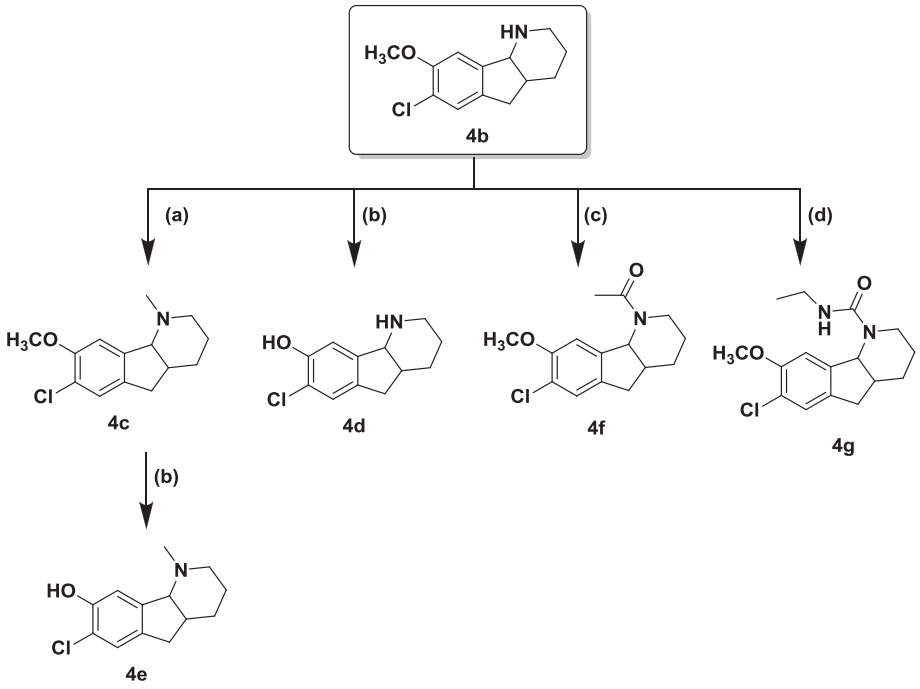

Scheme 6. Synthesis of HHIP **4c**–**4g**. Reagents and conditions: (a) 37% formaldehyde, formic acid, MeOH, refluxed, 1 h; $NaBH_4$, reflux, 1 h; (b) BBr_3, CH_2Cl_2, −78 °C, 2 h; (c) Ac_2O, pyr, rt, 2 h; (d) ethyl isocyanate, CH_2Cl_2, reflux, N_2 atmosphere, 2 h.

neurophysiological disorders, including depression and/or insomnia.

4. Experimental section

4.1. Chemistry

EIMS mass spectra were recorded on a VG Autospec Analytical Fisons (Manchester, UK) or a GC–MS instrument (PerkinElmer Clarus 500 gas chromatography, Shelton, EEUU) using a ZB-5 MS capillary column (Phenomenex, Torrance, CA, EEUU). High resolution (HRESIMS) data were recorded on a Waters Xevo quadrupole time-of-flight (Q-TOF) spectrometer (Waters Corp., Milford, MA, USA) coupled to an Acquity UPLC system (Waters Corp., Milford, MA, USA) via an electrospray ionization (ESI) interface operating in positive mode and using a Waters Acquity BEH C18 column (50 × 2.1 mm i.d., 1.7 μm); ^{1}H NMR and ^{13}C NMR spectra were recorded with $CDCl_3$ as solvent on a Bruker AC-500. Multiplicities of ^{13}C NMR resonances were assigned by DEPT experiments. COSY, HSQC and HMBC correlations were recorded at 400 MHz and 500 MHz (Bruker AC-400 or AC-500). The assignments of all compounds were made by COSY, DEPT, HSQC and HMBC. All the reactions were monitored by analytical TLC with silica gel 60 F254 (Merck 5554). Residues were purified by silica gel 60 (40–63 μm, Merck 9385) column chromatography. Solvents and reagents were purchased from commercial sources. Quoted yields are of purified material.

4.1.1. General procedure for the synthesis of (inden-3-yl)piperidines (*1a*-*4a*)

A solution of 1-indanone (**1**–**4**, 0.52 mmol) in dry toluene (10 mL) was stirred under nitrogen atmosphere at room temperature. Then, 0.31 mL of piperidine (3.1 mmol) was added and the mixture was cooled to −10 °C on an ice bath. The mixture was treated with $TiCl_4$ (0.32 mL, 0.31 mmol) and stirred at −10 °C for one additional hour. Then, the ice bath was removed and stirring was continued at room temperature for 3 days. The resulting suspension was filtered through Celite, which was washed with AcOEt, dried over Na_2SO_4 and concentrated to dryness. The enamines **1a**–**4a** were used in the following step with no further purification.

*4.1.1.1. 1-(5,6-Dimethoxy-1H-inden-3-yl)piperidine (**1a**).* From 5,6-dimethoxy-1-indanone (**1**), 160 mg (99%) **1a** was obtained (yield: 99%). ^{1}H NMR (500 MHz, $CDCl_3$) δ 7.00 (s, 1H, CH-7), 6.95 (s, 1H, CH-4), 5.43 (t, 1H, J = 2.0 Hz, CH-2), 3.90 (s, 6H, 2 × OCH_3), 3.23 (d, 2H, J = 2.0 Hz, CH_2-1), 3.01 (m, 4H, CH_2-2′ and CH_2-6′), 1.75 (m, 4H, CH_2-3′ and CH_2-5′), 1.55 (m, 2H, CH_2-4′); ^{13}C NMR (125 MHz, $CDCl_3$) δ 153.9 (C-3), 147.5 (C-5 and C-6), 137.0 (C-3a), 134.4 (C-7a), 108.1 (CH-2), 107.7 (CH-7), 103.8 (CH-4), 56.2 (2 × OCH_3), 52.2 (CH_2-2′ and CH_2-6′), 35.4 (CH_2-1), 25.9 (CH_2-3′ and CH_2-5′), 24.6 (CH_2-4′). EIMS *m/z* (%) 259 $[M]^+$ (70), 244 (60), 161 (50), 133 (50).

*4.1.1.2. 1-(5,6-Methylenedioxy-1H-inden-3-yl)piperidine (**2a**).* From 5,6-methylenedioxy-1-indanone (**2**), **2a** was obtained (yield: 99%). ^{1}H NMR (500 MHz, $CDCl_3$) δ 6.90 (s, 1H, CH-7), 6.88 (s, 1H, CH-4), 6.06 (s, 2H, OCH_2O), 5.44 (t, 1H, J = 2.3 Hz, CH-2), 3.61 (d, 2H, J = 2.3 Hz, CH_2-1), 2.97 (m, 4H, CH_2-2′ and CH_2-6′), 1.72 (m, 4H, CH_2-3′ and CH_2-5′), 1.58 (m, 2H, CH_2-4′); ^{13}C NMR (125 MHz, $CDCl_3$) δ 153.8 (C-3), 146.1 (C-5) 145.5 (C-6), 138.1 (C-3a), 135.6 (C-7a), 107.9 (CH-2), 105.3 (CH-7), 100.8 (CH-4 and OCH_2O), 52.0 (CH_2-2′ and CH_2-6′), 35.8 (CH_2-1), 26.11 (CH_2-3′ and CH_2-5′), 24.4 (CH_2-4′). EIMS *m/z* (%) 243 $[M]^+$ (80), 159 (100), 103 (70).

*4.1.1.3. 1-(5-Methoxy-1H-inden-3-yl)piperidine (**3a**).* From 5-methoxy-1-indanone (**3**), **3a** was obtained (yield: 92%). ^{1}H NMR (500 MHz, $CDCl_3$) δ 7.35 (d, 1H, J = 8.1 Hz, CH-7), 7.03 (d, 1H, J = 2.4 Hz, CH-4), 6.82 (dd, 1H, J = 2.4, 8.1 Hz, CH-6), 5.62 (t, 1H, J = 2.3 Hz, CH-2), 3.30 (d, 2H, J = 2.3 Hz, CH_2-1), 3.08 (m, 4H, CH_2-2′ and CH_2-6′), 1.82 (m, 4H, CH_2-3′ and CH_2-5′), 1.67 (m, 2H, CH_2-4′); ^{13}C NMR (125 MHz, $CDCl_3$) δ 158.3 (C-5), 153.3 (C-3), 147.9 (C-3a), 136.4 (C-7a), 124.2 (CH-7), 110.4 (CH-2), 110.1 (CH-6), 105.8 (CH-4),

Table 1
MT_1 and MT_2 receptor-binding affinities of hexahydroindenopyridines.

Compounds	MT_1 K_i (nM)[a]	MT_2 K_i (nM)[a]
1b	>10,000	>10,000
1c	>10,000	>10,000
1d	>10,000	>10,000
1e	>10,000	>10,000
1f	>10,000	>10,000
1g	>10,000	>10,000
1h	>10,000	>10,000
2b	>10,000	>10,000
2c	>10,000	>10,000
2d	>10,000	>10,000
2e	500 ± 34	>10,000
2f	>10,000	380 ± 42
2g	>10,000	>10,000
3b	>10,000	>10,000
3c	>10,000	>10,000
3d	>10,000	>10,000
3e	>10,000	>10,000
3f	>10,000	>10,000
3g	>10,000	>10,000
4b	>10,000	>10,000
4c	>10,000	>10,000
4d	>10,000	>10,000
4e	>10,000	>10,000
4f	>10,000	>10,000
4g	670 ± 62	190 ± 35
MLT	0.14 ± 0.03	0.41 ± 0.04

[a] Data are expressed as mean ± SEM of at least three independent experiments.

52.0 (CH_2-2′ and CH_2-6′), 34.7 (CH_2-1), 25.9 (CH_2-3′ and CH_2-5′), 24.5 (CH_2-4′); EIMS *m/z* (%) 229 $[M]^+$ (65), 145 (90), 102 (100).

*4.1.1.4. 1-(6-Chloro-5-methoxy-1H-inden-3-yl)piperidine (**4a**).* From 6-chloro-5-methoxy-1-indanone (**4**), **4a** was obtained (yield: 96%). ^{1}H NMR (500 MHz, $CDCl_3$) δ 7.37 (s, 1H, CH-7), 6.94 (s, 1H, CH-4), 5.57 (t, 1H, J = 2.3 Hz, CH-2), 3.93 (s, 3H, OCH_3), 3.23 (d, 2H, J = 2.3 Hz, CH_2-1), 3.00 (m, 4H, CH_2-2′ and CH_2-6′), 1.75 (m, 4H, CH_2-3′ and CH_2-5′), 1.61 (m, 2H, CH_2-4′); ^{13}C NMR (125 MHz, $CDCl_3$) δ 153.6 (C-3), 153.5 (C-5), 141.5 (C-3a), 137.1 (C-7a), 125.4 (CH-7), 119.2 (C-6), 110.7 (CH-2), 104.0 (CH-4), 56.4 (OCH_3), 52.2 (CH_2-2′ and CH_2-6′), 34.8 (CH_2-1), 25.8 (CH_2-3′ and CH_2-5′), 24.5 (CH_2-4′). EIMS *m/z* (%) 263 $[M]^+$ (50), 248 (40).

*4.1.2. General procedure for the synthesis of 2,3,4,4a,5,9b-hexahydro-1H-indeno[1,2-b]pyridines (**1b**–**4b**)*

To a well-stirred solution of 3-bromopropylamine hydrobromide (471 mg, 2.51 mmol) in dry DMF (5 mL), the enamine (**1a**–**4a**, 2.42 mmol) was added. The mixture was refluxed at 110 °C under nitrogen atmosphere for 8 h. Then, the reaction mixture was evaporated to dryness, dissolved in EtOH (15 mL) and treated with $NaBH_4$ (11.08 mmol). The mixture was stirred overnight at room temperature. Next, 10 mL of H_2O were added and the solvent partially removed. The resulting suspension was extracted with AcOEt (3 × 10 mL). The combined organic layers were dried over Na_2SO_4 and concentrated to dryness.

*4.1.2.1. 7,8-Dimethoxy-2,3,4,4a,5,9b-hexahydro-1H-indeno[1,2-b]pyridine (**1b**).* From 1-(5,6-dimethoxy-3*H*-inden-1-yl)piperidine (**1a**), **1b** was obtained after purification by silica gel column chromatography (CH_2Cl_2/MeOH/NH_4OH 96:4:0.2) (yield: 80%). ^{1}H NMR (500 MHz, $CDCl_3$) δ 6.86 (s, 1H, CH-9), 6.78 (s, 1H, CH-6), 3.84 (s, 3H, OCH_3), 3.83 (s, 3H, OCH_3), 3.50 (d, 1H, J = 10.0 Hz, CH-9b), 3.26 (dd, 1H, J = 4.5, 13.0 Hz, CH_2-2α), 2.84 (td, 1H, J = 3.16, 13.0 Hz, CH_2-2β), 2.74 (dd, 1H, J = 6.5, 14.5 Hz, CH_2-5α), 2.37 (m, 1H, CH_2-5β), 2.06 (m, 1H, CH_2-4α), 1.73 (m, 2H, CH_2-3α and CH-4a), 1.63 (m, 1H, CH_2-4β), 1.50 (m, 1H, CH_2-3β); ^{13}C NMR (125 MHz, $CDCl_3$) δ 147.9 (C-8), 147.8 (C-7), 136.5 (CH-9a), 133.9 (C-5a), 108.6 (CH-6), 105.3 (CH-9), 68.1 (CH-9b), 56.1 (OCH_3), 56.0 (OCH_3), 52.1 (CH-4a), 47.3 (CH_2-2), 35.2 (CH_2-5), 29.4 (CH_2-4), 27.4 (CH_2-3). EIMS *m/z* (%) 232 $[M - H]^+$ (100), 227 (81); HRESIMS *m/z* 233.1427 $[M]^+$ ($C_{14}H_{19}NO_2$, calc 233.1416).

*4.1.2.2. 7,8-Methylenedioxy-2,3,4,4a,5,9b-hexahydro-1H-indeno[1,2-b]pyridine (**2b**).* From 1-(5,6-methylenedioxy-3*H*-inden-1-yl) piperidine (**2a**), **2b** was obtained after purification by silica gel column chromatography (CH_2Cl_2/MeOH/NH_4OH 92:8:0.2) (yield: 60%). ^{1}H NMR (500 MHz, $CDCl_3$) δ 6.59 (s, 1H, CH-9), 6.56 (s, 1H, CH-6), 5.77 (s, 1H, OCH_2O-α), 5.74 (s, 1H, OCH_2O-β), 3.27 (d, 1H, J = 10.0 Hz, CH-9b), 3.10 (dd, 1H, J = 4.5, 13.0 Hz, CH_2-2α), 2.67 (td, 1H, J = 3.2, 13.0 Hz, CH_2-2β), 2.55 (dd, 1H, J = 6.5, 14.5 Hz, CH_2-5α), 2.20 (m, 1H, CH_2-5β), 1.86 (m, 1H, CH_2-4α), 1.60 (m, 2H, CH_2-3α and CH-4a), 1.47 (m, 1H, CH_2-4β), 1.37 (m, 1H, CH_2-3β); ^{13}C NMR (125 MHz, $CDCl_3$) δ 145.8 (C-8), 145.5 (C-7), 137.6 (C-9a), 134.9 (C-5a), 105.2 (CH-6), 102.1 (CH-9), 100.3 (OCH_2O), 67.2 (CH-9b), 51.4 (CH-4a), 46.7 (CH_2-2), 34.7 (CH_2-5), 28.8 (CH_2-4), 26.6 (CH_2-3). EIMS *m/z* (%) 216 $[M - H]^+$ (100), 174 (25), 102 (40); HRESIMS *m/z* 218.1187 $[M + H]^+$ (218.1181, calc for $C_{13}H_{16}NO_2$).

*4.1.2.3. 8-Methoxy-2,3,4,4a,5,9b-hexahydro-1h-indeno[1,2-b]pyridine (**3b**).* From 1-(5-methoxy-3*H*-inden-1-yl)piperidine (**3a**), **3b** was obtained after purification by silica gel column chromatography (CH_2Cl_2/MeOH/NH_4OH 95:5:0.2) (yield: 67%). ^{1}H NMR (500 MHz, $CDCl_3$) δ 7.10 (d, J = 8.1 Hz, 1H, CH-6), 7.05 (d, J = 2.1 Hz, 1H, CH-9), 6.70 (dd, J = 2.1, 8.1 Hz, 1H, CH-7), 3.78 (s, 3H, OCH_3), 3.64 (d, 1H, J = 10.5 Hz, CH-9b), 3.38 (m, 1H, CH_2-2α), 2.90 (td, 1H, J = 3.5, 12.9 Hz, CH_2-2β), 2.79 (dd, 1H, J = 6.4, 14.5 Hz, CH_2-5α), 2.39 (m, 1H, CH_2-5β), 2.07 (m, 1H, CH_2-4α), 1.90 (m, 2H, CH_2-3α and CH-4a), 1.70 (m, 1H, CH_2-4β), 1.62 (m, 1H, CH_2-3β); ^{13}C NMR (125 MHz, $CDCl_3$) δ 158.7 (C-8), 143.5 (C-9a), 133.6 (C-5a), 125.3 (CH-6), 113.4 (CH-7), 107.5 (CH-9), 67.3 (CH-9b), 55.4 (OCH_3), 50.1 (CH-4a), 46.6 (CH_2-2), 34.4 (CH_2-5), 28.8 (CH_2-4), 25.7 (CH_2-3). EIMS *m/z* (%) 202 $[M - H]^+$ (100), 160 (80), 115 (40); HRESIMS *m/z* 204.1383 $[M + H]^+$(204.1388, calc for $C_{13}H_{18}NO$).

*4.1.2.4. 7-Chloro-8-methoxy-2,3,4,4a,5,9b-hexahydro-1H-indeno[1,2-b]pyridine (**4b**).* From 1-(6-chloro-5-methoxy-3*H*-inden-1-yl) piperidine (**4a**), **4b** was obtained after purification by silica gel column chromatography (CH_2Cl_2/MeOH/NH_4OH 97:3:0.2) (yield: 57%). ^{1}H NMR (500 MHz, $CDCl_3$) δ 7.06 (s, 1H, CH-6), 6.78 (s, 1H, CH-9), 3.74 (s, 3H, OCH_3), 3.38 (d, 1H, J = 10 Hz, CH-9b), 3.14 (dd, 1H, J = 4.5, 13.0 Hz, CH_2-2α), 2.73 (td, 1H, J = 3.16, 13.0 Hz, CH_2-2β), 2.62 (dd, 1H, J = 6.5, 14.5 Hz, CH_2-5α), 2.26 (m, 1H, CH_2-5β), 1.94 (m, 1H, CH_2-4α), 1.64 (m, 2H, CH_2-3α and CH-4a), 1.50 (m, 1H, CH_2-4β), 1.40 (m, 1H, CH_2-3β); ^{13}C NMR (125 MHz, $CDCl_3$) δ 153.1 (C-8), 144.5 (C-9a), 134.5 (C-5a), 125.6 (CH-6), 119.4 (C-7), 105.5 (CH-9), 67.4 (CH-9b), 55.8 (OCH_3), 51.2 (CH-4a), 46.8 (CH_2-2), 34.1 (CH_2-5), 28.9 (CH_2-4), 26.6 (CH_2-3). EIMS *m/z* (%) 236 $[M - H]^+$ (100), 194 (75), 145 (40), 115 (40), 102 (40); HRESIMS *m/z* 238.0992 $[M + H]^+$ (238.0999, calc for $C_{13}H_{17}NOCl$).

4.1.3. General procedure for N-methylation

To a stirred solution of HHIP (**1b**–**4b**, 0.17 mmol) in MeOH (8 mL), 37% formaldehyde (2.5 mL) and one drop of formic acid were added. The mixture was refluxed for 1 h and cooled to room temperature. Next, it was treated with $NaBH_4$ (1.7 mmol) and refluxed an additional hour. The reaction mixture was cooled to room temperature and H_2O (3 mL) was added. The solvent was partially removed under reduced pressure, and the aqueous mixture extracted with CH_2Cl_2 (3 × 15 mL). The combined organic extracts were dried over Na_2SO_4 and concentrated to dryness under reduced pressure.

*4.1.3.1. 7,8-Dimethoxy-1-methyl-2,3,4,4a,5,9b-hexahydro-1H-indeno [1,2-b] pyridine (**1c**).* From **1b**, **1c** was obtained after purification by silica gel column chromatography (CH_2Cl_2/MeOH/NH_4OH 98:2:0.2) (yield: 60%). ^1H NMR (500 MHz, $CDCl_3$) δ 6.97 (s, 1H, CH-9), 6.77 (s, 1H, CH-6), 3.85 (s, 6H, 2×OCH_3), 3.34 (d, 1H, J = 10.5 Hz, CH-9b), 3.01 (dd, 1H, J = 1.8, 12.5 Hz, CH_2-2α), 2.75 (dd, 1H, J = 6.5, 14.0 Hz, CH_2-5α), 2.62 (td, 1H, J = 3.0, 12.5 Hz, CH_2-2β), 2.56 (s, 3H, NCH_3), 2.34 (m, 1H, CH_2-5β), 2.12 (m, 1H, CH_2-4α), 1.98 (m, 1H, CH_2-3α), 1.77 (m, 1H, CH-4a), 1.55 (m, 1H, CH_2-4β), 1.47 (m, 1H, CH_2-3β); ^{13}C NMR (125 MHz, $CDCl_3$) δ 147.9 (C-8), 147.5 (C-7), 135.8 (CH-9a), 134.6 (C-5a), 108.4 (CH-6), 107.6 (CH-9), 74.0 (CH-9b), 57.0 (CH_2-2), 56.2 (OCH_3), 55.9 (OCH_3), 44.1 (CH-4a), 39.9 (NCH_3), 35.3 (CH_2-5), 29.6 (CH_2-4), 22.8 (CH_2-3). HRESIMS *m/z* 247.1565 $[M]^+$ ($C_{15}H_{21}NO_2$, calc 247.1572).

*4.1.3.2. 7,8-Methylenedioxy-N-methyl-2,3,4,4a,5,9b-hexahydro-1H-indeno[1,2-b] pyridine (**2c**).* From **2b**, **2c** was obtained after purification by silica gel column chromatography (CH_2Cl_2/MeOH/NH_4OH 95:5:0.2) (yield: 60%). ^1H NMR (500 MHz, $CDCl_3$) δ 6.91 (s, 1H, CH-9), 6.88 (s, 1H, CH-6), 5.91 (s, 1H, OCH_2O-α), 5.88 (s, 1H, OCH_2O-β), 3.25 (d, 1H, J = 10.5 Hz, CH-9b), 2.95 (dd, 1H, J = 4.5, 13.0 Hz, CH_2-2α), 2.70 (dd, 1H, J = 6.5, 14.5 Hz, CH_2-5α), 2.55 (td, 1H, J = 3.2, 13.0 Hz, CH_2-2β), 2.53 (s, 3H, NCH_3), 2.29 (m, 1H, CH_2-5β), 2.09 (m, 1H, CH-4a), 1.96 (m, 1H, CH_2-4α), 1.74 (m, 1H, CH_2-3α), 1.56 (m, 1H, CH_2-3β), 1.46 (m, 1H, CH_2-4β); ^{13}C NMR (125 MHz, $CDCl_3$) δ 146.1 (C-8), 145.9 (C-7), 136.9 (C-9a), 135.8 (C-5a), 105.7 (CH-6), 104.7 (CH-9), 100.7 (OCH_2O), 73.9 (CH-9b), 57.2 (CH_2-2), 44.5 (CH-4a), 39.7 (NCH_3), 35.3 (CH_2-5), 29.5 (CH_2-4), 23.0 (CH_2-3). EIMS *m/z* (%) 230 $[M - H]^+$ (100), 160 (35), 102 (40); HRESIMS *m/z* 232.1330 $[M + H]^+$(232.1338, calc for $C_{14}H_{18}NO_2$).

*4.1.3.3. 8-Methoxy-N-methyl-2,3,4,4a,5,9b-hexahydro-1h-indeno [1,2-b]pyridine (**3c**).* From **3b**, **3c** was obtained after purification by silica gel column chromatography (CH_2Cl_2/MeOH/NH_4OH 93:7:0.2) (yield: 65%). ^1H NMR (500 MHz, $CDCl_3$) δ 7.09 (d, J = 8.1 Hz, 1H, CH-6), 6.99 (d, J = 2.1 Hz, 1H, CH-9), 6.70 (dd, J = 2.1, 8.1 Hz, 1H, CH-7), 3.78 (s, 3H, OCH_3), 3.33 (d, 1H, J = 10.7 Hz, CH-9b), 3.01 (m, 1H, CH_2-2α), 2.76 (dd, 1H, J = 6.5, 14.1 Hz, CH_2-5α), 2.61 (m, 1H, CH_2-2β), 2.57 (s, 3H, NCH_3), 2.35 (m, 1H, CH_2-5β), 2.05 (m, 2H, CH-4α and CH-4a), 1.78 (m, 1H, CH_2-3α), 1.57 (m, 1H, CH_2-4β), 1.48 (m, 1H, CH_2-3β); ^{13}C NMR (125 MHz, $CDCl_3$) δ 158.3 (C-8), 145.2 (C-9a), 134.6 (C-5a), 125.0 (CH-6), 111.7 (CH-7), 109.8 (CH-9), 74.1 (CH-9b), 57.2 (CH_2-2), 55.4 (OCH_3), 44.4 (CH-4a), 39.7 (NCH_3), 34.6 (CH_2-5), 29.7 (CH_2-4), 22.9 (CH_2-3). EIMS *m/z* (%) 216 $[M - H]^+$ (100), 174 (30), 146 (40); HRESIMS *m/z* 218.1539 $[M + H]^+$ (218.1545, calc for $C_{14}H_{20}NO$).

*4.1.3.4. 7-Chloro-8-methoxy-N-methyl-2,3,4,4a,5,9b-hexahydro-1H-indeno[1,2-b] pyridine (**4c**).* From **4b**, **4c** was obtained after purification by silica gel column chromatography (CH_2Cl_2/MeOH/NH_4OH 93:7:0.2) (yield: 62%). ^1H NMR (500 MHz, $CDCl_3$) δ 7.17 (s, 1H, CH-6), 7.00 (s, 1H, CH-9), 3.86 (s, 3H, OCH_3), 3.40 (d, 1H, J = 10.0 Hz, CH-9b), 3.00 (dd, 1H, J = 4.5, 13.0 Hz, CH_2-2α), 2.75 (m, 1H, CH_2-5α), 2.71 (dd, 1H, J = 3.2, 13.0 Hz, CH_2-2β), 2.54 (s, 3H, NCH_3), 2.31 (m, 1H, CH_2-5β), 2.28 (m, 1H, CH-4a), 2.01 (m, 1H, CH_2-4α), 1.75 (m, 1H, CH_2-3α), 1.52 (m, 1H, CH_2-3β), 1.47 (m, 1H, CH_2-4β); ^{13}C NMR (125 MHz, $CDCl_3$) δ 153.5 (C-8), 143.3 (C-9a), 135.3 (C-5a), 126.2 (CH-6), 120.4 (C-7), 108.0 (CH-9), 73.6 (CH-9b), 56.7 (CH_2-2), 56.4 (OCH_3), 43.4 (CH-4a), 38.7 (NCH_3), 34.5 (CH_2-5), 29.6 (CH_2-4), 22.1 (CH_2-3). EIMS *m/z* (%) 250 $[M - H]^+$ (100), 145 (60), 42 (90); HRESIMS *m/z* 252.1153 $[M + H]^+$(252.1155, calc for $C_{14}H_{19}NOCl$).

4.1.4. General procedure for O-demethylation

A solution of the appropriate HHIP (0.29 mmol) in dry CH_2Cl_2 (6 mL) was cooled to −78 °C. To this stirring solution, BBr_3 (1.02 mmol) was added dropwise. After 15 min, the reaction mixture was warmed up to room temperature and stirred for 2 h. The reaction was terminated by the addition of MeOH (1 mL) dropwise and the mixture was stirred for another 30 min. The solvent was concentrated to dryness under reduced pressure.

*4.1.4.1. 7,8-Dihydroxy-2,3,4,4a,5,9b-hexahydro-1H-indeno[1,2-b]pyridine (**1d**).* From HHIP **1b**, **1d** was obtained after purification by silica gel column chromatography (CH_2Cl_2/MeOH 90:10) (yield: 62%). ^1H NMR (500 MHz, pyridine) δ = 8.20 (s, 1H, CH-9), 7.14 (s, 1H, CH-6), 4.13 (d, 1H, J = 10.7 Hz, CH-9b), 3.75 (dd, 1H, J = 3.5, 12.8 Hz, CH_2-2α), 3.28 (td, 1H, J = 3.5, 12.8 Hz, CH_2-2β), 2.70 (dd, 1H, J = 5.7, 13.2 Hz, CH_2-5α), 2.44 (m, 1H, CH_2-5β), 2.35 (m, 1H, CH_2-4α), 1.85 (m, 2H, CH_2-3α and CH-4a), 1.61 (m, 1H, CH_2-4β), 1.52 (m, 1H, CH_2-3β); ^{13}C NMR (125 MHz, pyridine) δ 147.8 (C-8), 145.8 (C-7), 132.8 (C-9a), 129.6 (C-5a), 113.3 (CH-6), 111.6 (CH-9), 65.1 (CH-9b), 47.6 (CH-4a), 44.8 (CH_2-2), 34.6 (CH_2-5), 27.6 (CH_2-4), 23.6 (CH_2-3). EIMS *m/z* (%) 206 $[M + H]^+$ (100); HRESIMS *m/z* 206.1176 $[M + H]^+$ (206.1181, calc for $C_{12}H_{16}NO_2$).

*4.1.4.2. 7,8-Dihydroxy-N-methyl-2,3,4,4a,5,9b-hexahydro-1H-indeno [1,2-b]pyridine (**1e**).* From **1c**, **1e** was obtained after purification by silica gel column chromatography (CH_2Cl_2/MeOH 90:10) (yield: 97%). ^1H NMR (500 MHz, $CDCl_3$) δ 8.0 (s, 1H, CH-9), 7.14 (s, 1H, CH-6), 4.20 (d, 1H, J = 11.1 Hz, CH-9b), 3.36 (m, 2H, CH_2-2), 2.81 (s, 3H, NCH_3), 2.67 (dd, 1H, J = 4.9, 12.2 Hz, CH_2-5α), 2.31 (m, 1H, CH_2-5β), 2.25 (m, 1H, CH_2-4α), 1.85 (m, 1H, CH-4a), 1.74 (m, 1H, CH_2-3α), 1.60 (m, 1H, CH_2-4β), 1.45 (m, 1H, CH_2-3β); ^{13}C NMR (125 MHz, $CDCl_3$) δ 147.9 (C-8), 146.0 (C-7), 133.2 (C-9a), 127.7 (C-5a), 113.3 (CH-6), 112.5 (CH-9), 61.1 (CH-9b), 54.1 (CH_2-2), 41.6 (CH-4a), 34.6 (CH_2-5 and NCH_3), 27.5 (CH_2-4), 20.4 (CH_2-3). EIMS *m/z* (%) 220 $[M + H]^+$ (100); HRESIMS *m/z* 220.1333 $[M + H]^+$(220.1338, calc for $C_{13}H_{18}NO_2$).

*4.1.4.3. 8-Hydroxy-2,3,4,4a,5,9b-hexahydro-**1h**-indeno[1,2-b]pyridine (**3d**).* From **3b**, **3d** was obtained after purification by silica gel column chromatography (CH_2Cl_2/MeOH 90:10) (yield: 86%). ^1H NMR (500 MHz, $CDCl_3$) δ 8.15 (d, J = 1.9 Hz, 1H, CH-9), 7.11 (d, J = 7.9 Hz, 1H, CH-6), 7.06 (dd, J = 1.9, 7.9 Hz, 1H, CH-7), 4.25 (d, 1H, J = 10.5 Hz, CH-9b), 3.75 (m, 1H, CH_2-2α), 3.32 (td, 1H, J = 3.6, 12.3 Hz, CH_2-2β), 2.70 (dd, 1H, J = 6.1, 13.5 Hz, CH_2-5α), 2.45 (m, 1H, CH-4a), 2.33 (m, 1H, CH_2-5β), 1.94 (m, 1H, CH_2-4α), 1.82 (m, 2H, CH_2-3α and CH_2-4β), 1.55 (m, 1H, CH_2-3β); ^{13}C NMR (125 MHz, $CDCl_3$) δ 158.2 (C-8), 140.5 (C-9a), 131.9 (C-5a), 126.4 (CH-6), 116.6 (CH-7), 111.7 (CH-9), 65.1 (CH-9b), 47.6 (CH-4a), 45.2 (CH_2-2), 34.4 (CH_2-5), 27.5 (CH_2-4), 23.7 (CH_2-3). EIMS *m/z* (%) 188 $[M - H]^+$ (75), 146 (100), 131 (60), 77 (60), 41 (85); HRESIMS *m/z* 190.1225 $[M + H]^+$(190.1232, calc for $C_{12}H_{16}NO$).

*4.1.4.4. 8-Hydroxy-N-methyl-2,3,4,4a,5,9b-hexahydro-1h-indeno [1,2-b]pyridine (**3e**).* From **3c**, **3e** was obtained after purification by silica gel column chromatography (CH_2Cl_2/MeOH 90:10) (yield: 80%). ^1H NMR (500 MHz, $CDCl_3$) δ 7.58 (d, J = 1.9 Hz, 1H, CH-9), 7.13 (d, J = 8.2 Hz, 1H, CH-6), 7.09 (dd, J = 1.9, 8.2 Hz, 1H, CH-7), 4.20 (d, 1H, J = 11.3 Hz, CH-9b), 3.30 (m, 2H, CH_2-2), 2.78 (s, 3H, NCH_3), 2.69 (m, 1H, CH_2-5α), 2.31 (m, 1H, CH_2-5β), 2.24 (m, 1H, CH_2-4α), 1.80 (m, 2H, CH-3α and CH-4a), 1.59 (m, 1H, CH-4β), 1.43 (m, 1H, CH-3β); ^{13}C NMR (125 MHz, $CDCl_3$) δ 157.9 (C-8), 139.4 (C-9a), 132.2 (C-5a), 126.3 (CH-6), 116.3 (CH-7), 112.5 (CH-9), 71.2 (CH-9b), 54.6 (CH_2-2), 41.9 (CH-4a), 35.1 (CH_2-5), 34.0 (NCH_3) 27.9 (CH_2-4), 20.5 (CH_2-3). EIMS *m/z* (%) 202 $[M - H]^+$ (85), 160 (30), 131 (55), 77 (35), 42 (100); HRESIMS *m/z* 204.1385 $[M + H]^+$(204.1388, calc for $C_{13}H_{18}NO$).

*4.1.4.5. 7-Chloro-8-hydroxy-2,3,4,4a,5,9b-hexahydro-1H-indeno[1,2-b]pyridine (**4d**).* From **4b**, **4d** was obtained after purification by silica gel column chromatography (CH_2Cl_2/MeOH 90:10) (yield:

90%). ^{1}H NMR (500 MHz, Pyr-d_5) δ 8.20 (s, 1H, CH-9), 7.20 (s, 1H, CH-6), 4.20 (d, 1H, J = 11.1 Hz, CH-9b), 3.69 (dd, 1H, J = 3.3, 12.7 Hz, CH_2-2α), 3.28 (td, 1H, J = 3.6, 12.7 Hz, CH_2-2β), 2.67 (dd, 1H, J = 5.8, 13.5 Hz, CH_2-5α), 2.41 (m, 1H, CH-4a), 2.32 (m, 1H, CH_2-5β), 1.90 (m, 1H, CH_2-4α), 1.82 (m, 1H, CH_2-3α), 1.79 (m, 1H, CH_2-4β), 1.53 (m, 1H, CH_2-3β); ^{13}C NMR (125 MHz, $CDCl_3$) δ 153.7 (C-8), 139.1 (C-9a), 133.1 (C-5a), 127.1 (CH-6), 121.7 (C-7), 112.9 (CH-9), 64.6 (CH-9b), 47.5 (CH-4a), 45.1 (CH_2-2), 34.3 (CH_2-5), 27.4 (CH_2-4), 23.7 (CH_2-3). EIMS m/z (%) 222 $[M - H]^+$ (100), 180 (70), 131 (60), 77 (40), 41 (65); HRESIMS m/z 224.0841 $[M + H]^+$(224.0842, calc for $C_{12}H_{15}NOCl$).

*4.1.4.6. 7-Chloro-8-hydroxy-N-methyl-2,3,4,4a,5,9b-hexahydro-1H-indeno[1,2-b]pyridine (**4e**).* From **4c**, **4e** was obtained after purification by silica gel column chromatography (CH_2Cl_2/MeOH 90:10) (yield: 89%). ^{1}H NMR (500 MHz, Pyr-d_5) δ 7.80 (s, 1H, CH-9), 7.25 (s, 1H, CH-6), 3.85 (d, 1H, J = 10.5 Hz, CH-9b), 3.10 (m, 1H, CH_2-2α), 3.00 (m, 1H, CH_2-2β), 2.68 (m, 1H, CH_2-5α), 2.62 (s, 3H, NCH_3), 2.27 (m, 1H, CH_2-5β), 2.16 (m, 1H, CH-4a), 1.78 (m, 1H, CH_2-4α), 1.70 (m, 1H, CH_2-3α), 1.52 (m, 1H, CH_2-3β), 1.38 (m, 1H, CH_2-4β); ^{13}C NMR (125 MHz, $CDCl_3$) δ 153.3 (C-8), 140.0 (C-9a), 133.7 (C-5a), 126.8 (CH-6), 120.8 (C-7), 113.6 (CH-9), 71.9 (CH-9b), 55.4 (CH_2-2), 42.6 (CH-4a), 35.0 (NCH_3), 34.2 (CH_2-5), 28.5 (CH_2-4), 21.3 (CH_2-3). EIMS m/z (%) 236 $[M - H]^+$ (75), 131 (55), 115 (30), 77 (30), 42 (100); HRESIMS m/z 238.0951 $[M + H]^+$(238.0993, calc for $C_{13}H_{17}NOCl$).

4.1.5. General procedure for N-acetylation

To a solution of the appropriate HHIP (0.85 mmol), acetic anhydride (0.85 mmol) and pyridine (1 mL) were added at room temperature. After stirring for 2 h, solvent was evaporated under vacuum and the residue redissolved in CH_2Cl_2 (10 mL). The organic solution was washed by saturated aq. $NaHCO_3$ solution (5 × 10 mL). The organic layer was dried over Na_2SO_4 and the solvent evaporated under reduced pressure.

*4.1.5.1. 7,8-Dimethoxy-N-acetyl-2,3,4,4a,5,9b-hexahydro-1H-indeno [1,2-b]pyridine (**1f**).* From **1b**, **1f** was obtained after purification by silica gel column chromatography (CH_2Cl_2/MeOH 90:10) (yield: 89%). ^{1}H NMR (500 MHz, $CDCl_3$) δ 6.87 (s, 1H, CH-9), 6.73 (s, 1H, CH-6), 4.22 (d, 1H, J = 10.0 Hz, CH-9b), 3.86 (s, 3H, OCH_3), 3.85 (s, 3H, OCH_3), 3.20 (m, 2H, CH_2-2), 2.89 (dd, 1H, J = 6.3, 14.1 Hz, CH_2-5α), 2.37 (m, 1H, CH_2-5β), 2.36 (m, 1H, CH-4a), 2.15 (s, 3H, CH_3CO), 2.13 (m, 1H, CH_2-4α), 1.77–1.65 (m, 3H, CH_2-4β, CH_2-3); ^{13}C NMR (125 MHz, $CDCl_3$) δ 171.6 (CO), 148.7 (C-8), 148.6 (C-7), 133.7 (C-9a), 133.2 (C-5a), 108.9 (CH-6), 108.4 (CH-9), 70.0 (CH-9b), 56.5 (OCH_3), 56.4 (OCH_3), 48.1 (CH_2-2), 46.6 (CH-4a), 35.5 (CH_2-5), 28.7 (CH_2-4), 25.8 (CH_2-3), 22.5 ($COCH_3$). EIMS m/z (%) 275 $[M]^+$ (100), 246 (45), 204 (60); HRESIMS m/z 276.1503 $[M + H]^+$ (276.1594, calc for $C_{16}H_{22}NO_3$).

*4.1.5.2. 8-Methoxy-N-acetyl-2,3,4,4a,5,9b-hexahydro-1h-indeno[1,2-b]pyridine (**3f**).* From **3b**, **3f** was obtained after purification by silica gel column chromatography (CH_2Cl_2/MeOH 90:10) (yield: 94%). ^{1}H NMR (500 MHz, $CDCl_3$) δ 7.08 (d, J = 8.2 Hz, 1H, CH-6), 6.85 (d, J = 2.3 Hz, 1H, CH-9), 6.71 (dd, J = 2.3, 8.2 Hz, 1H, CH-7), 4.25 (d, 1H, J = 10.8 Hz, CH-9b), 3.77 (s, 3H, OCH_3), 3.25 (td, 1H, J = 3.2, 12.2 Hz, CH_2-2), 2.89 (dd, 1H, J = 5.5, 14.1 Hz, CH_2-5α), 2.35 (m, 1H, CH-4a), 2.34 (m, 1H, CH_2-5β), 2.09 (s, 3H, CH_3CO), 2.08 (m, 1H, CH_2-4α), 1.60–1.74 (m, 3H, CH_2-4β, CH_2-3); ^{13}C NMR (125 MHz, $CDCl_3$) δ 171.1 (CO), 158.4 (C-8), 133.2 (C-9a), 133.0 (C-5a), 125.2 (CH-6), 112.9 (CH-7), 110.6 (CH-9), 69.0 (CH-9b), 55.9 (OCH_3), 48.5 (CH_2-2), 47.5 (CH-4a), 34.9 (CH_2-5), 28.0 (CH_2-4), 25.8 (CH_2-3), 23.1 (CH_3CO). EIMS m/z (%) 246 $[M + H]^+$ (100); HRESIMS m/z 246.1502$[M + H]^+$ (246.1494, calc for $C_{15}H_{20}NO_2$).

*4.1.5.3. 7-Chloro-8-methoxy-N-acetyl-2,3,4,4a,5,9b-hexahydro-1H-indeno[1,2-b] pyridine (**4f**).* From **4b**, **4f** was obtained after purification by silica gel column chromatography (CH_2Cl_2/MeOH 90:10) (yield: 91%). ^{1}H RMN (500 MHz, $CDCl_3$) δ 7.09 (s, 1H, CH-6), 6.83 (s, 1H, CH-9), 3.80 (s, 3H, OCH_3), 4.10 (d, 1H, J = 10.3 Hz, CH-9b), 3.22 (m, 2H, CH_2-2), 2.81 (dd, 1H, J = 6.8, 13.9 Hz, CH_2-5α), 2.28 (m, 1H, CH-4a), 2.27 (m, 1H, CH_2-5β), 2.06 (s, 3H, CH_3CO), 2.05 (m, 1H, CH_2-4α), 1.57–1.74 (m, 3H, CH_2-4β, CH_2-3); ^{13}C RMN (125 MHz, $CDCl_3$) δ 171.2 (CO), 153.4 (C-8), 143.1 (C-9a), 133.0 (C-5a), 125.9 (CH-6), 120.8 (C-7), 109.3 (CH-9), 68.9 (CH-9b), 56.3 (OCH_3), 47.9 (CH_2-2), 45.8 (CH-4a), 34.4 (CH_2-5), 29.6 (CH_2-4), 25.4 (CH_2-3), 23.1 ($COCH_3$). EIMS m/z (%) 279 $[M]^+$ (100), 250 (65), 222 (45), 208 (60), 69 (40); HRESIMS m/z 280.1095 $[M + H]^+$ (280.1104, calc for $C_{15}H_{19}NO_2Cl$).

*4.1.6. Synthesis of ethyl-4-(8-methoxy-2,3,4,4a,5,9b-hexahydro-1H-indeno[1,2-b]pyridin-1-yl)-4-oxobutanoate (**3g**)*

To a solution of the appropriate HHIP **3b** (0.98 mmol) in CH_2Cl_2 (30 mL) and 5% aqueous NaOH (15 mL), the ethyl 4-chloro-4-oxobutanoate (0.98 mmol) was added dropwise at 0 °C. The reaction was stirred at room temperature for 2 h, and then, extracted with CH_2Cl_2 (3 × 10 mL). The combined organic phases were washed with brine and H_2O, dried over anhydrous Na_2SO_4, filtered and evaporated to dryness. The amide **3g** was obtained after purification by silica gel column chromatography (CH_2Cl_2/MeOH 95:5) (yield: 92%). ^{1}H NMR (500 MHz, $CDCl_3$) δ 7.06 (d, J = 8.0 Hz, 1H, CH-6), 6.82 (d, J = 2.1 Hz, 1H, CH-9), 6.70 (dd, J = 2.1, 8.0 Hz, 1H, CH-7), 4.23 (m, 1H, CH-9b), 4.10 (m, 2H, CO_2CH_2), 3.78 (m, 1H, CH_2-2α), 3.76 (s, 3H, OCH_3), 3.25 (td, 1H, J = 3.2, 12.2 Hz, CH_2-2β), 2.89 (m, 1H, CH_2-5α), 2.63 (m, 4H, $NCOCH_2CH_2$), 2.38 (m, 1H, CH-4a), 2.37 (m, 1H, CH_2-5β), 2.14 (m, 1H, CH_2-4α), 1.60–1.77 (m, 3H, CH_2-4β, CH_2-3), 1.24 (m, 3H, CH_3); ^{13}C NMR (125 MHz, $CDCl_3$) δ 173.6 (CONH), 171.6 (COO), 158.7 (C-8), 144.1 (C-9a), 132.7 (C-5a), 125.5 (CH-6), 113.2 (CH-7), 110.5 (CH-9), 70.2 (CH-9b), 60.8 (CO_2CH_2), 55.8 (OCH_3), 48.5 (CH_2-2), 46.0 (CH-4a), 34.9 (CH_2-5), 29.9 (2 × C, $NCOCH_2CH_2$), 29.8 (CH_2-4), 25.9 (CH_2-3), 14.6 (CH_3). EIMS m/z (%) 331 $[M]^+$ (30), 286 (25), 202 (100), 186 (40), 174 (40); HRESIMS m/z 332.1877 $[M + H]^+$ (332.1862, calc for $C_{19}H_{26}NO_4$).

4.1.7. General procedure for the synthesis of ureas and thioureas

A solution of the appropriate HHIP (0.42 mmol) in CH_2Cl_2 was treated with the corresponding isocyanate or thioisocyanate (0.42 mmol) and refluxed for 2 h. The reaction mixture was extracted with water (3 × 10 mL) and the combined organic layers were concentrated to dryness.

*4.1.7.1. 7,8-Dimethoxy-N-(2-(piperidin-yl)ethyl)-2,3,4,4a,5,9b-hexahydro-1H-indeno [1,2-b] pyridine-1-carbothioamide (**1g**).* From **1b** and 1-(2-isothiocyanatoethyl) piperidine, **1g** was obtained after purification by silica gel column chromatography (CH_2Cl_2/MeOH 97:3) (yield: 82%). ^{1}H NMR (500 MHz, $CDCl_3$) δ 6.83 (s, 1H, CH-9), 6.78 (s, 1H, CH-6), 6.54 (s, 1H, NH), 5.51 (m, 1H, CH_2-2α), 4.48 (d, 1H, J = 11.1 Hz, CH-9b), 3.85 (s, 3H, OCH_3), 3.83 (s, 3H, OCH_3), 3.56 (m, 2H, $CSNHCH_2$), 3.24 (m, 1H, CH_2-2β), 2.99 (dd, 1H, J = 6.2, 14.4 Hz, CH_2-5α), 2.44–1.20 (m, 10H, CH_2-piperidine), 2.37 (m, 1H, CH_2-5β), 2.25 (m, 1H, CH-4a), 2.16 (m, 2H, $NHCH_2CH_2$), 1.85 (m, 1H, CH_2-4α), 1.80 (m, 1H, CH_2-4β), 1.41 (m, 1H, CH_2-3α), 1.25 (m, 1H, CH_2-3β); ^{13}C NMR (125 MHz, $CDCl_3$) δ 181.1 (CS), 149.2 (C-8), 148.2 (C-7), 133.5 (C-9a), 130.2 (C-5a), 108.4 (CH-6), 107.8 (CH-9), 71.7 (CH-9b), 54.4-24.1 (5 × CH_2-piperidine), 56.2 (OCH_3), 56.1 (CH_2-2), 55.9 (OCH_3), 44.9 (CH-4a), 43.1 ($NHCH_2CH_2$), 42.0 ($CSNHCH_2$), 35.4 (CH_2-5), 25.7 (CH_2-4), 24.3 (CH_2-3). EIMS m/z (%) 404 $[M + H]^+$ (100); HRESIMS m/z 404.2384 $[M + H]^+$(404.2372, calc for $C_{22}H_{34}N_3O_2S$).

*4.1.7.2. 7,8-Dimethoxy-N-(2′,3′,4′-trifluorophenyl)-2,3,4,4a,5,9b-hexahydro-1H-indeno[1,2-b] pyridine-1-carbothioamide (**1h**).* From **1b** to 1,2,3-trifluoro-4-isothiocyanatobenzene, **1h** was obtained after purification by silica gel column chromatography (CH_2Cl_2/MeOH 97:3) (yield: 87%). ^{1}H NMR (500 MHz, $CDCl_3$) δ 7.30 (m, 1H, CH-6′), 7.04 (s, 1H, CH-9), 6.92 (m, 1H, CH-5′), 6.81 (s, 1H, CH-6), 5.59 (m, 1H, CH_2-2α), 4.68 (d, 1H, J = 11.3 Hz, CH-9b), 3.87 (s, 3H, OCH_3), 3.82 (s, 3H, OCH_3), 3.33 (m, 1H, CH_2-2β), 3.05 (dd, 1H, J = 5.8, 14.1 Hz, CH_2-5α), 2.44 (m, 2H, CH_2-5β and CH-4a), 2.27 (m, 1H, CH_2-4α), 1.82 (m, 2H, CH_2-3α and CH_2-4β), 1.78 (m, 1H, CH_2-3β); ^{13}C NMR (125 MHz, $CDCl_3$) δ 182.4 (CS), 152.3 (C-2′), 149.1 (C-8), 148.3 (C-7), 146.2 (C-4′), 138.1 (C-3′), 134.6 (C-9a), 130.1 (C-5a), 120.5 (CH-6′), 112.6 (C-1′), 111.3 (CH-5′), 109.2 (CH-6), 107.8 (CH-9), 73.3 (CH-9b), 56.4 (2×OCH_3 and CH_2-2), 46.5 (CH-4a), 35.6 (CH_2-5), 31.0 (CH_2-4), 25.5 (CH_2-3). HRESIMS *m/z* 423.1310 $[M + H]^+$(423.1349, calc for $C_{21}H_{22}N_3O_2SF_3$).

*4.1.7.3. N-(4-fluorophenyl)-7,8-methylenedioxy-2,3,4,4a,5,9b-hexahydro-1h-indeno [1,2-b] pyridine-1-carboxamide (**2d**).* From **2b** and 4-(fluorophenyl) isocyanate, **2d** was obtained after purification by silica gel column chromatography (CH_2Cl_2/MeOH 97:3) (yield: 79%). ^{1}H RMN (500 MHz, $CDCl_3$) δ 7.09 (dd, J = 5.7, 8.4 Hz, 2H, CH-2′ and CH-6′), 6.93 (s, 1H, CH-9), 6.90 (dd, J = 8.4, 8.9 Hz, 2H, CH-5′ and CH-3′), 6.78 (s, 1H, CH-6), 5.96 (s, 1H, OCH_2O-α), 5.75 (s, 1H, OCH_2O-β), 4.56 (dd, 1H, J = 4.3, 13.7 Hz, CH_2-2α), 4.28 (d, 1H, J = 10.5 Hz, H-9b), 2.91 (m, 2H, CH_2-5α and CH_2-2β), 2.33 (m, 2H, H-4a and CH_2-5β), 2.16 (m, 1H, CH_2-4α), 1.61 (m, 3H, CH_2-4β and CH_2-3); ^{13}C RMN (125 MHz, $CDCl_3$) δ 158.6 (C-4′, J_{FC} = 241 Hz), 155.7 (CO), 148.7 (C-8), 147.1 (C-7), 135.8 (C-5a), 134.8 (C-1′), 132.4 (C-9a), 120.9 (CH-2′ and CH-6′, J_{FC} = 7.50 Hz), 115.2 (CH-3′ and CH-5′, J_{FC} = 21.25 Hz), 106.7 (CH-6), 104.7 (CH-9), 101.5 (OCH_2O), 69.9 (CH-9b), 49.3 (CH_2-2), 46.2 (CH-4a), 35.3 (CH_2-5), 29.7 (CH_2-4), 24.9 (CH_2-3). EIMS *m/z* (%) 377 $[M + Na]^+$ (100), 355 (25) $[M + H]^+$, 326 (25), 309 (15), 241 (25); HRESIMS *m/z* 355.1457 $[M + H]^+$ (355.1458, calc for $C_{20}H_{20}N_2O_3F$).

*4.1.7.4. 7-Chloro-8-methoxy-N-ethyl-2,3,4,4a,5,9b-hexahydro-1H-indeno[1,2-b] pyridine-1-carboxamide (**4g**).* From **4b** and ethyl isocyanate, **4g** was obtained after purification by silica gel column chromatography (CH_2Cl_2/MeOH 97:3) (yield: 84%). ^{1}H RMN (500 MHz, $CDCl_3$) δ 7.26 (s, 1H, CH-6), 6.94 (s, 1H, CH-9), 4.57 (s, 1H, NH), 4.45 (dd, 1H, J = 4.8, 12.6 Hz, CH_2-2α), 4.20 (d, 1H, J = 10.7 Hz, CH-9b), 3.84 (s, 3H, OCH_3), 3.28 (m, 1H, CH_2-2′α), 3.04 (m, 1H, CH_2-2′β), 2.90 (m, 2H, CH_2-2β and CH_2-5α), 2.41 (m, 1H, CH_2-5β), 2.35 (m, 1H, CH-4a), 2.14 (m, 1H, CH_2-4α), 1.64 (m, 3H, CH_2-4β and CH_2-3), 0.96 (t, 3H, J = 7.0 Hz, CH_3-3′); ^{13}C RMN (125 MHz, $CDCl_3$) δ 158.2 (CO), 153.9 (C-8), 140.3 (C-9a), 134.4 (C-5a), 127.3 (CH-6), 121.9 (C-7), 107.8 (CH-9), 69.6 (CH-9b), 56.3 (OCH_3), 49.2 (CH_2-2), 44.9 (CH-4a), 35.3 (CONH*CH*$_2$), 34.6 (CH_2-5), 30.4 (CH_2-4), 24.7 (CH_2-3), 15.5 ($CONHCH_2$*CH*$_3$). EIMS *m/z* (%) 309 $[M + H]^+$ (40), 238 (100); HRESIMS *m/z* 309.1372 $[M + H]^+$ (309.1370, calc for $C_{16}H_{22}N_2O_2Cl$).

4.1.8. General procedure for the synthesis of N-alkyl amides

To a solution of the appropriate HHIP (0.23 mmol) in dry CH_3CN (10 mL) and Et_3N (0.23 mmol), the corresponding 2-bromo-acetamide (0.23 mmol) was added. The reaction mixture was refluxed under a N_2 atmosphere for 4 h. Then, H_2O was added and the reaction mixture partially evaporated and extracted with CH_2Cl_2 (3 × 10 mL). The combined organic layers were washed with H_2O, dried over Na_2SO_4 and concentrated to dryness.

*4.1.8.1. 7,8-Methylenedioxy-N-phenyl-2-(2,3,4,4a,5,9b-hexahydro-1H-indeno[1,2-b] pyridin-5-yl)acetamide (**2e**).* From **2b** and 2-bromo-*N*-phenylacetamide, **2e** was obtained after purification by silica gel column chromatography (CH_2Cl_2/MeOH 97:3) (yield: 93%). ^{1}H RMN (500 MHz, $CDCl_3$) δ 9.66 (s, 1H, NH), 7.65–7.12 (m, 5H, Ph), 6.70 (s, 1H, CH-6), 6.60 (s, 1H, CH-9), 5.89 (s, 2H, OCH_2O), 3.80 (d, 1H, J = 8.7 Hz, CH-9b), 3.32 (m, 2H, CH_2CO), 3.01 (m, 2H, CH_2-2), 2.75 (dd, 1H, J = 6.1, 14.2 Hz, CH_2-5α), 2.32 (m, 1H, CH_2-5β), 2.05 (m, 1H, CH_2-4α), 1.78 (m, 1H, CH-4a), 1.60 (m, 1H, CH_2-3α), 1.52 (m, 1H, CH_2-4β), 1.37 (m, 1H, CH_2-3β); ^{13}C RMN (125 MHz, $CDCl_3$) δ 169.9 (CO), 146.9 (C-8), 146.5 (C-7), 137.7 (C-5a), 135.6 (C-9a and C-1′), 129.0 (CH-3′ and CH-5′), 124.2 (CH-4′), 119.6 (CH-2′ and CH-6′), 106.1 (CH-6), 103.3 (CH-9), 100.9 (OCH_2O), 72.6 (CH-9b), 52.9 (CH_2-2), 51.7 (CH_2CO), 43.8 (CH-4a), 35.1 (CH_2-5), 29.7 (CH_2-4), 20.6 (CH_2-3). EIMS *m/z* (%) 351 $[M + H]^+$ (100), 282 (25); HRESIMS *m/z* 351.1707 $[M + H]^+$ (351.1709, calc for $C_{21}H_{23}N_2O_3$).

*4.1.8.2. 7,8-Methylenedioxy-N,N-diethyl-2-(2,3,4,4a,5,9b-hexahydro-1H-indeno[1,2-b] pyridin-5-yl)acetamide (**2f**).* From **2b** and 2-bromo-*N*,*N*-diethylacetamide, **2f** was obtained after purification by silica gel column chromatography (CH_2Cl_2/MeOH 97:3) (yield: 89%). ^{1}H RMN (500 MHz, $CDCl_3$) δ 6.76 (s, 1H, CH-9), 6.69 (s, 1H, CH-6), 5.92 (s, 1H, OCH_2O-α), 5.88 (s, 1H, OCH_2O-β), 3.80 (d, 1H, J = 9.4 Hz, CH-9b), 3.54 (d, 1H, J = 13.2 Hz, CH_2CO-α), 3.43 (m, 1H, CH_2CO-β), 3.36 (m, 4H, CH_2-2′ and CH_2-4′), 3.17 (m, 1H, CH_2-2α), 2.92 (td, 1H, J = 2.1, 12.1 Hz, CH_2-2β), 2.73 (dd, 1H, J = 6.2, 12.6 Hz, CH_2-5α), 2.28 (m, 1H, CH_2-5β), 2.12 (m, 1H, H-4a), 2.03 (m, 1H, CH_2-4α), 1.82 (m, 1H, CH_2-3α), 1.55 (m, 1H, CH_2-4β), 1.46 (m, 1H, CH_2-3β), 1.14 (m, 6H, CH_3-3′ and CH_3-5′); ^{13}C RMN (125 MHz, $CDCl_3$) δ 169.4 (CO), 146.6 (C-8), 146.3 (C-7), 135.8 (C-5a), 135.7 (C-9a), 106.0 (CH-6), 104.1 (CH-9), 100.9 (OCH_2O), 72.7 (CH-9b), 52.4 (CH_2-2), 49.9 (CH_2CO), 42.6 (CH-4a), 40.2 (CH_2-2′ and CH_2-4′), 35.3 (CH_2-5), 29.9 (CH_2-4), 20.7 (CH_2-3), 14.3 (CH_3-3′ and CH_3-5′). EIMS *m/z* (%) 330 $[M]^+$ (90), 282 (35). HRESIMS *m/z* 331.2033 $[M + H]^+$ (331.2022, calc for $C_{19}H_{27}N_2O_3$).

*4.1.8.3. 7,8-Methylenedioxy-1-(piperidin-1-yl)-(2,3,4,4a,5,9b-hexahydro-1H-indeno [1,2-b]pyridin-5-yl)ethanone (**2g**).* From **2b** and 2-bromo-1-piperidin-1-yl)ethanone, **2g** was obtained after purification by silica gel column chromatography (CH_2Cl_2/MeOH 97:3) (yield: 84%). ^{1}H RMN (500 MHz, $CDCl_3$) δ 6.76 (s, 1H, CH-9), 6.69 (s, 1H, CH-6), 5.93 (s, 1H, OCH_2O-α), 5.89 (s, 1H, OCH_2O-β), 3.80 (d, 1H, J = 9.4 Hz, H-9b), 3.64 (d, 1H, J = 12.9 Hz, CH_2CO-α), 3.55–1.15 (m, 10H, CH_2-piperidine), 3.44 (m, 1H, CH_2CO-β), 3.16 (dd, 1H, J = 4.1, 13.5 Hz, CH_2-2α), 2.91 (m, 1H, CH_2-2β), 2.73 (dd, 1H, J = 12.4, 6.4 Hz, CH_2-5α), 2.28 (m, 1H, CH_2-5β), 2.12 (m, 1H, CH-4a), 2.02 (m, 1H, CH_2-4α), 1.79 (m, 1H, CH_2-3α), 1.55 (m, 1H, CH_2-4β), 1.53 (m, 1H, CH_2-3β); ^{13}C RMN (125 MHz, $CDCl_3$) δ 168.4 (CO), 146.6 (C-8), 146.2 (C-7), 135.9 (C-5a and C-9a), 106.0 (CH-6), 104.3 (CH-9), 100.9 (OCH_2O), 72.7 (CH-9b), 52.5 (CH_2-2), 50.5 (CH_2CO), 46.4–24.5 (CH_2-piperidine), 43.0 (CH-4a), 35.3 (CH_2-5), 29.8 (CH_2-4), 20.9 (CH_2-3). EIMS *m/z* (%) 343 $[M + H]^+$ (10), 230 (100), 187 (10); HRESIMS *m/z* 343.2019 $[M + H]^+$ (343.2022, calc for $C_{20}H_{27}N_2O_3$).

4.2. Pharmacology

4.2.1. Cell culture

Human embryonic kidney 293 (HEK 293) cell line stably expressing the human melatonin MT_1 or MT_2 receptor were grown in DMEM medium supplemented with 10% fetal calf serum, 2 mM glutamine, 100 IU/mL penicillin, and 100 μg/mL streptomycin. Once they were grown at confluence at 37 °C, they were harvested in PBS containing EDTA (2 mM) and centrifuged at 1000 *g* for 5 min (4 °C). The resulting pellet was suspended in TRIS (5 mM, pH 7.5), containing EDTA (2 mM), and homogenized using a Kinematica polytron. The homogenate was then centrifuged (95,000 g, 30 min, 4 °C) and the resulting pellet suspended in 75 mM TRIS (pH 7.5), 12.5 mM $MgCl_2$, and 2 mM EDTA. Aliquots of membrane preparations were stored at −80 °C until use.

4.2.2. Binding assays

2-[^{125}I]Iodomelatonin (2200 Ci/mmol) was purchased from NEN (Boston, MA). Other drugs and chemicals were purchased from Sigma–Aldrich (Saint Quentin, France). The compounds were evaluated for their binding affinity towards human MT_1 and MT_2 receptors stably transfected in HEK 293 cells, using 2-[^{125}I]iodomelatonin as radioligand. Briefly, binding was initiated by addition of membrane preparations from stable transfected HEK cells (40 μg/mL) diluted in the binding buffer (50 mM TRIS-HCl buffer, pH 7.4, containing 5 mM $MgCl_2$) to 2-[^{125}I]iodomelatonin (0.025 and 0.2 nM, respectively, for MT_1 and MT_2 receptors) and the tested drug. Nonspecific binding was defined in the presence of 1 μM melatonin. After a 120 min incubation at 37 °C, reaction was stopped by rapid filtration through GF/B filters presoaked in 0.5% (v/v) polyethylenimine. The filters were washed three times with 1 mL of ice-cold 50 mM TRIS-HCl buffer, pH 7.4.

Data from the dose–response curves (seven concentrations in duplicate) were analyzed using the program PRISM (Graph Pad Software Inc., San Diego, CA) to yield IC_{50} (inhibitory concentration 50). Results are expressed as $K_i = IC_{50}/1 + ([L]/K_D)$, where [L] is the concentration of radioligand used in the assay and K_D, the dissociation constant of the radioligand characterizing the membrane preparation.

Acknowledgments

This study was supported by grant SAF2011-23777 Spanish Ministry of Economy and Competiveness, the European Regional Development Fund (FEDER) and research grants from Generalitat Valenciana (GVACOMP2013-015 and PROMETEO II/2013/014). A.G. is a recipient of a pre-doctoral grant (FPU) from the Spanish Ministry of Education.

Appendix A. Supplementary data

Supplementary data related to this article can be found at http://dx.doi.org/10.1016/j.ejmech.2014.09.038.

References

[1] B. Claustrat, J. Brun, G. Chazot, The basic physiology and pathophysiology of melatonin, Sleep. Med. 9 (2005) 11–24.
[2] M.M. Macchi, J.N. Bruce, Human pineal physiology and functional significance of melatonin, Front. Neuroendocrinol. 25 (2004) 177–195.
[3] R.J. Reiter, Oxidative damage in the central nervous system: protection by melatonin, Prog. Neurobiol. 56 (1998) 359–384.
[4] R.J. Reiter, Melatonin: clinical relevance, Best. Pract. Res. Clin. Endocrinol. Metab. 17 (2003) 273–285.
[5] J. Arendt, Melatonin: characteristics, concerns, and prospects, J. Biol. Rhythms 20 (2005) 291–303.
[6] P. Delagrange, J. Atkinson, J.A. Boutin, L. Casteilla, D. Lesieur, R. Misslin, S. Pelissier, P. Renard, Therapeutic perspectives for melatonin agonists and antagonists, J. Neuroendocrinol. 15 (2003) 442–448.
[7] J.A. Boutin, V. Audinot, G. Ferry, P. Delagrange, Molecular tools to study melatonin pathways and actions, Trends Pharmacol. Sci. 26 (2005) 412–419.
[8] M.L. Dubocovich, P. Delagrange, D.N. Krause, D. Sugden, D.P. Cardinali, J. Olcese, International union of basic and clinical pharmacology. LXXV. Nomenclature, classification, and pharmacology of G protein-coupled melatonin receptors, Pharmacol. Rev. 62 (2010) 343–380.
[9] F. Mailliet, G. Ferry, F. Vella, S. Berger, F. Coge, P. Chomarat, C. Mallet, S.P. Guénin, G. Guillaumet, M.C. Viaud-Massuard, S. Yous, P. Delagrange, J.A. Boutin, Characterization of the melatoninergic MT3 binding site on the NRH:quinone oxidoreductase 2 enzyme, Biochem. Pharmacol. 71 (2005) 74–88.
[10] E. Corruble, C. De Bodinat, C. Belaidi, G.M. Goodwin, Efficacy of agomelatine and escitalopram on depression, subjective sleep and emotional experiences in patients with major depressive disorder: a 24-wk randomized, controlled, double-blind trial, Int. J. Neuropsychopharmacol. 16 (2013) 2219–2234.
[11] I.B. Hickie, N.L. Rogers, Novel melatonin-based therapies: potential advances in the treatment of major depression, Lancet 378 (2011) 621–631.
[12] J. Augstein, A.L. Ham, P.R. Leeming, Relation between antihistamine and antidepressant activity in hexahydroindenopyridines, J. Med. Chem. 15 (1972) 466–470.
[13] R. Kunstmann, U. Lerch, H. Gerhards, M. Leven, U. Schacht, 2,3,4,4a,5,9b-Hexahydro-1H-indeno[1,2-b]pyridines: potential antidepressants, J. Med. Chem. 27 (1984) 432–439.
[14] R. Kunstmann, H. Gerhards, H. Kruse, M. Leven, E.F. Paulus, U. Schacht, K. Schmitt, P.U. Witte, Resolution, absolute stereochemistry, and enantioselective activity of nomifensine and hexahydro-lH-indeno[1,2-b]pyridines, J. Med. Chem. 30 (1987) 798–804.
[15] M.D. Meyer, J.F. DeBernardis, A.A. Hancock, Synthesis and structure activity relationships of cis- and trans-2,3,4,4a,9,9a-hexahydro-1H-indeno[2,1-c]pyridines for 5-HT receptor subtypes, J. Med. Chem. 37 (1994) 105–112.
[16] W. Chen, T. Lee, Substituted tricyclic heterocycles as serotonin receptor agonists and antagonists, US20070049613.
[17] C.R. Rasmussen, Antipsychotic hexahydro-2H-indeno[1,2-c]pyridine derivatives, WO 1991017992A1.
[18] C.E. Cook, M.C. Wani, J.M. Jump, Y.-W. Lee, P.A. Fail, S.A. Anderson, Y.-Q. Gu, V. Petrow, Structure-activity studies of 2,3,4,4a,5,9b-hexahydroindeno[1,2-c]pyridines as antispermatogenic agents for male contraception, J. Med. Chem. 38 (1995) 753–763.
[19] M. Eckhardt, S. Peters, H. Nar, F. Himmelsbach, L. Zhuang, Aryl- and heteroarylcarbonyl derivatives of hexahydroindenopyridine and octahydrobenzoquinoline, WO 2011057054A1.
[20] K. Van Emelen, T. De Wit, G.J. Hoornaert, F. Compernolle, Synthesis of cis-fused hexahydro-4aH-indeno[1,2-b]pyridines via intramolecular ritter reaction and their conversion into tricyclic analogues of NK-1 and dopamine receptor ligands, Tetrahedron 58 (2002) 4225–4236.
[21] B.-C. Hong, M.S. Hallur, J.-H. Liao, Hetero Diels-Alder cycloaddition of indene for the formal synthesis of onychnine, Synth. Commun. 36 (2006) 1521–1528.
[22] L. Moreno, I. Berenguer, A. Díaz, P. Marín, J. Párraga, D.-H. Caignard, B. Figadère, N. Cabedo, D. Cortes, Synthesis of new melatoninergic hexahydroindenopyridines, Bioorg. Med. Chem. Lett. 24 (2014) 3534–3536.
[23] R. Carlson, A. Nilsson, M. Strömqvist, Optimum conditions for enamine synthesis by an improved titanium tetrachloride procedure, Acta Chem. Scand. Ser. B 37 (1983) 7–13.
[24] S.G.R. Guinot, J.D. Hepworth, M. Wainwright, Synthesis of tertiary 1-naphthylamines via the enamine, Dyes Pigments 36 (1998) 387–393.
[25] R.F. Parcell, F.P. Hauck, The preparation of tetrahydropyridines from enamines and imines, J. Org. Chem. 28 (1963) 3468–3473.
[26] E. Landagaray, M. Ettaoussi, V. Leclerc, B. Traoré, V. Pérez, O. Nosjean, J.A. Boutin, D.-H. Caignard, P. Delagrange, P. Berthelot, S. Yous, New melatonin (MT1/MT2) ligands: design and synthesis of (8,9-dihydro-7H-furo[3,2-f]chromen-1-yl) derivatives, Bioorg. Med. Chem. 22 (2014) 986–996.
[27] V. Audinot, F. Mailliet, C. Lahaye-Brasseur, A. Bonnaud, A. Le Gall, C. Amossé, S. Dromaint, M. rodriguez, N. Nagel, J.-P. Galizzi, B. Malpaux, G. Guillaumet, D. Lesieur, F. Lefoulon, P. Renard, P. Delagrange, J.A. Boutin, New selective ligands of human cloned melatonin MT1 and MT2 receptors, Schmiedeb. Arch. Pharmacol. 367 (2003) 553–561.

Capítulo 3

Síntesis y estudios de actividad antimicrobiana y citotóxica de Isoquinoleínas lactámicas y benzo-quinolizidinas.

Artículo 6: "Synthesis of pyrido[2,1-a]isoquinolin-4-ones and oxazino[2,3-a]isoquinolin-4-ones: New inhibitors of mitochondrial respiratory chain"

(En: *European Journal of Medicinal Chemistry* **2013**, *69*, 69)

Artículo 7: "Synthesis of new antimicrobial pyrrolo [2,1-a]isoquinolin-3-ones"

(En: *Bioorganic & Medicinal Chemistry* **2012**, *20*, 6589)

European Journal of Medicinal Chemistry 69 (2013) 69–76

Contents lists available at ScienceDirect

European Journal of Medicinal Chemistry

journal homepage: http://www.elsevier.com/locate/ejmech

Original article

Synthesis of pyrido[2,1-*a*]isoquinolin-4-ones and oxazino[2,3-*a*]isoquinolin-4-ones: New inhibitors of mitochondrial respiratory chain

Laura Moreno [a], Nuria Cabedo [b,*], Agathe Boulangé [c], Javier Párraga [a], Abraham Galán [a], Stéphane Leleu [c], María-Jesús Sanz [d,e], Diego Cortes [a], Xavier Franck [c,**]

[a] Departamento de Farmacología, Facultad de Farmacia, Universidad de Valencia, Burjassot, 46100 Valencia, Spain
[b] Centro de Ecología Química Agrícola-Instituto Agroforestal Mediterráneo, Universidad Politécnica de Valencia, UPV, Campus de Vera s/n, Edificio 6C, 46022 Valencia, Spain
[c] Normandie Univ, COBRA, UMR 6014 et FR 3038, CNRS, Univ Rouen, INSA Rouen, 1 rue Tesnières, 76821 Mont-Saint-Aignan Cedex, France
[d] Departamento de Farmacología, Facultad de Medicina, Universidad de Valencia, 46013 Valencia, Spain
[e] Institute of Health Research-INCLIVA, University Clinic Hospital of Valencia, Valencia, Spain

ARTICLE INFO

Article history:
Received 13 May 2013
Received in revised form
9 August 2013
Accepted 10 August 2013
Available online 19 August 2013

Keywords:
Benzo[*a*]quinolizines
Bischler–Napieralski cyclodehydration
Acyl-ketene imine cyclocondensation
Respiratory chain inhibition
Cytotoxicity

ABSTRACT

Benzo[*a*]quinolizine is an important heterocyclic framework that can be found in numerous bioactive compounds. The general scheme for the synthesis of these compounds was based on the preparation of the appropriate dihydroisoquinolines by Bischler–Napieralski cyclization with good yields, followed by the Pemberton method to form the oxazinones or pyridones derivatives via acyl-ketene imine cyclocondensation. All the synthesized compounds were assayed in vitro for their ability to inhibit mitochondrial respiratory chain. Most of the tested compounds were able to inhibit the integrated electron transfer chain, measured as NADH oxidation, which includes complexes I, III and IV, in the low micromolar range. Oxazino[2,3-*a*]isoquinolin-4-ones displayed greater activity than their pyrido[2,1-*a*]isoquinolin-4-ones analogs. Indeed, the presence of a furan ring in C_2 position of oxazino[2,3-*a*]isoquinolin-4-ones provided the compound (**1g**) with the most potent biological activity. Therefore, these compounds and especially the oxazinone derivatives are in the tendency of the new less toxic antitumor agents that target mitochondrial electron transport chain in a middle range potency.

1. Introduction

Isoquinoline alkaloids are a large family of natural products with a variety of powerful biological activities [1–3], including the inhibition of cellular proliferation [4]. Our research group has for a long time been focused on the isolation and synthesis of isoquinoline-containing compounds and a variety of chemically diverse structures with dopaminergic activity were obtained [5–9]. In addition, we have also been interested in the search of new compounds with antitumor properties via inhibition of mitochondrial respiratory chain, such as Annonaceous acetogenins [10–12]. Mitochondrial electron transport chain, comprises the enzymatic respiratory complexes (I–IV), the coenzyme Q (ubiquinone) and cytochrome c. In the electron transport chain a transfer of electrons occurs during the oxidative phosphorylation and a proton gradient is established as the energy source for the ATP generation. In addition, when an electron escapes, it may react with molecular oxygen to form the superoxide radical ($O_2^{\bullet-}$) which can be converted to hydrogen peroxide (H_2O_2) and other reactive oxygen species (ROS). Therefore, mitochondria play essential roles in the ATP synthesis, ROS metabolism and apoptosis. It is important that cells preserve an apposite level of intracellular ROS to keep redox balance and signaling cellular proliferation [13]. An increase of intracellular ROS leads to cellular damage, including lipid peroxidation, oxidative DNA modifications, protein oxidation, enzyme inactivation and finally, the cell death. Furthermore, DNA damage and mutations in the enzymatic complexes are related to the most common human neurodegenerative diseases, including Parkinson's disease [14] and aging [15]. Damage to the mitochondria has been also detected in cancer cells that increase the glycolytic activity (Warburg effect) to produce the ATP required for cellular functions [16]. Some anticancer agents have the ability to inhibit mitochondrial electron transport and/or increase superoxide radical

* Corresponding author. Tel.: +34 963 87 90 58.
** Corresponding author. UMR-CNRS 6014 COBRA, Université de Rouen, 1 rue Tesnière, 76131 Mont Saint Aignan Cedex, France. Tel.: +33 (0) 2 35 52 24 59.
E-mail addresses: ncabedo@ceqa.upv.es, ncabedo@uv.es (N. Cabedo), xavier.franck@insa-rouen.fr (X. Franck).

0223-5234/$ – see front matter © 2013 Elsevier Masson SAS. All rights reserved.
http://dx.doi.org/10.1016/j.ejmech.2013.08.013

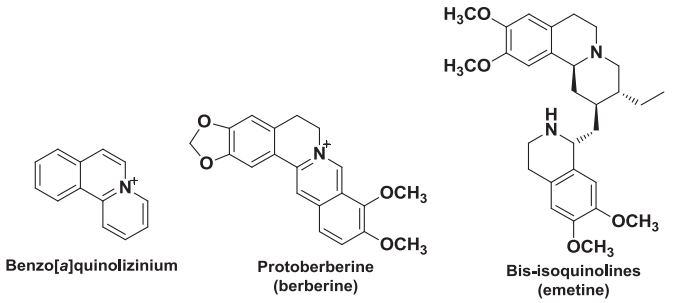

Fig. 1. Structure of benzo[*a*]quinolizine framework and examples of natural products containing it.

generation in tumor cells, causing apoptosis by reducing ATP levels and/or cell-damaging. Indeed, the research on respiratory chain inhibitors has been focused on pharmacological [17] and agrochemical targets, providing compounds with high potential for antitumor therapy [18] and pest control [19]. In addition, mitochondrial respiratory chain inhibitors have been also extremely useful to establish the functional mechanisms and crystal structures of complex I [20].

Benzo[*a*]quinolizine is an important heterocyclic framework that can be found in numerous bioactive compounds (Fig. 1) [1] such as berberine [21] and emetine [22]. Furthermore, many biologically-relevant 2-pyridones like the yohimbane-type alkaloid sempervilam [23] and the antineoplasic agent camptothecin are natural products that contain multi ring-fused systems (Fig. 2). Recently, synthetic benzo[*a*]quinolizine derivatives have shown effect in reversing tumor cell resistance with IC_{50} values in the micromolar range [24].

The biological properties and chemical features of these molecules have attracted the chemists' interest leading to the description of a large number of synthetic routes [25]. Therefore, both the attractive structure of the benzo[*a*]quinolizine moiety together with their potential activity as inhibitors of cellular proliferation, encouraged us to prepare pyrido[2,1-*a*]isoquinolin-4-ones and the oxygenated analogs oxazino[2,3-*a*]isoquinolin-4-ones in order to explore their properties as mitochondrial respiratory chain inhibitors.

Several approaches for the synthesis of benzo[*a*]quinolizines have been described in the literature [26], most of which involved B-ring closure by formation of de C_{11a}–C_{11b} bond either by Bischler–Napieralski cyclodehydration or by related palladium-catalyzed cyclization [27,28]. Other reported methods include the formation of C_1–C_{11b} bond via Mannich cyclization of a dihydroisoquinolinium ion [29] or B-ring closure by the formation of the C_7–C_{7a} bond from the appropriate N-substituted 2-arylpiperidine or pyridine derivatives [30]. Roy et al. [31] also showed an effective procedure for the synthesis of benzo[*a*]quinolizin-4-thiones through the reaction of 3,4-dihydroisoquinolines with different β-oxodithioesters. Furthermore, a conjugate addition-dipolar cycloaddition cascade has been described for the synthesis of benzo[*a*]quinolizines [32]. Among the different depicted approaches we are now interested in the study of the reactivity of imines since it can lead to original and biologically unexplored frameworks. Indeed, the microwave-assisted acyl-ketene imine cyclocondensation has been a useful strategy to generate oxazinones. In this regard, Presset et al. [33] reported the use of cyclic 2-diazo-1,3-diketones as acyl-ketene source by Wolff rearrangement, and Pemberton et al. [34] started from either Meldrum's acid derivatives or 1,3-dioxine-4-ones to react with dihydroisoquinolines. Therefore, we have applied the Pemberton method using dioxinones as acyl-ketenes precursors taking advantage of the chemical diversity generated by this procedure. The structure–activity relationship (SAR) of the synthesized products was further evaluated.

2. Results and discussion

2.1. Chemistry

The general synthetic plan to obtain these compounds was based on the preparation of the appropriate β-phenylacetamides (**1**–**3**) by standard methods [6,35] and further cyclization by Bischler–Napieralski cyclodehydration (Scheme 1). First, 3,4-dimethoxyphenethylamine was subjected to Ac_2O/Pyr or Schotten–Bauman conditions to give the appropriate amides (**1**–**3**). Then, amides **1**–**3** were treated with $POCl_3$ to lead to the expected dihydroisoquinolines **1a**–**3a** by Bischler–Napieralski cyclization with good yields.

Once the different imines were prepared following Pemberton's procedure [34], imine **1a** was reacted with the commercially available 2,2,6-trimethyl-4H-1,3-dioxin-4-one (**4a**) under neutral or basic conditions, either using microwave irradiation or conventional heating. Similar to Pemberton et al. [34], the formation of oxazinone **1c** was favored by basic conditions and it was almost exclusively formed by the use of conventional heating. Neutral conditions clearly favored the formation of pyridone **1b** under either conventional or microwave activation (Table 1, Scheme 2).

Once the reaction conditions were set up [38], this methodology was applied to the synthesis of oxazinones (**1c**–**3c**, **1e**, **1g**) and pyridones (**1b**–**3b**, **1d**, **1f**) from different 1-substituted dihydroisoquinolines (**1a**–**3a**) and dioxinones (**4a**–**4c**). When 1-benzyldihydroisoquinolines (**2a**, **3a**) were used, yields were lower than those for 1-methyldihydroisoquinoline (**1a**) (Schemes 3 and 4). In addition, in order to explore their biological activity, deprotection of the methoxy groups of compound **1b** was performed. Catechol **1h** was then obtained in good yield using BBr_3. To our knowledge, compounds **1c**, **1f**–**1h**, **2b**, **2c**, **3b** and **3c** are here reported for the first time and their structures were confirmed by NMR spectral data and mass spectrometry.

2.2. Respiratory chain inhibition (SAR)

All the synthesized compounds were assayed in vitro against the NADH oxidase activity of beef-heart submitochondrial particles, as a model of mammalian respiratory chain. Most of the tested

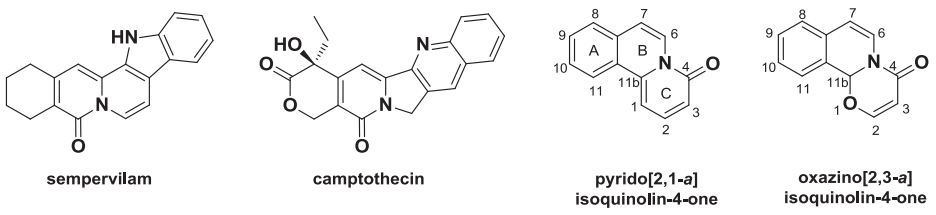

Fig. 2. Examples of natural 2-pyridones and structures of pyrido[2,1-*a*]isoquinolin-4-ones and oxazino[2,3-*a*]isoquinolin-4-ones.

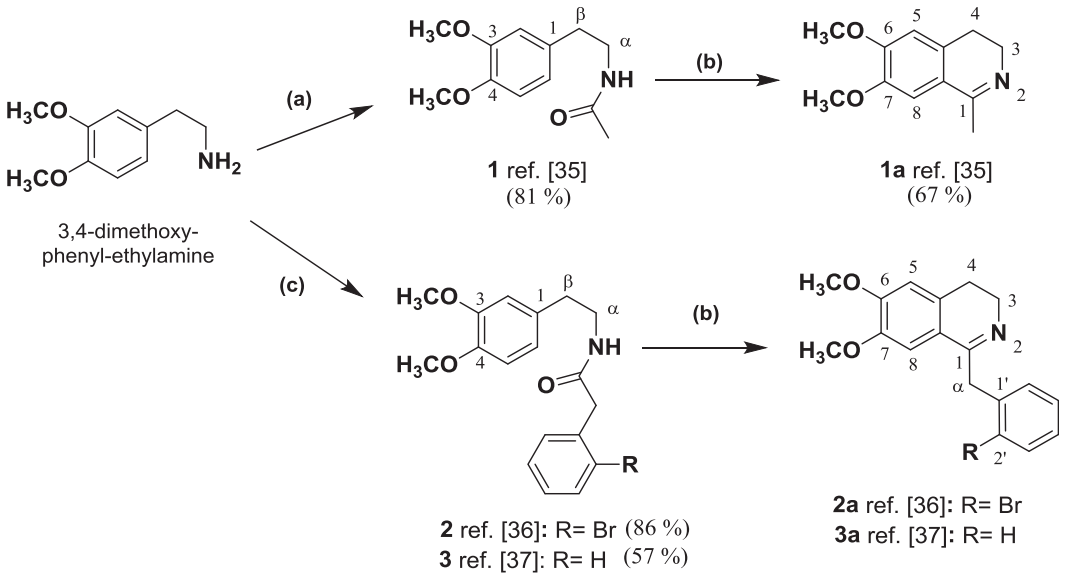

Scheme 1. Synthesis of dihydroisoquinolines **1a**–**3a**. Reagents and Conditions: (a) Ac_2O, Pyr, rt, 3 h; (b) $POCl_3$, CH_3CN, N_2, reflux, 1 h; (c) 2-bromophenylacetyl chloride or 2-phenylacetyl chloride, CH_2Cl_2, 5% aq NaOH, rt, 16 h.

Table 1
Reaction of dihydroisoquinoline **1a** with 2,2,6-trimethyl-4H-1,3-dioxin-4-one under different reaction conditions.

Solvent	Heating	Pyridone (1b)	Oxazinone (1c)
Toluene	MW	70%	-
TEA + Toluene	MW	Complex mixture	
Toluene	Conventional	78%	1%
TEA + Toluene	Conventional	2%	68%

compounds were able to inhibit the whole respiratory chain in the micromolar range. Indeed, this enzymatic assay detected a decay of the NADH oxidase activity in the integrated electron transfer chain which involves all three energy-conserving enzymatic complexes: NADH:ubiquinone oxidoreductase (complex I), ubiquinol:cytochrome *c* reductase (complex III) and cytochrome *c* oxidase (complex IV). NADH is the physiological electron donor of complex I that catalyzes the reduction of lipid soluble endogenous coenzyme Q or ubiquinone (CoQ_{10} in beef heart). In fact, in the integrated electron transfer chain, electrons are first carried from complex I or from complex II (succinate:cytochrome *c* reductase) to complex III by ubiquinone, and then from complex III to complex IV by the peripheral membrane protein cytochrome c. Thus, the inhibitory action of the active compounds might be affecting one or more of the electron transfer chain enzymatic complexes [39].

Compared with the highly toxic rotenone (a high-affinity inhibitor of complex I), the pyridone (**1b**, **1f**, **1h**, **2b** and **3b**) and oxazinone (**1c**, **1e**, **1g**, **2c** and **3c**) cytotoxic derivatives showed a moderate inhibitor activity that was in the same order of magnitude that the structural-related mycotoxins such as circumdatins (circumdatin E and H, IC_{50} = 2.5 and 1.5 μM, respectively) and flavacol (IC_{50} = 13 μM) [40]. Given that most of the respiratory chain inhibitors with potential therapeutic interest act in the high nanomolar and low micromolar ranges to avoid an extreme toxicity, as it happens with Annonaceus acetogenins (IC_{50} values in the low nanomolar range), these compounds and especially the oxazinone derivatives can be consider effective inhibitors of the whole respiratory chain [41] (Table 2).

In general, oxazino[2,3-*a*]isoquinolin-4-ones seemed to display greater activity than their respective pyrido[2,1-*a*]isoquinolin-4-

Table 2
Inhibitory potency of compounds **1b**–**3c** against the NADH oxidase activity of mammalian respiratory chain.

Compound	IC_{50} (μM) ± SE[a]
1b	8.23 ± 0.98*
1c	1.36 ± 0.50*
1d	>30
1e	1.32 ± 0.03*
1f	12.50 ± 1.66*
1g	0.90 ± 0.03*
1h	3.44 ± 0.05*
2b	4.24 ± 0.03*
2c	1.39 ± 0.20*
3b	4.69 ± 0.11*
3c	1.53 ± 0.10*
Rotenone	5.10 ± 0.90* (nM)

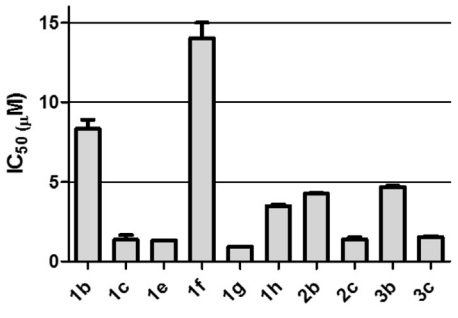

*$p < 0.05$.
[a] Data are presented as the mean ± SD of thee independent determinations for each compound.

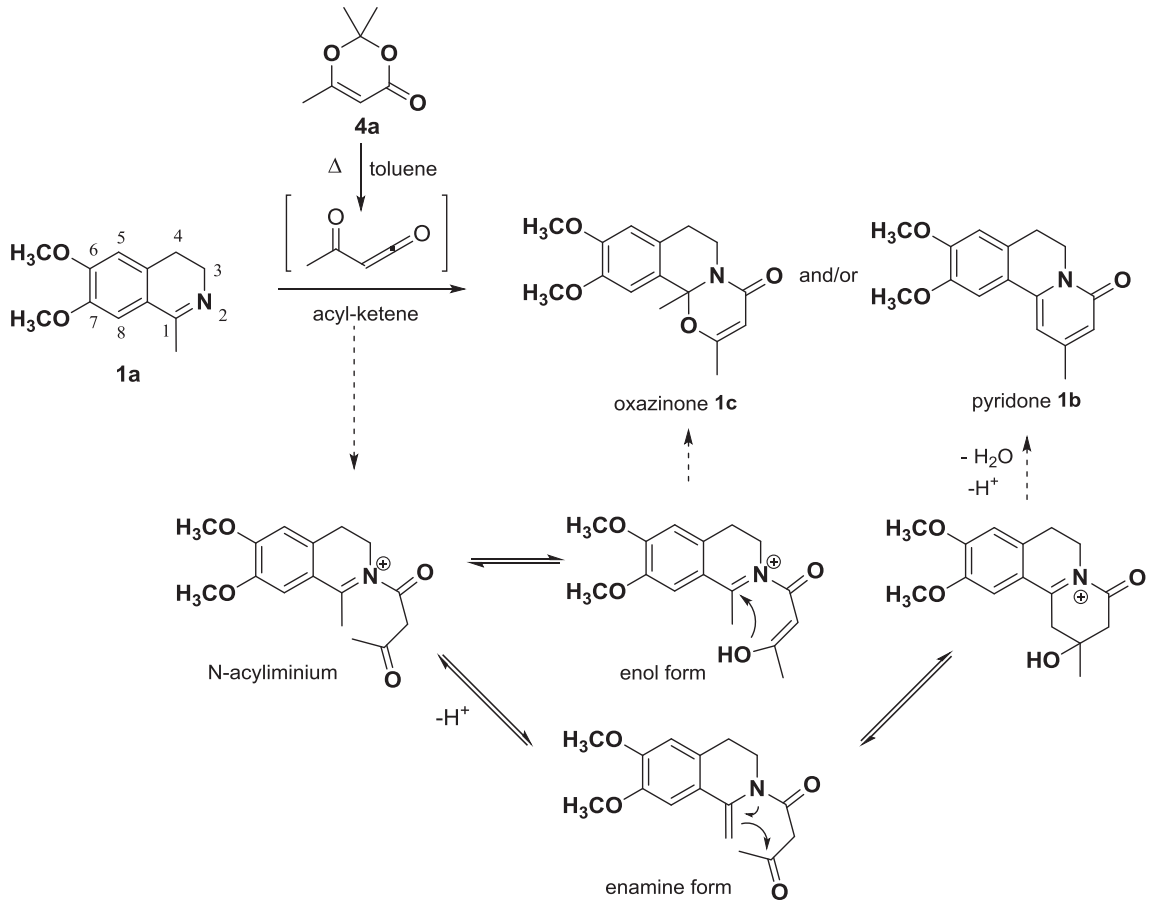

Scheme 2. Mechanism of reaction.

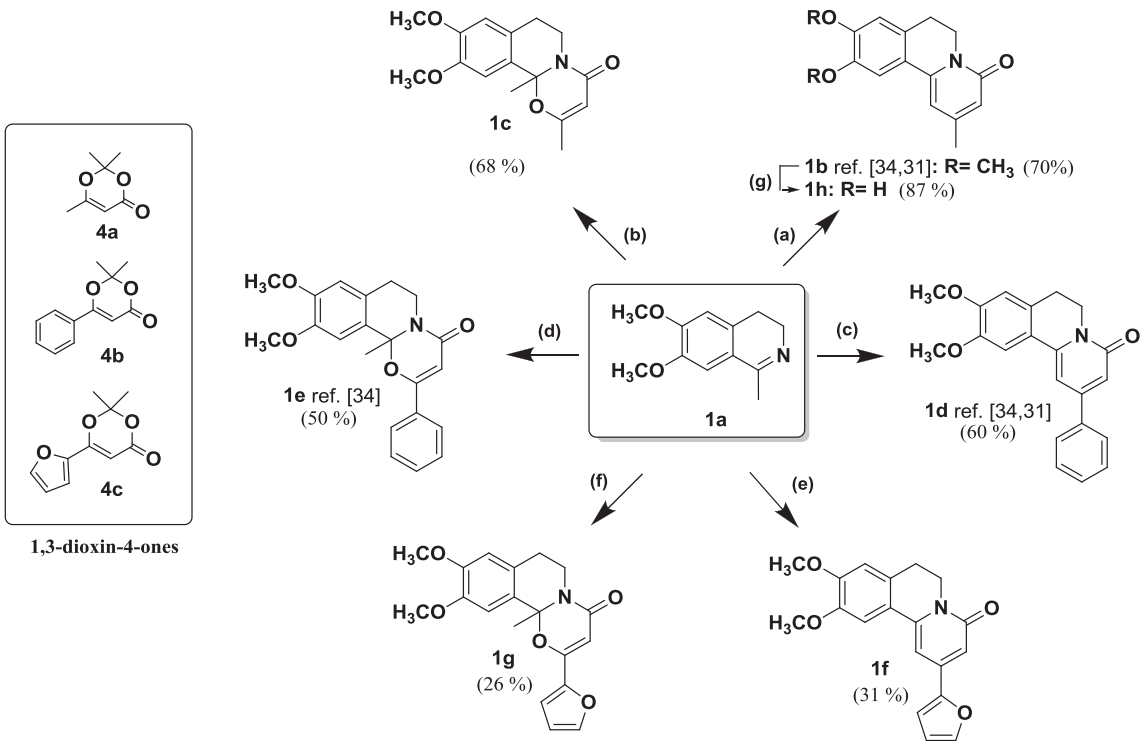

Scheme 3. Synthesis of pyrido[2,1-*a*]isoquinolin-4-ones and oxazino [2,3-*a*]isoquinolin-4-ones **1b**–**1g**. Reagents and Conditions: (a) 2,2,6-trimethyl-4H-1,3-dioxin-4-one **4a**, toluene, N_2, MW, 150 °C, 5 min; (b) 2,2,6-trimethyl-4H-1,3-dioxin-4-one **4a**, Et_3N, toluene, N_2, reflux, 3 h; (c) 2,2-dimethyl-6-phenyl-4H-1,3-dioxin-4-one **4b**, toluene, N_2, MW, 110 °C, 5 min; (d) 2,2-dimethyl-6-phenyl-4H-1,3-dioxin-4-one **4b**, Et_3N, toluene, N_2, reflux, 3h; (e) 6-(furan-2-yl)-2,2-dimethyl-4H-1,3-dioxin-4-one **4c**, toluene, N_2, MW, 110 °C, 5 min; (f) 6-(furan-2-yl)-2,2-dimethyl-4H-1,3-dioxin-4-one **4c**, Et_3N, toluene, N_2, reflux, 3 h; (g) BBr_3, CH_2Cl_2, N_2, rt, 2 h.

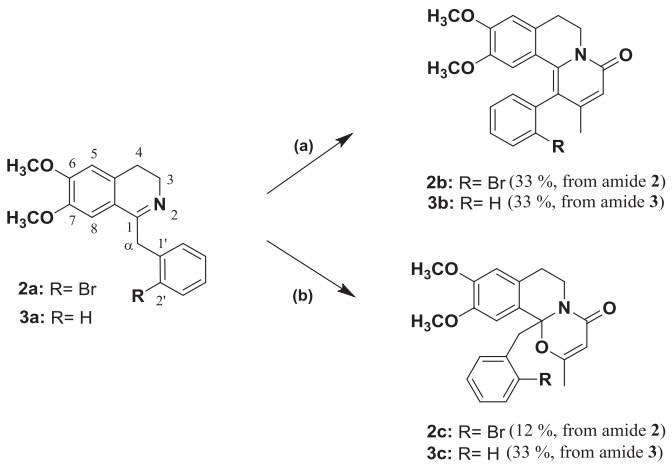

Scheme 4. Synthesis of pyrido[2,1-*a*]isoquinolin-4-ones and oxazino[2,3-*a*]isoquinolin-4-ones **2b**–**3c**. Reagents and Conditions: (a) 2,2,6-trimethyl-4H-1,3-dioxin-4-one **4a**, toluene, N_2, reflux, 3 h; (b) 2,2,6-trimethyl-4H-1,3-dioxin-4-one **4a**, Et_3N, toluene, N_2, reflux, 3 h.

ones analogs. For instance, while the IC_{50} of the compound **1c** was 1.36 μM, its pyridone analog (**1b**) showed decreased NADH oxidase activity (IC_{50} = 8.33 μM). In addition, when the methyl group in C_2 position of the pyridone was replaced by an aromatic group, the activity decreased or almost disappeared (**1d** and **1f**). By contrast, the size and nature of the substituent in 2-position of the oxazine did not seem to affect NADH oxidase activity. In this regard, not only the existence of a phenyl group (**1e**) kept the activity but the presence of a furan ring in C_2 position provided the most potent compound **1g**. Interestingly, the deprotection of the methoxy groups in A ring to obtain a catechol (**1h**) maintained the activity.

On the other hand, when the aromatic ring was placed on C_1 position (series 2 and 3), the pyrido[2,1-*a*]isoquinolin-4-ones were able to inhibit respiratory chain at moderated potencies (compounds **2b** and **3b** with IC_{50} of 4.24 μM and 4.69 μM respectively) without any noticeable influence of the halogen group. However and in agreement with the previous observations, the oxazine analogs displayed greater NADH oxidase inhibition than their respective pyridones (compounds **2c** and **3c** with IC_{50} of 1.39 μM and 1.53 respectively). Likewise, the presence of a bromine atom in the aromatic ring did not seem to affect the activity. Therefore, pyridone and mainly oxazine derivatives can interfering with the mitochondrial respiratory chain by direct inhibition of one or more enzyme complexes and/or, similar to many potent inhibitors that mimic the quinoid head of ubiquinone, they can function as false electron acceptors (carriers) by extracting electrons from intermediates in the respiratory chain in competition with their natural substrates [42]. We could hypothesize that the different electron density of oxazine and pyridone nucleus might establish their different electron acceptor properties whereas substituents on C_1 or C_2 positions favors the passage through the hydrophobic environment of the ubiquinone catalytic binding site.

3. Conclusions

In conclusion, we have synthesized via Pemberton method eleven benzo[*a*]quinolizines including pyrido[2,1-*a*]isoquinolin-4-ones (**1b**, **1d**, **1f**, **1h**, **2b** and **3b**) and oxazino[2,3-*a*]isoquinolin-4-ones (**1c**, **1e**, **1g**, **2c** and **3c**). Most of these compounds were found to be moderate inhibitors of the electron transport chain in the same range that known mycotoxins. Oxazino[2,3-*a*]isoquinolin-4-ones displayed greater activity than their pyrido[2,1-*a*]isoquinolin-4-ones analogs. Indeed, the presence of a furan ring in C_2 position of oxazino[2,3-*a*]isoquinolin-4-ones provided the compound (**1g**) with the most potent biological activity. Therefore, these compounds and especially the oxazinone derivatives are in the tendency of the new less toxic antitumor agents that target mitochondrial electron transport chain in a middle range potency.

4. Experimental section

4.1. Chemistry

Melting points were taken on a Cambridge microscope instrument coupled with a Reichert-Jung. EIMS was recorded in a VG Auto Spec Fisons spectrometer instrument (Fisons, Manchester, United Kingdom). Microwave reactions were performed using a CEM Focused Microwave Synthesis System apparatus, Model Discover. The device is a continuous focused microwave power delivery system with operator selectable power output from 0 to 300 W. All the reactions were performed in special 10 mL glass vessels under argon atmosphere. Reaction mixture temperatures were measured during microwave heating with an IR surface sensor located at the base of the Discover. The temperature was fixed at 150 °C or 110 °C and maintained for 5 min (i.e., hold time: time in which the system maintains the control parameters) and was usually reached within 1 min (i.e., run time: maximum run time for the method in situations where the control point is not reached). ^1H NMR and ^{13}C NMR spectra were recorded with $CDCl_3$ as a solvent in a Bruker AC-300, AC-400 or AC-500. Multiplicities of ^{13}C NMR resonances were assigned by DEPT experiments. COSY, HSQC and HMBC correlations were recorded at 400 and 500 MHz (Bruker AC-400 or AC-500). The assignments of all compounds were made by COSY, DEPT, HSQC and HMBC. All the reactions were monitored by analytical TLC with silica gel 60 F_{254} (Merck 5554). Residues were purified by silica gel 60 (40–63 μm, Merck 9385) column chromatography. Solvents and reagents were purchased from commercial sources. Quoted yields are of purified material.

4.1.1. General procedure for the synthesis of dihydroisoquinolines (*1a*–*3a*)

*4.1.1.1. 6,7-Dimethoxy-1-methyl-3,4-dihydroisoquinoline (**1a**).* A solution of 3,4-dimethoxyphenethylamine (1 g, 5.52 mmol) in dry Ac_2O (10 mL) and pyridine (0.5 mL) was stirred under nitrogen atmosphere at room temperature for 3 h. Then, the reaction mixture was diluted with water (15 mL) and extracted with CH_2Cl_2. The combined organic phases were dried over Na_2SO_4 and evaporated to dryness to give 1.02 g (81%) of **1** as a white solid, which was used in the next step with no further purification. Next, a solution of *N*-(3,4-dimethoxyphenethyl)acetamide **1** (500 mg, 2.24 mmol) in dry CH_3CN (20 mL) was treated with $POCl_3$ (0.37 mL, 4.1 mmol) and refluxed for 1 h in a nitrogen atmosphere. The reaction mixture was concentrated to dryness, re-dissolved in water and basified with NH_4OH until pH = 9. The mixture was extracted with CH_2Cl_2. The organic solution was dried over Na_2SO_4 and evaporated to dryness to give 312 mg of **1a** (67%) which was used in the next step with no further purification. Characterization data for **1** and **1a** were in agreement with published data [35].

*4.1.1.2. 6,7-Dimethoxy-1-(2-bromobenzyl)-3,4-dihydroisoquinoline (**2a**).* 2-Bromophenylacetyl chloride (1.2 mL, 8.25 mmol) was added dropwise at 0 °C to a solution of 3,4-dimethoxyphenetylamine (2 g, 5.50 mmol) in 15 mL of CH_2Cl_2 and 5% aqueous NaOH (2.5 mL). The reaction was stirred at room temperature overnight and then extracted with CH_2Cl_2 (3 × 10 mL). The combination of the organic phases was washed with brine (2 × 10 mL) and H_2O (2 × 10 mL), dried over Na_2SO_4 and evaporated to dryness. The residue was purified by silica gel column chromatography (hexane-EtOAc, 5:5) to afford 1.8 g

of amide **2** as a white powder (4.73 mmol, 86%). Next, a solution of **2** (100 mg, 0.27 mmol) in dry CH_3CN (5 mL) was treated with $POCl_3$ (0.07 mL, 0.75 mmol) and refluxed for 1 h in a nitrogen atmosphere under the same conditions described above to obtain **1a**. The residue was used in the next step with no further purification. Characterization data for **2** and **2a** were in agreement with published data [36].

*4.1.1.3. 6,7-Dimethoxy-1-benzyl-3,4-dihydroisoquinoline (**3a**).* The compound was **3** prepared according to the procedure described above to obtain **2a**. Firstly, 2-phenylacetyl chloride (2.18 mL, 16.5 mmol), 3,4-dimethoxyphenetylamine (2 g, 11 mmol) and NaOH 5% (2.5 mL). The residue was purified by silica gel column chromatography (hexane/EtOAc 5:5) to afford 1.9 g of amide **3** as a white powder (6.27 mmol, 57%). Next, a solution of **3** (200 mg, 0.65 mmol) in dry CH_3CN (15 mL) was treated with $POCl_3$ (0.12 mL, 1.35 mmol) and refluxed for 1 h in a nitrogen atmosphere under the same conditions described above to obtain **1a**. The residue was used in the next step with no further purification. Characterization data for **3** and **3a** were in agreement with published data [37].

*4.1.2. General procedure for the synthesis of pyrido[2,1-a] isoquinolin-4-ones (**1b**, **1d**, **1f**)*

*4.1.2.1. 9,10-Dimethoxy-2-methyl-6,7-dihydro-4H-pyrido[2,1-a]isoquinolin-4-one (**1b**).* 2,2,6-Trimethyl-4H-1,3-dioxin-4-one (0.065 mL, 0.48 mmol) was added to a stirred solution of imine **1a** (50 mg, 0.24 mmol) dissolved in dry toluene (0.5 mL). The mixture was irradiated at 150 °C, 300 W, for 5 min and then cooled to room temperature. The resulting solution was diluted with CH_2Cl_2 and washed with saturated aq. $NaHCO_3$, water and brine. The combined organic extracts were dried with Na_2SO_4, filtered and concentrated. Purification by column chromatography (CH_2Cl_2—MeOH, 98:2) gave **1b** (42 mg, 70%) as a white powder. Characterization data were in agreement with published data [33,31].

*4.1.2.2. 9,10-Dimethoxy-2-phenyl-6,7-dihydro-4H-pyrido[2,1-a]isoquinolin-4-one (**1d**).* This compound was prepared following the same procedure described above for the synthesis of **1b**, and using **1a** (0.24 mmol) and 2,2-dimethyl-6-phenyl-4H-1,3-dioxin-4-one (89 mg, 0.46 mmol). The mixture was irradiated at 110 °C, 300 W, for 5 min and then cooled to room temperature. Purification by column chromatography (CH_2Cl_2-AcOEt, 60:40) gave **1d** (35 mg, 60%) as a yellow powder. Characterization in agreement with published data [33,31].

*4.1.2.3. 2-(Furan-2-yl)-9,10-dimethoxy-6,7-dihydro-4H-pyrido[2,1-a]isoquinolin-4-one (**1f**).* This compound was prepared following the same procedure described above for the synthesis of **1b**, and using **1a** (0.24 mmol) and 6-(furan-2-yl)-2,2-dimethyl-4H-1,3-dioxin-4-one (93 mg, 0.48 mmol). The mixture was irradiated at 110 °C, 300 W, for 5 min and then cooled to room temperature. Purification by column chromatography (CH_2Cl_2-AcOEt, 70:30) gave **1f** (23 mg, 31%) as a yellow oil. IR (cm^{-1}): 2932, 1648, 1566, 1504, 1459, 1341; ^1H NMR (500 MHz, $CDCl_3$): $\delta = 7.57$ (d, $J = 1.3$ Hz, 1H, H-3′), 7.23 (s, 1H, H-11), 6.87 (d, $J = 3.3$ Hz, 1H, H-5′), 6.85 (d, $J = 1.7$ Hz, 1H, H-1), 6.79 (d, $J = 1.7$ Hz, 1H, H-3), 6.75 (s, 1H, H-8), 6.54 (dd, $J = 3.5$, 1.8 Hz, 1H, H-4′), 4.27 (m, 2H, CH_2-6), 3.98 (OCH_3-9), 3.94 (OCH_3-10), 2.92 (m, 2H, CH_2-7); ^{13}C NMR (125 MHz, $CDCl_3$): $\delta = 162.7$ (CO), 151.1 (C-9), 151.0 (C-10), 148.5 (C-2), 144.0 (CH-3′), 143.5 (C-11b), 139.6 (C-1′), 129.1 (C-7a), 121.5 (C-11a), 112.1 (CH-4′), 110.4 (CH-8), 109.9 (CH-3), 109.4 (CH-5′), 108.2 (CH-11), 98.0 (CH-1), 56.3 (OCH_3-9), 56.0 (OCH_3-10), 39.1 (CH_2-6), 27.6 (CH_2-7); ESMS *m/z* (%) 324 $[M + H]^+$ (100).

*4.1.2.4. 9,10-Dihydroxy-2-methyl-6,7-dihydro-4H-pyrido[2,1-a]isoquinolin-4-one (**1h**).* A solution of **1b** (75 mg, 0.33 mmol) in dry CH_2Cl_2 (5 mL) was cooled to −78 °C. Then, BBr_3 (0.05 mL, 0.50 mmol) was added dropwise under nitrogen atmosphere. After 15 min, the reaction mixture was warmed up to room temperature and stirred for 2 h. The reaction was terminated by the addition of MeOH (1 mL) dropwise and the mixture was further stirred for another 30 min. The solvent was concentrated to dryness. The residue was purified by silica gel column chromatography (CH_2Cl_2—MeOH, 90:10) to afford 70 mg of **1h** (87%) as a brown solid. Mp: 281—283 °C; IR (cm^{-1}): 3328, 2971, 2734, 2589, 1646, 1509, 1298; ^1H NMR (500 MHz, $CDCl_3$): $\delta = 7.59$ (s, 1H, H-11), 6.98 (s, 1H, H-8), 6.46 (d, $J = 1.1$ Hz, 1H, H-3), 6.37 (d, $J = 1.1$ Hz, 1H, H-1), 4.19 (m, 2H, CH_2-6), 2.66 (m, 2H, CH_2-7), 2.03 (s, 3H, CH_3); ^{13}C NMR (125 MHz, $CDCl_3$): $\delta = 165.2$ (CO), 153.3 (C-9), 151.9 (C-10), 148.6 (C-2), 145.8 (C-11b), 130.5 (C-7a), 120.9 (C-11a), 117.6 (CH-1), 117.4 (CH-8), 115.6 (CH-11), 106.6 (CH-3), 41.9 (CH_2-6), 29.5 (CH_2-7), 23.3 (CH_3); ESMS *m/z* (%) 234 (100) $[M]^+$

*4.1.3. General procedure for the synthesis of oxazino[2,3-a] isoquinolin-4-ones (**1c**, **1e**, **1g**)*

*4.1.3.1. 9,10-Dimethoxy-2,11b-dimethyl-7,11b-dihydro-4H,6H- [1,3]oxazino[2,3-a]isoquinolin-4-one (**1c**).*
2,2,6-Trimethyl-4H-1,3-dioxin-4-one (0.06 mL, 0.44 mmol) was added to a stirred solution of imine **1a** (46 mg, 0.22 mmol) dissolved in dry toluene (5 mL). Et_3N (0.06 mL, 0.44 mmol) was added and the heated mixture was refluxed for 3 h and then cooled to room temperature. The resulting solution was diluted with CH_2Cl_2 and washed with saturated aq. $NaHCO_3$, water and brine. The combined organic extracts were dried with Na_2SO_4, filtered and concentrated. Purification by column chromatography (CH_2Cl_2-AcOEt, 60:40) gave **1c** (43 mg, 68%). IR (cm^{-1}): 2932, 1662, 1515, 1409; ^1H NMR (500 MHz, $CDCl_3$): $\delta = 6.99$ (s, 1H, H-8), 6.96 (s, 1H, H-11), 5.26 (s, 1H, H-3), 4.62 (ddd, $J = 12.7$, 5.1, 2.7 Hz; 1H, H-6α), 3.91 (s, 3H, OCH_3-9), 3.66 (s, 3H, OCH_3-10), 3.01 (m, 1H, H-6β), 2.91 (m, 1H, H-7α), 2.66 (m, 1H, H-7β), 1.97 (CH_3-2), 1.81 (CH_3-11b); ^{13}C NMR (125 MHz, $CDCl_3$): $\delta = 163.4$ (CO), 162.1 (C-2), 149.2 (C-10), 148.8 (C-9), 128.5 (C-11a), 126.9 (C-7a), 110.7 (CH-8), 108.8 (CH-11), 98.4 (CH-3), 90.3 (C-11b), 56.1 (OCH_3-10), 55.8 (OCH_3-9), 35.9 (CH_2-6), 27.6 (CH_2-7), 23.1 (CH_3-11b), 19.8 (CH_3-2); ESMS *m/z* (%) 290 $[M + H]^+$ (100)

*4.1.3.2. 9,10-Dimethoxy-11b-methyl-2-phenyl-7,11b-dihydro-4H,6H-[1,3]oxazino[2,3-a]isoquinolin-4-one (**1e**).* This compound was prepared following the same procedure described above for the synthesis of **1c**, and using **1a** (75 mg, 0.36 mmol) and 2,2-dimethyl-6-phenyl-4H-1,3-dioxin-4-one (178 mg, 0.88 mmol), Et_3N (0.12 mL, 0.88 mmol), and dry toluene (3 mL). Purification by column chromatography (CH_2Cl_2-AcOEt, 90:10) gave **1e** (40 mg, 50%). Characterization data were in agreement with published data [33].

*4.1.3.3. 2-(Furan-2-yl)-9,10-dimethoxy-11b-methyl-7,11b-dihydro-4H,6H- [1,3]oxazino[2,3-a]isoquinolin-4-one (**1g**).* This compound was prepared following the same procedure described above for the synthesis of **1c**, and using **1a** (50 mg, 0.24 mmol) and 6-(furan-2-yl)-2,2-dimethyl-4*H*-1,3-dioxin-4-one (126 mg, 0.66 mmol), Et_3N (0.06 mL, 0.33 mmol), and dry toluene (2 mL). Purification by column chromatography ($CHCl_2$-AcOEt, 90:10) gave **1g** (20 mg, 26%) as a white powder. Mp: 123—125 °C; IR (cm^{-1}): 2943, 1653, 1515, 1414, 1364; ^1H NMR (500 MHz, $CDCl_3$): $\delta = 7.53$ (d, $J = 1.1$ Hz, 1H, H-3′), 7.02 (s, 1H, H-11), 6.80 (d, $J = 3.3$ Hz, 1H, H-5′), 6.62 (s, 1H, H-8), 6.50 (dd, $J = 3.4$, 1.8 Hz, 1H, H-4′), 5.89 (s, 1H, H-3), 4.67 (ddd, $J = 13.0$, 5.3, 2.8 Hz, 1H, H-6α), 3.94 (OCH_3-10), 3.87 (OCH_3-9), 3.09 (m, 1H, H-6β), 2.97 (m, 1H, H-7α), 2.70 (dt, $J = 13.5$, 3.3 Hz, 1H, H-7β), 1.89 (CH_3-11b); ^{13}C NMR (125 MHz, $CDCl_3$): $\delta = 162.2$ (CO), 152.3 (C-2), 149.4 (C-9), 148.1 (C-10), 147.1 (C-1′), 145.1 (CH-3′), 128.4 (C-11a), 127.1 (C-7a), 111.8 (CH-4′, CH-5′), 110.7 (CH-8), 108.9 (CH-11), 94.9

(CH-3), 90.7 (C-11b), 56.1 (OCH_3-10), 55.9 (OCH_3-9), 36.2 (CH_2-6), 27.6 (CH_2-7), 23.0 (CH_3-11b); ESMS *m/z* (%) 341 $[M]^+$ (100).

4.1.4. General procedure for the synthesis of pyrido[2,1-a] isoquinolin-4-ones **2b**–**3b**

*4.1.4.1. 1-(2-Bromophenyl)-9,10-dimethoxy-2-methyl-6,7-dihydro-4H-pyrido[2,1-a]isoquinolin-4-one (**2b**).* A residue of the imine **2a** (from 100 mg, 0.27 mmol of amide **2**) was dissolved in dry toluene (5 mL), and treated with 2,2,6-trimethyl-4H-1,3-dioxin-4-one (0.06 mL, 0.44 mmol). The reaction mixture was refluxed under nitrogen atmosphere for 3 h and then cooled to room temperature. The resulting solution was diluted with CH_2Cl_2 and washed with saturated aq. $NaHCO_3$, water and brine. The combined organic extracts were dried with Na_2SO_4, filtered and concentrated. Purification by column chromatography (CH_2Cl_2-AcOEt, 10:90) gave **2b** (40 mg, 33% from amide **2**) as a white solid. Mp: 216–218 °C. IR: 2961, 1639, 1491, 1466, 1450, 1212; ^{1}H NMR (500 MHz, $CDCl_3$): δ = 7.65 (dd, 1H, J = 8.02, 1.12 Hz, CH-2′), 7.31 (td, 1H, J = 7.49, 1.19 Hz, CH-6′), 7.20 (td, 1H, J = 7.77, 1.71 Hz, CH-4′), 7.14 (dd, 1H, J = 7.55, 1.65 Hz, CH-4′), 6.66 (s, 1H, H-8), 6.52 (s, 1H, H-3), 6.43 (s, 1H, H-11), 4.45 (m, 1H, H-6α), 3.97 (m, 1H, H-6β), 3.86 (OCH_3-9), 3.23 (OCH_3-10), 2.85 (m, 2H, CH_2-7), 1.88 (s, 3H, CH_3); ^{13}C NMR (125 MHz, $CDCl_3$): δ = 161.7 (CO), 150.2 (C-9), 149.5 (C-10), 146.5 (C-2), 140.4 (C-1), 140.1 (C-1′), 133.2 (CH-3′), 132.7 (CH-5′), 131.6 (C-11b), 129.2 (CH-4′), 128.2 (CH-6′), 126.5 (C-2′), 121.4 (C-11a), 118.4 (C-7a), 117.7 (CH-3), 112.4 (CH-11), 109.6 (CH-8), 55.7 (OCH_3-9), 55.3 (OCH_3-10), 40.3 (CH_2-6), 28.6 (CH_2-7), 21.0 (CH_3); ESMS *m/z* (%) 425 $[M + H]^+$ (100).

*4.1.4.2. 9,10-Dimethoxy-2-methyl-1-phenyl-6,7-dihydro-4H-pyrido [2,1-a] isoquinolin-4-one (**3b**).* This compound was prepared following the same procedure described above for the synthesis of **2b**, and using a residue of the imine **3a** (from 200 mg, 0.65 mmol of amide **3**) and treated with 2,2,6-trimethyl-4H-1,3-dioxin-4-one (0.18 mL, 1.30 mmol) in dry toluene (10 mL). Purification by column chromatography (CH_2Cl_2–MeOH, 95:5) gave **3b** (75 mg, 33% from amide **3**). IR (cm^{-1}): 2933, 1690, 1517, 1373, 1262, 1212; ^{1}H NMR (500 MHz, $CDCl_3$): δ = 7.45 (m, 2H, CH-3′, CH-5′), 7.30 (m, 1H, CH-4′), 7.29 (m, 2H, CH-2′, CH-6′), 6.96 (s, 1H, H-8), 6.89 (s, 1H, H-11), 6.16 (s, 1H, H-3), 4.63 (m, 1H, H-6α), 3.98 (m, 1H, H-6β), 3.83 (OCH_3-9), 3.25 (OCH_3-10), 2.92 (m, 2H, CH_2-7), 1.93 (s, 3H, CH_3); ^{13}C NMR (125 MHz, $CDCl_3$): δ = 161.0 (CO), 148.9 (C-9), 148.1 (C-2), 146.5 (C-10), 140.2 (C-1), 135.6 (C-11b), 132.5 (C-1′), 128.9 (CH-2′, CH-6′), 128.7 (C-7a), 128.6 (CH-3′, CH-5′), 127.9 (CH-4′), 123.5 (C-11a), 118.7 (CH-3), 111.4 (CH-8), 109.7 (CH-11), 55.8 (OCH_3-9), 55.4 (OCH_3-10), 41.3 (CH_2-6), 27.2 (CH_2-7), 19.0 (CH_3); ESMS *m/z* (%) 347 (100) $[M]^+$

4.1.5. General procedure for the synthesis of oxazino[2,3-a] isoquinolin-4-ones (**2c**–**3c**)

*4.1.5.1. 11B-(2-Bromobenzyl)-9,10-dimethoxy-2-methyl-7,11b-dihydro-4H,6H- [1,3]oxazino[2,3-a]isoquinolin-4-one (**2c**).* A residue of the imine **2a** (from 100 mg, 0.27 mmol of amide **2**) in dry toluene (5 mL) was treated with 2,2,6-trimethyl-4H-1,3-dioxin-4-one (0.06 mL, 0.44 mmol) and Et_3N (0.06 mL, 0.44 mmol). The reaction mixture was refluxed under nitrogen atmosphere for 3 h and then cooled to room temperature. The resulting solution was diluted with CH_2Cl_2 and washed with saturated aq. $NaHCO_3$, water and brine. The combined organic extracts were dried with Na_2SO_4, filtered and concentrated. Purification by column chromatography (Toluene-AcOEt, 70:30) gave **2c** (15 mg, 12% from amide **2**). IR (cm^{-1}): 2938, 1664, 1515, 1460, 1264, 1212; ^{1}H NMR (500 MHz, $CDCl_3$): δ = 7.44 (m, 1H, C-2′), 7.16 (m, 1H, CH-5′), 7.07 (m, 1H, CH-4′), 6.94 (m, 1H, CH-6′), 6.56 (s, 1H, H-11), 6.55 (s, 1H, H-8), 5.29 (s, 1H, H-3), 4.33 (m, 1H, H-6α), 3.84 (OCH_3-9), 3.80 (m, 1H, CH_2Ph-α), 3.66 (OCH_3-10), 3.65 (m, 1H, CH_2Ph-β), 3.18 (m, 1H, H-6β), 2.81 (m, 1H, H-7α), 2.50 (m, 1H, H-7β), 2.05 (s, 3H, CH_3); ^{13}C NMR (125 MHz, $CDCl_3$): δ = 162.7 (CO), 161.9 (C-2), 149.3 (C-9), 147.3 (C-10), 134.6 (C-1′), 132.8 (CH-3′), 132.5 (CH-6′), 128.6 (CH-4′), 127.5 (C-2′), 126.9 (CH-5′), 126.8 (C-7a), 126.4 (C-11a), 110.3 (CH-8), 109.6 (CH-11), 98.8 (CH-3), 91.7 (C-11b), 55.8 (OCH_3-9), 55.8 (OCH_3-10), 41.8 (CH_2Ph), 36.7 (CH_2-6), 27.1 (CH_2-7), 19.8 (CH_3); ESMS *m/z* (%) 444 (100) $[M+1]^+$

*4.1.5.2. 11B-Benzyl-9,10-dimethoxy-2-methyl-7,11b-dihydro-4H,6H-[1,3]oxazino[2,3-a]isoquinolin-4-one (**3c**).* This compound was prepared following the same procedure described above for the synthesis of **2c**, and using a residue of the imine **3a** (from 200 mg, 0.65 mmol of amide **3**) in dry toluene (10 mL), and treated with 2,2,6-trimethyl-4H-1,3-dioxin-4-one (0.18 mL, 1.30 mmol) and Et_3N (0.18 mL). The reaction mixture was refluxed under nitrogen atmosphere for 2.5 h and then cooled to room temperature. Purification by column chromatography (CH_2Cl_2–MeOH, 95:5) gave **3c** (80 mg, 33% from amide **3**). IR (cm^{-1}): 2933, 1698, 1515, 1373, 1324, 1212; ^{1}H NMR (500 MHz, $CDCl_3$): δ = 7.18 (m, 3H, CH-3′, CH-4′, CH-5′), 7.83 (m, 2H, CH-2′, CH-6′), 6.70 (s, 1H, H-11), 6.54 (s, 1H, H-8), 5.36 (s, 1H, H-3), 4.16 (m, 1H, H-6α), 3.86 (OCH_3-9), 3.75 (OCH_3-10), 3.53 (m, 2H, CH_2Ph), 2.87 (m, 1H, H-6β), 2.72 (m, 1H, H-7α), 2.35 (m, 1H, H-7β), 2.04 (s, 3H, CH_3); ^{13}C NMR (125 MHz, $CDCl_3$): δ = 163.1 (CO), 162.2 (C-2), 149.2 (C-9), 147.4 (C-10), 134.6 (C-1′), 130.9 (CH-2′, CH-6′), 128.0 (CH-3′, CH-5′), 127.8 (C-7a), 127.0 (CH-4′), 126.3 (C-11a), 110.4 (CH-11), 109.7 (CH-8), 99.1 (CH-3), 91.8 (C-11b), 55.9 (OCH_3-9), 55.8 (OCH_3-10), 42.7 (CH_2Ph), 37.2 (CH_2-6), 27.2 (CH_2-7), 19.8 (CH_3); ESMS *m/z* (%) 366 (100) $[M + H]^+$.

4.2. Biological assays

NADH and other biochemical reagents were purchased from Sigma–Aldrich Chemical Co. Stock solutions (30 mM in absolute EtOH) of target compounds were prepared and kept in the dark at −20 °C. Appropriate dilutions (10–30 mM) were made before the experiments. Inverted submitochondrial particles (SMP) from beef heart were obtained following Fato's method [39] by extensive ultrasonic disruption of frozen-thawed mitochondria to produce open membrane fragments where permeability barriers to substrates were lost, and they were stored at −70 °C at 28 mg/mL (protein measured by the Bradford method). The beef heart SMP were transferred to glass test tubes, diluted to 0.5 mg/mL in 250 mM sucrose and 10 mM Tris–HCl buffer, pH 7.4, and treated with 300 μM NADH to activate complex I before starting the experiments. Aliquots of the stocks solutions (1 μL) were added successively to 500 μL of the SMP preparations with 5 min of incubation on ice after each addition (ethanol never exceeded 2% of the total volume). After incubation, aliquots of the treated SMP (25 μL) were diluted to 6 μg/mL in 50 mM potassium phosphate buffer (pH 7.4) and 1 mM EDTA, in a cuvette at 22 °C, always in the presence of 75 μM NADH. Immediately, NADH oxidase activity was measured as the aerobic oxidation of NADH. Reaction rates were calculated for each inhibitor (at increasing concentrations) from the linear decrease of NADH concentration (λ = 340 nm, ε = 6.22 mM^{-1} cm^{-1}) measured in an end-window photomultiplier spectrophotometer ATI-Unicam UV4-500. The inhibitory concentration (IC_{50}) was taken as the final compound concentration in the assay cuvette that yielded 50% inhibition of the NADH oxidase activity. Data from individual titrations were used to assess the means and standard deviations of three independent assays for each compound.

Acknowledgments

This study was supported by grants SAF2011-23777, Spanish Ministry of Economy and Competitiveness, RIER RD08/0075/0016,

Carlos III Health Institute, Spanish Ministry of Health and the European Regional Development Fund (FEDER). A. Galán was the recipient of a fellowship from FPU program of Spanish Ministry of Education, Culture and Sport.

Appendix A. Supplementary data

Supplementary data related to this article can be found at http://dx.doi.org/10.1016/j.ejmech.2013.08.013.

References

[1] K.W. Bentley, β-Phenylethylamines and the isoquinoline alkaloids, Nat. Prod. Rep. 22 (2005) 249–268.
[2] S.S. Kulkarni, S. Singh, J.R. Shah, W.-K. Low, T.T. Talele, Synthesis and SAR optimization of quinazolin-4(3H)-ones as poly(ADP-ribose)polymerase-1 inhibitors, Eur. J. Med. Chem. 50 (2012) 264–273.
[3] O.P.J. van Lindena, C. Farenc, W.H. Zoutmanc, L. Hameetmanc, M. Wijtmans, R. Leurs, C.P. Tensenc, G. Siegal, I.J.P. de Escha, Fragment based lead discovery of small molecule inhibitors for the EPHA4 receptor tyrosine kinase, Eur. J. Med. Chem. 47 (2012) 493–500.
[4] R.J. Juszczak, J.H. Russell, Inhibition of cytotoxic T lymphocyte-mediated lysis and cellular proliferation by isoquinoline sulfonamide protein kinase inhibitors. Evidence for the involvement of protein kinase C in lymphocyte function, J. Biol. Chem. 264 (1989) 810–815.
[5] A. Bermejo, P. Protais, M.A. Blázquez, K.S. Rao, M.C. Zafra-Polo, D. Cortes, Dopaminergic isoquinoline alkaloids from roots of *Xylopia papuana*, Nat. Prod. Lett. 6 (1995) 57–62.
[6] I. Berenguer, N. El Aouad, S. Andujar, V. Romero, F. Suvire, T. Freret, A. Bermejo, M.D. Ivorra, R.D. Enriz, M. Boulouard, N. Cabedo, D. Cortes, Tetrahydroisoquinolines as dopaminergic ligands: 1-butyl-7-chloro-6-hydroxy-tetrahydroisoquinoline, a new compound with antidepressant-like activity in mice, Bioorg. Med. Chem. 17 (2009) 4968–4975.
[7] N. El Aouad, I. Berenguer, V. Romero, P. Marín, A. Serrano, S. Andujar, F. Suvire, A. Bermejo, M.D. Ivorra, R.D. Enriz, N. Cabedo, D. Cortes, Structure-activity relationship of dopaminergic halogenated 1-benzyl-tetrahydroisoquinoline derivatives, Eur. J. Med. Chem. 44 (2009) 4616–4621.
[8] N. Cabedo, I. Berenguer, B. Figadère, D. Cortes, An overview on benzylisoquinoline derivatives with dopaminergic and serotonergic activities, Curr. Med. Chem. 16 (2009) 2441–2467.
[9] S. Andujar, F. Suvire, I. Berenguer, N. Cabedo, P. Marín, L. Moreno, M.D. Ivorra, D. Cortes, R.D. Enriz, Tetrahydroisoquinolines acting as dopaminergic ligands. A molecular modeling study using MD simulations and QM calculations, J. Mol. Model. 18 (2012) 419–431.
[10] A. Bermejo, B. Figadere, M.C. Zafra-Polo, I. Barrachina, E. Estornell, D. Cortes, Acetogenins from annonaceae. Recent progress in isolation, synthesis, and mechanisms of action, Nat. Prod. Rep. 22 (2005) 269–303.
[11] S. Granell, I. Andreu, D. Marti, A. Cave, R. Aragon, E. Estornell, D. Cortes, M.C. Zafra-Polo, Bisbenzyltetrahydroisoquinolines, a new class of inhibitors of the mitochondrial respiratory chain complex I, Planta Med. 70 (2004) 266–268.
[12] I. Andreu, N. Cabedo, J.R. Tormo, A. Bermejo, R. Mello, D. Cortes, Synthesis of *N*-diisopropyl phosphoryl benzyltetrahydroisoquinoline, a new class of mitochondrial complexes I and III inhibitors, Bioorg. Med. Chem. Lett. 10 (2000) 1491–1494.
[13] D. Trachootham, W. Lu, M.A. Ogasawara, N. Rivera-del Valle, P. Huang, Redox regulation of cell survival, Antioxid. Redox Signal. 10 (2008) 1343–1374.
[14] T.M. Dawson, V.L. Dawson, Molecular pathways of neurodegeneration in Parkinson's disease, Science 302 (2003) 819–822.
[15] R.S. Balaban, S. Nemoto, T. Finkel, Mitochondria, oxidants, and aging, Cell 120 (2005) 483–495.
[16] H. Pelicano, L. Feng, Y. Zhou, J.S. Carew, E.O. Hileman, W. Plunkett, M.J. Keating, P. Huang, Inhibition of mitochondrial respiration. A novel strategy to enhance drug-induced apoptosis in human leukemia cells by a reactive oxygen species-mediated mechanism, J. Biol. Chem. 278 (2003) 37832–37839.
[17] A. Szewczyk, L. Wojtczak, Mitochondria as a pharmacological target, Pharmacol. Rev. 54 (2002) 101–127.
[18] V. Gogvadze, S. Orrenius, B. Zhivotovsky, Mitochondria in cancer cells, what is so special about them? Trends Cell Biol. 18 (2008) 165–173.
[19] F. Schuler, J.E. Casida, The insecticide target in the PSST subunit of complex I, Pest. Manag. Sci. 57 (2001) 932–940.
[20] R. Baradaran, J.M. Berrisford, G.S. Minhas, L.A. Sazanov, Crystal structure of the entire respiratory complex I, Nature 494 (2013) 443–448.
[21] G. Memetzidis, J. Stambach, L. Jung, C. Schott, C. Heitz, J.C. Stocklet, Structure-affinity relationships of berbines or 5,6,13,13a-tetrahydro-8H-dibenzo[*a*,*g*]quinolizines at α-adrenoceptors, Eur. J. Med. Chem. 26 (1991) 605–611.
[22] C. Szantay, L. Toke, P. Kolonits, Synthesis of protoemetine. A new total synthesis of emetine, J. Org. Chem. 31 (1966) 1447–1451.
[23] N. Kogure, C. Nishiya, M. Kitajima, H. Takayama, Six new indole alkaloids from *Gelsemium sempervirens* Ait. f. Tetrahedron Lett. 46 (2005) 5857–5861.
[24] Y. Kanintronkul, R. Worayuthakarn, N. Thasana, P. Winayanuwattikun, K. Pattanapanyasat, R. Surarit, S. Ruchirawat, J. Svasti, Overcoming multidrug resistance in human lung cancer with novel benzo[*a*]quinolizin-4-ones, Anticancer Res. 31 (2011) 921–927.
[25] W. Du, Towards new anticancer drugs: a decade of advances in synthesis of camptothecins and related alkaloids, Tetrahedron 59 (2003) 8649–8687.
[26] S.U. Saraf, The chemistry of the benzo(*a*)- and benzo(*c*)quinolizinium ions, Heterocycles 16 (1981) 803–841.
[27] S. Kirschbaum, H. Waldeman, Construction of the tricyclic benzoquinolizine ring system by combination of a tandem Mannich-Michael reaction with a Heck reaction, Tetrahedron Lett. 38 (1997) 2829–2832.
[28] S. Kirschbaum, H. Waldeman, Three-step access to the tricyclic benzo[a]quinolizine ring system, J. Org. Chem. 63 (1998) 4936–4946.
[29] M. Strandtmann, M.P. Cohen, J. Shravel, A new general synthesis of benzo[a] quinolizines, dibenzo[a, f]quinolizines, and related compounds, J. Org. Chem. 31 (1966) 797–802.
[30] M. Rubiralta, A. Diez, A. Balet, J. Bosch, New synthesis of benzo[*a*]quinolizidin-2-ones via protected 2-aryl-4-piperidones, Tetrahedron 43 (1987) 3021–3030.
[31] A. Roy, S. Nandi, H. Ila, H. Junjappa, An expedient route to 2,3-substituted and fused benzo[*a*]quinolizine-4-thione framework via ring annulation with β-oxodithioesters, J. Org. Lett. 3 (2001) 229–232.
[32] C.J. Stearman, M. Wilson, A. Padwa, Conjugate addition-dipolar cycloaddition cascade for the synthesis of benzo[a]quinolizine and indolo[*a*]quinolizine scaffolds: application to the total synthesis of (±)-yohimbenone, J. Org. Chem. 74 (2009) 3491–3499.
[33] M. Presset, Y. Coquerel, J. Rodriguez, Microwave-assisted domino and multicomponent reactions with cyclic acylketenes: expeditious syntheses of oxazinones and oxazindiones, Org. Lett. 11 (2009) 5706–5709.
[34] N. Pemberton, L. Jakobsson, F. Almqvist, Synthesis of multi ring-fused 2-pyridones via an acyl-ketene imine cyclocondensation, Org. Lett. 8 (2006) 935–938.
[35] M.R. Pitts, J.R. Harrison, C.J. Moody, Indium metal as a reducing agent in organic synthesis, J. Chem. Soc. Perkin Trans. 1 (2001) 955–977.
[36] M. Lafrance, N. Blaquière, K. Fagnou, Direct intramolecular arylation of unactivated arenes: application to the synthesis of aporphine alkaloids, Chem. Commun. 24 (2004) 2874–2875.
[37] M. Ariza, A. Díaz, R. Suau, M. Valpuesta, Synthesis of new dopamine D1 antagonist SCH 23390 analogues by the stereoselective Stevens rearrangement, Eur. J. Org. Chem. (2011) 6507–6518.
[38] P.A. Peixoto, A. Boulangé, S. Leleu, X. Franck, Versatile synthesis of acylfuranones by reaction of acylketenes with α-hydroxy ketones: application to the one-step multicomponent synthesis of cadiolide B and its analogues, Eur. J. Org. Chem. (2013) 3316–3327.
[39] R. Fato, E. Estornell, S. Bernando, F. Palloti, G. Parenti-Castelli, G. Lenaz, Steady-state kinetics of the reduction of coenzyme Q analogs by complex I (NADH:ubiquinone oxidoreductase) in bovine heart mitochondria and submitochondrial particles, Biochemistry 35 (1996) 2705–2716.
[40] M.P. López-Gresa, M.C. González, J. Primo, P. Moya, V. Romero, E. Estornell, Circumdatin H, a new inhibitor of mitochondrial NADH oxidase from *Aspergillus ochraceous*, J. Antibiot. 58 (2005) 416–419.
[41] A. Bermejo, J.R. Tormo, N. Cabedo, E. Estornell, B. Figadère, D. Cortes, Enantiospecific semisynthesis of (+)-almuheptolide-A, a novel natural heptolide inhibitor of the mammalian mitochondrial respiratory chain, J. Med. Chem. 41 (1998) 5158–5166.
[42] M. Degli Esposti, A. Ngo, A. Ghelli, B. Benelli, V. Carelli, H. McLennan, A.W. Linnane, The interaction of Q analogs, particularly hydroxydecyl benzoquinone (idebenone), with the respiratory complexes of heart mitochondria, Arch. Biochem. Biophys. 330 (1996) 395–400.

Bioorganic & Medicinal Chemistry 20 (2012) 6589–6597

Contents lists available at SciVerse ScienceDirect

Bioorganic & Medicinal Chemistry

journal homepage: www.elsevier.com/locate/bmc

Synthesis of new antimicrobial pyrrolo[2,1-*a*]isoquinolin-3-ones

Laura Moreno [a], Javier Párraga [a], Abraham Galán [a], Nuria Cabedo [b], Jaime Primo [b], Diego Cortes [a,*]

[a] Departamento de Farmacología, Facultad de Farmacia, Universidad de Valencia, 46100 Burjassot, Valencia, Spain
[b] Centro de Ecología Química Agrícola-Instituto Agroforestal Mediterraneo, UPV, Campus de Vera, Edificio 6C, 46022 Valencia, Spain

ARTICLE INFO

Article history:
Received 21 April 2012
Revised 13 September 2012
Accepted 15 September 2012
Available online 24 September 2012

Keywords:
Pyrrolo[2,1-*a*]isoquinolin-3-ones
Bischler-Napieralski cyclodehydration
Bactericide
Fungicide

ABSTRACT

The attractive structure of the pyrroloisoquinoline moiety, together with its potential antimicrobial activity, encouraged us to prepare six 8-substituted and seven 8,9-disubstituted-1,2,3,5,6,10b-hexahydropyrrolo[2,1-*a*]isoquinolin-3-ones in a few steps with good yields. We applied a convenient methodology via double intramolecular cyclization conducted by a Bischler-Napieralski cyclodehydration-imine reduction sequence, which is widely employed in the synthesis of isoquinoline alkaloids. Therefore, we synthesized three series of these pyrrolo[2,1-*a*]isoquinolin-3-ones characterized by the substituent at the 8-position or 8,9-positions of the aromatic ring: (a) different side chains are attached to an 8-OH group (series 1); (b) a chlorine atom is attached to the 8-position (series 2); and (c) 8- and 9-carbons are bearing an identical group (series 3). The compounds bearing a benzylic moiety at the 8-position, for example, 8-benzyloxy-pyrrolo[2,1-*a*]isoquinolin-3-one (**1a**) and 8-(4-fluorobenzyloxy)-pyrrolo[2,1-*a*]isoquinolin-3-one (**1e**), as well as, a 8-chloro-9-methoxy moiety including the 8-chloro-9-methoxy-pyrrolo[2,1-*a*]isoquinolin-3-one (**2a**), provided the most fungicide and bactericide agents, respectively.

1. Introduction

Isoquinoline alkaloids are a large family of natural products with a variety of powerful biological activities,[1] including inhibition of cellular proliferation.[2] Within the isoquinoline family, pyrroloisoquinoline alkaloids have been paid considerable attention in recent years because they display interesting biological activities such as antidepressant,[3] muscarinic agonist,[4] antiplatelet[5] and antitumor activity.[6] In 1968, the first natural pyrroloisoquinoline alkaloids were isolated from the peyote cactus and were identified as peyoglutam and mescalotam.[7] Since then, the pyrrolo[2,1-*a*]isoquinoline ring system is the main core of a wide variety of biologically active alkaloids, including antitumor crispine A, isolated from *Carduus crispus*,[8] tetracyclic compounds such as antiglycemic jamtine, isolated from the climbing shrub *Cocculus hirsutus*,[9] and erythrina type alkaloids with curare-like neuromuscular blocking activities.[10,11] In 1984, a tetracyclic framework bearing a pyrroloisoquinoline lactam was found in nuevamine[12] which displayed anti-inflammatory, antimicrobial, anti-leukemic and antitumor properties.[13] In 2004, tricyclic lactam trolline was isolated from *Trollius chinensis*. This alkaloid exhibited in vitro significant antibacterial activity against some strains of *Klebsiella pneumoniae*, *Pseudomonas aeruginosa*, *Haemophilus influenza*, *Staphylococcus aureus*, *Streptococcus pneumonia*, *S. pyogenes*, and moderate antiviral activity against influenza viruses A and B.[14]

Actually, pyrrolo[2,1-*a*]isoquinolines were synthesized long before they were isolated as natural products, and were incorporated into larger ring systems; for example, in the lamellarins skeleton.[15] Nevertheless, given their attractive biological activities, the synthesis of new compounds bearing this structural framework has greatly increased in recent years.[16] One representative synthetic strategy involves the annulation of the pyrrole ring by intramolecular reaction of a 1,3-difunctionalized three-carbon building block with a 3,4-dihydroisoquinoline.[17–19] Other strategies proceed principally via phenethyl succinimides, in which a *N*-acyliminium ion undergoes different types of intramolecular aromatic π-cyclization reactions to provide the C10a–C10b bond formation. In this case, some broadly used approaches involve: (1) tandem carbophilic addition of the organolithium reagent-*N*-acyliminium ion cyclization sequence to obtain the isoquinolone skeleton;[20] (2) application of Parham-type cyclization to halogenated imides, giving the corresponding enamides;[21,22] and (3) the Pummerer/Mannich induced cyclization cascade, which involves a thionium-*N*-acyliminium ion cyclization to give the azabicyclic ring system.[23]

Our research group is focusing since a long time on isolating and synthesizing isoquinoline-containing compounds to obtain a variety of chemically diverse structures with dopaminergic activity.[24–28] However, the discovery of new antimicrobial agents in the last few years has become a need since some microorganisms develop resistance to classic drugs due to their extensive use. As mentioned above, previous works have shown the antimicrobial properties of pyrroloisoquinolines, including the nuevamine-type and trolline-type alkaloids.[13,14] The attractive structure of the

* Corresponding author.
E-mail address: dcortes@uv.es (D. Cortes).

0968-0896/$ - see front matter © 2012 Elsevier Ltd. All rights reserved.
http://dx.doi.org/10.1016/j.bmc.2012.09.033

pyrroloisoquinoline moiety, together with its potential antimicrobial activity, encouraged us to synthesize trolline analogs containing a lactam-ring pharmacophore similar to antibiotic β-lactams. Although several methods have been portrayed for the synthesis of this framework, we applied a typical methodology that we widely employed in the course of our research into isoquinoline synthesis. It is based on double intramolecular cyclization, conducted by Bischler-Napieralski cyclodehydration from an ester β-phenylethylamide and involves the subsequent reduction of the imine intermediate. Therefore, we prepared six 8-substituted and seven 8,9-disubstituted-1,2,3,5,6,10b-hexahydropyrrolo[2,1-*a*]isoquinolin-3-ones, including the known alkaloid (±)-trolline, in a few steps with good yields for the purpose of exploring their antimicrobial activities. Specifically, we followed the same approach to synthesize three series of these pyrrolo[2,1-*a*]isoquinolinones characterized by the substituent at the 8-position of the aromatic ring. In these series: (a) different side chains are attached to an 8-OH group (series 1); (b) a chlorine atom is attached to the 8-position (series 2); and (c) 8- and 9-carbons are bearing an identical group (series 3). The biological results of these thirteen compounds have enabled us to draw conclusions on these groups' influence on antimicrobial activity.

2. Results and discussion

2.1. Chemistry

The general synthetic plan for these compounds focused on preparing the appropriate β-phenyl acetamides (**1**–**3**) by standard methods[25,26] to be cyclized by Bischler-Napieralski cyclodehydration. Firstly, these were prepared by starting with benzaldehyde derivatives: 3-hydroxybenzaldehyde (series 1, Scheme 1) and 3-chloro-4-methoxy-benzaldehyde (series 2, Scheme 2); and from the 3,4-dimethoxy-β-phenyl-ethylamine (series 3, Scheme 3). Therefore, by commencing with these benzaldehydes, and by a successive nitromethane-reduction sequence, β-phenylethylamine intermediates were obtained and then condensed with the ethyl succinyl chloride under Shotten-Bauman conditions to give the β-(3-benzyloxy-phenyl)acetamide (**1**), β-(3-chloro-4-methoxy-phenyl)acetamide (**2**) and β-(3,4-dimethoxy-phenyl)-acetamide (**3**), as outlined in Schemes 1–3, respectively. These amides **1**–**3** were treated with a $POCl_3$ reagent to lead us to the expected dihydroisoquinolines by Bischler-Napieralski cyclization. The obtained imine was reduced with $NaBH_4$ to give the tetrahydroisoquinoline skeleton and, simultaneously, the formed nucleophilic amine quickly attacked the carbonyl ester leading to C ring closure by a second intramolecular cyclization to give 8-benzyloxy-1,2,3,5,6,10b-hexahydropyrrolo[2,1-*a*]isoquinolin-3-one (**1a**), 8-chloro-9-methoxy-1,2,3,5,6,10b-hexahydropyrrolo[2,1-*a*]isoquinolin-3-one (**2a**) and 8,9-dimethoxy-1,2,3,5,6,10b-hexahydropyrrolo[2,1-*a*]isoquinolin-3-one (**3a**) for series 1–3, respectively. In order to obtain different substitutions at the 8 and 9-positions to explore their influence on antimicrobial activity, the benzylic and the methoxy groups of **1a** (series 1) and **2a** (series 2) were deprotected under acid medium to give 8-hydroxy-1,2,3,5,6,10b-hexahydropyrrolo[2,1-*a*]isoquinolin-3-one (**1b**), and by BBr_3 to obtain 8-chloro-9-hydroxy-1,2,3,5,6,10b-hexahydropyrrolo[2,1-*a*]isoquinolin-3-one (**2b**) (Schemes 1 and 2). In addition, those substituents that seemed to enhance the antimicrobial activity were placed in both 8 and 9-positions on the aromatic A-ring (series 3), also by previous deprotection of **3a** by BBr_3 to obtain (±)-trolline (**3b**) (Scheme 3).

Secondly, in series 1, one carbamate and three O-alkylated derivatives were prepared from 8-hydroxy-pyrroloisoquinolone **1b** (Scheme 4) to give: 8-ethylcarbamate- (**1c**), 8-(1-piperidinethoxy)- (**1d**), 8-(4-fluorobenzyloxy)- (**1e**) and 8-phenylacetamide-1,2,3,5,6,10b-hexahydropyrrolo[2,1-*a*]isoquinolin-3-ones (**1f**). In series 2, one carbamate derivative was prepared from 8-chloro-9-hydroxy-pyrroloisoquinolone **2b** to obtain 8-chloro-9-ethylcarbamate-1,2,3,5,6,10b-hexahydropyrrolo[2,1-*a*]isoquinolin-3-one (**2c**) (Scheme 2). In series 3, one 8,9-bis(4-fluorobenzyloxy)- (**3c**) and one 8,9-bis(phenylacetamide)-1,2,3,5,6,10b-hexahydropyrrolo[2,1-*a*]isoquinolin-3-ones (**3d**), were prepared from (±)-trolline (**3b**) (Scheme 3). All the target compounds were synthesized using a short approach with good yields. In addition, and to our knowledge, compounds **1a**–**1f**, **2a**–**2c**, **3c** and **3d** are reported for the first time. Their structures were confirmed by NMR spectral data and MS spectrometry.

2.2. Antimicrobial activity

All the synthesized pyrrolo[2,1-*a*]isoquinolines were assayed in vitro for their ability to inhibit bacterial and fungal growth. In the antimicrobial assays, our compounds were tested against several human pathogenic and economically important phytopathogenic bacteria and/or fungi. The bacterial agents were distributed over Gram(+) and Gram(−) bacteria: *B. cereus*, *S. aureus*, and *E. faecalis* as Gram(+) and *S. typhii*, *E. coli* and *E. carotovora* as Gram(−) (Table 1). The inhibition zones exhibited by compounds **1a**–**1f**, **2a**–**2c** and **3a**–**3c** are summarized in Tables 1 and 2 for

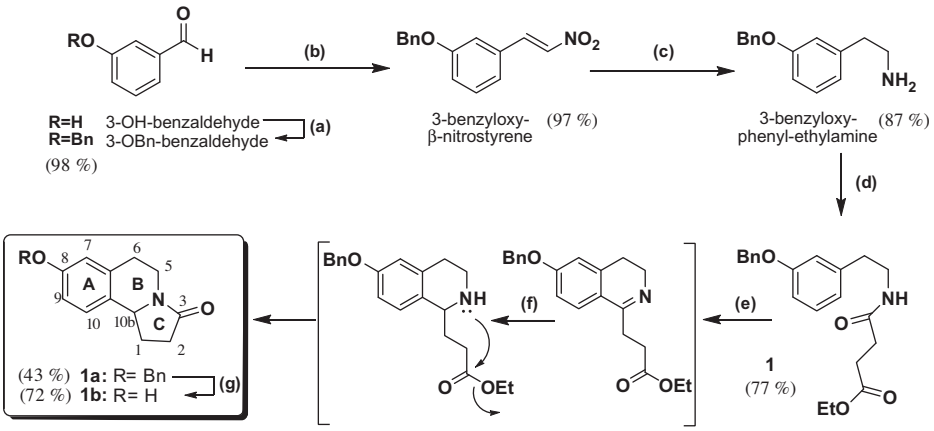

Scheme 1. Synthesis of pyrroloisoquinolin-3-ones **1a,1b** (series 1). Reagents and conditions: (a) Benzyl chloride, K_2CO_3, EtOH, reflux, 6 h; (b) Nitromethane, NH_4OAc, AcOH, reflux, overnight; (c) $LiAlH_4$, THF/Et_2O, N_2, reflux, 2 h; (d) Ethyl succinyl chloride, NaOH 5%, CH_2Cl_2, rt, overnight; **(e)** $POCl_3$, CH_2Cl_2, N_2, reflux, 6 h; (f) $NaBH_4$; MeOH, rt, 2 h; (g) concd HCl–EtOH 1:1, reflux, 3 h.

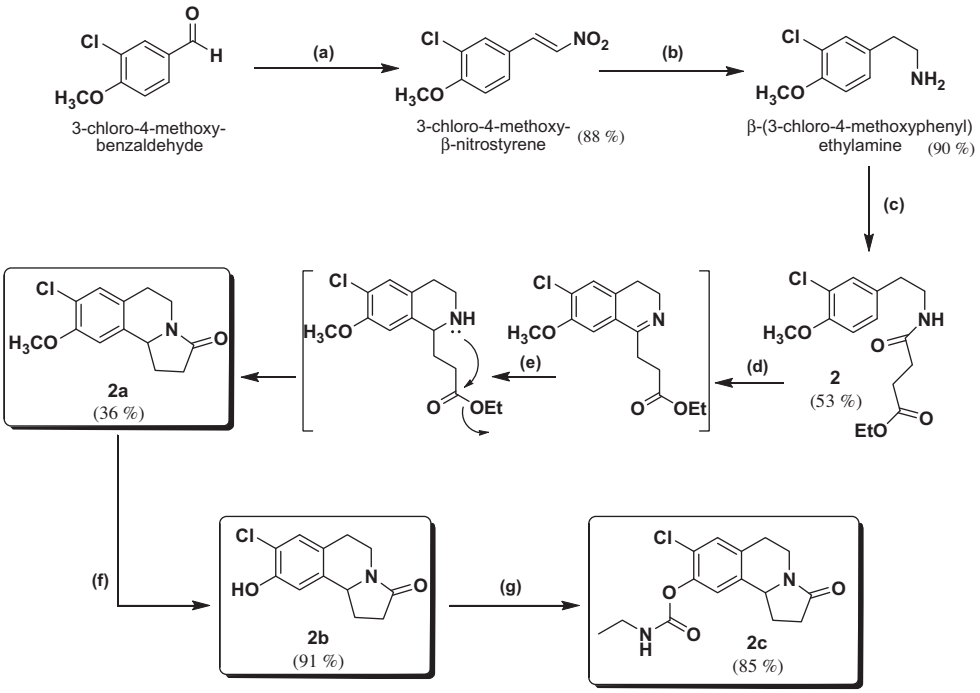

Scheme 2. Synthesis of pyrroloisoquinolin-3-one **2a–2c** (series 2). Reagents and conditions: (a) Nitromethane, NH_4OAc, AcOH, reflux, 6 h; (b) $LiAlH_4$, THF/Et_2O, N_2, reflux, 2 h; (c) Ethyl succinyl chloride, NaOH 5%, CH_2Cl_2, rt, overnight; (d) $POCl_3$, CH_3CN, N_2, reflux, 4 h; (e) $NaBH_4$; MeOH, rt, 2 h; (f) BBr_3, CH_2Cl_2, rt, 2 h; (g) Ethyl isocyanate, acetone, reflux, 3 h.

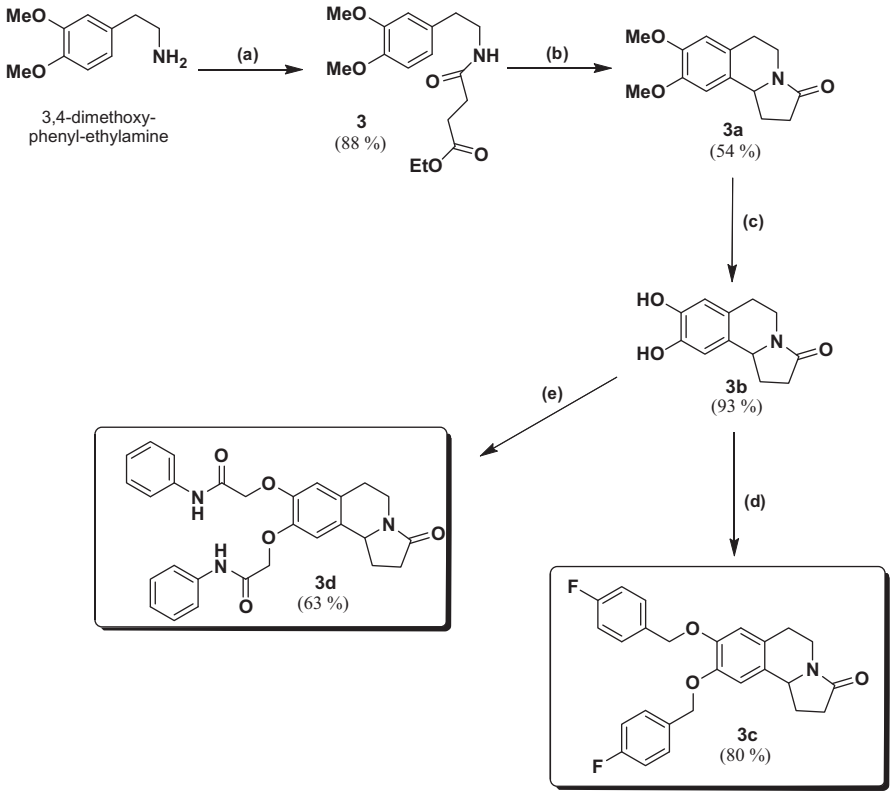

Scheme 3. Synthesis of pyrroloisoquinolin-3-ones **3a–3d** (series 3). Reagents and conditions: (a) Ethyl succinyl chloride, NaOH 5%, CH_2Cl_2, rt, overnight; (b) $POCl_3$, CH_2Cl_2, N_2, reflux, 3 h; and $NaBH_4$; MeOH, rt, 2 h; (c) BBr_3, CH_2Cl_2, rt, 2 h; (d) *p*-fluorobenzyl chloride, K_2CO_3, EtOH, reflux, overnight; (e) 2-bromo-*N*-phenylacetamide, K_2CO_3, EtOH, reflux, 6 h.

bactericidal and antifungal activity, respectively. In general, a lipophilic group at the 8- and/or 9-position seemed to provide moderate activity if compared with a free hydroxyl group such as **1b** and (±)-trolline (**3b**). The introduction of the *O*-benzyl group (**1a**) was adequate for activity, and a halogen atom (**1e**) over the benzyl moiety or even two *p*-fluorobenzyloxy groups (**3c**), did

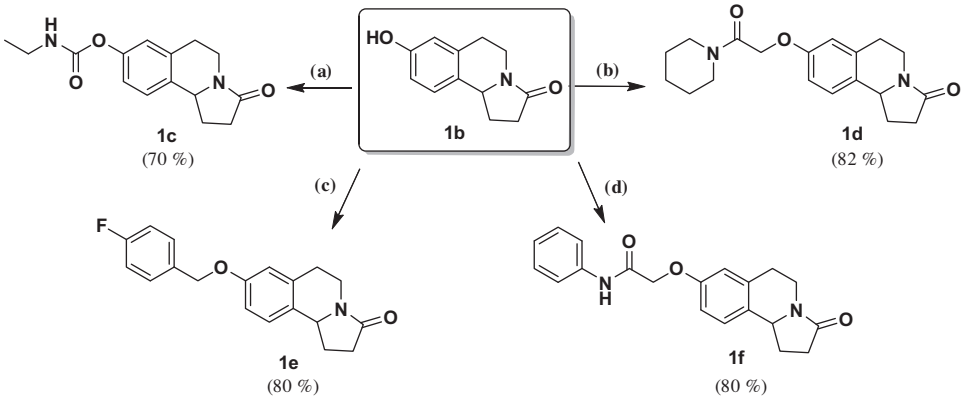

Scheme 4. Synthesis of pyrroloisoquinolin-3-ones **1c–1f**. Reagents and conditions: (a) Ethyl isocyanate, acetone, reflux, 3 h; (b) 2-bromo-1-(piperidin-1-yl)ethanone, K_2CO_3, EtOH, reflux, 6 h; (c) *p*-fluorobenzyl chloride, K_2CO_3, EtOH, reflux, overnight; (d) 2-bromo-N-phenylacetamide, K_2CO_3, EtOH, reflux, 6 h.

Table 1

Strains	Bactericidal activity Inhibition zone (mm) 24 h (means ± SE)[a]								
	1a[b]	**1b**[b]	**2a**[b]	**1c**[b]	**1e**[b]	**1f**[b]	**3b**[b]	**3c**[b]	Tetracycline[b]
B. cereus	8.66 ± 0.20^{A}	7.50 ± 0.35^{B}	7.33 ± 0.41^{BC}	6.50 ± 0.35^{C}	7.50 ± 0.61^{B}	8.83 ± 0.20^{A}	6.66 ± 0.41^{BC}	7.33 ± 0.41^{BC}	24.33 ± 0.41^{D}
S. aureus	0 ± 0	0 ± 0	7.83 ± 0.20^{A}	0 ± 0	6.33 ± 0.20^{B}	0 ± 0	0 ± 0	0 ± 0	27.0 ± 0.71^{C}
E. faecalis	6.83 ± 0.20^{AB}	0 ± 0	6.83 ± 0.20^{AB}	8.50 ± 0.35^{C}	0 ± 0	7.33 ± 0.41^{B}	0 ± 0	6.33 ± 0.20^{A}	26.0 ± 0.71^{D}
S. typhii	6.0 ± 0^{A}	0 ± 0	7.33 ± 0.73^{B}	7.50 ± 0.35^{B}	0 ± 0	7.33 ± 0.20^{B}	0 ± 0	5.83 ± 0.20^{A}	24.33 ± 0.41^{C}
E. coli 405	6.33 ± 0.20^{A}	0 ± 0	6.83 ± 0.20^{AB}	6.83 ± 0.54^{AB}	6.16 ± 0.20^{A}	7.50 ± 0.35^{B}	0 ± 0	6.83 ± 0.20^{AB}	25.66 ± 0.41^{C}
E. carotovora	7.26 ± 0.18^{AB}	0 ± 0	10.33 ± 0.41^{C}	8.83 ± 0.20^{D}	8.0 ± 0.61^{B}	8.0 ± 0.35^{BD}	0 ± 0	7 ± 0^{A}	13.33 ± 0.41^{E}
E. coli 100	0 ± 0	0 ± 0	6.16 ± 0.20^{A}	6.33 ± 0.41A	0 ± 0	0 ± 0	0 ± 0	0 ± 0	25.66 ± 0.41^{B}

[a] Each value represents the average and the standard error of three independent experiments. Within each line, the mean values labeled with the same superscript (A–E) do not present statistically significant differences ($P > 0.05$).

[b] Dose: 0.2 mg/disk. Compounds **1d, 2b, 2c** and **3d** did not show bactericidal activity. Compound **3a** showed bactericidal activity at 0.3 mg/disk for *S. aureus*, *E. faecalis*, *E. coli 405* and *E. carotovora*.

Table 2

Strains	Antifungal activity Inhibition zone (mm) 72 h (means ± SE)[a]				
	1a[b]	**2a**[b]	**1c**[b]	**1e**[b]	Benomyl
A. parasiticus	6.83 ± 0.20^{A}	7.50 ± 0.35^{B}	0 ± 0	7.83 ± 0.20^{B}	$29.33 \pm 0.41^{C,c1}$
T. viride	6.0 ± 0^{A}	0 ± 0	0 ± 0	8.10 ± 0.25^{B}	$29.33 \pm 0.81^{C,c1}$
F. culmorum	12.0 ± 0.71^{A}	7.50 ± 0.35^{B}	0 ± 0	10.50 ± 0.35^{C}	$27.66 \pm 1.08^{D,c2}$
G. candidum	6.16 ± 0.20^{A}	6.33 ± 0.41^{A}	0 ± 0	7.0 ± 0.35^{A}	0 ± 0
P. citrophthora	11.33 ± 0.41^{A}	6.83 ± 0.20^{B}	9.66 ± 0.41^{C}	10.66 ± 0.41^{A}	$44.33 \pm 0.41^{D,c3}$

[a] Each value represents the average and the standard error of three independent experiments. Within each line, the mean values labeled with the same superscript (A–D) do not present statistically significant differences ($P > 0.05$).

[b] Dose: 0.2 mg/disk.

[c1] Dose: 20 μg/disk.

[c2] Dose: 0.2 mg/disk.

[c3] Dose: 30 μg/disk. Compounds **1b**, **1d, 1f** did not show antifungal activity.

not significantly improve it. Moreover, a carbamate bond at the 8-position (**1c**) also provided activity against most of the tested strains but not at 9-position (**2c**) on the aromatic A-ring. A similar effect was observed for **1f** and **3d** with one and two aromatic amide side chains, respectively. However, saturated amide **1d** at 8-position did not display any bactericidal activity. The most noteworthy compound was **2a**, which possessed both a chlorine atom which draws electron density away from the π system and an electron donating methoxyl group at the 8- and 9-position, respectively. This compound displayed bactericidal activity against all the tested strains. However, the presence of two methoxyl groups (**3a**) at 8 and 9-positions was detrimental to the activity of the compound and doses of 0.3 mg/disk were required to get a moderate bactericidal effect. Furthermore, **2a** showed the highest inhibition zone against *S. aureus* and *E. carotovora* among all the tested pyrroloisoquinolines. For this latter microorganism, **2a** possessed a potency that almost fell in the same range as the reference compound (tetracycline), suggesting that it could be a potential alternative bactericidal agent to this ubiquitous plant pathogen with a wide host range. Thus, the presence in **2a** of a chlorine atom and a methoxyl group at the 8-position and the 9-position, respectively, appeared to enhance activity.

Fungicide activity was tested against some phytopathogen fungi strains: *A. parasiticus, T. viridae, F. culmorum, G. candidum* and *P. citrophthora* (Table 2). Compounds **1a**, **2a**, **1c** and **1e** inhibited fungal growth in vitro. Compounds **1d** and **1f**, in which the substitution at the 8-position was an amide side chain, did not display growth inhibition of the selected fungi at 0.2 mg/disk, unlike

the bactericidal test. In series 1, the most active compounds were **1a** and their fluorinated analog **1e**, which showed similar potency. Consequently, it seems that the benzylic moiety located at the 8-position on the pyrroloisoquinoline structure contributed positively to its antifungal properties, even if there was, or was not, a halogen atom. Compound **2a,** which was seen to be the most potent bactericidal agent among the tested pyrroloisoquinolines, had a moderate antifungal effect. Its derivatives **2b** and **2c** did not display any antifungal activity even at 0.4 mg/disk. Surprisingly, other disubstituted series 3 analogous (**3a**–**3d**) also showed no fungicidal effect at the highest dose tested (0.4 mg/disk).

In conclusion, we prepared new eleven 8-substituted pyrrolo[2,1-*a*]isoquinolinones together with the known **3a** and trolline (**3b**) via a double cyclization unleashed by Bischler-Napieralski cyclodehydration and an imine reduction sequence in a few steps with good yields. The SAR studies reveal that the benzylic moiety at the 8-position, as in compounds **1a** (*O*-benzyl group) and **1e** (*O*-*p*-fluoro-benzyl group), and the 8-chloro-9-methoxy substitution as in **2a**, provide the most fungicide and bactericide agents, respectively.

3. Material and methods

3.1. General instrumentation

Melting points were taken on a Cambridge microscope instrument coupled with a Reichert-Jung. EIMS was recorded in a VG Auto Spec Fisons spectrometer instrument (Fisons, Manchester, United Kingdom). ^{1}H NMR and ^{13}C NMR spectra were recorded with $CDCl_3$ as a solvent in a Bruker AC-300, AC-400 or AC-500. Multiplicities of ^{13}C NMR resonances were assigned by DEPT experiments. COSY, HSQC and HMBC correlations were recorded at 400 and 500 MHz (Bruker AC-400 or AC-500). The assignments of all compounds were made by COSY, DEPT, HSQC and HMBC. All the reactions were monitored by analytical TLC with silica gel 60 F_{254} (Merck 5554). Residues were purified by silica gel 60 (40–63 μm, Merck 9385) column chromatography. Solvents and reagents were purchased from commercial sources. Quoted yields are of purified material.

3.2. General procedure for the synthesis of amides (1–3)

3.2.1. 3-Benzyloxy-benzaldehyde

A mixture of 3-hydroxybenzaldehyde (3 g, 24.59 mmol), benzyl chloride (4.1 mL, 35.79 mmol) and anhydrous K_2CO_3 (2.4 g, 17.39 mmol) in absolute EtOH (30 mL) was refluxed for 6 h. Then the reaction mixture was concentrated to dryness, redissolved in 10 mL of CH_2Cl_2 and washed with 5% aqueous NaOH (3 × 10 mL). The organic layer was dried with anhydrous Na_2SO_4 and evaporated to dryness. The residue was purified by silica gel column chromatography (hexane/EtOAc, 8:2) to afford 5.1 g of 3-benzyloxy-benzaldehyde (98%) as a white solid. Mp: 54–56 °C; ^{1}H NMR (300 MHz, $CDCl_3$): δ = 9.85 (s, 1H, CHO), 7.32 (m, 9H, H-2, H-4, H-5, H-6, Ph), 5.11 (s, 2H, OCH_2Ph); ^{13}C NMR (75 MHz, $CDCl_3$) δ 192.5 (CHO), 159.7 (C-3), 138.2 (C-1), 136.7 (C-1′), 130.5 (CH-5), 129.1 (CH-3′, CH-5′), 128.6 (CH-4′), 127.9 (CH-2′, CH-6′), 124.1 (CH-6), 122.6 (CH-4), 113.6 (CH-2), 70.6 (OCH_2Ph); ESMS *m*/*z* (%): 213 (100) $[M+1]^+$.

3.2.2. 3-Benxyloxy-β-nitrostyrene

A mixture of 3-benzyloxy-benzaldehyde (1 g, 4.71 mmol), nitromethane (0.7 mL, 12.89 mmol) and NH_4OAc (0.8 g, 10.41 mmol) in AcOH (12.5 mL) was refluxed overnight. After cooling, the mixture was diluted with water and extracted with CH_2Cl_2 (3 × 10 mL). The organic solution was washed with brine (2 × 10 mL) and water (2 × 10 mL), dried with anhydrous Na_2SO_4 and evaporated to dryness to obtain the 3-benzyloxy-β-nitrostyrene (1.2 g, 97%) as yellow needles, which was used in the following step with no further purification. Mp: 80–83 °C; ^{1}H NMR (300 MHz, $CDCl_3$): δ = 7.88 (d, *J* = 13.8 Hz, 1H, H-β), 7.48 (d, *J* = 13.8 Hz, 1H, H-α), 7.40 (m, 7H, H-2, H-5, Ph), 7.01 (m, 2H, H-4, H-6), 5.11 (s, 2H, OCH_2Ph); ^{13}C NMR (75 MHz, $CDCl_3$) δ = 159.6 (C-3), 139.4 (CH-β), 137.8 (C-1), 136.7 (C-1′), 130.9 (CH-α), 129.1-127.9 (6C, CH-5, CH2′-CH-6′), 122.4 (CH-6), 119.2 (CH-4), 115.5 (CH-2), 70.6 (OCH_2Ph); ESMS *m*/*z* (%): 256 (100) $[M+1]^+$.

3.2.3. 3-Chloro-4-methoxy-β-nitrostyrene

3-Chloro-4-methoxy-benzaldehyde (1.0 g, 5.87 mmol) was submitted to the same conditions depicted above to obtain the 3-chloro-4-methoxy-β-nitrostyrene (1.1 g, 88%) as yellow needles, which was used in the following step with no further purification.[26] Mp: 143–145 °C; ^{1}H NMR (400 MHz, $CDCl_3$): δ = 7.91 (d, *J* = 13.7 Hz, 1H, H-β), 7.59 (d, *J* = 2.2 Hz, 1H, H-2), 7.52 (d, *J* = 13.7 Hz, 1H, H-α), 7.44 (dd, *J* = 8.6, 2.2 Hz, 1H, H-6), 6.97 (d, *J* = 8.6 Hz, 1H, H-5), 3.90 (s, 3H, OCH_3-4); ^{13}C NMR (100 MHz, $CDCl_3$) δ = 158.4 (C-4), 138.4 (CH-β), 136.4 (CH-α), 130.9 (CH-2), 130.1 (CH-6), 124.2 (C-1), 123.7 (C-3), 112.7 (CH-5), 56.8 (OCH_3); MS (EI) *m*/*z* (%): 213.5 (55) $[M]^+$, 185 (100).

3.2.4. β-(3-Benzyloxy-phenyl)ethylamine

A mixture of 3-benzyloxy-β-nitrostyrene (600 mg, 2.35 mmol) in 10 mL of anhydrous THF was added dropwise to a well-stirred suspension of $LiAlH_4$ (0.3 g, 8.7 mmol) in 13 mL of anhydrous Et_2O under nitrogen atmosphere, and was refluxed for 2 h. Then the reaction mixture was cooled and the excess of reagent destroyed by a dropwise addition of H_2O. After a partial evaporation of the filtered portion, the aqueous solution was extracted with CH_2Cl_2 (3 × 10 mL). The organic layers were washed with brine, dried over Na_2SO_4 and the solvent was removed to give the β-(3-benzyloxy-phenyl)ethylamine (465 mg, 87%) as a yellow oil. ^{1}H NMR (300 MHz, $CDCl_3$): δ = 7.20 (m, 6H, H-5, Ph), 6.83 (m, 3H, H-2, H-4, H-6), 5.03 (s, 2H, OCH_2Ph), 2.88 (t, *J* = 13.5 Hz, 2H, CH_2-β), 2.65 (t, *J* = 13.5 Hz, 2H, CH_2-α); ^{13}C NMR (75 MHz, $CDCl_3$): δ = 159.3 (C-3), 140.1 (C-1′), 137.4 (C-1), 130.0 (CH-5), 129.9 (CH-3′, CH-5′), 128.3 (CH-4′), 127.9 (CH-2′, CH-6′), 121.9 (CH-6), 116.0 (CH-2), 112.8 (CH-4), 70.3 (OCH_2Ph), 43.7 (CH_2-β), 40.3 (CH_2-α); ESMS *m*/*z* (%): 228 (100) $[M+1]^+$.

3.2.5. β-(3-Chloro-4-methoxyphenyl)ethylamine

3-Chloro-4-methoxy-β-nitrostyrene (1.0 g, 4.70 mmol) was submitted to the same conditions depicted above to obtain the 2-(3-chloro-4-methoxyphenyl)ethylamine (905 mg, 90%) as a yellow oil. The compound was used in further reaction without purification.[26] ^{1}H NMR (400 MHz, $CDCl_3$): δ = 7.30 (d, *J* = 2.2 Hz, 1H, H-2), 7.20 (dd, *J* = 8.5, 2.2 Hz, 1H, H-6), 6.80 (d, *J* = 8.5 Hz, 1H, H-5), 3.90 (s, 3H, OCH_3-4), 3.10 (m, 2H, H-β), 2.80 (m, 2H, H-α); ^{13}C NMR (100 MHz, $CDCl_3$): δ = 153.8 (C-4), 133.3 (C-1), 130.8 (CH-2), 128.4 (CH-6), 122.6 (C-3), 112.5 (CH-5), 56.5 (OCH_3), 43.8 (CH_2-α), 39.1 (CH_2-β); MS (EI) *m*/*z* (%): 185 (45) $[M]^+$.

3.2.6. Ethyl [β-(3-benzyloxy)phenethylamino]-oxobutanoate (1)

An amount of 0.47 mL of ethyl succinyl chloride (3.31 mmol) was added dropwise at 0 °C to a solution of β-(3-benzyloxy-phenyl)ethylamine (446 mg, 2.12 mmol) in CH_2Cl_2 and 5% aqueous NaOH (4 mL). The reaction was stirred at room temperature overnight to be then extracted with CH_2Cl_2 (3 × 10 mL). The combination of the organic phases was washed with brine (2 × 10 mL) and H_2O (2 × 10 mL), dried over Na_2SO_4 and evaporated to dryness. The residue was purified by silica gel column chromatography (hexane/EtOAc 6:4) to afford 540 mg of amide **1** (77%) as a yellow powder. Mp: 68–71 °C; ^{1}H NMR (500 MHz, $CDCl_3$): δ = 7.22 (m, 6H, H-5, Ph), 6.76 (m, 3H, H-2, H-4, H-6), 5.09 (s, 2H, OCH_2Ph), 4.01 (q, *J* = 7.9 Hz,

2H, $CO_2C\underline{H_2}CH_3$), 3.40 (q, J = 6.3 Hz, 2H, CH_2-α), 2.81 (t, J = 6.3 Hz, 2H, CH_2-β), 2.65 (t, J = 6.5 Hz, 2H, $C\underline{H_2}CO$), 2.37 (t, J = 6.5 Hz, $C\underline{H_2}CONH$), 1.10 (t, J = 7.9 Hz, 3H, $CO_2CH_2C\underline{H_3}$); ^{13}C NMR (125 MHz, $CDCl_3$): δ = 172.9 ($\underline{C}O_2CH_2CH_3$), 171.3 (CONH), 159.0 (C-3), 140.5 (C-1′), 136.9 (C-1), 129.6 (CH-5), 128.5 (CH-3′, CH-5′), 127.9 (CH-4′), 127.4 (CH-2′, CH-6′), 121.3 (CH-6), 115.3 (CH-2), 112.8 (CH-4), 69.8 ($O\underline{CH_2}Ph$), 60.6 ($CO_2\underline{CH_2}CH_3$), 40.5 (CH_2-α), 35.6 (CH_2-β), 31.0 ($\underline{CH_2}CONH$), 29.5 ($\underline{CH_2}CO$), 14.1 ($CO_2CH_2\underline{CH_3}$); ESMS m/z (%): 356 (100) $[M+1]^+$.

3.2.7. Ethyl [β-(3-chloro-4-methoxy)phenethylamino]-oxobutanoate (2)

β-(3-Chloro-4-methoxyphenyl)ethylamine (1 g, 5.39 mmol) was submitted to the same conditions depicted above. The residue was purified by silica gel column chromatography (hexane/EtOAc 5:5) to afford 900 mg of amide **2** (53%) as a yellow powder. Mp: 109–112 °C; ^1H NMR (500 MHz, $CDCl_3$): δ = 7.17 (d, J = 2.1 Hz, 1H, H-2), 7.04 (dd, J = 8.3, 2.1 Hz, 1H, H-6), 6.84 (d, J = 8.3 Hz, 1H, H-5), 4.11 (q, J = 7.9 Hz, 2H, $CO_2C\underline{H_2}CH_3$), 3.85 (s, 3H, OCH_3_4), 3.43 (q, J = 6.3 Hz, 2H, CH_2-α), 2.70 (t, J = 6.3, 2H, CH_2-β), 2.60 (t, J = 6.5 Hz, 2H, $C\underline{H_2}CO$), 2.41 (t, J = 6.5 Hz, $C\underline{H_2}CONH$), 1.22 (t, J = 7.9 Hz, 3H, $CO_2CH_2C\underline{H_3}$); ^{13}C NMR (125 MHz, $CDCl_3$): δ = 173.1 ($\underline{C}O_2CH_2CH_3$), 171.8 (CONH), 153.5 (C-4), 131.9 (C-1), 130.3 (CH-2), 127.8 (CH-6), 122.2 (CH-3), 112.1 (CH-5), 60.7 ($CO_2\underline{CH_2}CH_3$), 56.1 (OCH_3), 40.6 (CH_2-α), 34.3 (CH_2-β), 30.9 ($\underline{CH_2}CONH$), 29.5 ($\underline{CH_2}CO$), 14.0 ($CO_2CH_2\underline{CH_3}$); ESMS m/z (%): 314.5 (100) $[M+1]^+$.

3.2.8. Ethyl [β-(3,4-dimethoxy)phenethylamino]-oxobutanoate (3)

β-(3,4-Dimethoxyphenyl)ethylamine (1 g, 5.52 mmol) was submitted to the same conditions depicted above. The residue was purified by silica gel column chromatography (hexane/EtOAc 5:5) to afford 1.5 g of amide **3** (88%) as a white powder. Mp: 48–51 °C. ^1H NMR (500 MHz, $CDCl_3$): δ = 6.81 (d, J = 2.1 Hz, 1H, H-5), 6.70 (m, 2H, H-2, H-6), 4.11 (q, J = 7.9 Hz, 2H, $CO_2CH_2CH_3$), 3.85 (s, 3H, OCH_3-4), 3.84 (s, 3H, OCH_3-3), 3.43 (q, J = 6.3 Hz, 2H, CH_2-α), 2.70 (t, J = 6.3, 2H, CH_2-β), 2.60 (t, J = 6.5 Hz, 2H, CH_2CO), 2.41 (t, J = 6.5 Hz, CH_2CONH), 1.22 (t, J = 7.9 Hz, 3H, $CO_2CH_2CH_3$); ^{13}C NMR (125 MHz, $CDCl_3$): δ = 173.4 ($CO_2CH_2CH_3$), 171.9 (CONH), 149.4 (C-3), 148.0 (C-4), 131.9 (C-1), 121.1 (CH-6), 112.4 (CH-5), 111.8 (CH-2), 61.0 ($CO_2CH_2CH_3$), 56.2 (2× OCH_3), 41.2 (CH_2-α), 35.6 (CH_2-β), 31.4 (CH_2CONH), 29.8 (CH_2CO), 14.5 ($CO_2CH_2CH_3$); ESMS m/z (%): 310 (100) $[M+1]^+$.

3.3. General procedure for the synthesis of 1,2,3,5,6,10b-pyrrolo[2,1-*a*]isoquinolin-3-ones (1a–3a)

3.3.1. 8-Benzyloxy-1,2,3,5,6,10b-hexahydropyrrolo[2,1-*a*]isoquinolin-3-one (1a)

A solution of ethyl 4-[β-(3-benzyloxyphenyl)ethylamino]-4-oxobutanoate (**1**) (300 mg, 0.84 mmol) in dry CH_2Cl_2 (30 mL) was treated with $POCl_3$ (0.39 mL, 4.20 mmol) and was refluxed for 6 h in a nitrogen atmosphere. The reaction mixture was diluted with H_2O (10 mL) and extracted with CH_2Cl_2 (3 × 10 mL). The organic solution was dried over Na_2SO_4 and evaporated to dryness. The residue was dissolved in MeOH (25 mL) and treated with $NaBH_4$ (400 mg, 10.57 mmol) at room temperature. The reaction mixture was stirred for 2 h. Afterward, H_2O (5 mL) was added and the organic solvent was removed under reduced pressure. The aqueous mixture was made basic and extracted with CH_2Cl_2 (3 × 10 mL), dried over Na_2SO_4 and concentrated. The residue was purified by silica gel column chromatography (toluene/EtOAc/MeOH/Et_3N, 6:3:1:0.1) to obtain 105 mg of the 8-benzyloxy-pyrrolo[2,1-*a*]isoquinolin-3-one **1a** (43%) as a yellow oil. ^1H NMR (500 MHz, $CDCl_3$): δ = 7.36 (m, 5H, Ph), 7.02 (d, J = 8.5 Hz, 1H, H-10), 6.87 (dd, J = 8.5, 2.5 Hz, 1H, H-9), 6.75 (d, J = 2.5 Hz, 1H, H-7), 5.04 (s, 2H, OCH_2Ph), 4.71 (t, J = 8 Hz, 1H, H-10b), 4.23 (ddd, J = 12.4, 5.8, 2.7 Hz, 1H, H-5α), 3.05 (m, 1H, H-5β), 2.91 (m, 1H, H-6α), 2.71 (m, 1H, H-6β), 2.61 (m, 1H, H-1α), 2.54 (m, 1H, H-2α), 2.45 (m, 1H, H-2β), 1.82 (m, 1H, H-1β); ^{13}C NMR (125 MHz, $CDCl_3$): δ = 173.2 (NCO), 157.4 (C-8), 136.7 (C-1′), 134.8 (C-6a), 130.0 (C-10a), 128.5 (CH-3′, CH-5′), 127.9 (CH-4′), 127.3 (CH-2′, CH-6′), 125.8 (CH-10), 114.6 (CH-7), 113.8 (CH-9), 69.9 (OCH_2Ph), 56.3 (CH-10b), 36.8 (CH_2-5), 31.6 (CH_2-2), 28.7 (CH_2-6), 27.5 (CH_2-1); ESMS m/z (%): 293 (100) $[M]^+$.

3.3.2. 8-Chloro-9-methoxy-1,2,3,5,6,10b-hexahydropyrrolo[2,1-*a*]isoquinolin-3-one (2a)

Ethyl β-(3-chloro-4-methoxy-phenethylamino)-4-oxobutanoate (**2**) (100 mg, 0.31 mmol) was submitted to the same conditions depicted above. The residue was purified by silica gel column chromatography (toluene/EtOAc/MeOH/Et_3N, 6:3:1:0.1) to obtain 28 mg of 8-chloro-9-methoxy-pyrrolo[2,1-*a*]isoquinolin-3-one **2a** (36%) as a yellow oil. ^1H NMR (500 MHz, $CDCl_3$): δ = 7.15 (s, 1H, H-7), 6.62 (s, 1H, H-10), 4.72 (t, J = 8.0 Hz, 1H, H-10b), 4.28 (ddd, J = 12.9, 6.2, 2.7 Hz, 1H, H-5α), 3.86 (s, 3H, OCH_3), 2.99 (m, 1H, H-5β), 2.84 (m, 1H, H-6α), 2.68 (m, 1H, H-6β), 2.66 (m, 1H, H-1α), 2.56 (m, 1H, H-2α), 2.48 (m, 1H, H-2β), 1.85 (m, 1H, H-1β); ^{13}C NMR (125 MHz, $CDCl_3$): δ = 173.0 (NCO), 153.6 (C-9), 136.9 (C-10a), 130.5 (CH-7), 127.8 (C-6a), 121.1 (C-8), 108.3 (CH-10), 56.2 (CH-10b), 56.1 (OCH_3), 36.9 (CH_2-5), 31.6 (CH_2-2), 27.5 (CH_2-6), 27.4 (CH_2-1); ESMS m/z (%): 251 (100) $[M]^+$.

3.3.3. 8,9-Dimethoxy-1,2,3,5,6,10b-hexahydropyrrolo[2,1-*a*]isoquinolin-3-one (3a)

Ethyl β-(3,4-dimethoxy-phenethylamino)-4-oxobutanoate (**3**) (1.2 g, 3.88 mmol) was submitted to the same conditions depicted above. The residue was purified by silica gel column chromatography (CH_2Cl_2/MeOH/NN_4OH, 95:5:0.1) to obtain 520 mg of 8, 9-dimethoxy-pyrrolo[2,1-*a*]isoquinolin-3-one **3a** (54%) as a green oil. ^1H NMR (500 MHz, CDCl3): δ = 6.59 (s, 1H, H-7), 6.54 (s, 1H, H-10), 4.70 (t, J = 8.0 Hz, 1H, H-10b), 4.26 (ddd, J = 12.9, 6.2, 2.7 Hz, 1H, H-5α), 3.83 (s, 3H, OCH_3-9), 3.82 (s, 3H, OCH_3-8), 2.99 (m, 1H, H-5β), 2.85 (m, 1H, H-6α), 2.65 (m, 1H, H-6β), 2.60 (m, 1H, H-1α), 2.55 (m, 1H, H-2α), 2.44 (m, 1H, H-2β), 1.80 (m, 1H, H-1β); ^{13}C NMR (125 MHz, CDCl3): δ = 173.1 (NCO), 148.0 (C-8), 147.8 (C-9), 129.2 (C-10a), 125.4 (C-6a), 111.6 (CH-7), 107.6 (CH-10), 56.5 (CH-10b), 55.9 (OCH_3-8), 55.8 (OCH_3-9), 36.9 (CH_2-5), 31.6 (CH_2-2), 27.9 (CH_2-6), 27.6 (CH_2-1); ESMS m/z (%): 247 (100) $[M]^+$.

3.4. General procedure for the synthesis of 1,2,3,5,6,10b-hexahydropyrrolo[2,1-*a*]isoquinolin-3-ones (1b–1f)

3.4.1. 8-Hydroxy-1,2,3,5,6,10b-hexahydropyrrolo[2,1-*a*]isoquinolin-3-one (1b)

8-benzyloxy-1,2,3,5,6,10b-hexahydropyrrolo[2,1-*a*]isoquinolin-3-one (**1a**) (200 mg, 0.68 mmol) was refluxed for 3 h in a mixture of equal volumes of ethanol and concentrated HCl (50 mL). The reaction mixture was evaporated to dryness and the residue purified by silica gel column cromatography (CH_2Cl_2/MeOH 94:6) to give 101 mg of 8-hydroxy-pyrrolo[2,1-*a*]isoquinolin-3-one **1b** (72%) as a white oil. ^1H NMR (500 MHz, $CDCl_3$): δ = 6.76 (d, J = 8.3 Hz, 1H, H-10), 6.53 (dd, J = 8.3, 2.0 Hz, 1H, H-9), 6.42 (d, J = 2.0 Hz, 1H, H-7), 4.56 (t, J = 8 Hz, 1H, H-10b), 3.90 (m, 1H, H-5α), 2.91 (m, 1H, H-5β), 2.67 (m, 1H, H-6α), 2.56 (m, 1H, H-6β), 2.45 (m, 1H, H-1α), 2.37 (m, 1H, H-2α), 2.22 (m, 1H, H-2β), 1.65 (m, 1H, H-1β); ^{13}C NMR (125 MHz, $CDCl_3$): δ = 174.0 (NCO), 155.3 (C-8), 134.2 (C-6a), 128.0 (C-10a), 125.4 (CH-10), 114.7 (CH-7), 113.9 (CH-9), 56.5 (CH-10b), 36.9 (CH_2-5), 31.3 (CH_2-2), 28.1 (CH_2-6), 27.1 (CH_2-1); ESMS m/z (%): 203 (100) $[M]^+$.

3.4.2. 8-Ethylcarbamate-1,2,3,5,6,10b-hexahydropyrrolo[2,1-*a*]isoquinolin-3-one (1c)

A solution of 8-hydroxy-1,2,3,5,6,10b-hexahydropyrrolo[2,1-*a*]-isoquinolin-3-one (**1b**) (35 mg, 0.17 mmol) in dry acetone (10 mL) was treated with ethyl isocyanate (0.34 mmol, 0.03 mL). After refluxing for 3 h, the reaction mixture was concentrated to dryness, redissolved in 10 mL of CH_2Cl_2 and washed with H_2O (3 × 10 mL). The organic layer was dried with anhydrous Na_2SO_4, filtered and evaporated under reduced pressure. The residue was purified through a silica gel column (CH_2Cl_2/MeOH 97:3) to afford 8-ethylcarbamate-pyrrolo[2,1-*a*]isoquinolin-3-one **1c** (34 mg, 70%) as a yellow oil. ^{1}H NMR (500 MHz, $CDCl_3$): δ = 7.09 (d, J = 8.3 Hz, 1H, H-10), 7.00 (dd, J = 8.3, 2.0 Hz, 1H, H-9), 6.91 (d, J = 2.0 Hz, 1H, H-7), 4.71 (t, J = 8.0 Hz, 1H, H-10b), 4.26 (m, 1H, H-5α), 3.30 (m, 2H, $CH_3C\underline{H_2}NHCO$), 3.07 (m, 1H, H-5β), 2.92 (m, 1H, H-6α), 2.77 (m, 1H, H-6β), 2.63 (m, 1H, H-1α), 2.53 (m, 1H, H-2α), 2.45 (m, 1H, H-2β), 1.86 (m, 1H, H-1β), 1.20 (m, 3H, $\underline{CH_3}CH_2NHCO$); ^{13}C NMR (125 MHz, $CDCl_3$): δ = 173.2 (NCO), 154.4 (C-8), 149.6 (NHCO), 134.8 (C-6a), 134.4 (C-10a), 128.7 (CH-10), 125.1 (CH-7), 120.3 (CH-9), 56.5 (CH-10b), 36.8 (CH_2-5), 36.7 ($CH_3\underline{CH_2}NHCO$), 31.3 (CH_2-2), 28.5 (CH_2-6), 27.5 (CH_2-1), 15.0 ($\underline{CH_3}CH_2NHCO$); ESMS m/z (%): 297 (100) $[M+Na]^+$.

3.4.3. 8-(1-Piperidinethoxy)-1,2,3,5,6,10b-hexahydropyrrolo[2,1-*a*]isoquinolin-3-one (1d)

A mixture of 8-hydroxy-1,2,3,5,6,10b-hexahydropyrrolo[2,1-*a*]isoquinolin-3-one (**1b**) (30 mg, 0.14 mmol), 2-bromo-1-(piperidin-1-yl)ethanone (19 mg, 0.14 mmol) and anhydrous K_2CO_3 (19 mg, 0.14 mmol) in absolute EtOH (10 mL) was refluxed for 6 h. Afterward, the reaction mixture was concentrated to dryness, redissolved in 10 mL of CH_2Cl_2 and washed with 5% aqueous NaOH (3 × 10 mL). The organic layer was dried with anhydrous Na_2SO_4, filtered and evaporated to dryness. The residue was purified by silica gel column chromatography (toluene/EtOAc/MeOH/Et_3N, 6:3:1:0.1) to afford 40 mg of 8-(1-piperidinethoxy)-pyrrolo[2,1-*a*]isoquinolin-3-one **1d** (82%) as a green oil. ^{1}H NMR (500 MHz, $CDCl_3$): δ = 7.02 (d, J = 8.5 Hz, 1H, H-10), 6.84 (dd, J = 8.5, 2.6 Hz, 1H, H-9), 6.70 (d, J = 2.6 Hz, 1H, H-7), 4.71 (t, J = 6.7 Hz, 1H, H-10b), 4.65 (s, 2H, $OC\underline{H_2}CO$), 4.23 (m, 1H, H-5α), 3.55 (t, J = 5.3 Hz, 2H, $C\underline{H_2}N$), 3.46 (t, J = 5.3 Hz, 2H, $C\underline{H_2}N$), 3.04 (m, 1H, H-5β), 2.89 (m, 1H, H-6α), 2.73 (m, 1H, H-6β), 2.56 (m, 1H, H-1α), 2.52 (m, 1H, H-2α), 2.44 (m, 1H, H-2β), 1.82 (m, 1H, H-1β), 1.64–1.54 (m, 6H, $(C\underline{H_2})_3N$); ^{13}C NMR (125 MHz, $CDCl_3$): δ = 173.2 (NCO-3), 166.0 ($N\underline{C}OCH_2O$), 156.7 (C-8), 135.0 (C-6a), 130.6 (C-10a), 125.9 (CH-10), 114.5 (CH-7), 113.6 (CH-9), 67.5 ($O\underline{CH_2}CO$), 56.4 (CH-10b), 46.3 and 43.2 (2 × $\underline{CH_2}N$), 36.9 (CH_2-5), 31.7 (CH_2-2), 28.6 (CH_2-6), 27.5 (CH_2-1), 26.4 and 25.4 (2 × $\underline{CH_2}CH_2N$), 24.3 ($\underline{CH_2}(CH_2)_2N$); ESMS m/z (%): 328 (100) $[M]^+$.

3.4.4. 8-(4-Fluorobenzyloxy)-1,2,3,5,6,10a-hexahydropyrrolo[2,1-*a*]isoquinolin-3-one (1e)

A mixture of 8-hydroxy-1,2,3,5,6,10b-hexahydropyrrolo[2,1-*a*]isoquinolin-3-one (**1b**) (20 mg, 0.10 mmol), *p*-fluorobenzyl chloride (0.01 mL) and anhydrous K_2CO_3 (10 mg) in absolute ethanol (10 mL) was refluxed overnight. Afterward, the reaction mixture was concentrated to dryness, redissolved in 10 mL of CH_2Cl_2 and washed with 5% aqueous NaOH (3 × 10 mL). The organic layer was dried with anhydrous Na_2SO_4, filtered and evaporated to dryness under reduced pressure. The residue was purified by silica gel column chromatography (CH_2Cl_2/MeOH 97:3) to afford 25 mg of 8-(4-fluorobenzyloxy)-pyrrolo[2,1-*a*]isoquinolin-3-one **1e** (80%) as a yellow oil. ^{1}H NMR (500 MHz, $CDCl_3$): δ = 7.38 (m, 2H, PhF), 7.07 (m, 3H, PhF, CH-10), 6.86 (dd, J = 8.5, 2.5 Hz, 1H, H-9), 6.74 (d, J = 2.5 Hz, 1H, H-7), 5.00 (s, 2H, $OC\underline{H_2}Ph$), 4.73 (t, J = 7.8 Hz, 1H, H-10b), 4.25 (m, 1H, H-5α), 3.04 (m, 1H, H-5β), 2.91 (m, 1H, H-6α), 2.75 (m, 1H, H-6β), 2.63 (m, 1H, H-1α), 2.56 (m, 1H, H-2α), 2.46 (m, 1H, H-2β), 1.82 (m, 1H, H-1β); ^{13}C NMR (125 MHz, $CDCl_3$): δ = 173.4 (NCO), 162.5 (C-4′, $^1J_{CF}$ = 246 Hz), 157.3 (C-8), 135.0 (C-1′), 132.5 (C-6a), 130.2 (C-10a), 129.3 (2CH, CH-2′, CH-6′), 125.9 (CH-10), 115.5 (2CH, CH-3′, CH-5′, $^2J_{CF}$ = 21.7 Hz), 114.5 (CH-7), 113.9 (CH-9), 69.3 (OCH_2Ph), 56.4 (CH-10b), 36.9 (CH_2-5), 31.7 (CH_2-2), 28.7 (CH_2-6), 27.6 (CH_2-1); ESMS m/z (%): 311 (100) $[M]^+$.

3.4.5. 8-Phenylacetamide-1,2,3,5,6,10a-hexahydropyrrolo[2,1-*a*]isoquinolin-3-one (1f)

A mixture of 8-hydroxy-1,2,3,5,6,10a-hexahydropyrrolo[2,1-*a*]isoquinolin-3-one (**1b**) (30 mg, 0.14 mmol), 2-bromo-*N*-phenylacetamide (29 mg, 0.14 mmol) and anhydrous K_2CO_3 (19 mg, 0.14 mmol) in EtOH (10 mL) was refluxed for 6 h. Then the reaction mixture was concentrated to dryness, redissolved in 10 mL of CH_2Cl_2 and washed with 5% aqueous NaOH (3 × 10 mL). The organic layer was dried with anhydrous Na_2SO_4 and evaporated to dryness. The residue was purified by silica gel column chromatography (toluene/EtOAc/MeOH/Et_3N, 6:3:1:0.1) to afford 40 mg of 8-phenylacetamide-pyrrolo[2,1-*a*]isoquinolin-3-one **1f** (80%) as a yellow oil. ^{1}H NMR (500 MHz, $CDCl_3$): δ = 7.58 (d, 2H, J = 7.6 Hz, H-2′, H-6′), 7.36 (t, 2H, J = 7.5 Hz, H-3′, H-5′), 7.16 (t, 1H, J = 7.5 Hz, H-4′), 7.10 (d, J = 8.5 Hz, 1H, H-10), 6.90 (dd, J = 8.5, 2.5 Hz, 1H, H-9), 6.78 (d, J = 2.5 Hz, 1H, H-7), 4.74 (t, J = 7.9 Hz, 1H, H-10b), 4.60 (s, 2H, $OC\underline{H_2}CO$), 4.28 (ddd, J = 12.9, 6.2, 2.7 Hz, 1H, H-5α), 3.06 (m, 1H, H-5β), 2.93 (m, 1H, H-6α), 2.87 (m, 1H, H-6β), 2.65 (m, 1H, H-1α), 2.57 (m, 1H, H-2α), 2.47 (m, 1H, H-2β), 1.84 (m, 1H, H-1β); ^{13}C NMR (125 MHz, $CDCl_3$): δ = 173.2 ($PhN\underline{C}O$), 166.0 (NCO-3), 155.7 (C-8), 136.7 (C-1′), 135.6 (C-6a), 131.8 (C-10a), 129.1 (2CH, CH-2′, CH-6′), 126.3 (CH-10), 124.9 (CH-4′), 120.1 (2CH, CH-3′, CH-5′), 114.9 (CH-7), 113.7 (CH-9), 67.7 ($O\underline{CH_2}CO$), 56.3 (CH-10b), 36.8 (CH_2-5), 31.7 (CH_2-2), 28.7 (CH_2-6), 27.6 (CH_2-1); ESMS m/z (%): 336 (100) $[M]^+$.

3.5. General procedure for the synthesis of 1,2,3,5,6,10b-hexahydropyrrolo[2,1-*a*]isoquinolin-3-ones (2b and 3b)

3.5.1. 8-Chloro-9-hydroxy-1,2,3,5,6,10b-hexahydropyrrolo[2,1-*a*]isoquinolin-3-one (2b)

8-Chloro-9-methoxy-1,2,3,5,6,10b-hexahydropyrrolo[2,1-*a*]isoquinolin-3-one (**2a**, 0.23 mmol, 60 mg) in dry CH_2Cl_2 was stirred at −78 °C. Then, 0.10 mL of BBr_3 were added under nitrogen atmosphere and the resulting mixture was stirred for 2 h at room temperature. The reaction mixture was evaporated to dryness and purified by silica gel column chromatography (CH_2Cl_2/MeOH 90:10) to afford 50 mg of 8-chloro-9-hydroxy-1,2,3,5,6,10b-hexahydropyrrolo[2,1-*a*]isoquinolin-3-one **2b** (91%) as a colorless oil. ^{1}H NMR (500 MHz, CDCl3): δ = 7.18 (s, 1H, H-7), 6.97 (s, 1H, H-10), 4.48 (t, J = 8.0 Hz, 1H, H-10b), 4.30 (ddd, J = 12.9, 6.2, 2.7 Hz, 1H, H-5α), 2.87 (m, 1H, H-5β), 2.67 (m, 1H, H-6α), 2.51 (m, 1H, H-6β), 2.42 (m, 1H, H-1α), 2.35 (m, 1H, H-2α), 2.31 (m, 1H, H-2β), 1.62 (m, 1H, H-1β); ^{13}C NMR (125 MHz, CDCl3): δ = 172.5 (NCO), 149.3 (C-9), 138.1 (C-10a), 131.3 (CH-7), 130.3 (C-6a), 119.9 (C-8), 113.6 (CH-10), 56.2 (CH-10b), 37.0 (CH_2-5), 31.7 (CH_2-2), 27.5 (CH_2-6), 27.4 (CH_2-1); ESMS m/z (%): 237.5 (100) $[M]^+$.

3.5.2. (±)-Trolline (3b)

8,9-Dimethoxy-1,2,3,5,6,10b-hexahydropyrrolo[2,1-*a*]isoquinolin-3-one (**3a**, 0.80 mmol, 200 mg) in dry CH_2Cl_2 was stirred at −78 °C. Then, 0.25 mL of BBr_3 were added under nitrogen atmosphere and the resulting mixture was stirred for 2 h at room temperature. The reaction mixture was evaporated to dryness and purified by silica gel column chromatography (CH_2Cl_2/MeOH 85:15) to afford 165 mg of 8,9-dihydroxy-1,2,3,5,6,10b-hexahydropyrrolo[2,1-*a*]isoquinolin-3-one **3b** (93%) as a white powder. Mp: 245–247 °C; ^{1}H NMR (500 MHz, CDCl3): δ = 6.99 (s, 1H, H-7),

6.98 (s, 1H, H-10), 4.54 (t, J = 8.0 Hz, 1H, H-10b), 4.32 (ddd, J = 12.9, 6.2, 2.7 Hz, 1H, H-5α), 2.89 (m, 1H, H-5β), 2.74 (m, 1H, H-6α), 2.48 (m, 1H, H-6β), 2.43 (m, 1H, H-2α), 2.35 (m, 1H, H-2β), 2.33 (m, 1H, H-1α) 1.66 (m, 1H, H-1β); ^{13}C NMR (125 MHz, CDCl3): δ = 172.6 (NCO), 146.3 (C-8), 146.1 (C-9), 129.3 (C-10a), 124.7 (C-6a), 118.7 (CH-10), 116.5 (CH-7), 56.4 (CH-10b), 37.4 (CH_2-5), 31.9 (CH_2-2), 28.1 (CH_2-6), 28.0 (CH_2-1); ESMS m/z (%): 219 (100) $[M]^+$.

3.6. General procedure for the synthesis of 9-substituted-1,2,3,5,6,10b-hexahydropyrrolo[2,1-*a*]isoquinolin-3-ones (2c, 3c and 3d)

3.6.1. 8-Chloro-9-ethylcarbamate-1,2,3,5,6,10b-hexahydropyrrolo[2,1-*a*]isoquinoline-3-one (2c)

A solution of 8-chloro-9-hydroxy-1,2,3,5,6,10b-hexahydropyrrolo[2,1-*a*]isoquinolin-3-one **2b** (20 mg, 0.084 mmol) in dry acetone (10 mL) was treated with ethyl isocyanate (0.17 mmol, 0.01 mL). After refluxing for 3 h, the reaction mixture was concentrated to dryness, redissolved in 10 mL of CH_2Cl_2 and washed with H_2O (3 × 10 mL). The organic layer was dried with anhydrous Na_2SO_4, filtered and evaporated under reduced pressure. The residue was purified through a silica gel column (CH_2Cl_2/MeOH 95:5) to afford 8-chloro-9-ethylcarbamate-1,2,3,5,6,10b-hexahydropyrrolo[2,1-*a*]isoquinolin-3-one **2c**. (85%) as a yellow oil. ^{1}H NMR (500 MHz, $CDCl_3$): δ = 7.10 (s, 1H, H-7), 6.78 (s, 1H, H-10), 4.68 (t, J = 8.0 Hz, 1H, H-10b), 4.42 (ddd, J = 12.9, 6.2, 2.7 Hz, 1H, H-5α), 3.72 (m, 2H, CH_3CH_2NHCO), 3.01 (m, 1H, H-5β), 2.83 (m, 1H, H-6α), 2.63 (m, 1H, H-6β), 2.61 (m, 1H, H-1α), 2.55 (m, 1H, H-2α), 2.46 (m, 1H, H-2β), 1.80 (m, 1H, H-1β), 1.20 (m, 3H, CH_3CH_2NHCO); 13C NMR (125 MHz, $CDCl_3$): δ = 173.3 (NCO), 158.5 (C-9), 150.5 (NHCO), 137.4 (C-10a), 130.6 (CH-7), 126.0 (C-6a), 119.3 (C-8), 112.5 (CH-10), 56.5 (CH-10b), 37.4 (CH_3CH_2NHCO), 37.0 (CH_2-5), 31.7 (CH_2-2), 27.4 (CH_2-6), 27.3 (CH_2-1), 15.4 (CH_3CH_2NHCO); ESMS m/z (%): 308.5 (100) $[M]^+$.

3.6.2. 8,9-Bis(4-fluorobenzyloxy)-1,2,3,5,6,10a-hexahydropyrrolo[2,1-*a*]isoquinolin-3-one (3c)

A mixture of 8, 9-dihydroxy-1,2,3,5,6,10b-hexahydropyrrolo[2,1-*a*]isoquinolin-3-one (**3b**) (50 mg, 0.22 mmol), *p*-fluorobenzyl chloride (0.04 mL) and anhydrous K_2CO_3 (40 mg) in absolute ethanol (20 mL) was refluxed overnight. Afterward, the reaction mixture was concentrated to dryness, redissolved in 10 mL of CH_2Cl_2 and washed with 5% aqueous NaOH (3 × 10 mL). The organic layer was dried with anhydrous Na_2SO_4, filtered and evaporated to dryness under reduced pressure. The residue was purified by silica gel column chromatography (CH_2Cl_2/MeOH 97:3) to afford 70 mg of 8-(4-fluorobenzyloxy)-pyrrolo[2,1-*a*]isoquinolin-3-one **1e** (80%) as a yellow oil. ^{1}H NMR (500 MHz, $CDCl_3$): δ = 7.38 (m, 4H, PhF), 7.04 (m, 4H, PhF, CH-10), 6.69 (s, 1H, H-7), 6.64 (s, 1H, H-10), 5.05 (s, 4H, OCH_2Ph), 4.66 (t, J = 7.8 Hz, 1H, H-10b), 4.26 (m, 1H, H-5α), 2.99 (m, 1H, H-5β), 2.84 (m, 1H, H-6α), 2.65 (m, 1H, H-6β), 2.56 (m, 1H, H-1α), 2.51 (m, 1H, H-2α), 2.42 (m, 1H, H-2β), 1.76 (m, 1H, H-1β); ^{13}C NMR (125 MHz, $CDCl_3$): δ = 173.1 (NCO), 163.4 (C-4′, $^1J_{CF}$ = 246 Hz), 161.4 (C-4″, $^1J_{CF}$ = 246 Hz), 147.9 (C-8), 147.7 (C-9), 132.8 (C-1′, C-1″), 130.4 (C-10a), 129.2 (4CH, CH-3′, CH-5′, CH-3″, CH-5″), 126.9 (C-6a), 115.4 (4CH, CH-2′, CH-6′, CH-2″, CH-6″), 115.2 (CH-7), 112.2 (CH-10), 71.2 (OCH_2Ph), 70.7 (OCH_2Ph), 56.4 (CH-10b), 36.9 (CH_2-5), 31.7 (CH_2-2), 28.0 (CH_2-6), 27.5 (CH_2-1); ESMS m/z (%): 435 (100) $[M]^+$.

3.6.3. 8,9-Bis(phenylacetamide)-1,2,3,5,6,10a-hexahydropyrrolo[2,1-*a*]isoquinolin-3-one (3d)

A mixture of 8, 9-dihydroxy-1,2,3,5,6,10b-hexahydropyrrolo[2,1-*a*]isoquinolin-3-one (**3b**) (30 mg, 0.13 mmol), 2-bromo-*N*-phenylacetamide (61 mg, 0.26 mmol) and anhydrous K_2CO_3 (30 mg, 0.22 mmol) in EtOH (10 mL) was refluxed for 6 h. Then the reaction mixture was concentrated to dryness, redissolved in 10 mL of CH_2Cl_2 and washed with 5% aqueous NaOH (3 × 10 mL). The organic layer was dried with anhydrous Na_2SO_4 and evaporated to dryness. The residue was purified by silica gel column chromatography (CH_2Cl_2/MeOH, 98:2) to afford 40 mg of 8,9-bis(phenylacetamide)-1,2,3,5,6,10a-hexahydropyrrolo[2,1-*a*]isoquinolin-3-one **3d** (63%) as a brown oil. ^{1}H NMR (500 MHz, $CDCl_3$): δ = 7.52 (m, 4H, H-2′, H-6′, H-2″, H-6″), 7.26 (m, 4H, H-3′, H-5′, H-3″, H-5″), 7.10 (m, 2H, H-4′, H-4″), 6.75 (s, 1H, H-7), 6.72 (s, 1H, H-10), 4.68 (s, 2H,OCH_2CO), 4.67 (t, J = 7.9 Hz, 1H, H-10b), 4.25 (ddd, J = 12.9, 6.2, 2.7 Hz, 1H, H-5α), 2.98 (m, 1H, H-5β), 2.82 (m, 1H, H-6α), 2.66 (m, 1H, H-6β), 2.62 (m, 1H, H-2α), 2.53 (m, 1H, H-2β), 2.43 (m, 1H, H-1α), 1.74 (m, 1H, H-1β); ^{13}C NMR (125 MHz, $CDCl_3$): δ = 173.0 (NCO-3), 165.9 (PhNCO), 146.9 (C-9), 146.2 (C-8), 136.6 (C-1′), 132.4 (C-10a), 128.9 (C-3′, C-5′, C-3″, C-5″), 124.9 (CH-4′, CH-4″), 128.7 (C-6a), 120.0 (4CH, CH-2′, CH-6′, CH-2″, CH-6″), 115.7 (CH-7), 111.9 (CH-10), 69.6 (OCH_2CO), 56.2 (CH-10b), 36.7 (CH_2-5), 31.6 (CH_2-6), 27.9 (CH_2-2), 27.4 (CH_2-1); ESMS m/z (%): 485 (100) $[M]^+$.

3.7. Pharmacological assays

3.7.1. Target microorganisms

Fungicidal activity was measured against 5 phytopathogens: *Aspergillus parasiticus* (CECT 2681), *Trichoderma* V*iride* (CECT 2423), *Fusarium culmorum* (CCM 172), *Phytophthora citrophthora* (CECT 2353) and *Geotrichum candidum* (CCM 245). Seven different bacterial strains were used to determine bactericidal activity: *Bacillus cereus* (CECT 148), *Staphylococcus aureus* (CECT 86), *Enterococcus faecalis* (CECT 481), *Salmonella typhi* (CECT 409), *Escherichia coli* (CECT 405), *Escherichia coli* (CECT 100) and *Erwinia carotovora* (CECT 225). The strains were provided by the Colección Española de Cultivos Tipo (CECT) or by the Colección de la Cátedra de Microbiología (CMM) of the Biotechnology Department (Universidad Politécnica de Valencia).

3.7.2. Antifungal and antibacterial activities

These assays were determined in triplicate by the paper disk-agar diffusion assay according to Cole.[29] The doses used in the assays were 10, 15 or 20 μg/mm^2 (0.2, 0.3 or 0.4 mg/disk). Fungal strains were seeded in Petri dishes containing PDA culture medium and were incubated for 7 days at 28 °C. Then, a Tween 80 solution (0.05%) in sterile distilled water was used to obtain a suspension containing ~106 conidia/mL. Next 1 mL of this conidia suspension was added to 15 mL of PDA in a Petri dish. After solidification, four Whatman disks (No. 113, 0.5 cm diameter) impregnated with the tested products, at appropriate doses, were added to these Petri dishes. The PDA plates containing disks impregnated with only the solvent used to dissolve the tested compounds were used as negative controls, and the disks with benomyl (methyl-1-[butylcarbamoyl]-2-benzimidazolecarbamate) (Sigma), at different concentrations according to the fungal species assayed, were used as positive controls. Fungicidal activity was determined by measuring the inhibition zone developed around the paper disk, indicating a zone of no growth.

In the bactericidal tests, 24-h cultures of each bacterium, maintained in inclined tubes on solid culture medium, were reactivated with a Nutrient Broth (Difco) and were incubated for 24 h at 28 or 37 °C according to the bacterium. Then, 1 mL of this suspension was inoculated in a Petri plate, and 15 mL of the culture medium Plate Count Agar (Difco) was added. When the medium was completely solidified, five paper disks loaded with the tested products were placed in the dish. These plates were incubated for 24 h in the dark at 28 or 37 °C, according to the bacterium. The plate Count Agar plates containing disks impregnated with only the solvent used to dissolve the tested compounds were used as negative

controls, and a positive control with tetracycline chlorhydrate (0.2 mg/disk) was performed to appraise the level of activities. Bactericidal activity was determined by measuring the halo developed around the paper disk.

3.8. Statistical analysis

Analysis of variance (ANOVA) was performed for the fungicidal and bactericidal data (Tables 1 and 2), and the least significant difference (LSD) test was used to compare means (Statgraphics centurion XVI version).

References and notes

1. Bentley, K. W. *Nat. Prod. Rep.* **2005**, *22*, 249.
2. Juszczak, R. J.; Russell, J. H. *J. Biol. Chem.* **1989**, *264*, 810.
3. Elwan, N. M.; Abdelhadi, H. A.; Abdallah, T. A.; Hassaneen, H. M. *Tetrahedron* **1996**, *52*, 3451.
4. Loesel, W.; Roos O.; Schonorrenberg, G. US Patent 4694085 1987; *Chem. Abstr.* **1988**, *108*, 204513.
5. Kuo, R.-Y.; Wu, C.-C.; Chang, F.-R.; Yeh, J.-L.; Chen, I.-J.; Wu, Y.-C. *Bioorg. Med. Chem. Lett.* **2003**, *13*, 821.
6. Anderson, W. K.; Heider, A. R.; Raju, N.; Yucht, J. A. *J. Med. Chem.* **1988**, *31*, 2097.
7. Kapadia, G. J.; Fales, H. M. *Chem. Commun.* **1968**, 1688.
8. Zhang, Q.; Tu, G.; Zhao, Y.; Cheng, T. *Tetrahedron* **2002**, *58*, 6795.
9. Ahmad, V. U.; Rahman, A.-U.; Rasheed, T.; Rehman, H.-U. *Heterocycles* **1987**, *26*, 1251.
10. Tanaka, H.; Tanaka, T.; Etoh, H.; Goto, S.; Terada, Y. *Heterocycles* **1999**, *51*, 2759.
11. Zhang, F.; Simpkins, N. S.; Blake, A. J. *Org. Biomol. Chem.* **2009**, *7*, 1963–1979.
12. Valencia, E.; Freyer, A. J.; Shamma, M. *Tetrahedron Lett.* **1984**, *25*, 599.
13. Moreau, A.; Couture, A.; Deniau, E.; Grandclaudon, P.; Lebrun, S. *Tetrahedron* **2004**, *60*, 6169.
14. Wang, R. F.; Yang, X. W.; Ma, C. M.; Cai, S. Q.; Li, J. N.; Shoyama, Y. *Heterocycles* **2004**, *63*, 1443.
15. Andersen, R. J.; Faulkner, D. J.; He, C. H.; Van Duyne, G. D.; Clardy, J. *J. Am. Chem. Soc.* **1985**, *107*, 5492.
16. Pässler, U.; Knölker, H.-J. The Pyrrolo[2,1-*a*]isoquinoline Alkaloids In *The Alkaloids: Chemistry and Biology*; Knölker, H.-J., Ed.; Elsevier: San Diego, 2012; Vol. 70, pp 79–151.
17. Shono, T.; Hamaguchi, H.; Sasaki, M.; Fujita, S.; Nagami, K. *J. Org. Chem.* **1983**, *48*, 1621.
18. Knölker, H. J.; Agarwal, S. *Tetrahedron Lett.* **2005**, *46*, 1173.
19. Wu, T. R.; Chong, J. M. *J. Am. Chem. Soc.* **2006**, *128*, 9646.
20. Hiemstra, H.; Speckamp, W. N. Additions to *N*-Acyliminium Ions In *Comprehensive Organic Chemistry*; Trost, B. M., Fleming, I., Eds.; Pergamon Press: Oxford, 1991; Vol. 2, pp 1047–1082.
21. Parham, W. E.; Bradsher, C. K. *Acc. Chem. Res.* **1982**, *15*, 300.
22. Collado, M. I.; Manteca, I.; Sotomayor, N.; Villa, M. J.; Lete, E. *J. Org. Chem.* **1997**, *62*, 2080.
23. Padwa, A.; Henning, R.; Kappe, C. O.; Reger, T. S. *J. Org. Chem.* **1998**, *63*, 1144.
24. Bermejo, A.; Protais, P.; Blázquez, M. A.; Rao, K. S.; Zafra-Polo, M. C.; Cortes, D. *Nat. Prod. Lett.* **1995**, *6*, 57.
25. Berenguer, I.; El Aouad, N.; Andujar, S.; Romero, V.; Suvire, F.; Freret, T.; Bermejo, A.; Ivorra, M. D.; Enriz, R. D.; Boulouard, M.; Cabedo, N.; Cortes, D. *Bioorg. Med. Chem.* **2009**, *17*, 4968.
26. El Aouad, N.; Berenguer, I.; Romero, V.; Marín, P.; Serrano, A.; Andujar, S.; Suvire, F.; Bermejo, A.; Ivorra, M. D.; Enriz, R. D.; Cabedo, N.; Cortes, D. *Eur. J. Med. Chem.* **2009**, *44*, 4616.
27. Cabedo, N.; Berenguer, I.; Figadère, B.; Cortes, D. *Curr. Med. Chem.* **2009**, *16*, 2441.
28. Andujar, S.; Suvire, F.; Berenguer, I.; Cabedo, N.; Marín, P.; Moreno, L.; Ivorra, M. D.; Cortes, D.; Enriz, R. D. *J. Mol. Model.* **2012**, *18*, 419.
29. Cole, M. D. *Biochem. Syst. Ecol.* **1994**, *22*, 837.

Resumen ~ Discusión de los Resultados

Resumen – Discusión de los resultados

En la presente **Tesis Doctoral** se han desarrollado diversas rutas de síntesis para la obtención de alcaloides isoquinoleínicos, con diferentes esqueletos, y de hexahidroindenopiridinas. Además se han realizado sus correspondientes ensayos farmacológicos, sobre distintas dianas biológicas basándonos en los resultados obtenidos previamente con este tipo de alcaloides de síntesis y/o aislados de la naturaleza, y de moléculas estructuralmente similares. Se ha observado, a lo largo de muchos años, que las IQ son uno de los metabolitos secundarios activos (MSA) más abundantes y de mayor interés farmacológico de los aislados en especies de la familia de las Annonáceas. Las azafluorenonas, alcaloides piridínicos presentes también en Annonáceas, y con propiedades antipalúdicas, nos has servido de inspiración para la síntesis de las HHIP.

Los dianas biológicas para las que se ha desarrollado la síntesis de estos nuevos fármacos son:

a)- IQ con afinidad por los Receptores Dopaminérgicos D_1 y D_2.

b)- HHIP con afinidad por los Receptores Melatoninérgicos MT_1 y MT_2.

c)- IQ con actividad antimicrobiana.

d)- IQ con actividad antitumoral.

Así pues, los Artículos que forman parte de la presente Tesis Doctoral se pueden dividir en tres capítulos:

Capítulo 1: Alcaloides Isoquinoleínicos con afinidad por los Receptores Dopaminérgicos - Modelización Molecular sobre Receptores Dopaminérgicos: Artículos 1, 2 y 3.

Capítulo 2: Alcaloides Indenopiridínicos con afinidad por los Receptores Melatoninérgicos: Artículos 4 y 5.

Capítulo 3: Alcaloides Isoquinoleínicos con actividad antimicrobiana y antitumoral: Artículos 6 y 7.

Capítulo 1.

Artículo 1: **"2,3,9- and 2,3,11- Trisubstituted tetrahydroprotoberberines as D_2 dopaminergic ligands "** (En: *European Journal of Medicinal Chemistry*, **2013**, *68*, 150)

La dopamina es un neurotransmisor que tiene una importante función en el sistema nervioso central. Un desorden en el sistema dopaminérgico conduce a la aparición de alteraciones neurológicas y psiquiátricas importantes como la esquizofrenia y/o la enfermedad de Parkinson. Por lo tanto, la investigación en este campo tratará de sintetizar nuevos fármacos que posean una mayor afinidad por los RD D_1 y D_2 y poder paliar este tipo de enfermedades.

Las tetrahidroprotoberberinas (THPB) son compuestos naturales existentes en diferentes especies vegetales, presentes como MSA. Este tipo de alcaloide isoquinoleínico contiene diversas actividades farmacológicas, incluyendo entre ellas la afinidad por los receptores dopaminérgicos (RD). Con el objetivo de mejorar la unión a dichos receptores, se desarrolló una ruta sintética mediante la que se obtuvieron tres series de THPB, obteniendo once moléculas finales a ensayar (**Figura 19**).

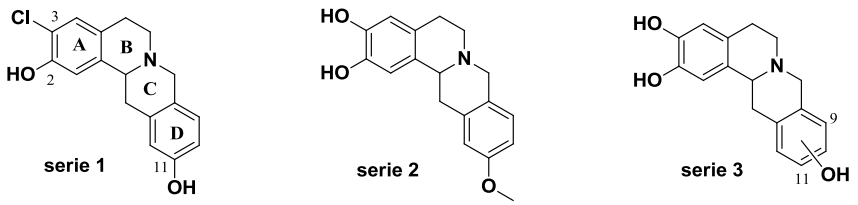

Figura 19. Series de THPB.

Existen diferentes métodos para la obtención de THPB. La ruta sintética que seguimos consta de cinco etapas. La primera es una reacción de Henry, mediante la cual se obtiene el β-nitroestireno. Esta va seguida de una reducción para conseguir la feniletilamina, producto de partida en la siguiente etapa, para dar lugar, reaccionando con el cloruro de ácido adecuado, a la fenilacetamida correspondiente. A continuación, mediante una ciclodeshidratación de Bischler-Napieralski y posterior reducción, la fenilacetamida genera la 1-bencil-THIQ, producto de partida en la ciclación de Mannich mediante la cual se obtiene la THPB de interés.

En este trabajo se ha estudiado la influencia de los sustituyentes sobre los anillos A y D de las THPB sintetizadas, en la afinidad por los RD. Así pues, se observó que la presencia de hidroxilos en el anillo A da lugar a un aumento de la afinidad por los RD D_1 y D_2 con respecto a los análogos que presentan las funciones oxigenadas bloqueadas. La presencia de un átomo de cloro en el anillo A provoca un aumento de la afinidad por los RD D_1, disminuyendo así la selectividad por los RD D_2. Además se observó que la existencia de un grupo metilendioxi en las posiciones 2,3 produce una disminución de la selectividad por RD D_2. En cuanto a los sustituyentes en el anillo D, la presencia de un grupo hidroxilo en posición 9 causa un aumento de la afinidad tanto por el RD D_1 como por el D_2, mientras que un hidroxilo en posición 11 disminuye dicha afinidad (**Figura 20**). Así, podemos destacar entre las 11 moléculas ensayadas **9f** (2,3-OCH_2O-9-OH), **6b** (2,3-diOH-11-MeO) y **9d** (2,3,9-triOH) por presentar mayor afinidad por los RD D_2, siendo esta última (**9d**) la que mostró mayor selectividad (ratio Ki D_1/D_2 de 40.6).

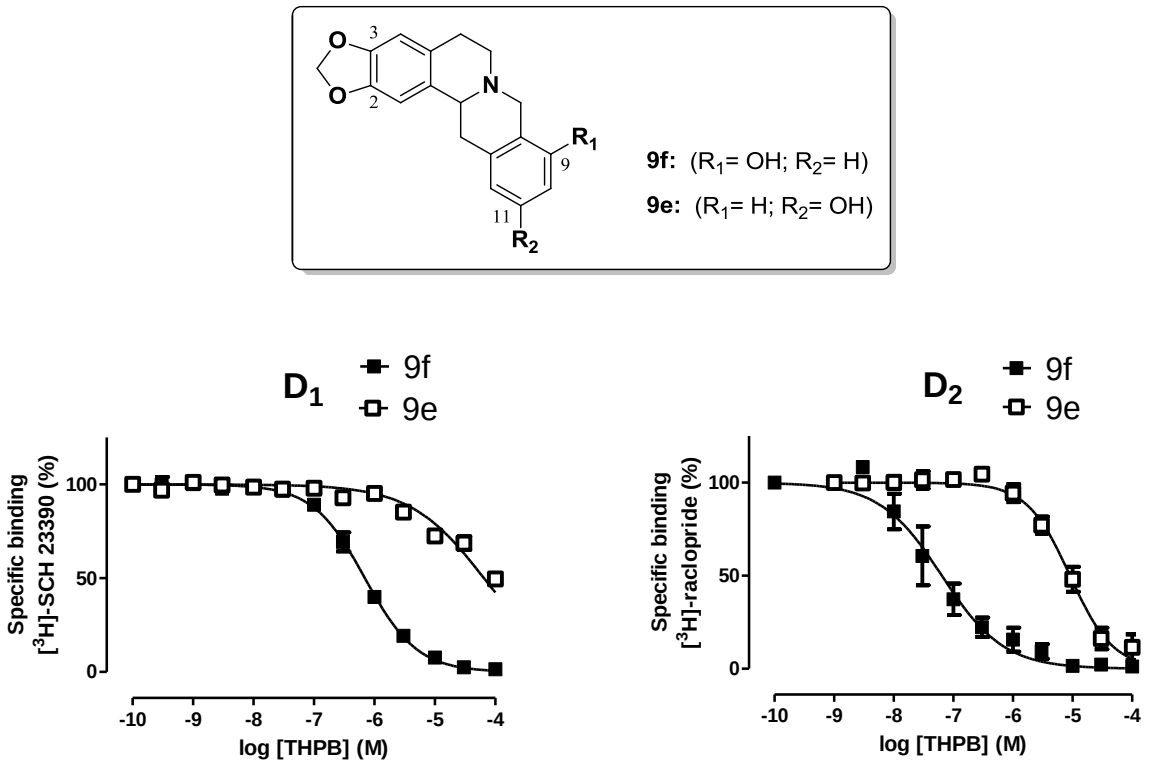

Figura 20. Curvas de desplazamiento de [^{3}H]-SCH 23390 (D_1) y [^{3}H] raclopride (D_2) de binding específico para **9e** y **9f**. Datos obtenidos de 3-5 experimentos.

Para entender mejor la interacción molecular que se establece entre los fármacos sintetizados y los RD D_2, se realizaron estudios de modelización molecular mediante simulaciones moleculares dinámicas y cálculos mecánico cuánticos de tres de las THPB más activas (**9c**, **9d** y **6b**). De estas simulaciones se pudo concluir que las interacciones más importantes en la unión fármaco-receptor son las establecidas entre el Asp 114 y la amina protonada con carga positiva de la THPB y entre Ser 193 y/o Ser 194 y el grupo catecol del anillo A. Además, se observó que de las tres moléculas ensayadas la THPB **9d** era la que mostraba ser más afín sobre el RD D_2, puesto que poseía una elevada energía en la interacción con dicho receptor.

Además, se realizaron ensayos de toxicidad celular en neutrófilos humanos, mediante técnica de MTT y de citometría de flujo, en las que se determinó que ninguna de las THPB sintetizadas eran citotóxicas.

Artículo 2: **"Synthesis of hexahydrocyclopenta[*ij*]isoquinolines as a new class of a dopaminergic agents"** (En: *European Journal of Medicinal Chemistry*, **2015**, *90*, 101)

Las THIQ son alcaloides naturales presentes en multitud de especies vegetales biosintetizados a partir de la tirosina y de la dopamina, por lo que se ha estudiado la afinidad de estos compuestos por los RD.

En el Artículo 2 se ha desarrollado la síntesis de una serie de alcaloides tricíclicos llamados 1,2,3,7,8,8a-hexahidrociclopenta[*ij*]-isoquinoleínas (HCPIQ) con la finalidad de optimizar y mejorar la afinidad por los RD D_1 y D_2.

La síntesis de este tipo de IQ comienza con la condensación de una feniletilamina y de un cloruro de ácido, que mediante condiciones de Schotten-Baumann darán lugar a la correspondiente fenilacetamida. Una ciclodeshidratación de Bischler-Napieralski seguida de una reducción de la imina intermediaria, genera el esqueleto IQ. La última etapa es una ciclación intramolecular mediante condiciones de Friedel-Crafts en la que se usa el reactivo de Eaton, generando en esta etapa el anillo ciclopentano (**Figura 21**).

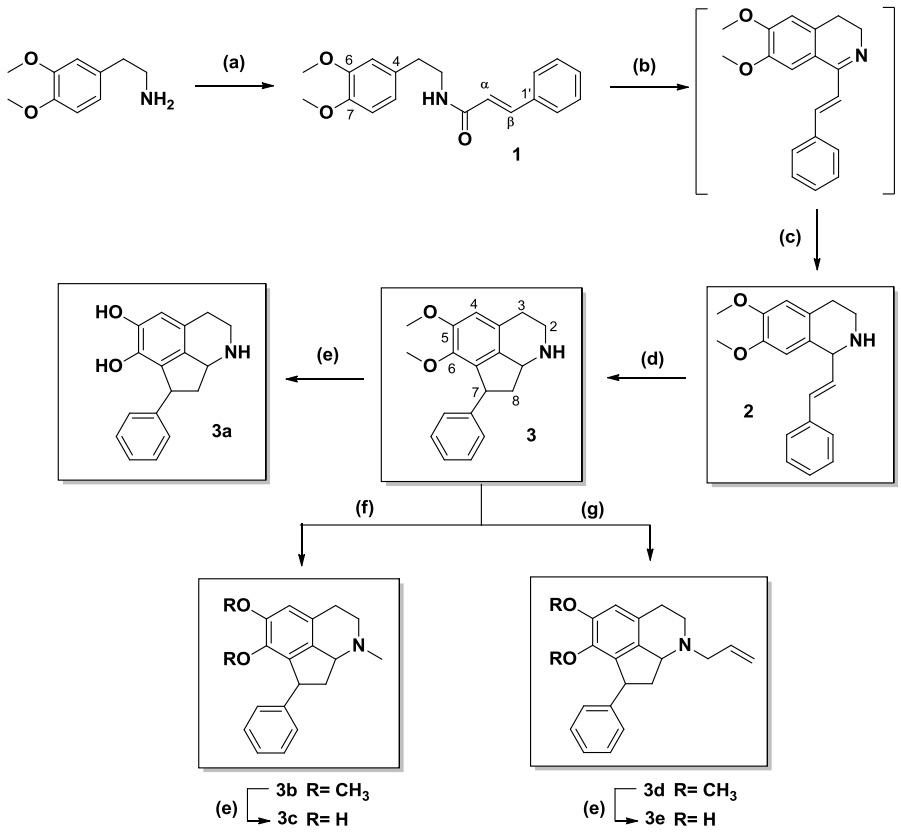

Reactivos y condiciones: (a) cloruro de cinnamoilo, CH_2Cl_2, NaOH 5 %, ta, 3h; (b) $POCl_3$, acetonitrilo, N_2, reflujo, 5h; (c) $NaBH_4$; MeOH, ta, 2h; (d) Reactivo de Eaton (P_2O_5-CH_3SO_3H, 1:10 w/w), reflujo, 15h; (e) CH_2Cl_2, BBr_3, ta, 2h; (f) metanol, formaldehido, acido fórmico, reflujo, 1h, seguido de $NaBH_4$, reflujo, 1h; (g) CH_3CN, K_2CO_3,cloruro de alilo, reflujo, 10h.

Figura 21. Esquema sintético de las HCPIQ.

En cuanto a la afinidad por los RD D_1 y D_2, se observó que todas las HCPIQ sintetizadas eran capaces de desplazar a los radioligandos específicos ([^{3}H]-SCH 23390 (D_1) y [^{3}H] raclopride (D_2)). Como en el caso de las THPB, aquellas que presentaban los hidroxilos libres poseían mayor capacidad de unión por los RD que los análogos correspondientes con los grupos oxigenados bloqueados. Las HCPIQ **3a**, **3c** y **3e** poseían valores excepcionales de afinidad sobre los RD D_2, 29, 13 y 18 nM respectivamente. Además, se observó, en toda la serie de este tipo de IQ, una muy elevada selectividad sobre los RD D_2, destacando los compuestos **3a** y **3c**, con un valor de ratio D_1/D_2 de 2465 y 1010 respectivamente.

En este trabajo también se realizaron ensayos de toxicidad celular sobre neutrófilos humanos, determinándose que ninguna de las HCPIQ sintetizadas eran citotóxicas.

Artículo 3: **"3-Chlorotyramine Acting as Ligand of the D_2 Dopamine Receptor. Molecular Modeling, Synthesis and D_2 Receptor Affinity"** (En: *Molecular informatics*, **2014**, *in press*)

En este trabajo, se realizaron estudios de modelización molecular en los cuales se evaluaron las interacciones entre los compuestos y el RD D_2 mediante la combinación de simulaciones de dinámica molecular (MD), semiempírica, ab initio y cálculos teóricos basados en el funcional de la densidad (DFT). En el segundo, se hizo uso de sistemas modelo reducido que nos permitió llevar a cabo cálculos de mecánica cuántica y estudios tipo teoría cuántica de átomos en moléculas (QTAIM).

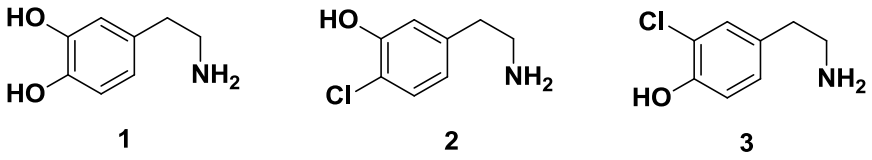

Figura 22. Dopamina y análogos clorados

De las energías de unión obtenidas en las simulaciones se puede observar que la sustitución de un hidroxilo por un átomo de cloro (**Figura 22**, compuesto **3**), aumenta la afinidad por el RD D_2 en comparación con la dopamina (**1**). Sin embargo, la sustitución del OH en posición *para* por el cloro (**2**) ejerce el efecto contrario.

Como ya se había sugerido en artículos anteriores del grupo del profesor Ricardo D. Enriz, que colabora activamente con nuestro grupo de investigación, la existencia de un resto carboxilo en el lugar de unión es muy importante para la interacción ligando-receptor, puesto que la fuerte interacción de los ligandos con el Asp 114 se mantuvo para todos los complejos evaluados. Respecto a la Val 115 (**Figura 23**), este aminoácido forma diversas interacciones con el anillo aromático de la dopamina. En cuanto a los restos serina, la Ser 197 aporta la mayor contribución a las energías de interacción de los complejos con los compuestos que poseen un hidroxilo en *meta* (**1** y **2**), mientras que la Ser 193 es más importante para el compuesto que tiene un cloro en esta posición (**3**). Por otro lado, el análisis de descomposición de residuos también revela una destacable contribución de la Phe 389, siendo más importante en el caso de los compuestos con hidroxilo en *para* (**1** y **3**).

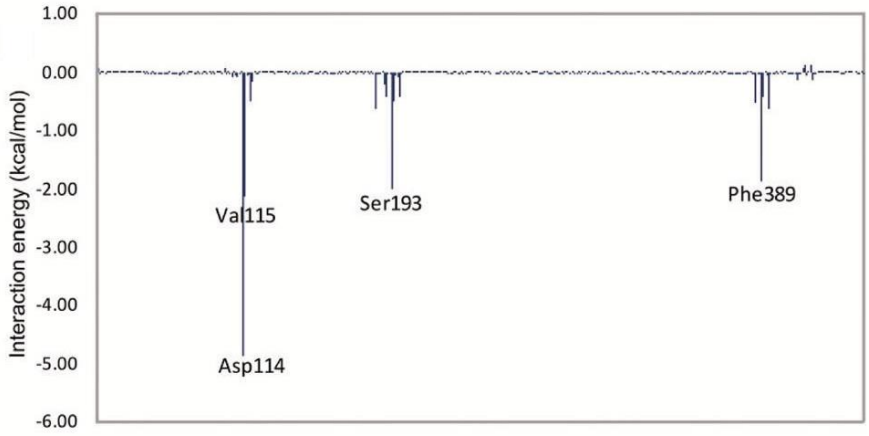

Figura 23. Energías de interacción para el compuesto **3**.

Capítulo 2.

Artículo 4: **"Synthesis of new melatoninergic hexahydroindenopyridines"** (En: *Bioorganic & Medicinal Chemistry Letters*, **2014**, *24*, 3534)

Las hexahidroindenopiridinas (HHIP) son moléculas alcaloídicas con un esqueleto novedoso que genera una nueva clase de compuestos con posible utilidad como agentes terapéuticos. Las HHIP se conocen por poseer varias actividades farmacológicas como lo son su actividad antiespermatogénica, antidepresiva y serotoninérgica, entre otras.

Con objeto de obtener HHIP con diferentes sustituciones sobre posiciones clave dentro del esqueleto: posiciones 1, 7 y 8, que pudieran interaccionar selectivamente sobre los receptores de la melatonina, se desarrolló la siguiente ruta sintética (**Figura 24**).

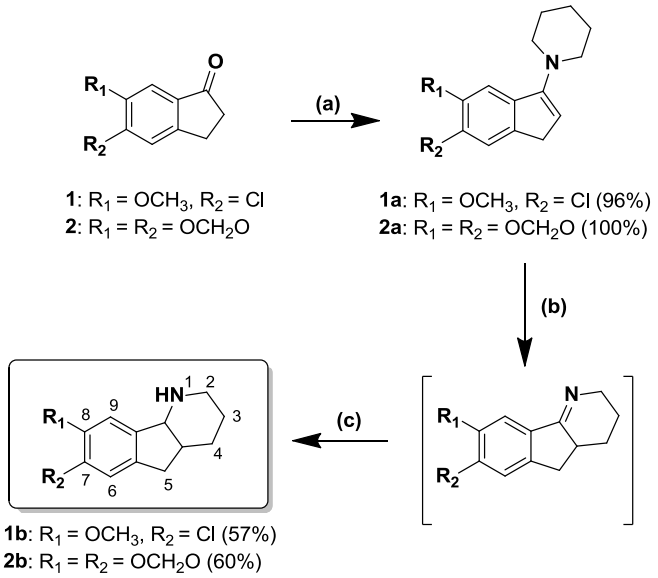

Reactivos y condiciones: (a) piperidina, $TiCl_4$, tolueno seco, N_2, ta, 3 días; (b) Hidrobromuro de 3-bromopropilamina, DMF seco, 110 ºC, 8 h; (c) $NaBH_4$, EtOH, ta, 16 h.

Figura 24. Ruta sintética para la obtención de HHIP **1b** y **2b**.

En ella, se parte de 1-indanonas sustituidas en posiciones 5 y/o 6, comercialmente disponibles, y mediante una reacción catalítica con $TiCl_4$ y piridina se produce la formación de la enamina correspondiente; la cual es sometida a una reacción de ciclación en la que se hace reaccionar con el hidrobromuro de 3-bromopropilamina, seguida de una reducción con borohidruro sódico, obteniendo así el esqueleto HHIP. A continuación se llevó a cabo la funcionalización del nitrógeno de las HHIP sintetizadas, para dar lugar a los compuestos que pudieran mimetizar los efectos de la melatonina sobre sus receptores específicos. De esta forma se prepararon por métodos clásicos los derivados *N*-acetilados, carbamatos y *N*-alquilados.

Estudios preliminares de binding melatoninérgico de las HHIP sintetizadas, mostraron que dicho esqueleto convenientemente funcionalizado, constituye un farmacóforo adecuado con capacidad para unirse a los receptores de la melatonina MT_1 y/o MT_2, y de esta forma conseguir un nuevo agente inductor del sueño.

Artículo 5: **"Efficient synthesis of hexahydroindenopyridines and their potencial as melatoninergic ligands"** (En: *European Journal of Medicinal Chemistry*, **2014**, *86*, 700)

La melatonina es una neurohormona que está implicado en procesos celulares, neuroendocrinos y neurofisiológicos. Se ha observado que alteraciones en el sistema melatoninérgico conducen a la aparición de enfermedades como insomnio y depresión, por lo que la investigación en este campo tiene como objetivo crear fármacos nuevos que posean una elevada afinidad por MT_1 y MT_2.

Las hexahidroindenopiridinas (HHIP) son alcaloides tricíclicos que muestran semejanza estructural con la melatonina y con otros fármacos recientemente comercializados, como la agomelatina (Valdoxan®), indicados en problemas de insomnio. Es por ello que las HHIP han sido estudiadas por nuestro grupo, con objeto de obtener análogos con una mayor afinidad por los receptores melatoninérgicos (**Figura 25**).

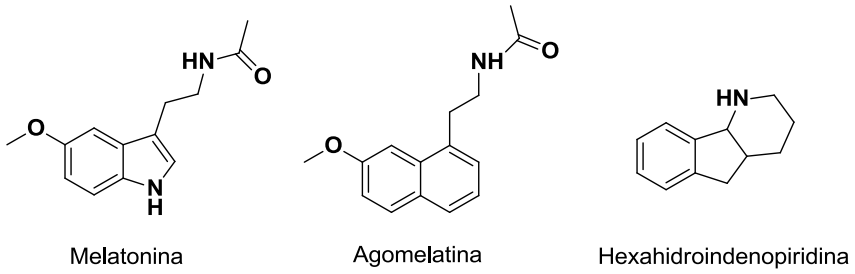

Figura 25. Melatonina, Agomelatina y HHIP.

En este artículo se sintetizaron 25 HHIP, clasificados en 4 series, con una diferente sustitución sobre las posiciones 7 y 8 (Anillo A), dependiendo de la indanona de partida utilizada. A continuación preparamos los derivados correspondientes mediante funcionalización del nitrógeno de la amina secundaria.

Todas estas moléculas sintetizadas fueron evaluadas como ligandos melatoninérgicos MT_1 y MT_2 mediante ensayos de binding. Así se observó que el compuesto **4g** era capaz de desplazar al radioligando específico para MT_1 y MT_2 (2-[^{125}I]-melatonina) en el rango nanomolar (Ki MT_1 = 670 nM y Ki MT_2 = 190 nM). Además se pudo concluir que el compuesto **2e** fue selectivo para MT_1 con una Ki = 500 nM y el compuesto **2f** lo fue para MT_2 con un valor de Ki = 380 nM (**Figura 26**).

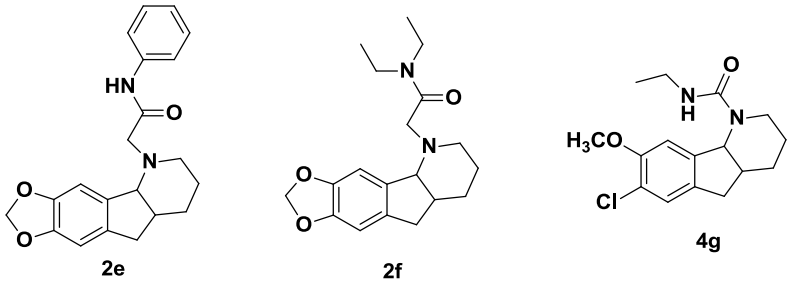

Figura 26. HHIP con afinidad por los receptores MT_1 y MT_2

Capítulo 3.

Artículo 6. **"Synthesis of pyrido[2,1-*a*]isoquinolin-4-ones and oxazino[2,3-*a*]isoquinolin-4-ones: New inhibitors of mitochondrial respiratory chain"** (En: *European Journal of Medicinal Chemistry* **2013**, *69*, 69)

La cadena respiratoria mitocondrial (CRM) de transporte electrónico comprende cuatro complejos enzimáticos (del I al IV), el coenzima Q (ubiquinona) y el citocromo C. Este sistema juega un papel esencial en la síntesis del ATP, el metabolismo de las especies reactivas del oxígeno y la apoptosis. Por ello, sus inhibidores presentan importantes perspectivas para convertirse en nuevos agentes antitumorales.

Los alcaloides benzo[*a*]quinolicidínicos poseen interesantes propiedades biológicas, así como una similitud estructural con algunos inhibidores de la CRM conocidos. En este trabajo decidimos realizar la síntesis de moléculas con dicho esqueleto. Entre los métodos descritos en la literatura, elegimos el de Pemberton, puesto que nos permitía explorar la reactividad de las iminas y aprovecharnos de la diversidad estructural que proporcionaba, dado que con él se obtienen pirido[2,1-*a*]-IQ y oxazino[2,3-*a*]-IQ.

Las diferentes iminas se sintetizaron mediante la ciclación de Bischler-Napieralski y se hicieron reaccionar con diferentes dioxinonas. El producto mayoritario obtenido de esta reacción depende del pH del medio: en condiciones neutras, los productos mayoritariamente aislados fueron las pirido[2,1-*a*]-IQ mientras que al añadir una base, se formaron preferentemente las oxazino[2,3-*a*]-IQ. Siguiendo este procedimiento se sintetizaron tres series de compuestos, a partir de tres iminas diferentes, dando un total de 11 compuestos a ensayar como posibles inhibidores de la CRM.

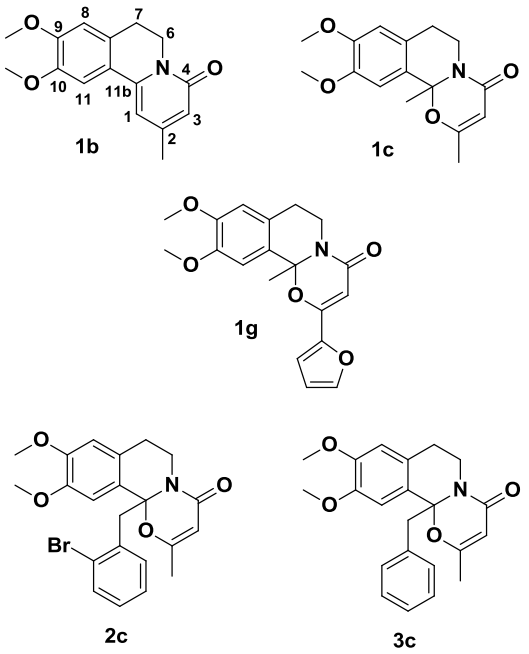

Figura 27. Pirido[2,1-*a*]-IQ y oxazino[2,3-*a*]-IQ inhibidoras de la CRM.

En general, las oxazino[2,3-*a*]-IQ mostraron mayor potencia que sus respectivos análogos piridínicos. Por ejemplo: el compuesto **1b** (**Figura 27**) mostró una CI_{50} de 8.33 µM mientras que su análogo oxigenado **1c** presentó una capacidad de inhibición cinco veces superior. Una tendencia similar se observa en todos los productos ensayados. En cuanto al sustituyente en posición 2, un grupo fenilo mantuvo la actividad (**1e**) y un anillo furánico proporcionó el compuesto más activo, **1g**. La desprotección de los metoxilos del anillo A (**1h**) también mantuvo la actividad. En el mismo sentido, cuando se introdujo un anillo aromático en posición 1 (series 2 y 3), las pirido[2,1-*a*]-IQ (**2b**, **3b**) inhibieron la CRM con potencias moderadas, mientras que sus respectivos análogos oxazino[2,3-*a*]-IQ (**2c**, **3c**) mostraron una mayor actividad. La presencia de un átomo de bromo sobre el anillo aromático no afectó significativamente a su actividad (ver **Artículo 6**).

Comparando con el compuesto de referencia, rotenona (un potente inhibidor del complejo I, altamente tóxico), tanto las pirido[2,1-*a*]-IQ como las oxazino[2,3-*a*]-IQ mostraron actividad inhibidora de la CRM con potencias moderadas. Dado que la mayoría de inhibidores de la CRM con potenciales aplicaciones en terapéutica actúan en el rango alto nanomolar o bajo micromolar, estos compuestos ensayados, y especialmente las oxazino[2,3-*a*]-IQ, pueden considerarse inhibidores efectivos de la CRM.

Artículo 7: **"Synthesis of new antimicrobial pyrrolo [2,1-*a*]isoquinolin-3-ones"** (En: *Bioorganic & Medicinal Chemistry* **2012**, *20*, 6589)

Las pirrolo[2,1-*a*]isoquinoleínas (IQ), MSA poco frecuentes en la naturaleza, presentan una estructura original y han mostrado una cierta actividad antimicrobiana. La búsqueda de nuevos antibióticos y antifúngicos que puedan sustituir a fármacos poco eficaces, a causa de las resistencias generadas por los microorganismos, fue lo que nos impulsó a realizar la síntesis de nuevas pirrolo[2,1-*a*]-IQ con actividad antimicrobiana.

Existen diversos métodos de síntesis de pirrolo-IQ. Nosotros hemos desarrollado un nuevo procedimiento basado en una doble ciclación intramolecular a partir de β-fenilacetamidas (**Figura 28**). Mediante este método, las pirrolo-IQ fueron obtenidas con buenos rendimientos.

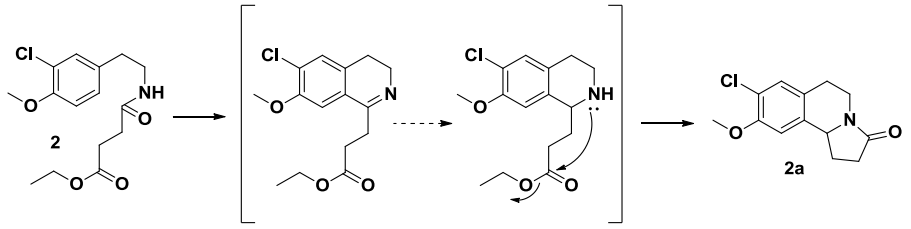

Figura 28. Mecanismo de ciclación de pirrolo[2,1-*a*]-IQ.

Utilizando este procedimiento, realizamos la síntesis de tres series de pirrolo[2,1-*a*]-IQ (**Figura 29**). Entre ellas, se sintetizó el compuesto natural **trollina** (**3b**).

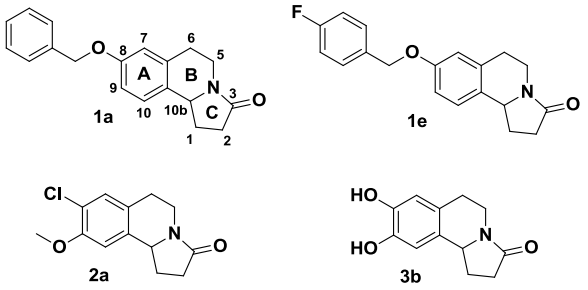

Figura 29. Pirrolo[2,1-*a*]-IQ antimicrobianas.

Los 13 compuestos sintetizados fueron evaluados como bactericidas y antifúngicos, mediante la técnica de difusión en agar. En lo que respecta a los test bactericidas, nuestros compuestos fueron ensayados frentes a diversas especies bacterianas patógenas humanas: *Bacillus cereus*, *Staphylococcus aureus*,*Enterococcus faecalis*, *Salmonella typhi*, *Escherichia coli* y *Erwinia carotovora*.

En general, pudimos observar que la introducción de un grupo lipofílico en posición 8 y/o 9 resultó adecuada para aumentar la actividad antimicrobiana, en comparación con los compuestos con hidroxilos libres en estas posiciones, como en el caso del compuesto **1b** y de la **trollina** (**3b**) (**Figura 29**). El compuesto que presentó una actividad más relevante fue **2a**, que posee un átomo de cloro en posición 8 y un grupo metoxilo en posición 9. Este compuesto demostró actividad bactericida frente a todas las cepas ensayadas. Además, mostró el mayor halo de inhibición frente a *S. aureus* y *E. carotovora* de entre todas las pirrolo-IQ sintetizadas. En el caso de esta última, la potencia bactericida de **2a** fue equiparable a la del compuesto de referencia (tetraciclina).

La actividad fungicida fue comprobada frente a algunas cepas de hongos fitopatógenos: *Aspergillus parasiticus*, *Trichoderma viride*, *Fusarium culmorum, Geotrichum candidum y Phytophthora citrophthora*. Dentro de la serie 1, las pirrolo-IQ más activas fueron **1a** y su análogo fluorado **1e**. Estos compuestos mostraron una potencia similar entre ellos, lo que sugiere que el grupo *O*-bencilo en posición 8 de las pirrolo-IQ contribuye positivamente a sus propiedades antifúngicas, independientemente de que contenga o no un grupo halógeno. El compuesto **2a**, el más activo en los ensayos bactericidas, demostró un efecto antifúngico moderado.

Summary – Results and Discussion

Summary – Results and Discussion

In the present **Thesis**, we have developed several synthetic routes in order to obtain different scaffolds of isoquinolines (IQ) alkaloids and hexahydroindenopyridines (HHIP). In addition, we have made their corresponding pharmacological tests, based on results previously obtained for these compounds with synthetic and/or natural origin and other structurally similar compounds. It has been observed, throughout many years, IQ alkaloids are one of the active secondary metabolites (ASM) most abundant in nature and with highest pharmacological interest, isolated in species of Annonaceae family. Azafluorenones are pyridin alkaloids with antimalarial properties also present in Annonaceae, which inspired us for the synthesis of HHIP.

We have developed the synthesis of these new drugs for the following biological targets:

a)- IQ with affinity towards Dopaminergic Receptors D_1 y D_2.

b)- HHIP with affinity towards Melatoninergic Receptors MT_1 y MT_2.

c)- IQ with antimicrobial activity.

d)- IQ with antitumor activity.

This Thesis is composed of seven articles which have been classified in three chapters:

Chapter 1: Isoquinoline Alkaloids with Affinity for Dopaminergic Receptors – Molecular Modeling on Dopaminergic Receptors: Articles 1, 2 and 3.

Chapter 2: Indenopyridine Alkaloids with Affinity for Melatoninergic Receptors: Articles 4 and 5.

Chapter 3: Isoquinoline Alkaloids with Antimicrobial and Antitumor Activities: Articles 6 and 7.

Chapter 1

Article 1. **"2,3,9- and 2,3,11- Trisubstituted tetrahydroprotoberberines as D_2 dopaminergic ligands"** (in: *European Journal of Medicinal Chemistry*, **2013**, *68*, 150)

Dopamine-mediated neurotransmission plays an important role in the central nervous system. A disorder in the dopaminergic system may cause neurological and psychiatric disorders as schizophrenia or Parkinson's disease. Therefore, there is an increased interest in the discovery of novel dopaminergic ligands, with high affinity for D_1 and D_2 dopamine receptors (DR), as potential drugs in the therapy of these neurological disorders.

Tetrahydroprotoberberines (THPB) are natural compounds which exist in different plant species as MSA. This kind of IQ alkaloids contains several pharmacological activities including affinity for DR. In order to improve the binding affinity towards DR, a synthetic route was developed to obtain three series of THPB. Finally, we synthesized 11 molecules to assay (**Figure 19**).

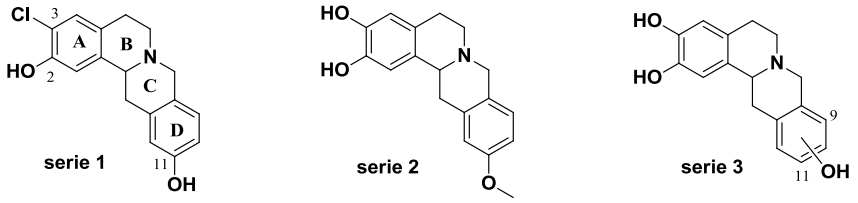

Figure 19. Series of THPB.

There are different methods for synthesizing THPB. We carried out a synthetic route that consists in five steps. The first step is a Henry reaction, whereby the β-nitrostyrene is obtained. This is followed by a reduction reaction to achieve the phenylethylamine, which was treated with the corresponding acid chloride to give the corresponding phenylacetamide. Next, a Bischler-Napieralski cyclodehydration followed by the imine reduction will result in the benzyl-THIQ. This compound is the starting material to obtain our THPB of interest by means of Mannich cyclization.

In the present work, we have studied the influence of A- and D-ring substituents of the THPB synthesized towards DR. It was observed that the presence of a hydroxyl group in A-ring increased the affinity for both D_1 and D_2 DR in comparison with blocked oxygenated function analogues. The presence of a chlorine atom in the A-ring increased the affinity for D_1 DR and decreased the selectivity over D_2 DR. Furthermore, it was observed that the presence of a methylenedioxy group in 2 and 3-positions decreased the selectivity over D_2 DR. On the other hand, it was observed that substituents in the D-ring also produced changes in the affinity for DR. The presence of a hydroxyl group in 9-position, increased the affinity for D_1 and D_2 DR. Among the 11 THPB tested, the most active molecule was **9f**, while a hydroxyl group in the 11-position substantially decreased the affinity for both DR (**Figure 20**).

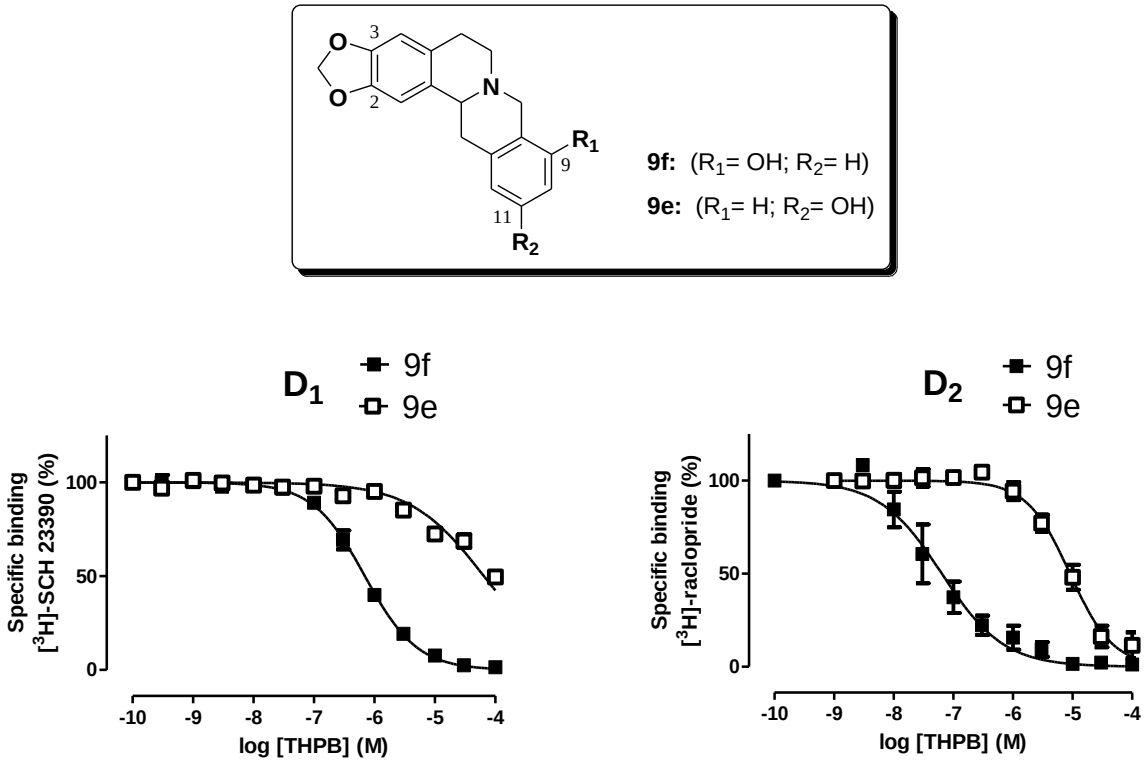

Figure 20. Displacement curves of the specific binding of D_1 and D_2 DR ligands by the compounds **9e** and **9f**. Data were displayed as mean ± SEM for 3-5 experiments.

Molecular modeling studies were carried out to better understand the interaction between the synthesized drugs and the D_2 DR. These studies were performed using molecular dynamics simulations and quantum mechanical calculations of three of the most active THPB (**9c**, **9d** and **6b**). In these simulations it was concluded that the most important interactions in the drug-receptor binding are: the interaction between Asp 114 and the protonated amine with positive charge of the THPB and the interaction between Ser 193 and/or Ser 194 and catechol group of the A-ring. In addition, we observed that **9d** is the drug with better interaction of the three molecules tested, since this compound has a high energy of interaction with D_2 DR.

Furthermore, cell toxicity assays were performed on human neutrophils by MTT and flow cytometry assays. In this study we observed that none of THPB synthesized were cytotoxic.

Article 2. **"Synthesis of hexahydrocyclopenta[*ij*]isoquinolines as a new class of a dopaminergic agents"** (in: *European Journal of Medicinal Chemistry*, **2015**, *90*, 101)

THIQ are natural compounds present in many plant species. The isoquinoline alkaloids were biosynthesized from tyrosine and dopamine, therefore we have been studied the affinity of these synthesized compounds towards DR.

In the Article 2, we have developed the synthesis of a series of tricyclic alkaloids called 1,2,3,7,8,8a-hexahydrociclopent[*ij*]-isoquinolines (HCPIQ), in order to optimize and improve the affinity for D_1 and D_2 DR.

The synthetic route of this class of compounds begins with the synthesis of the phenylacetamide by Schotten-Baumann conditions. The second step is the Bischler-Napieralski cyclodehydration to obtain the corresponding imine, which after reduction will result in the THIQ. The last step is an intramolecular cyclization by Friedel-Crafts conditions and using Eaton's reagent to generate the cyclopentane ring (**Figure 21**).

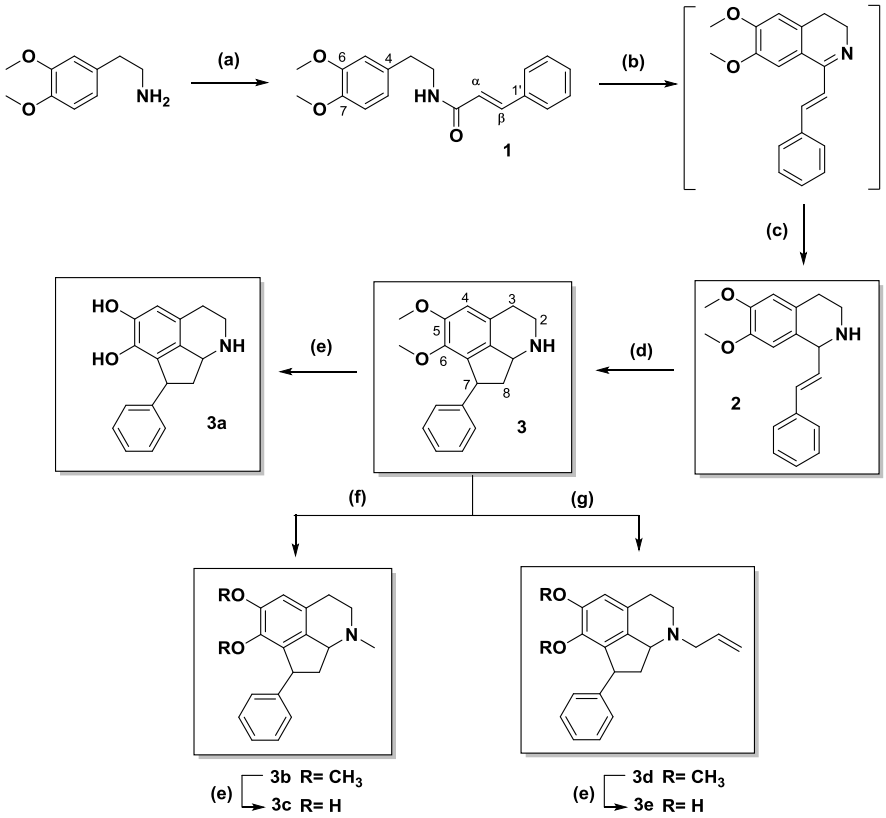

Reagents and conditions: (a) cynnamoyl chloride, CH_2Cl_2, NaOH 5 %, rt, 3h; (b) $POCl_3$, acetonitrile, N_2, refluxe, 5h; (c) $NaBH_4$; MeOH, rt, 2h; (d) Eaton's reagent (P_2O_5-CH_3SO_3H, 1:10 w/w), refluxe, 15h; (e) CH_2Cl_2, BBr_3, rt, 2h; (f) methanol, formaldehyde, formic acid, refluxe, 1h, followed of $NaBH_4$, refluxe, 1h; (g) CH_3CN, K_2CO_3,allyl chloride, refluxe, 10h.

Figure 21. Synthetic scheme of HCPIQ.

It was observed that all the HCPIQ synthesized were able to displace the specific radioligands ([^{3}H]-SCH 23390 (D_1) and [^{3}H] raclopride (D_2)) from its D_1 and D_2 DR binding sites, respectively. As in the case of THPB, the hydroxyl group produces greater binding activity than their corresponding blocked oxygenated function analogues. The HCPIQ **3a**, **3c** and **3e** had outstandingly affinity values for D_2 DR, being 29, 13 and 18 nM respectively. In addition, it was observed in all series a very high selectivity for the D_2 DR. The most selective compounds were **3a** and **3c**, with a ratio D_1/D_2 of 2465 and 1010 respectively.

In this work, we also assayed cell toxicity on human neutrophils by MTT assay, and we found that HCPIQ synthesized did not show cytotoxicity.

Article 3. **"3-Chlorotyramine Acting as Ligand of the D_2 Dopamine Receptor. Molecular Modeling, Synthesis and D_2 Receptor Affinity"** (in: *Molecular informatics*, **2014***, in press*)

This study was carried out in three steps. Firstly, molecular dynamic simulations (MD) to evaluate the molecular interactions between the compounds and the D_2 DR were performed. Secondly, a reduced model system for the binding pocket was used. Finally, the most representative complexes obtained in the previous steps were further analyzed theoretically by Density Functional Theory (DFT) calculations with the Quantum Theory of Atoms in Molecules (QTAIM) approach to the electron density distribution analysis.

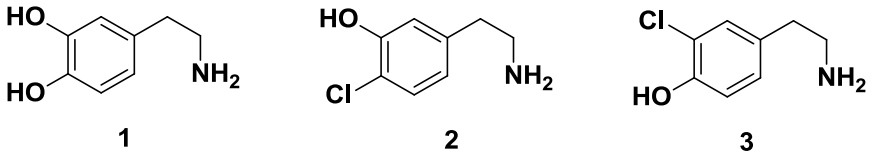

Figure 22. Dopamine and chlorinated analogues

From the relative binding energies obtained in the MD simulations, it can be observed that the replacement of the OH group in *meta* respect to the aminoethyl chain by a chlorine atom (**Figure 22**, compound **3**) increases the affinity towards D_2 DR when compared with DA (**1**). In contrast, the replacement of the OH group in *para* position (**2**) resulted in the opposite effect.

As it was earlier suggested in previous articles of Prof. Ricardo D. Enriz's group which collaborates actively with our research group, the strong interaction with the carboxylic group of an aspartate is very important for ligand's binding, since the interaction with the Asp 114 was maintained for all the tested complexes (**Figure 23**). On the other hand, Val 115 can form several interactions with the DA aromatic ring. In regard to other serine residues of the binding site, Ser 197 is the residue that exerted the largest contribution to the interaction energy for complex with **1** and **2**. In addition, Ser 193 showed the most important contribution in the complex with compound **3**. Finally, the residue decomposition analysis exhibited a significant contribution of Phe 389. The contribution of this residue was greater for **1**/D_2 DR or compound **3**/D_2 DR complexes than for compound **2**/D_2 DR complex.

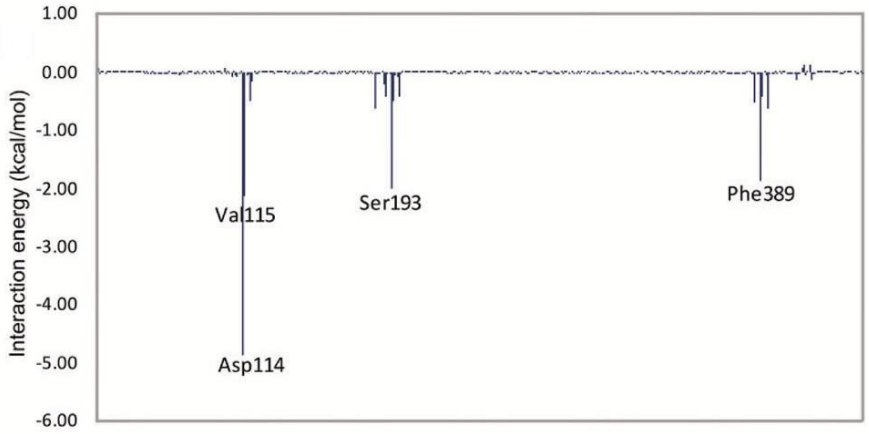

Figure 23. Interaction energies for compound **3**.

Chapter 2.

Article 4. **"Synthesis of new melatoninergic hexahydroindenopyridines"** (in: *Bioorganic & Medicinal Chemistry Letters*, **2014**, *24*, 3534)

Hexahydroindenopyridines (HHIP) are alkaloids with a novel scaffold which generates a new class of compounds with a potential utility as therapeutic agents. HHIP possess several pharmacological activities such as antispermatogenic and serotoninergic activity, among others.

In order to obtain HHIP with different substitutions on important positions of this skeleton, 1-, 7-, and 8- positions, and to make an extensive study on the capacity of these compounds to bind to the melatonin receptors MT_1 and MT_2, the following synthetic route was developed (**Figure 24**).

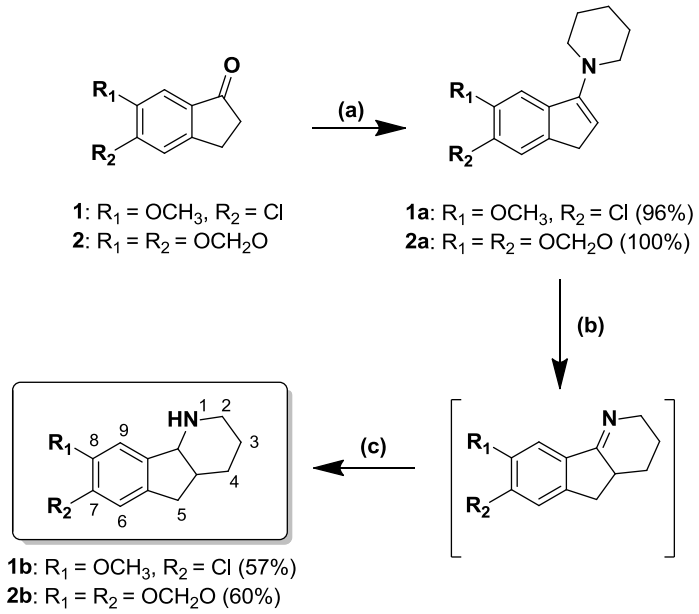

Reagents and conditions: (a) piperidine, $TiCl_4$, dry toluene, N_2, rt, 3 days; (b) 3-bromopropylamine hydrobromide, dry DMF, 110 ºC, 8 h; (c) $NaBH_4$, EtOH, rt, 16 h.

Figure 24. Synthetic route for synthesis of HHIP **1b** and **2b**.

Therefore, the commercially available 1-indanone substituted in 5- and/or 6- position was the starting material which was treated by catalytic reaction with $TiCl_4$ and pyridine to obtain the corresponding enamine. This was subjected to a cyclization by reaction with 3-bromo-propylamine hydrobromide followed of a reduction reaction with sodium borohydride to give the HHIP scaffold. Then, we made a functionalization of the nitrogen atom in the HHIP to obtain the compounds capable of mimicking melatonin's behavior on its receptors. Thus, we synthesized *N*-acetylated, carbamates and *N*-alkylated derivatives by classical conditions.

Preliminary melatoninergic binding affinity studies of synthesized HHIP showed that the appropriately functionalized skeleton is a pharmacophore with capacity to bind to melatonin receptors MT_1 and/or MT_2, which could provide new sleep-inducing agents.

Article 5. **"Efficient synthesis of hexahydroindenopyridines and their potencial as melatoninergic ligands"** (in: *European Journal of Medicinal Chemistry*, **2014**, *86*, 700)

Melatonin is a neurohormone involved in cell, neuroendocrine and neurophysiological processes. It has been observed that alterations in melatoninergic system can produce diseases such as insomnia or depression. Thus, research in this field aims at creating new drugs with a high affinity for melatonin receptors (MT).

Hexahydroindenopyridines (HHIP) are tricyclic alkaloids with structure related to melatonin and with other marketed drugs such as Agomelatine (Valdoxan®) used in insomnia. For this reason, our group paid attention to obtain the HHIP compounds with a high affinity for the MT receptors (**Figure 25**).

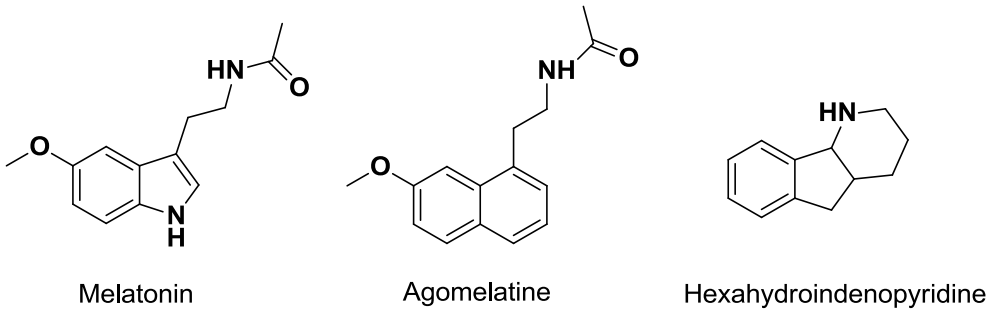

Figure 25. Melatonin, Agomelatine and HHIP.

In this article, we synthesized 25 HHIP, classified into four series, with a different substitution at the 7- and 8-position (A-ring), according to the indanona used as starting material. Then, we prepare the corresponding derivatives by functionalization of nitrogen atom of the secondary amine.

All synthesized molecules were evaluated as MT_1 and MT_2 melatoninergic ligands by binding assays. Thus, we can observe that compound **4g** was able to displace the specific radioligand to MT_1 and MT_2 (2-[^{125}I]-melatonin) in the nanomolar range (Ki MT_1 = 670 nM and Ki MT_2 = 190). Furthermore, it was concluded that compound **2e** was selective for MT_1 (Ki MT_1 = 500 nM) and compound **2f** was selective for MT_2 (Ki MT_2 = 380 nM) (**Figure 26**).

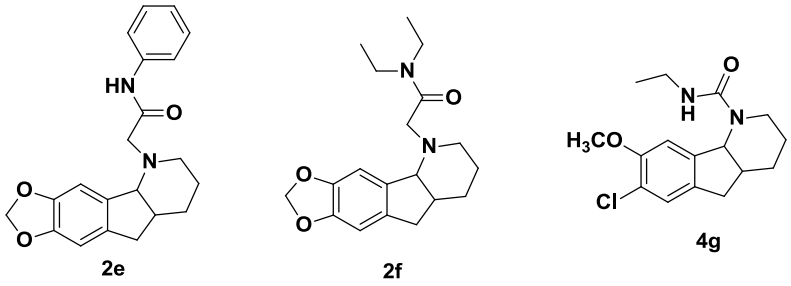

Figure 26. HHIP with affinity for MT_1 and MT_2 receptors.

Chapter 3.

Article 6. **"Synthesis of pyrido[2,1-*a*]isoquinolin-4-ones and oxazino[2,3-*a*]isoquinolin-4-ones: New inhibitors of mitocondrial respiratory chain"** (in: *European Journal of Medicinal Chemistry* **2013**, *69*, 69)

Mitochondrial electron transport chain comprises the enzymatic respiratory complexes (I-IV), the coenzyme Q (ubiquinone) and cytochrome c. Mitochondria play essential roles in the ATP synthesis, ROS metabolism and apoptosis. It is important that cells preserve an appropriate level of intracellular ROS to keep redox balance and signaling cellular proliferation. Some anticancer agents have the ability to inhibit mitochondrial electron transport and/or increase superoxide radical generation in tumor cells, resulting in cell apoptosis through ATP levels reduction and/or cell-damaging.

Benzo[a]quinolizidine is an important heterocyclic framework that can be found in numerous bioactive compounds. Benzo[*a*]quinolizidines are structurally related to some mitochondrial respiratory chain (MRC) inhibitors (mycotoxins, such as circumdatins) and we have carried out their synthesis as target of this study. Among the different depicted approaches, we have applied the Pemberton's method that uses dioxins as acyl-ketenes precursors. Therefore, taking advantage of the chemical diversity generated by this procedure, different pyrido[2,1-*a*]isoquinolines and oxazino[2,3-*a*]isoquinolines were obtained.

Several imines were prepared using Bischler-Napieralski cyclization and then reacted with dioxinones. The major product obtained relied on the pH of the medium. Under neutral conditions, the formation of pyridones was clearly favored, and under basic conditions oxazinones were preferentially formed. Following this procedure, we synthesized three series of compounds, starting from the three different imines to get a total of 11 compounds. Then, their potential effect on respiratory chain inhibition was evaluated.

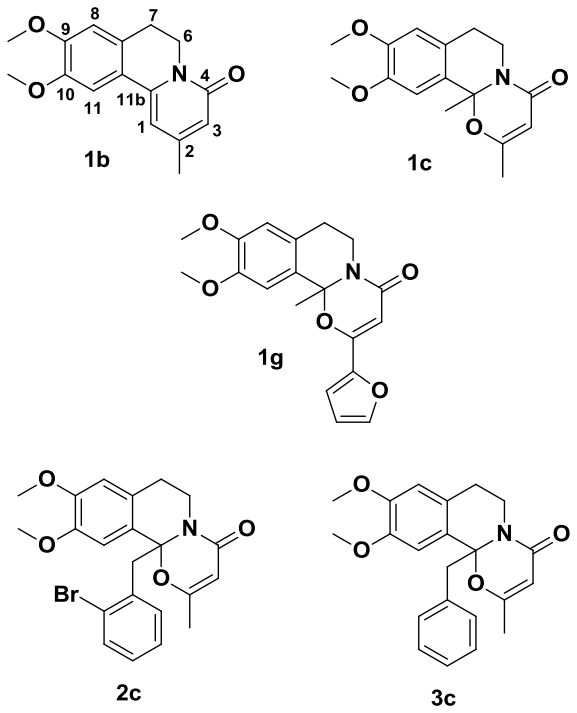

Figure 27. Pyrido[2,1-*a*]- and oxazino [2,3-*a*]-IQ MRC inhibitors.

In general, oxazino[2,3-*a*]-IQ-4-ones seemed to display greater activity than their respective pyrido[2,1-*a*]-IQ-4-ones analogues. For instance, while compound **1c** (**Figure 27**) IC_{50} was 1.36 µM, its pyridine analogue (**1b**) showed a decrease NADH oxidase activity (IC_{50} = 8.33 µM). By contrast, the size and nature of the substituent at 2-position of the oxazine did not seem to affect NADH oxidase activity. In this regard, not only the existence of a phenyl group (**1e**) kept the activity but the presence of a furan ring at C2 position provided the most potent compound **1g**. Moreover, the deprotection of the methoxyl groups in the A ring to obtain a catechol **1h**, maintained the activity. On the other hand, when the aromatic ring was placed on C1 position (series 2 and 3), the pyrido- and oxazino-IQ-4-ones were able to inhibit respiratory chain without any noticeable influence of the halogen group.

Compared with the highly toxic compound, rotenone (a high-affinity inhibitor of complex I), the pyridine and oxazinone derivatives showed a moderated inhibitory activity. Given that most of the respiratory chain inhibitors with potential therapeutic interest act in the high nanomolar and low micromolar ranges, these compounds and especially the oxazinone derivatives, can be considered effective inhibitors of the whole respiratory chain.

Article 7: **"Synthesis of new antimicrobial pyrrolo [2,1-*a*]isoquinolin-3-ones"** (in: *Bioorganic & Medicinal Chemistry* **2012**, *20*, 6589)

Pyrroloisoquinolines are secondary active metabolites scarce in nature, which present an original structure with certain antimicrobial properties. Inasmuch, the discovery of new antimicrobial agents has turned into a clear need in the last few years, due to the development of resistance to classic drugs as a consequence of their extensive use.

Althought several methods have been employed for the synthesis of these compounds, we have applied a new methodology based on double intramolecular cyclization, conducted by Bischler-Napieralski cyclodehydration from an ester phenylethylamide. It involves the subsequent reduction of the imine intermediate (**Figure 28**).

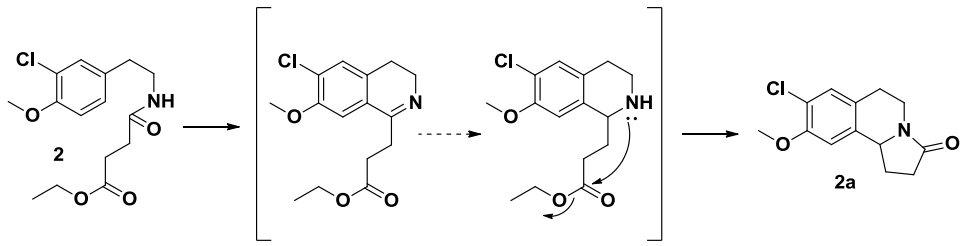

Figure 28. Mechanism of cyclization of pyrrolo[2,1-*a*]isoquinolines.

Using this method we performed the synthesis of three series of compounds with pyrroloisoquinoline structure, obtaining a total of 13 different molecules (**Figure 29**). The natural product **trolline** (**3b**) was synthesized, among other compounds.

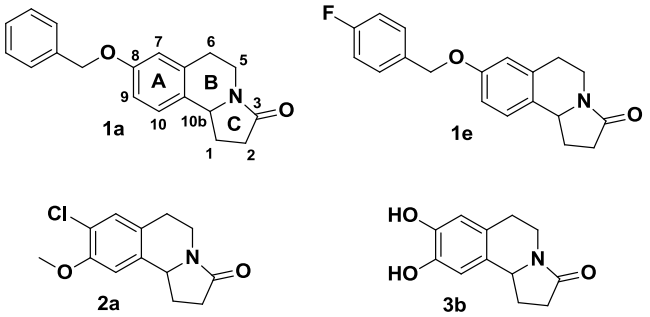

Figure 29. Antimicrobial pyrrolo[2,1-*a*]isoquinolines

All the synthesized pyrrolo[2,1-*a*]isoquinolines were assayed in vitro for their ability to inhibit bacterial and fungal growth. In the antimicrobials assays, our compounds were tested against several human pathogenic bacteria as well as economically important phytopathogenic bacteria and/or fungi. The bacterial agents were: *Bacillus cereus*, *Staphylococcus aureus*, *Enterococcus faecalis*, *Salmonella typhi*, *Escherichia coli* and *Erwinia carotovora*

In general, a lipophilic group at the 8- and/or 9- position seemed to provide moderate activity compared with that displayed by a free hydroxyl group such as **1b** and **trolline** (**3b**) (**Figure 29**). The most noteworthy compound was **2a**, which possessed both a chlorine atom and a methoxyl group at the 8- and 9- position, respectively. This compound exerted bactericidal activity against all tested strains. Furthermore, **2a** showed a potency within the range displayed by the reference compound tetracycline.

Fungicide activity was tested against some phytopathogen fungi strains: *Aspergillus parasiticus*, *Trichoderma viride*, *Fusarium culmorum, Geotrichum candidum* and *Phytophthora citrophthora*. Compounds **1a**, **2a**, **1c** and **1e** inhibited fungal growth in vitro. In series 1, the most active compounds were **1a** and its fluorinated analogue **1e**, which showed similar potency. Consequently, it seems that the benzylic moiety located at the 8-position on the pyrroloisoquinoline structure contributed positively to its antifungal properties regardless the presence of a halogen atom. By contrast, compound **2a**, which was the most potent bactericidal agent against human pathogens, only exerted a moderated antifungal activity.

Therefore, 8-chloro-9-mtehoxy compound (**2a**) was the most relevant in bactericidal assays and 8-benzyl-pyrroloisoquinolines **1a** and **1e** in the fungicidal assays.

Conclusiones

Conclusiones

1. Se han sintetizado 11 derivados de estructura 2,3,9- y 2,3,11-tetrahidro-protoberberinas (THPB) con afinidad por las familias de RD D_1 y D_2, a través de una ciclación de Mannich de un intermedio 1-bencil-tetrahidroisoquinoleína (**Artículo 1**). De los resultados de REA se pudo establecer que: i) los grupos hidroxilo libres en el anillo A, incrementan la afinidad por ambos tipos de RD; ii) la presencia de un átomo de cloro en el anillo A favorece la afinidad por los RD D_1; iii) en cuanto a la sustitución en el anillo D, la presencia de un grupo hidroxilo en posición 9 aumenta la afinidad por los RD D_2, siendo la 2,3-metilendioxi-9-hidroxi-THPB (compuesto **9f**) y la 2,3,9-trihidroxi-THPB (compuesto **9d**), los más activos; mientras que un hidroxilo en posición 11, disminuye la afinidad por ambos RD. Por otra parte, los estudios de modelización molecular mostraron que el compuesto **9d** se comporta como un agonista D_2 ya que los residuos de Serina parecen cruciales para la unión y activación a este receptor. Además, ninguna de las THPB trisustituídas sintetizadas mostraron citotoxicidad.

2. Seis derivados de un esqueleto isoquinoleínico novedoso, las hexaciclopenta-isoquinoleínas (HCPIQ), fueron sintetizadas a través de una ciclación intramolecular de Friedel-Crafts de un intermedio (*Z*)-1-estiril-THIQ, utilizando el reactivo de Eaton (**Artículo 2**). Las HCPIQ sintetizadas mostraron gran afinidad por los RD D_2, destacando los compuestos catecólicos **3a** (7-fenil-5,6-dihidroxi-HCPIQ), **3c** (1-metil-7-fenil-5,6-dihidroxi-HCPIQ), y **3e** (1-alil-7-fenil-5,6-dihidroxi-HCPIQ), con unos valores de afinidad de rango nanomolar frente a los RD D_2, y una importante selectividad por dichos RD, situándose el ratio D_1/D_2 entre 2500 y 400.

3. Los estudios de modelización molecular sobre 3-clorotiramina, nos ha permitido conocer la importancia que tiene la carga negativa del aspartato sobre el ligando que se une al receptor (**Artículo 3**). El grupo ácido carboxílico terminal interacciona con el grupo amino protonado del ligando en cuestión. Además, el resto serina también contribuye a la estabilización puesto que interacciona con los grupos fenólicos del ligando.

4. Las hexahidroindenopiridinas (HHIP) son un tipo de esqueleto tricíclico muy poco frecuente en la naturaleza, pero con semejanza estructural con la melatonina, neurohormona implicada en procesos fisiológicos como el sueño. Las HHIP fueron sintetizadas partiendo de indanonas comerciales, mediante una reacción catálitica con $TiCl_4$ y piridina, y posterior ciclación de la enamina correspondiente con un bromoalquilamina y reducción. A continuación se prepararon derivados HHIP con objeto de estudiar su afinidad por los receptores de la melatonina (**Artículo 4**).

5. Las HHIP sintetizadas con grupos carbamatos, mostraron una importante afinidad por los receptores melatoninérgicos. El compuesto **4g** (7-cloro-8-metoxi-1-*N*-etilcarboxamida-HHIP) presentó afinidad tanto por el receptor MT_1 como por el MT_2. Sin embargo, los derivados amídicos mostraron selectividad por uno de los dos receptores: el compuesto **2e** (7,8- metilendioxi-2-*N*-acetamida-HHIP) fue selectivo para MT_1 con una Ki = 500 nM, mientras que el compuesto **2f** (7,8-metilendioxi-*N*,*N*-dietilacetamida-HHIP) lo fue para MT_2 con un valor de Ki = 380 nM (**Artículo 5**).

6. Finalmente, sintetizamos IQ con esqueletos diversos, unas con capacidad para inhibir la cadena respiratoria mitocondrial (CRM), otras con actividad antibacteriana o antifúngica. A) Las pirido y oxazino-isoquinoleínas se sintetizaron mediante ciclación de Bischler-Napieralski, haciendo reaccionar la imina resultante con diversas dioxinonas. En general, las oxacino-IQ mostraron mayor capacidad para inhibir los complejos de la CRM, que los correspondientes pirido-IQ (**Artículo 6**). B) Las pirrolo-isoquinoleínas (pirrol-IQ) fueron sintetizadas mediante un nuevo procedimiento basado en una doble ciclación intramolecular a partir de fenilacetamidas. De las moléculas sintetizadas, el compuesto **2a** (8-cloro-9-metoxi-pirrol-IQ), disustituído en el anillo A, fue el que mostró mayor actividad antibacteriana, frente a diversas bacterias patógenas; mientras que los compuestos monosustituidos en el anillo A, **1a** (8-benziloxi-pirrol-IQ) y **1e** (8-(4-fluorobenziloxi)-pirrol-IQ), resultaron los más potentes frente a cepas de hongos fitopatógenos (**Artículo 7**).

Conclusions

Conclusions

1. Eleven derivatives of 2,3,9- and 2,3,11- tetrahydroprotoberberine (THPB) structure with affinity for DR families D_1 and D_2, have been synthesized through Mannich cyclization of an intermediate 1-benzyl-tetrahydroisoquinoline (**Article 1**). It was established from REA studies that: i) free hydroxyl groups on A-ring, increase the affinity for both types of DR; ii) the presence of halogens in the A-ring such as chlorine atom, favors affinity for D_1 DR; iii) concerning D-ring substitution, the presence of a hydroxyl group at 9-position increases the affinity for D_2 RD, being 9-hydroxy-2,3-methylenedioxy-THPB (compound **9f**) and 2,3,9-trihydroxy-THPB (compound **9d**) the most active compounds; while a hydroxyl group at 11-position, decreases the affinity for both DR. In addition, molecular modeling studies showed that the compound **9d** behaves as an agonist D_2 because the serine residues seem to be crucial for binding and activation of this receptor. Finally, none of the synthesized trisubstituted THPB showed any cytotoxicity.

2. Six isoquinoline derivatives with a novel skeleton, the hexacyclopentaisoquinoline (HCPIQ), were synthesized by intramolecular cyclization of Friedel-Crafts acylation of an intermediate (*Z*) -1-styryl-THIQ using Eaton's reagent (**Article 2**). The synthesized HCPIQ showed high affinity for D_2 DR. It was noteworthy the catecholic compounds **3a** (7-phenyl-6,5-dihydroxy-HCPIQ), **3c** (1-methyl-7-phenyl-6,5-dihydroxy-HCPIQ), and **3e** (1-allyl-7-phenyl-6,5-dihydroxy-HCPIQ), with nanomolar affinity values for D_2 DR, and also a significant selectivity with a D_1/D_2 ratio between 2500 and 400.

3. Molecular modeling studies of 3-chlorotyramine allowed us to know the importance of negatively charged aspartate on the ligand that binds to the receptor (**Article 3**). The terminus carboxylic acid group interacts with the protonated amine group of the ligand. In addition, the serine residue also contributes to stabilization since it interacts with the ligand phenolic groups.

4. The hexahydroindenopyridines (HHIP) are a type of unusual tricyclic skeleton in nature, but with structural similarity with melatonin, a neurohormone involved in physiological processes such as sleep. The HHIP were synthesized starting from commercial indanones, by catalytic reaction with $TiCl_4$ and pyridine, and subsequent cyclization of the corresponding enamine with a bromoalkylamine and reduction. Then HHIP derivatives were obtained in order to study their affinity for melatonin receptors (**Article 4**).

5. The HHIP synthesized with carbamate groups showed a significant affinity for melatoninergic receptors. Compound **4g** (7-chloro-8-methoxy-1-*N*-ethylcarboxamide-HHIP) displayed affinity for both MT_1 and MT_2 receptors. However, the amide derivatives showed selectivity for one of the two receptors: Compound **2e** (7,8-methylenedioxy-2-*N*-acetamide-HHIP) was selective for MT_1 with a Ki of 500 nM, while compound **2f** (7,8-methylenedioxy-*N,N*-diethylacetamide-HHIP) was for MT_2 with a Ki of 380 nM (**Article 5**).

6. Finally, we synthesize IQ with varied skeletons, some of them with ability to inhibit mitochondrial respiratory chain (MRC), and others with antibacterial or antifungal activity. A) pyrido- and oxazino-isoquinolines were synthesized by Bischler-Napieralski cyclization, treating the resulting imine with a variety of dioxinones. In general, oxazino-IQ showed greater ability to inhibit the complexes of the MRC than the corresponding pyrido-IQ (**Article 6**). B) pyrrolo-isoquinolines (pirrol-IQ) were synthesized by a novel process based on a double intramolecular cyclization from phenylacetamides. Among synthesized molecules, compound **2a** (8-chloro-9-methoxy-pirrol-IQ), disubstituted on A-ring, exhibited the highest antibacterial activity against various pathogenic bacteria; while compounds monosubstituted on A-ring, the **1a** (8-benzyloxy-pirrol-IQ) and **1e** (8-(4-fluorobenzyloxy)-pirrol-IQ), were the most potent against phytopathogenic fungi strains (**Article 7**).

Anexo: Elucidación estructural

Espectros de RMN representativos

Espectros Capítulo 1

Espectros referentes al Artículo 1.

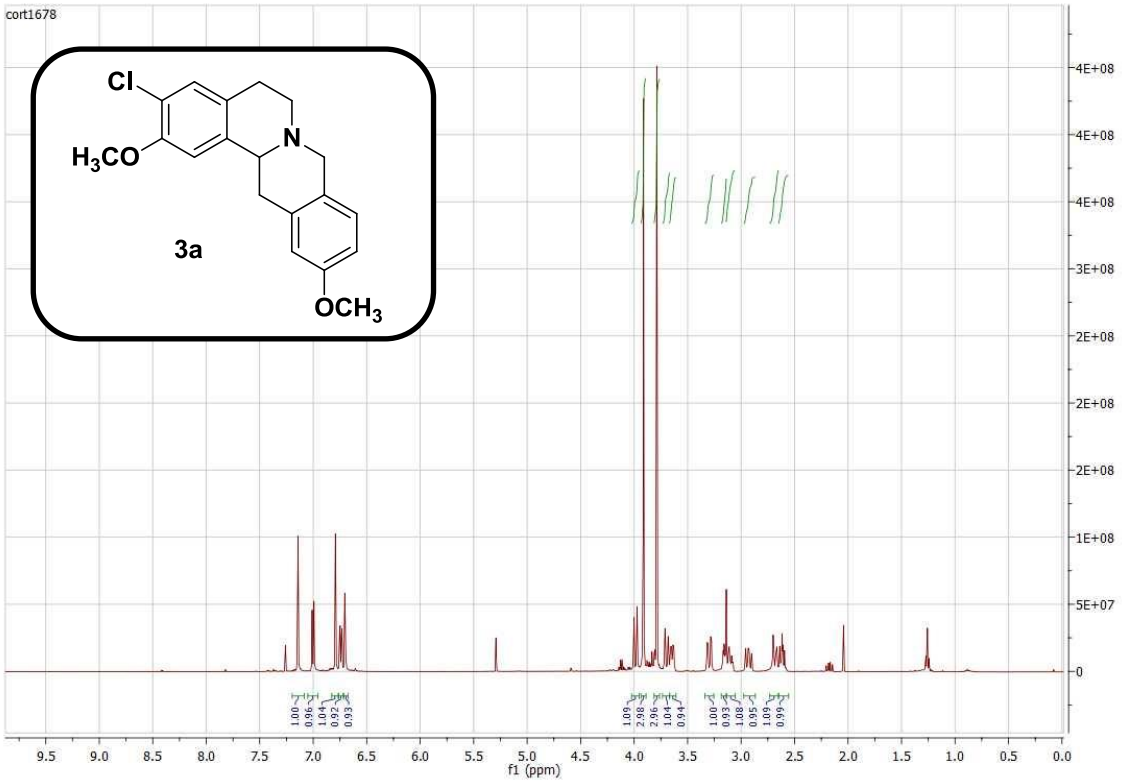

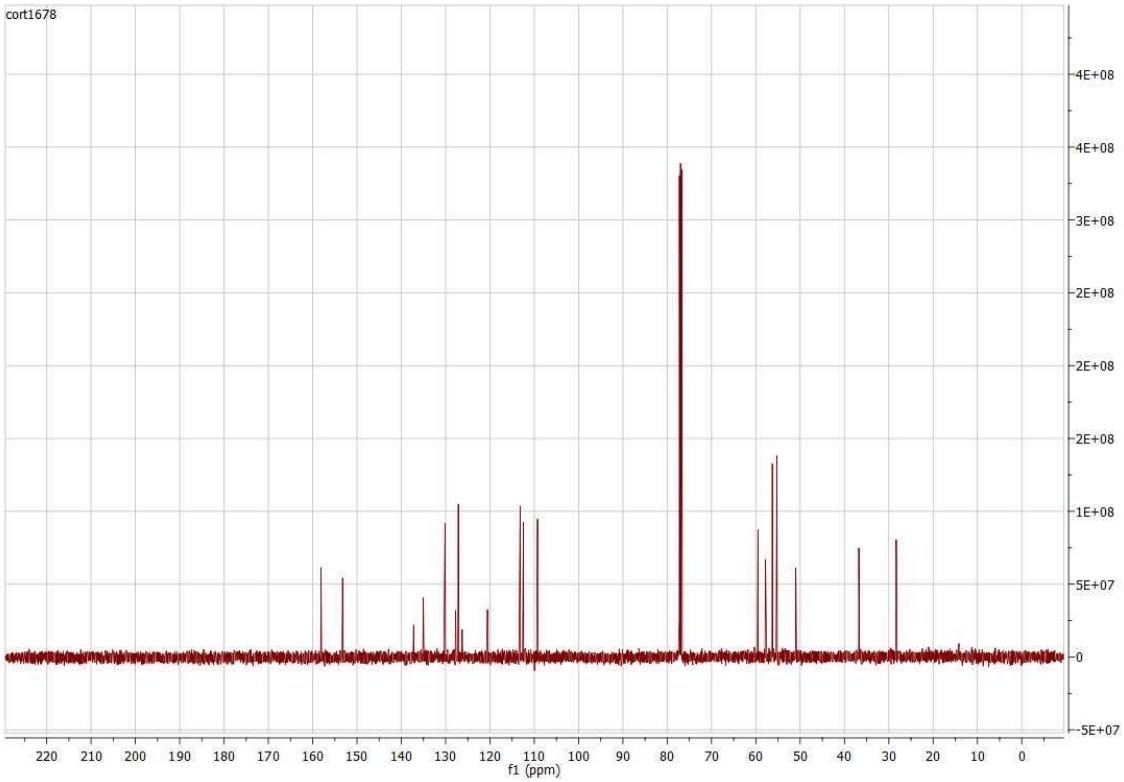

Espectros en $CDCl_3$ de ^{1}H-RMN (500 MHz) y ^{13}C-RMN (125 MHz) de **3a**

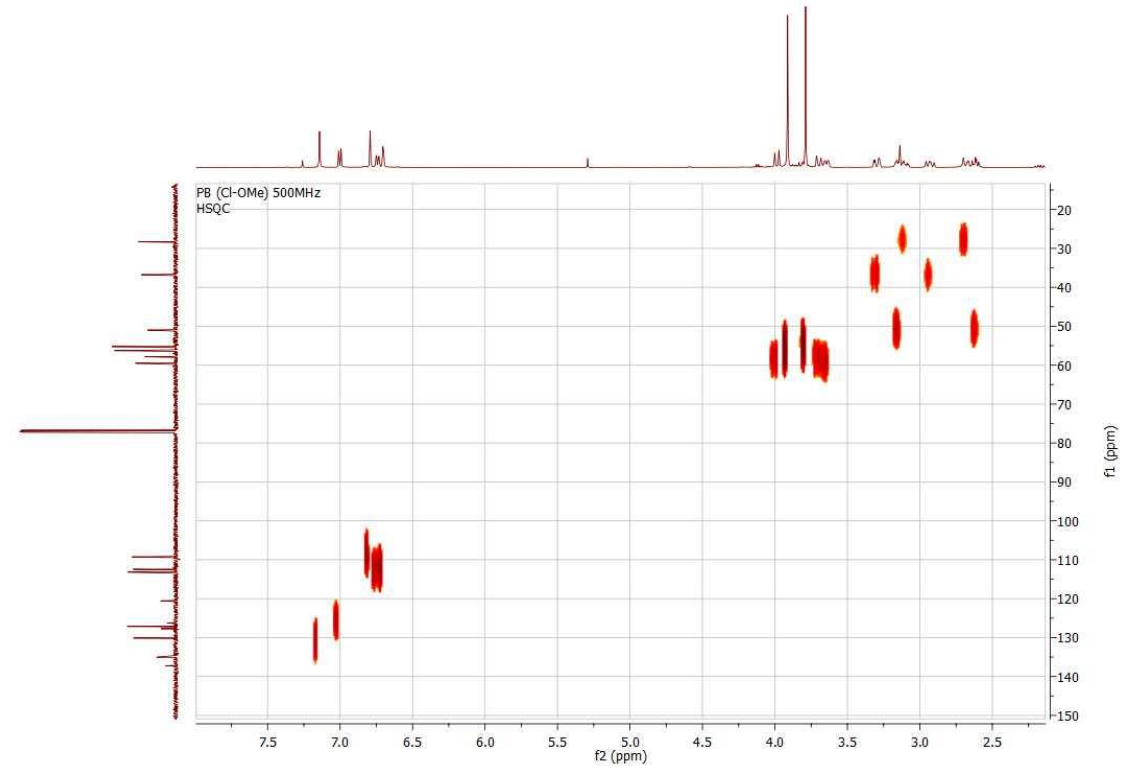

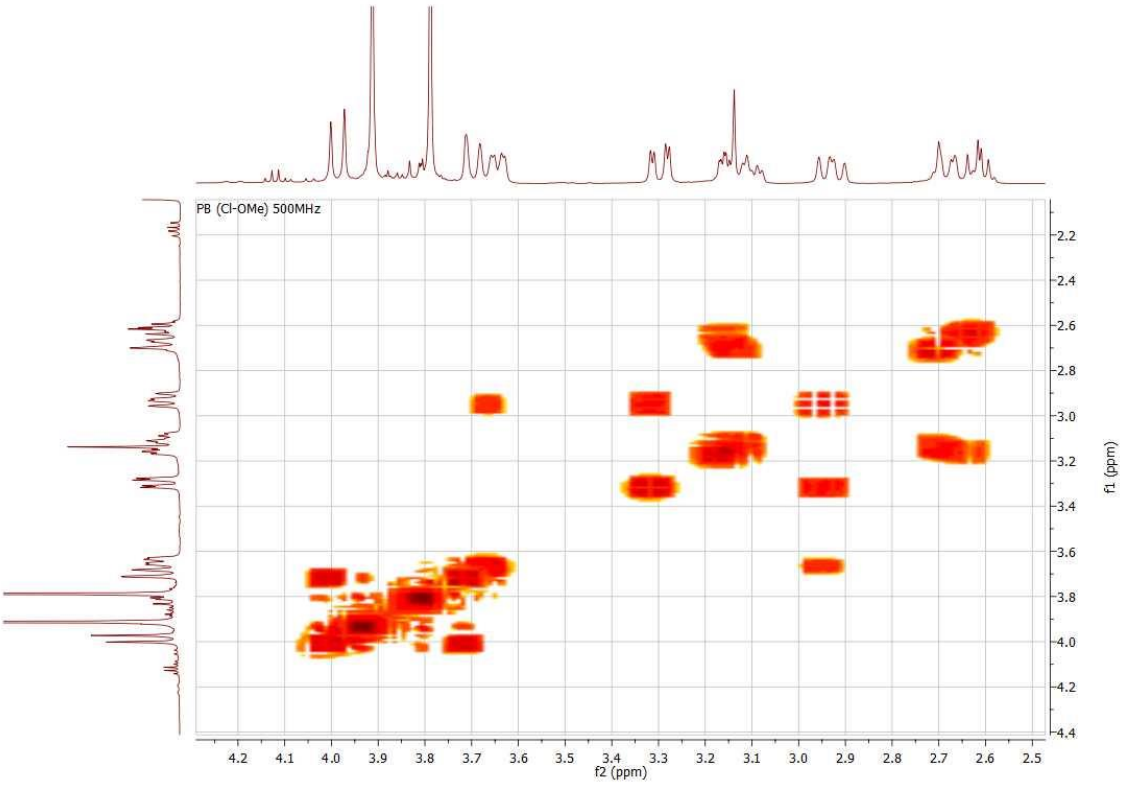

Espectros en $CDCl_3$ de HSQC y COSY 45 de **3a**

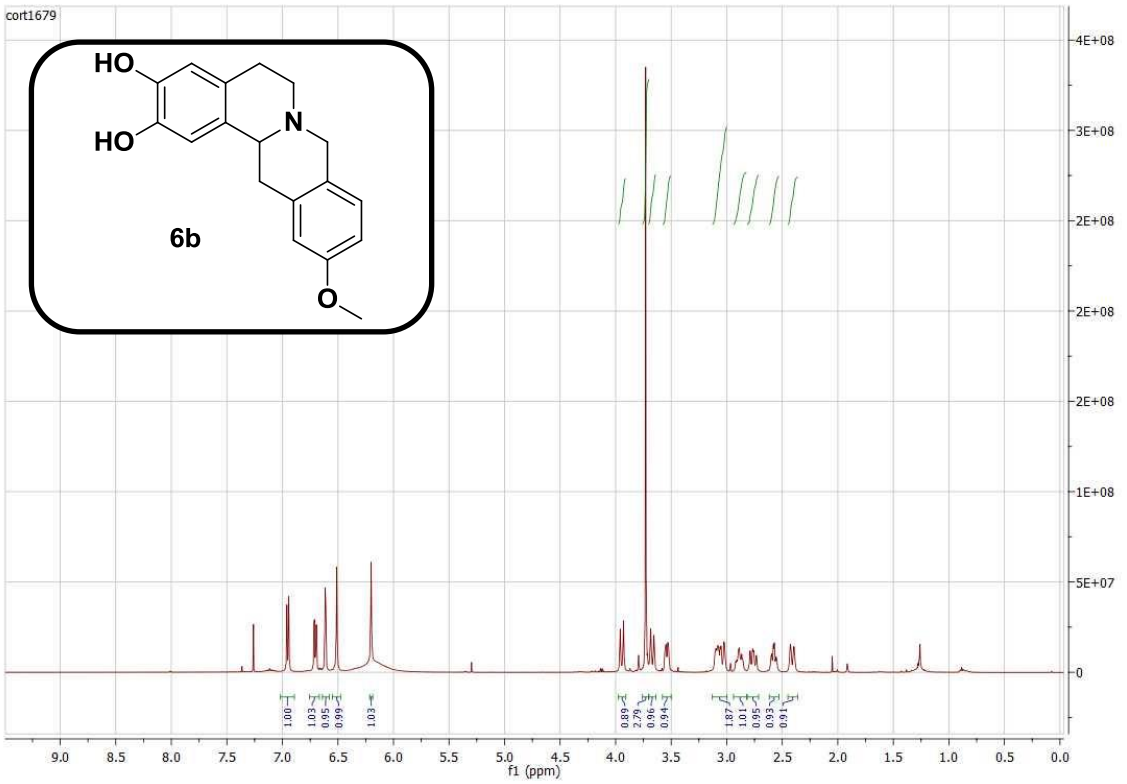

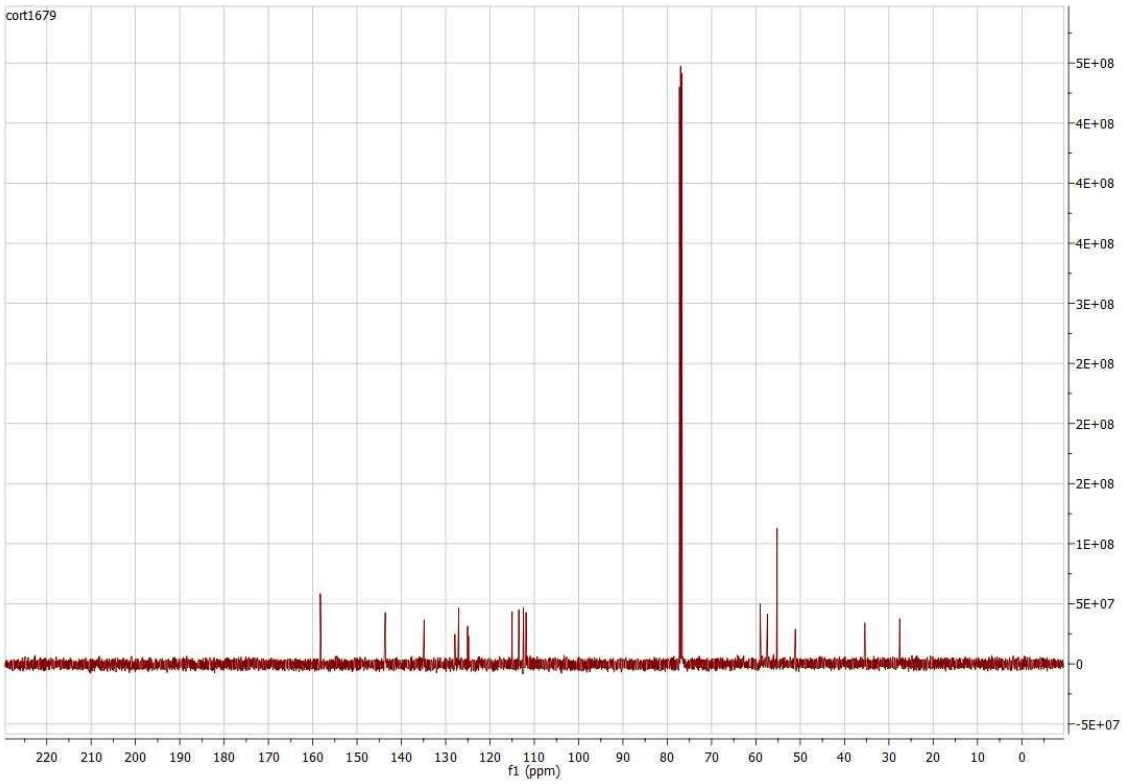

Espectros en $CDCl_3$ de ^{1}H-RMN (500 MHz) y ^{13}C-RMN (125 MHz) de **6b**

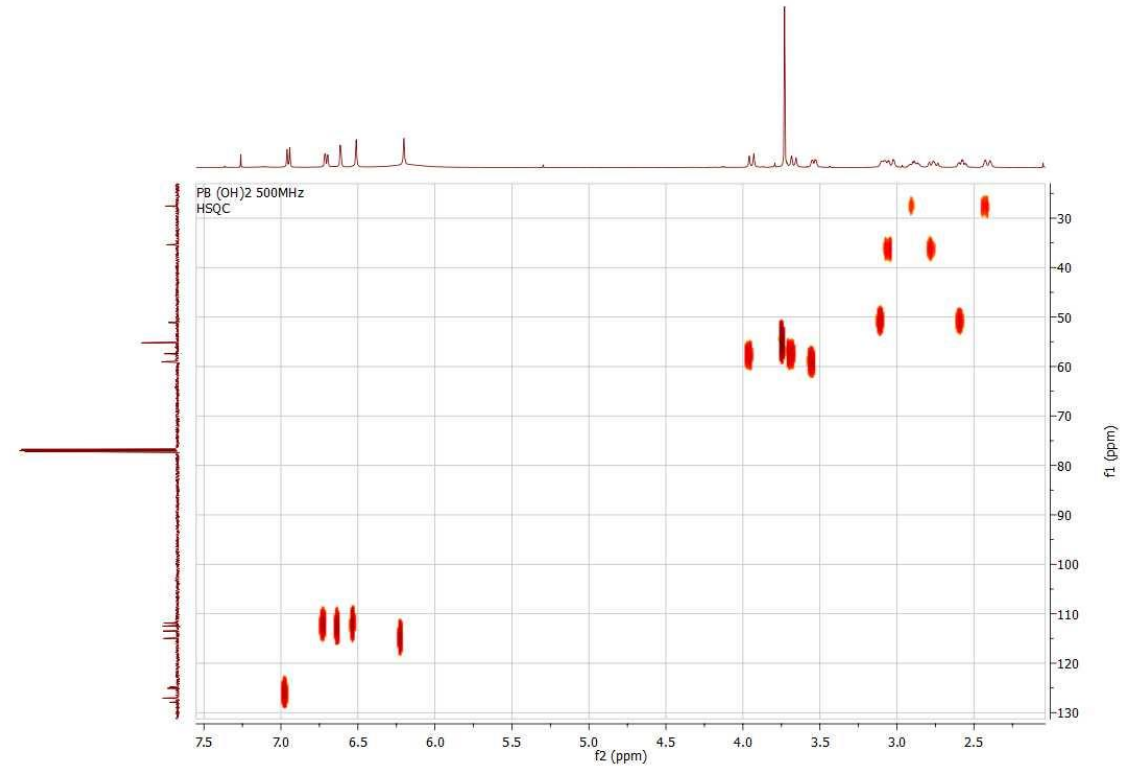

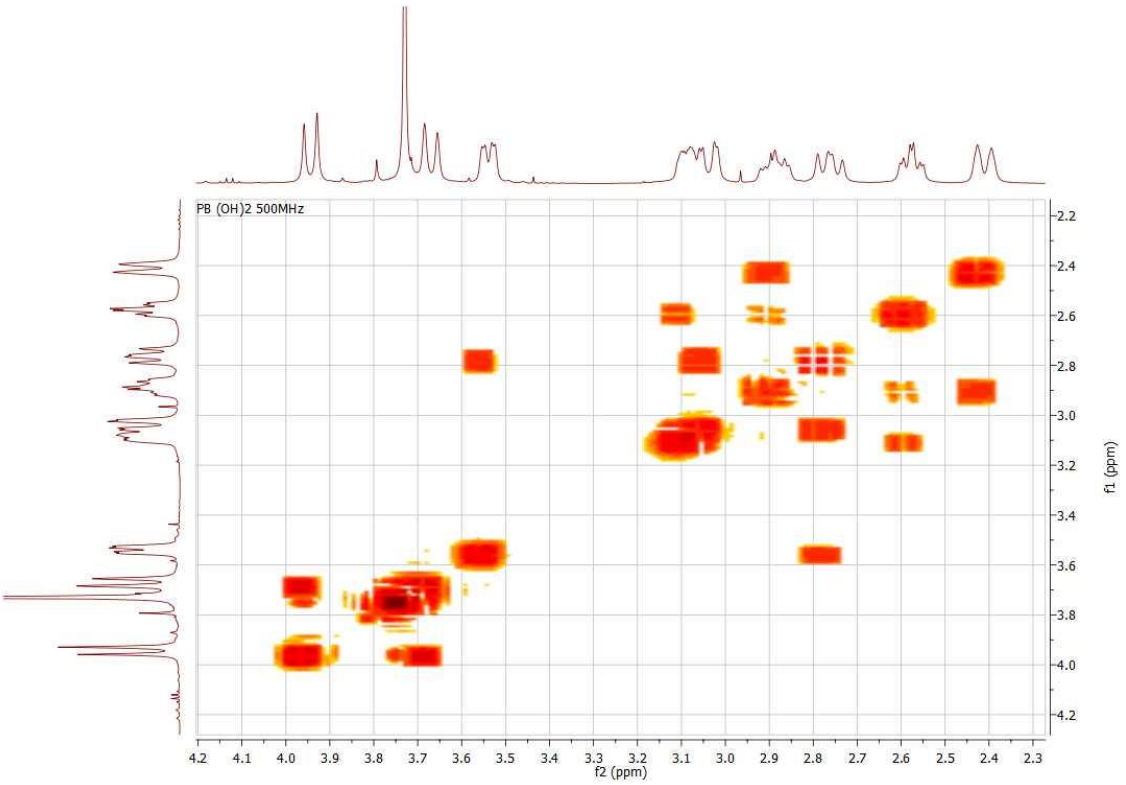

Espectros en $CDCl_3$ de HSQC y COSY 45 de **6b**

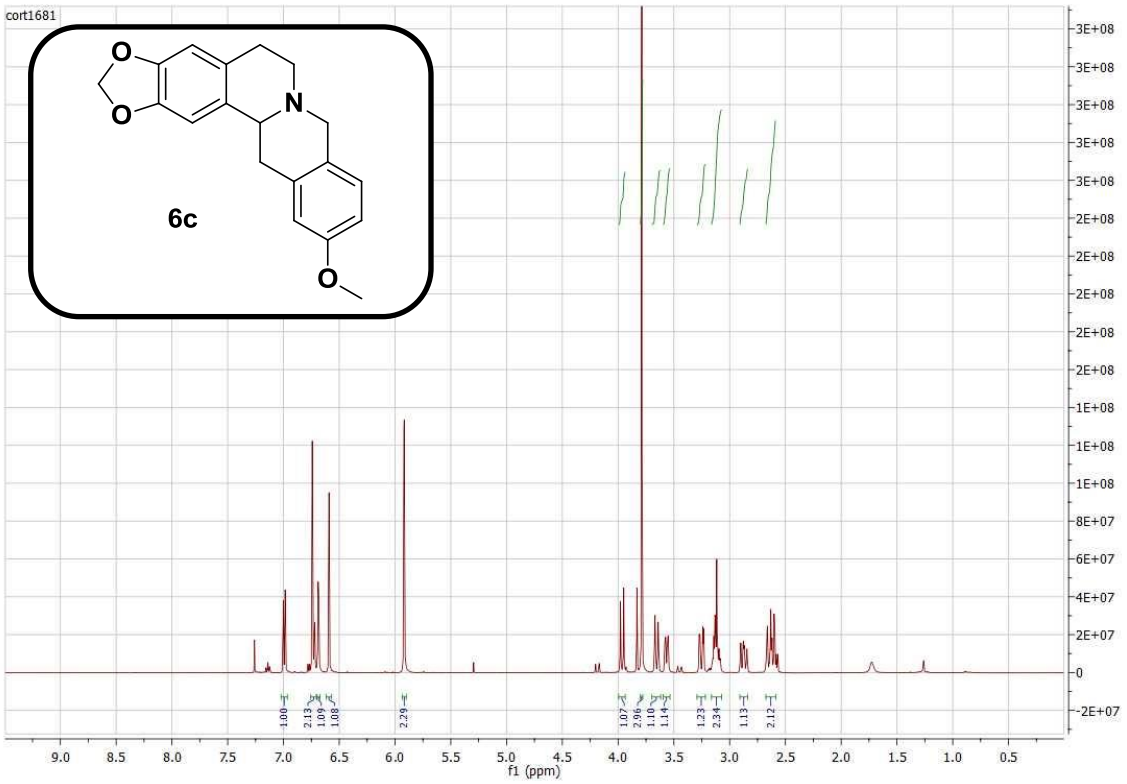

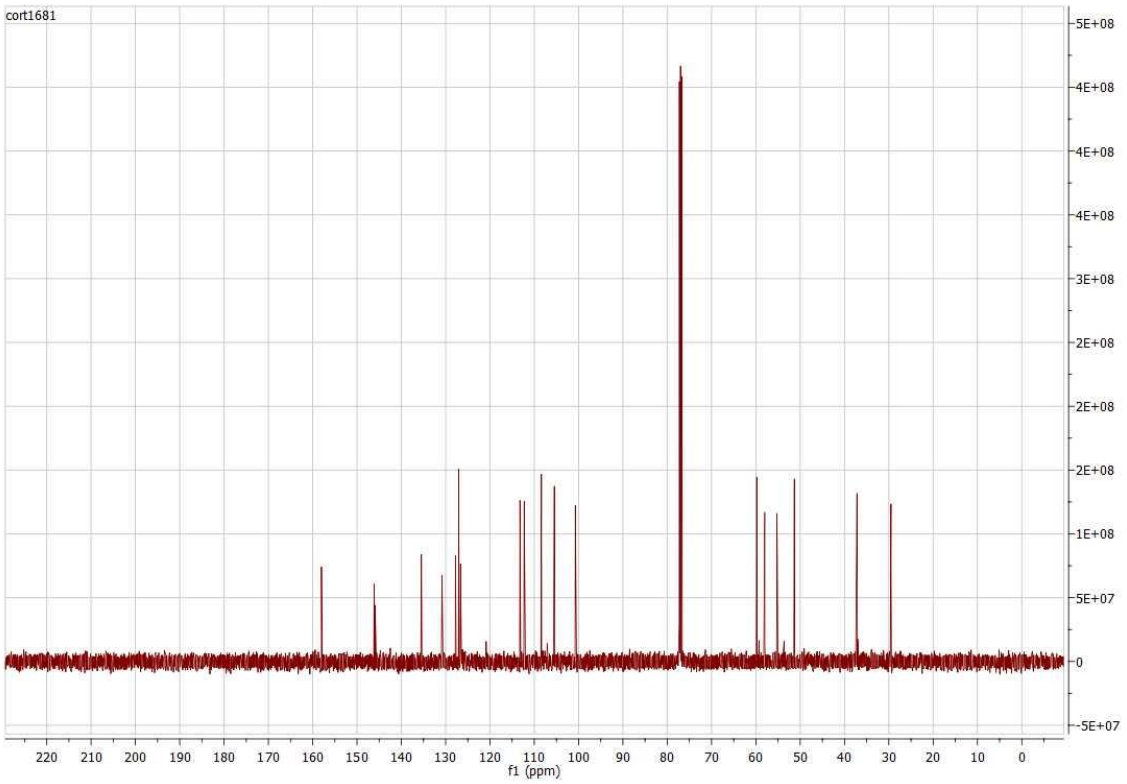

Espectros en $CDCl_3$ de ^{1}H-RMN (500 MHz) y ^{13}C-RMN (125 MHz) de **6c**

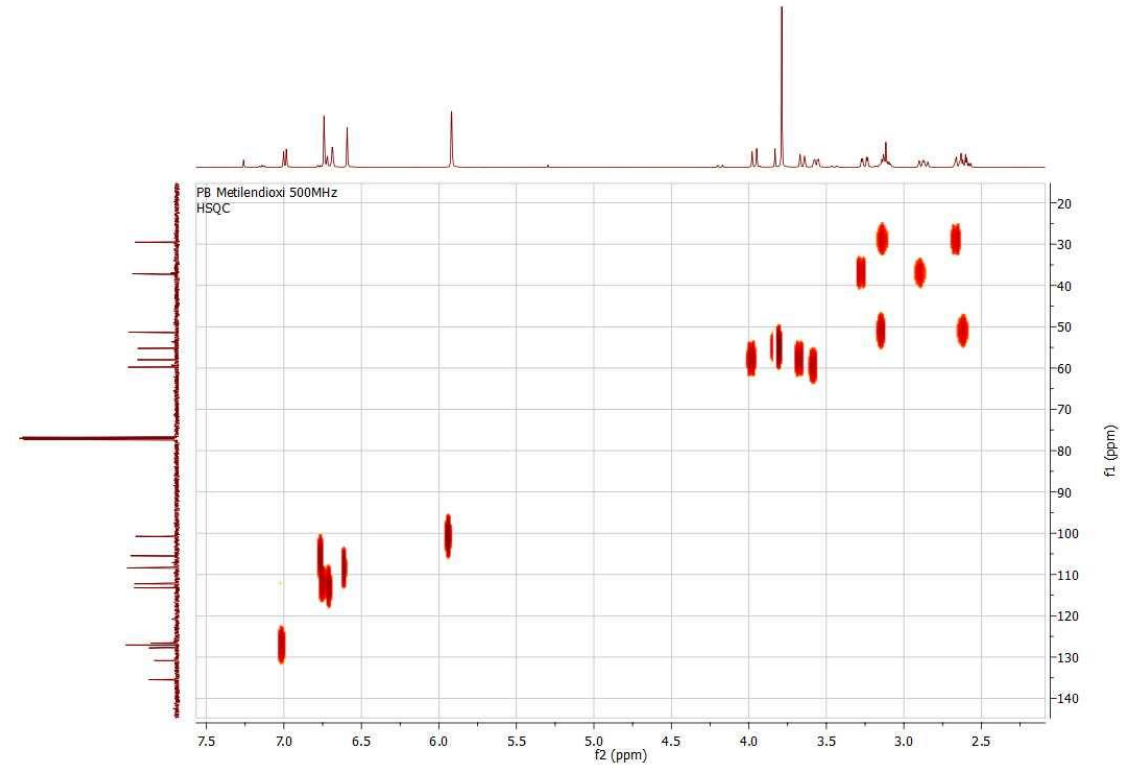

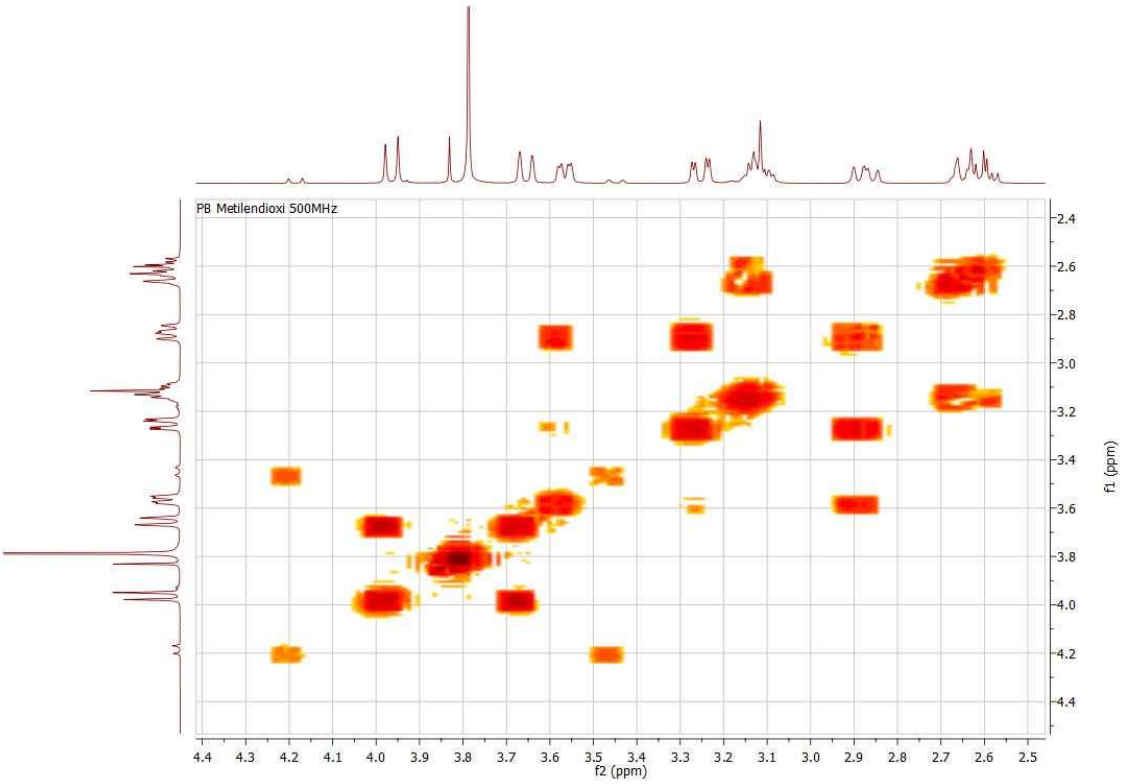

Espectros en $CDCl_3$ de HSQC y COSY 45 de **6c**

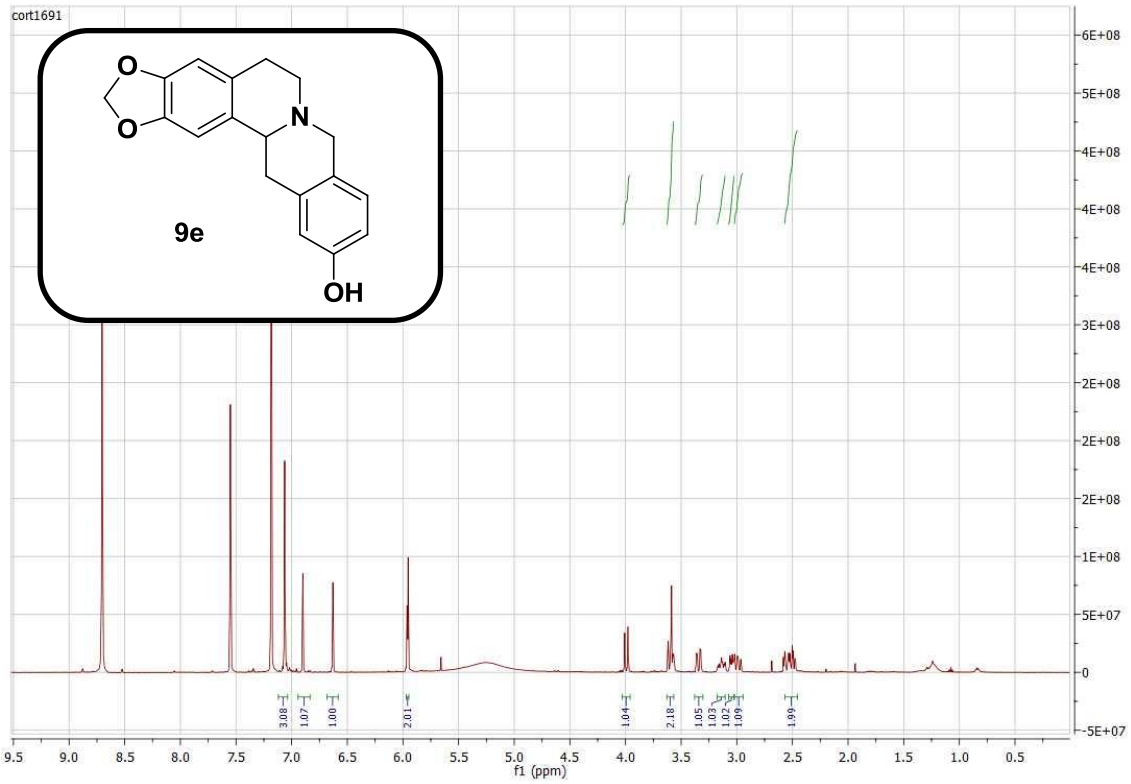

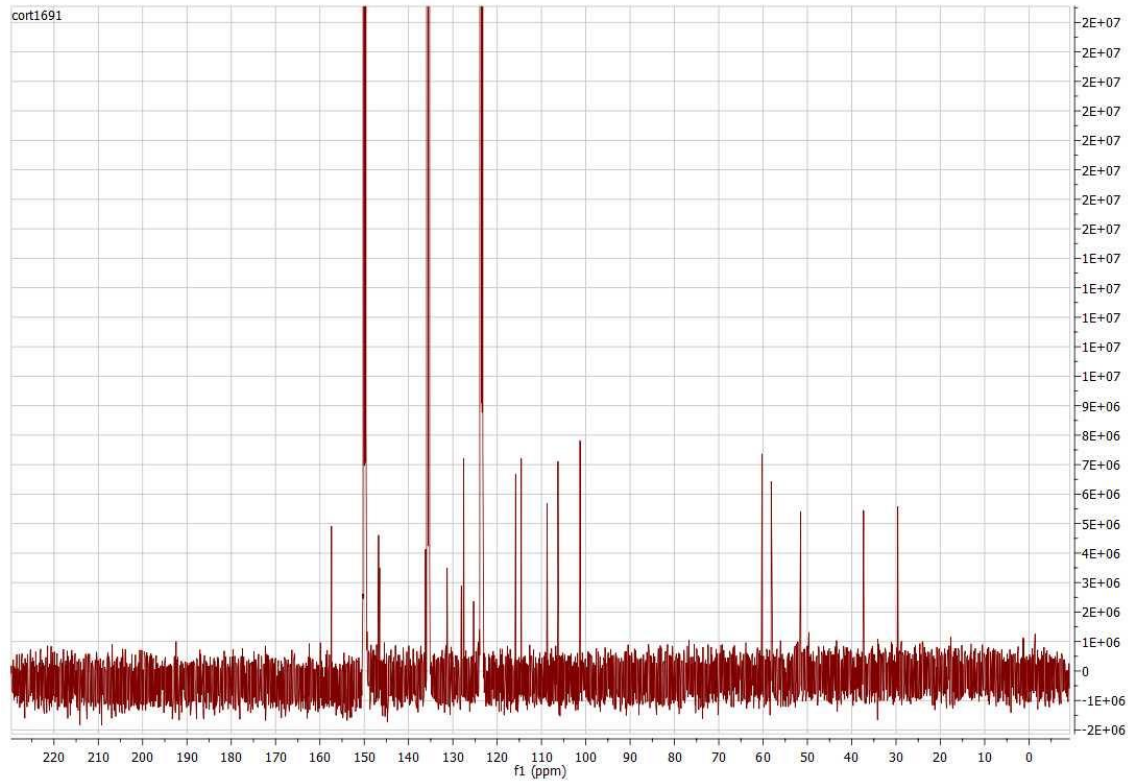

Espectros en C_5D_5N de ^{1}H-RMN (500 MHz) y ^{13}C-RMN (125 MHz) de **9e**

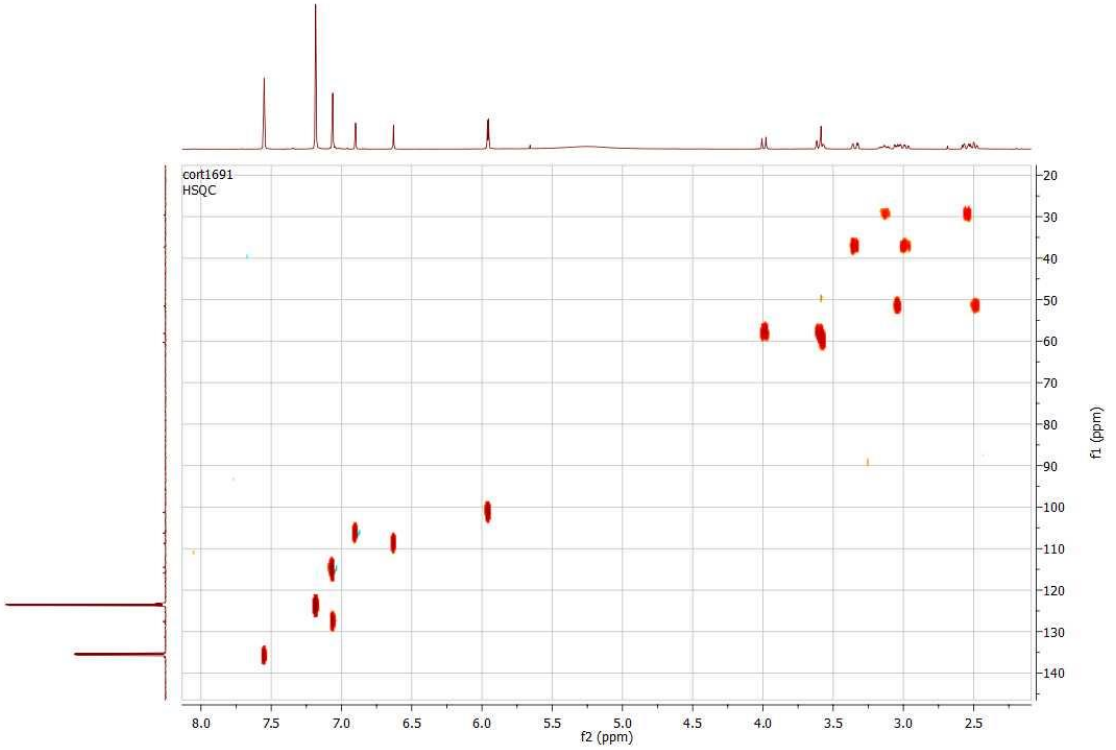

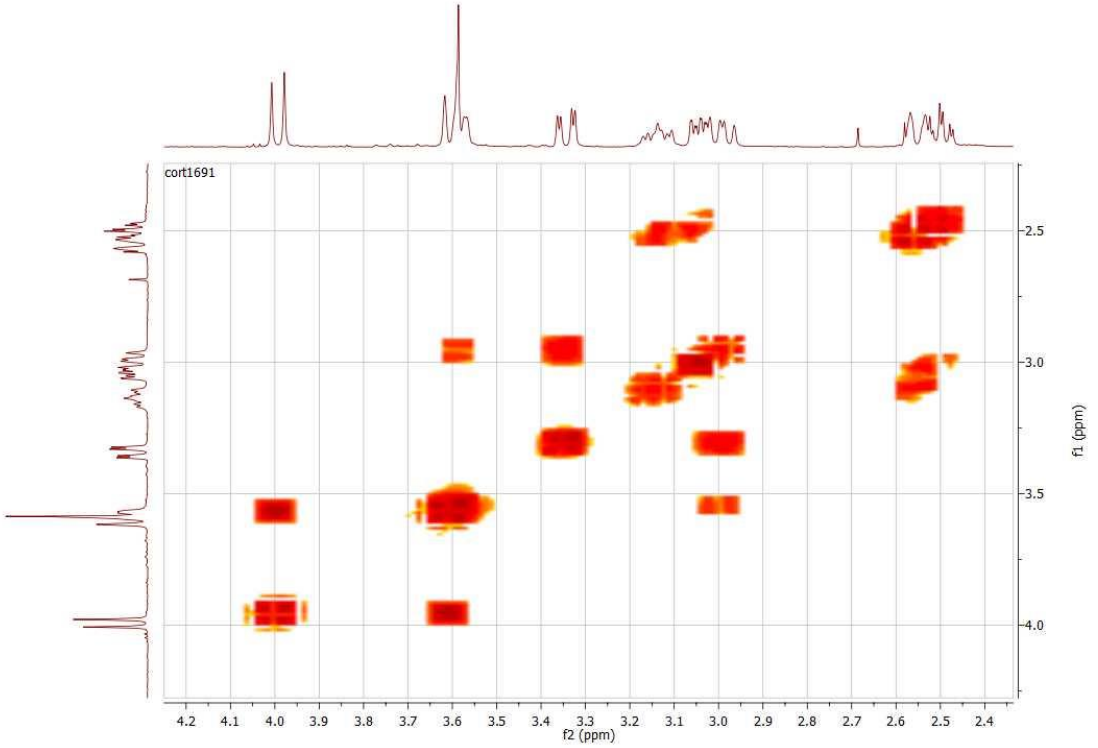

Espectros en C_5D_5N de HSQC y COSY 45 de **9e**

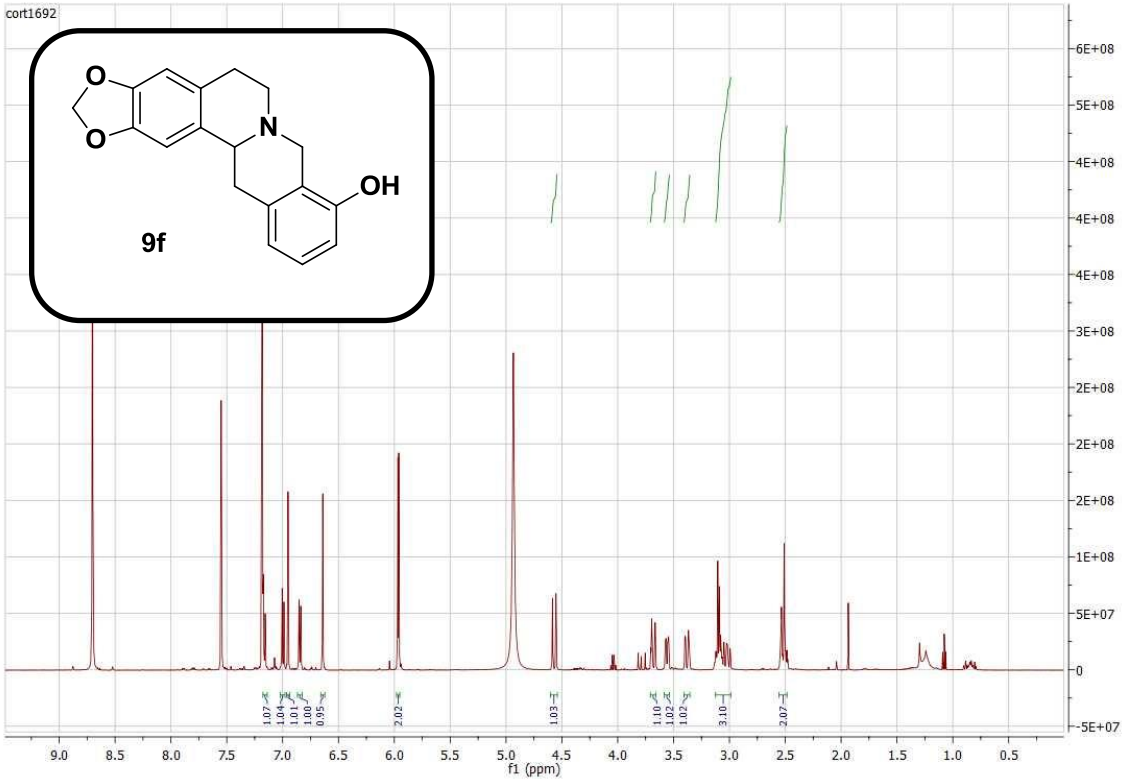

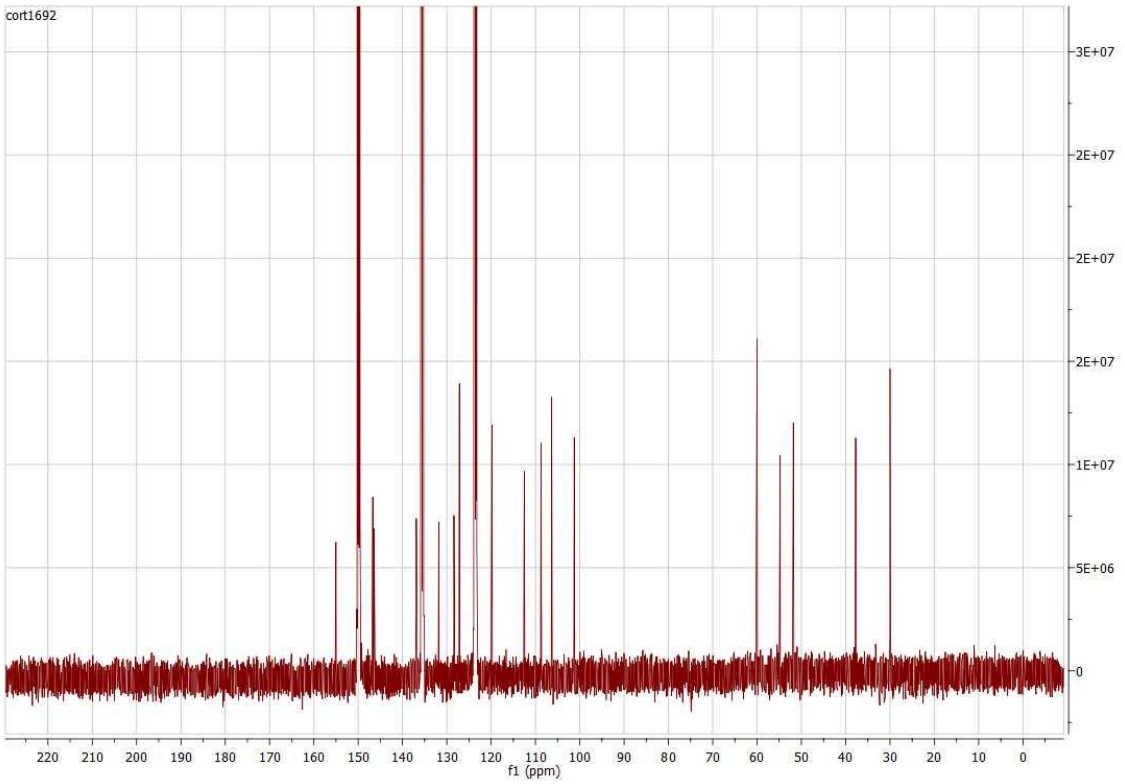

Espectros en C_5D_5N de ^{1}H-RMN (500 MHz) y ^{13}C-RMN (125 MHz) de **9f**

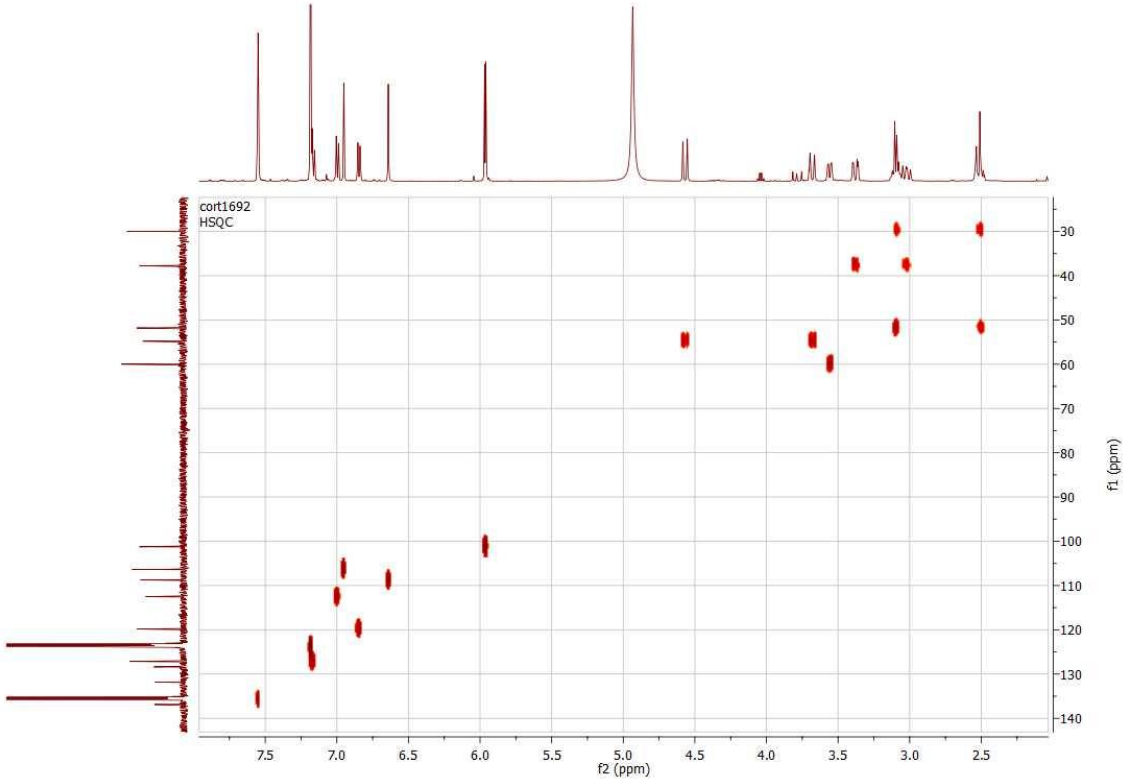

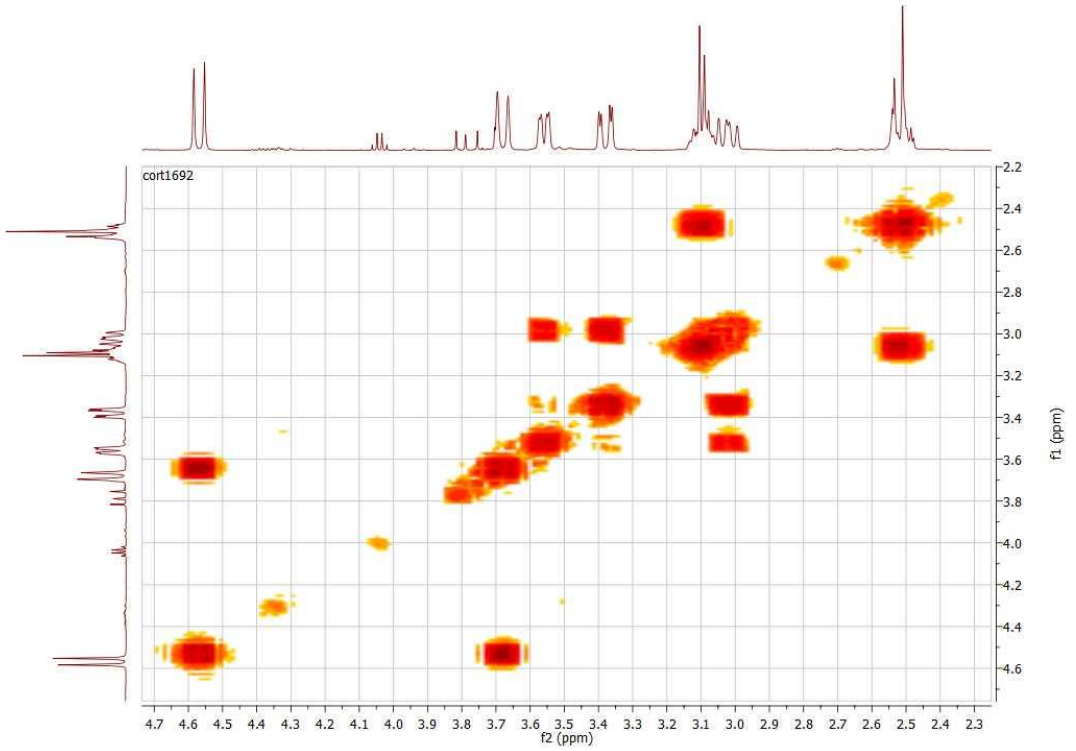

Espectros en C_5D_5N de HSQC y COSY 45 de **9f**

Espectros relativos al Artículo 2

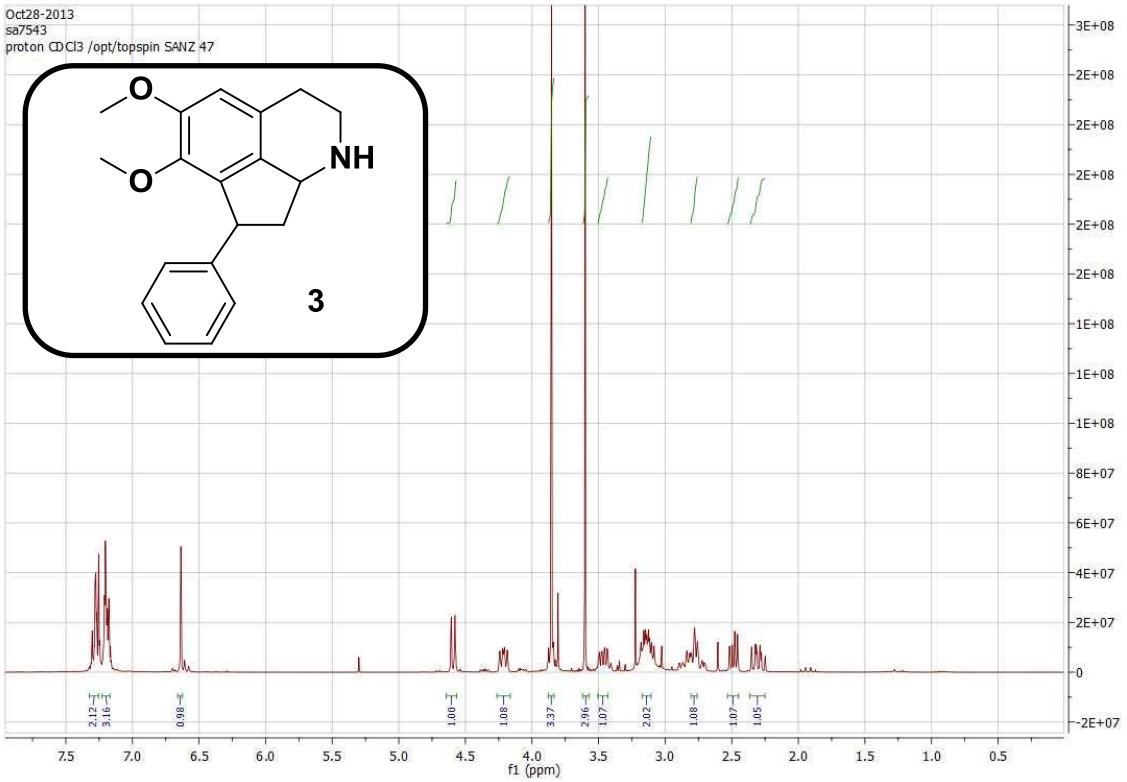

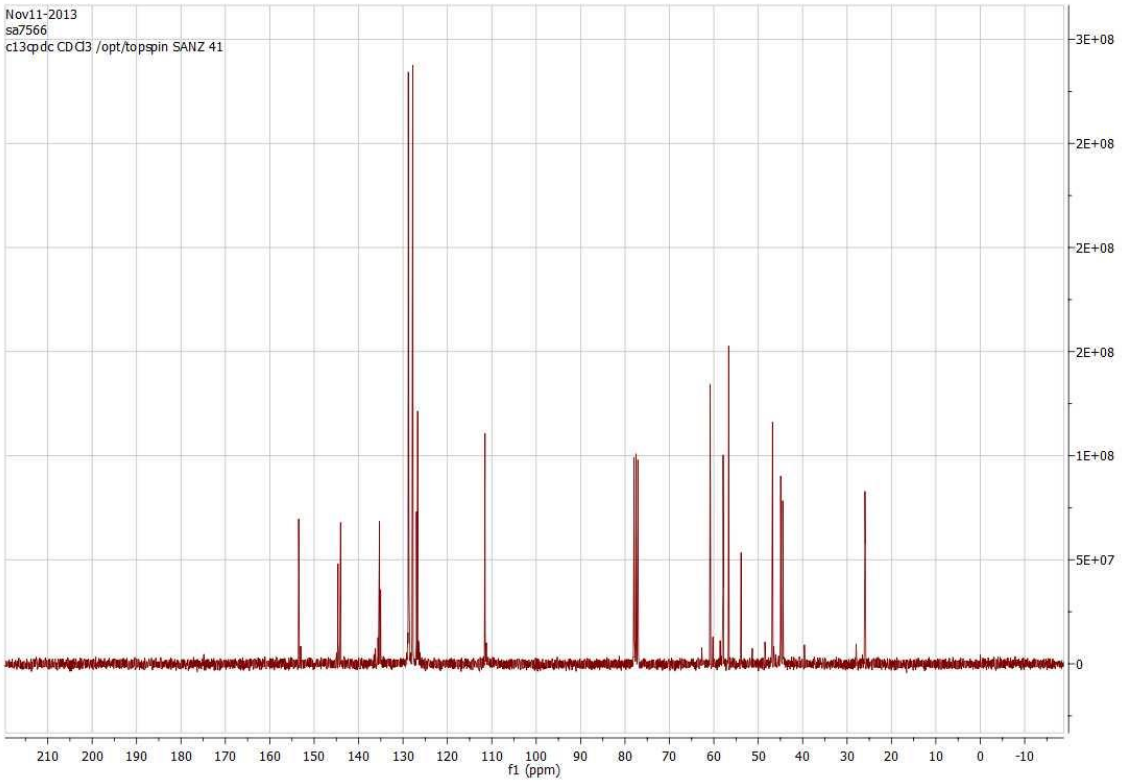

Espectros en $CDCl_3$ de ^{1}H-RMN (500 MHz) y ^{13}C-RMN (125 MHz) de **3**

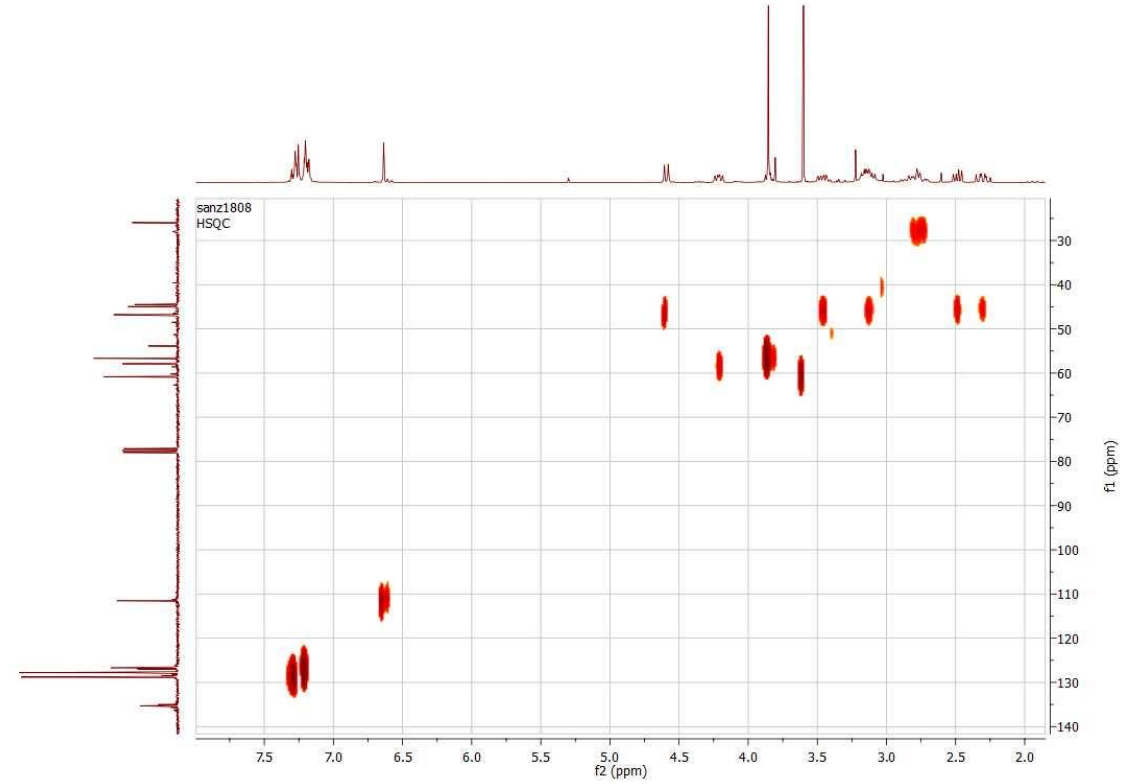

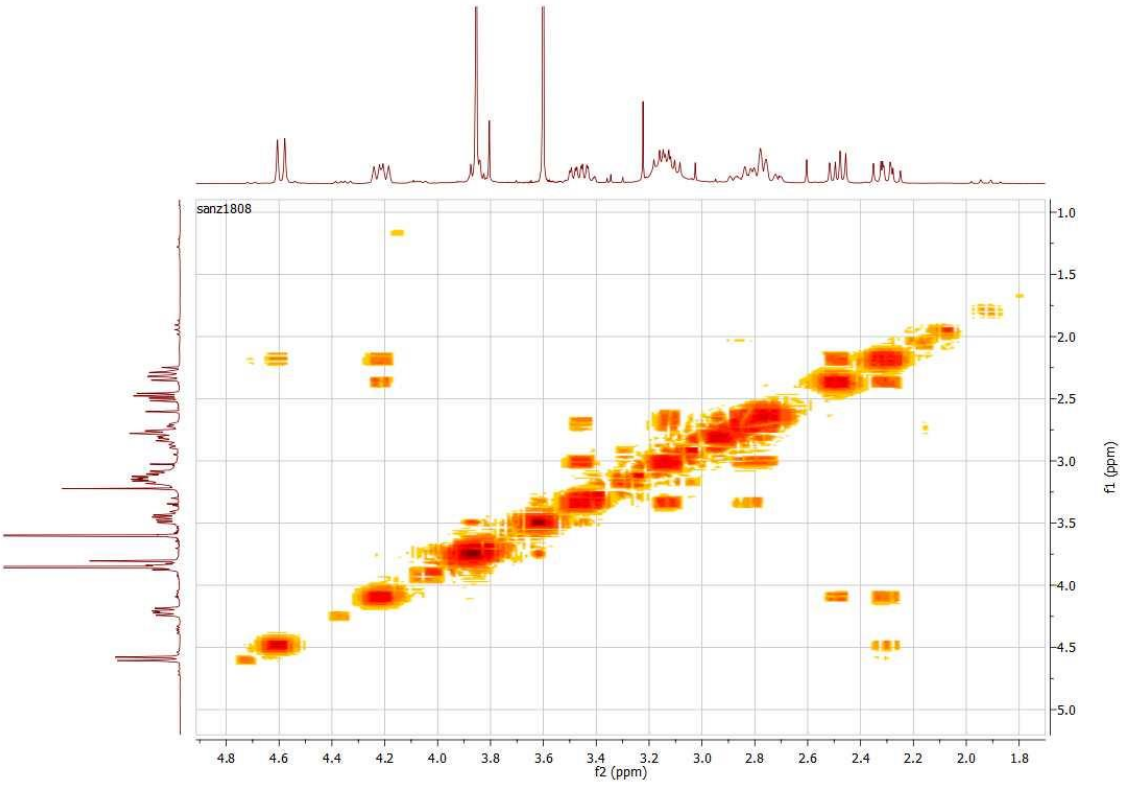

Espectros en $CDCl_3$ de HSQC y COSY 45 de **3**

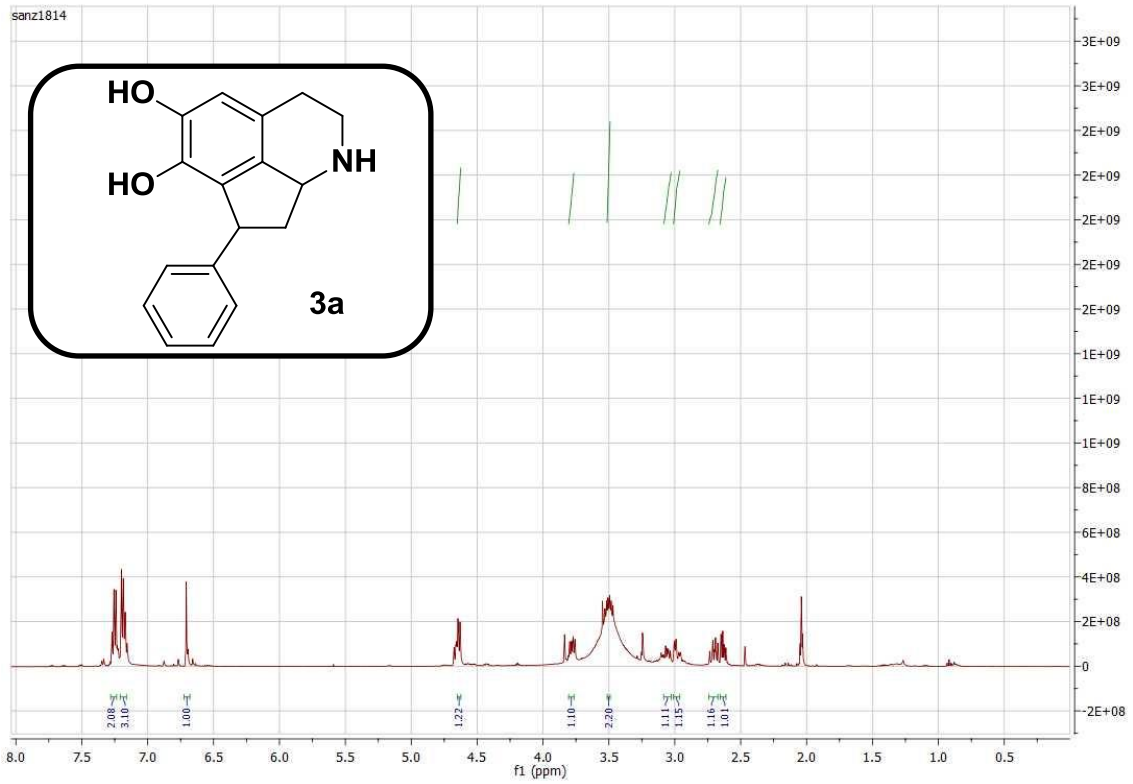

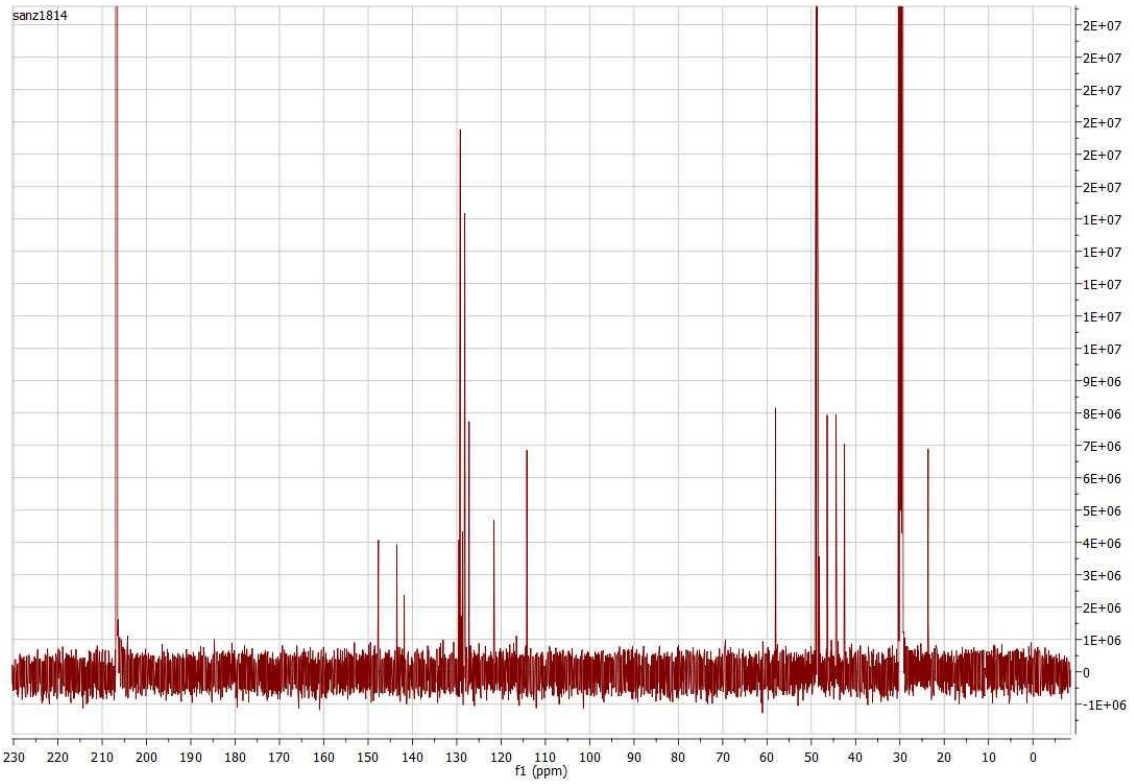

Espectros en $(CD_3)_2CO$ y CD_3OD de ^{1}H-RMN (500 MHz) y ^{13}C-RMN (125 MHz) de **3a**

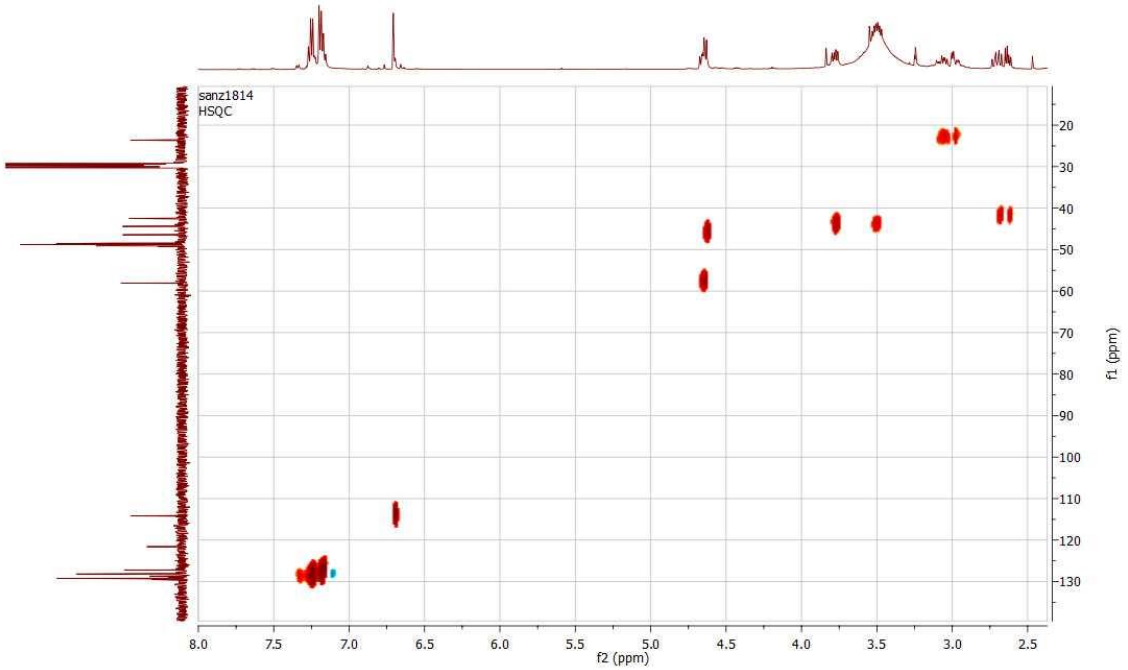

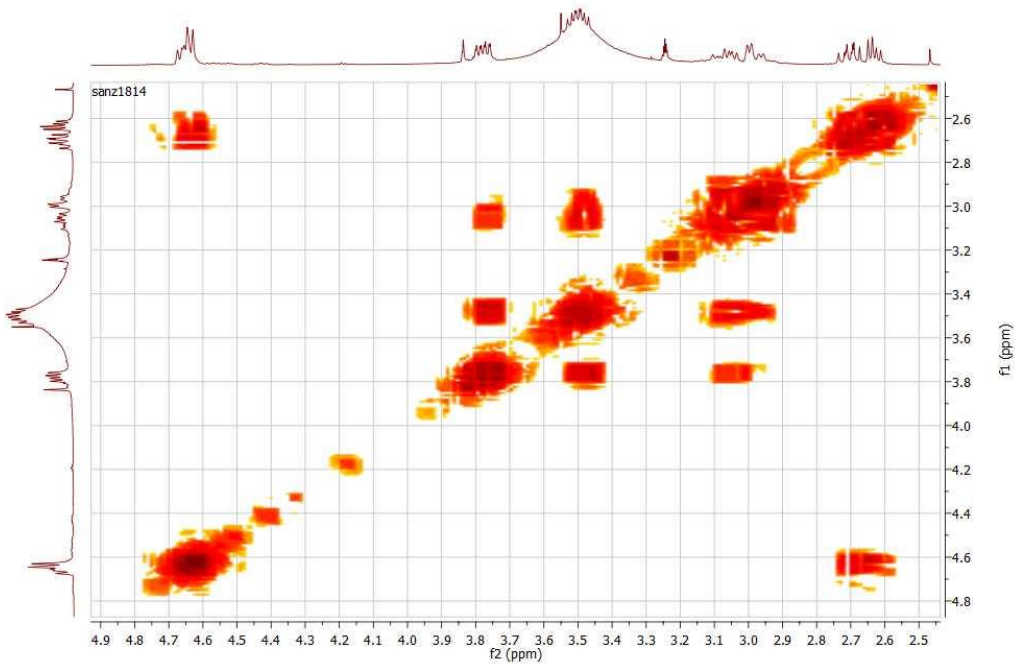

Espectros en $(CD_3)_2CO$ y CD_3OD de HSQC y COSY 45 de **3a**

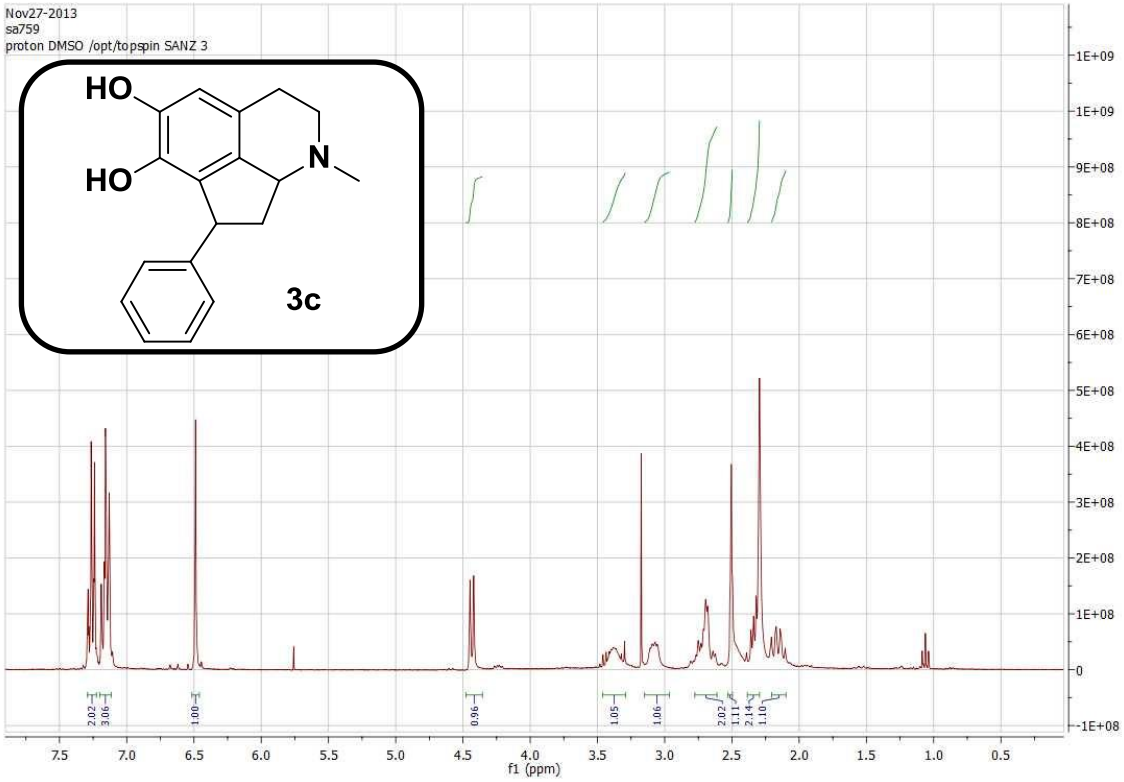

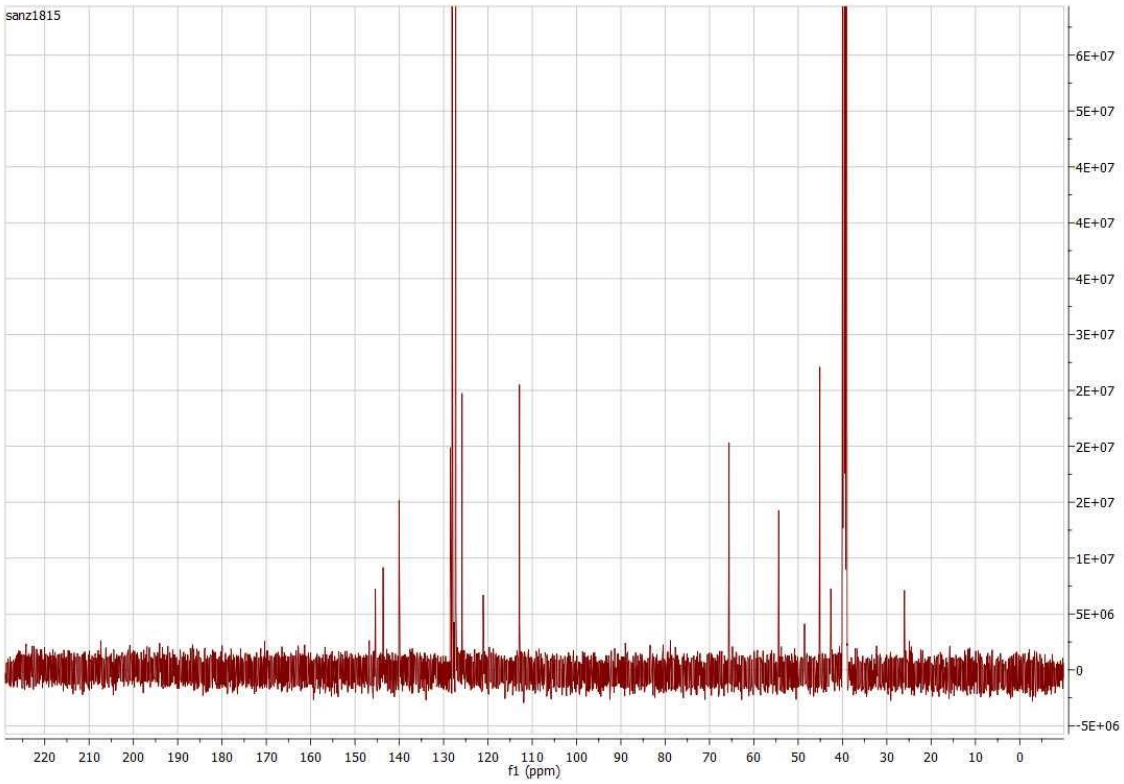

Espectros en $CDCl_3$ de ^{1}H-RMN (500 MHz) y ^{13}C-RMN (125 MHz) de **3c**

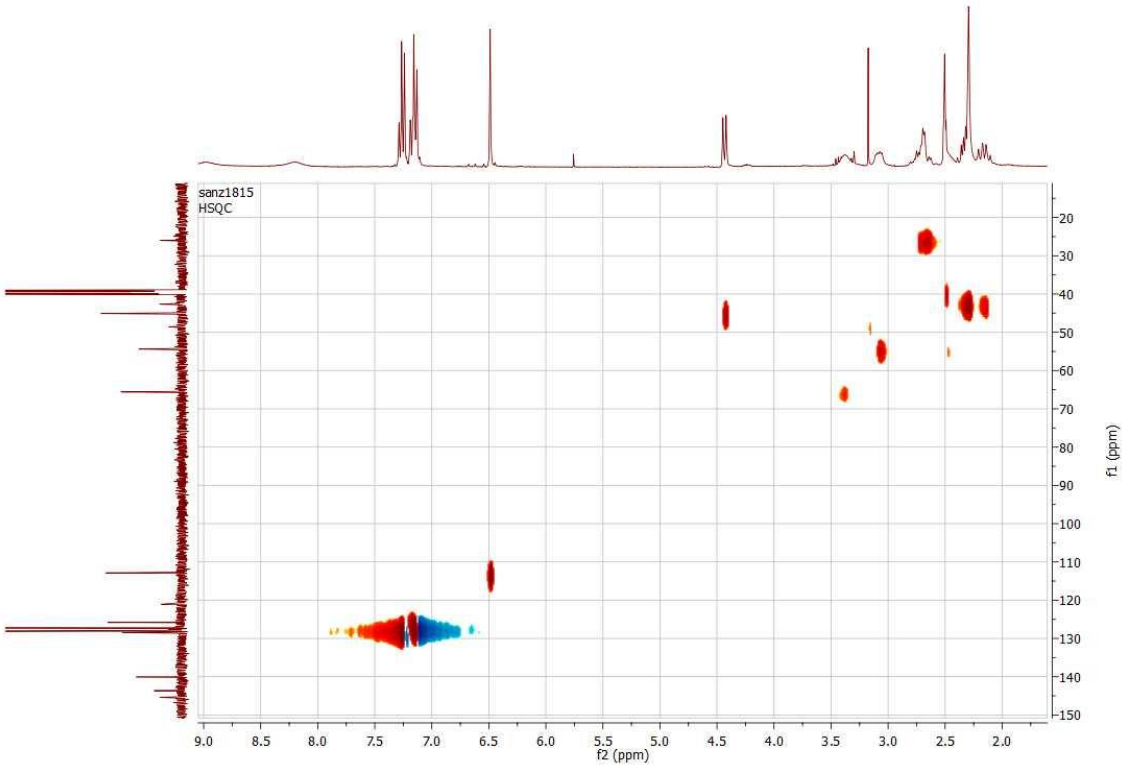

Espectro en $CDCl_3$ de HSQC de **3c**

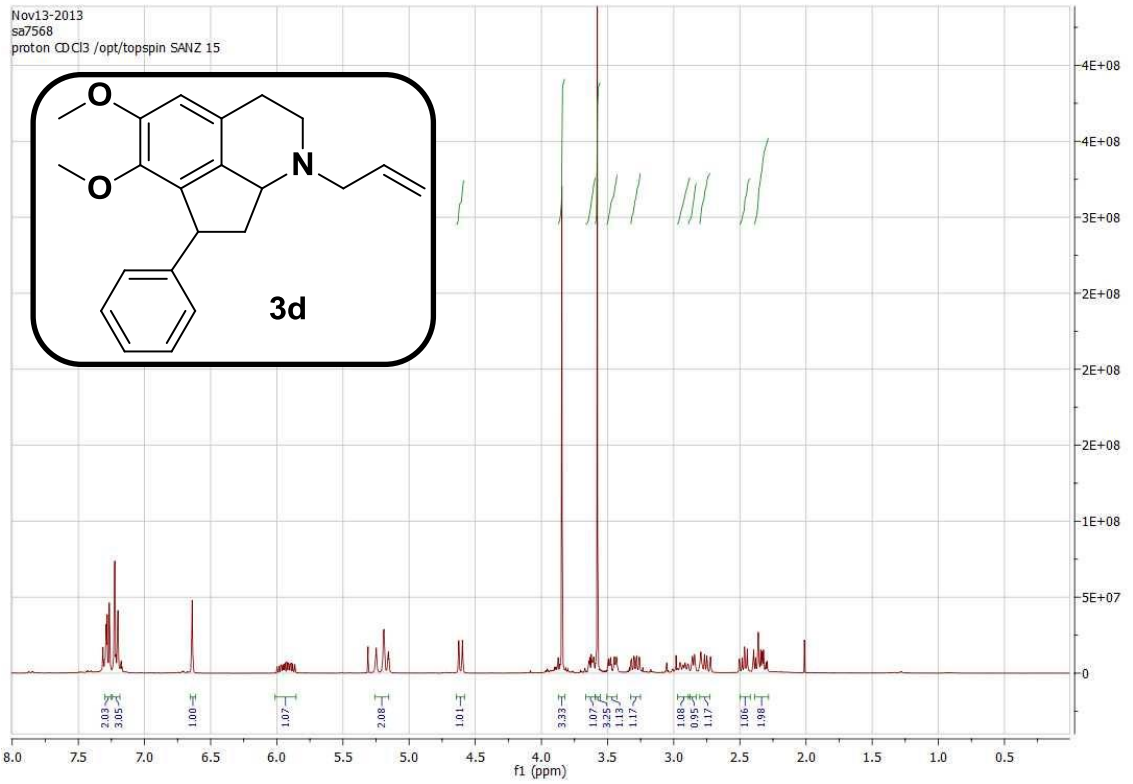

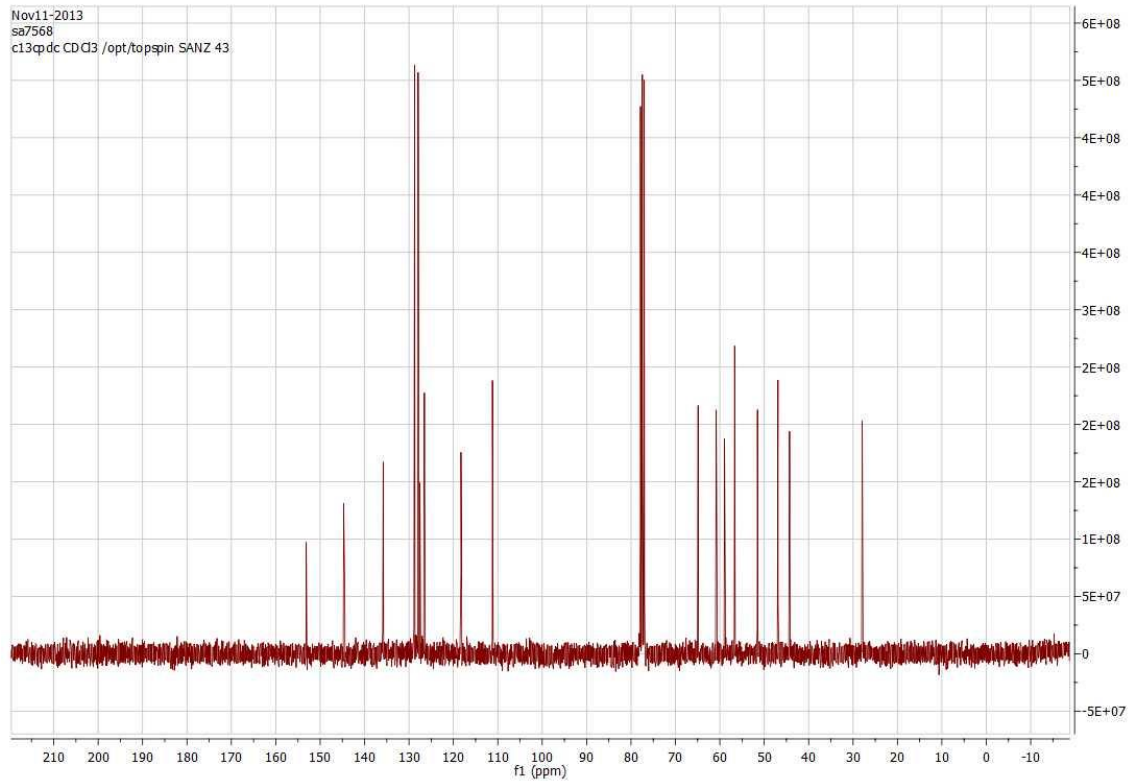

Espectros en $CDCl_3$ de ^{1}H-RMN (500 MHz) y ^{13}C-RMN (125 MHz) de **3d**

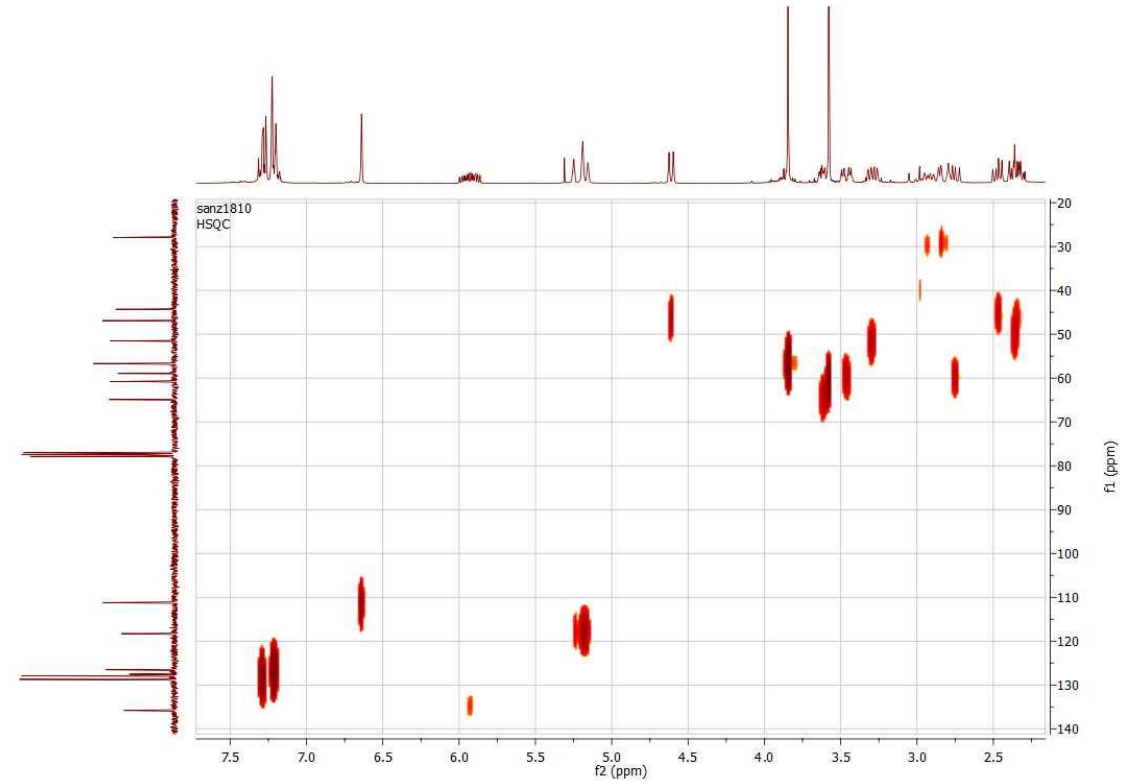

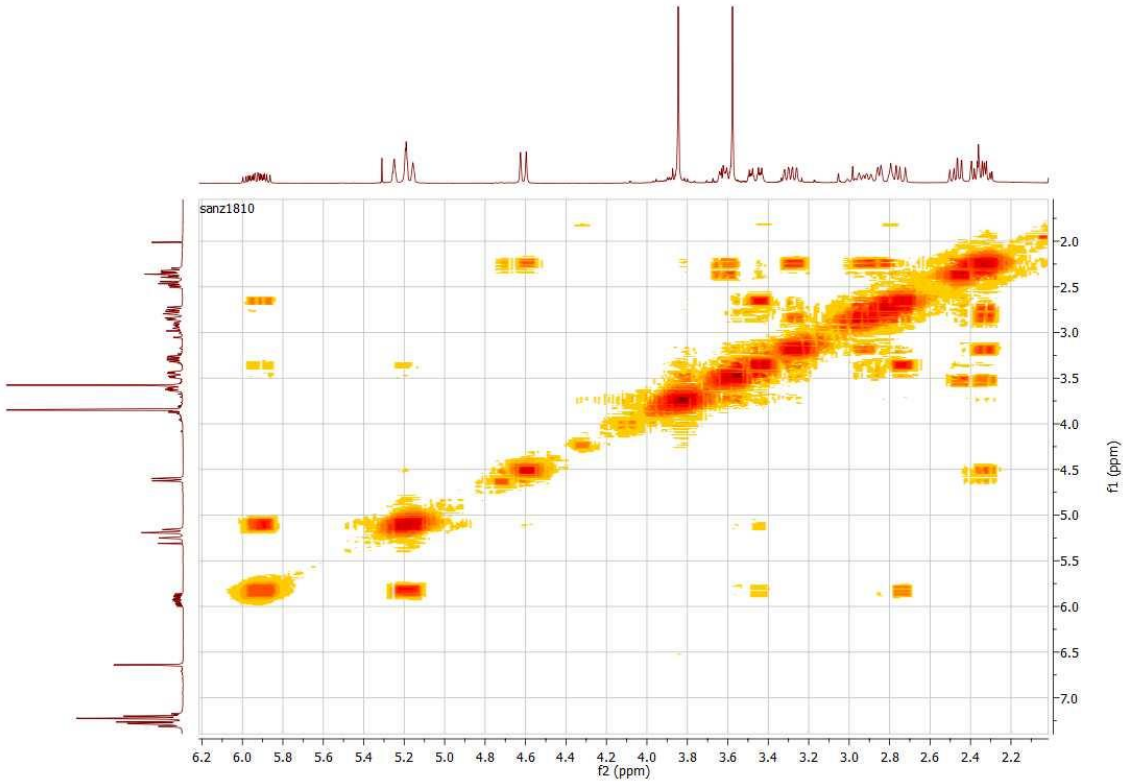

Espectros en $CDCl_3$ de HSQC y COSY 45 de **3d**

Espectros Capítulo 2

Espectros referentes a los Artículos 4 y 5

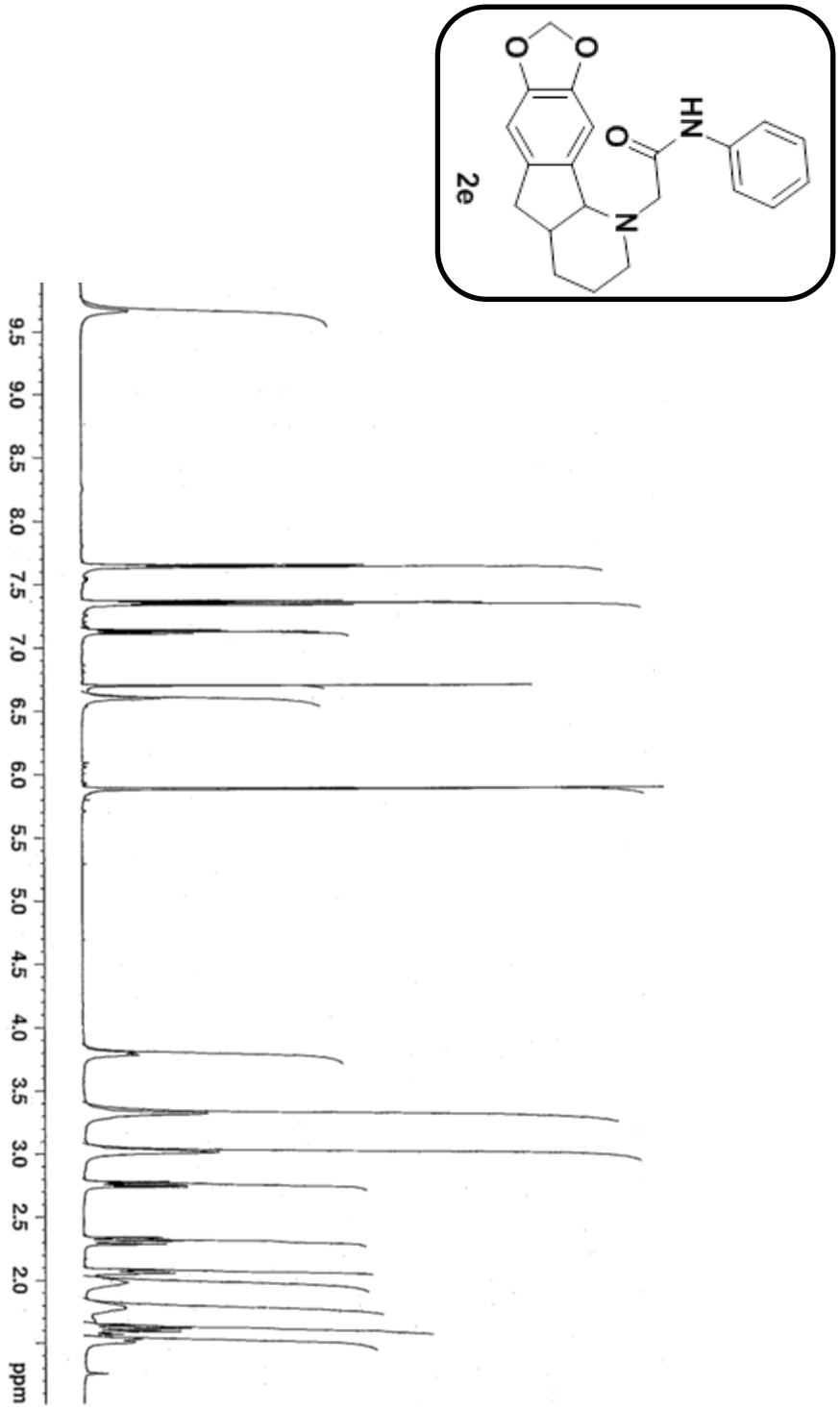

Espectros en $CDCl_3$ de ^{1}H-RMN (500 MHz) y ^{13}C-RMN (125 MHz) de **2e**

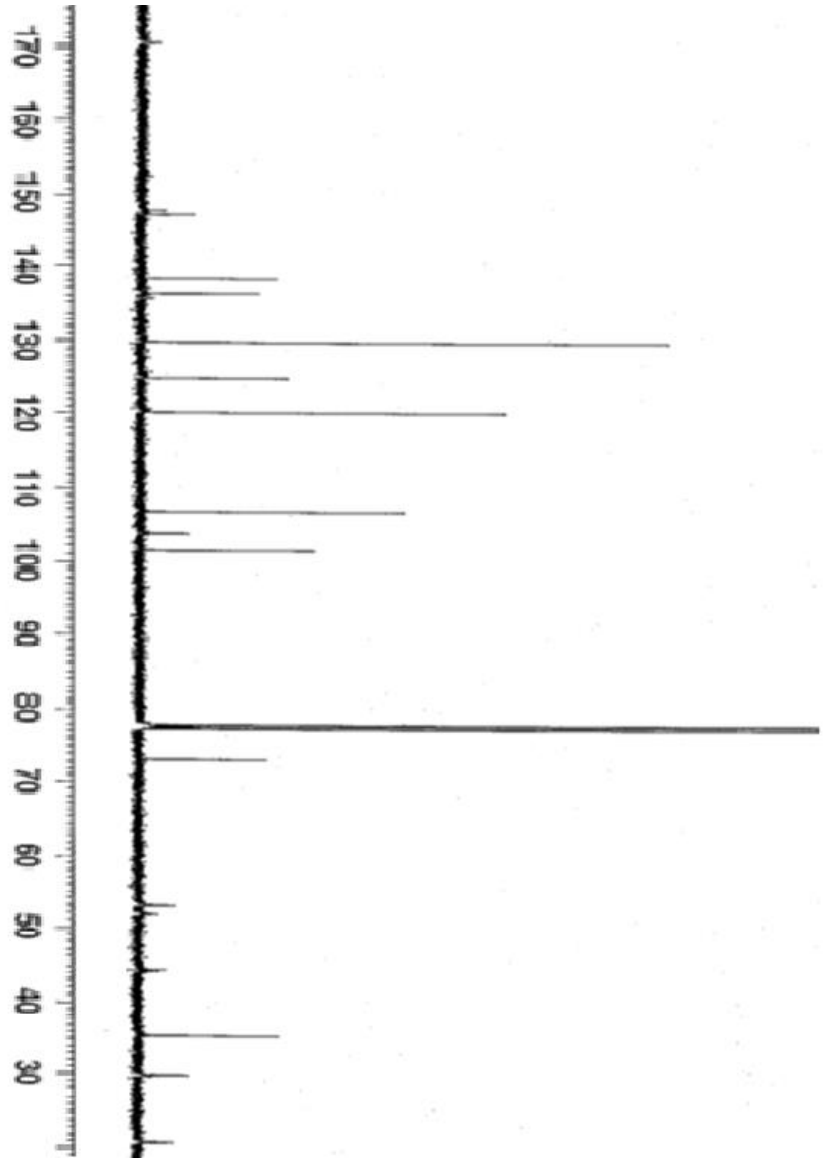

Espectros en $CDCl_3$ de ^{1}H-RMN (500 MHz) y ^{13}C-RMN (125 MHz) de **2e**

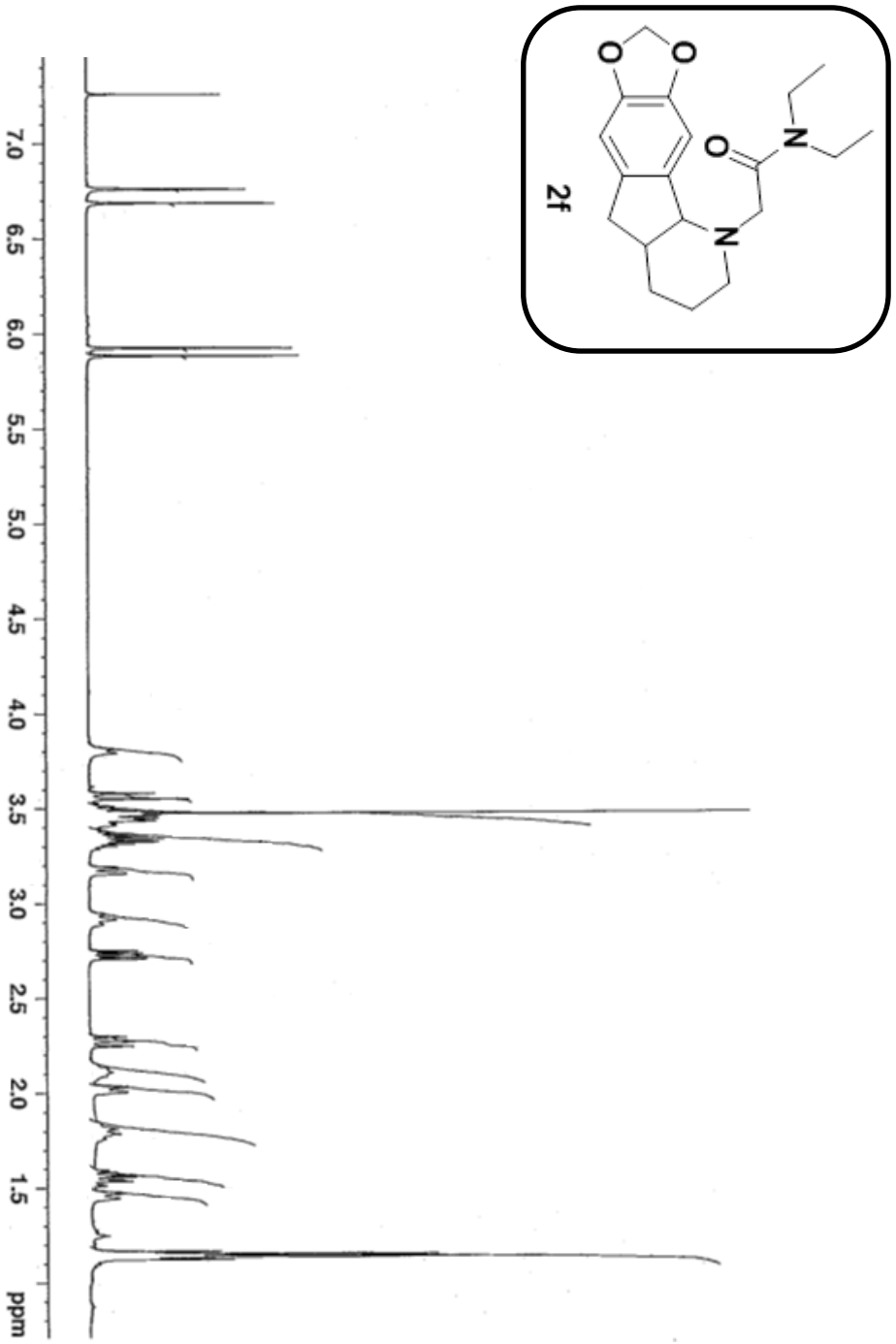

Espectros en $CDCl_3$ de ^{1}H-RMN (500 MHz) y ^{13}C-RMN (125 MHz) de **2f**

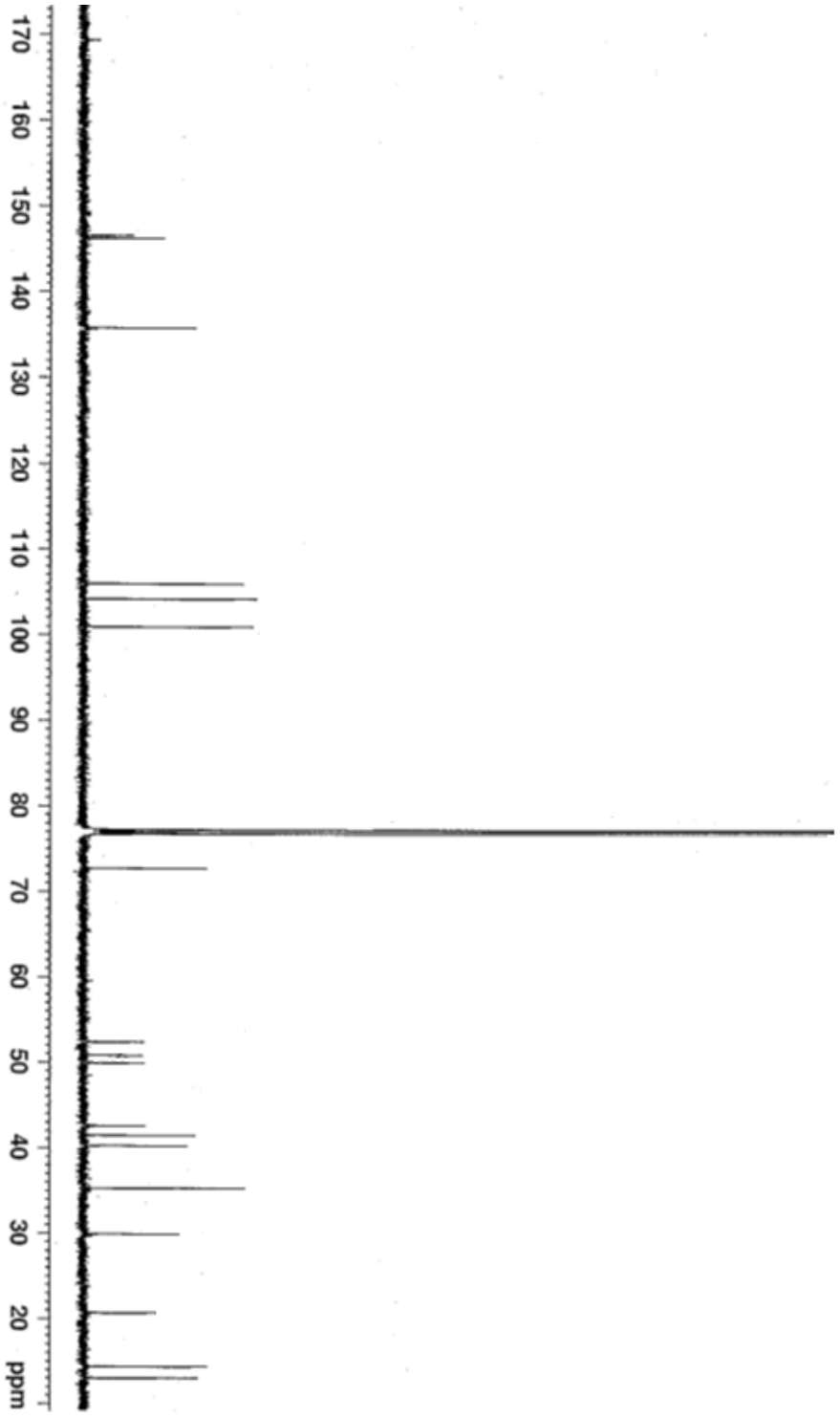

Espectros en $CDCl_3$ de ^{1}H-RMN (500 MHz) y ^{13}C-RMN (125 MHz) de **2f**

Espectros Capítulo 3

Espectros referentes a los Artículos 6

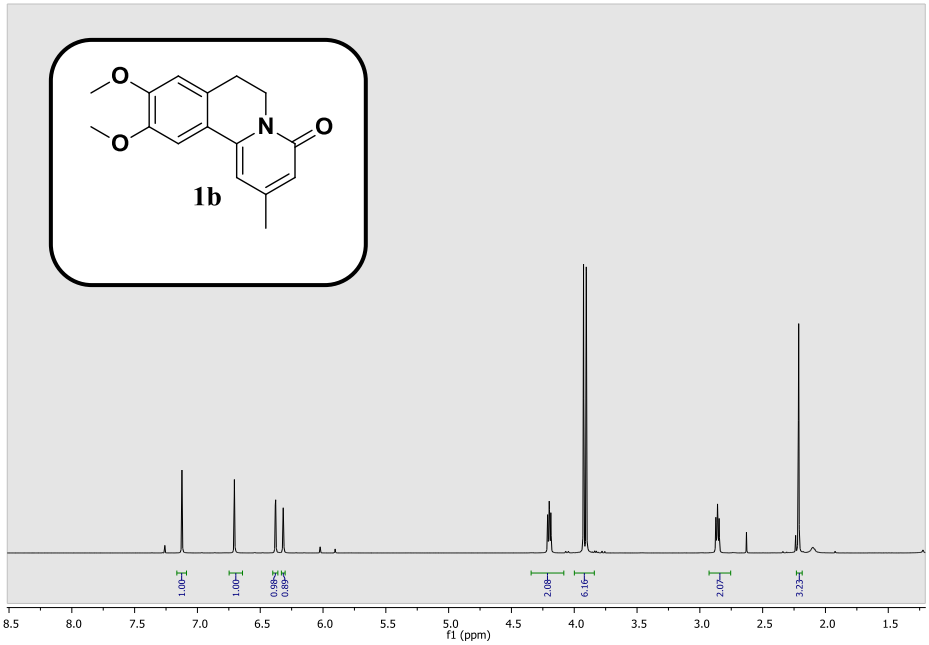

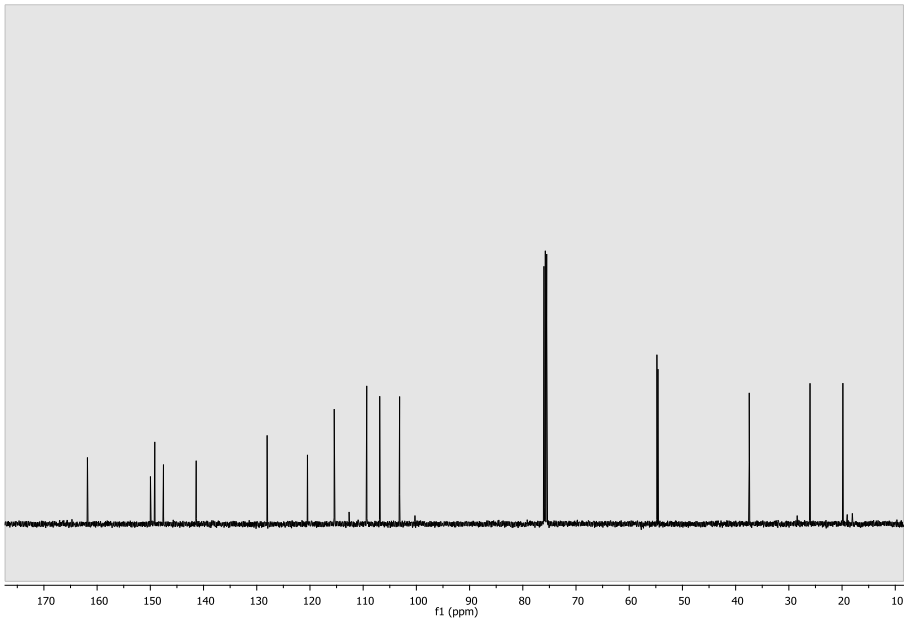

Espectros en $CDCl_3$ de ^{1}H-RMN (500 MHz) y ^{13}C-RMN (125 MHz) de **1b**

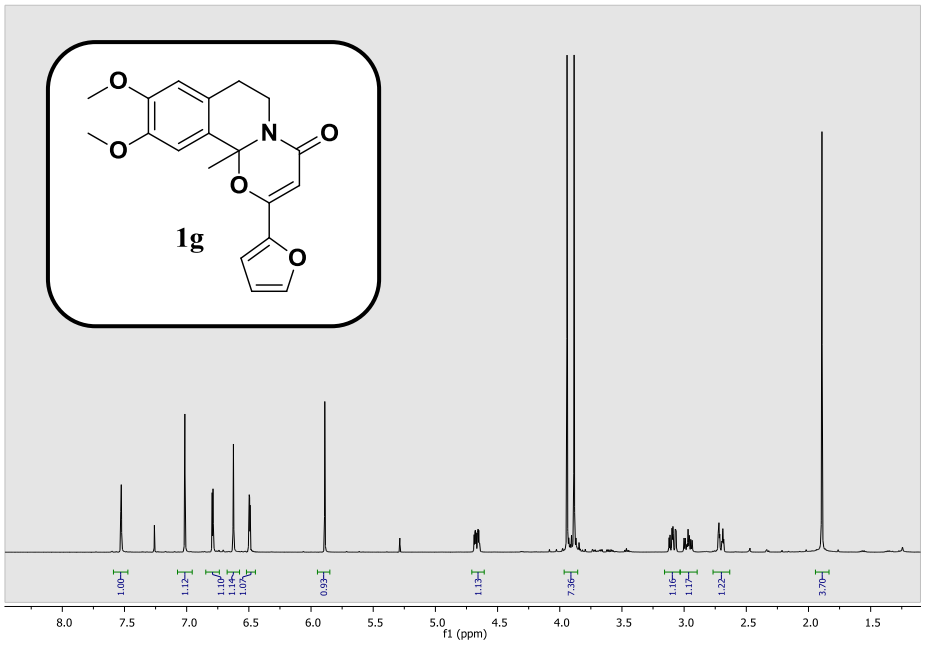

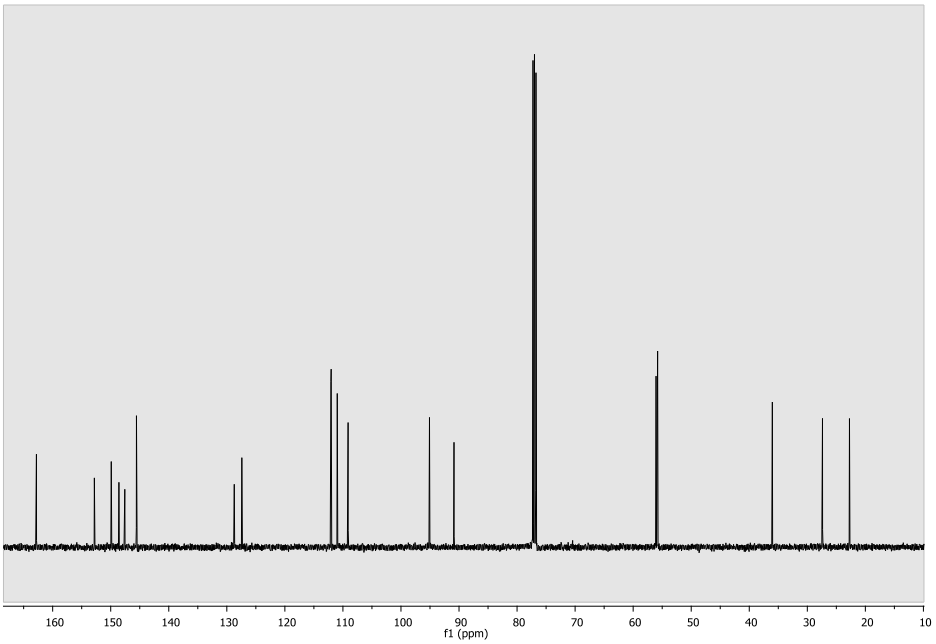

Espectros en $CDCl_3$ de ^{1}H-RMN (500 MHz) y ^{13}C-RMN (125 MHz) de **1g**

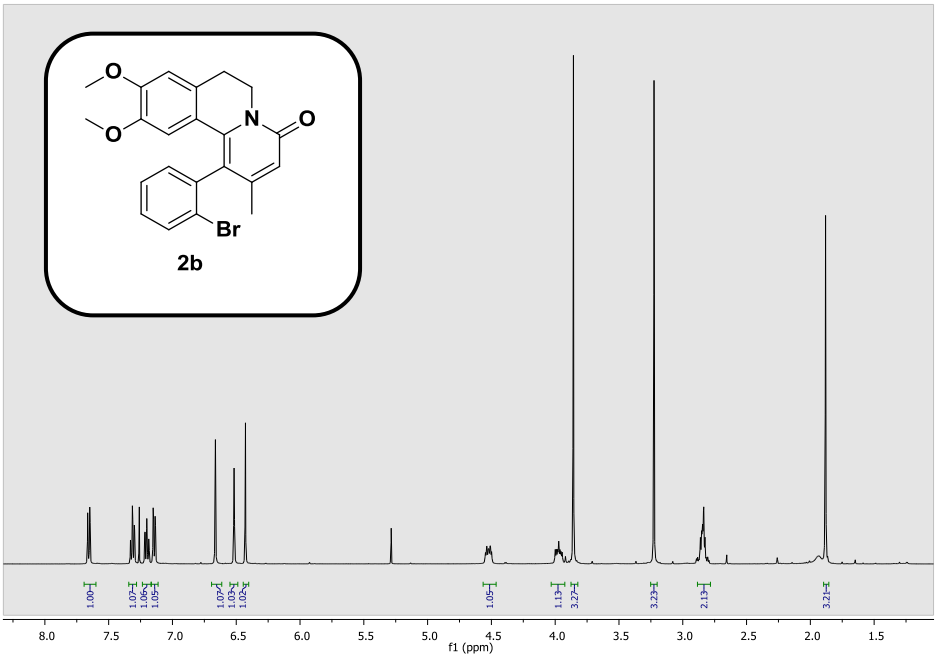

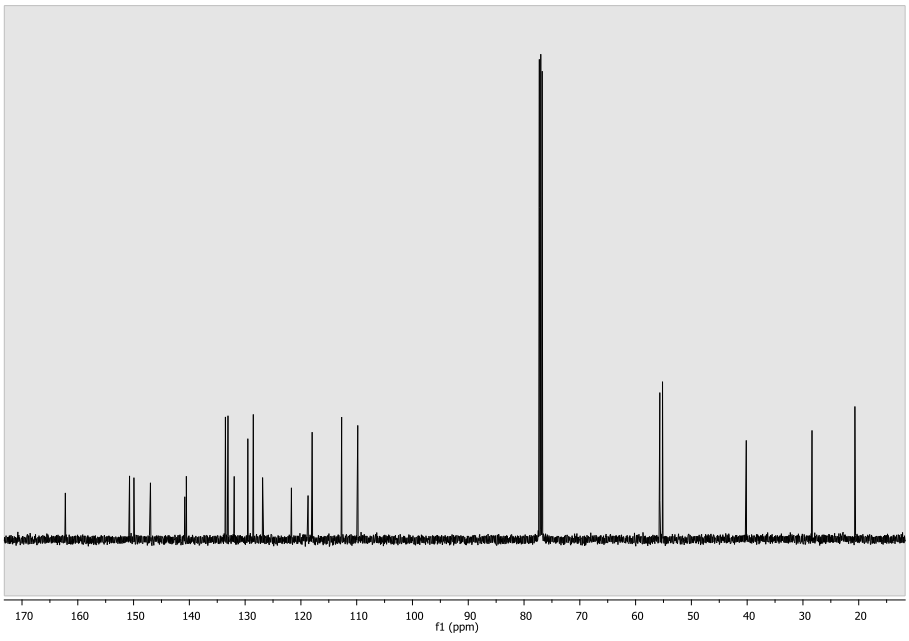

Espectros en $CDCl_3$ de ^{1}H-RMN (500 MHz) y ^{13}C-RMN (125 MHz) de **2b**

Espectros referentes a los Artículos 7

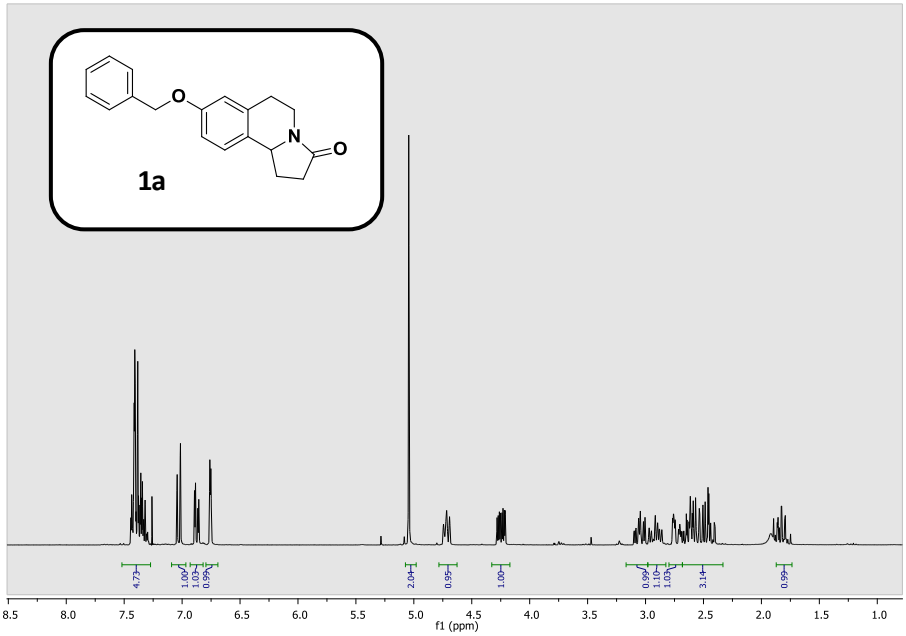

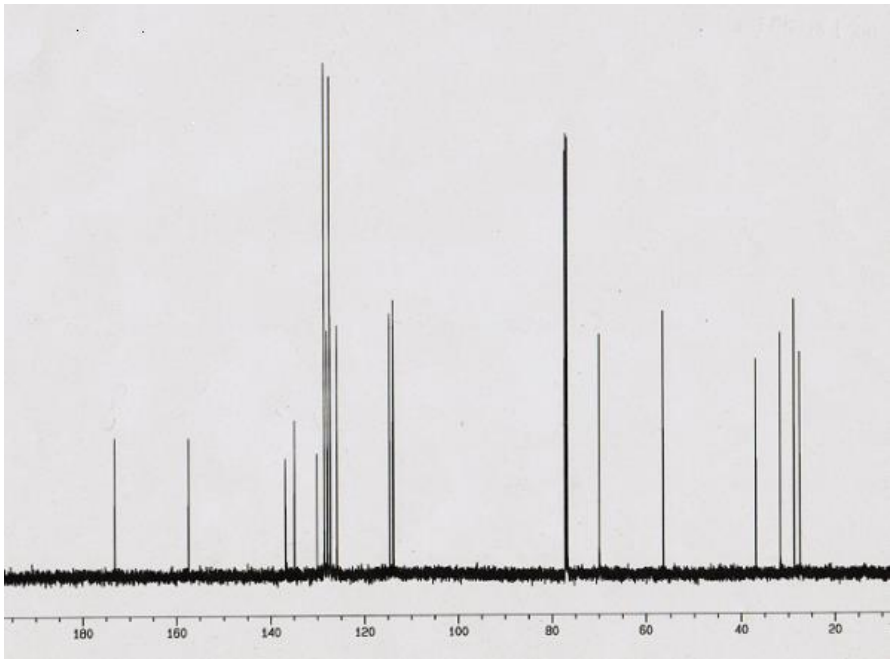

Espectros en $CDCl_3$ de ^{1}H-RMN (500 MHz) y ^{13}C-RMN (125 MHz) de **1a**

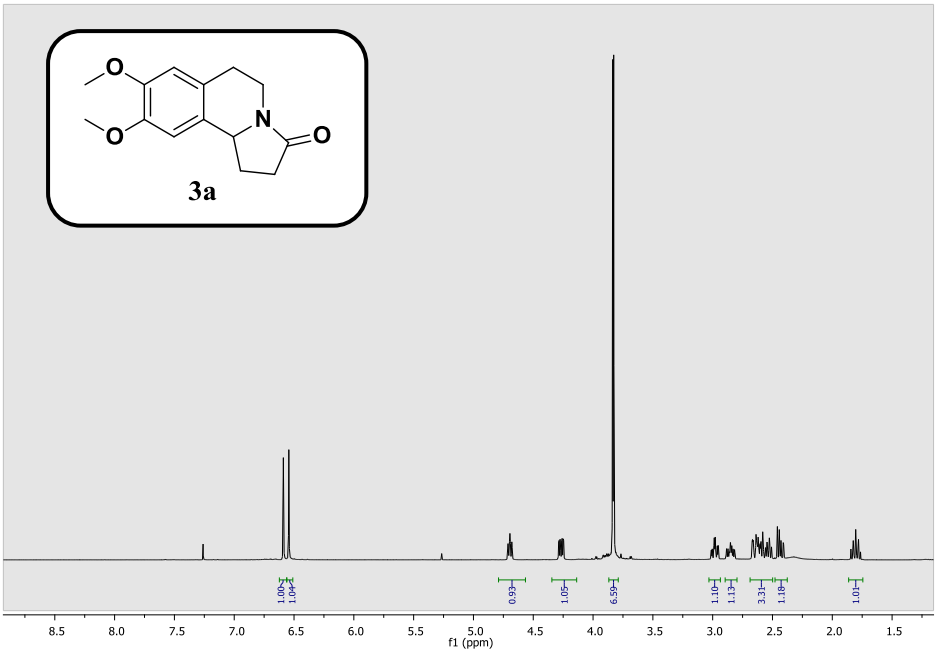

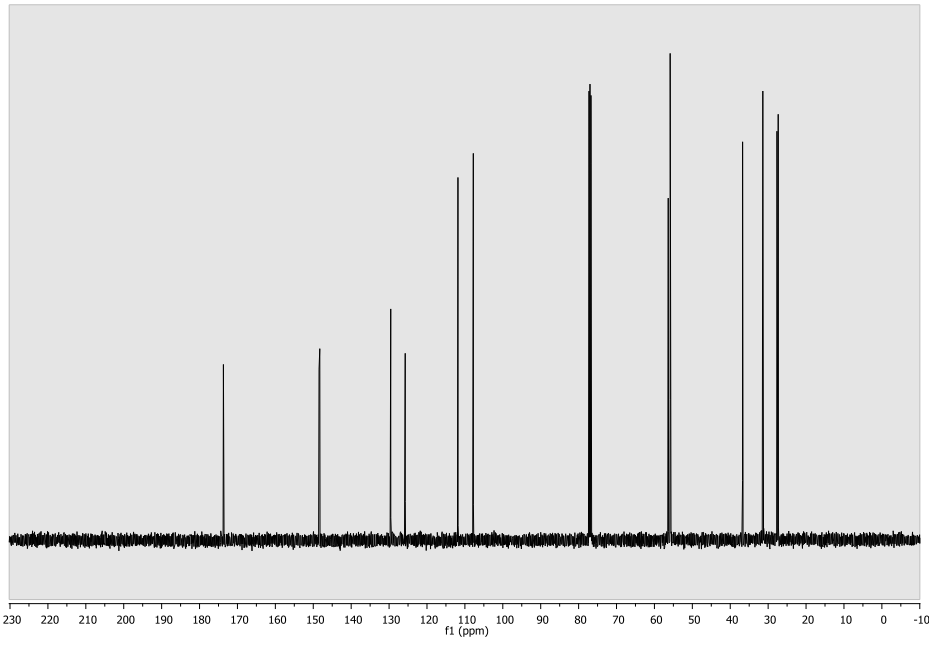

Espectros en $CDCl_3$ de ^{1}H-RMN (500 MHz) y ^{13}C-RMN (125 MHz) de **3a**

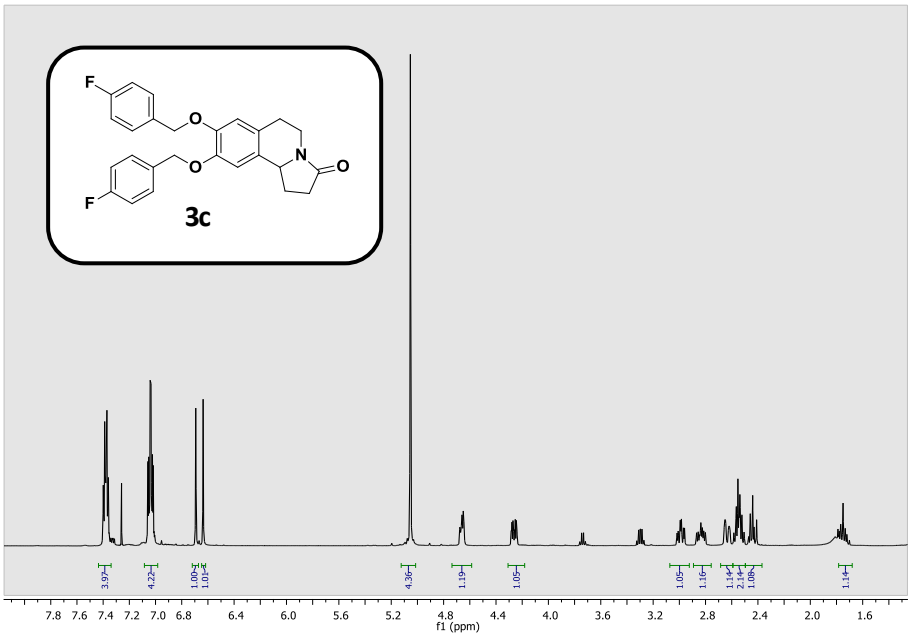

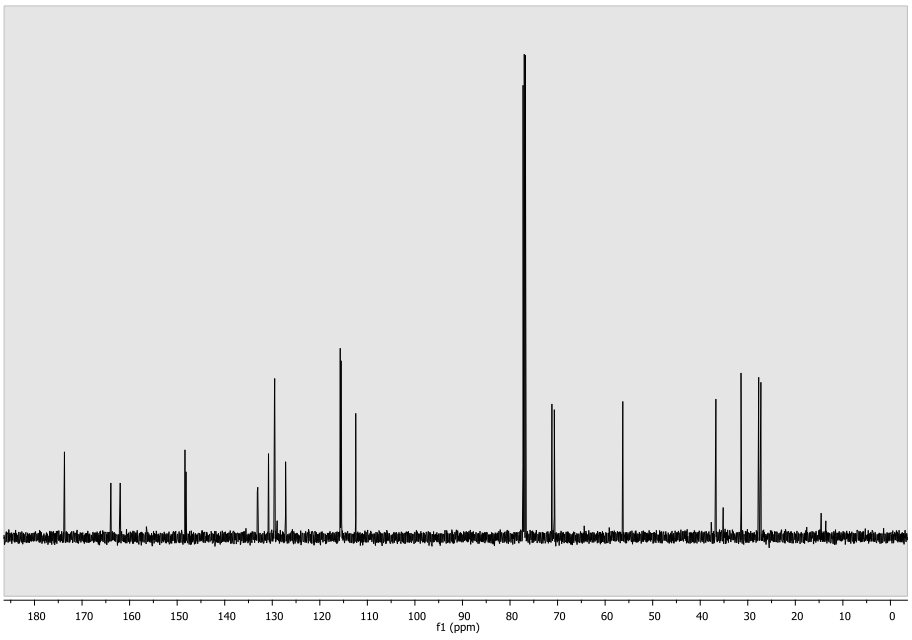

Espectros en $CDCl_3$ de ^{1}H-RMN (500 MHz) y ^{13}C-RMN (125 MHz) de **3c**